Minerals, Rocks and Mountains 17

Frederick J. Sawkins

Metal Deposits in Relation to Plate Tectonics

Second Edition

Minerals and Rocks 17

F. J. Sawkins

Metal Deposits in Relation to Plate Tectonics

Second Revised and Enlarged Edition

With 246 Figures

Springer-Verlag Berlin Heidelberg GmbH

Dr. FREDERICK J. SAWKINS
Department of Geology and Geophysics
University of Minnesota
108 Pillsbury Hall
310 Pillsbury Drive S.E.
Minneapolis, MN 55455, USA

Volumes 1 to 9 in this series appeared under the title
Minerals, Rocks and Inorganic Materials

ISBN 978-3-662-08683-4 ISBN 978-3-662-08681-0 (eBook)
DOI 10.1007/978-3-662-08681-0

Originally published by Springer-Verlag Berlin Heidelberg New York in 1990.

Typesetting: Overseas Typographers, Inc., Makati, Philippines
2132/3145-543210 – Printed on acid-free paper

Preface to the Second Edition

Almost all the reviews of the first edition of *Metal Deposits in Relation to Plate Tectonics* have been positive, some enthusiastically so. The dissenters either represent the diminishing ranks of those still dubious about the far-reaching implications of plate tectonic theory, or they seem to be tied to rather special interests. Whatever the level of acceptance of the first edition, I am keenly aware of certain serious shortcomings, some related to omissions, others to matters of balance in emphasis.

This edition attempts to rectify these faults and to incorporate at least some of the significant advances in the available data and conceptual thinking that the last five years have brought to the science of economic geology. In addition, in recognition of current and, almost certain, future emphasis on gold within the exploration community, I have paid particular attention to the geological settings and generative models of gold deposits of all kinds.

There doubtless will be much scepticism in certain quarters regarding the emphasis that has been placed on the importance of magmatic-hydrothermal processes for the vast majority of the metal deposits that are formed in arc systems. My position on this matter has been long standing, influenced by due consideration for the geology of arc-related metal deposits and for the specifics of their distribution in time and space, as well as by the constraints of geochemistry. Geochemical modelling certainly has its place in the spectrum of ore deposits research, but its use without tight geologic constraints and concern for physical processes has led some investigators up some very blind alleys.

The basic format of the first edition has been retained, including the suggestions for exploration. I fully appreciate that parts of these latter segments will seem naive to advanced practitioners of the exploration business, but, as explained in the original preface, my intent is only to help the student or more general reader to appreciate the fundamental connection between genetic concepts and their utilization in exploration strategy. Few books dealing with ore deposits offer this additional information.

As before, I have attempted to assemble a bibliography that is as current as possible and that is not replete with entries that have limited availability. One is always conscious, however, that all around the world a great deal of excellent work is either in publication or in progress and thus lies undiscovered by the writer. R. H. Sillitoe again kindly agreed to edit and review my initial, somewhat raw, typescript, and in the process readily shared his enormous experience and expertise regarding the occurrence and formation of hydrothermal metal deposits.

Finally, my thanks to those who, either through published reviews or personal contact, have voiced their support for my efforts. It is in large measure because of them that I find encouragement to attempt a second edition relatively soon after the appearance of the original.

Frederick J. Sawkins

Preface to the First Edition

I attempt this volume with no small degree of trepidation, for despite the near universal acceptance of plate tectonic theory, and the undeniable sweep and power of the concepts involved, points of controversy and uncertainty still abound. This is especially true with regard to the limited extent to which many ancient geologic terranes, however well studied, lend themselves to plate tectonic interpretation. There is also considerable controversy regarding the genesis of many metal deposits, and this impacts upon the degree to which such deposits can be meaningfully related to the tectonic settings in which they occur.

It is relatively simple matter to point out that certain types of ore deposits exhibit impressive time-space associations with certain kinds of more recent plate boundary environments. It is also all too easy to posit plate tectonic-ore deposit relationships in ancient geologic terranes. What is more challenging is the recognition of the boundaries beyond which speculation is idle, but within which useful new insights regarding the relationship of certain ores to their lithologic and tectonic environments may emerge.

My interest in plate tectonic-metal deposit relationships was initially motivated by a desire to find a suitable framework within which students could be introduced to the wide variety of distinctive metal deposit types. Somewhat later it was fostered by the desire to investigate the degree to which such concepts could be used in creative planning of exploration programs. However, I have encountered a certain degree of confusion about metal deposits and their divergent types amongst students, exploration geologists, and geochemists interested in ore genesis problems. We all have much to learn regarding these matters, but an attempt at synthesis seems warranted at this time, especially in view of our increasing dependence on earth resources. I make no claim that application of plate tectonic concepts can pinpoint new metal deposits. The main tool available to the exploration geologist is that of analogy with respect to other deposits and to their lithologic settings, i.e., certain types of

metal deposits occur in association with certain types of rocks. The importance of plate tectonics is simply that plate interactions spawn various types of lithologic assemblages and, thus, such concepts can considerably sharpen our perceptions and interpretations of geologic terranes. As such, they can aid the exploration geologist in his (her) evaluation of various lithologic sequences and the types of metal deposits that might have been generated within them.

The study of metal deposits has accelerated a great deal in the last two decades, in particular through geochemical research. The application of fluid inclusion, stable isotope, and various experimental techniques to the study of metal deposits has broadened our insights into the chemical and hydrodynamic aspects of ore formation. These advances have, in turn, allowed the formation of more realistic conceptual models for various types of ore generating systems. Such models are of considerable aid to the exploration and mining geologist in areas of known mineralization, but are of more limited utility in terms of the search for new mineral districts.

The problem of the geographic distribution of metal deposits must be addressed initially in terms of geologic and tectonic environments rather than the nuances of ore solution geochemistry. Endeavors in this field, it seems, have not kept pace with those of a more geochemical nature (e.g. Barnes 1979). In part, this is because geochemical research tends to be more 'tidy' and amenable to institutional funding and publication than the rather less rigorous and more empirical aspects of regional synthesis and compilation. The latter have to be based on some combination of personal experience and literature research. An important point in this regard is that metal deposits and the systems that generate them need to be viewed not as geochemical accidents, but rather as fortunate culminations of normal geologic and geochemical processes.

No one has made this point with more eloquence than Wyllie (1981), who states that metal deposits are not "the illegitimate offspring from random couplings of rocks and fluids from indeterminate sources," but "have respectable ... family lineages, with ancestors deep within the continental crust, or below it."

The extent to which ore generating systems can proceed to fruition and where they develop depends on a host of local factors, but the broad environmental controls in each case will be tectonic. It follows that if these tectonic controls result in the main from plate interactions, and if plate tec-

tonics have operated throughout much of earth history, then a variety of environments favorable for ore generation must have repeated themselves through geologic time. A consequence of these observations, if correct, is that major irregularities in the time distribution of various metal deposit types require explanation.

Ore deposits can be broadly divided into those generated by endogenetic processes and those generated by exogenic processes. The former are invariably associated with thermal processes and, in general, can be related more readily to magmatic and tectonic events instigated by plate activity. Deposits formed by surficial processes such as weathering or shallow marine sedimentation will have relationships to their tectonic environment that are more tenuous.

This volume represents an attempt to provide a rational basis for the observed time-space distribution of metal deposits, at least those of endogenous type. Such deposits can form by a wide variety of mechanisms in a highly diverse spectrum of geologic environments, and it follows that their relationships to plate tectonics will vary from significant in some instances to more tenuous in others. In fact, it is important to realize that even in cases where an impressive association between plate tectonics and certain ore types is manifest, plate interactions merely provide the master control for the particular geologic environments within which such deposits tend to form.

What I propose to do in the chapters that follow is deal with specific plate tectonic environments and cover the ore deposits that can be associated with each. Descriptions of individual type examples for which abundant data exist are provided to add substance to the volume. Additional examples are catalogued, where feasible, but any exhaustive compilation of world metal deposits is clearly beyond the scope of this book. Certain of my interpretations of distant ore deposits garnered from the literature will inevitably be in error, and possibly enrage some of those with first-hand local knowledge. To such people I can only offer an advance apology and an exhortation to publish and set the record straight. The line between creative synthesis and idle speculation is an extremely fuzzy one. I have included, wherever feasible, some thoughts on how the relationship between tectonics, geologic terranes, and metal deposits can be used in the context of exploration planning. Inevitably, such thoughts will be of a speculative nature, but the literature on ore deposits is notably lacking in attempts to do this. A concerted attempt has been made to include up to date ref-

erences and to avoid references pertaining to obscure sources or unpublished material, so that the interested reader with access to a good geological library can backtrack on any particular subject.

It is hoped that this book will prove useful to students at the advanced undergraduate and graduate levels, and to mining and exploration geologists. I owe no small debt of gratitude to various company geologists around the world for their willingness to share freely of their time and local expertise with an itinerant academic. Without their enormous, and sometimes unheralded, contributions, the science of economic geology would be sad shape indeed, and in recognition of this, I dedicate this volume to them. I am also indebted to the front line troops such as Richard Sillitoe, who, not only have covered vast amounts of territory, but have written lucidly and imaginatively about their observations.

Finally, it is hoped that we will be able eventually, to use "fundamental ore deposit geology to elucidate plate tectonics, not (only) the reverse" (Guilbert 1981).

Acknowledgments. The initial typescript of this book was produced by Kathy Ohler, for whose competent, patient, and always cheerful help I am most grateful. The figures were drafted by Jim Kiehne, and I thank him for his timely aid.

I owe a special debt of gratitude to Richard Sillitoe who reviewed nearly all stages of the manuscript and corrected a number of my misconceptions. Discussions with my colleagues at the University of Minnesota were also most helpful. Finally, my thanks to my wife Patricia Davis for many sound editorial suggestions, and to Peter Wyllie for initially suggesting the project and for encouragement during its evolution.

Frederick J. Sawkins

Contents

Chapter 3 Metal Deposits of Arc-Related Rifts

Chapter 4 Additional Aspects of Arc-Related Metallogeny

Chapter 7 Metal Deposits Associated with the Early Stages of Continental Rifting

Chapter 8 Metal Deposits Related to Advanced Stages of Rifting

Introduction: Plate Tectonics and Geology

Plate tectonics, as it operates in the modern earth, represents in a fundamental sense a mechanism by which excess thermal energy from the mantle is dissipated (Sclater et al. 1980). Substantial evidence now exists for the operation of plate tectonics during Phanerozoic time, and evidence for similar tectonic activity during Proterozoic time is steadily growing, both in quantity and quality (Hoffman 1988). Furthermore, concrete evidence for the operation of essentially analogous forms of plate tectonics during Archean time is now appearing (Condie 1982; Helmstaedt et al. 1986) supporting the notion that the provocative similarities that exist between certain elements of Archean terranes and plate boundary-related terranes of late Phanerozoic age can be reasonably interpreted in terms of uniformitarianism.

Before we proceed further, the spectrum of tectonic activity that can, I believe, be included under the rubric of plate tectonics requires clarification. Thus, hotspot activity, aborted rifting, and even Basin and Range-type extensional tectonics (Allmendinger et al. 1987) are all considered legitimate facets of plate tectonic activity. The last 200 million years of earth history have been rather rigorously interpreted in terms of plate interactions, thanks primarily to the recognition and dating of seafloor magnetic anomaly patterns. Reconstructions of earlier plate interactions have to be made on the basis of the geologic record of the continents and paleomagnetic studies, and we have to operate by comparing the older lithologic assemblages with those of the last 200 million year period. Nevertheless, plate tectonic interpretations of more ancient continental geologic terranes have met with success in many instances, and exercises of this type continue apace.

There are certain fundamental principles, in addition to that of uniformitarianism, that must be adhered to in attempting such reconstructions. One of the most important is isostasy. Thus, thicknesses of sedimentary and/or volcanic rocks in excess of a few 1000 m cannot accumulate, and be preserved, in intracontinental areas unless extensional attenuation of the crust takes place. It follows that ancient accumulations of such rocks with thicknesses greater than approximately 5 km must have initially accumulated either at continental edges, or in intracontinental areas subject to some sort of rifting activity. By the same token, plate convergence that results in major thickening of the continental crust (e.g., Andes, Himalaya) must be followed by massive supracrustal (and possibly some subcrustal) erosion. By the time erosion has removed the topographic expression of such areas and isostatic equilibrium is reestablished, ancient examples of these orogenic belts will bear little re-

semblance to their modern analogs. As we shall see later, this has important implications for understanding the time distribution of certain types of metal deposits.

Another important clue to ancient tectonic regimes is the petrochemistry of igneous rocks. Martin and Piwinskii (1972) pointed out that igneous rocks generated at modern convergent plate boundaries tend to be characterized by unimodal petrochemistry, whereas those generated in rift zones are characterized by strongly bimodal petrochemistry. This bimodality, especially with regard to silica content of volcanic rocks, although as yet controversial in petrogenetic terms, provides a powerful tool for the recognition of ancient rifting events. Since the pioneering studies of Pearce and Cann (1973), major effort has been expended in attempts to utilize various trace element patterns of igneous rocks as clues to the tectonic setting in which they were generated (e.g., Floyd and Winchester 1975; Pearce et al. 1984; Leeman and Hawkesworth 1986).

Petrochemical signatures of igneous rocks, together with lithologic assemblages, are the main tools, other than structural analysis, that geologists have at their disposal for tectonic interpretation of older geologic terranes. Despite the assumptions involved, they have been used with success, both in areas where definitive structures (e.g., normal faults, nappes) are still observable, and to some extent where metamorphism and orogenesis have largely erased the original structural relationships. What is pertinent here, both in terms of ancient tectonics and the distribution of ore deposits, is that certain similar lithologic assemblages with distinctive petrochemical features have been generated and welded into the fabric of the continents repeatedly during much of earth history. Inasmuch as many ore-generating systems can be viewed as the culminations of normal geologic processes, it follows that such systems have undoubtedly repeated themselves through geologic time.

This is not the place for an exhaustive review of the full spectrum of geologic terranes spawned by various types of plate boundaries, but certain points do need to be made preparatory to the main sections of the volume that follow. Plate convergence involving subduction can occur entirely in oceanic areas or adjacent to continental margins. Subduction-related magmatism, as we shall see later, is the key factor to understanding convergent plate boundary metallogenesis, and thus a somewhat more detailed examination of current knowledge regarding tectonic interactions and magma generation in this environment is in order.

A preliminary concensus appears to have been reached that the bulk of the materials that build volcanoplutonic arcs are fluxed from the asthenospheric wedge overlying the subducting slab (Anderson et al. 1978), but there is considerable circumstantial and growing isotopic evidence for a certain degree of involvement of the subducting slab in the process (Gill 1981; Woodhead 1987; Woodhead et al. 1987). In addition, styles of subduction can vary in terms of rates, angle of dip, thermal maturity of slab, plate vectors, and imposed stress field (Dewey 1980; Uyeda and Nishiwaki 1980; Jarrard 1986). These variables affect the intensity of earthquake activity, and the tectonic, mag-

matic, and sedimentation patterns of arcs at all stages of their development. Dewey (1980) defines arcs as extensional, neutral, or compressional, depending on the relative motions of the overriding plate, and the degree to which rollback of the subduction hinge is occurring (Fig. 1). He also demonstrates that arc segmentation tends to correlate with breaks in the subducting plate, originally inherited from transform offsets at a spreading ridge system. Finally, Dewey draws attention to the fact that an extensional arc system will have the tendency to evolve through a neutral stage to one in which the original intraoceanic arc is welded to a continental margin to become the fore-arc portion of a compressional continental margin arc. At least some of the allochthonous terranes of the western United States, Canada, and Alaska seem to provide clear examples of this scenario (Coney 1981). Isotopic studies by Farmer and DePaolo (1983) on Mesozoic and Tertiary granitic rocks of the western United States support this notion and indicate that most of the accretion that has occurred in this area took place at the edge of the Precambrian craton (Ernst 1988).

The physical parameters of the subduction process in 39 modern subduction zones have recently been more rigorously examined by Jarrard (1986).

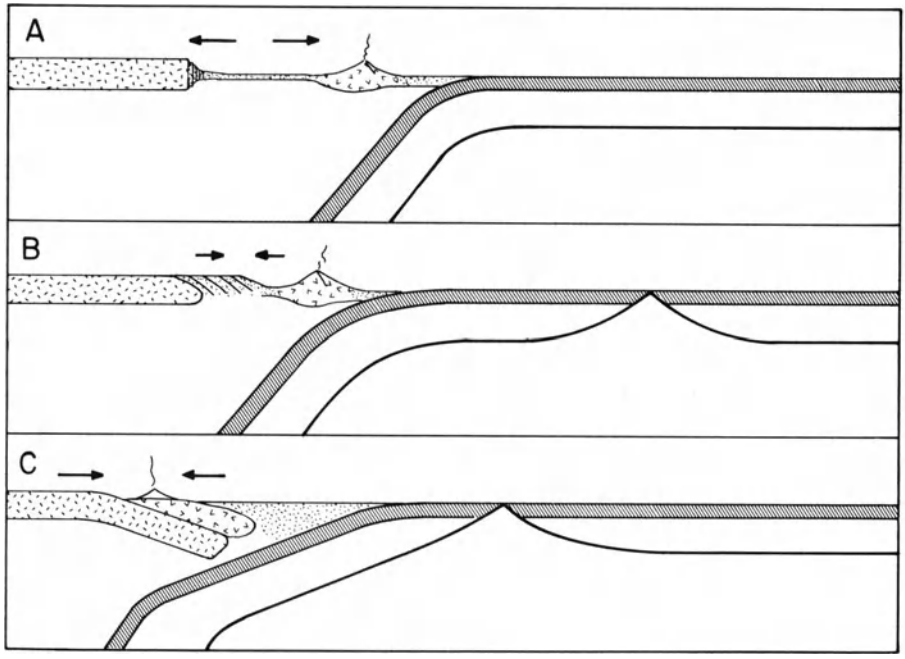

Fig. 1. Three types of arc systems. **A** Subduction is steep, rollback of the subducting plate hinge is taking place, and backarc extension is creating new crust of oceanic type. **B** The angle of subduction has shallowed and compression is taking place in the backarc area. **C** The angle of subduction has shallowed still more and the arc system is actively overthrusting the continental edge. This sequence appears to be characteristic of the successive evolutionary stages of many volcanoplutonic arc systems (Dewey 1980)

Using multivariate analysis of the data set, he found excellent correlation between the length of the Benioff zone and the product of convergence rate and slab age. Stress states in overriding plates were found to vary in a continuum from strongly compressional to strongly extensional. Arc-parallel strike slip faulting emerges as a common feature of such systems and is probably a prime cause of the structural complexity and terrane juxtaposition that characterizes many longer-lived convergent margins (Karig 1983).

The variations in style of arc development discussed above will have profound effects on the magmatic, sedimentary, and structural evolution of individual arc systems. For example, extensional arcs tend to be dominated by basaltic-andesite and basalt-dacite bimodal volcanic rocks and their plutonic equivalents and tend to have subdued topographic expression. As a consequence, associated volcaniclastic sedimentary fans are restricted, and in composition reflect their rather mafic source terranes.

At the other end of the spectrum compressional arcs develop a thick crust, and exhibit andesitic-dacitic-rhyolitic volcanic and associated tonalitic-granodioritic plutonic igneous rocks. As a result of isostatic uplift and consequent erosion, such arcs generate extensive and thick, more felsic, sedimentary fans. These conditions are typified by the Andean arc system of Peru and Chile, although in detail the dominant compression probably varied in intensity with time and was interspersed with periods of extension. Simple continental margin compressional arcs of this type tend to manifest a well-defined inward younging of magmatism with time (Farrar et al. 1970), and can be divided into principal arc and backarc segments (Sillitoe 1981a). Principal arcs encompass the main linear focus of volcanoplutonic activity, whereas backarc zones exhibit more diffuse magmatism manifest as isolated stocks and limited volcanism. In some instances the general tendency of the angle of subduction to flatten with time will be reversed, and the locus of magmatism will swing trenchward. Such appears to have been the case in the southwestern United States and northern Mexico (Fig. 2; Coney and Reynolds 1977; Keith 1978) during Cretaceous and Tertiary time.

Physical variations in the subduction process are thus important, but it is the nature of the slab material (i.e., degree of alteration and hydration) that exerts a fundamental control on magma genesis and composition. As we shall see later, this becomes critical to an understanding of most aspects of convergent boundary metallogenesis. Models for arc magma generation have grown increasingly complex since the inception of plate tectonic concepts (e.g., Gill 1981; Arculus and Powell 1986) in part due to recognition that alteration of oceanic crust strongly influences the rates of H_2O and Cl exchange between mantle and surface reservoirs (Ito et al. 1983). In addition to consuming oceanic crust of varied degrees of layer 2 and 3 alteration, Benioff zones can ingest significant amounts of pelagic and trench sediment, intraplate oceanic basalt, and perhaps slivers of older material tectonically eroded from a continental edge (Rutland 1971; Shreve and Cloos 1986).

Recent studies in modern arc systems provide support for sediment contamination of subduction zones. Combined Nd and Sr isotope data from

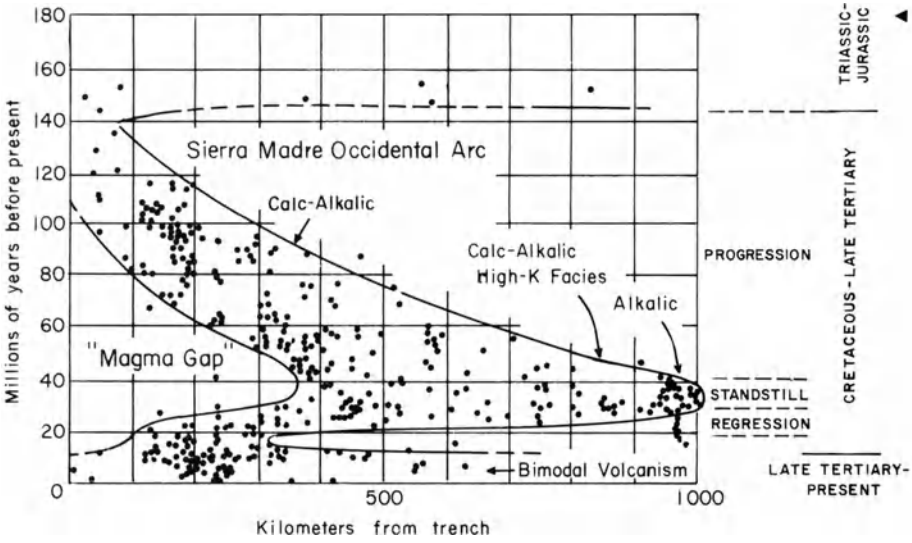

Fig. 2. Time-space relationships of magmatism in northern Mexico during Cretaceous and Tertiary time. The migration of magmatism eastwards and then westwards is interpreted mainly in terms of changes with respect to the dip and motion of the subducting lithosphere slab (After Clark et al. 1982)

the Aleutians (von Drach et al. 1986) and the Lesser Antilles (White and Dupre 1986) indicate that some sedimentary material must be reaching depths at which magma genesis is initiated. Similar conclusions are permitted by ^{10}Be studies of recent volcanic rocks in the Marianas arc, western Pacific (Woodhead and Fraser 1985), and from studies of accretionary wedge development or lack thereof at circum-Pacific convergent plate boundaries (Hilde 1983).

Further geochemical studies on the Marianas arc system by Woodhead and Fraser (1985) and Woodhead (1987) have demonstrated that fluids derived from the subducting slab convey substantial amounts of the mobile elements from the slab to the overlying asthenosphere. Basing his conclusions on results from radiogenic (Sr, Pb, Nd, and Hf) and stable isotope (O, S, and H) systems, Woodhead suggests that over half the elements of low ionic potential, such as Pb, K, Sr, Rb, Ba, and La, are removed from the slab and added to the overlying mantle wedge, where arc magmas are generated.

Perhaps the most striking evidence for the subduction of sediment, together with interstitial brines, has come from magnetotelluric soundings made across Vancouver Island (Kurtz et al. 1986). Furthermore, in studies of arc magmatism one must consider the modification of subduction-related magmas during their upward journey to shallow crustal or volcanic sites (Leeman 1983). In this regard Hollister and Crawford (1986) point out that the melts themselves may be important in terms of lubrication of shear zones in lower crustal environments.

The extent to which the geologic terranes present in Cenozoic arc systems are recognizable in more ancient terranes is a matter of inevitable controversy. However, this author concurs with the arguments originally advanced by Burke et al. (1976) that the granite-greenstone terranes of Archean and certain younger cratons are related to ancient subduction processes (Thomas and Gibb 1985). Tarney et al. (1976) have produced cogent arguments that the Rocas Verdes marginal basin in southern Chile (deWit and Stern 1981) represents a young example of greenstone belt formation (Fig. 3). It is important, however, to realize that the suprastructural (volcanic) portions of neutral and compressional arcs are rapidly lost to the forces of erosion and will be less likely to have preserved ancient analogs (see also Windley 1984 and pertinent references therein). Recent results from tectonic, petrologic, and geochemical studies of greenstone belts (see deWit and Ashwal 1986) indicate that many features of these belts can be explained within a plate tectonic framework involving generation of subduction-related volcanic arcs and their subsequent accretion.

This brief review of the development of arc systems is admittedly sketchy but provides a skeleton to flesh out in following chapters. It is worth noting that as understanding of the complexities and variations of arc environments grows in parallel with a clearer comprehension of arc metallogeny, the concept that the tectonic environment significantly controls the formation of arc-hosted metal deposits appears to be increasingly validated.

Divergent plate boundary environments in the modern earth are very much dominated by sites at which seafloor spreading is taking place. However, within the fabric of the continents are many terranes within which evidence for past rifting events can be found. Some of the older systems occur as identifiable failed rifts, others have undergone extensive later orogenesis, at least in part due to complete revolutions of the Wilson Cycle (Burke et al. 1977), and can only be identified by careful attention to definitive lithologic associations, now much obscured by metamorphism and tectonism.

The main variability exhibited by spreading ridge systems within the ocean basins relates to spreading rates. Slow spreading ridges tend to exhibit a well-defined axial rift and greater structural and petrochemical diversity in comparison to fast spreading ridges (Fig. 4). In broad terms, magma genesis by partial melting of underlying welts of asthenosphere, and its emplacement as a layered complex of basaltic pillow lavas, sheeted dikes, and underlying gabbros is relatively well understood. Nevertheless, complexities relating to magma budgets near fracture zones and distinctions between the seismic Moho and petrologic Moho (Karson and Elthon 1987 and references therein) await resolution.

Much of the dissipation of the heat transferred from the mantle during seafloor spreading processes is achieved through the action of seawater-dominated hydrothermal convective systems at or near ridge crests (Sclater et al. 1980). Actualistic examples of such systems are currently receiving considerable research attention, especially along the East Pacific Rise and along the Galapagos and Juan de Fuca spreading systems.

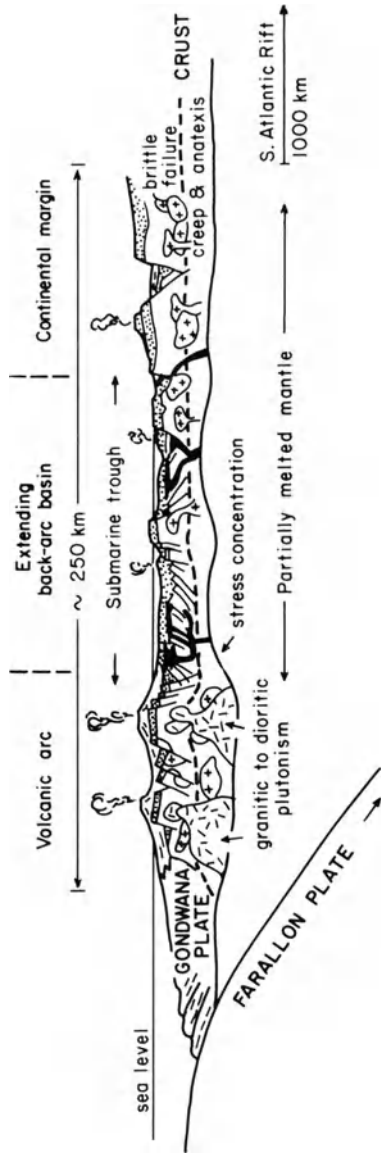

Fig. 3. Generalized cross-section illustrating the tectonic setting of the Rocas Verdes Complex in southern Chile. Many workers consider that most Precambrian greenstone belts originally formed in analogous tectonic settings (After de Wit and Stern 1981)

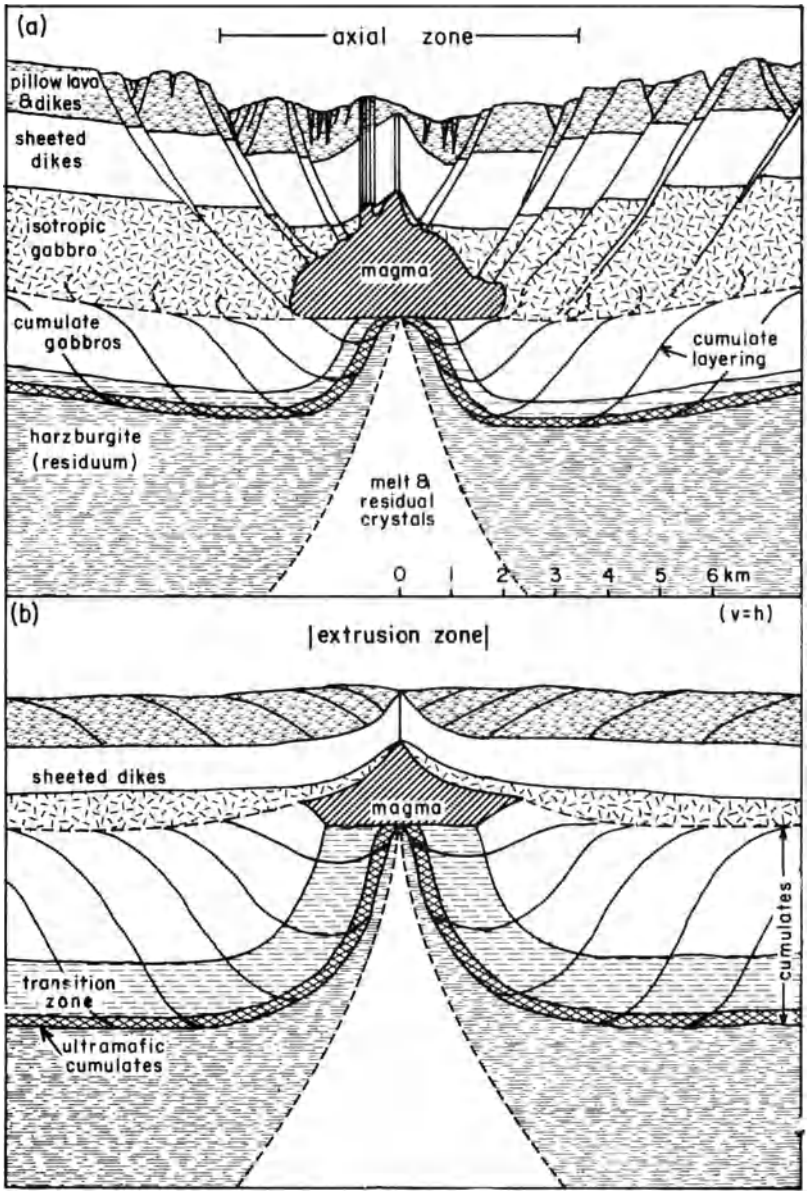

Fig. 4. Cross-sections of **a** slow-spreading and **b** fast-spreading ocean ridge systems. Note the more pronounced fault-induced topography associated with slow-spreading systems (After Burke and Kidd 1980)

Only miniscule amounts of the oceanic lithosphere produced at "midoceanic" divergent plate boundaries become incorporated into continental geologic terranes. It is now recognized that most ophiolite complexes (Coleman 1977) represent patches of oceanic crust and lithosphere that were generated by spreading systems in backarc basins and subsequently embedded in the continents by arc-continent accretionary collision events (Pearce et al. 1984). These suprasubduction zone slices of oceanic crust can suffer considerable degrees of tectonic disruption, but despite this, recognizable ophiolite complexes are known from many Cenozoic, Mesozoic, and Paleozoic orogenic belts (e.g., Bird et al. 1971). Unequivocal pre-Paleozoic ophiolite complexes are known only in Pan-African (1000–500 Ma) accretionary terranes in Saudi Arabia (Nasseef et al. 1980), in Morocco (Leblanc 1976), and in the Baikal orogen, USSR (Kiltin and Pavlova 1974). Burke and Kidd (1980) pointed out that dismembered fragments of even older oceanic crust remain to be discovered in early Proterozoic orogenic belts and even in Archean terranes. Recent work on Archean greenstone belts has shown this prediction to be correct (Helmstaedt et al. 1986; de Wit and Ashwal 1986). The paucity of ophiolitic materials in older terranes vis-a-vis Cenozoic orogenic belts is entirely explicable in terms of erosional loss because collision events tend to elevate the ophiolite complexes. At depth these sutures tend to be "cryptic", and are marked only by fault planes.

Hotspot activity represents an interaction of lithosphere and underlying asthenosphere and as such is considered a valid plate tectonic process. Most hotspots do little more than leave a track of basaltic lavas on the plate overriding their source regions (Fig. 5). However, in cases where hotspots impinge on an overlying continental lithosphere that is more or less stationary with respect to them, the basaltic volcanism tends to be accompanied by processes that can result in continental rifting (Sengor and Burke 1978) and perhaps the initiation of a new Wilson Cycle (Burke and Dewey 1973). The sequence of events by which subcontinental hotspot activity can lead to rifting and onset of a Wilson Cycle is illustrated in Fig. 6. The connection between hotspot activity, manifest as the eruption of flood basalts, and successful continental rifting is clearly demonstrated by the rifting history of the Atlantic Ocean. The Iceland and Tristan/Gough hotspots sit astride or close to active spreading systems, and are connected to continental flood basalts on neighboring continents by aseismic volcanic ridges (see Fig. 5).

The current doming, rifting, and volcanic activity occurring in the East African Rift System (Girdler 1983) almost certainly represent the early stages of an ocean opening event. As noted by Burke and Kidd (1980), most identifiable flood basalt events in the geologic record were manifestations of continental rifting-ocean opening events. Notable exceptions are the Columbia River basalts, the Siberian Traps, and the Keweenawan basalts (Burke et al. 1981). The Proterozoic record contains numerous examples of rifting events associated with basaltic magmatism. Many of these cluster around 1 Ga (Sawkins 1976a), but major dike swarms also penetrated the North American craton approximately 2 Ga (Fahrig et al. 1986; Halls 1986;

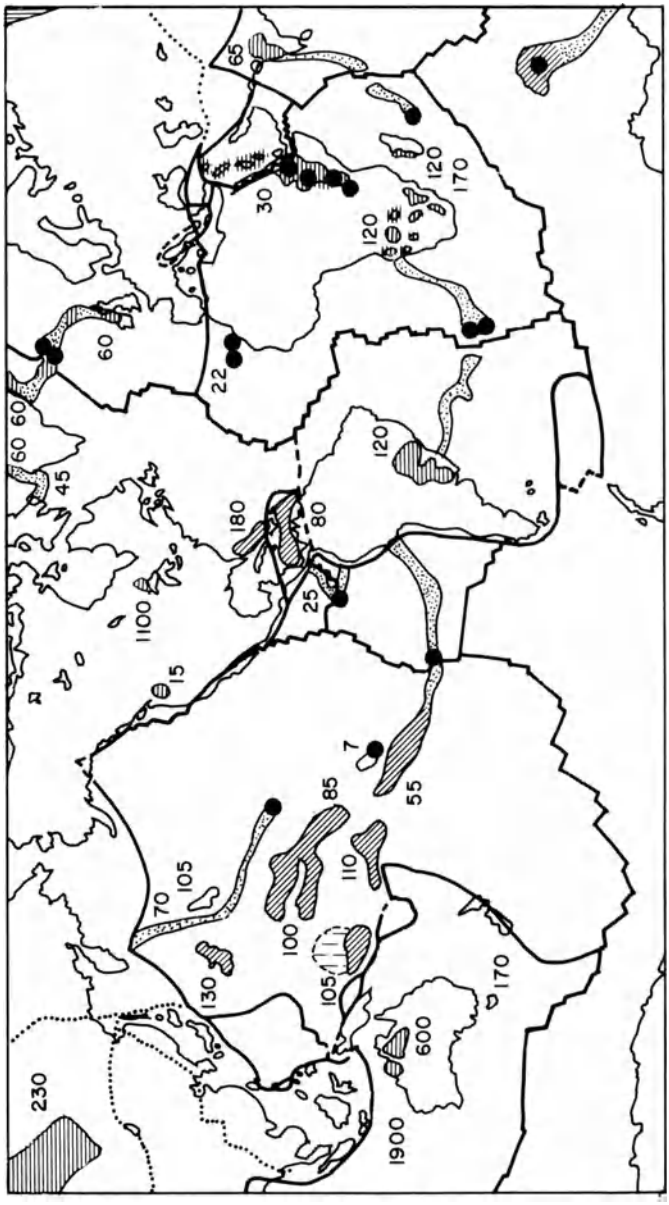

Fig. 5. Distribution of major sites of basaltic magmatism in most of the world, exclusive of that generated by normal seafloor spreading processes. Linear trends record plate motions relative to the hotspots (*black dots*). *Diagonal ruling* indicates submarine equivalent of flood basalts, *horizontal ruling* indicates continental flood basalts. *Numbers* give approximate ages of flood basalts in millions of years (After Burke and Kidd 1980). *Stippled areas* represent aseismic volcanic ridges and *lined areas* represent basalt lava plateaus

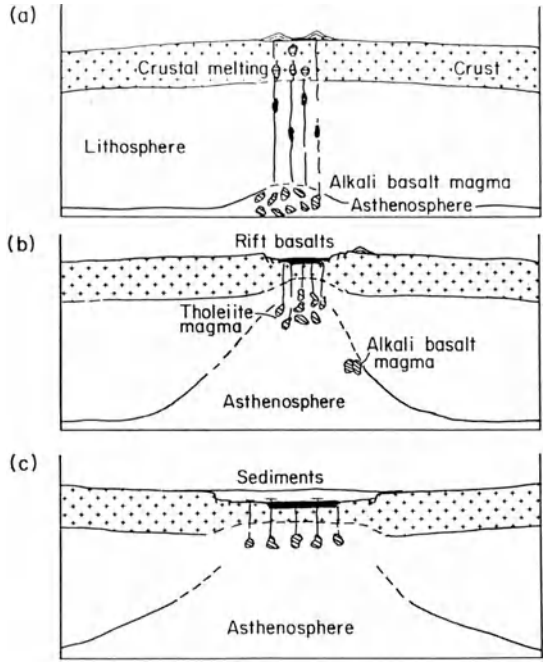

Fig. 6a-c. Generalized cross-sections illustrating the sequence of events commonly associated with intracontinental rift formation (sketch by author)

Southwick and Halls 1987). Even earlier examples of this rifting-basalt magmatism phenomenon may be represented by the Great Dyke, Zimbabwe (2.6 Ga; J. Hamilton 1977) and the Ameralik dikes in West Greenland (3.0 Ga and older; Bridgewater et al. 1978).

Although most rifting events that produce new ocean basins are basically simple pull-apart features, important rift structures and attendant basaltic magmatism can develop by transtension along essentially transform fault features (Biddle and Christie-Blick 1985). The Dead Sea Rift (Freund and Garfunkel 1981) and the Gulf of California-Salton Sea system (Crowell 1979) are obvious, modern examples. A major reevaluation of the structural mechanisms involved in continental extension and rifting has occurred in recent years (e.g., Wernicke and Burchfiel 1982; Coward 1986; Etheridge 1986). Deep seismic studies of young extensional terranes (e.g., Allmendinger et al. 1987) and along passive continental margins (Keen et al. 1987) indicate that shallow-dipping detachment faults may be a key factor in rift development and continental breakup (Fig. 7). Lister et al. (1986) have demonstrated that certain features of passive continental margins can be interpreted in terms of the upper or lower plates of an original detachment fault transecting the lithosphere.

The relationships between doming, rifting, and continental breakup are particularly well illustrated by the post-Paleozoic history of Africa (Burke and Whiteman 1973). Crustal melting, in response to hotspot activity, can produce anorogenic alkali granites such as those of the Jos Plateau, Nigeria (Jacobson

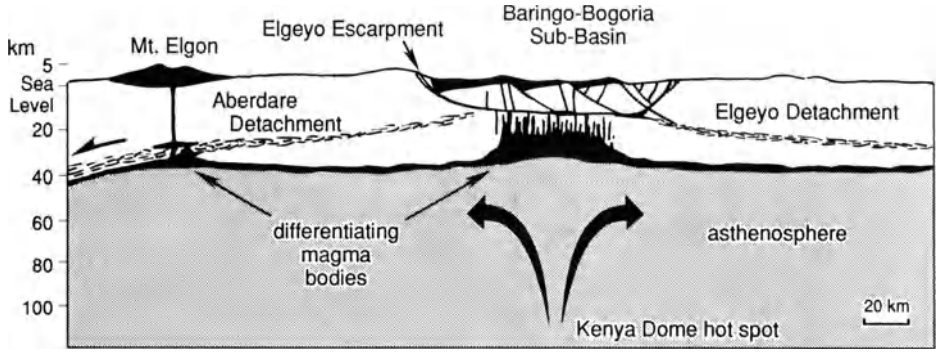

Fig. 7. Cross-section of the Gregory Rift in northern Kenya, as envisaged by recent rifting concepts. Note emphasis on shallow-dipping detachment zones starting at midcrustal levels (After Bosworth 1987)

et al. 1958; Bonin 1986), prior to rifting. However, the volcanic and sedimentary rocks that fill rift basins and the broader downwarps that postdate them (see Milanovsky 1981) are the most important products of rifting in terms of environments for metallogenesis. Such rocks and their metamorphosed equivalents have wide distribution on the continents and, as we shall see, host a number of major metal deposits.

The lower portions of rift troughs are typically occupied by basalts and lesser amounts of felsic igneous rocks (bimodal volcanism). Overlying these volcanic rocks, nonmarine arkosic arenites and local conglomerates tend to accumulate. Local lacustrine environments may also develop within these oxidized subaerial settings and isolated evaporite-rich or organic-rich zones can be created. The former provide critical constituents to aid metal mobility, and the latter can act as efficient redox traps for elements transported in oxidizing groundwaters. As rifting progresses and lithospheric attenuation continues, the rift floor drops below sea level and marine sediments, both clastic and nonclastic, will accumulate. Real world examples of this scenario (Burke and Dewey 1973) are numerous, but inevitably each rift system contains its own set of (typically minor) variations. Because orogenic activity and metamorphism so commonly follow eventually from rifting, the metamorphosed equivalents of these supracrustal rocks can be found locally in many Proterozoic metamorphic terranes. They occur typically in synforms between domes of reactivated basement as quartzofeldspathic gneisses associated with lesser amounts of amphibolite, marble, and minor iron formation.

An inevitable result of ocean opening and closing events (Wilson Cycles) is continental collision, and some workers (Burke et al. 1977; Thomas and Gibb 1985) favor this mechanism as the fundamental cause of virtually all ancient orogenic belts. This interpretation has not gone unchallenged by those (e.g., Kroner 1977a,b, 1985; Etheridge et al. 1987) who find support, especially in Proterozoic orogenic belts, for concepts of ensialic orogeny. Space does not

permit a more detailed examination of this dichotomy here, but an early rifting episode can be recognized in almost all orogenic belts (e.g., Martin and Porada 1978; Miller 1983a,b). Thus, the crux of the matter seems to be the amount of extension and ocean opening that must occur prior to the onset of compression and orogenesis.

Dewey (1977) has pointed out that continental collision events tend to spawn terranes of enormous geologic and structural complexity. The geology of the Himalaya and Tibet provides eloquent testament to this (Gupta 1987), and it is not surprising that attempts at the unraveling of much older collisional orogens are fraught with uncertainty. An important advance in tectonics has been the realization that the effects of continental collisions can be found to extend far into continental interiors (Tapponnier et al. 1982), and many students of tectonics now see collisional events as a major factor in the initiation of continental rifts (Burke and Sengor 1986). However, it is still puzzling as to why many rifts, that clearly have not evolved into ocean basins and undergone Wilson Cycles, tend to experience subsequent compressive stress regimes (Milanovsky 1981).

In recent years, structural geologists have had to broaden their thinking regarding the spectrum of fundamental settings in which orogenesis can occur. Many orogenic belts are now recognized to be a collage of accreted terranes (Schermer et al. 1984; Scholl et al. 1986; Hoffman 1988). Within these belts major shear zones suggest the local importance of transcurrent movements (Daly 1986), and elsewhere thermal diapirism related to crustal extension can be recognized (Coward et al. 1987; Allmendinger et al. 1987). Thus, the theoretical gamut of structural, sedimentary, and magmatic events that can occur during these orogenic interludes is considerable, and it is hardly surprising that a certain degree of controversy surrounds the tectonic interpretation of many ancient orogenic belts.

In the preceding pages we have considered various plate environments and touched on evidence supportive of their presence during more remote geologic epochs. Much of this evidence can be integrated into a comprehensive theory of plate tectonic-controlled continental growth, for it seems abundantly clear that the subduction process builds new continental-type crust in intraoceanic areas, and adds to the volume of the continents at continental margin subduction sites. The contribution of ensialic orogeny and underplating to continental growth (Etheridge et al. 1987) is still poorly understood.

During Archean time the capacity of the mantle to produce heat was considerably greater due to larger budgets of radioactive elements (Fig. 8), and thus the necessity for some type of heat-dissipating convective activity was more acute. This fact, taken in conjunction with the striking similarities of the Archean rock record to certain younger terranes, and Hoffman's (1980, 1988) compelling evidence for the operation of Wilson Cycle tectonics in northwestern Canada 2 billion years ago, supports the notion that plate-like activity and attendant continental growth were features of earth evolution since early Archean times. Moorbath (1980) has reviewed the implications of the

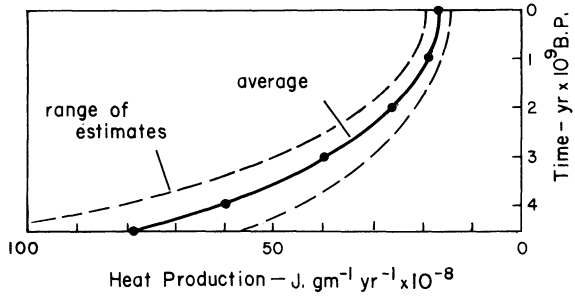

Fig. 8. Heat production-time relationships in the earth. The progressive decrease is due to decay-related reduction in the budget of heat-producing radioactive isotopes of U, Th, and K (After Lee 1967)

geochronologic data base for the oldest continental rocks, and argues cogently for progressive continental growth from those times onward. The requirements for greater rates of mantle heat dissipation at that time can be accomodated merely by increasing the number of plates and/or their rates of rotation without the necessity for greatly increased geothermal gradients. Opposing concepts of a very early permobile sialic crust (e.g., Hargraves 1978; Fyfe 1980) seem not only at odds with much of the geologic and isotopic evidence, but run aground on available P-T estimates derived from Archean granulites and related rocks (see Tarney and Windley 1978; Wells 1979).

This very brief review of the role plate tectonics is believed to have played in the evolution of continental-type crust and the assembly of the continents represents a mere skeleton on which to hang the various geologic environments which will be encountered in the chapters that follow, and it provides an indication of the writer's own conceptual baggage. Readers who feel a need for more substance are strongly encouraged to avail themselves of *The Evolving Continents* (2nd edition, Windley 1984).

Part I
Convergent Plate Boundary Environments

Chapter 1 Principal Arcs and Their Associated Metal Deposits

1.1 Introduction

Principal arcs are relatively narrow, well-defined zones of volcanic and plutonic igneous activity that occur above intermediate to steeply dipping subduction zones. These important metallogenic elements are characterized by the formation Cu, Fe, Mo, Au, and Ag deposits that exhibit a close time-space association with calc-alkaline magmatism. In fact, principal arcs and their metal deposits provide the most compelling evidence for direct causative relationships between purely plate tectonic events (i.e., subduction) and magmato-metallogenic events. In the early 1970's this concept became known as "geostill", but the initial enthusiasm of its proponents had to be tempered when it became clear that processes of magma generation in arc systems were complex, and involved a broader range of potential source materials than originally realized

In the previous section, the complexities attendant to subduction-related magmagenesis were briefly considered. Data are now emerging which support earlier suggestions (e.g., Sillitoe 1976b) that some of the critical components of ore-generating systems in arc environments (i.e., sulfur, chlorine, and water) are recycled from the subducting slab and are ultimately related to processes that fix these components at sites of newly generated oceanic crust. Studies of the 1982 El Chicon volcanic eruption demonstrate that arc volcanism can be characterized by large amounts of isotopically heavy sulfur ($\delta^{34}S \approx +6$ ‰, Luhr et al. 1984). The most plausible source of this "excess" heavy sulfur are sulfides previously deposited by black smoker activity at ridge crests. Furthermore, the δD signature of magmatic-hydrothermal fluids in arcs (~ -50 ‰) can be explained in terms of subduction of hydrated oceanic crust. The most extensive hydration of oceanic crust near ridge crests involves low temperature, off-axis convection of seawater (Fehn and Cathles 1986). Hydrous minerals such as chlorite formed under such conditions will incorporate hydrogen with δD values of approximately -50 ‰.

The comparatively oxidized nature of many subduction-related magmas, especially those associated with metal deposits (Burnham 1981), has been interpreted to indicate the involvement of oxidized, subducted sedimentary materials in their genesis, providing yet another link to the downgoing slab. It seems probable that similar considerations apply to the critically important chloride component of ore-associated magmatic systems in volcanoplutonic arcs (Ito et al. 1983).

The complexities of magma generation in volcanoplutonic arcs, including significant lower-crustal inputs, especially along continental margins, are manifold (see Roddick 1983; Sillitoe 1987). Despite this, empirical evidence clearly supports the notion that many of the critical components of arc-related, ore-generating systems have a lineage that stretches back to a spreading ridge system.

1.2 Porphyry-Type Deposits

Porphyry-type deposits can be defined as low-grade, large, disseminated deposits emplaced either in shallow porphyritic intrusions and/or in the country rocks adjacent to such intrusions. Diagnostic features are an intimate fracturing of the host rock and pervasive wall-rock alteration. An important corollary is that such deposits are amenable to bulk mining techniques.

Porphyry copper deposits, the major type of porphyry deposit, range in size from about 10 million tons to several billion tons and exhibit grades of hypogene mineralization that range from 0.2% to about 2% Cu. In many instances, especially in continental margin deposits, supergene enrichment is an important facet of orebody formation (J.A. Anderson 1982; Brimhall et al. 1985). Porphyry-type mineralization with grades of less than 0.2% copper also tends to be widespread in porphyry copper belts, but in most instances supergene enrichment cannot create viable orebodies from protore that lean.

Porphyry-type deposits, especially those of copper, occur overwhelmingly along linear, calc-alkaline volcanoplutonic arcs related to the subduction process. The spatial association of porphyry copper deposits and volcanoplutonic arcs formed above current or former subduction zones (Fig. 1.1) was first detailed by Sillitoe (1972a). More recently, Uyeda and Nishiwaki (1980) have demonstrated that porphyry copper deposits tend to form in compressional arc systems, and appear to be notably scarce in extensional arcs (see also Sillitoe 1980b). Thus, the volcanoplutonic arcs along the western margins of North and South America are well endowed with porphyry copper deposits (Sutherland Brown 1976; Sillitoe 1976a,b, 1981a,b; Hollister 1978), whereas arc systems that have undergone considerable interarc and backarc spreading (e.g., Japan) appear to be largely devoid of porphyry copper deposits.

Around the Pacific rim the age distribution of porphyry copper deposits is distinctly episodic, and basically reflects a similar time variation in the intensity of calc-alkaline magmatism along this belt. An important episode of porphyry copper generation took place, for example, from 74 to 48 Ma ago in the Cordilleras of North America, but this was followed by a lean period between 48 and 40 Ma ago. The main episode of such metallization in the western Pacific occurred during Miocene through Pleistocene time (Titley and Beane 1981, pp. 228–229; Sillitoe 1987), although it should be noted that most western Pacific arcs are themselves no older than mid-Tertiary.

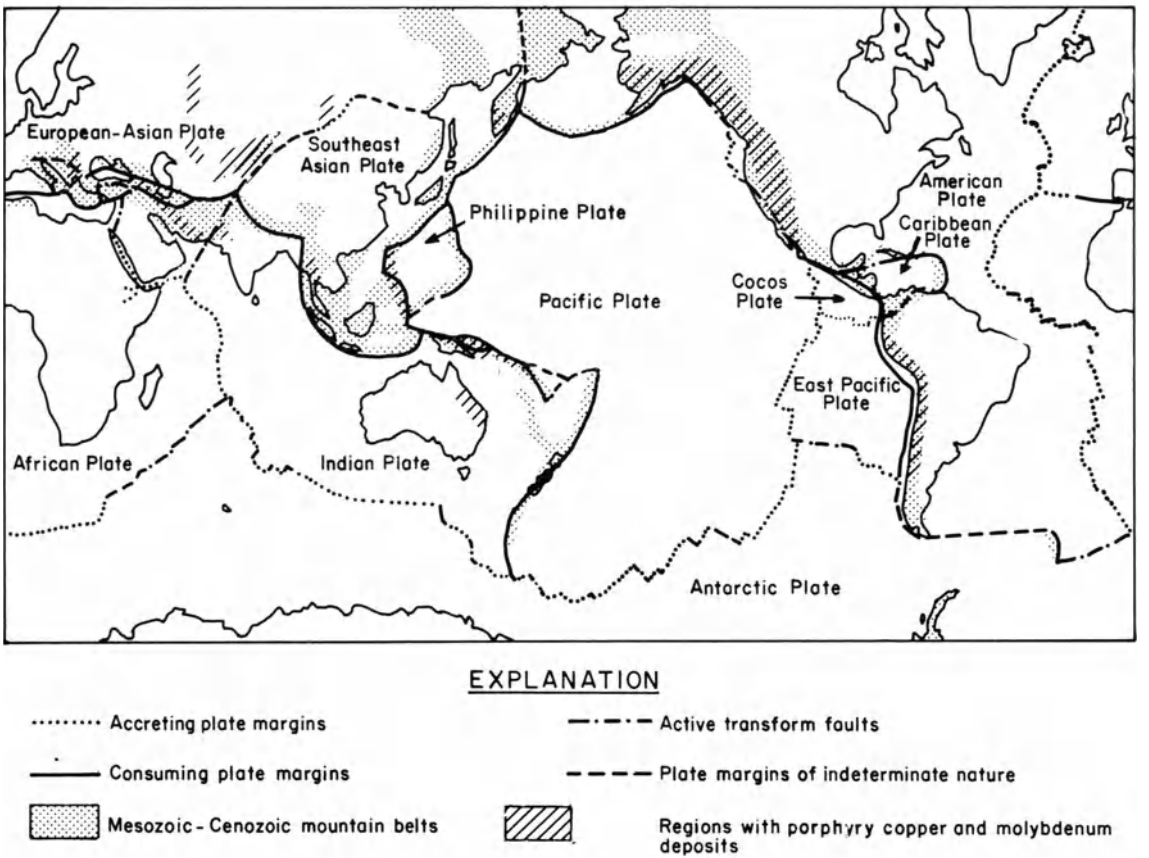

Fig. 1.1. Porphyry copper belts of the world. Note that all, with the exception of those in the USSR and eastern Australia, are associated with zones of present or recent subduction activity. The belts in the USSR north of the Alpine-Himalayan zone, and that in eastern Australia, can be related to Paleozoic convergent boundaries (After Sillitoe 1972a)

The plate tectonic history of the Pacific is complex, but the flourish of porphyry copper metallization represented by the Laramide deposits of Arizona and surrounding areas coincided with a change from oblique to normal subduction of the Farallon Plate beneath southwestern North America, and a marked increase in convergence rate (Coney 1972; Engebretson et al. 1985). The strong pulse of magmatism and related porphyry copper (and other) metallization around the Pacific rim during Miocene time may have a causal connection to a readjustment in plate motions at that time.

1.2.1 Associated Igneous Rocks

The igneous rocks associated with porphyry copper deposits occupy a spectrum from quartz diorites to adamellites. In island arc settings, calc-alkalic hornblende and hornblende-biotite diorites and quartz diorites predominate (Griffin 1983; Sillitoe and Gappe 1984), whereas in continental margin settings the ore-associated intrusions tend to be granodiorites and quartz monozonites (Burnham 1981). In the Galore Creek area of British Columbia, a group of Triassic age porphyry copper deposits is associated with a suite of silica-deficient, alkalic intrusives (Barr et al. 1976). The igneous systems that generate porphyry copper deposits are typically manifest as complex subvolcanic centers consisting of a variety of rock types emplaced during a number of intrusive/extrusive events. The major metallization event, however, can generally be shown to be primarily associated with a single member of the intrusive suite.

The host rocks to these intrusions include a wide variety of lithologies, from coeval volcanics in some instances through older clastic or even crystalline basement rocks in others, although the most common situation involves volcanic rocks of approximately similar age to the intrusions. Although the composition of the country rocks tends to influence the nature and extent of the hydrothermal alteration associated with such deposits, the ores themselves display a striking disregard for the character of their surrounding, older, country rocks.

In essentially all cases, the igneous rocks fall within the I-type grouping of the granitoid classification scheme of Chappell and White (1974), and the magnetite series of Ishihara's (1977) system. Their source is most probably the subjacent mantle, and their generation is unquestionably closely tied to operation of the subduction process, although complex, multistage processes must operate in the genesis of arc magmas (Wyllie 1981). One reflection of this complexity is the range of initial strontium ratios that porphyry-associated intrusions display (< 0.703 to > 0.709), although Sillitoe (1987) interprets these data (Fig. 1.2) merely to indicate that the mantle-derived magmatic systems can undergo considerable crustal contamination without impairment of their ability to generate porphyry-style copper deposits.

Sillitoe (1973, 1980c) contends that the formation of porphyry copper deposits occurs within the subvolcanic environment below andesitic-dacitic

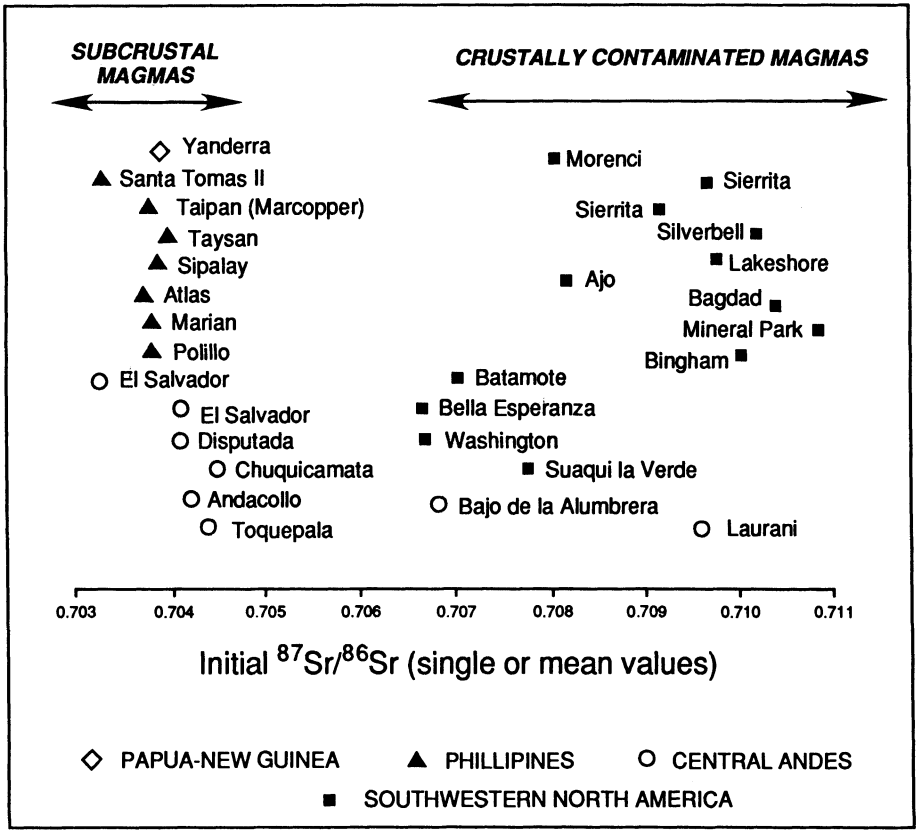

Fig. 1.2. Plot illustrating the range of initial $^{87}Sr/^{86}Sr$ ratios displayed by the intrusions associated with the formation of porphyry copper deposits in the circum-Pacific belt. The implication of this data set is that subduction-related magmatic systems capable of generating porphyry copper deposits will do so despite considerable crustal contamination in some instances (After Sillitoe 1987)

stratovolcanoes (Fig. 1.3). Whether all porphyry systems develop below actual volcanoes is not clear, for in most instances erosion has removed the critical evidence. It does seem possible, nevertheless, that porphyry copper deposits could also develop in the apical portions of stocks that protrude above larger igneous bodies, but that do not connect to overlying volcanics. The critical point, however, is that porphyry systems form in upper crustal environments (~ 1 to 6 km depth), although the shallower end of this spectrum is probably most common.

Kesler (1973) has demonstrated that porphyry copper deposits can be divided into either molybdenum- or gold-rich subclasses, and gold-enriched examples tend to be more prominent in island arc settings. There are, however, some important exceptions to this rule, and the occurrence of porphyry molybdenum mineralization in the Philippines principal arc has been reported

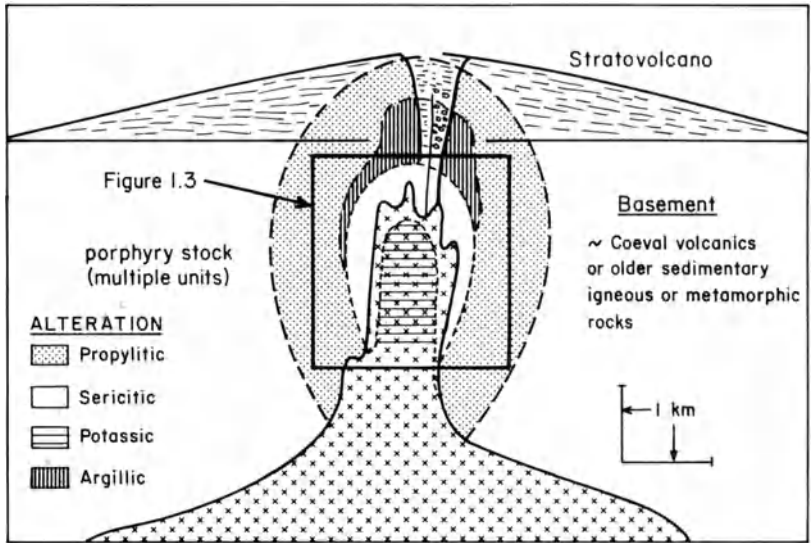

Fig. 1.3. Generalized model of porphyry copper formation. The salient feature of this model is the development of porphyry copper mineralization in the subvolcanic zone below a stratavolcano and above an intrusive body of some magnitude at depth. Within this critical zone geometries of individual intrusions can vary considerably, as can the geometries of the various alteration envelopes (After Sillitoe 1973)

(Sillitoe 1980a; Sillitoe and Gappe 1984). A more thorough investigation of precious metal contents of porphyry copper deposits in western Canada has been recently carried out by Sinclair et al. (1982), who demonstrated that silver tends to be most enriched in alkaline-type porphyries, whereas gold is higher in volcanic as opposed to more plutonic porphyry settings.

1.2.2 Mineralization and Alteration Patterns

The mineralization and alteration patterns manifest in porphyry copper deposits are closely interrelated (J.D. Lowell and Guilbert 1970; Beane and Titley 1981). In general terms, the central, deeper portions of porphyry copper deposits are characterized by disseminated or microveinlet mineralization and potassic (qtz-biotite ± K-feldspar-anhydrite) alteration. Copper:iron ratios are high, and a low-grade core zone of low total sulfide content may be present (Fig. 1.4). The deep zones of some porphyry systems tend to contain magnetite, actinolite, epidote, chlorite, and perhaps albite as additional alteration phases. Outward and upward from this zone, the copper:iron ratios in the total sulfide assemblage decrease and potassic alteration gives way to phyllic assemblages (qtz-sericite-pyrite). In such zones, mineralization is exclusively of veinlet type and total sulfide content tends to reach a maximum. These zones are inevitably surrounded by a broad zone of diffuse propylitic alteration (chlorite-

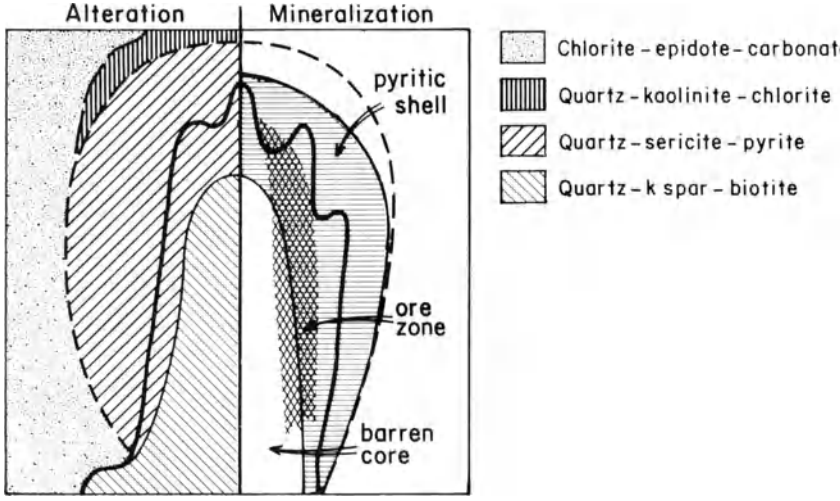

Fig. 1.4. Mineralization and alteration envelopes that develop in a typical porphyry copper system (After Beane and Titley 1981)

epidote-carbonate) that may be interrupted locally by zones of intense argillic alteration (qtz-kaolinite-chlorite; see Fig. 1.4). Mineralization, where present in these outer zones, occurs as sporadic, discrete veins that in many intances contain minor lead, zinc, and precious metals in addition to copper.

1.2.3 Fluid Inclusions and Stable Isotopes

The fluid inclusion data base for porphyry systems has expanded considerably since the pioneering studies of Roedder (1971). The temperature and salinity patterns obtained from fluid inclusions mimic the zonal alteration-mineralization patterns. The highest temperature (up to 700°C) and salinity (up to 60 wt% alkali chlorides) inclusions characterize the central portions of porphyry systems (e.g., Chivas and Wilkins 1977; Eastoe 1978). Fluid inclusion temperatures and salinities decrease both as a function of distance from the core zone, and of time during the mineralization process. Another important observation is that evidence for boiling tends to be virtually ubiquitous during the higher temperature ($>$ 400°C) phase of hydrothermal activity.

Stable isotope studies of porphyry systems (Sheppard et al. 1971; Sheppard and Gustafson 1976) indicate that potassic alteration and initial emplacement of copper sulfides are effected by hydrothermal fluids of magmatic provenance, whereas the phyllic alteration, and a certain amount of redistribution of metals, involve the participation of nonmagmatic waters. The involvement of nonmagmatic fluids in porphyry systems is clearly a complex matter and varies in degree from one deposit to another. However, where careful studies have been carried out (Gustafson and Hunt 1975; Eastoe 1978,

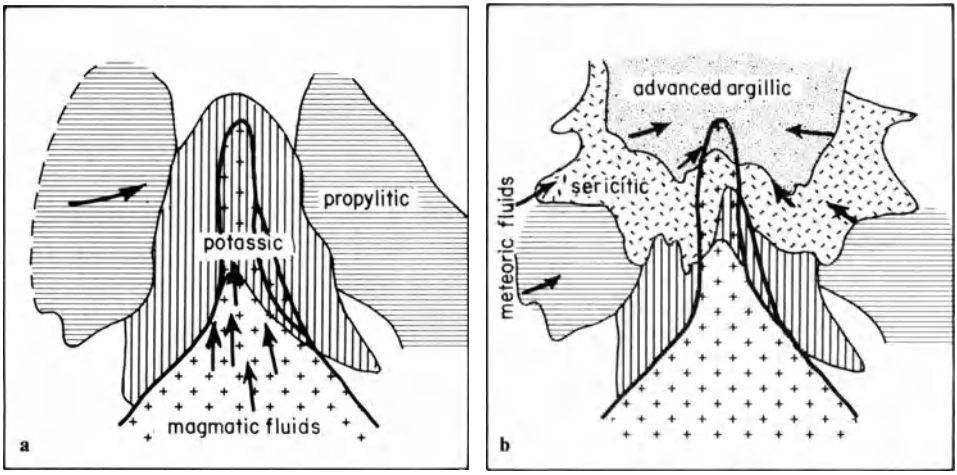

Fig. 1.5. Simplified cross-sectional illustration of the early and later stages of alteration and fluid movement deduced by Gustafson and Hunt (1975) from their study of the El Salvador porphyry copper deposit, Chile

1982), the evidence supports a genetic model in which a magmatic-hydrothermal system is surrounded by a cooler meteoric-hydrothermal system that collapses inward and downwards as the magmatic-hydrothermal system wanes (Fig. 1.5).

1.2.4 The El Salvador Porphyry Copper Deposit, Chile

The most complete study of a porphyry copper system undertaken to date is that of the El Salvador deposit in northern Chile (Gustafson and Hunt 1975). Here, Cretaceous andesitic volcanics and sedimentary rocks, overlain uncomformably by lower Tertiary volcanics, were subjected to a series of intrusive events from 50–41 Ma ago. Early rhyolite domes were followed 46 Ma ago by subvolcanic intrusions of quartz rhyolite and quartz porphyry. The main alteration and mineralization events were associated with emplacement of a steep-walled granodioritic porphyry complex, dated at 41 Ma (Fig. 1.5). A number of separate porphyry intrusive events occurred at this time, the latest of which postdated the major metallization event. Wide ranges of textural variation occur in these intrusions, including obliteration of porphyry textures locally. Compositional trends are obscured by hydrothermal events, but the ore-associated intrusions are definitely less felsic than earlier, unrelated siliceous extrusives and domes. Initial $^{87}Sr/^{86}Sr$ ratios throughout the igneous-hydrothermal complex exhibit consistent values of 0.704.

Early mineralization accounts for the bulk of the copper in the system, and occurs either in quartz veinlets or disseminated in alkali feldspar-biotite-anhydrite-chalcopyrite-bornite (K-silicate) alteration assemblages. Biotitization

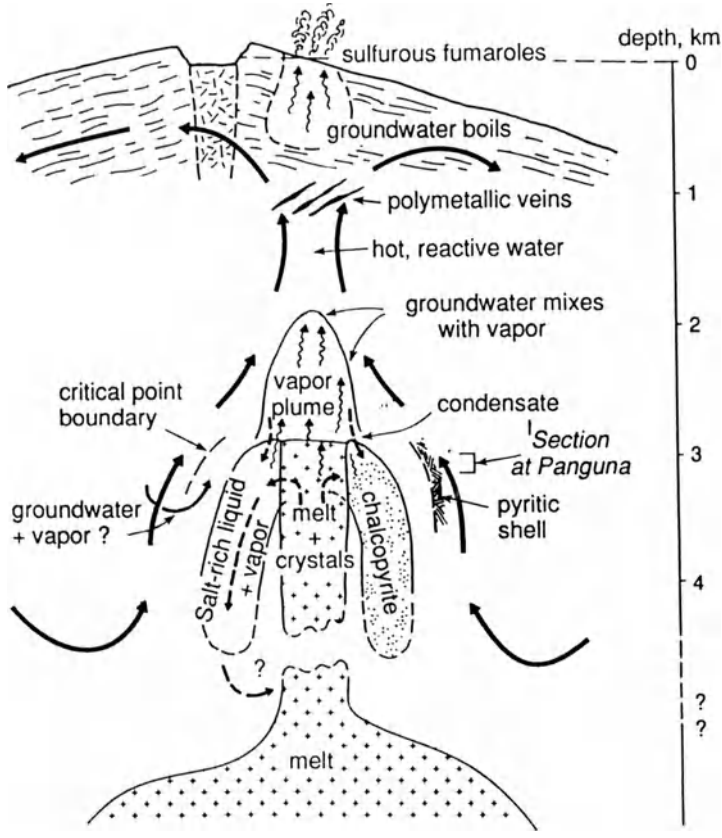

Fig. 1.6. Model of porphyry copper genesis developed by Eastoe based on his studies of the Panguna deposits in Papua New Guinea. On *right* side of the diagram at the level indicated for Panguna the mineralization is shown. On the *left* side of the diagram the fluids responsible for that mineralization (as indicated by fluid inclusion studies) are shown. Note presence of surrounding meteoric waters that will collapse inwards as soon as the flux of magmatic waters ceases (After Eastoe 1982)

of andesitic volcanics and development of an outer halo of propylitic alteration apparently accompanied this event. Outward from the central zone of potassic alteration and mineralization, bornite decreases and is supplanted by pyrite, which increases outward until decreasing in the propylitic zone. The pyrite is closely associated with sericite or sericite plus chlorite, and pyrite-sericite-chlorite veins definitely postdate K-silicate and propylitic alteration assemblages.

This feldspar-destructive phyllic alteration is characterized by abundant pyrite and exhibits strong fracture control. These late sulfide veins and veinlets cut all earlier mineralized rock and contain minor, but upward-increasing amounts of chalcopyrite, bornite, tennantite, enargite, sphalerite, or galena, plus quartz and anhydrite as gangue minerals. At high levels above the sulfide enrichment blanket, advanced argillic assemblages containing pyrophyllite,

diaspore, alunite, amorphous material, and local corundum are strongly developed.

Fluid inclusion assemblages associated with main-stage mineralization contain both high salinity and vapor-dominant types, both of which homogenize in the range 360° to > 600°C. Low-salinity, two-phase inclusions are the only type found in late pyritic veins but also occur as inclusions of probable secondary origin in earlier veins. These low salinity inclusions homogenize at less than 360°C. Stable isotope studies of the El Salvador deposit (Sheppard and Gustafson 1976; Field and Gustafson 1976) indicate that the sulfur involved in main-stage sulfide mineralization was of magmatic origin ($\delta^{34}S = +1.6‰$), and that water involved in the hydrothermal events was initially of magmatic origin but became increasingly meteoric after main-stage metallization. The water involved in advanced argillic alteration was enriched in deuterium and ^{18}O, presumably by near-surface evaporation processes.

The considerable body of data available for the El Salvador deposit is entirely consistent with an initial metallization event of magmatic-hydrothermal origin at a depth of approximately 2 km. This main-stage mineralization underwent subsequent modification due to the effects of deeply circulating meteoric waters driven by heat from underlying cooling intrusives. The actual orebody was formed by later supergene enrichment during the early and mid-Miocene (pre-12 Ma; Sillitoe 1988a) that produced a secondary enrichment blanket containing approximately 300 million tons of 1.6% Cu.

1.2.5 Porphyry Copper Deposits in Island Arcs

The data base for porphyry copper deposits along the North and South American continental margins is far more extensive than that for the porphyry copper deposits of island arcs. Nevertheless, excellent studies on the Panguna porphyry system (see Fig. 1.6) are available (Eastoe 1978, 1982) and a major compilation of data on Philippine porphyry copper deposits is now at hand (Sillitoe and Gappe 1984). This latter study covers 48 porphyry copper deposits and prospects in the Philippine archipelago and is summarized below.

The greatest concentration of porphyry copper deposits and prospects occurs in a north-south trending belt in northern Luzon, but significant clusters of deposits also occur to the south, especially on Marinduque, Cebu, Negros, and eastern Mindanao. Host rocks to the deposits mainly comprise late Mesozoic to Neogene volcanic and volcaniclastic rocks. With few exceptions, deposits are centered on small stocks of diorite or quartz diorite porphyry. Magmatic histories tend to be complex in nearly all instances with intramineral and postmineral phases present, the former characterized by dacite porphyry, the latter by andesite porphyry. Postmineral events also include large diatremes. Regionally extensive strike-slip fault systems, including the Philippine fault zone, appear to have controlled emplacement of the porphyry-generating intrusions.

The major alteration types found are K-silicate, sericite-clay-chlorite, and propylitic. Sericitic, advanced argillic, and calc-silicate alteration are more restricted. The main chalcopyrite-bornite-magnetite ore zones (low pyrite) are cogenetic with K-silicate alteration, which was overprinted by sericite-clay-chlorite alteration. Surrounding pyritic halos developed in propylitically altered rocks. Advanced argillic alteration, in places containing economically important massive pyrite-enargite bodies within alunite-chalcedonic silica zones, occurs at high levels with respect to the porphyry stocks.

The relative amounts of copper, molybdenum, and gold vary considerably between deposits (Fig. 1.7) and, although most are distinctly gold rich, several contain significant amounts of molybdenum. Sillitoe and Gappe (1984) also note that copper sulfides and gold distribution patterns correlate closely and a number of deposits contain copper- and gold-rich cores. Typical copper grades in Philippine porphyries range from 0.4–0.55% Cu, and the gold-rich examples average nearly 1 ppm Au. Mineralization is closely tied to K-silicate alteration and is not influenced by host rock lithologies, erosion level, or quartz veinlet abundance. Many of the deposits manifest intra- and post mineralization hydrothermal breccias, some of which carry copper ore.

Secondary enrichment of hypogene ores tends to be limited by rapid erosion rates, but most deposits exhibit thin (< 100 m) post-Pliocene supergene profiles, some containing poorly developed chalcocite blankets. Sillitoe and Gappe (1984) consider the Philippine porphyry copper deposits to typify the island-arc type of such ores and use their data base to generate a generalized model for such deposits (Fig. 1.8). This model exhibits many

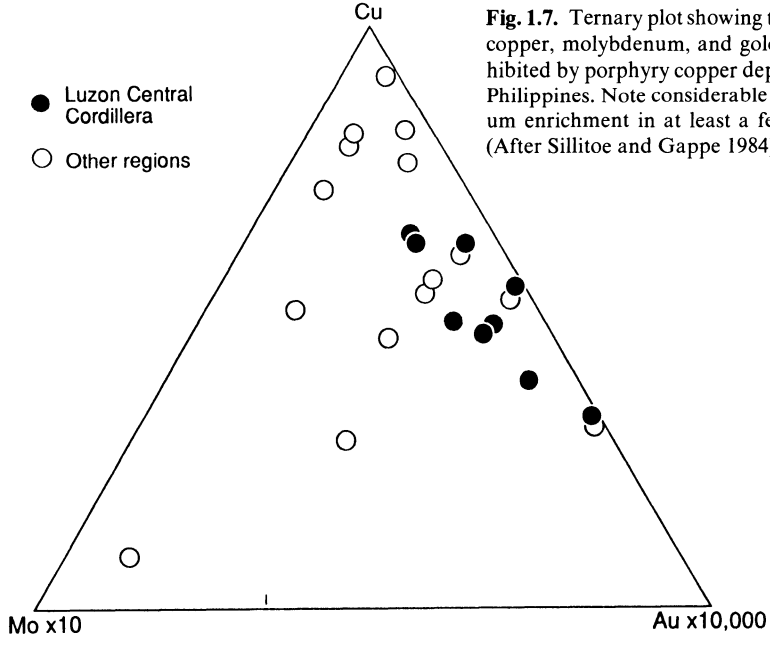

Fig. 1.7. Ternary plot showing the range of copper, molybdenum, and gold ratios exhibited by porphyry copper deposits in the Philippines. Note considerable molybdenum enrichment in at least a few deposits (After Sillitoe and Gappe 1984)

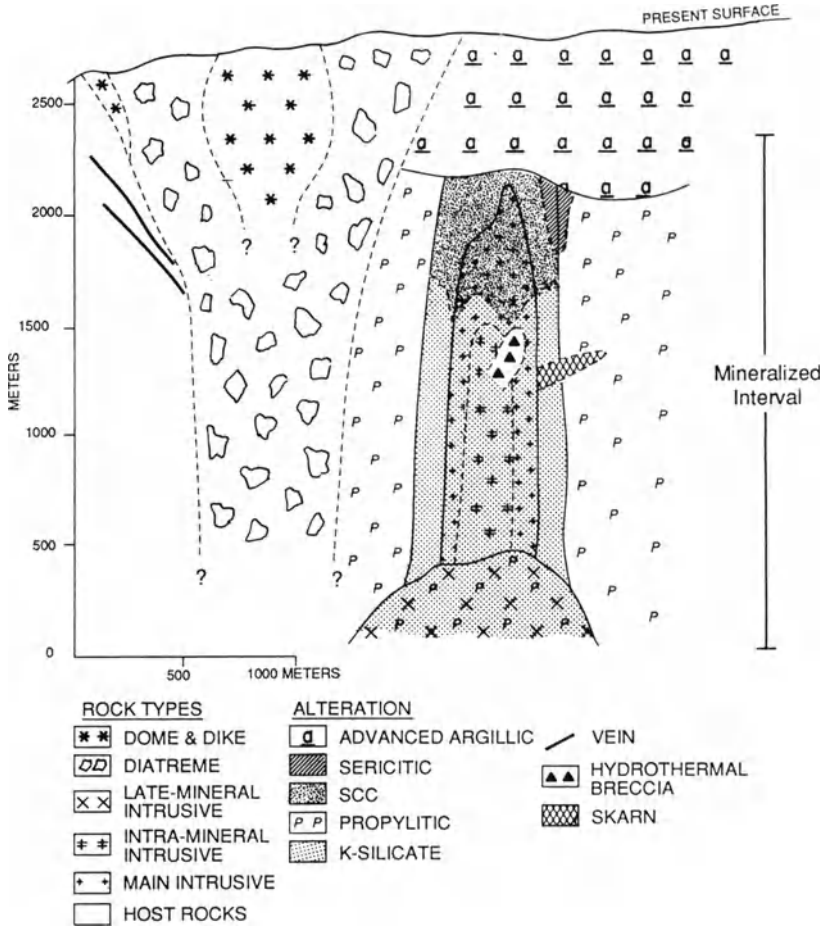

Fig. 1.8. Generalized model of island arc porphyry copper deposits based on examples from the Philippines. Most mineralization is coincident with the zone of k-silicate alteration (After Sillitoe and Gappe 1984)

similarities to continental margin porphyry systems, but also some important differences. In broad terms, island arc porphyries tend to be smaller, contain higher gold, and lack well-defined barren core zones. Mineralized breccia pipes (see next section) and tourmaline as an indicator phase of mineralization are also lacking. Finally, the spatial relationship of porphyry copper deposits, especially those rich in gold, to major transcurrent faults as seen in the Philippines is not mirrored by continental margin porphyries.

1.2.6 The Panguna Porphyry Copper Deposit, Bougainville, Papua New Guinea

The Panguna porphyry deposit is a well-studied example of a gold-rich porphyry copper deposit in an island arc setting (Fig. 1.9). This mineralized system contains over 1 billion metric tons of ore grading 0.5% Cu and 0.55 g/t Au (Sillitoe 1979). Geologic studies of the deposit (Baumer and Fraser 1975; Ford 1978; Baldwin et al. 1978) have revealed a major andesite unit, probably part of a stratavolcano, intruded by a biotite diorite which is cut by a biotite granodiorite which, in turn, is cut by feldspar porphyry dikes and various breccia bodies. Potassium-argon dating of the various magmatic and hydrothermal events at Panguna (Page and McDougall 1972) indicate that the early diorites were intruded between 4 and 5 Ma, that the feldspar porphyries and mineralization followed within the next million years, and that the

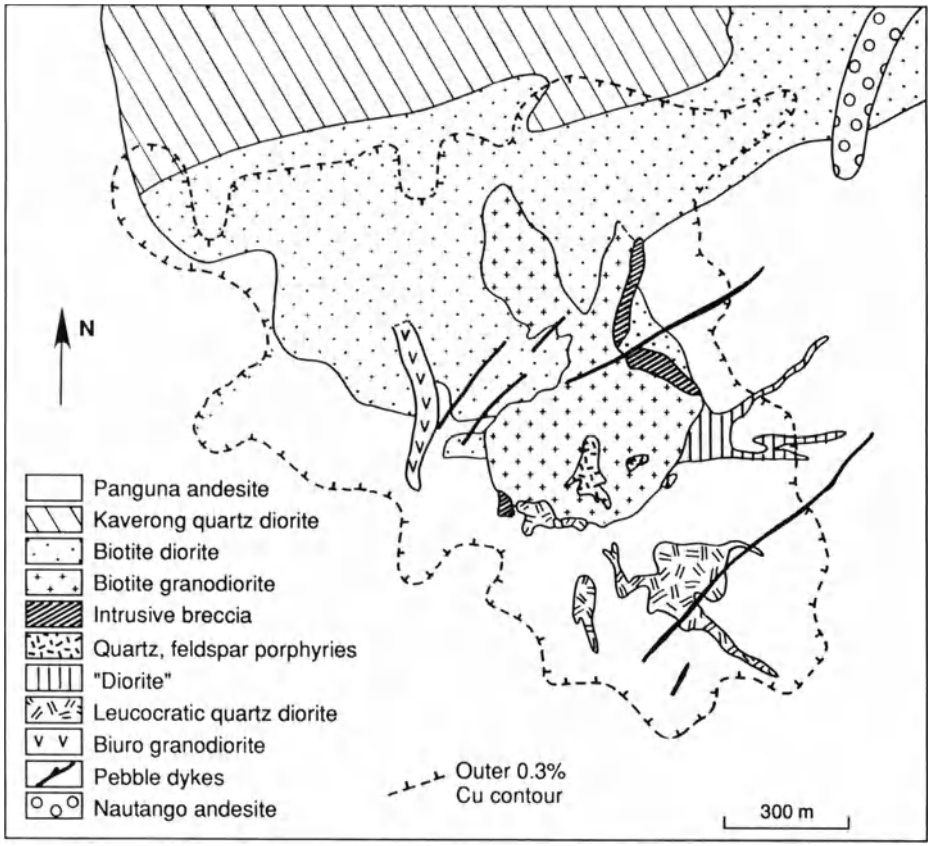

Fig. 1.9. Simplified map of the Panguna porphyry copper deposit. Note that the zone of copper mineralization encompasses a range of preexisting rock units (After Eastoe 1978)

metallization process had essentially ceased by the time intrusion of the Biuro Granodiorite occurred at close to 3.5 Ma.

Baldwin et al. (1978) noted that a number of large breccia bodies have been exposed by mining and that these breccias tend to contain significantly higher copper grades. In well-mineralized areas alteration is of K-silicate type, characterized mainly by biotite, which within some intrusions and breccias is overprinted by K-feldspar. Surrounding the K-silicate zone is a halo of propylitic alteration in which chlorite-epidote-quartz-calcite-pyrite assemblages occur. More intense alteration within the biotite granodiorite is manifest by a silica-sericite-kaolinite-chlorite assemblage (cf. SCC alteration in Philippine porphyries), and is a late-stage feature, as are 3- to 20-m-wide zones of intense quartz-sericite-kaolinite-pyrite alteration that cross-cut earlier K-feldspar alteration.

Mineralization at Panguna is of relatively low total sulfur content (1–4 wt% sulfides). Pyrite and chalcopyrite vary inversely and a pyritic halo surrounds the copper-gold orebody, which is 60% in andesite, 40% in intrusive units. Veins containing quartz plus sulfides correlate with higher-grade ore in nonbrecciated material. Information on the spatial relationship of gold values to copper values is not available, but gold is concentrated mainly in bornite (300–400 ppm). Molybdenum is uniformly low and reaches maximum levels of only 80 ppm in the biotite granodiorite.

Geochemical (Ford 1978) and fluid inclusion studies (Eastoe 1978) indicate that copper mineralization occurred by saline solutions in the 350–700°C temperature range. An outward decrease in temperature from the central portions of the deposit is indicated by both the alteration patterns (Fig. 1.10) and the fluid inclusion data, but time-related changes are also important. Eastoe's (1978, 1982) studies indicate the presence of many veining episodes at Panguna, ranging from pre-copper mineralization amphibole-quartz-magnetite veins through various quartz-sulfide and sulfate veins containing copper minerals to late carbonate, clay or sulfate veins essentially devoid of sulfides. Furthermore, although some uncertainties exist, two major periods of copper introduction, perhaps separated by a million years during which groundwater inundation occurred, are suggested.

Copper metallization, however, was clearly associated with dense, hot saline fluids that were actively boiling and may themselves in part have condensed from vapor phases. Further work on the Panguna hydrothermal system (Eastoe 1982) resulted in a rather complete detailing of many of the physical and chemical parameters during ore formation that tie the ore generation to a relatively oxidized ($\log f_{O_2} = -11.0$), sulfur-rich magmatic system.

1.2.7 Genetic Models for Porphyry Copper Deposits

The extent to which the El Salvador model, the Panguna model, and the more general models of mineralization and alteration of porphyry systems discussed

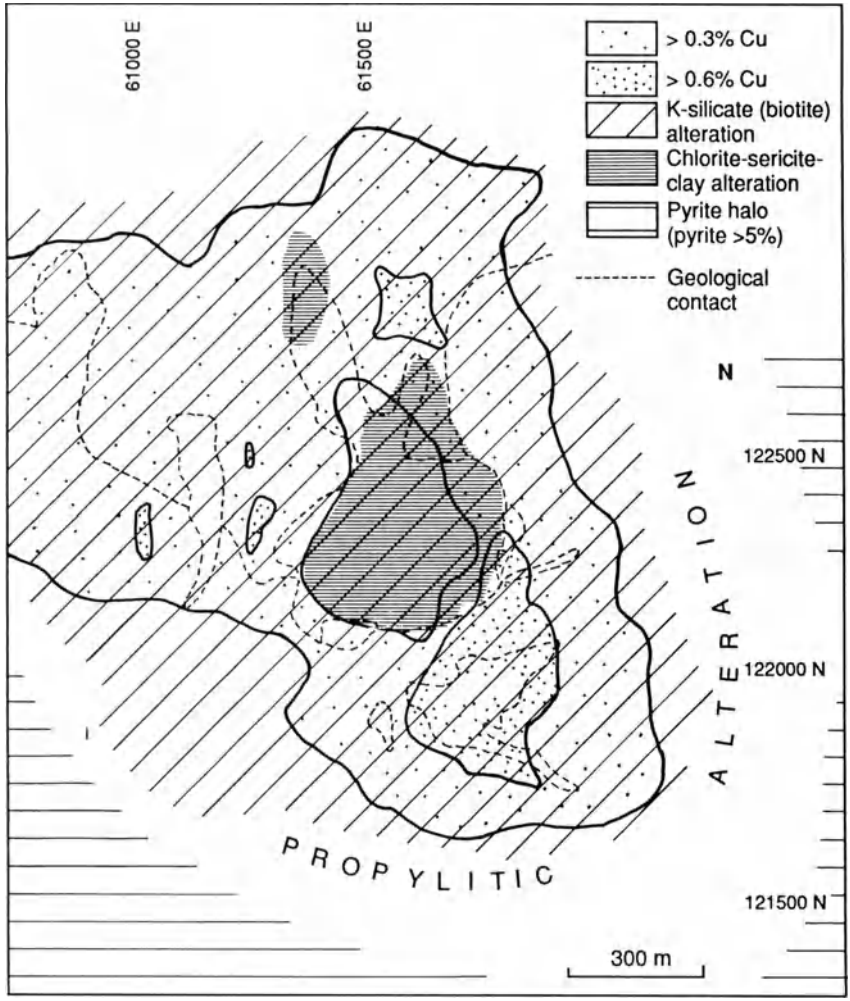

Fig. 1.10. Distribution of principal alteration types and copper grades at the Panguna porphyry copper deposit (After Ford 1978)

earlier, can be applied to all porphyry copper deposits is unclear. Sillitoe (1973) offers evidence that some entire porphyry copper systems may have considerable vertical extent (up to 8 km) and "effectively span the boundary between the plutonic and volcanic environments." Burnham (1981) has considered the physicochemical constraints on porphyry copper genesis. These include the H_2O content of porphyry magma ($\sim$ 2–3 wt%), which must be such that it can reach depths between 2 and 6 km without solidifying, crystallize hornblende and biotite as phenocryst phases, and release sufficient energy from exsolved aqueous fluids to fracture large volumes of rock. Magma temperatures must be sufficiently high ($>$ 800°C) to allow melts to reach

depths of about 4 km in a largely liquid state. In addition, the metal, sulfur, and chlorine contents of such magmas must be sufficient to allow the extraction, transport, and deposition of large amounts of copper sulfides. Finally, the oxidation state of the magmas must be relatively high to permit transport of large quantities of sulfur, together with metal chlorides. The data obtained from studies of the El Chichon eruption of 1982 (Luhr et al. 1984; Varekamp et al. 1984, Table 1–2) indicate that most of the constraints enumerated by Burnham were met by this magmatic system. Furthermore, the discovery of lithic clasts containing chalcopyrite plus pyrite mineralization within the volcanic ejecta strongly suggest that porphyry copper-style mineralization is currently occurring or has occurred in the subsurface.

The magmatic origin for virtually all the essential components of porphyry copper deposits can be considered to be firmly established, not only on the basis of the evidence reviewed above, but also on the basis of thermochemical studies (Candela and Holland 1986) and various isotope studies (H.P. Taylor Jr 1979 and references therein).

One of the unresolved problems of porphyry copper genesis is the extent to which superimposed meteoric-hydrothermal activity (see Fig. 1.5) is a necessary and integral part of orebody formation (e.g., Norton 1978; Henley and McNabb 1978; Eastoe 1982), or merely a likely consequence of the cooling history of fractured and mineralized subvolcanic igneous complexes. As pointed out by Burnham (1981), the main impetus for the formation of phyllic alteration zones in porphyry systems may be the HCl released by deposition of metal sulfides from metal chloride-rich brines. This observation, taken in conjunction with experimental results (e.g., Montoya and Hemley 1975), suggests that typical porphyry copper zonal alteration patterns could develop without incursion of meteoric fluids. The stable isotope data base, however, indicates that this condition is probably rare in the evolution of porphyry systems. An extreme case of the redistribution of primary porphyry copper mineralization and alteration patterns is provided by the important vein deposits at Butte, Montana (Brimhall 1979). Here, a combination of permeable volcanics surrounding the Butte Quartz Monzonite ($\sim$ 70 Ma), later magmatic events, and the development of an extensive fracture system resulted in major modification of the previously formed K-silicate alteration and low-grade copper mineralization, and emplacement of the extensive system of high-grade veins, now termed Main-Stage mineralization. Stable isotope data (Sheppard and Taylor 1974) indicate a meteoric origin for the hydrous fluids involved in this vein-forming event, which occurred over a temperature range of 200–350°C (Roedder 1971).

Brimhall has demonstrated, however (Brimhall 1980; Brimhall and Ghiorso 1983), that not only was the original metallization at Butte magmatic, but that the addition of magmatic volatiles (sulfur gases mainly) to the meteoric water-dominated Main-Stage system controlled all aspects of Main-Stage (vein) ore deposition at Butte. Thus, the high oxygen and sulfur fugacities attendant on the advanced argillic alteration were critical to the initiation and continuation of base metal remobilization and deposition

processes. Furthermore, because of negative volume changes induced by these reactions, the high porosities necessary for circulation of very large volumes of water were attained.

In island arc porphyry systems evidence for the incursion of late meteoric fluids is certainly present, but the actual copper metallization is invariably centered on the K-silicate alteration facies. This is distinct from the F.D. Lowell and Guilbert (1970) model, developed on the basis of North American continental margin porphyry copper deposits, which emphasizes the interface between the K-silicate potassic and phyllic zones as the principal locus of copper deposition.

Farmer and DePaolo (1987) have added further evidence for a wholly magmatic source of components during porphyry copper mineralization with their study of Nd and Sr isotope patterns in wall rocks adjacent to the San Manuel porphyry copper deposit in Arizona. They demonstrate that Nd is essentially immobile during alteration events associated with porphyry copper development and can thus be used to categorize magma sources. Sr is mobile under alteration conditions, and at San Manuel a steep $^{87}Sr/^{86}Sr$ gradient can be demonstrated that propagated outward from the porphyry-wall rock contact with time.

Important corroborative evidence for a magmatic source of the copper in porphyry deposits has come from analytical work on minerals from mineralized and barren stocks in North America (Hendry et al. 1985). Three types of intrusions were recognized in the study: (1) mineralized, (2) barren, but deep level temporal equivalents of mineralized intrusions, and (3) barren and removed in time and space from mineralization. The latter exhibit higher overall copper contents of certain mafic minerals (biotite and magnetite) than mineralized or mineralization-associated intrusions. Thus, the process of copper concentration leading to porphyry copper formation is reflected in copper depletion of certain minerals, thereby demonstrating the fundamental magmatic nature of porphyry copper ore-generating systems.

1.2.8 Suggestions for Exploration

In terms of exploration for porphyry copper deposits, principal arc-hosted intermediate to felsic subvolcanic complexes characterized by multiple igneous events and pervasive wall-rock alteration obviously merit close investigation. Erosion levels are of major significance, for compressive arcs tend to form thick crustal roots and stand high, and their uppermost few kilometers, where porphyry deposits form, are vulnerable to removal. Few of the porphyry deposits of the Andes or those of the Philippines, for example, would survive 20 million years into the future, given continuation of current uplift and erosion rates in these areas.

In arid areas porphyry copper-type mineralization is marked by strong color anomalies but the initial location of occurrences of porphyry copper-type mineralization in vegetated areas is best accomplished by geochemical pro-

specting techniques (Chafee 1982). Once anomalous sites have been found, recognition of zonal or distal alteration patterns is important, but it must be borne in mind that such patterns can exhibit a wide variety of geometries. The ability to interpret leached cappings (F.A. Anderson 1982) and to "see through" supergene overprinting of hypogene alteration assemblages is a valuable skill in this regard. Furthermore, the distinctive fluid inclusion assemblages that characterize porphyry copper deposits can be used (Nash 1976), for even in areas of strong alteration and surficial weathering fragments of veinlet quartz will tend to survive and be amenable to study. In the evaluation of oxidized and leached surface showings it is also important to bear in mind that maximum sulfide and maximum copper contents seldom coincide. This caveat also applies to the results of geophysical surveys (e.g., I.P.) that essentially measure total sulfide content. Ground magnetometry can distinguish between K-silicate (magnetite present) and sericitic (no magnetite present) alteration. In this regard it is noteworthy that high-Au porphyry systems typically contain significant amounts of magnetite (Sillitoe 1979). Generally, a combination of rock geochemistry, careful alteration mapping, and application of suitable geophysical techniques will provide a sufficient basis for meaningful exploratory drilling.

The spacing of porphyry copper deposits along principal arc systems is of interest in exploration, and Sawkins (1980) has attempted to show that average spacing of porphyry copper deposits exhibit a relationship to the average spacing of volcanoes along volcanoplutonic arc systems. Clearly, any regularities in this parameter within a specific arc system will have major implications for exploration, especially where gaps in an otherwise regular spacing pattern are apparent. It is noteworthy that the recently discovered major porphyry copper deposit, La Escondida in Chile (Brimhall et al. 1985 and references therein), occurs in one of the significant gaps in the linear array of porphyry copper deposits in that country. Finally, the spatial relationship of many Philippine porphyry copper systems to transcurrent faults, especially the Philippine Fault System, is clearly important and may provide an exploration guideline in other island arc environments (Sillitoe and Gappe 1984).

1.3 Copper-Bearing Breccia Pipes

Mineralized breccia pipes that are not integral parts of porphyry copper deposits are of relatively minor economic importance compared to the huge tonnages of many porphyry copper systems, but are attractive in that they tend to be higher-grade targets that require less capital investment to develop. In addition, they tend to provide excellent material for mineralogic and fluid inclusion studies, and present some intriguing problems with respect to their genesis (Sillitoe 1985).

1.3.1 Distribution and Associated Igneous Rocks

In general terms, the igneous rock associations discussed in the preceding section on porphyry deposits in principal arcs apply equally to copper-bearing breccia pipe deposits. Breccia pipes occur, either singly or in clusters of up to 100 or more, in the roofs of intermediate composition batholiths or stocks, and in their volcanic roof rocks. Their most common occurrence is in granodioritic plutons that represent typical products of volcanoplutonic arc formation (e.g., Sillitoe and Sawkins 1971). Many porphyry copper deposits contain breccia bodies. In some instances these are clearly phreatic breccias formed relatively late in the mineralization sequence (Gustafson and Hunt 1975), but, in others, irregular bodies of brecciated rock occur whose origin is enigmatic (Sillitoe 1985).

Mineralized breccia pipes that are not integral parts of porphyry copper deposits occur widely in Chile (Sillitoe and Sawkins 1971), northern Mexico (Sillitoe 1976a), and the southwestern USA (Kuhn 1941; Johnson and Lowell 1961), but examples are also known from Peru (Carlson and Sawkins 1980), Korea (Fletcher 1977), and northern Australia (Knutson et al. 1979).

1.3.2 Mineralization and Alteration

Although volumes of brecciated and mineralized rock can display a variety of geometries, the majority occur as steeply inclined circular or elliptical pipes. In areas where nests of pipes are found, the intensity of mineralization and the grades of metal they contain are highly variable. Typically, a few pipes will contain ore grade material, whereas the majority will be hydrothermally altered and contain hydrothermal gangue minerals, but low metal values.

Two distinct end-member types of breccia pipe can be identified, one that contains highly rounded fragments of various sizes set in a matrix of rock flour, and another characterized by highly angular fragments and an absence of rock flour. Intermediate types are also known, but are less common. Ore grade mineralization is more common in the pipes that contain angular fragments, presumably because of their enhanced permeability characteristics.

Copper-iron and molybdenum sulfides are the principal economic minerals in the breccia pipes found in principal arcs, but some pipes contain significant amounts of tungsten as scheelite. A large array of other minerals are also present in some pipes, including pyrite, magnetite, specular hematite, arsenopyrite, sphalerite, tetrahedrite, bismuthinite, fluorite, apatite, and gold, although the quantities of these are generally minor. Quartz is ubiquitous as a gangue mineral, and tourmaline is an important constituent of many pipes, especially those in the Andes. Additional gangue minerals that may be present are carbonates, actinolite, K-feldspar, biotite, anhydrite, sericite, and chlorite.

In pipes that are not integral parts of porphyry copper systems, alteration tends to be rather localized, and in few instances extends more than a few meters beyond pipe margins (see Sillitoe and Sawkins 1971). The majority of

pipes exhibit phyllic alteration (sericite-quartz-pyrite), but this tends to give way to K-silicate alteration at depth (Sillitoe 1976b).

Mineral zoning is strongly developed in some breccia pipes and is less prominent in others. In the Washington pipe, Sonora (Simmons and Sawkins 1983) there is intense development of pyrite, accompanied by quartz, sericite, and tourmaline at near-surface levels. Downward, pyrite and tourmaline decrease, whereas chalcopyrite and scheelite increase. In the deepest levels the assemblage chalcopyrite-chlorite-calcite is dominant, although numerous patches of K-silicate alteration are found. The molybdenite content of the pipe increases downward. In the Cumobabi area, about 12 km to the east, metal zoning patterns are irregular, but tourmaline only occurs in outlying pipes that crop out at the highest elevations and lack obvious mineralization (Scherkenbach et al. 1985). The Turmalina pipe in northern Peru (Carlson and Sawkins 1980) is strongly zoned with respect to copper and molybdenum values and, surprisingly, changes from high molybdenum values near surface to high copper values at depth (Fig. 1.11).

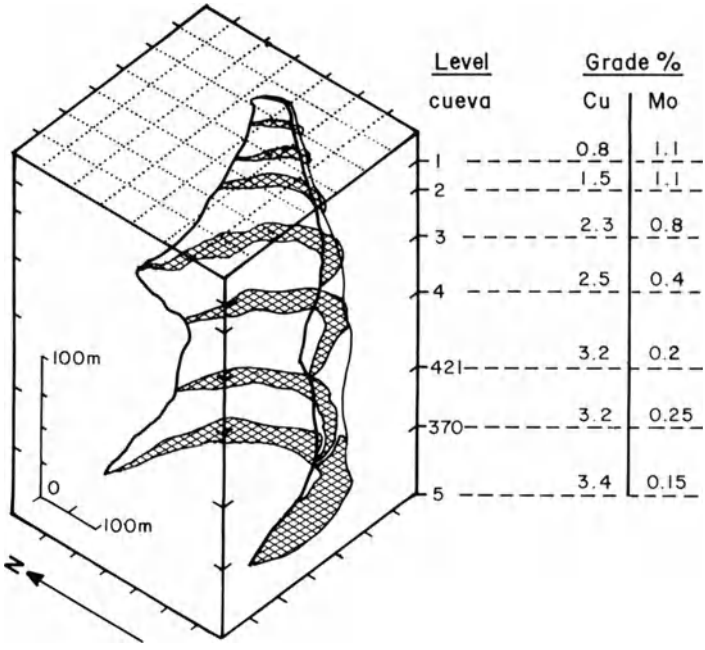

Fig. 1.11. The ore-bearing margin of the Turmalina breccia pipe, northern Peru, showing the marked vertical zoning with respect to copper and molybdenum values (After Carlson and Sawkins 1980)

1.3.3 Formation and Mineralization of Breccia Pipes

Available fluid inclusion data on breccia pipe mineralization (Sillitoe and Sawkins 1971; Fletcher 1977; Sawkins 1979; Carlson and Sawkins 1980; Sawkins and Scherkenbach 1981; Scherkenbach et al. 1985) indicate temperatures in the range 300–475°C and a wide range of salinities (5–45 wt% alkali chlorides). Broad distribution of vapor-dominated inclusions indicates that boiling of hydrothermal fluids was common. To date, no comprehensive stable isotope studies have been published on this type of deposit, but a series of $\delta^{18}O$ measurements on quartz from the Cumobabi deposit are consistent with a magmatic origin for the mineralizing fluids.

The close time-space association of mineralized breccia pipes in principal arcs with felsic magmatism and/or porphyry copper emplacement indicates that important aspects of their genesis must be essentially similar to those of porphyry copper deposits. The modes of formation of breccia bodies and pipes are, however, more equivocal, but both theoretical approaches (Burham 1985) and experimental studies (McCallum 1985) suggest that their formation is related to the release of P-V energy from aqueous fluids in subvolcanic environments. As noted by Sillitoe (1985), the aqueous fluids can be of either magmatic or meteoric provenance.

The breccia pipes formed in these subvolcanic principal arc environments can vary from major magmatic or phreatomagmatic diatremes to columns of hydrothermal breccia, containing angular fragments of local derivation, that pass upward into altered, but unbrecciated rock (Fig. 1.12). The mechanisms by which space is created to accommodate the expanded volume occupied by the broken rock in these blind breccia pipes remain puzzling. Whatever their precise genesis, columns of breccia afford excellent channels for the passage of hydrothermal fluids and large surface areas for mineral deposition, accounting perhaps for the attractive grades encountered in many breccia-hosted ores (see Sillitoe 1985).

1.3.4 The Cumobabi Breccia Pipe Deposits, Mexico

The molybdenum- and copper-bearing breccia pipes at Cumobabi, Mexico (Fig. 1.13) occur in a typical subvolcanic setting with a series of calc-alkaline volcanic units intruded sequentially by various intrusions and apophyses of quartz monzonite, diorite porphyry, and finally microgranite (Scherkenbach et al. 1985). High-angle faulting with dominant N-S and E-W trends is pronounced in the area.

At least 36 breccia bodies are known to occur, and in broad terms a ring of unmineralized, tourmaline-bearing breccias surrounds the central, lower elevation mineralized breccias. Alteration patterns are complex in detail, but essentially mineralization is associated with strong development of K-silicate alteration in the breccia pipes, with outlying diffuse propylitization. Sericitic

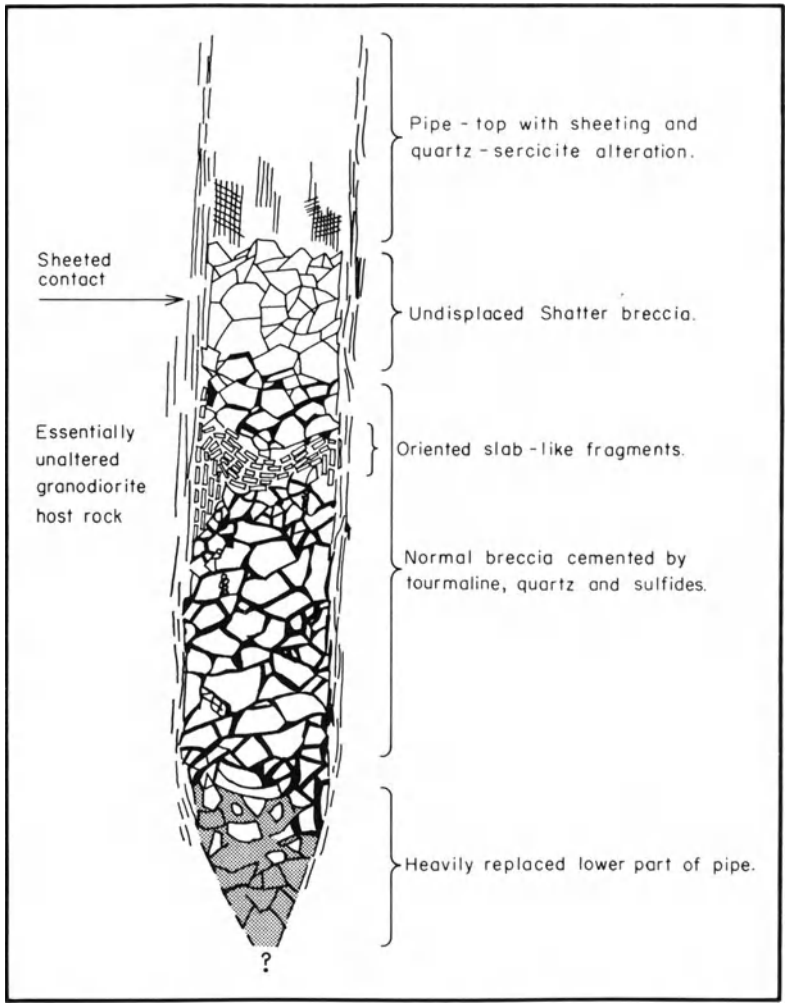

Fig. 1.12. Mineralized breccia pipe inferred to be formed by a mechanism of solution collapse. Note that the pipe structure passes upward into unbrecciated altered rock (After Sillitoe and Sawkins 1971)

alteration is demonstrably later and overprinted earlier alteration patterns along highly permeable zones.

Breccia mineralization associated with the K-silicate alteration event comprises molybdenite, and lesser chalcopyrite, whereas accompanying gangue minerals are quartz, orthoclase, biotite, anhydrite, and minor apatite and fluorite. Adjacent to some of the pipes, disseminated chalcopyrite mineralization of porphyry type is present. In general terms, molybdenite deposition is early and closely associated with strong K-silicate alteration, whereas minor sphalerite and tetrahedrite deposition postdate chalcopyrite and are more closely associated with sericitic alteration.

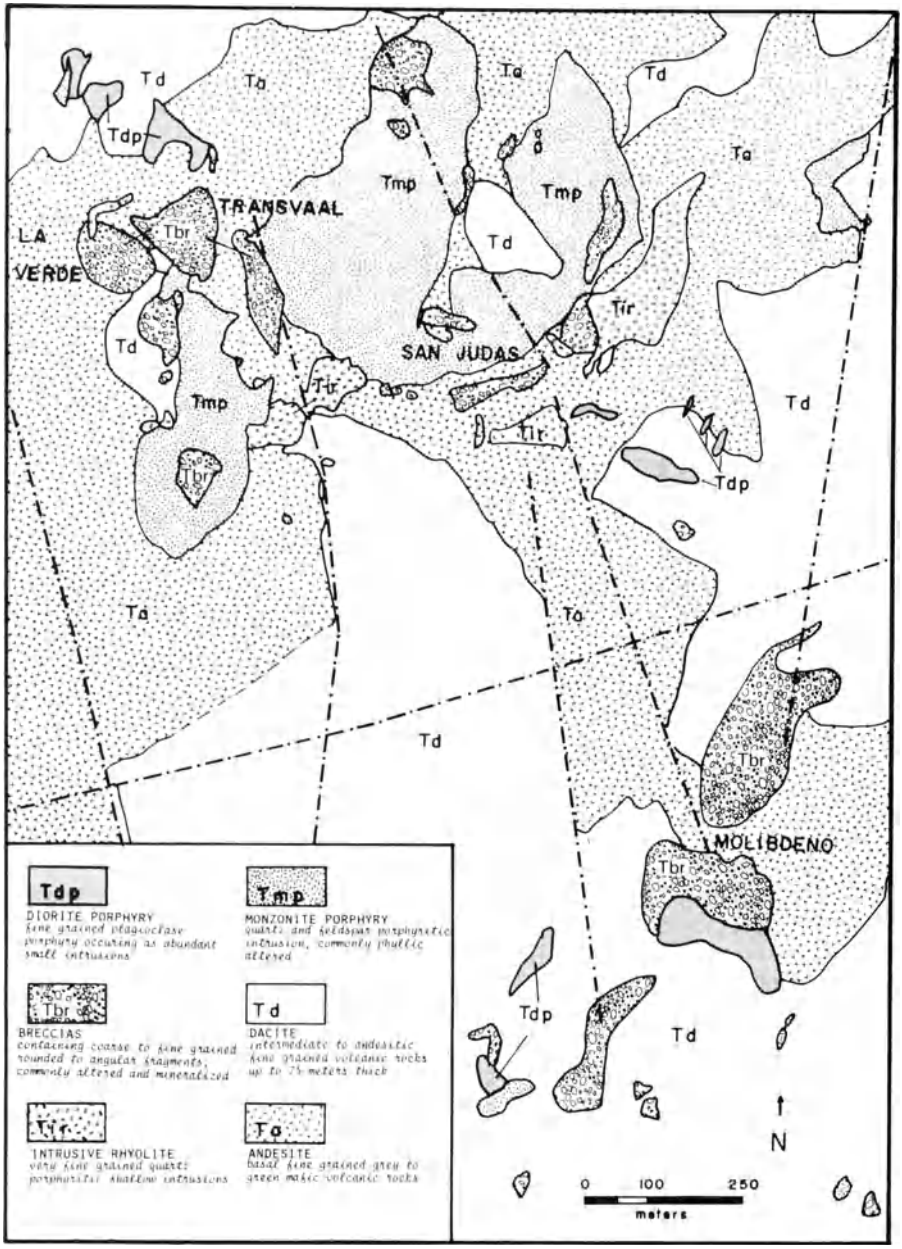

Fig. 1.13. Map of the central zone of breccias at Cumobabi, northern Mexico. Numerous breccia bodies beyond this zone are known, but most are unmineralized at current exposure levels (After Scherkenbach et al. 1985)

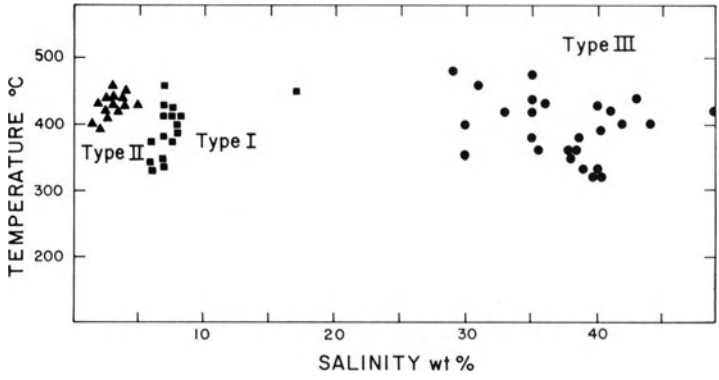

Fig. 1.14. Plot of temperature and salinity data obtained from fluid inclusions in quartz from the central zone of mineralized breccia at Cumobabi, northern Mexico. Note three types (*I-III*) of fluid inclusion populations that can be differentiated on the basis of salinity and liquid-vapor ratios (After Scherkenbach et al. 1985)

Euhedral quartz crystals from the mineralized breccias have yielded a considerable body of fluid inclusion data (Scherkenbach et al. 1985). Temperature and salinity measurements from these inclusions (Fig. 1.14) indicate the presence of hot (340–410°C), boiling fluids during mineralization. In addition, scanning electron microscope studies of the high salinity inclusions indicate that the fluids they represent carried copper and iron in amounts up to 10 000 ppm each. Quantitative chemical analysis of these trapped fluids have indicated mean contents of 2150 ppm copper and 1160 ppm zinc in addition to considerable sodium, calcium, potassium, and chlorine (Scherkenbach et al. 1985). These fluids are essentially equivalent to those found in fluid inclusion studies of porphyry copper deposits (see preceding section).

1.3.5 Mineralized Tourmaline Breccias at Los Bronces-Rio Blanco, Chile

The Los Bronces-Rio Blanco breccia complex of central Chile represents a major copper resource that produces 10 000 tons/day of ore grading 1.25% Cu (Warnaars et al. 1985). The complex consists of seven contiguous copper-bearing tourmaline breccias that occupy the western edge of the Rio Blanco porphyry copper deposit, and formed between 7.4 and 4.9 Ma ago.

Geologic studies (Warnaars et al. 1985) indicate that at least seven brecciation events occurred, each producing a steep-sided breccia body of distinctive character in terms of clast size and shape, texture, mineralization, and alteration. Contacts of the various breccia bodies against the surrounding andesites or intrusive rocks are sharp, but internal contacts between breccia units vary from sharp to ill-defined in places.

The northern end of the breccia complex is occupied by the Donoso Breccia (Fig. 1.15). It apparently formed late and contains clasts of two other

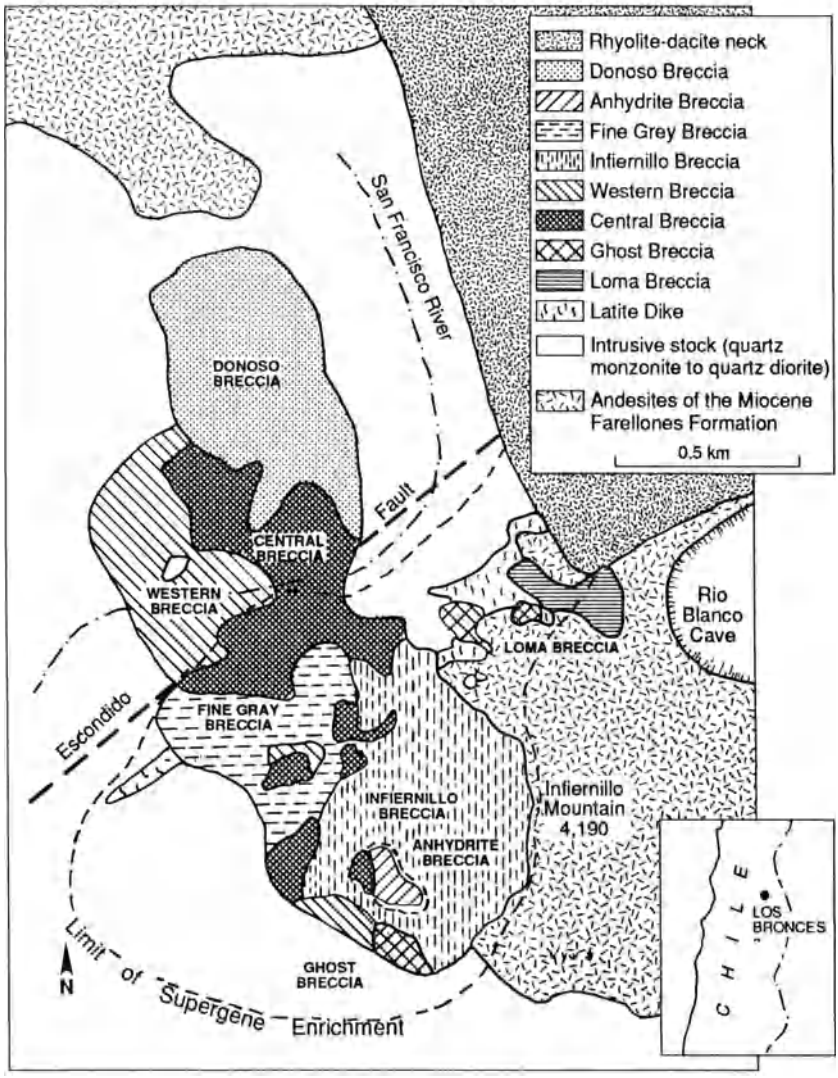

Fig. 1.15. Simplified map of the Los Bronces breccia complex, central Chile (After Warnaars et al. 1985)

breccia types in an otherwise monolithologic population of quartz monzonite clasts. The matrix consists of tourmaline, specularite, quartz, and sulfides (py, cpy ± bn, cc). The average copper grade of the Donoso Breccia is 0.92%, but grade distribution studies indicate that relative amounts of pyrite, specularite, and chalcopyrite vary, and irregular, almost vertical shells of chalcopyrite-rich material occur within the body. A summary of the mineralization and brecciation events as deduced by Warnaars et al. (1985) is shown in Fig. 1.16.

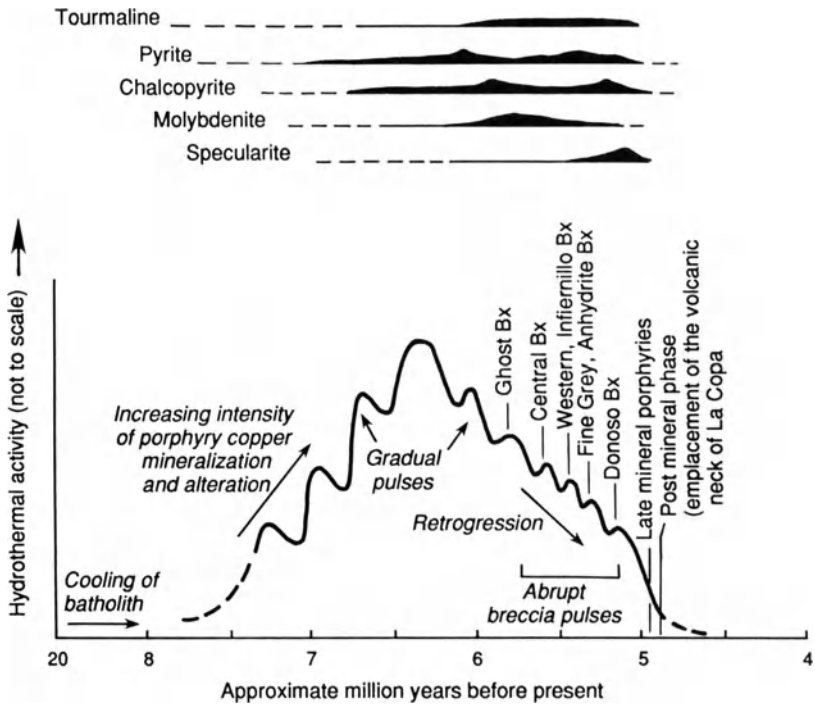

Fig. 1.16. Sequence of mineralization and brecciation events at the Los Bronces deposit. The time axis is based on a number of K-Ar age determinations primarily on biotite (After Warnaars et al. 1985)

1.3.6 Suggestions for Exploration

Notwithstanding the enigmas surrounding their formation, pipes and bodies of broken rock formed in the vicinity of cooling igneous intrusions are obviously highly favorable loci for mineralization by metal sulfides. However, inasmuch as such pipes only intersect the erosion surface at a single point or may be blind, they present an interesting challenge to the exploration geologist.

Many pipes, especially those that contain considerable amounts of quartz, crop out boldly relative to their immediate host rocks. Such pipes are easy to locate and recognize in arid terrane, but typically any metal sulfides they may contain have been leached and oxidized. In addition, the vertical zoning present in many pipes can create situations where pipes are essentially barren at the extant erosion surface, but contain ore-grade material at depth.

In areas where arrays of pipes occur, careful attention should be paid to the occurrence of limonite types, breccia textures, interstitial material, and the alteration characteristics and geochemistry of each pipe exposure, for typically only a small proportion of the total number of pipes will contain ore-grade

mineralization. Geophysical techniques aimed at assessing the content of metal sulfides below the zone of oxidation should also be considered.

Ultimately, diamond drilling is required to evaluate those pipes whose surface characteristics are most favorable, and in planning of drilling programs cognizance should be taken of the tendency for many pipes to be most heavily mineralized along their margins.

1.4 Skarn Deposits

The excellent and extensive review of skarn deposits by Einaudi et al. (1981) has provided an indispensable source for this and later sections on skarn deposits. The term "skarn" has been applied to a variety of coarse-grained assemblages of metamorphogenic silicates developed primarily in carbonate-bearing rocks, but it is used more restrictively here to categorize mineral assemblages formed as the result of metasomatic and hydrothermal processes related in time and space to the cooling of intermediate to felsic igneous bodies. It is worth noting, however, that some very mafic intrusions can be associated with Fe skarns, and that in certain instances skarns can form from host rocks that are essentially lacking in carbonate components.

Einaudi et al. divide skarns on the basis of primary metal type, but they point out that skarns can also be classified by their dominant calc-silicate mineral assemblages. The purpose of this book, however, is to explore the degree to which plate tectonic environments can be utilized to understand diversity within various ore deposit types, and more importantly perhaps, their geographic distribution. Accordingly, the text will be restricted here to a discussion of those skarns that form in principal arc environments.

1.4.1 Distribution and Associated Igneous Rocks

Mineralized contact metasomatic skarns are developed in continental margin and oceanic principal arcs, mainly where intrusions encounter carbonate-rich country rocks, Along continental margin arcs such lithologies are more common, having resulted from sedimentation in earlier miogeoclinal environments. In true oceanic arc systems, however, carbonate rocks are less common, and tend to be limited to local development of reef limestones.

Principal arc terranes that contain this type of mineralization include the batholiths of the Sierra Nevada (Kerrick 1970), Aconchi, Sonora (Newberry and Einaudi 1981), and less deeply eroded terranes in Japan (Shimazaki 1980), the Philippines (Bryner 1969), Indonesia (Djumhani 1981), and Iran Jaya (R.H. Sillitoe, pers. comm.). Although porphyry copper-associated skarns represent an important subgroup, such deposits also occur prominently in inner arc environments where carbonate country rocks tend to be more widespread (see later).

The majority of skarn deposits are associated with magnetite series, I-type granitoids, but in Japan a number of skarn deposits are associated with ilmenite-series granitoids (Shimazaki 1980), especially those that contain tin-wolframite mineralization. The late Mesozoic and Cenozoic patterns of granitoid magmatism in Japan are particularly complex, but these ilmenite-series intrusions are not related to principal arc magmatism.

The literature on Russian ore deposits is replete with descriptions of skarn ores of all types, but apart from those that occur in late Paleozoic arcs accreted to the southern margin of the Siberian craton (Laznicka 1976), and those within the Urals, assignment of these deposits to specific plate tectonic categories is deemed premature, at least in terms of the author's knowledge.

1.4.2 Mineralization

Magnetite skarn deposits can be divided into calcic types that form in island arc settings, and magnesium types found in Cordilleran arcs and on their inner margins (Einaudi et al. 1981). Calcic, island arc-related magnetite skarns are typically associated with dioritic or even gabbroic intrusions. They are characterized by formation of significant amounts of skarn from igneous rocks, widespread sodium metasomatism, and anomalous cobalt and in some instances nickel concentrations. Examples include Larap, Philippines (Frost 1965), Daiquiri, Cuba (Lindgren and Ross 1916), the Empire Mine, Vancouver Island (Sangster 1969; Haug 1976; Meinert 1984), and some large ($>$ 100 million tons) deposits in the Urals (Sokolov and Grigorev 1977; see Einaudi et al. 1981, Table 3).

Magnesian magnetite skarn deposits in Cordilleran settings are associated with more felsic intrusions such as quartz monzonites and tend to form only in dolomitic country rocks. Skarn silicate minerals in these deposits are magnesium-rich, leaving the iron available for magnetite formation. Examples that can be placed with any confidence into a principal arc setting are limited, but include the Eagle Mountain mine, California ($>$ 50 million tons; Dubois and Brummett 1968). Two large deposits in Russia appear to belong to this class, based on mineral associations (see Einaudi et al. 1981, Table 4), but their assignment to a principal arc setting would involve pure conjecture. The well-known Fierro deposit, Central mining district, New Mexico (Hernon and Jones 1968) represents another example, but it occurs in what may be more appropriately designated as a backarc setting.

Tungsten skarns associated with coarse-grained granodioritic stocks and batholiths are widespread in the principal arc terranes of the western USA and northern Mexico. Based on stratigraphic reconstructions, prograde skarn mineralogy and the nature of the associated intrusions, Newberry and Einaudi (1981) suggest that most North American scheelite-bearing skarns developed at depths of 5 km or more. Furthermore, they hypothesize that areal concentrations of such deposits reflect the coincidence of suitable intrusion and country rocks and appropriately deep erosion levels, rather than discrete tungsten-rich geochemical provinces (Fig. 1.17).

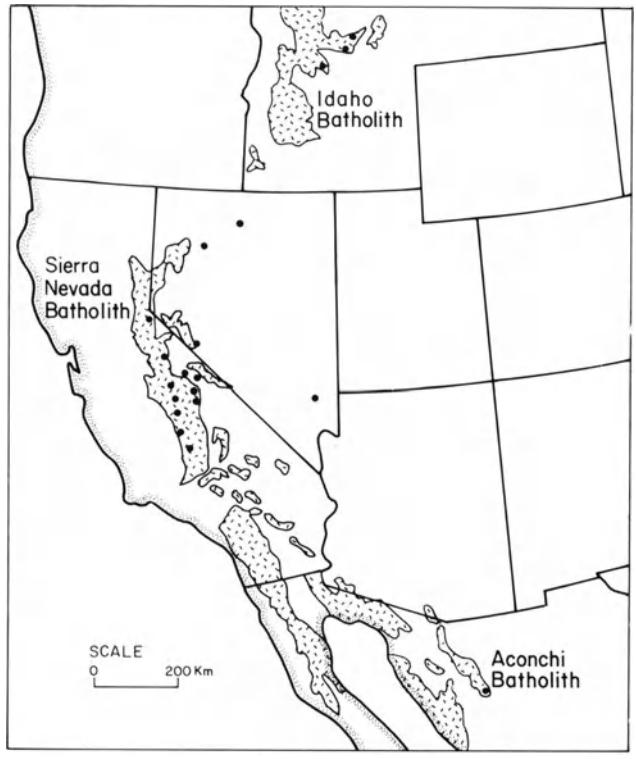

Fig. 1.17. Distribution of tungsten skarn deposits in the western USA and northwest Mexico. Note the association of these deposits with granitic intrusions of batholithic dimensions (After Meinert et al. 1980)

Studies of typical skarns associated with roof pendants in the Sierra Nevada batholith (Morgan 1975; Nokleberg 1981) indicate that, although the geometry of individual skarn bodies tends to be complex, they can be subdivided into distinctive zones, based on mineralogy. The distal zone adjacent to the marble is typically represented by wollastonite skarn with lesser grossularite, idocrase, and diopside. Progressively closer to the intrusive contact are zones of garnet skarn with andradite-grossularite, diopside-hedenbergite, and scheelite, and, finally, adjacent to intrusive rock, hornblende skarn containing mainly hornblende, plagioclase, microcline, magnetite, and scheelite. The whole sequence, which can vary markedly in thickness along igneous contacts, can be viewed as a layered metasomatic front between intrusive rock and marble in which CaO and CO_2 are progressively removed by metasomatizing fluids, and SiO_2, total Fe, MgO, MnO, Al_2O_3, and Na_2O, K_2O, and WO_3 added. Variability in these types of skarns from one deposit to another is probably controlled more by host-rock lithologies and fluid-flow patterns than fundamental differences in the chemistry of the aqueous fluids emanating from the adjacent intrusions.

Only one major ($>$ 10 million tons) deposit occurs in this Sierra Nevada principal arc terrane, the Pine Creek mine (Gray et al. 1968; P.E. Brown et al. 1985). Other world-class tungsten skarns are the Sangdong deposit, Korea (John 1978), King Island, Tasmania (Kwak 1978), the MacMillan Pass (Dick

1976) and Canada Tungsten deposits (Zaw 1976) in N.W. Territories, Canada. Sillitoe (1981a) has suggested a backarc setting for the MacMillan Pass and Canada Tungsten deposits and this appears more appropriate to their locale (see later). The same may also be true for the Sangdong deposit. Of these deposits, all except the King Island deposit belong to Einaudi et al.'s (1981, Table 7 p. 338) grouping of reduced tungsten skarns. Such reduced skarns are characterized by hedenbergitic pyroxene, almandine-rich garnet, Fe-rich biotite and hornblende, minor magnetite, and low sulfidation states. Late-stage, cross-cutting zones of hydrous minerals containing hornblende, biotite, actinolite, and epidote are present locally in these skarns and tend to contain enhanced tungsten grades, and assorted sulfide minerals.

The other main group of skarn deposits formed in principal arc settings are base metal ores, primarily of copper. A few such deposits are known from island arc terranes (see Einaudi et al. 1981, p. 340), where they occur adjacent to quartz diorite or granodiorite plutons, but most occur in continental margin environments. Skarn copper deposits along such arcs can be divided into those associated with porphyry copper deposits and those associated with unmineralized intrusions. The former tend to be finer-grained and exhibit more marked retrograde hydrothermal alteration than the latter. In many instances zinc mineralization is significant, but many large base metal skarns, especially those containing significant amounts of lead, develop in backarc rather than principal arc environments (see later).

In broad terms, sulfide skarn deposits differ from tungsten skarns in having more oxidized silicate assemblages and developing at shallower crustal levels (Newberry and Einaudi 1981, Fig. 1.18). A detailed study of the Mason Valley mine deposit in Nevada (Einaudi 1977a) indicates that the zonal arrangement of skarn minerals from country rock marble toward maximum skarn development is: talc-magnetite-calcite, tremolite-magnetite-calcite, pyroxene-sulfides, garnet-pyroxene-sulfides, and garnet. Composition changes in silicate minerals are complex in detail and appear to reflect chemical controls and sharp compositional gradients during skarn production.

These and similar skarns in the region are distal in type and occur from 1–2 km from mapped contacts of Jurassic granodiorites of the Yerington batholith. Proximal skarns in the region differ in having lower total sulfide (5% or less), much higher chalcopyrite/pyrite ratios (10 or greater), absence of iron oxides, a gangue dominated by andradite, and stronger brecciation. This general sequence of minerals in zoned skarn deposits as detailed above (see also Burt 1974) is repeated in skarn deposits elsewhere in the western USA and in British Columbia, Mexico, Japan, and the USSR (Einaudi et al. 1981). However, in skarns developed in dolomitic host rocks, significant amounts of forsterite and serpentine develop, and in some calcium skarns an outer zone of wollastonite is present.

Certain sulfide skarns, in particular those rich in copper or magnetite, tend to contain appreciable quantities of gold (Shimazaki 1980; Sillitoe 1988a). A series of gold-rich skarn deposits occur in the Battle Mountain area of Nevada (Blake et al. 1978; Theodore et al. 1986; Wotruba et al. 1988). Ore deposition

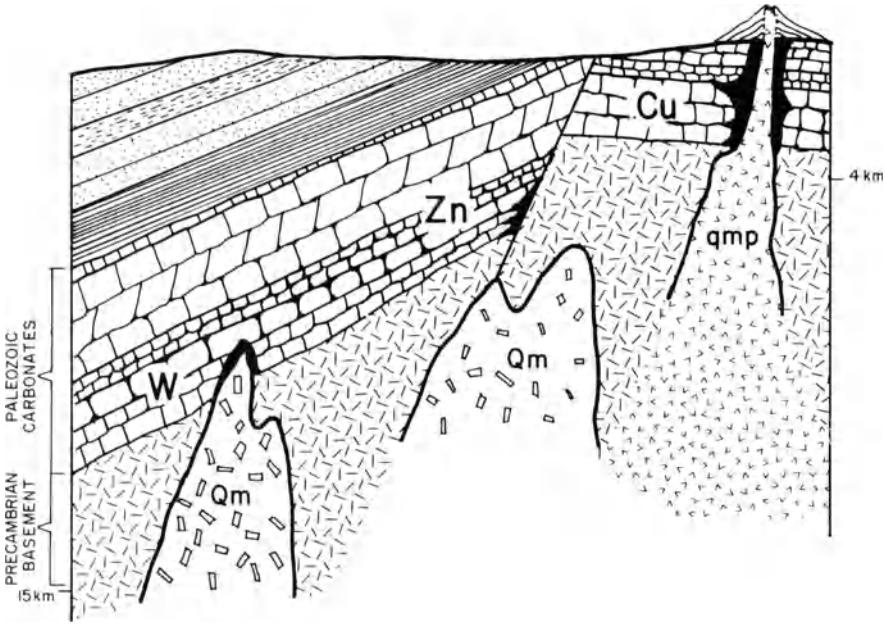

Fig. 1.18. Idealized skarn-forming environments in continental margin principal arcs. Note variation of skarn metallogeny as a function of depth of formation. *Qm* Quartz monzonite; *qmp* quartz monzonite porphyry (After Meinert et al. 1980)

involved the retrograde hydration (actinolite, chlorite) of calc-silicate-rich limy horizons in sedimentary units of late Paleozoic age adjacent to a mid-Tertiary granodiorite stock, itself a host to porphyry copper mineralization. In the Fortitude deposit (Wotruba et al. 1988) 6.7 million tons grading 8 g/ton Au and 200 g/ton Ag have been blocked out. The ores contain 10 to > 50% iron sulfides and minor base metal sulfides, and exhibit strong control by a steep N-S normal fault. It is not clear, however, whether central Nevada can be considered as a principal or backarc environment during mid-Tertiary time (see Chap. 4).

1.4.3 Genesis of Contact Metasomatic Skarn Deposits

Although a number of detailed studies on the mineralogy and zoning of mineralized skarns have been carried out, the fluid inclusion and stable isotope data base is more limited. However, the available data of this type indicate that scheelite skarns typically form at temperatures in excess of 500°C (Newberry and Einaudi 1981), whereas base metal skarns mainly in the temperature range 500–350°C (Meinert et al. 1980).

Stable isotope studies (e.g., Taylor and O'Neil 1977; P.E. Brown et al. 1985) indicate that prograde skarn formation and metallization are effected by

fluids of magmatic origin, but that meteoric waters tend to become increasingly important toward the final stages of hydrothermal activity, and can be responsible for retrograde alteration and perhaps some redistribution of ore minerals. Understandably, these effects tend to be more marked in sulfide skarn deposits than in deeper-seated scheelite skarns.

Detailed studies of the King Island scheelite deposits (Kwak and Tan 1981; Kwak 1987) provide a scenario of mineralizing fluids that progressively decreased in both temperature (maximum 800°C) and salinity (max 65 wt% alkali chlorides), both with respect to distance from the associated Devonian granodiorite and with time. These changes were accompanied by systematic changes in the chemistry of garnets, pyroxenes, and amphiboles. Pressure estimates based on fluid inclusion data suggest about 650 bar during mineralization. This relatively shallow environment plus indicated movement on the North Boundary fault apparently allowed mixing of meteoric and magmatic fluids during mineralization, and one result thereof was the partial dissolution of early Mo-rich scheelite and its redistribution and redeposition as Mo-poor scheelite and molybdenite. Unfortunately, although the King Island deposits exhibit strong similarities to principal arc scheelite skarns in western North America, it must be stressed that the complex associations of Paleozoic granitoid rocks in Tasmania (Solomon 1981; Kwak 1987) have not as yet yielded to plate tectonic interpretation, so the designation of the King Island deposits as representative of principal arc metallization is, as stated earlier, premature.

The Darwin silver-lead-zinc skarn deposit in California (Hall and Mackevett 1962) has also been the subject of detailed isotope studies (Rye et al. 1974). Here, massive replacement sulfide ores occur within contact skarns composed mainly of diopside, garnet, and idocrase adjacent to a quartz monzonite stock of Jurassic age (~ 180 m.y.; Fig. 1.19). Prograde skarn formation is separated from sulfide mineralization by a period of fracturing, and isotope and fluid inclusion studies of this later stage of metallization indicate ore fluids of about 325°C with salinities up to 25 wt% alkali chlorides. The fluids averaged $\delta^{34}S$ values of +3‰, $\delta^{13}C$ of -3.5‰, and δD of -66‰. Initial pH was estimated at 4.8 and final pH after interaction with skarn and limestones at 6.7. Rye et al. (1974) conclude that metallization was effected by fluids of magmatic origin from the adjacent quartz monzonite, but that the carbon in ore-associated calcite is a mixture of host rock and magmatic carbon. Recent geologic work in the area, however, has indicated previously unrecognized complexities including the possibility that the deposit is not directly related to the adjacent quartz monzonite (L. Meinert, pers. comm.). Notwithstanding these uncertainties, the Darwin deposit is of interest for it appears to represent an example, albeit small, of lead-zinc mineralization in the Sierra Nevada principal arc setting.

Overall, it appears that most sulfide skarn deposits in principal arcs form in two stages. An initial high temperature zoned stage of lime silicate development and a subsequent lower temperature stage of sulfide metallization; although scheelite may accompany prograde skarn formation, and

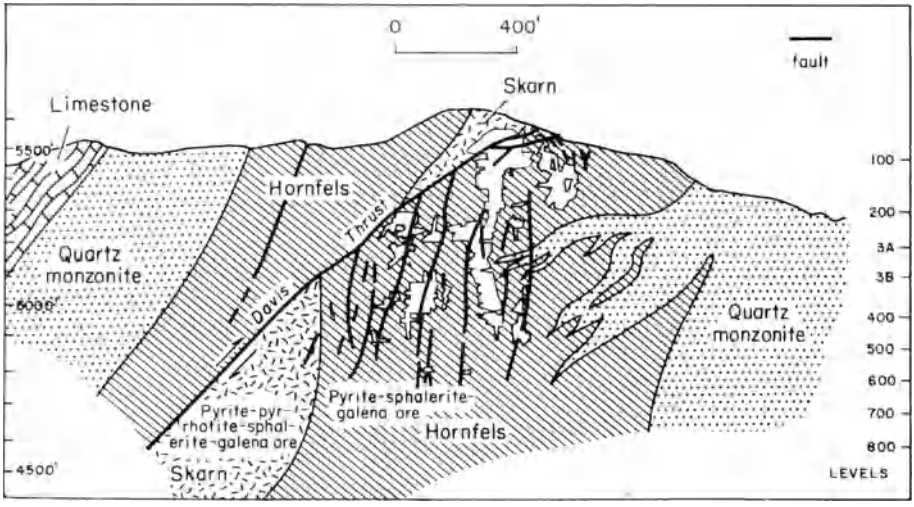

Fig. 1.19. Cross-section of the Darwin skarn ores, California (After Rye et al. 1974)

typically scheelite mineralization precedes sulfide mineralization. Nonmagmatic fluids can impinge on skarn ore-generating systems, but their role is probably limited to minor redistribution and alteration of previously deposited phases.

1.4.4 Discussion and Suggestions for Exploration

As detailed above, most skarns occur in close proximity to igneous contacts, but some are up to 2 km or more distant from their related intrusions. In the latter case, a combination of good access structures for the metasomatizing fluids and carbonate-silicate host-rock contacts will control the sites of skarn development (Fig. 1.20). Skarn development and associated mineralization (Fig. 1.21) tend to be limited in spatial extent compared with porphyry or vein-type mineralization, and thus subsurface exploration for blind skarn orebodies can be particularly difficult. By the same token, the potential for the discovery of important blind orebodies of this type always exists in principal arc areas where carbonate units are intruded by intermediate to felsic plutons, but especially so in areas of known skarn mineralization. Also, many base metal skarns are transitional to porphyry copper deposits. Tungsten skarns, on the other hand, are best sought above plutons or in the roof pendants of batholiths.

Another problem facing the explorationist is the location of optimum metallization within skarn complexes. This requires a knowledge of the zoning characteristics of a particular skarn, both in terms of mineralogy and mineral chemistry. Broad relationships between sulfide concentrations and minerals such as andradite with specific chemistries are now emerging (Einaudi et al.

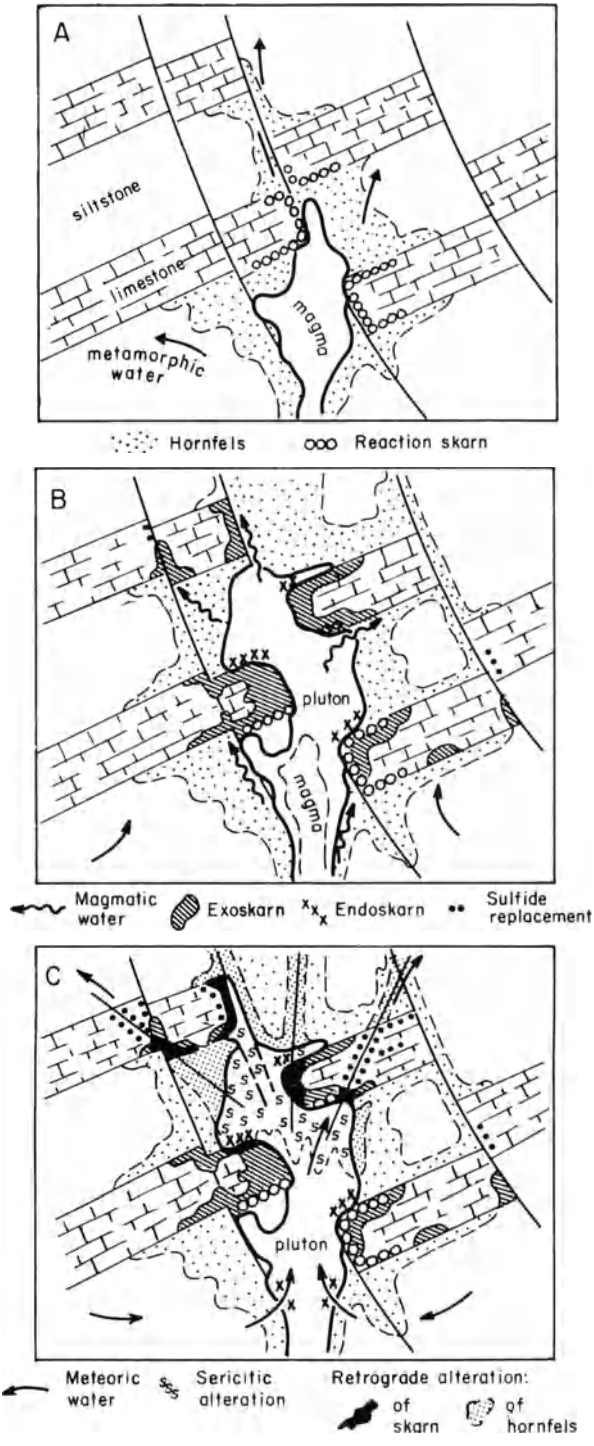

Fig. 1.20. Generalized model for the evolutionary stages of skarn ore formation. **A** Initial magma emplacement drives off connate and groundwaters and produces a metamorphic aureole and local reaction skarns. **B** Magmatic fluids generated from crystallizing magma form exoskarns in limestones along stock and fault contacts and local endoskarns. Some peripheral sulfide replacement bodies in limestone may also form at this time. **C** Cooling of the system allows progressive influx of meteoric waters, leading to sericitic alteration of the stock, retrograde alteration of skarn and hornfels, and sulfide-silica-carbonate replacement along major structures and bedding in limestone (After Einaudi et al. 1981)

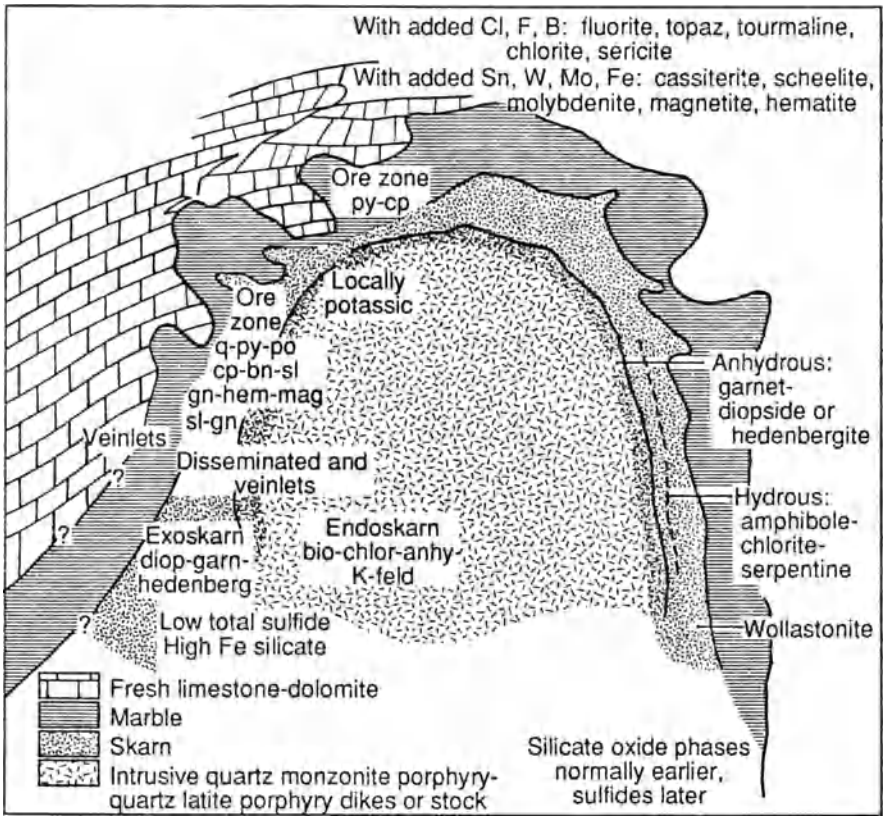

Fig. 1.21. Skarns in contact with an intrusive stock. Skarn types are illustrated on the contact on the *right* and ore types on the contact on the *left* (After Guilbert and Lowell 1974)

1981; Kwak 1987), and with careful work such relationships can probably be used to develop trends from surface and drill-core samples that will aid in the siting of drill holes seeking blind orebodies.

Geophysical methods of exploration such as magnetics can be used to delineate skarn zones containing magnetite, and igneous contacts in the subsurface. Obviously subsurface skarns containing significant amounts of conductive sulfide minerals will give good conductivity or induced polarization response provided they are not too deep, but the presence of graphite developed from the recrystallization of carbonaceous materials in the host rocks can be problematic for interpretation of these types of geophysical anomaly.

1.5 Epithermal Deposits

1.5.1 Distribution and Associated Igneous Rocks

Epithermal deposits are best defined as epigenetic, principally vein-type deposits formed at shallow levels (< 1 km depth) within the crust. The original temperature conotation intended by Lindgren (1933) is no longer valid and epithermal deposits can form over a wide temperature range (100–400°C). These deposits, mainly in the form of discrete veins, but also as disseminated ore, and in a few instances, massive deposits, are widespread in the high-level volcanic portions of principal arcs and within the uppermost portions of underlying intrusive systems. Deposits of this type are prone to removal by erosion but occur throughout the arc systems of the circum-Pacific belt, and elsewhere, where erosion has not cut too deeply. They include ± bonanza gold-silver vein deposits, enargite-bearing vein, and massive gold deposits, and, of increasing significance in terms of current economics, a spectrum of bulk mineable, disseminated precious metal deposits.

Examples of this general type of mineralization can be followed from the important gold-copper-silver vein system at El Indio, Chile (Siddeley and Araneda 1986) through the silver deposits of Charñarcillo and Caracoles, Chile (Ruiz et al. 1965), through the somewhat deeper-seated copper and gold-quartz veins associated with the Coastal Batholith of Peru (Bellido and de Montreuil 1972; Agar 1981), to precious and base metal veins in Ecuador and Colombia (Goossens 1972, 1976; Baum and Gobel 1980). Farther north, the precious metal veins of Central America (Ferencic 1971; Kesler 1978) continue the line to those of the Sierra Madre Occidental of Mexico (e.g., Tayoltita, D.M. Smith et al. 1982). Deposits of similar type are widespread in the western USA, but with the exception of the Cascades province the plate setting is more complex and they will be discussed separately (see later). In western Canada, epithermal precious metal deposits occur through much of British Columbia and the Yukon (Wolfhard and Ney 1976; Panteleyev 1986 and references therein).

The principal arc systems of the western Pacific and Indonesia also contain numerous vein deposits. In Japan, a complex series of vein deposits of different ages and different metal content are known (Ishihara 1978), but the scheelite-gold deposits associated with Cretaceous magnetite-series granitoids and some of the precious metal deposits of Neogene age can be assigned to principal arc settings. Vein gold deposits in the Philippines are widespread (Balce et al. 1981), with the large majority lying within a well-defined Miocene-Pleistocene belt that runs the length of the Philippine archipelago from eastern Mindanao to northern Luzon. Similar vein deposits occur along the Indonesian arc system and in Kalimantan (Djumhani 1981). Farther to the southeast, several epithermal precious metal deposits in Papua New Guinea and nearby island arcs are known. Prominent among these are the Wau deposit (Sillitoe et al. 1984) and Porgera (Fleming et al. 1986). Epithermal vein deposits are also scattered along the collided arc systems in the southern USSR, the Caucasus, (Kovalev and Karyakin 1980), along the Neogene volcanic chain of the Carpathian arc (Lang 1979), and through the Balkans.

1.5.2 Mineralization and Alteration: Low Sulfidation Type

Bonham (1988) identifies three major types of epithermal, volcanic-hosted, precious metal deposits, two of which occur primarily in principal arc systems. The most widespread type is characterized by a low total sulfidation environment of ore deposition, a quartz-adularia-carbonate-sericite (illite) alteration assemblage, high silver/gold ratios, and minor amounts of base metals. Many such deposits occur within andesitic volcanic sequences that exhibit broad zones of propylitic alteration (see Lang 1979), but Bonham states (1988) that either high or low silica rhyolites are the most common, genetically associated igneous rocks.

Low sulfidation type epithermal precious metal veins in principal arcs occur most typically as well-defined, volcanic-hosted fissure fillings in which quartz is the dominant gangue mineral. Calcite and/or adularia are also important gangue constituents in some cases. Metallization consists of native gold ($\pm$ gold tellurides) and silver sulfides and sulfosalts, and locally selenides; contents of base metals in such veins are notably low, commonly less than 1–2%. Alteration assemblages can vary with depth, but most veins are surrounded by an envelope of chlorite-dominated propylitic alteration. In many instances illite or sericite is developed close to veins, and disseminations of pyrite are inevitably developed in the host rocks.

Buchanan (1981), by assembling the data from a large number of epithermal vein deposits in western North America, has attempted to encapsulate the variables of typical epithermal vein systems (Fig. 1.22). He envisages precious metal deposition occurring at shallow depth ($\sim$ 200–350m) below an intensely altered, acid-leached zone that passes upward into a hot spring system. Below the precious metal horizon, base metals are deposited in the vein system. This generalized model does serve to demonstrate many features found in epithermal vein systems, but it should be emphasized that the model was developed prior to the recognition of high- and low-sulfur end-member types. Nevertheless, it fits the more widespread low sulfidation type well.

1.5.3 The Baguio, Philippines and Tayoltita, Mexico Vein Systems

Two important low-sulfur precious metal vein systems of which the writer has personal experience are those of Baguio and Tayoltita. Both have sustained mining for many decades and continue to produce precious metals. Furthermore, both have been the subject of research studies (Sawkins et al. 1979; D.M. Smith et al. 1982).

In the Baguio district, which has produced over 800 tons of gold, the Acupan and Atamok mines have been the major producers and each exploits an extensive set of fissure veins (Fig. 1.23). The steeply dipping veins, which are dominated by quartz gangue, are hosted either in andesitic volcanics or volcaniclastic sediments. In addition, at Acupan breccia zones in andesite adjacent to a phreatomagmatic diatreme are mineralized where veins impinge upon them (Callow and Worley 1965; Fig. 1.24), and many tens of millions of

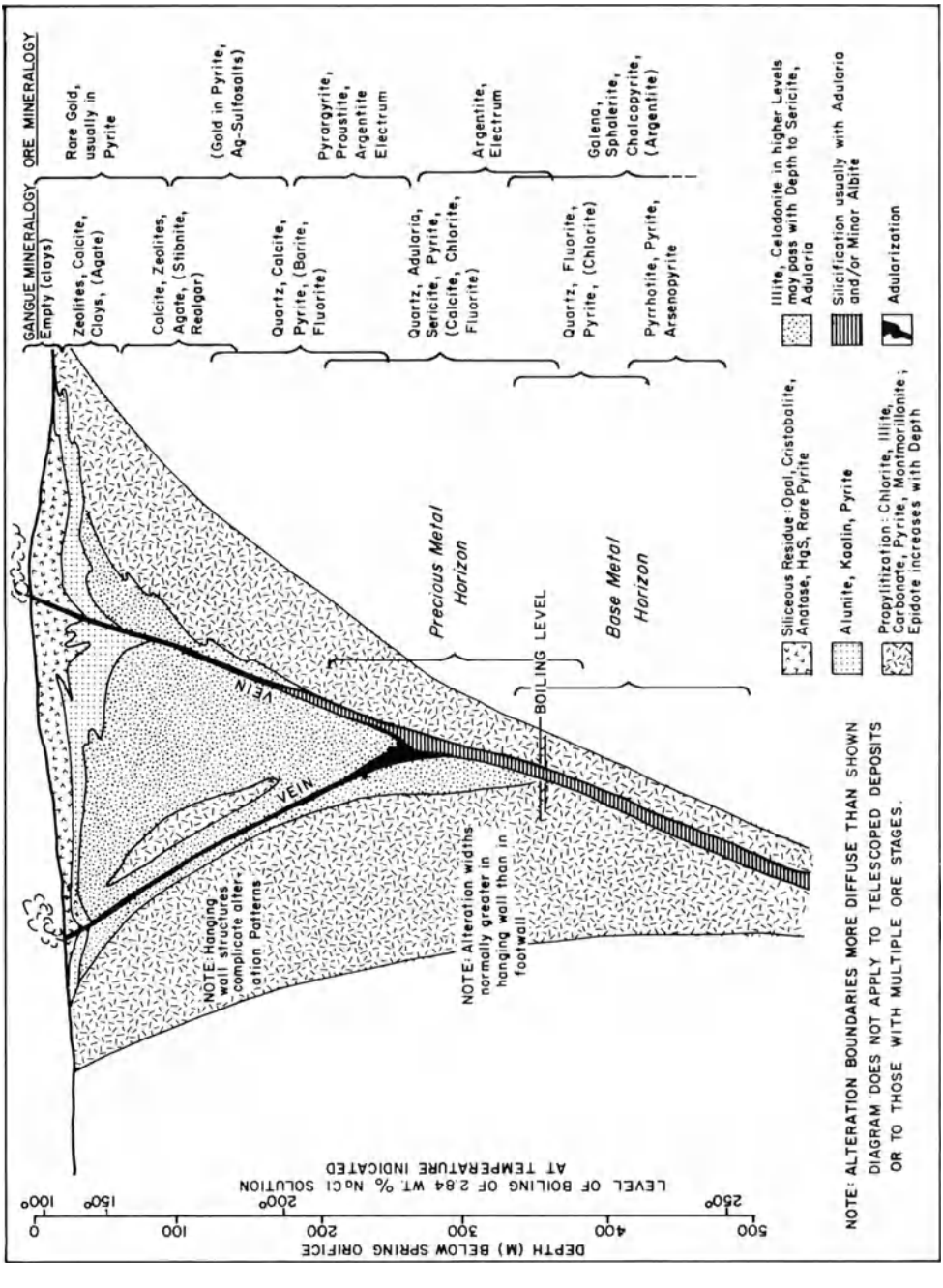

Fig. 1.22. Idealized model for an epithermal precious metal vein system incorporating many of the features found in such systems. In any one system only some of features shown are manifest; for example, not all epithermal precious metal deposits pass downwards into base metal veins

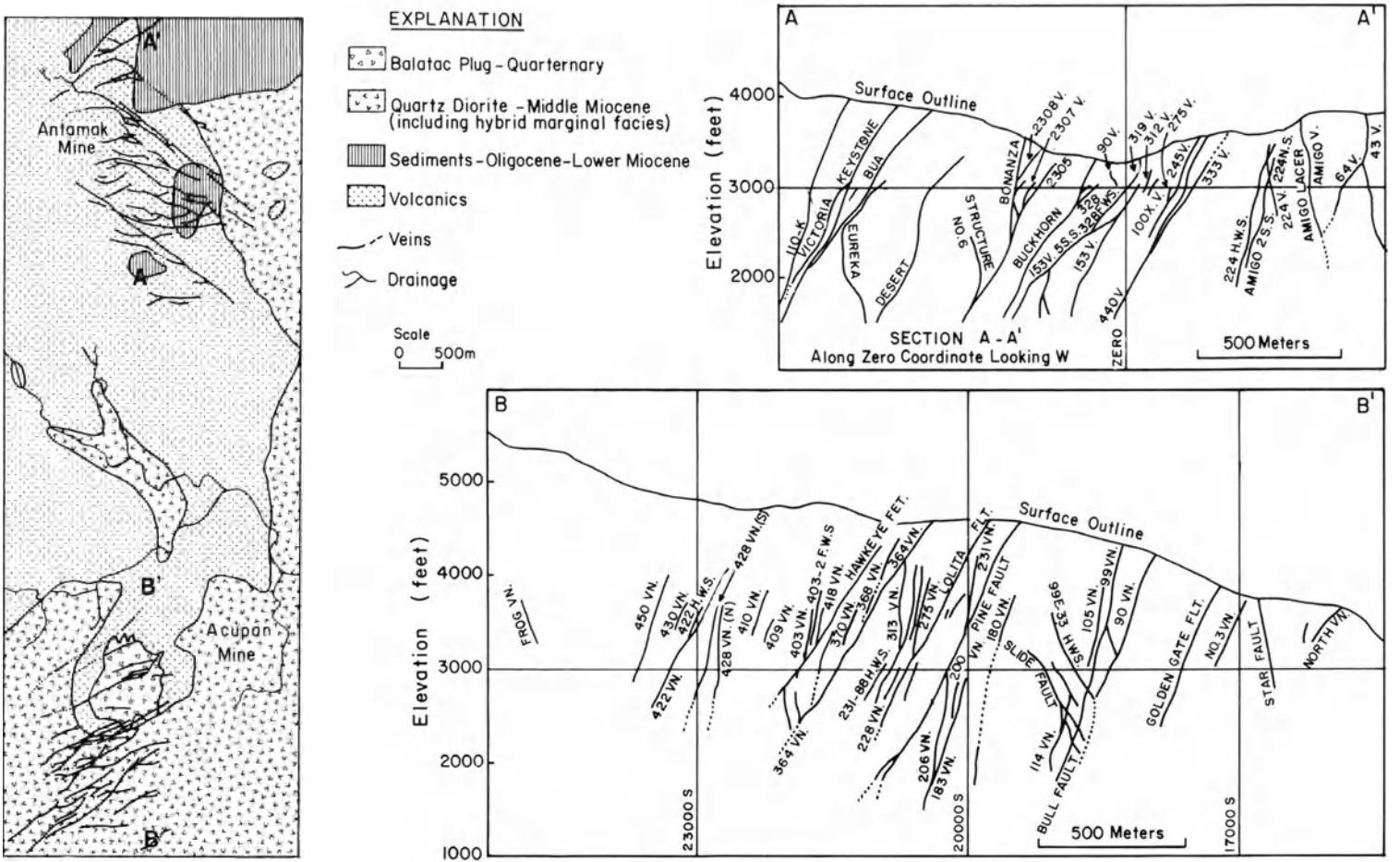

Fig. 1.23. Map **a** and cross-sections **b** of two major vein systems in the Baguio district, Luzon, Philippines. Cross-sections are through central portions of each vein system (After Sawkins et al. 1979)

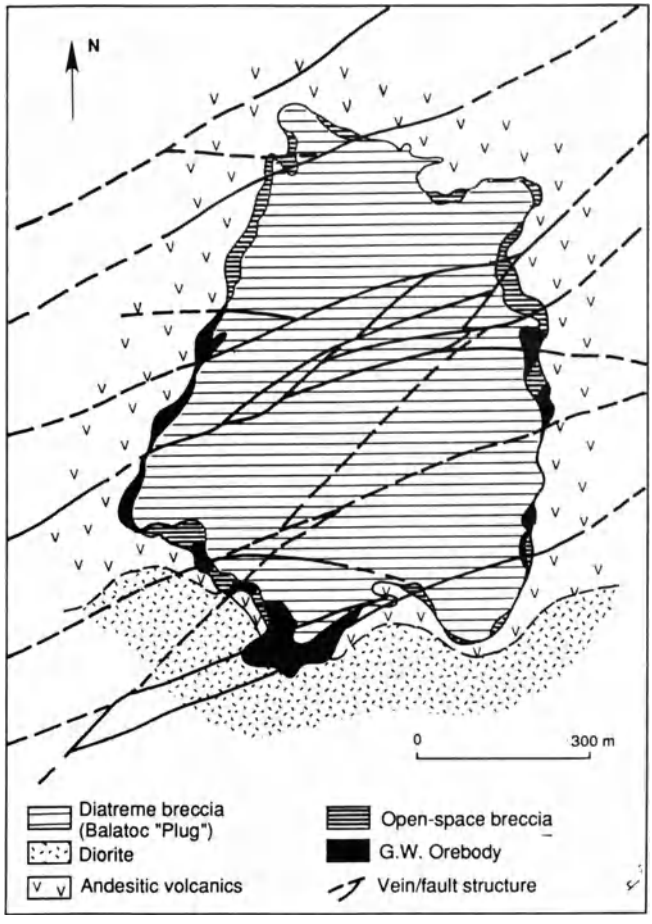

Fig. 1.24. Map of the breccia-hosted (*G.W.*) orebodies adjacent to the Balatoc "Plug" in the Acupan Mine, Baguio district (After Damasco and de Guzman 1977)

tons of ore are present. The gold in both veins and breccias occurs predominantly as native gold in gray, granular quartz containing disseminated pyrite. Later stages of mineralization are represented by white quartz, rhodonite, calcite, and anhydrite with minor base metal sulfides and gold tellurides.

A series of discrete ore shoots (up to 75 g/ton Au) occur within the vein structures (Fernandez and Damasco 1979). Some pitch at angles of about 45° or less, whereas most are much steeper, and can be related to vein intersections of splits, or changes in the strike of vein structures. It is noteworthy that the maximum vertical extent of mineralization is 500 m. Upward, vein structures pass into intensely altered ground and ore shoots do not appear to approach closer than about 250 m from the elevation of the Baguio erosion surface, a Plio-Pleistocene surface upon which a stratovolcano probably existed during the period of mineralization (Sawkins et al. 1979). Wall-rock alteration in the

Baguio district has produced mainly chlorite and lesser sericite. In vein breccias rock fragments are strongly silicified, and development of disseminated pyrite in these and adjacent wall rocks is ubiquitous. In detail, however, the intensity of alteration adjacent to vein structures is highly variable.

Fluid inclusion studies indicate ore fluids of low salinity (0.6–4.6 equiv. wt% NaCl) at temperatures between 205° and 300°C. No evidence of consistent spatial variations in temperature was observed, but sporadic evidence of boiling of ore fluids was noted. Pressure estimates based on the fluid inclusion data are compatible with the notion that the surface during mineralization was at elevations not much higher than that of the Baguio surface. Stable isotope studies indicated that the ore fluids were essentially similar to modern day thermal and ground waters in the area. The considerable lateral extent of the Baguio ore shoots, as opposed to their more limited vertical extent, the subhorizontal pitch of certain ore shoots, and the restricted temperature range of vein filling, all suggest that ore deposition was affected by predominantly meteoric fluids with a major horizontal flow direction (Sawkins et al. 1979). The source of the gold is most probably the gold-rich porphyry copper type mineralization that is extensive in the district (Sillitoe 1988a).

The Tayoltita vein system in Durango, Mexico (D.M. Smith et al. 1982; Fig. 1.25) exhibits strong similarities to that of Baguio, although silver-gold ratios are considerably higher (> 40 vs 2:1). The Tayoltita vein system is particularly instructive, for postore tilting combined with steep topography have allowed exposure of the subjacent rock units to depths of almost 1.5 km below the mineralized zone (Fig. 1.26). This mineralized interval lies within an alternating sequence of andesites and rhyolites that overlie and are intruded by granodiorite and related plutonic rocks, representative of the uppermost portions of an extensive batholith. Quartz monozonite encountered in the Tayoltita tunnel has been dated at 42.8 Ma.

Veins and vein breccias of the extensive Tayoltita system are dominated by quartz gangue, accompanied by lesser amounts of adularia, johannsenite-rhodonite, and calcite locally. Gold and silver metallization is associated with grayish quartz discolored by occluded materials, and distinguishable from earlier and later generations of essentially barren white quartz. Gold occurs mainly as electrum, and silver as argentite and various silver sulfosalts. Base metal sulfides are minor and in most areas represent less than 2% of the ore.

Fluid inclusion studies of mineral-stage quartz indicate deposition largely in the range 250–280°C (D.M. Smith et al. 1982) by fluids of 2–5 equiv. wt% NaCl. Considerable evidence for boiling exists, especially toward the top of the ore-bearing interval. Contours of Ag/Au ratios within the veins of the Tayoltita system are predominantly horizontal (pretilting) and the flat tongue-like shapes of mineralization with lower ratios (higher gold contents) in the central parts of the veins strongly suggest largely horizontal flow of the ore fluids (M. Clarke and T. Albinson, pers. comm.). The fluid inclusion temperature data from ore-stage quartz indicate slightly higher temperatures in the mineralized interval than both above and below it, and this is also suggestive of horizontal flow.

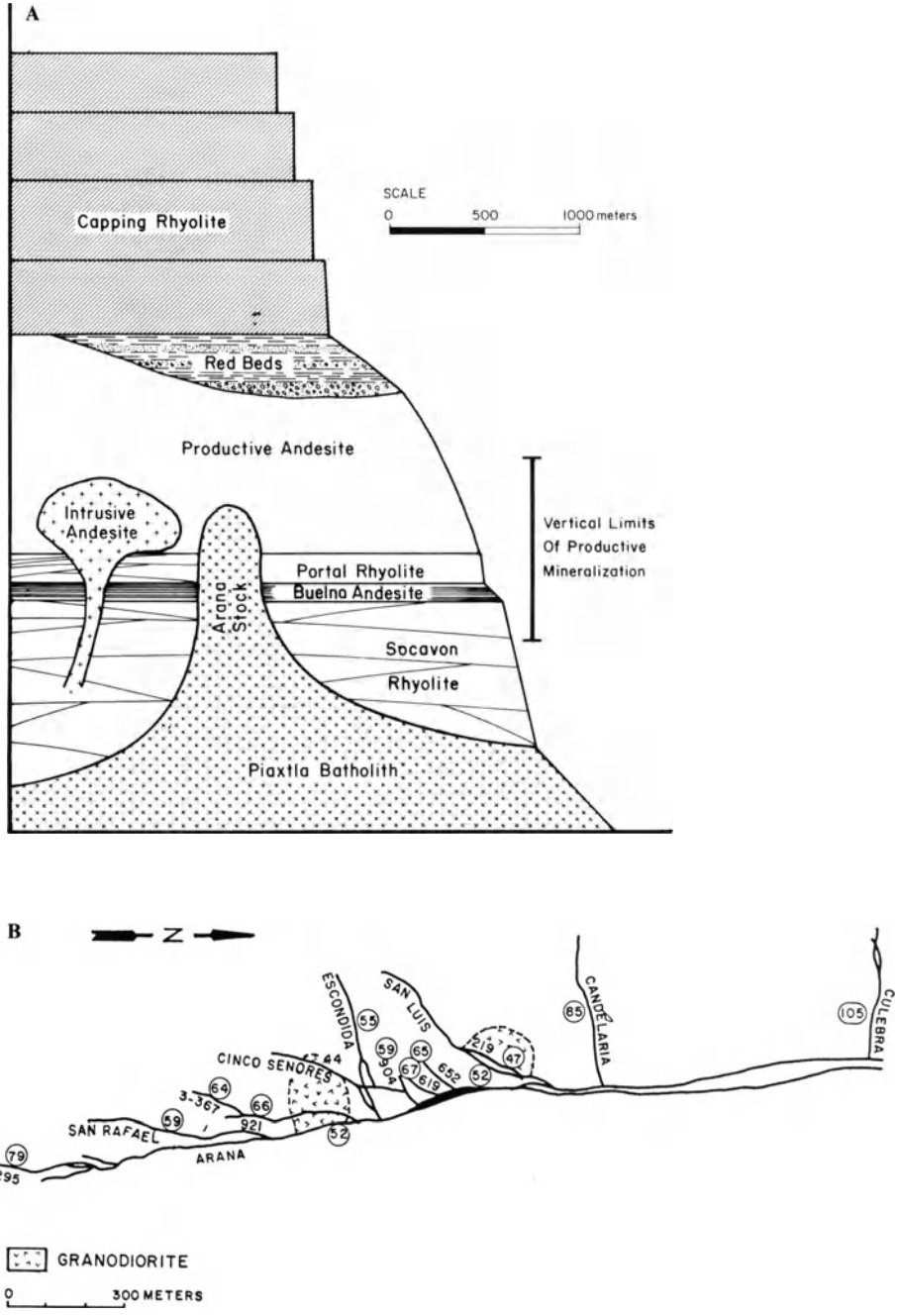

Fig. 1.25A. Diagrammatic section of the stratigraphy and intrusive phases in the area of the Tayoltita Mine, Mexico (courtesy of M. Clarke and Cia. Luismin, Mexico). **B** Plan of Tayoltita vein system showing bulk Ag:Au ratios of the major veins (After D.M. Smith et al. 1982)

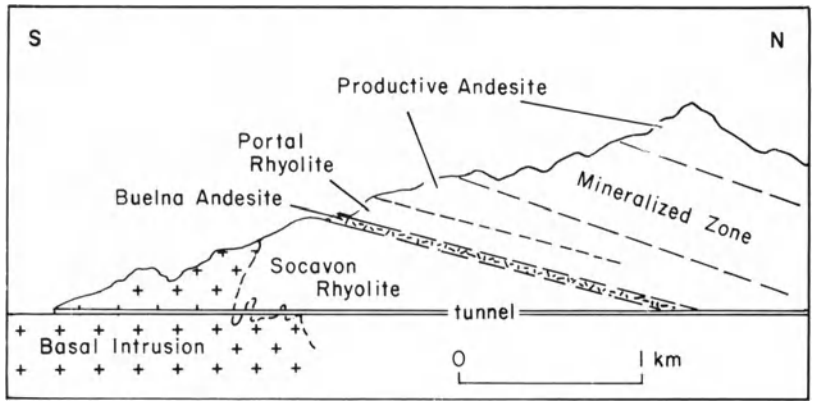

Fig. 1.26. Longitudinal section of the Tayoltita system showing how combination of tilting, erosion, and development of the Tayoltita tunnel allows interpretation of the geologic relationships well below parts of the system (Courtesy of Cia. Luismin, Mexico)

Stable isotope data obtained on vein materials, host rocks, and selvages adjacent to alteration veinlets in the subjacent volcanic and intrusive rocks (Churchill 1980) define the presence of a large meteoric water-dominated convection system during mineralization. However, high-precision analysis for gold and silver in altered versus fresh volcanic and intrusive rocks from below the mineralized zone failed to provide evidence for a host-rock leaching origin for the precious metals in the vein ores.

1.5.4 Mineralization and Alteration: High Sulfidation Type

It has been recognized by several workers (e.g., Ashley 1982; Heald et al. 1987; Bonham 1988) that certain epithermal precious metal deposits are characterized by high sulfidation states and a distinctive mineralogy. Typical features of such deposits are intense argillic or advanced argillic alteration, especially the quartz-alunite assemblage, and the presence of enargite group ore minerals. In addition,they exhibit a spatial, temporal, and genetic relationship to calc-alkaline igneous rocks of andesitic to rhyodacitic composition. Deposits occur mainly as veins, but occur locally also as breccias and massive replacements (Sillitoe 1983a). In some cases, evidence for a surficial hot spring environment is preserved (Urashima et al. 1981). Major examples of this type of deposit include El Indio, Chile, Pueblo Viejo, Dominican Republic (Russell et al. 1981), Lepanto, Philippines (Bryner 1969), and Julcani, Peru (Petersen et al. 1977).

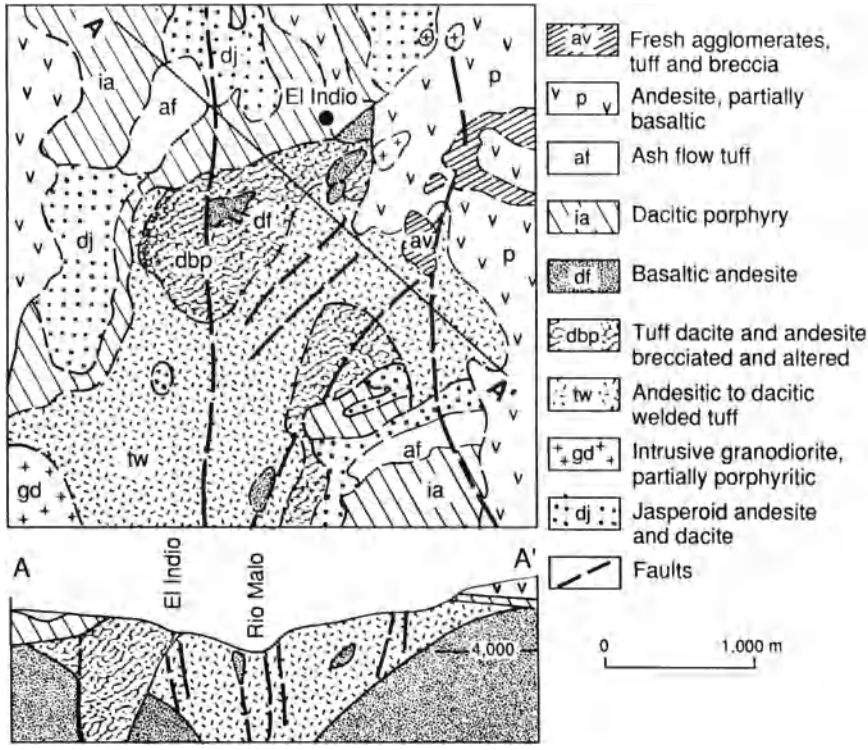

Fig. 1.27. Generalized map of the El Indio district, Chile (After Walthier et al. 1985)

1.5.5 The El Indio Gold Deposit, Chile

Currently, one of the most important examples of high sulfidation systems in economic terms is the El Indio deposit, Chile (Siddeley and Araneda 1986). Between initiation of large-scale mining in 1981 and the end of 1985 the El Indio district produced > 50 tons of gold, > 100 tons silver, and 60 000 tons copper. Reserves in January 1986 included > 45 000 tons high-grade (197 g/ton) direct smelting ore, and nearly 6 million tons of plant grade ore (1.7 g/ton). This latter figure will unquestionably increase as exploration in the area continues.

The El Indio district lies at > 4 000 m, close to the crest of the Andes at approximately 30° S (Fig. 1.27). The volcanic country rocks consist of a calc-alkaline assemblage that evolved from andesite flows (11.4 Ma) to rhyolitic and dacitic pyroclastic rocks (8.2 Ma), which are related to nearby vents. This Upper Tertiary sequence overlies a more extensive Mid-Tertiary accumulation of andesites that is preserved in a north trending tectonic depression. The western margin of this feature is marked by the Baños del Toro

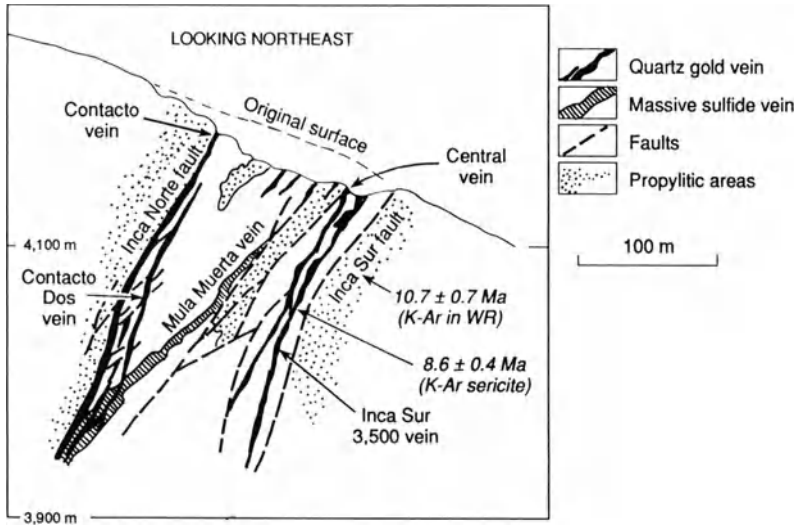

Fig. 1.28. Cross-sectional view of the major vein faults and lithologies encountered at the El Indio gold deposit (After Walthier et al. 1985)

high-angle reverse fault, which brings Paleozoic granitoid basement rocks in contact with the Tertiary volcanic belt (see Fig. 1.27).

Both the El Indio vein system and the nearby El Tambo system, which lies 6 km south-southeast, occur within a complex of highly altered rocks that are as yet poorly understood. The vein systems at El Indio trend mainly northeast to east and are hosted by strongly altered and bleached rhyolite and dacite tuffs. Minor intrusive bodies of dacite porphyry and quartz porphyry are common along the ridge of dacitic tuffs that separates the El Indio and El Tambo mines, and porphyry Cu-Mo mineralization occurs only 2 km SE of El Indio (R.H. Sillitoe, pers. comm.).

Based on mineralogic assemblages, three distinct vein types can be recognized: massive sulfide, quartz-gold, and, at El Tambo, barite-alunite-gold. The massive sulfide veins consist almost entirely of enargite-pyrite and are confined to the central portions of the El Indio mine. They occur as massive anastomosing veins and stockworks up to 6 m wide with horizontal extents of over 400 m (Fig. 1.28). Typical grades range from 6–10% Cu, 4–10 g/t Au, and 60–120 g/t Ag.

The gold-quartz veins cut massive sulfide veins and occur mainly at the northwest and southeast margins of the massive sulfide vein zone. Some of these veins are phenomenally rich and one single structure, the Indio Sur 3500 vein, will eventually yield over 40 tons of gold. Pyrite, enargite, and tennantite occur in the quartz-gold veins, which are enveloped by an ill-defined silica-sericite alteration. The quartz exhibits banded, colloform, cryptocrystalline,

jasperoidal, and drusy forms and there is evidence of multiple hydrothermal events, manifest as repeated fracturing and rehealing of vein material.

The barite-alunite-gold association is restricted to the El Tambo deposit. Orebodies of this type occur either as irregularly shaped breccia bodies or in vein structures. Silicification represents the first stage of mineralization, but gold is preferentially associated with barite. Alunite, which follows barite in the paragenetic sequence, exhibits little association with gold deposition. Some of the veins containing barite-alunite-gold change to silicified enargite veins at depth. Gold is largely in the native form, but gold tellurides, arsenates, and silver minerals are also present.

The phenomenal richness of some of the El Indio-El Tambo bonanza ores has sparked a wave of intense exploration activity in the numerous alteration zones present along the crest of the Andes in Chile and neighboring countries, and additional discoveries of high sulfidation-type gold systems will surely be made. Fluid inclusion and stable isotope data are as yet unavailable for the El Indio district, but, given the principal arc subaerial setting, the abundant sulfur that distinguishes this system is almost certainly of magmatic origin. Presumably the gold, silver, and copper are from the same source, although involvement of local meteoric water may be important in the final stages of metal transport and deposition.

1.5.6 Discussion and Suggestions for Exploration

Epithermal precious metal deposits in principal arcs contain both silver and gold but are typically more important for their gold contents. Graybeal and Smith (1978) have observed that the eastern side of the Pacific Rim (i.e., the Cordilleran belts of North and South America) contain 25 silver deposits with over 100 million oz Ag, but that the western Pacific Rim, which is also dominated by subduction-related arc systems, contains no silver deposits. They also demonstrate that porphyry copper deposits formed on the eastern rim typically exhibit higher Ag/Au ratios ($>$ 50) than those formed in the Philippines and S.W. Pacific ($\leq$ 15).

The two most obvious parameters that relate to these variations are the greater crustal thicknesses and stronger development of felsic (rhyolitic) magmatism in Cordilleran Belts. These observations infer a fundamental magmatic control, but, in addition, Ag/Au ratios increase from principal arc toward back-arc terranes and I would allocate the major silver deposits of western North and South America probably to such backarc environments (see next chapter).

Except in areas of aridity most of the pre-Quaternary, uppermost volcanic portions of the principal arcs along the eastern Pacific Rim have been lost to erosion. Thus, major gold deposits of principal arc setting are relatively uncommon in North and South America. It is noteworthy that the volcanics hosting the El Indio district lie within a graben and have thus been shielded from erosion.

The genesis of epithermal precious metal deposits has been a matter of some uncertainty. The regularities of occurrence of such deposits in terms of specific volcanic environments (Sillitoe and Bonham 1984) and petrochemical associations (Bonham 1986) suggest a fundamental link to magmatism, but stable isotope studies (cf. Field and Fifarek 1985 and references therein) rather consistently indicate the overwhelming predominance of meteoric water in such systems. Conventional wisdom among geochemists who study epithermal systems (Ohmoto 1986) is that ore genesis occurs through convection of meteoric fluids and leaching of metals from ambient host rocks. This model is based on data that have predominantly been obtained from gangue minerals, especially quartz. Thus, the large bulk of fluid inclusion and stable isotope data obtained from such gangue materials may fail to provide information regarding the critical, and possibly very short-lived, episodes when precious metal transport and deposition are occurring. Another possibility is that geothermal convection systems rework metal enrichments of magmatic-hydrothermal origin and focus them into high-level structures as epithermal vein deposits. This is analogous to the situation at Butte, Montana, discussed earlier. Another ambiguity affecting interpretation of H/D data may be Rayleigh distillation effects operating under the open-system conditions of magmatic devolatilization. Such effects have been cogently detailed in rhyolitic magmatic systems by B.E. Taylor (1986), who demonstrates that highly depleted δD values ($< -100‰$) can characterize the final hydrous fluids generated during magmatic crystallization.

In reality, both a direct contribution of precious metals from magmatic sources, and staging and redistribution of magmatic-hydrothermal protores are probably dominant processes in individual cases, or even at different times during the development of the same epithermal deposit (see Sillitoe 1988b). However, the formation of significant epithermal deposits solely by convective circulation of heated meteoric water through average rocks is considered unlikely in the extreme.

The extraordinary gold values that characterize the El Indio and Hishikari (Japan) vein systems have rekindled the enthusiasm of mining companies for epithermal vein-type precious metal deposits, despite the high costs and low tonnages associated with the exploitation of such deposits. Furthermore, it is increasingly clear that large tonnages of disseminated lower grade ore amenable to bulk extraction can occur near or adjacent to vein systems, and that the inherently high-level nature of these deposits involves the possibility that they could represent the distal manifestations of much larger mineralized systems at depth.

In terms of exploration strategy the most valuable aids to the geologist are the conceptual models developed by Buchanan (1981), Giles and Nelson (1983), and Bonham (1988) linking paleosurface manifestations, alteration and geochemical patterns, structural features, and ore distribution. Field exploration consists of looking for alteration and analyzing altered rock, primarily for gold. In areas of heavy vegetation stream-sediment geochemistry for pathfinder elements such as Sb, As, and Hg is required. Those epithermal

systems that await discovery must largely consist of those that lie intact in the subsurface, and thus recognition of the paleosurface or near-paleosurface features of such systems (e.g., sinter deposits and/or hydrothermal eruption breccia aprons) is of prime importance to the explorationist. In some areas recognition of high-level alteration is no problem. It is the definition of realistic drilling targets within extensive areas of alteration that is more problematic.

1.6 Additional Deposits of Principal Arcs

1.6.1 Massive Magnetite Deposits

There are a number of massive magnetite deposits around the Pacific margin that represent important local sources of iron ore (Park 1972). The majority of these occur as contact metasomatic replacements adjacent to diorite or granodiorite stocks intruded into volcanics or sediments, and in some cases the

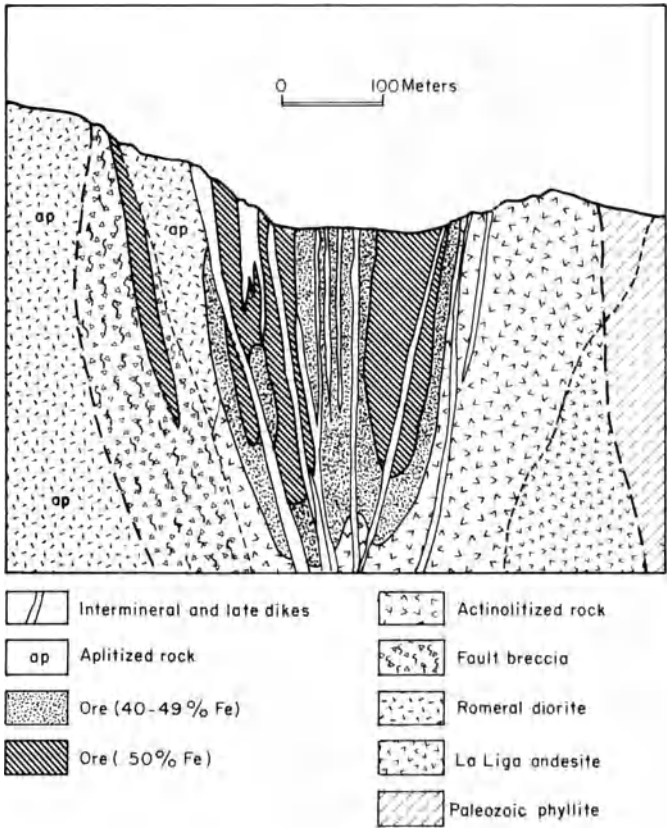

Fig. 1.29A

distinction of these from magnetite skarn deposits is difficult. In reality there is probably a complete spectrum between end-member types. A well-defined north-south zone of these deposits, 600 km long, occurs in central Chile (Ruiz et al. 1965; Fig. 1.29A), and several other deposits are known in Peru (Park 1972). Essentially similar magnetite deposits occur at Las Truchas, Michoacan, Mexico (Salas 1975), and Texada Island, British Columbia (Swanson 1925).

Detailed studies of the El Romeral magnetite ores, central Chile are reported by Bookstrom (1977). Here, a series of steeply dipping, lenticular, magnetite-rich masses occurs in a north-south array adjacent to the El Romeral fault, which cuts the El Romeral diorite along the ore trend (Fig. 1.29B). Field evidence indicates both pre- and postore intrusive and faulting events. The ores consist of fine-grained assemblages of magnetite-actinolite replacing either andesite porphyry (e.g., main orebody) or Paleozoic schists (e.g., north orebody). The orebodies exhibit gradational boundaries, and altered rocks within and around them contain magnetite, actinolite, plagioclase (An_{22-32}), diopside, clinozoisite, sphene, chloroapatite, scapolite, tourmaline, chlorite, pyrite, calcite, micas, and clays. Minor element contents of the magnetite ore

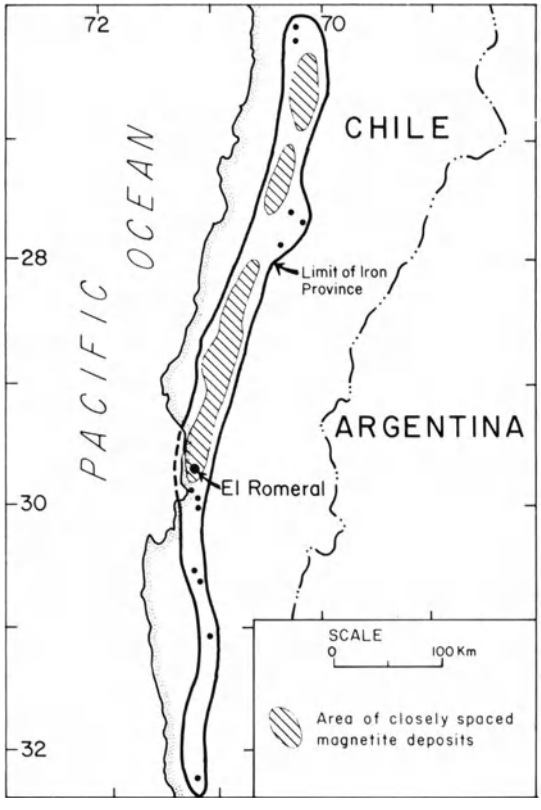

Fig. 1.29B

Fig. 1.29A. Belt of magnetite deposits in north-central Chile (After Ruiz 1965). **B** Cross-section of the Main orebody at El Romeral iron deposit, Chile (After Bookstrom 1977)

are low, especially with respect to base metals. Based on experimental data of equilibrium phase relationships for similar mineral assemblages, a temperature range of 475–550°C and pressures of approximately 2 kb are suggested.

Whether the ores of El Romeral and similar deposits of massive magnetite in principal arcs are truly hydrothermal in origin, or represent intrusive equivalents of the massive magnetite flows at El Laco, Chile (Park 1961) and Cerro Mercado, Durango, Mexico, is not clear at present. These magnetite flow deposits are associated with felsic volcanics and appear to represent apatite-rich immiscible fractions separated from andesitic magmas, but how such magnetite-rich melts achieved the bouyancy to permit their extrusion at $>$ 4000 m is problematic. Some of the circum-Pacific iron deposits may be intermediate between contact-metasomatic and flow types, but this is simply not clear at the present time. The iron orebody at Acari, Peru occurs as a long plunging rod in undeformed granodiorite and may be of magmatic segregation origin.

1.6.2 Manto-Type Copper Deposits

Manto-type copper deposits are essentially limited to Chile in their occurrence, although possibly similar examples are found in Peru and British Columbia (Sillitoe 1981a). Despite their rarity elsewhere, manto-type copper deposits are an important facet of Chilean metallogeny, and at Buena Esperanza, Antofogasta Province, 25 000 000 tons of 3% copper ore were discovered. There, and elsewhere in Chile, manto-type deposits consist of broadly stratiform bodies in volcanic rocks, volcaniclastic sediments, and in minor instances in limestones. Maximum thicknesses of mineralized intervals are about 30 m, but the deposits may extend for kilometers along strike (Sillitoe 1977). The ore minerals consist of hypogene chalcocite, bornite, and chalcopyrite emplaced as disseminations, vesicle fillings, and short veinlets, commonly in the upper parts of permeable volcanic units. Development of gangue minerals and alteration assemblages is subtle, and orebodies tend to exhibit well-defined tops but gradational lower contacts.

The Mantos Blancos deposits (Chavez 1983, 1984) contain both oxide and sulfide ores and cumulative production in the district is expected to exceed 1.8 million tons of copper metal from well over 100 million tons of ore. The silver-rich copper ores are hosted by a gently dipping sequence of andesite to rhyolite flows, breccias, and tuffs containing a discontinuous volcaniclastic sandstone unit. Based on K-Ar dating of postore dikes, the host rocks and their contained mineralization are at least 150 Ma old. Numerous steeply dipping normal faults, both small- and large-scale, traverse the area, although many of the larger structures have a small strike-slip component to their displacement.

The bulk of the mineable copper ore originally existed in the form of oxides in which atacamite and chrysocolla occur in a 3:1 ratio. The oxide ores have apparently formed from oxidation and very minor enrichment of pyrite plus chalcopyrite mineralization, and not from the sulfide ores which exhibit

bornite-digenite-covellite assemblages. The Marina deposit, the largest known sulfide orebody, contains some 5 million tons of material grading 1.65% Cu and 20 g/ton silver. It is of lense-like shape and approximately parallel to stratigraphic contacts. Mineralogic zoning patterns are complex but overall involve decreasing copper/iron + sulfur downward through the ore.

At Buena Esperanza (Ruiz et al. 1971) 28 mineralized horizons occur within a 270-m-thick sequence of Jurassic andesites. Individual ore horizons range in thickness from 2 to 28 m and occur within vesicular flow tops and intercalated clastic sediments. Chalcocite and bornite represent the ore minerals and occur in a 4:1 ratio. Farther south, between latitudes 30° and 34° disseminated bornite mineralization occurs in the tops of lower Cretaceous andesite flows. Irregular disseminations of copper sulfides in volcanics also occur elsewhere in Chile and are probably of similar origin; for example, at Lo Aguirre in Santiago Province, ores of this type containing 10 million tons of 2% copper are known (Ruiz et al. 1965).

A smaller group of copper-silver deposits in continental rhyolites and associated lacustrine sediments occurs just south of Copiapo, Atacama Province. Lortie and Clark (1987) conclude that the mineralization here is a hybrid style that displays features of both red-bed and epithermal ore types. These deposits are much younger, however, for they are hosted by early Tertiary formations.

Much remains to be learned about this unusual but economically important class of deposits in Chile; however, it seems clear that they are closely connected to the copper-rich principal arc volcanism that characterizes this part of the Andean arc system (Sillitoe 1977).

1.7 Discussion

Principal arcs are linear, typically continuous, belts of batholiths, stocks, and coeval volcanics generated above actively subducting lithospheric slabs. In arcs where the dip angle of subduction remains constant for significant periods of time (tens of millions of years) principal arcs tend to be narrow, but if the dip angle changes with time the principal arc axis will shift and the resultant arc will be broader and more diffuse. In the principal arcs of the Andes, Mexico, and the southwestern USA there has been a tendency for the angle of subduction to decrease with time and as a result a well-defined inward younging of magmatic events (Fig. 1.30) is discernible (e.g., Clarke et al. 1976). In such instances it becomes difficult to separate magmatic events that pertain to bona fide principal arcs from those more appropriately assigned to backarc environments. Perhaps backarc magmatism merely represents igneous activity related to low-angle subduction.

Table 1.1. Relative importance of ore-deposit types in principal arcs

Volcano-plutonic arc	Age	Base-ment	Porph Cu	Massive Magnetite
W. Andes, N. Chile-S. Chile	Jurassic-Pliocene	C	P	I
West and Central Cordillera, Colombia	Triassic-Piocene	O (W) C (E)	I	–
West Mexico	Cretaceous-Eocene	O (W) C (E)	P	I
Costa Rica-Panama	Miocene-Pliocene	O	P	–
Philippines	Paleocene-Pliocene	O	P	–
Papua New Guinea	Miocene-Pleistocene	O (NE)	P	–
Solomon Islands	Pliocene-Pleistocene	O	m	–
Fiji	Miocene-Pliocene	O	I	–
E. Lachlan belt, NSW, Australia	Silurian-Devonian	?O	I	–
W. British Columbia, Canada	Triassic-Eocene	O + C	P	?m
N. Honshu, Japan	Cretaceous	?C	m	–
Balkans, Bulgaria	U. Cretaceous Paleocene	C	P	?–
Chagai belt, Pakistan	?Late Cretaceous-Miocene	?C	I	m

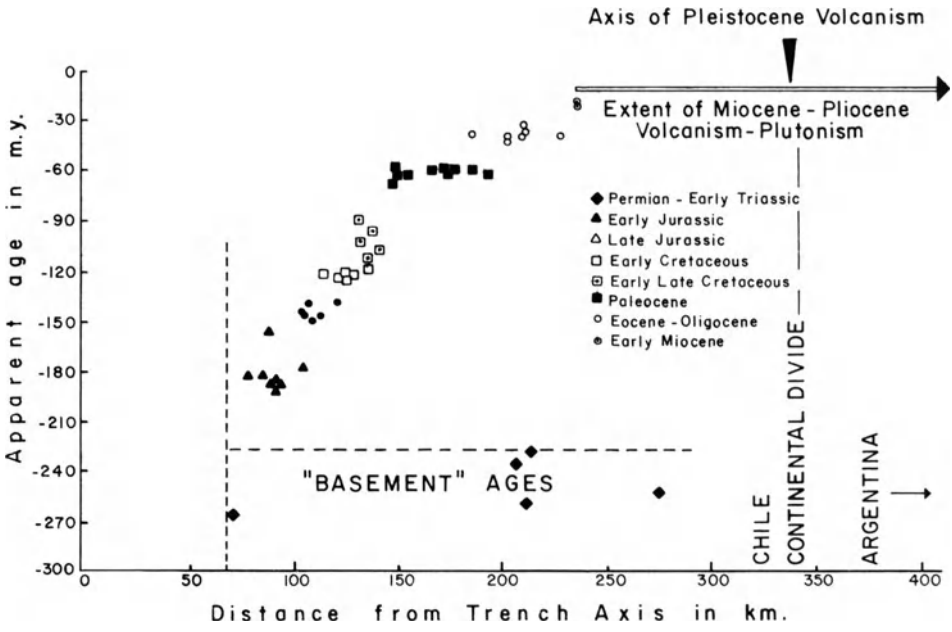

Fig. 1.30. Plot illustrating progressive shift of calc-alkaline magmatism with time in northern Chile (After Clarke et al. 1976)

Table 1.1. (continued)

Skarn Fe-Cu-Au	Skarn W-Mo	Manto Cu	Pluton-Related Veins	Epi-thermal Au-Ag	Reference
I	–	I	I	I	Sillitoe (1976b)
m	–	–	I	I	Barrero (1976)
m	m	–	m	P	Salas (1975)
–	–	–	–	I	Kesler (1978)
I	m	–	m	P	Gervasio (1971)
m	–	–	m	P	Grainger and Grainger (1974)
–	–	–	–	m	Taylor (1976)
m	–	–	m	P	Colley and Greenbaum (1980)
P	–	m	I	–	Gilligan (1978)
P	I	m	I	–	Sutherland Brown et al. (1971)
I	I	–	I	–	Isihara (1978)
I	–	–	–	–	Bogdanov et al. (1974)
m	–	m	m	–	Sillitoe (1978)

O = oceanic; C = continental; P = principal and economically viable ore-deposit type;
I = important ore-deposit type; m = minor ore-deposit type;
– = essentially absent (from Sillitoe 1981a)

From the previous sections it is clear that the metallogeny of principal arcs is dominated by copper, iron, and precious metal deposits together with lesser tungsten and molybdenum mineralization locally. Arrays of deposits in almost all instances parallel the trench axis, but their distribution tends to be controlled in part by across-arc tectonic segmentation (Sillitoe 1974a). The intrusive rocks associated with these deposits are mainly tonalites, granodiorites, and lesser adamellites, but more mafic types (diorite, quartz diorite) and more alkaline types (monzodiorite, monzonite, and syenite) are important locally.

Sillitoe (1981a) has detailed the relative importance of ore deposit types within specific principal arcs (Table 1.1). The fact that the same spectrum of ore deposit types characterizes these arcs, despite their variations in maturity, crustal setting, and age, indicates that magma generation and subsequent ore deposition must not be influenced in any significant way by these variations.

It has been noted that porphyry copper deposits in island arc settings tend to be gold-rich and molybdenum-poor and that the converse is true for

porphyries in Cordilleran (continental margin) arcs (Kesler 1973). Exceptions to this rule do occur, however, and include the gold-rich Bajo de La Alumbrera porphyry deposit in Argentina, and the molybdenum-rich Sipalay porphyry copper, Philippines (Sillitoe 1979, 1980a). The metal chemistry of porphyry deposits, and, for that matter, of the majority of deposits found in principal arcs is apparently more closely related to magmatic evolution and crustal thickness than regional variations in the lithochemistry of the country and basement rocks in different areas. Thus, both the restriction of tungsten deposits to Cordilleran principal arcs and the larger average size of porphyry copper deposits within such arcs may be influenced by the greater crustal thickness inherent in Cordilleran arcs vis-a-vis oceanic arcs (Sillitoe 1981a).

Chapter 2 Metal Deposits on the Inner Sides of Principal Arcs

In mature island arc systems (e.g., Japan) and Cordilleran belts, a spectrum of metal deposits form that are sufficiently distinctive from those of principal arcs to merit separate consideration. They tend to exhibit a close spatial association with isolated stocks that intrude the zone on the inner side of principal arcs. The precise demarcation of this zone is not easy and is particularly tenuous in situations where the principal arc itself has migrated back and forth relative to the trench axis. As suggested in the previous chapter, backarc magmatism and related metallogenesis is probably a function of subduction attaining some critical low angle (Fig. 2.1), and thus backarc metal deposits differ in degree rather than kind from principal arc deposits.

2.1 Contact Metasomatic Deposits

Contact-metasomatic deposits, characterized by major amounts of zinc, lead, and silver, occur on the eastern side of the Coastal Batholith of central Peru (Petersen 1965), east of the Sierra Madre Occidental in Mexico (Salas 1975) and on the eastern side of magmatic arcs related to subduction in the western United States during Cretaceous to mid-Tertiary time (Sillitoe 1981a). Similar occurrences possibly include the skarn deposits of the Sanin belt, Honshu, Japan (Shimazaki 1980) and related deposits in southern Korea. The isolated stocks that are typically adjacent to such deposits range in composition from diorite to granite, but are most commonly granodiorite or quartz monzonite. The carbonate host rocks of the deposits typically represent earlier miogeoclinal or stable platform environments.

2.1.1 Mineralization

The development of these contact-metasomatic deposits results from replacement of the carbonate units adjacent to stocks, and a wide spectrum of orebody geometries can result (Fig. 2.2). At Naica, Chihuahua, Mexico, for example, flat-lying mantos controlled by bedding are interspersed with pipe or chimney-like deposits (Stone 1959), whereas in other instances (e.g., Morococha and Yauricocha, Peru; Petersen 1965) ore occurs mainly in steeply plunging chimneys. Many of the deposits in this category are associated with strong development of skarns, but others contain relatively minor amounts of

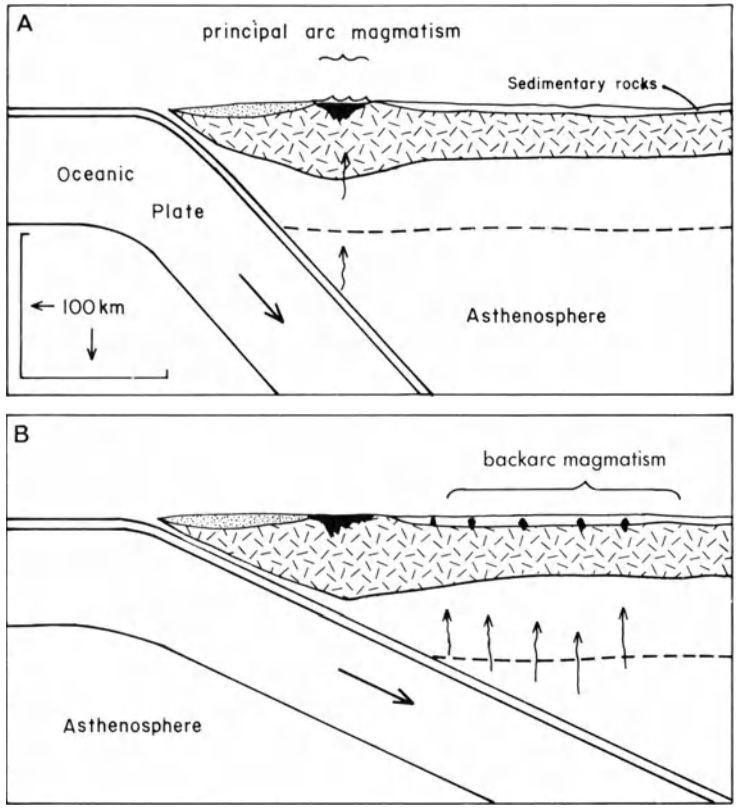

Fig. 2.1.A A narrow belt of magmatic activity (principal arc) above a steeply dipping lithospheric slab; **B** a broad diffuse zone of magmatic activity (backarc) above a shallow dipping lithospheric slab

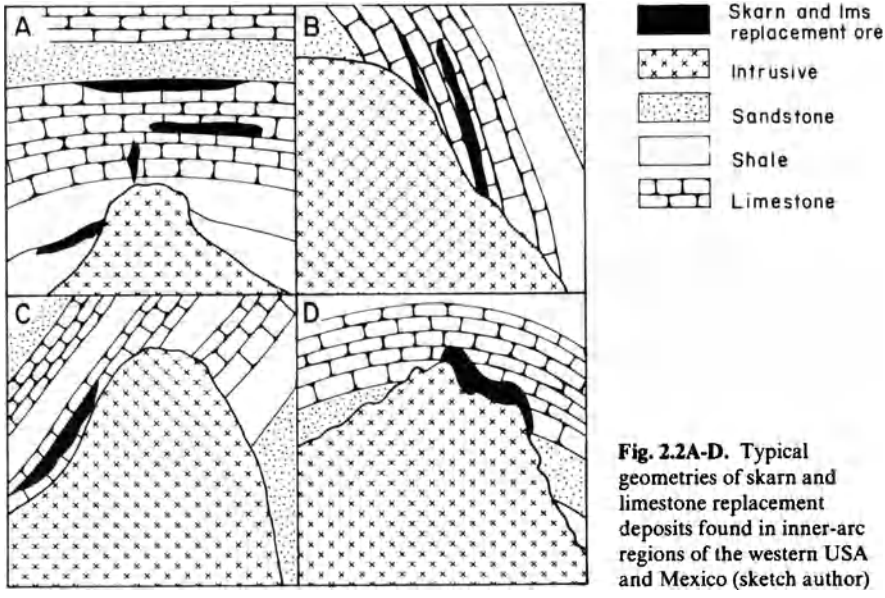

Fig. 2.2A-D. Typical geometries of skarn and limestone replacement deposits found in inner-arc regions of the western USA and Mexico (sketch author)

skarn. The orebodies either crosscut their host rocks at high angles or merely follow shallow or steeply dipping carbonate units.

Zinc, lead, and silver are the most characteristic metals of these backarc deposits, but most contain a certain amount of copper, and in some instances it may represent the major metal of economic significance. In the latter case, deposits generally exhibit a well-defined zonal pattern with the lead-zinc ores lying peripheral to those of copper (Petersen 1965). For the most part the intrusive stocks spatially associated with the deposits are unmineralized, but some important exceptions to this rule are known. At Bingham, Utah, for example, a major porphyry copper deposit lies at the center of the district (see Econ Geol., v. 73, no. 7). Adjacent to the stock that hosts the Bingham porphyry deposit, are important bedding-controlled copper skarn deposits (Atkinson and Einaudi 1978), and fringing these, beyond the skarn front, are lead-zinc-silver replacement deposits (Rubright and Hart 1968; Fig. 2.3). The ores of these deposits tend to be massive in character, especially where skarn development is restricted. Iron sulfides typically represent a significant fraction of the massive ore and occur as pyrite, in some instances accompanied by lesser pyrrhotite.

The Cerro de Pasco replacement deposit in central Peru (Einaudi 1977b) is of particular interest, both in terms of its size and its unusual setting on the margin of a diatreme. It is estimated that the deposit contained $>$ 500 million tons of pyrite, 4 million tons Zn, 2 million tons Pb, over 1 million tons Cu, 10 000 tons Ag, and lesser quantities of gold and bismuth. This quantity of contained metals clearly marks it as a world-class deposit. Adjacent to the diatreme, hydrothermal solutions formed a steep, funnel-shaped, massive quartz-pyrite body by replacement of Mesozoic limestone and possibly diatreme breccia (Fig. 2.4). This large iron sulfide body was itself replaced locally by pyrrhotite pipes and lead-zinc orebodies. The latter also extend into carbonate host rocks locally. Most of the copper ores occur as steep veins cutting the diatreme, and consist primarily of pyrite-enargite, with minor associated quartz, barite, and alunite. Alteration of quartz monzonite domes and pyroclastic breccia produced sericite-pyrite-quartz assemblages, but advanced argillic alteration envelopes are present around some of the copper-bearing veins (Sillitoe and Bonham 1984). Einaudi (1977b) has demonstrated that the considerable complexity of the ores probably relates to rapid sulfide deposition from an ore fluid that fluctuated widely in sulfidation-oxidation state. Although the Cerro de Pasco ores are in many respects unique, partial similarities to other backarc contact-metasomatic deposits (e.g., Magma and Bisbee, Arizona), porphyry copper-related vein deposits (e.g., Butte, Montana), and massive enargite-bearing deposits (e.g., Lepanto, Philippines) can be recognized.

The calc-silicate assemblages present in some backarc contact-metasomatic deposits are complex, but resemble those described in more detail for principal arc sulfide skarns. However, in many cases (e.g., Naica: Stone 1959), garnet tends to be grossularitic rather than andraditic in composition. Pathways of ore fluids were inevitably controlled by structural breaks in the host

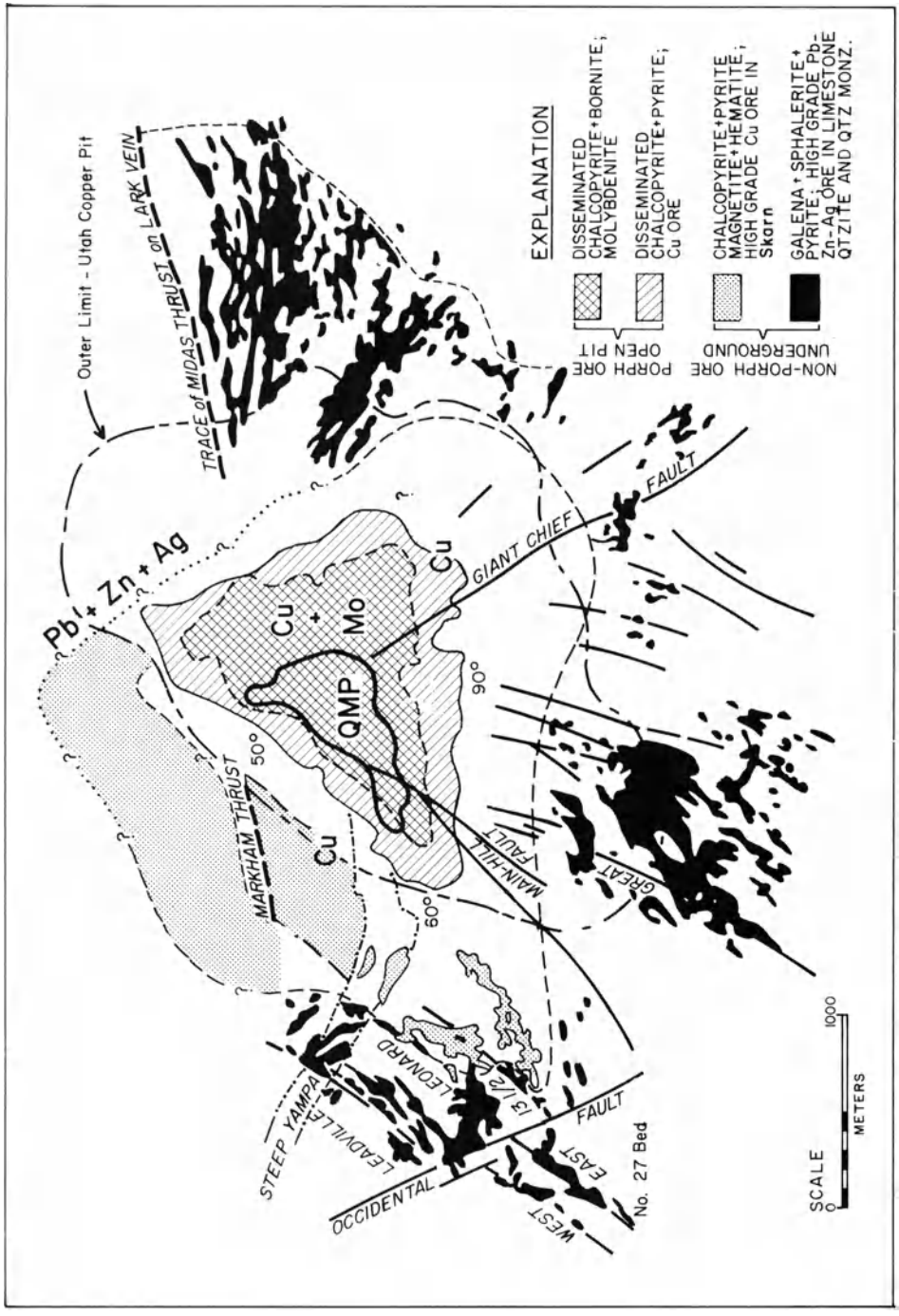

Fig. 2.3. Zonal distribution of porphyry, skarn, and limestone replacement ores centered on the Bingham stock. Such district-wide zoning is characteristic of strongly mineralized areas in backarc regions (After Atkinson and Einaudi 1978)

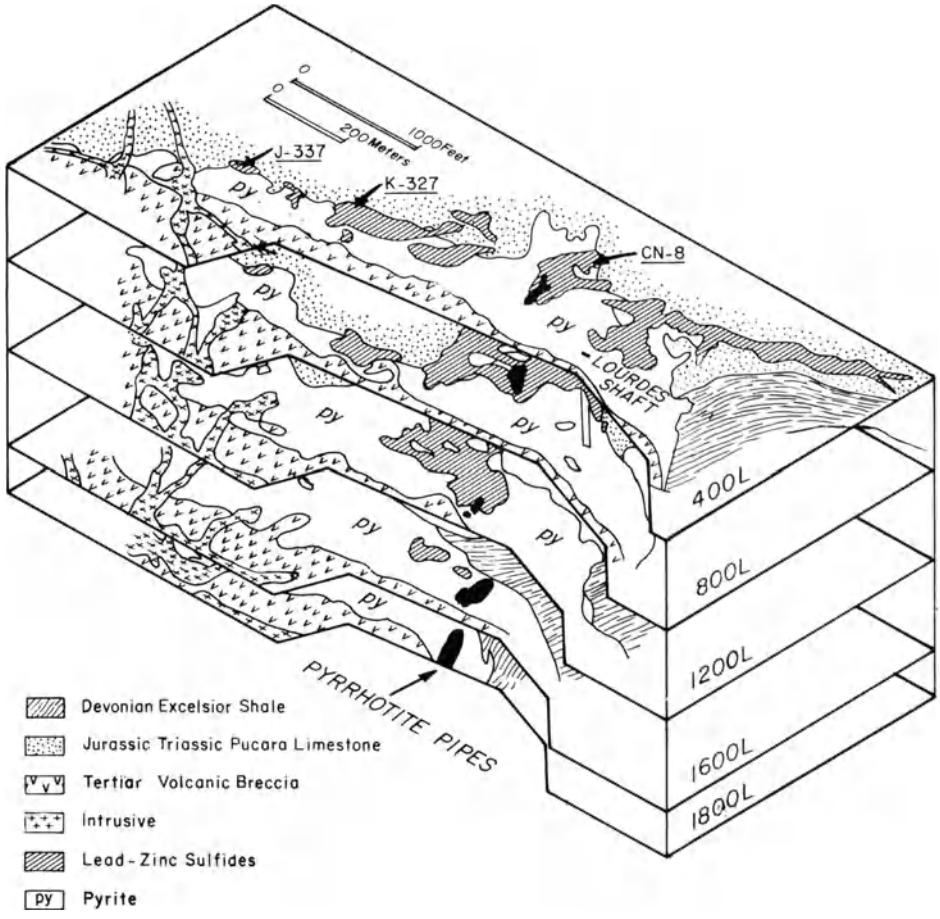

Fig. 2.4A. Isometric diagram of the Cerro de Pasco ore deposit showing relationships between lithologic units, pyrite body, pyrrhotite pipes, and lead-zinc ores. Slight vertical exaggeration of scale. **B** Vertical, north-south cross-sections, looking east through the central portions of the Cerro de Pasco ore deposit (After Einaudi 1977b)

rocks, and the carbonate units just above older noncarbonate basement tend to be important hosts for mineralization. However, the precise reason why certain carbonate units are mineralized preferentially to others is in many instances unclear. In addition, the structures involved in channeling the ore fluids are commonly subtle and difficult to map.

2.1.2 The Providencia Ag-Pb-Zn-Cu Deposit, Zacatecas, Mexico

The massive sulfide chimneys at Providencia have produced over 7 million tons of high-grade base metal ore rich in silver, and represent a well-studied

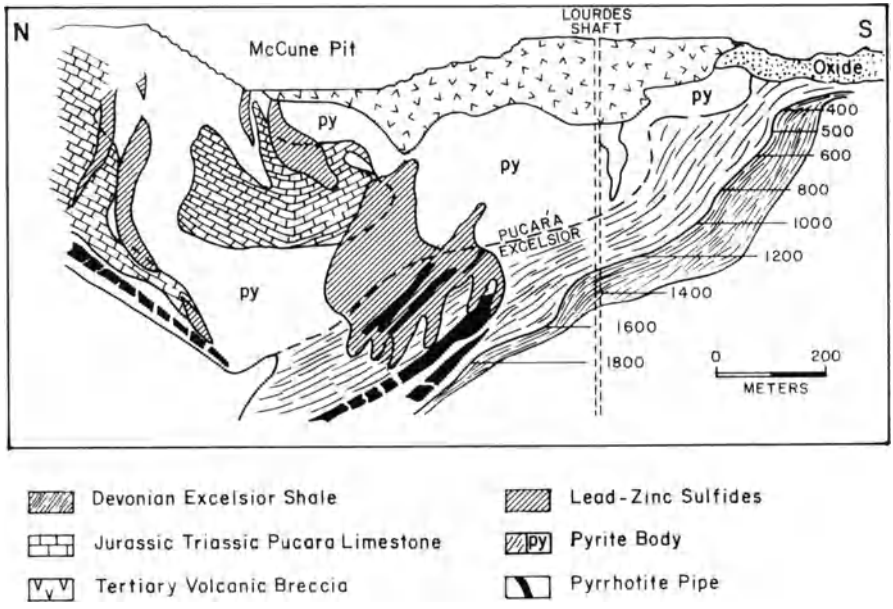

Fig. 2.4 B

example of backarc, contact-metasomatic ore deposition (Sawkins 1964; Rye 1966). Elongate pipe-like bodies of lead-zinc sulfide ore occur in steeply dipping Upper Jurassic and Cretaceous limestones adjacent to and near the southern margin of the Providencia stock (Fig. 2.5). This granodiorite intrusion is continuous in the subsurface with the Concepción del Oro granodiorite to the southeast where important copper skarn deposits occur (Buseck 1966), and where substantial additional tonnages of copper-tungsten skarn ore have recently been discovered. K-Ar and Rb-Sr age determinations of minerals from the granodiorite and from the ores indicate an age of close to 40 Ma for both intrusions and mineralization. Initial strontium ratios are 0.705 (Ohmoto et al. 1966).

The Providencia massive sulfide pipes exhibit a combination of fracture and bedding control and contain predominantly pyrite, sphalerite, and galena. Silver occurs largely in tetrahedrite and much lesser bournonite and geocronite. Small amounts of chalcopyrite occur in the ores and appear to increase somewhat in abundance with depth. The principal gangue mineral is pink manganiferous calcite, but minor amounts of dolomite occur locally, and kutnahorite and rhodochrosite are present in one of the pipes (Salaverna). Lime silicates, mainly grossular garnet, are admixed with sulfide minerals in the deepest levels of the larger pipes (e.g., Zinc West, Animas), whereas quartz is rare or absent at depth, but increases steadily in amount upward within the pipes. Unreplaced shale bands partly altered to muscovite may be observed locally in the Animas and Salaverna pipes, and this material was used in part in the age determination studies cited above.

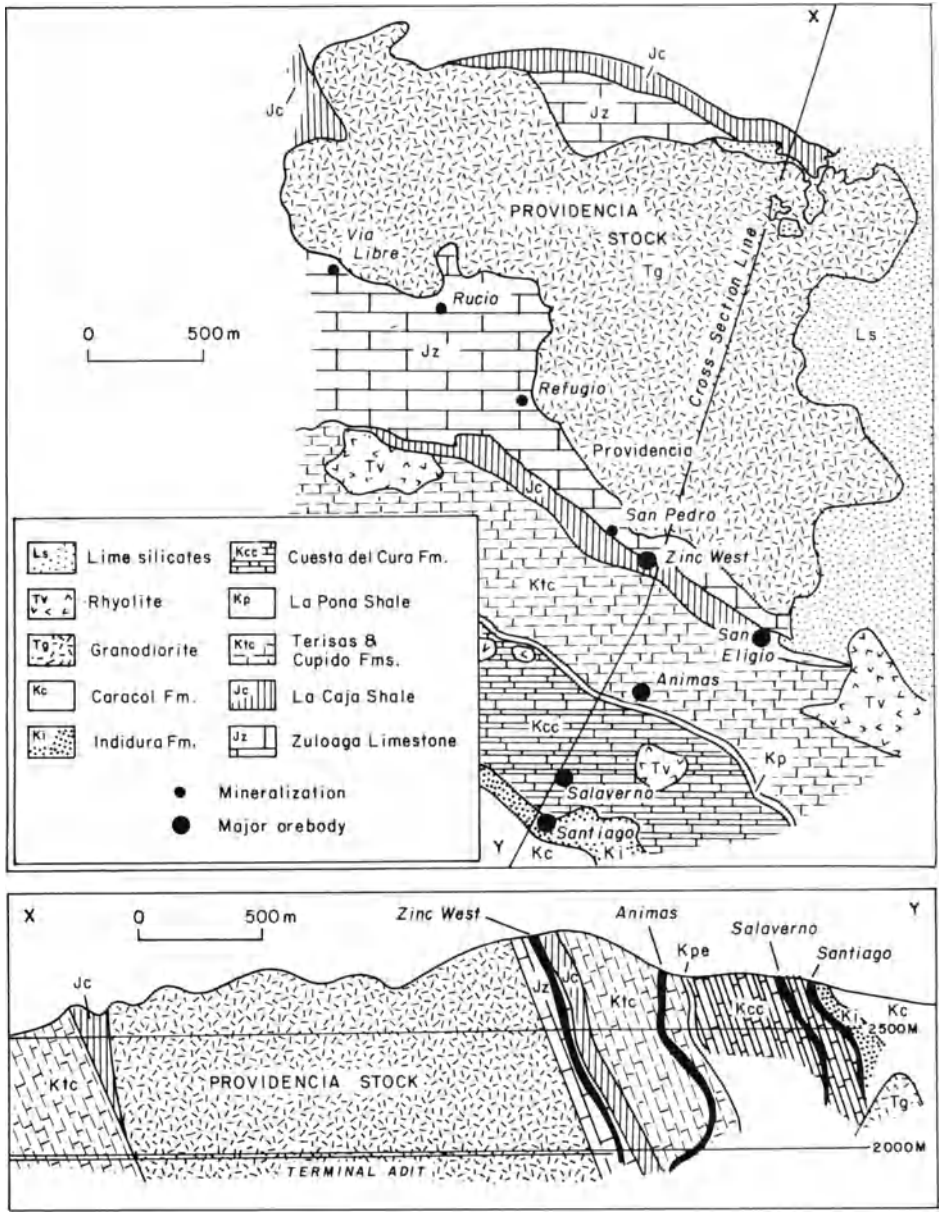

Fig. 2.5. Map and cross-section of the Providencia Mine area, Mexico. In detail the Pb-Zn-Ag sulfide replacement pipes exhibit considerable irregularities in their shapes (After Sawkins 1964)

Fluid inclusion studies, utilizing mainly zoned sphalerite crystals, indicate that the last third of ore deposition at Providencia took place mainly from 370–300°C, with very minor amounts of sulfide deposition continuing to 200°C (Sawkins 1964). Although temperature decreased steadily, no evidence of a drop in temperature relative to elevation was found over the 400-m interval sampled. The salinity of the ore fluids varied erratically between 5 and 40 wt% alkali chlorides during mineralization, with evidence that episodes of high salinity were accompanied by boiling. A pressure of approximately 500 bar during mineralization is indicated by the fluid inclusion data.

Stable isotope studies of the Providencia ores (Rye 1966, 1974; Rye and O'Neil 1968) support a magmatic origin for the sulfur, carbon, and ore fluids involved in ore deposition at Providencia. $\delta^{34}S$ values from sulfides fall within the restricted range of −3 to +6 ‰, whereas $\delta^{13}C$ values for carbonates are close to −7 ‰, except at the end of ore deposition where they tend toward marine limestone (~ 0 ‰). The $\delta^{18}O$ values, both from minerals and fluid inclusions, indicate that the ore fluids ranged in composition from 8.8–7.9 ‰. These isotope results, taken in conjunction with the −68 to −83 ‰ δD values obtained from fluid inclusions, all reinforce the conclusion that ore deposition at Providencia was effected by fluids of magmatic origin, that underwent little modification between their source and the sites of ore deposition. Chemical analysis of these fluids preserved in fluid inclusions (Rye and Haffty 1969) indicate chloride was the major anion and sodium, potassium, and calcium the major cations. Maximum base metal concentrations of inclusion water in quartz, a late-stage mineral, were found to be 890 ppm Zn and 530 ppm Cu.

2.1.3 Limestone Replacement Deposits of Leadville, Colorado

At current metal prices, the value of base and precious metals produced from the Leadville district since its inception in 1860 must be well in excess of $2 billion. Exploitation of the complex Zn-Pb-Ag-Au sulfide replacement ores commenced in 1931 and still continues.

The Leadville district is one of several mining districts that are hosted in Upper Paleozoic carbonate rocks that flank the largely Precambrian Sawatch Uplift (Fig. 2.6). The Leadville Dolomite, the major host for sulfide replacement ores at Leadville, exhibits a complex history of dolomitization on a regional scale. This is in part a diagenetic feature, manifest as early, fine-grained, dark gray dolomite, and in part a later, coarse-grained hydrothermal dolomitization that has been related to emplacement of the extensive batholithic masses that underlie the Colorado Mineral Belt (Lovering et al. 1978).

The most recent work on the Leadville district has been carried out by Thompson and his students (Thompson and Arehart, in press; Thompson and Beaty, in press), and much of the following summarizes their work. The Leadville area is characterized by complexity, both in structural and igneous terms. Several episodes of normal and high-angle reverse faulting occurred between 70 and 64 Ma and the largest faults guided the ascent of magmas. The

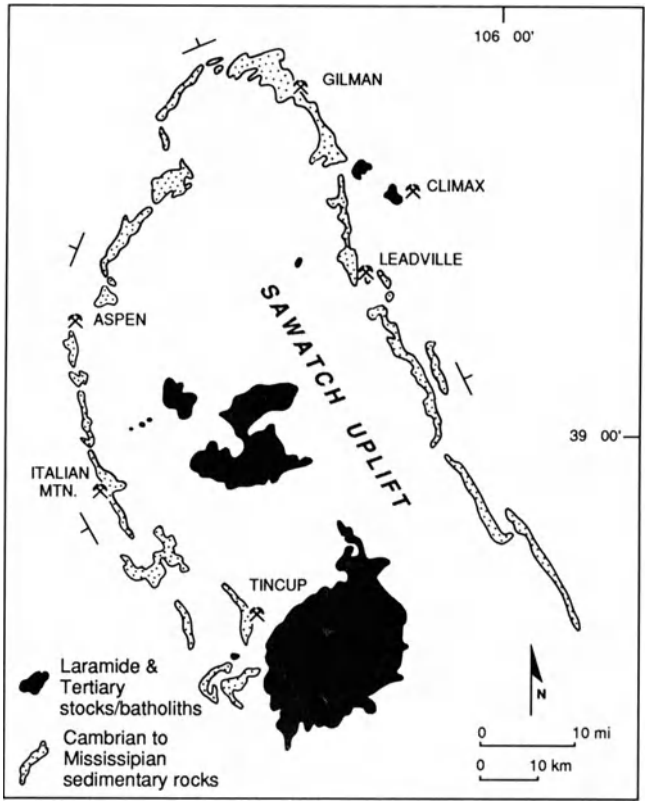

Fig. 2.6. Map of the Sawatch Uplift in Colorado showing the large Tertiary intrusions within it and the metal deposits that surround it (After Thompson et al. 1983)

major result was a series of blocks downstepped to the west, each composed of igneous and/or sedimentary lithologies (Fig. 2.7). The ore deposits, however, have been shown by fission track dating to be considerably younger than the earlier intrusions and have a 34 Ma age of formation.

Various types of economic mineralization have been exploited in the Leadville district. These include base metal veins, precious metal veins, magnetite skarns, silver-barite-minor base metal replacement ores, and base and precious metal replacement ores, but the latter have been the most important metal producers and are the focus of current mining activity. These "Leadville-type" (LTM) orebodies occur as massive replacements ($>$ 60% sulfides) within the Manitou, Dyer, and Leadville Dolomites. Locally, faults, impermeable beds, magnetite skarns, and even karst cave sediments have played a role in their localization, and all the orebodies are cut by veins or veinlets. Dimensions of LTM orebodies range from 100 to 1200 m in length, with widths up to 200 m and thicknesses from a few meters to 30 m. Typical ore grades are Zn + Pb = 8–20%; Cu $<$ 0.5%; Ag = 60–180 g/ton; and Au $<$ 3 g/ton.

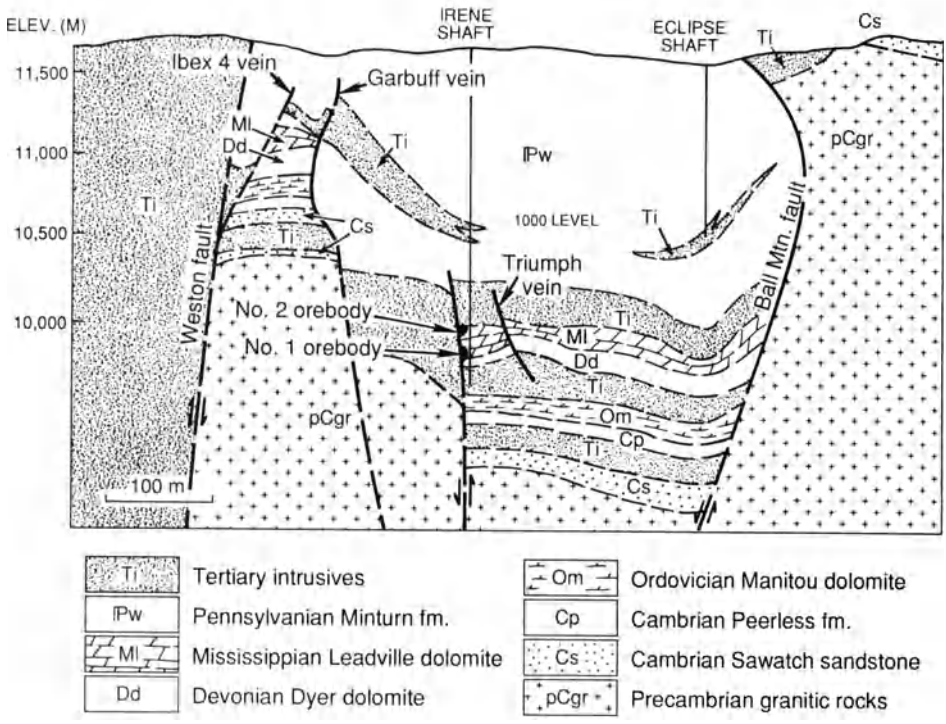

Fig. 2.7. Cross-section of a portion of the Leadville district showing replacement orebodies in the down-dropped block (Courtesy of T.B. Thompson and ASARCO)

A well-defined paragenesis (Fig. 2.8) consisting of early iron sulfides followed by base and precious metal replacement and open-space filling, and a final deposition of barite, dolomite, and fluorite has been worked out. Sulfides are massive or finely banded, the latter being due to grain size or mineralogic variations. Zoning within orebodies is manifest as base metal-rich cores and pyritic margins. Copper, silver, and gold occur in greater concentrations outside of the core zones, and the main silver-bearing mineral in these areas is tetrahedrite. Immediately adjacent to orebodies the host dolomite is invariably disaggregated (sanded), whereas wall-rock alteration of adjacent igneous rocks involves an argillic-sericitic zone (10–50 m), with development of kaolinite-nontronite-sericite-montmorillonite assemblages beyond this.

Lead isotope analyses for LTM ores, from both Leadville itself and from the important Gilman district to the north (see Fig. 2.6), indicate a tight grouping of data that are the same as analyses of feldspar lead from Laramide and mid-Tertiary plutons (Doe and Zartman 1979). This situation does not hold for the lead in the silver-rich replacement ores however. In addition to the lead data, isotope values for sulfur, oxygen, and hydrogen/deuterium all indicate operation of a magmatic-hydrothermal system during formation of the LTM orebodies. $\delta^{18}O$ and δD values are +5 to +7 and −50 to −70‰,

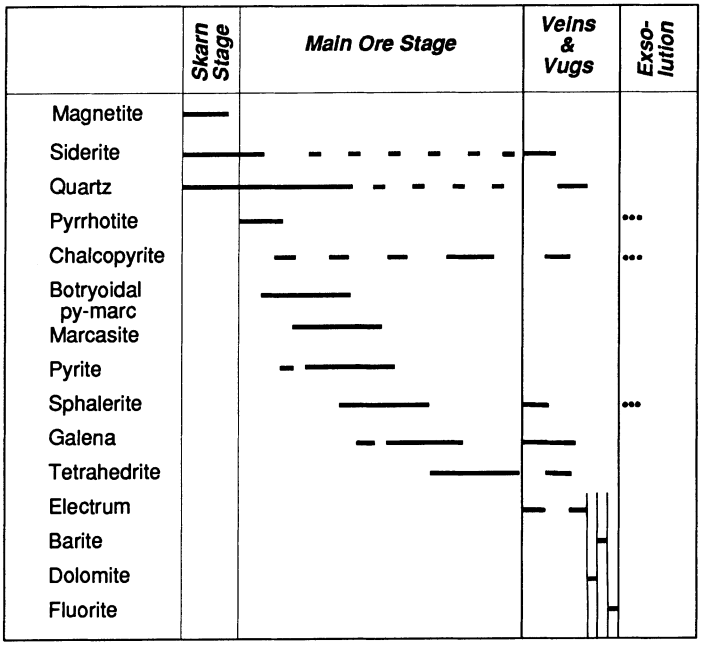

Fig. 2.8. Generalized paragenesis of the vein and replacement ores at Leadville (Thompson et al. 1983)

respectively, and are in strong contrast to the highly depleted character of the local meteoric water during mid-Tertiary time.

Fluid inclusion data define a temperature range of 459–310°C and an absence of boiling during mineralization. Salinities of the ore fluids were in the 5 equiv. wt% NaCl range. These salinities may seem low for a magmatic-hydrothermal system, but accord well with the salinities of many such systems during nonboiling episodes (cf. data in this volume pertaining to type 1 inclusions in various comparable deposits).

In summary, the sulfide replacement mantos at Leadville exhibit fundamental similarities to lead-zinc carbonate-hosted deposits adjacent to shallow felsic intrusions in backarc environments of Cenozoic age in both North and South America.

2.1.4 Discussion and Suggestions for Exploration

The contact metasomatic deposits that form in the vicinity of isolated intermediate to felsic stocks intruded on the landward side of principal arcs are important sources of base metals and silver. In the Andes and northern Mexico, the combination of such stocks and carbonate country rocks almost invariably produces some indications of mineralization. The position of orebodies relative to an intrusive stock can vary however. In the case of the

Santa Eulalia and Naica deposits in Mexico, the orebodies are above the roofs of stocks, whereas at San Martin, Mexico (Burton 1975), Providencia, and Bingham the orebodies occur mainly along the steeply dipping flanks of intrusions (see Fig. 22).

Inasmuch as contacts between ore and host rocks are typically sharp and geometries of individual pipes or mantos can be complex, the search for blind orebodies is inevitably difficult. If ores are zinc-poor, EM geophysical techniques may be effective, but in the final analysis drilling is the only way to truly test unexplored ground. Careful attention to the subtle effects of limestone recrystallization and to the distribution of lime silicates, especially in impure carbonate units, however, can isolate areas of higher potential. Recognition of structural and lithologic features that may have influenced the pathways of ore fluids is also important.

The massive or semimassive nature of lead-zinc contact-metasomatic deposits tends to generate strong electromagnetic and induced polarization responses. Furthermore, magnetic geophysical techniques can be used to help define intrusive contacts and ore, if pyrrhotite is present, in the subsurface. Application of all these techniques is warranted in areas where prior geologic work indicates the possible presence of subsurface mineralization near intermediate composition stocks intrusive into carbonate sequences.

2.2 Polymetallic Vein Systems

Polymetallic vein systems containing silver-lead-zinc (± copper) also characterize the inner sides of principal arc systems and exhibit a similar areal distribution to the contact metasomatic deposits discussed in the preceding section. The major difference is that these vein systems develop primarily in noncarbonate host rocks. In many of the more important backarc mineral districts, such vein deposits occur intermixed with contact metasomatic ores (e.g., Morococha, Peru: Petersen 1965; Fresnillo, Mexico: Ruvalcaba-Ruiz and Thompson 1988). Where zoning is well developed in such districts, the distal veins contain primarily silver, and merge in character with typical epithermal vein deposits. Gold contents, however, tend to be much subordinate to those of silver.

Major polymetallic vein deposits in the central Andes include San Cristobal, Casapalca, Huaron, and Morococha (see Petersen 1965; Bellido and de Montreuil 1972), and there are a host of smaller vein systems mined primarily for their silver content (e.g., Finlandia, Kamilli, and Ohmoto 1977; Julcani, Petersen et al. 1977; Caudalosa, Sawkins, and Rye 1976). It is noteworthy that most of these vein systems exhibit control by fractures that intersect the regional northwest-trending structural grain of the Andes at high angles.

In these vein deposits, the major base metals occur as sphalerite, galena, and chalcopyrite, although in some cases enargite or tetrahedrite-tennantite are the major copper-bearing phases. Silver is present mainly in a variety of

sulfosalt minerals, and quartz and calcite are the predominant gangue minerals in the veins.

In most examples the host rocks for such vein systems are Tertiary volcanics, and locally red beds or even schists (e.g., San Cristobal) host the vein systems, but it is rare to find such systems developed significantly in intrusive rocks. Wall-rock alteration is generally represented by some combination of sericitization, silicification, and chloritization.

Essentially similar vein-type mineralization occurs in Mexico at places such as Taxco, Pachuca, Fresnillo, San Luis Potosi, and Parral (Salas 1975), and a number of polymetallic and precious metal vein deposits occur in the western United States (Guild 1978). Vein deposits are especially widespread in the Colorado Mineral Belt (Tweto and Sims 1963), but they are largely of post-30 Ma age, and are more properly discussed later under arc-related rift environments.

2.2.1 The Fresnillo Ag-Pb-Zn District, Zacatecas, Mexico

The vein and lesser replacement deposits of the Fresnillo district constitute a world-class silver deposit with cumulate production to date of close to 10 000 tons of silver, 18 tons of gold, 1 000 000 tons of zinc, 700 000 tons of lead, and 75 000 tons of copper. In addition, current reserves of silver ore stand at 2 000 000 tons grading approximately 500 g/ton. Initially, ore was mined from oxide capping beneath Cerro Proaño (Fig. 2.9), but during this century almost all mining has been from either manto and chimney replacement deposits, or from the extensive vein system (see Fig. 2.10) that contains the bulk of the ore. Significant contributions to an understanding of the geology and genesis of the Fresnillo district include Stone and McCarthy (1948), de Cserna (1976), Macdonald et al. (1986), Ruvalcaba-Ruiz and Thompson (1988), Gemmell et al. (1988), and Simmons et al. (1988).

The units that host mineralization at Fresnillo consist of a sequence of lower Cretaceous graywacke and calcareous and carbonaceous shale that lie in fault contact with a sequence of basaltic to andesitic pillow lava, breccia, and tuff intercalated with shale, siltstone, and graywacke. Unconformably overlying these units is the Tertiary Fresnillo Formation, and a sequence of felsic pyroclastic rocks that pertain to the widespread ignimbritic volcanic episode of the Sierra Madre Occidental (Clark et al. 1982). Intrusive into the sedimentary rocks in the central and northern portions of the Fresnillo district are minor granodioritic and quartz porphyry dikes and the Fortuna stock, a small cylindrical body of quartz monzonite present only at depth (see Fig. 2.10). K-Ar age dating of the intrusive and felsic volcanic rocks in the Fresnillo region indicates a sequence of magmatic and hydrothermal events that spanned the interval from 38 to 27 Ma, with intrusion and hydrothermal activity occurring close to 30 Ma (Lang et al. 1988; see Fig. 2.10).

Of particular interest at Fresnillo is the vertical spectrum of sulfide ores, from deep replacement Pb-Zn ores of skarn type through sulfide-rich veins and

locally associated mantos with relatively low silver content (< 300 g/ton), to sulfide-poor veins with high silver contents (> 500 g/ton). The deep chimney and manto ores that cluster around the Fortuna stock are associated with skarn development in calcareous graywacke and shale. Tremolite, epidote, hedenbergite, and Ca-Mn garnet occur in the graywacke, whereas axinite is accompanied by silicification in the shales. The replacement sulfide mantos and chimneys in this area are up to 150 m in maximum dimension and consist of massive, commonly layered, bodies of sphalerite, galena, chalcopyrite, and pyrite accompanied by minor amounts of pyrrhotite, argentite, and lesser sulfosalts (Kreczmer 1977).

The Pb-Zn vein-associated manto replacement orebodies have many similarities to the deeper mantos, but axinite is the sole "skarn" mineral developed. Only the high-sulfide Pb-Zn veins extend over vertical distances of up to 1000 m, for the high-silver veins are restricted to the shallower portions of the Fresnillo system and exhibit classical "favorable zone" control. Fluid inclusion studies of the various ore types at Fresnillo (Macdonald et al. 1986; Ruvalcaba-Ruiz and Thompson 1988; Simmons et al. 1988) indicate that skarn-related ores were emplaced mostly in the range 400–300° C, whereas at the other end of the spectrum the shallow high-silver veins were formed at temperatures of less than 240° C. Salinity patterns of the ore fluids at Fresnillo indicate that the chimney, manto, and deep veins were formed from fluids ranging from 4–12 equiv. wt% NaCl, but that salinities for the shallow-level vein mineralization were typically less than 2 equiv. wt% NaCl (Macdonald et al. 1986).

Recent research efforts at Fresnillo have focused on the important, high-grade Santo Niño vein (Gemmell et al. 1988; Simmons et al. 1988), which extends in an ENE-WSW direction for approximately 3 km in the southern part of the district. In this area a set of high-silver veins has been found in recent years (see Fig. 2.9), but several remain undeveloped. Geologic and mineralogic studies of the Santo Niño vein (Gemmell et al. 1988) indicate that the productive portions of the vein, which average > 600 g/ton Ag and < 2% combined Pb + Zn, extend over a vertical interval of approximately 400 m, but do not reach the present surface. Sphalerite is the most abundant ore mineral in the vein, but other sulfides include galena, pyrite, chalcopyrite, and arsenopyrite. The silver occurs mainly as acanthite, native silver, and as the sulfosalt pyrargyrite. Additional antimony-rich sulfosalts are polybasite and tetrahedrite. Quartz is the predominant gangue mineral, but calcite, clay, chlorite, and sericite are also present. Textural studies of vein fill, including breccias, indicate that four stages of vein development occurred. In the first three, metallization was followed by deposition of considerable quartz and other gangue prior to initiation of the next stage. The fourth stage is characterized by deposition of largely barren quartz and major amounts of calcite.

Fluid inclusion studies (Simmons et al. 1988) indicate that temperatures ranged from 180–260° C and that the fluids lay close to or on the boiling-point curve as they traversed the vein structure. Fluids responsible for quartz deposition were low salinity (av. 2 equiv. wt% NaCl), whereas fluids respon-

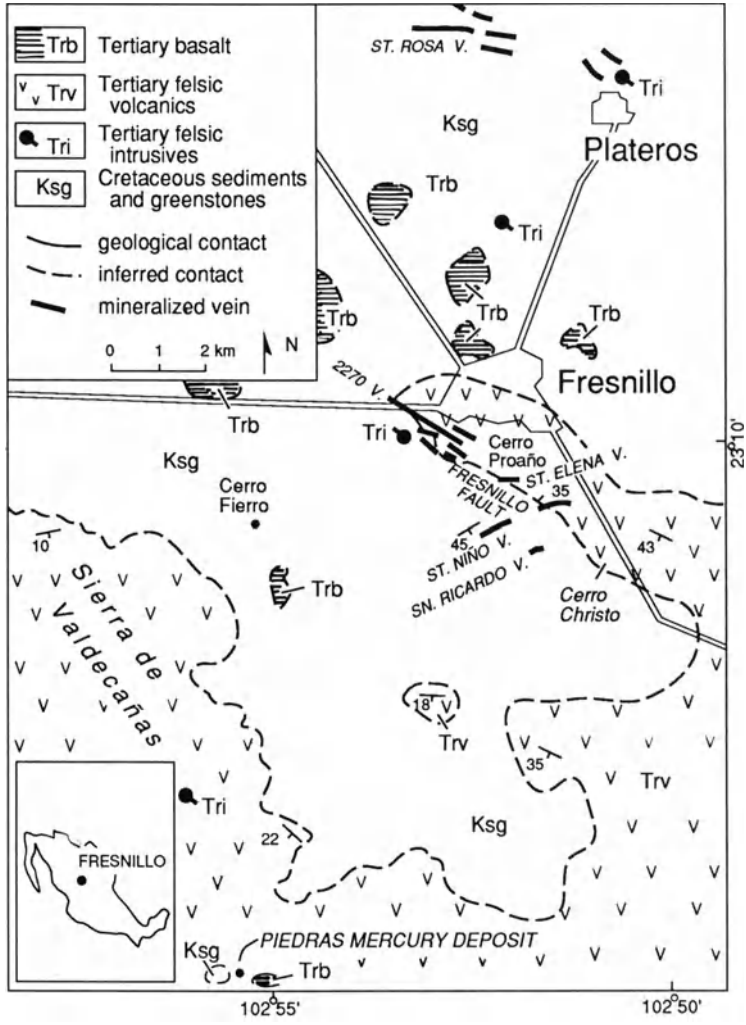

Fig. 2.9A. Simplified map of the Fresnillo mining district. The deeper replacement ores are found to the northwest of Cerro Proano (After Simmons et al. 1988). **B** Schematic cross-section to illustrate the ages of the main intrusive and volcanic units in the Fresnillo district based on K-Ar measurements. Age of 29.1 Ma was obtained on adularia obtained from veins in altered volcanics. Sketch is highly diagrammatic and not to scale (After Lang et al. 1988)

sible for sphalerite deposition ranged from 8.5 to 12 equiv. wt% NaCl. These more saline fluids were introduced repeatedly during the early parts of the first three stages of mineralization, but were apparently displaced rapidly by low salinity fluids each time. Complexities of this kind, involving repeated fracturing events and occupation of the open spaces by increments of quite dissimilar fluids are probably commonplace during the development of epithermal vein systems, and would explain the banding that develops.

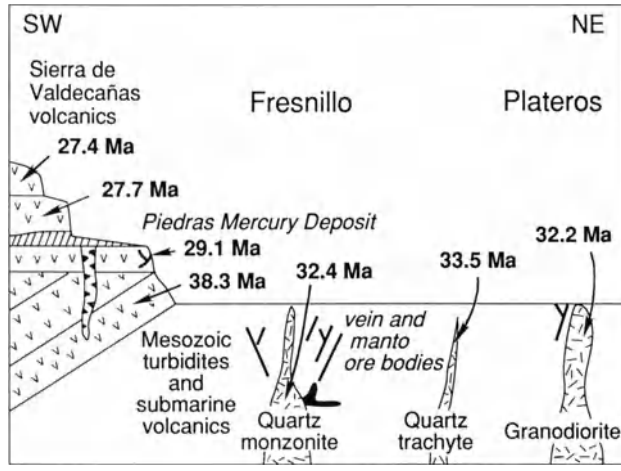

Fig. 2.9B

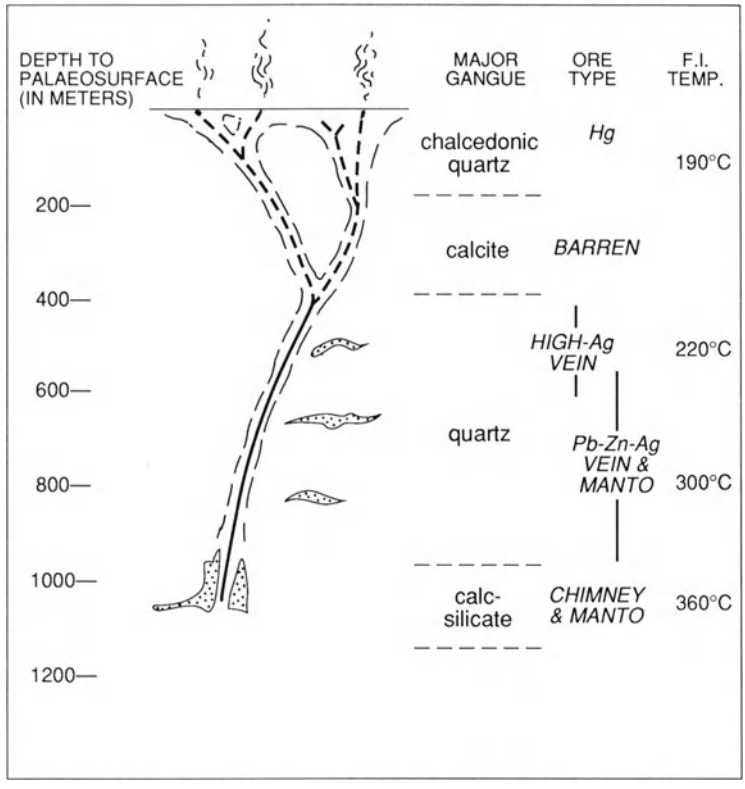

Fig. 2.10. Reconstruction of the complete ore-generating system at Fresnillo based on geologic relationships, mineralogy, and fluid inclusion data (After Sawkins 1988)

Limited stable isotope and $^3He/^4He$ studies of Fresnillo mineralization (Macdonald et al. 1986; Simmons et al. 1988) indicate that the sulfur in the ore could be entirely magmatic in origin or could be in part of sedimentary derivation. Oxygen, H/D, and helium data all point toward a significant magmatic contribution to the hydrothermal system, and it is probable that the minor amounts of intrusive rocks in the district represent the upward extremities of a major intrusion at depth.

The mid-Tertiary volcanic rocks exposed several kilometers west of the Fresnillo camp (see Fig. 2.10) exhibit widespread, albeit patchy, alteration and silicification in their lowermost units. In the Piedras area (Fig. 2.10) intense kaolinization, mercury mineralization, and major development of jasperoid indicates close proximity to the paleosurface (Albinson 1988). The rhyodacitic volcanic unit immediately above the jasperoid ledges is completely unaltered, and has provided a K-Ar date of 27 Ma (Lang et al. 1988). This indicates that the alteration immediately below the paleosurface is part of the Fresnillo hydrothermal event, and that the Fresnillo system may extend much farther westward than currently known.

The underground workings and surface exposures in the Fresnillo district provide a continuous spectrum of mineralization and alteration features that span a vertical interval of $>$ 1000 m, from contact-metasomatic skarn ores deposited at temperatures in the 300–400°C range to jasperoid with related mercury mineralization and kaolin deposits that formed virtually at, or very close to, the paleosurface during mid-Tertiary time. This demonstrates that the paleogeothermal system operating at Fresnillo had deep ore-generating roots which, based on geologic, geochemical, and isotope data, were of magmatic-hydrothermal origin.

2.2.2 The Casapalca Ag-Pb-Zn-Cu Deposit, Peru

This important vein system in central Peru has produced 1600 tons of silver, and been the subject of detailed fluid inclusion, stable isotope, and mineralogic studies (Rye and Sawkins 1974; Wu and Petersen 1977). Here, an extensive system of northeast-trending veins was emplaced in a series of folded volcanics and red beds of early Tertiary age (Fig. 2.11).

Veins are mostly narrow ($\sim$ 1 m) and the wall rocks adjacent to them exhibit pyritization, silicification, and sericitization. In the central part of the vein system this alteration affected a substantial volume of country rock, but toward the extremities of the system alteration envelopes narrow down to widths comparable to those of the vein itself. Although the veins are well defined, some mineralization occurs in small, parallel fractures adjacent to them, and this is important from an economic viewpoint because it partially negates the dilution problem involved in mining some narrow veins.

Most veins are relatively tightly filled, but some splits that dip vertically are extremely vuggy locally. Paragenetic studies on such material indicates a depositional sequence in which sphalerite, galena, and chalcopyrite accom-

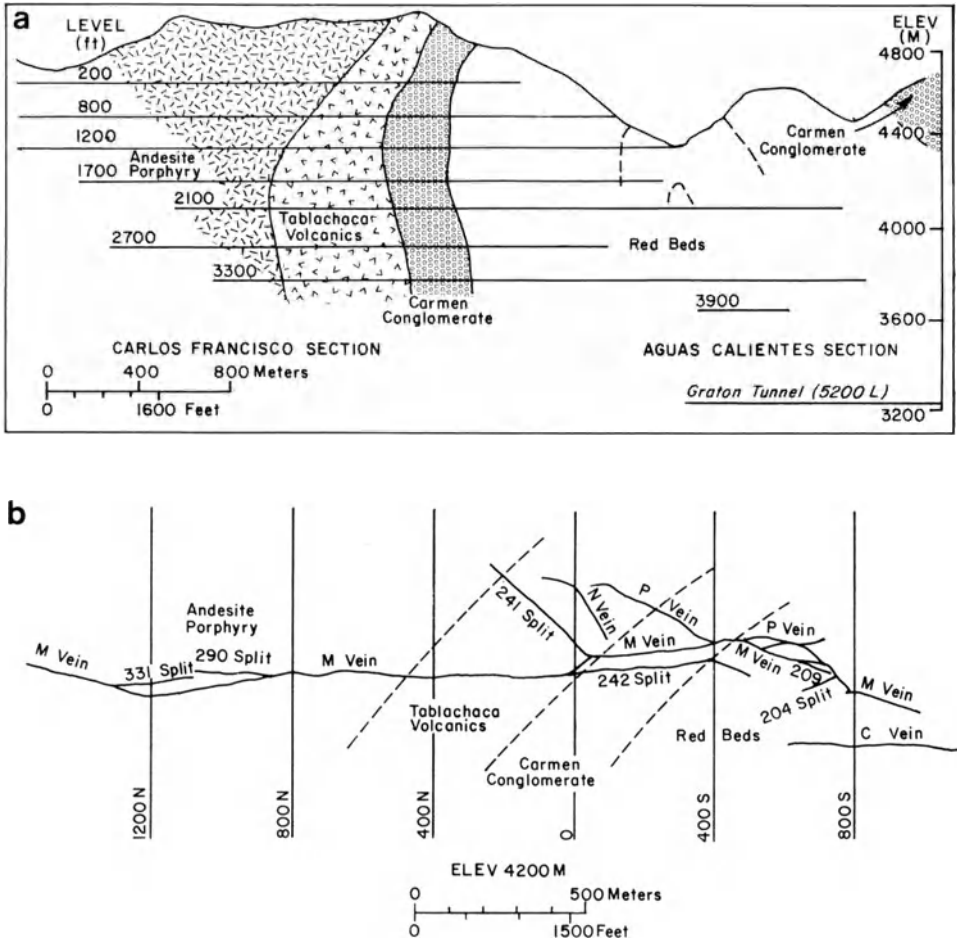

Fig. 2.11a. Longitudinal cross-section and **b** 1700 level plan of the Casapalca vein system, central Andies, Peru (Rye and Sawkins 1974)

panied by pyrite and quartz (main stage) are succeeded by lesser amounts of pale sphalerite, galena, tetrahedrite, and other sulfosalts, again with pyrite and quartz (late stage). The final stage of vein filling is represented by calcite in various crystallographic forms, essentially barren of metallic minerals (postsulfide stage). Fluid inclusion studies indicate that temperatures dropped steadily from 370° to 280°C during the main and late stages of ore deposition, whereas the calcites were deposited at still lower temperatures (Rye and Sawkins 1974). During main-stage deposition, salinities of the ore fluids varied from 5–40 wt% alkali chlorides and sporadic boiling occurred.

Stable isotope analysis on both inclusion fluids and vein quartz representative of main- and late-stage materials generated a tight data set indicative of fluids of magmatic origin. However, δD and $\delta^{18}O$ values from fluids in

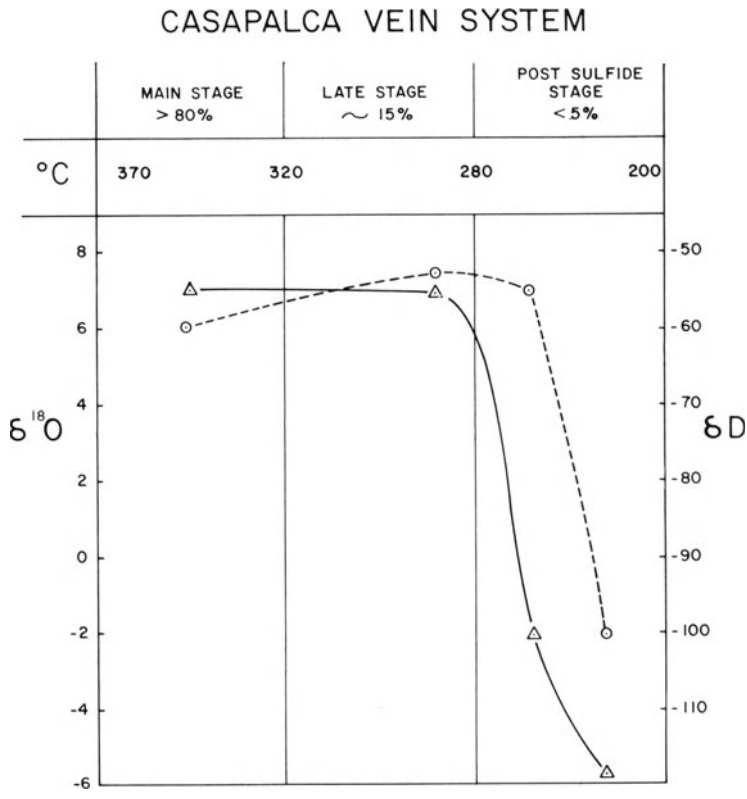

Fig. 2.12. Generalized plot of $\delta^{18}O$ (*circles*) and δD (*triangles*) values of Casapalca ore and postore fluids versus paragenetic stage. Note sharp change in isotope values from late stage to postsulfide (carbonate) stage of vein filling (After Rye and Sawkins 1974)

calcites exhibit a sharp trend toward waters strongly depleted in deuterium and ^{18}O, similar to present-day meteoric waters in the region (Fig. 2.12). Overall, the data provide a clear picture of incursion of local meteoric waters into the vein system, but only after metallization had essentially ceased. The $\delta^{34}S$ values obtained from sulfides indicate a narrow isotope range for sulfur and an average value of sulfur in the ore fluids of close to $+1$ ‰ $\delta^{34}S$. $\delta^{13}C$ values suggest an increasing marine carbonate component in the later calcite stages.

Despite their profound differences in terms of geometry and host-rock character, the Casapalca and Providencia (see previous section) deposits exhibit an almost uncanny similarity in terms of paragenesis, depositional temperatures, ore fluid salinities, and isotope systematics. The important inference that can be drawn from this observation is that the fundamental control of such deposits lies primarily in the evolution of ore fluids from magmatic source regions.

2.3 Epithermal Vein Deposits

As in the case of principal arc metallogeny, epithermal vein deposits occur and form part of the continuum of deposits that can develop outward from igneous systems capable of generating hydrothermal metal deposits. The epithermal vein mineralization can be of either low- or high-sulfidation type, just as documented in the previous chapter for principal arc settings. An example of the former is the upper part of the Fresnillo system (see Sect. 2.2.2), whereas an example of the latter is provided below.

2.3.1 The Julcani Deposit, Peru

The Julcani district is located in the central Andes of Peru at an altitude of approximately 4300 m. The deposit (Fig. 2.13), which consists of a series of fracture-controlled veins hosted by late Miocene dacitic to rhyolitic domes (Petersen et al. 1977; Shelnutt and Noble 1985; Drexler and Munoz 1985; Deen et al. 1987), has been a major producer of silver, together with appreciable Cu, Bi, and Pb, and lesser Au and W. Detailed K-Ar dating studies (Noble and Silberman 1984) have shown that the igneous and hydrothermal evolution of the Julcani district commenced at 10.1 Ma and continued for 0.7 Ma. Petrologic studies of the main-stage volcanic dome-forming event have demonstrated that the rhyodacite magma was sulfur-rich and highly oxidized (Drexler and Munoz 1985). Careful attention to microphenocrysts in these rocks has revealed a phenocrystic assemblage consisting of apatite-Fe-Ti oxides-hornblende-biotite-pyroxene-plagioclase-pyrrhotite-anhydrite. Based on this assemblage, the following magmatic intensive parameters were calculated: T = 833–908°C, $\log f_{O_2} = -10.1$ to -11.3, $H_2O = 2.5$ to 8.2%, $\log f_{S_2} = -0.25$ to -0.5, $\log f_{SO_2} = 1.7$ to 2.4, $\log f_{SO_3} = -2.9$ to -4.1, $\log f_{H_2S} = 0.6$ to 1.2. This was undoubtedly an oxidized, volatile-rich magmatic system, and, as noted in Chapter 1, such highly oxidized, highly sulfurized magmas are proposed (Burnham 1981) for the generation of porphyry copper deposits.

The vein system (Fig. 2.13) exhibits a well-defined zoning pattern, both in terms of ore mineralogy and alteration asemblages (Goodell and Petersen 1974). A central breccia area contains pyrite-wolframite-gold with attendant pyrophyllite-quartz-pyrite + alunite alteration. This is succeeded outward by enargite-tetrahedrite-barite veins enveloped in alunite-kaolinite-quartz-pyrite alteration, then tetrahedrite-bismuthinite-stibnite-silver and lead sulfosalts with kaolinite-quartz-pyrite + alunite alteration. The high-sulfidation nature of the system is clearly indicated by the presence of both enargite and alunite in the paragenesis.

Fluid inclusion studies demonstrate that main-stage mineralization temperatures declined from > 300°C in the central area (Wo + Au) to < 200°C in distal zones. The data also indicate depths of 100 to 700 m for the mineralized veins during their formation. Both the temperature data and the zoning patterns based on various metal ratios suggest a strong component of

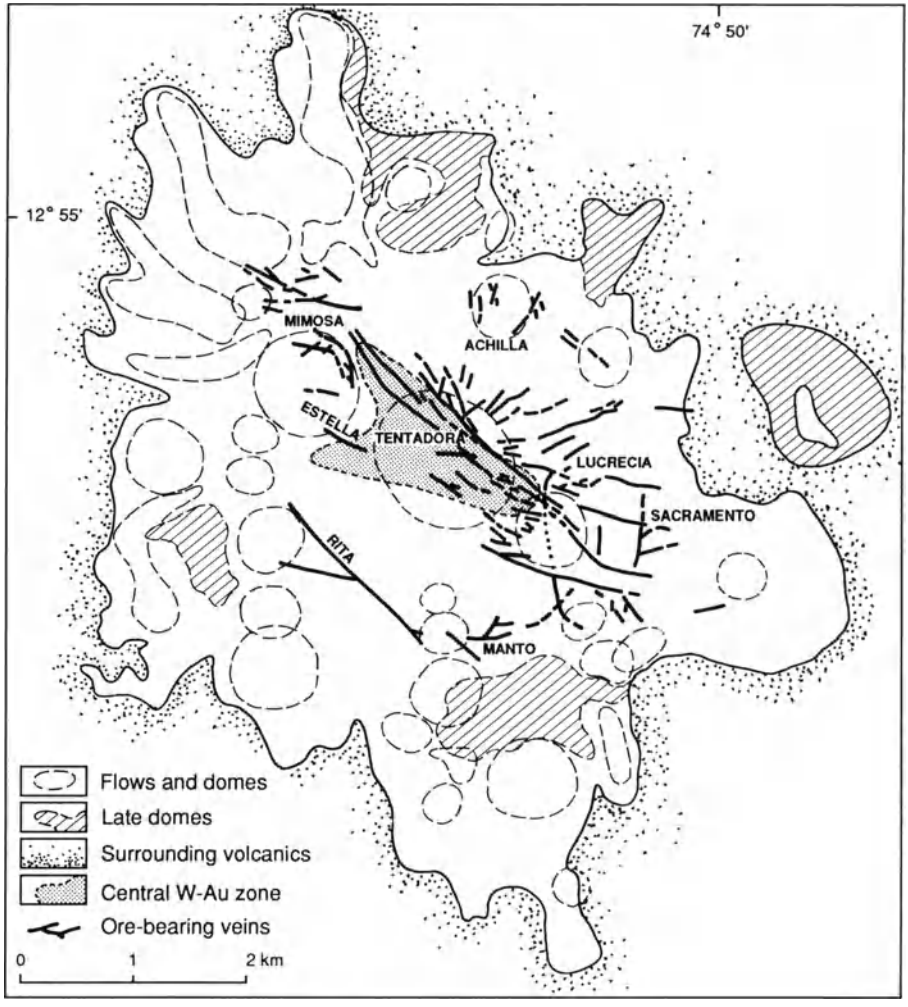

Fig. 2.13. Map of the Julcani district, central Peru. The entire district is hosted by felsic flows and domes of mid-Tertiary age (After Shelnutt and Noble 1985)

lateral flow as the ore fluids moved through the vein system. Deen et al. (1987) report the results of stable isotope studies (O, H/D, and S), all of which clearly indicate a magmatic-hydrothermal origin for main-stage mineralization, with incursion of local meteoric water only during late-stage vein filling.

2.3.2 Discussion and Suggestions for Exploration

Although many vein systems in backarc regions can be properly designated as polymetallic, many others contain relatively minor amounts of base metals

and are perhaps more correctly assigned to the epithermal precious metal category. In fact, the existence of a spectrum from polymetallic to true precious metal epithermal deposits is indicated in the examples just discussed in previous sections. Of particular interest in this regard is the Caudalosa vein deposit in central Peru (Sawkins and Rye 1976). Here, fluid inclusion studies indicate temperatures ranging from 320–200°C, and low to intermediate ore fluid salinities. δD values of inclusion fluids indicate the mixing of two fluids in the vein system with ore minerals deposited mainly by fluids of more magmatic character and gangue minerals by fluids characterized by more isotopically depleted meteoric signatures (Fig. 2.14). Isotope studies of the Finlandia polymetallic vein, central Peru, by Kamilli and Ohmoto (1977) gave two sets of δD values for the ore fluids, in the range -48 to -75 ‰ and approximately -100 ‰, and $\delta^{18}O$ values of -10 to +2 ‰, which led the authors to suggest a mixing of waters of connate origin and meteoric origin during ore deposition.

Vein systems, because of their extent and associated alteration, are generally easy to discover in the rugged arid terranes that characterize the backarc regions of the western USA, northern Mexico, and central Peru. However, once in production they represent a challenge in terms of location of splits and other mineralized structures parallel to major veins that may be blind upward.

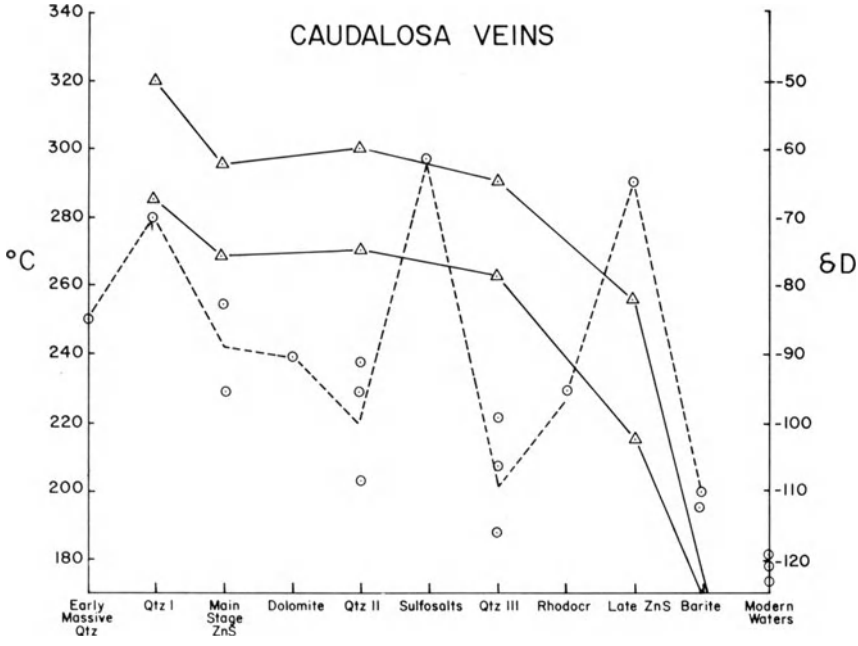

Fig. 2.14. Plot of temperature and δD variations versus paragenetic stage for the Caudalosa ore fluids. *Triangles* show maximum and minimum temperatures for each stage. The sharp variations of the δD values (*circles*) suggest differing involvement of magmatic (less depleted) and meteoric (more depleted) waters in each stage of the paragenesis (After Sawkins and Rye 1976)

There is also the ever present problem of maintaining ore reserves in such operations. Careful attention to all aspects of the local geology, especially structure, is important. Furthermore, studies of metal ratio zoning patterns in known veins (see Goodell and Petersen 1974) can provide an important tool in terms of understanding the anatomy of any particular vein system.

2.4 Tin-Tungsten Deposits

On the inner sides of many Cordilleran arc systems some felsic igneous rocks have important tin and/or tungsten deposits associated with them. Examples of this type of backarc metallogenesis in the Andes include the important Bolivian tin belt (Fig. 2.15), the Pasto Bueno (Landis and Rye 1974; Norman and Landis 1983) and San Cristobal (A.R. Campbell et al. 1984) tungsten deposits in Peru, and the important group of tungsten deposits in the Yukon, northwestern Canada (Fig. 2.16). To this list can probably be added many of the Korean tungsten deposits (So et al. 1983; Lee 1986) and some of the tin deposits in New South Wales, Australia (Sillitoe 1981a). Recent work on the world-class tungsten deposits of the Jiangxi Province (Simpson et al. 1987 and references therein) suggests that these extensive deposits and those of neighboring provinces also formed in a backarc environment during periods of late-Paleozoic and Mesozoic plate convergence (Hsü et al. 1988). Assessing

Fig. 2.15. Major igneous provinces of the Eastern Cordillera of Bolivia and associated tin deposits (After Grant et al. 1979)

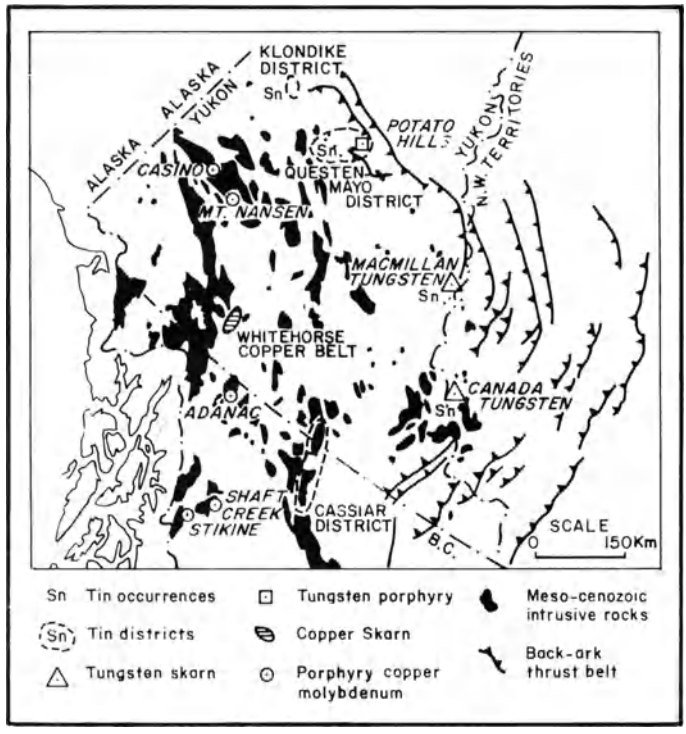

Fig. 2.16. Map showing location of major backarc tungsten deposits of northwestern Canada. Note that both here and in Bolivia there is a strong flexure in the trend of the arc system (After Sillitoe 1981a)

the geotectonic settings of Russian ore deposits is difficult on a number of counts, but it seems that many of the tin-tungsten deposits of the Transbaikalian region (Denisenko 1986) may well be of backarc setting.

The igneous rocks associated with this group of deposits are primarily quartz monzonites and granites and appear to represent both I- and S-types. In Bolivia, tin-tungsten veins are associated with Triassic granodiorite intrusions in the Cordillera Real (see Fig. 2.15). Farther south, the tin-silver deposits of Miocene age largely occur with subvolcanic complexes of felsic calc-alkaline composition and presumed I-type (Grant et al. 1977, 1980). Sillitoe (1981a); however, cites several observations that suggest that both the older Cordillera Real igneous suite and the Miocene suite may have S-type affiliations.

The important tungsten province of mid- to late-Cretaceous age in the Northwest Territories and Yukon provinces of Canada (Archibald et al. 1978; Noble et al. 1984; Bowman et al. 1985; see Fig. 2.16) is associated with quartz monzonite and granodiorite plutons (Gabrielse and Reesor 1974; Dick and Hodgson 1982). Geochemical work (e.g., Kuran et al. 1982) indicates that these intrusions are of S-type. There are also a number of skarn-type tin prospects in the vicinity of the tourmaline-bearing leucocratic Seagull Batholith (Dick

1979), but the position of these, about 200 km southwest of the main tungsten belt is puzzling, however.

A belt of tin and tungsten-bearing granites, which extends for about 1400 km from southwestern Burma to Phuket in southern Thailand (Mitchell and Garson 1981; Hutchinson 1983) forms the so-called Western Tin Belt of southeast Asia (Fig. 2.17). Isotope age studies (Beckinsale et al. 1979) indicate that the plutons along this belt range in age from early Cretaceous to early Tertiary. In Burma, cassiterite and wolfram mineralization occurs in quartz veins and greisen zones marginal to biotite adamellites and two-mica granites.

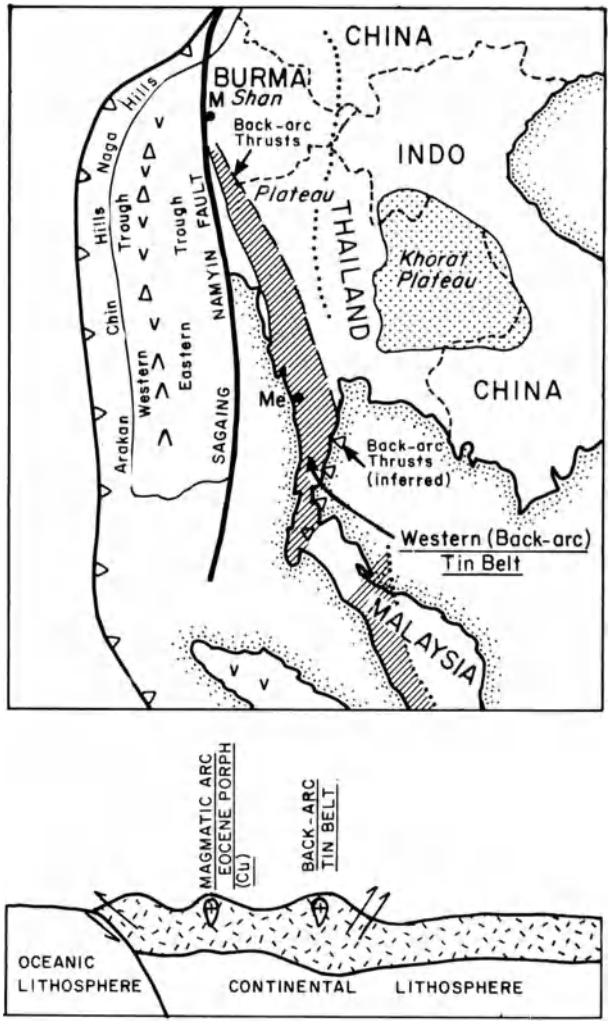

Fig. 2.17. Sketch map and cross-section of the Western Tin belt of Southeast Asia during the Eocene. Western Burma is restored to its inferred position prior to late-Cenozoic opening of the Andaman Sea (After Mitchell and Garson 1981)

In peninsular Thailand, the tin mineralization is restricted to biotite and two-mica granites of predominantly S-type, and occurs in quartz veins, stockworks in hornfels, and pegmatites (Ishihara et al. 1980).

The tectonic setting of these deposits is complicated by subsequent tectonic events such as late Tertiary movement along the Sagaing Fault, which has resulted in several 100 km of northward movement of a principal arc terrane originally lying west of the tin belt (Curray et al. 1980). The belt was thus developed between an arc system to the west and a zone of backarc thrusts to the east (Mitchell and Garson 1981), and as such, it is comparable with the backarc tin belt of Bolivia. There is also a belt of peraluminous muscovite granites that overlaps the Cordilleran thrust belt of the western United States (Miller and Bradfish 1980). Minor tin and tungsten deposits are known to be associated with some of these granites, certain of which have been shown to be of probable anatectic origin, due to their high initial strontium ratios.

The important belt of Mesozoic granites in southeastern China that contains a significant portion of the world's tungsten resources (Chongke and Zengqi 1986), consists almost entirely of S-type intrusives (Tu et al. 1980). An opposing view is offered by Simpson et al. (1987) who argue, on the basis of structural styles and geochemistry, that the granitoid rocks associated with the Jiangxi Province tungsten deposits are of dominantly mantle origin. The mechanics of plate tectonic assembly of the various crustal blocks that created this part of the Asian continent has recently been at least partially clarified by Hsü et al. (1988). It would be surprising indeed if the porphyry deposits of Cu, Cu-Mo, and Cu-W type and the roughly parallel but separate zones of vein-type W-Sn deposits, and the igneous rocks with which they are associated, are unrelated to convergent plate environments, for they are clearly of orogenic as opposed to anorogenic type.

2.4.1 Mineralization

This group of tin and/or tungsten deposits is a somewhat heterogeneous one in terms of deposit type and associated metals. In Bolivia, the older deposits in the Cordillera Real are tin-tungsten deposits (Turneaure and Welker 1947), whereas the Miocene tin-silver deposits farther south include veins, breccia pipes, and tin porphyries (Sillitoe et al. 1975; Grant et al. 1980). Such porphyry deposits are known at Llallagua, Oruro, and Potosi and are characterized by large tonnages of low-grade cassiterite ore within stockwork veinlets or breccias, within or adjacent to subvolcanic quartz latite porphyry stocks. Alteration associated with mineralization has sericitized and tourmalinized the host rocks.

In northwestern Canada most of the tungsten deposits are of skarn type and contain scheelite and, commonly, lesser chalcopyrite. The skarns themselves are characterized by early anhydrous assemblages of garnet (grossular-andradite) and hedenbergitic pyroxene, but exhibit retrograde effects with development of amphiboles and biotite during tungsten miner-

alization (Dick 1979; Dick and Hodgson 1982). Here, the host rocks are adamellite and diorite stocks. A good example of porphyry tungsten mineralization in this area is the Logtung deposit at Logjam Creek (Templeman-Kluit 1981; Sillitoe 1982; Noble et al. 1984).

Sillitoe (1981a) suggests that the Sangdong tungsten-molybdenum-bismuth skarn of Cretaceous age in southern Korea, and the important cassiterite-bearing limestone replacement deposits of Paleozoic age in Tasmania may also have formed in backarc tectonic settings. In eastern Australia tin and tungsten deposits occur mainly as vein or pipe deposits associated with greisens. At Ardlethan, New South Wales, pipe-like breccias mineralized with quartz, cassiterite, pyrrhotite, and lesser lead-zinc sulfides occur within highly differentiated S-type granites cut by quartz porphyry dikes (Paterson 1976). Tourmaline, sericite, and chlorite are developed as alteration phases.

No single genetic model is likely to be appropriate for this diverse group of deposits, but their invariable time-space association with felsic magmatism indicates that magmatic hydrothermal processes must have been a common denominator in the genesis of most. This conclusion is supported by the relatively few in-depth studies available. Kelly and Turneaure (1970), for example, reported high temperatures (up to 500°C) and high salinities (up to 46 wt% NaCl) for fluid inclusions in minerals from northern Bolivian vein tin-tungsten deposits. Similar results have been generated from studies of the Chorolque subvolcanic tin deposits in southern Bolivia (Grant et al. 1980). Genetic models for the tungsten deposits of northwestern Canada (e.g., Mathieson and Clark 1984; Noble et al. 1984) also favor magmatic-hydrothermal models four ore deposition.

2.4.2 The Llallagua Porphyry Tin Deposit, Bolivia

The Llallagua deposit occurs approximately in the center of the 800-km-long Bolivian tin belt (see Fig. 2.15), and with a production in excess of half a million tons of metallic tin, it is probably the largest hard-rock tin deposit in the world.

The tin mineralization is closely associated with the Salvadora stock, a small quartz latite body (Fig. 2.18), intruded into an overturned anticline of Silurian-Devonian graywacke, sandstone, and shale (Turneaure 1935, 1971). Any comagmatic extrusive rocks that may have been present have been removed by erosion. Hydrothermal breccias, containing both igneous and sedimentary fragments in a matrix of rock flour, are widely developed, both within the stock and at its margins. The breccias have the form of irregular pipes and dikes that exhibit widths from tens of meters down to a few centimeters (Grant et al. 1977, 1980). The intrusive porphyry and some of the adjacent sedimentary rocks show pervasive sericitic alteration, whereas the breccias are mainly altered to quartz and tourmaline (Sillitoe et al. 1975). Beyond the main zone of sericitic alteration, chlorite occurs as a replacement of mafic minerals in porphyry dikes.

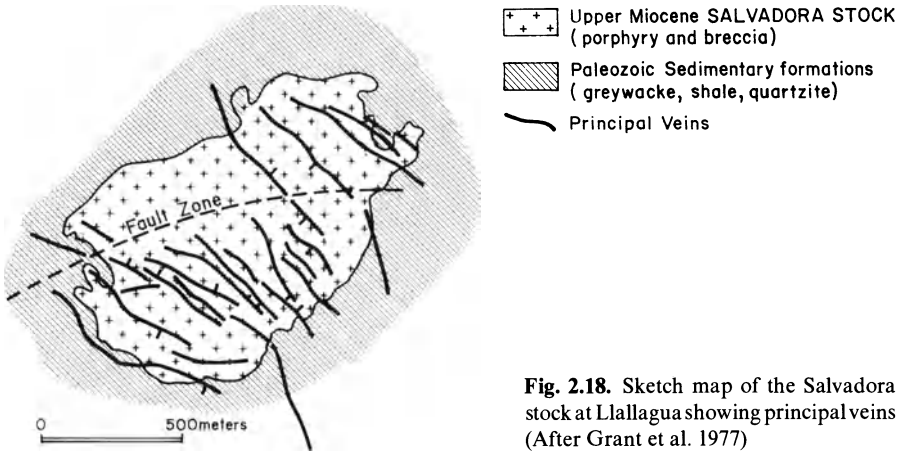

Fig. 2.18. Sketch map of the Salvadora stock at Llallagua showing principal veins (After Grant et al. 1977)

Bulk mineralization at Llallagua consists predominantly of cassiterite and pyrite in a stockwork of veinlets, and as disseminations in altered rocks. Mineralized fragments in breccias and mineralized veinlets that cut breccia indicate that brecciation was both preceded and followed by mineralization events. Tin values appear to be higher in the breccias, especially as replacements along fragment rims, but Sillitoe et al. (1975) report that the stock and breccias average 0.3% Sn. There is local evidence that pyrite is more concentrated around the margins of the deposit in a manner reminiscent of the pyritic halos around porphyry copper deposits.

In addition to this porphyry-type tin mineralization, the Salvadora stock is also cut by a series of northeast-trending veins (see Fig. 2.18) that postdate both sericitic alteration, brecciation, and bulk mineralization. These quartz veins exhibit an early stage of bismuthinite-cassiterite deposition followed by pyrrhotite and frankeite, and finally stannite, sphalerite, and chalcopyrite. A late-stage alteration of the pyrrhotite to pyrite-marcasite-siderite, similar to that reported by Kelly and Turneaure (1970), is also evident, and there is a group of late veinlets that contain sphalerite, siderite, fluorite, and hydrous phosphates.

Fluid inclusion studies of the Llallagua hydrothermal system (Grant et al. 1977) indicate temperatures of approximately 400° C and salinities of less than 26 wt% NaCl. Both temperature and salinity of the fluids tended to decrease as the system evolved (Fig. 2.19), but maximum temperatures and salinities are lower than those reported by Grant et al. (1980) for the Chorolque system. The observations of Sillitoe et al. (1975) and the more detailed studies of Grant et al. (1980) on porphyry tin mineralization in Bolivia have led to the formation of a comprehensive genetic model for these deposits (Fig. 2.20). Based on their detailed geologic, alteration, fluid inclusion and stable isotope studies, Grant et al. (1980) envisage four stages in the evolution of such systems. The intrusive

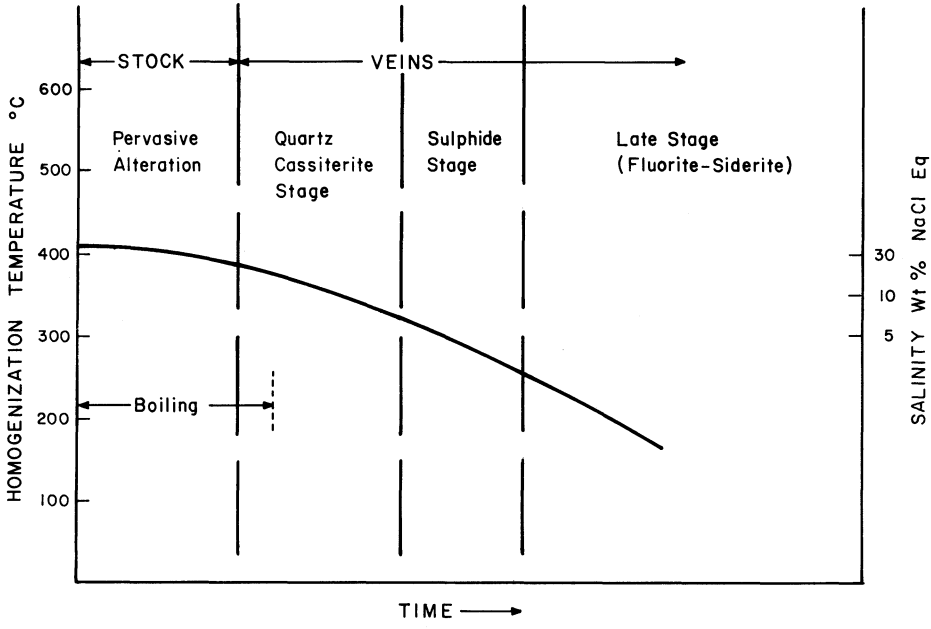

Fig. 2.19. Summary diagram of fluid inclusion data for the Llallagua hydrothermal system (After Grant et al. 1977)

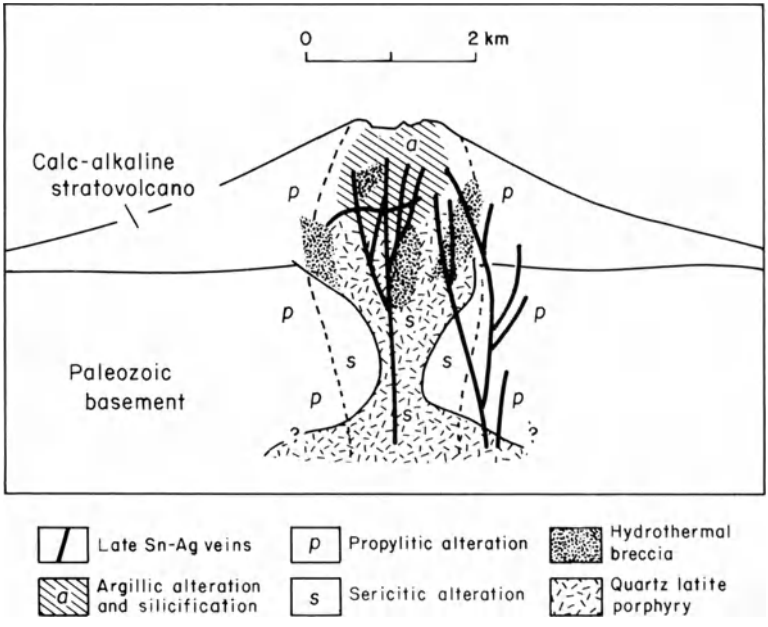

Fig. 2.20. Generalized model for the development of porphyry tin deposits. Note the broad similarity to that suggested for porphyry copper deposits (After Sillitoe et al. 1975)

and hydrothermal events which they detail are remarkably similar to those postulated for porphyry copper systems, in particular the brecciation and fracturing events, the evolution of high salinity and high temperature magmatic fluids, and the later involvement of a meteoric water convection system. However, the main precipitation of cassiterite takes place under conditions of dropping temperature and hence the tin mineralization is associated with sericite rather than K-silicate alteration (see Grant et al. 1980). Another difference of note is that the porphyry tin ores are cut by later quartz-cassiterite vein ores that were the primary focus of mining activity prior to recognition of the bulk-tonnage mineralization (see Fig. 2.20).

2.4.3 Discussion and Suggestions for Exploration

As emphasized above, the tin and/or tungsten deposits that form in backarc environments embrace a variety of deposit types from porphyries to pipes, skarns, and veins. In view of this fact, and the possible association of some deposits with highly evolved I-type granitic intrusives and others with more prevalent S-types, it is not possible to view them as a cohesive group, other than that most deposits occur on the innermost side of the backarc environment (see Mulligan 1971).

From an economic standpoint, large skarn and porphyry-type deposits amenable to bulk mining techniques are clearly the most important, given viable tin prices. In terms of future discoveries, it seems likely that the major potential lies with skarn and limestone replacement deposits, for they form in somewhat deeper environments, have less vertical extent and less obvious peripheral alteration than porphyry deposits. The existence of blind skarn and carbonate replacement orebodies is thus more likely. Porphyry tin deposits, on the other hand, are emplaced at shallow subvolcanic levels, and are thus susceptible to removal by erosion. The mid-to late-Tertiary age of all the known examples of porphyry tin mineralization (Grant et al. 1979) is in accord with this observation. Additional examples of such deposits may lie buried beneath the two substantial areas of Neogene ignimbrites present in the central parts of the Bolivian tin belt (see Fig. 2.15), but exploration for these would be difficult.

Exploration for blind tungsten skarn deposits would also be extremely challenging, unless there are sufficient associated sulfides to generate conductivity anomalies that could be sought using appropriate geophysical techniques. The margins of small and intermediate size stocks intruded into carbonate terranes along the innermost zones of backarc regions should be optimum areas to concentrate such exploration efforts.

2.5 Backarc Gold Deposits

A small but important group of gold deposits has been recognized that is associated with alkalic igneous rocks such as syenite, trachytes, and phonolites, (Giles 1982; Mutschler et al. 1985; Bonham 1986). The major examples of this class of gold deposits are Cripple Creek, Colorado (Thompson et al. 1985) and possibly the Emperor deposit, Fiji (Colley and Greenbaum 1980; W.B. Anderson et al. 1987; Ahmad et al. 1987), but a number of additional deposits are known in the alkalic province of Montana, in Colorado, and in New Mexico. Noteworthy are Zortman-Landusky, Montana (Hastings 1987), the La Plata district, Colorado (Saunders and May 1986), Jamestown, Colorado (Nash and Cunningham 1973), and Ortiz, New Mexico (Wright 1983). The almost 21 million oz of gold produced at Cripple Creek, however, make it the overwhelmingly important example of alkalic-type gold deposits.

The most prominent geochemical feature of many of these deposits is the occurrence of much of the gold in the form of Au-Ag tellurides. The minor importance of base metal sulfides, and the common presence of fluorite as a gangue mineral are also characteristic features. The Cripple Creek and Emperor deposits are associated with explosive volcanic settings (Sillitoe and Bonham 1984), but others such as the Zortman-Landusky deposits were emplaced in intrusive syenite.

Studies of the Cripple Creek deposit by Thompson et al. (1985) have done much to further understanding of the whole ore-generating system. At approximately 30 Ma, explosive alkalic volcanism generated a nested diatreme-intrusive complex that became host to the gold deposits (Fig. 2.21). The igneous activity involved two magma types, phonolite and alkali basalt, and intermediate types apparently created by magma mixing. Attendant on some of the phases of volcanic activity was major subsidence, and as a result basins above or on top of the diatreme complex were formed and filled with fluvial-lacustrine sediments (see Fig. 2.21).

The gold ores can be divided into vein type and bulk tonnage, breccia-hosted type. Results of studies on the vein-type ores of the Ajax mine (Thompson et al.1985) indicate that gold deposition occurred over a vertical interval of $>$ 1000 m with little apparent change in gold tenor (20–30 g/ton). The vein system cuts both the granodiorite Precambrian country rocks and the Cripple Creek breccias, although veins occur as narrow, well-defined sheeted zones in the former, and change to broader zones of irregular branching fractures in the latter. Wall-rock alteration is of limited extent and occurs as an inner zone composed of secondary K-feldspar, dolomite, vanadium mica, and pyrite, surrounded by an outer zone in which sericite, montmorillonite, magnetite, minor K-feldspar, and pyrite are developed. Paragenetic studies indicate five stages of vein filling with the deposition of gold tellurides restricted to stage four.

Fluid inclusion studies on quartz, fluorite, and sphalerite indicate that vein filling was initiated by high salinity fluids (30–40 equiv. wt% NaCl) of rather variable temperature (200–500°C), and that salinities and temperatures

decreased with time. During stage 4 gold telluride deposition, temperatures had declined to about 140°C, and salinities of the ore fluids ranged from 1.4–3.5 equiv. wt% NaCl. Observations of the fluid inclusion populations suggest that the fluids were weakly boiling during their ascent, and clathrate melting temperatures indicate CO_2 pressures of 44 bar during stage 3 and 4 deposition (Thompson et al. 1985).

The Globe Hill bulk-tonnage ores (see Fig. 2.21) are hosted within an alkali trachyte intrusive rock that intrudes the Cripple Creek breccia. At Globe Hill, Thompson et al. (1985) recognize a series of structural events that occurred prior to mineralization. These include formation of breccia bodies, faulting, and finally formation of a vertical pipe-like mass of intense hydrothermal brecciation. Alteration and mineralization events, each somewhat distinctive, accompanied each structural stage; however, gold mineralization is largely restricted to stage 1 and 2 structures.

The gold ores of the Cripple Creek camp thus occur both within vertically extensive vein systems and within shallow breccia bodies and were formed subsequent to mid-Tertiary diatreme development. CO_2 pressures were relatively high during hydrothermal activity, and at shallower levels where the vapor-dominated system became overpressured, significant development of hydrothermal breccias resulted. These breccias became sites for fluid channeling with consequent alteration and mineralization.

2.5.1 Discussion

The association of distinctive gold telluride ores with alkalic igneous activity in backarc belts in western North America strongly suggests a tectonomagmatic control of this type of mineralization. It could perhaps be argued that these deposits are more properly connected to mid- to late-Tertiary rifting events (Van Alstine 1976), but some deposits are both clearly older than the onset of rifting and also distant from the Rio Grande rift system and its northern extensions (Werle et al. 1984). It is also noteworthy that the Allard syenite stock, in the La Plata gold-telluride district (Saunders and May 1986), is at the southwestern extremity of the Colorado Mineral Belt, whereas the Boulder County gold telluride deposits (Kelly and Goddard 1969) are at the northeastern extremity. Furthermore, there is no recognized association of gold ores with rift-type alkalic magmatism.

Based on studies of the Allard stock in the La Plata district of Colorado and analogies to alkaline suite porphyry copper deposits in British Columbia, Werle et al. (1984) have suggested that epithermal gold telluride deposits in subvolcanic settings may grade downward into alkalic porphyry copper-precious metal deposits. Fluid inclusion studies of alkaline gold deposits (e.g., Nash and Cunningham 1973; Thompson et al. 1985) indicate the participation of saline fluids of probable magmatic origin during the early stages of hydrothermal activity, and the late-stage gold telluride deposition in the systems is presumably of similar origin.

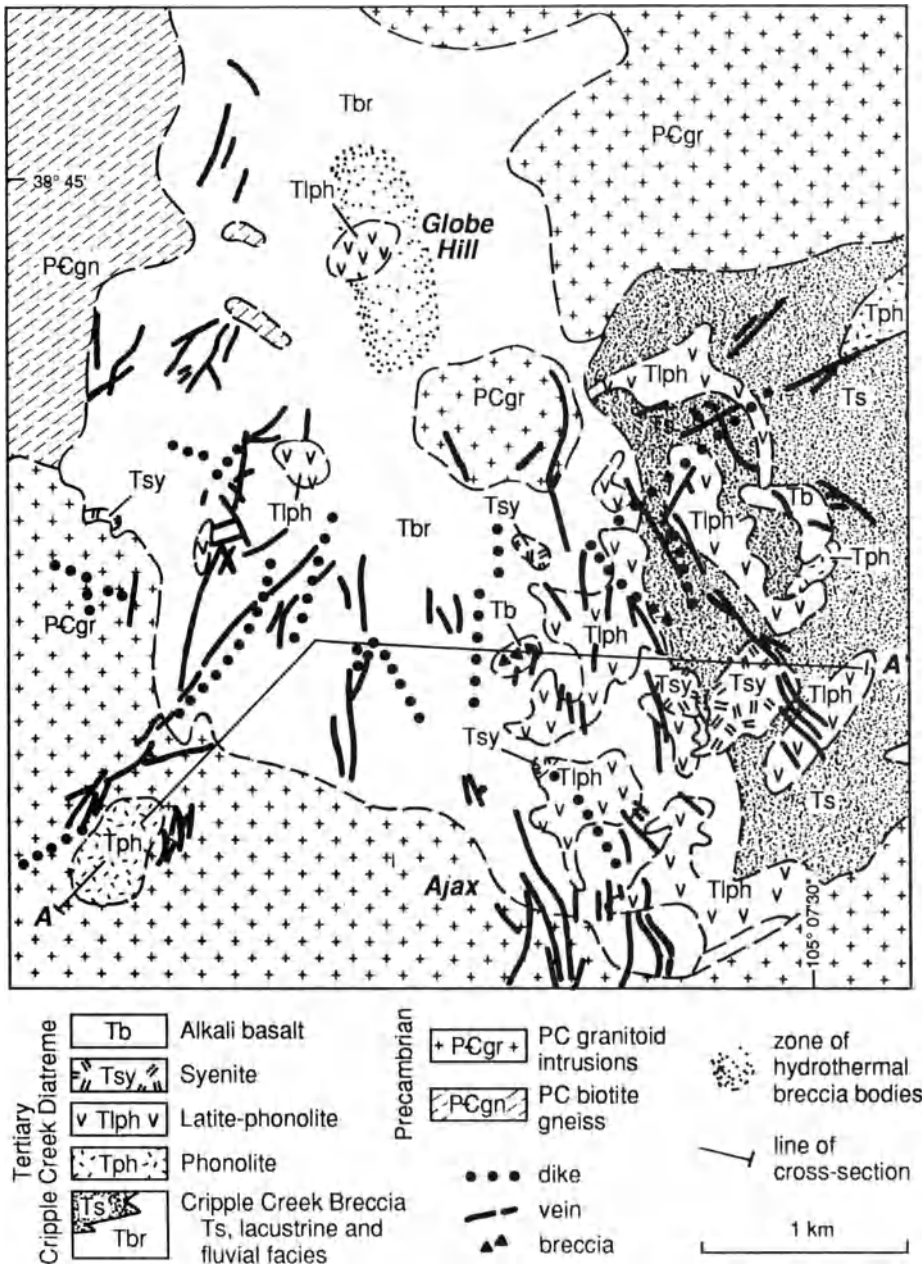

Fig. 2.21a. Simplified map and **b** cross-section of the Cripple Creek district, Colorado, which is hosted in a diatreme complex (After Thompson et al. 1985)

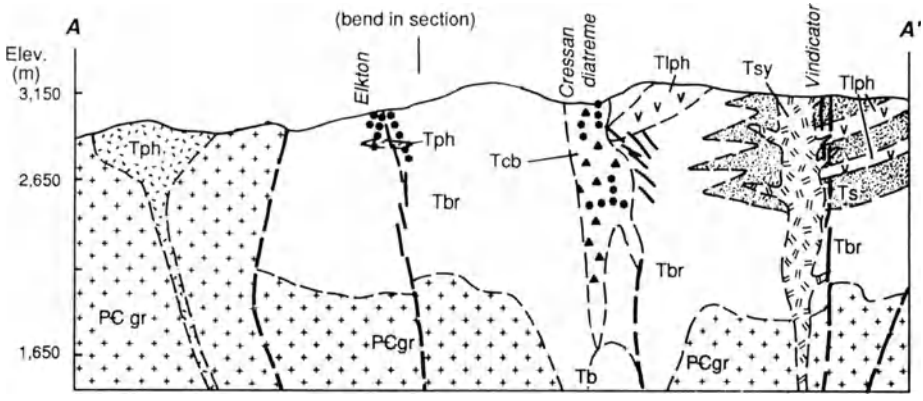

Fig. 2.21b

Recent studies of the Emperor mine, Vatukoula caldera, Fiji (Ahmad et al. 1987) have provided a considerable body of data pertaining to the formation of this alkalic-type gold deposit, developed in an oceanic setting. The ore fluids ranged in temperature from 150–300°C, and in salinity from 5–7 equiv. wt% NaCl, and on the basis of stable isotope analyses are of basically magmatic origin with a component of admixed seawater. The only other stable isotope data available at present for alkalic-type Au deposits pertains to the Golden Sunlight breccia-hosted ores in southwest Montana. Porter and Ripley (1985) report oxygen, hydrogen, and sulfur isotope data from this deposit that all point to a magmatic-hydrothermal origin for the gold mineralization.

Chapter 3 Metal Deposits of Arc-Related Rifts

As discussed briefly in the introductory chapter, the development of extensional tectonic regimes behind or within convergent plate boundary arcs is not an uncommon phenomenon (Vine and Smith 1981). Such regimes develop more readily perhaps in or behind island arc systems constructed in oceanic settings, or adjacent to, rather than within continental margins. However, the extensional tectonics that characterize the western United States and northern Mexico after about 30 Ma ago may in part represent an example of this same phenomenon developed within the continental portion of the North American plate (Keith 1978; Eaton 1979; Lipman 1980). Lorenz and Nicholls (1976) have suggested that an environment similar to that of the Basin and Range was maintained during Permian time in central and western Europe, although it was clearly less significant in metallogenic terms. In the case of the Andes of South America, extensional regimes are only well documented in the extreme south, where the Rocas Verdes terrane is representative of a Cretaceous arc-related rifting event (Dalziel 1981).

Modern examples of arc-related rifts are most clearly represented by the current rifting activity in certain of the western Pacific volcanoplutonic arc systems (Karig 1971). Of particular interest is the Lau Basin, an active rift in the Tonga-Kermadec arc system, for at its southern extremity this extensional feature, the Havre Trough, crosses from oceanic to continental crust (Cole 1984), and becomes the Taupo-Rotarua depression (Taupo Volcanic Zone) on the North Island of New Zealand (Fig. 3.1).

3.1 The Taupo Volcanic Zone, New Zealand

The Taupo Volcanic Zone has attracted the attention of volcanologists, geothermal engineers, hydrologists, and geochemists because of historic volcanic activity (Cole 1979; C.J.N. Wilson et al. 1984), and because of the abundant geothermal systems that occur within it (Henley and Ellis 1983). More recently, the Taupo Zone has attracted the attention of economic geologists, not only because of gold deposition in surface hot-spring environments (Weissberg 1969), but also because they see the geothermal systems as modern replicas of epithermal precious metal ore-generating systems (Henley 1985; Krupp and Seward 1987).

The Taupo Volcanic Zone hosts a number of major rhyolitic ash-flow calderas within which the large majority of New Zealand geothermal fields are

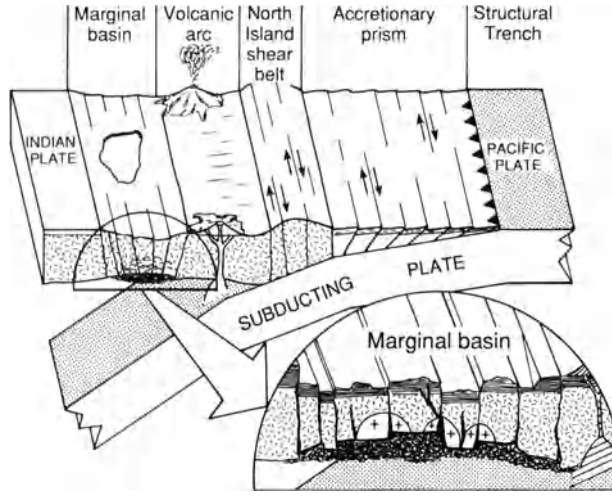

Fig. 3.1. Schematic block diagram illustrating the various tectonic components present in North Island, New Zealand, and the area to the north including the Lau Basin (After Cole 1979)

sited (Fig. 3.2). The felsic volcanics, which were virtually all erupted within the last 1 Ma, overlie a basement composed of late Paleozoic and Mesozoic graywacke and shale, and the caldera structures are clearly controlled by crustal extension related to the southward continuation of the Lau Basin-Havre Trough (Cole 1979). C.J.N. Wilson et al. (1984) estimate that a volume of rhyolitic material of $> 10^4$ km^3 has been erupted during the last million years at an average rate of 2.27 m^3/s and that this activity still continues. They also estimate that the volume of intruded material is six to seven times that of the extrusions. These estimates imply that a volume of magma of $>$ 60 000 km^3 has been emplaced in the subsurface of the Taupo zone during the last million years.

Current heat flux from the eastern Central Volcanic Region of the Taupo Zone is estimated at $4 \pm 1 \times 10^9$ W (Stern 1987 and references therein). Maintenance of this heat flux for 10 000 years requires a volume of felsic magma in the subsurface of approximately 1000 km (Hochstein 1976). Empirical evidence for the presence of these magmas is provided by ^{3}He anomalies in the gases collected from the geothermal systems (Hulston et al. 1986; Sano et al. 1987).

Studies of obsidian and glass inclusions in pyroxene phenocrysts (Hervig et al. 1986) indicate that at least some of the Taupo magmas contained 2.5–4.0 wt% H_2O, 0.18–0.24 wt% Cl, 400 ppm F, and $<$ 200 ppm S. These data indicate potential for a significant magmatic flux into the base of the large meteoric water systems that are currently active in the Taupo Volcanic Zone.

The recognition of small sinter deposits containing precious metals at ore-grade levels (Weissberg 1969) within the Waiotapu geothermal system has been followed by additional discoveries of precious metal-rich sinters in other geothermal systems associated with the Maroa caldera (see Fig. 3.2). Krupp and Seward (1987) suggest that the sulfur-rich Rotokawa geothermal system could have transported and deposited over 50 metric tons (1.7 million troy ounces)

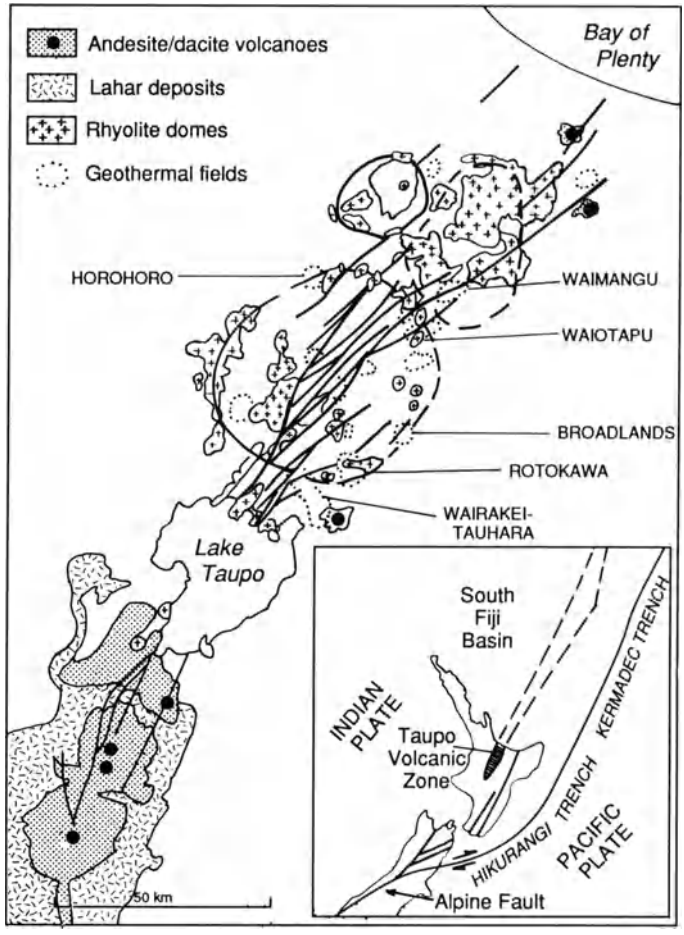

Fig. 3.2. Map of the Taupo Volcanic Zone, North Island, New Zealand. Note that this zone is the continental crustal equivalent of an extending intra-arc basin (After Krupp and Seward 1987)

of gold since the craters that are now occupied by Lake Rotokawa were formed by hydrothermal explosions approximately 6000 years ago.

The subsurface conditions in the Taupo geothermal fields are known mainly from drilling to exploit thermal energy, but close monitoring of these boreholes and study of the materials retrieved from them have allowed workers to reconstruct the subsurface anatomy, mineralogy, and geochemistry of the systems in some detail (Fig. 3.3). One of the most important results of this work has been the realization that these geothermal systems are close analogs of the conceptual models developed from well-documented epithermal systems (Henley 1985 and references therein).

Despite the close similarity between explored geothermal systems in New Zealand and elsewhere, genetic models for epithermal gold and silver deposits based solely on concepts of fluid chemistry need to be approached with

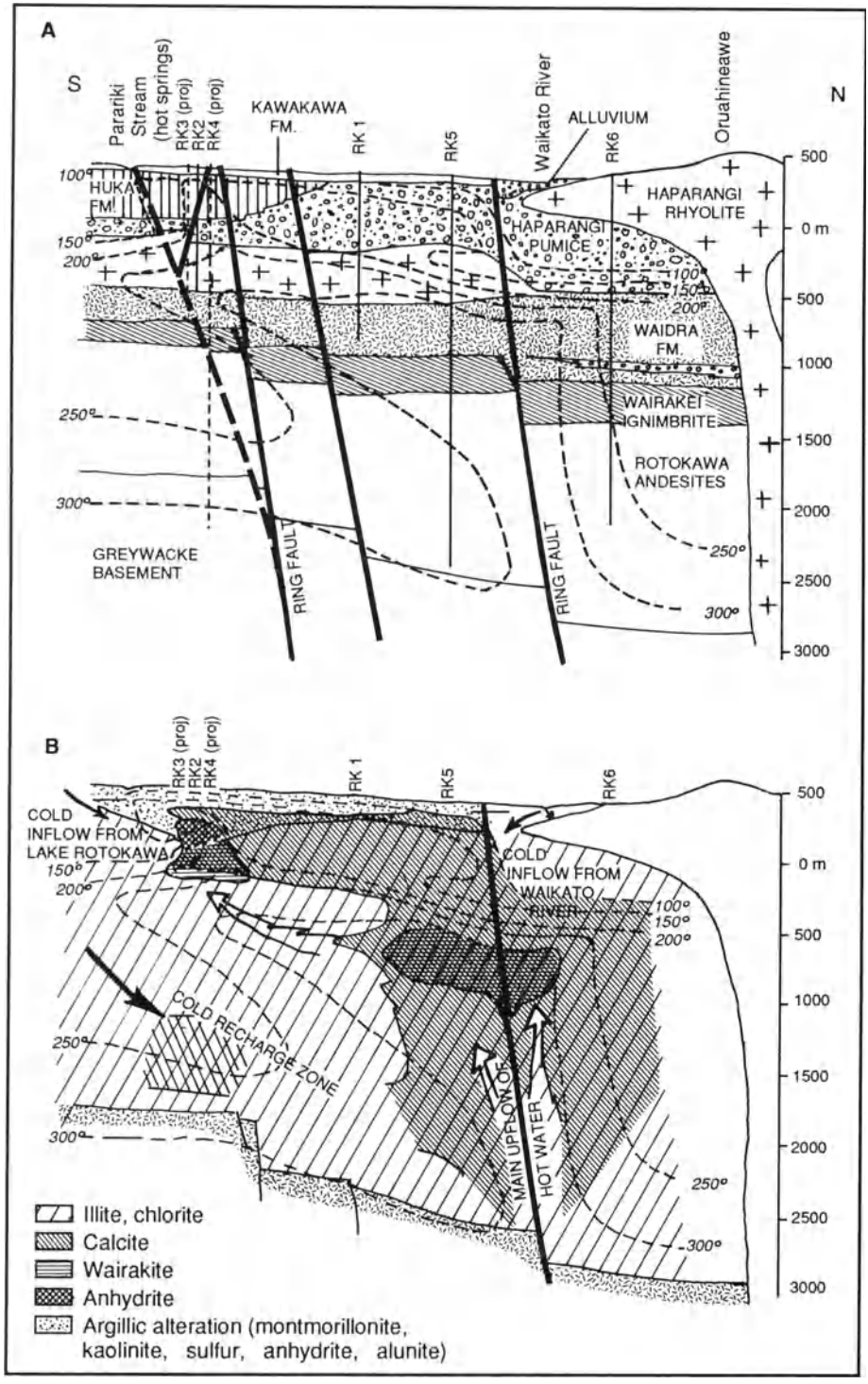

Fig. 3.3. North-south cross-section through the Rotokawa geothermal field, Taupo Volcanic Zone, New Zealand. **A** Section showing stratigraphy, faults and isotherms. **B** Wall-rock alteration and fluid flow paths for the same section. Data are based on study and monitoring of numerous drill holes, some of which are shown (After Krupp and Seward 1987)

caution, for additional factors such as availability of metals and plumbing systems are critical constraints on ore-generating systems. Thus, despite active exploration and study of geothermal systems, significant occurrences of subsurface mineralization in modern examples have proved to be elusive. As noted in this volume, many of the richest epithermal systems have strong magmatic antecedents, and occur within principal arc or backarc environments, as well as in arc-related rifts. It must be acknowledged, however, that all three of these geotectonic elements spawned by plate convergence are transitional to one another.

In terms of the geologic and ore-deposit record, the current hydrothermal activity in the North Island, New Zealand is perhaps more pertinent to exhalative types of metal deposits. These will be discussed in Section 3.4 of this chapter and in Section 4.6.1 of the following chapter.

3.2 Climax-Type Porphyry Molybdenum Deposits

A significant fraction of world molybdenum production comes from a series of large molybdenum deposits that are spatially associated with the Rio Grande Rift System and/or the Colorado Mineral Belt (Fig. 3.4). The northeast-trending Colorado Mineral Belt (Tweto and Sims 1963; Warner 1978) is recognized as a major crustal zone of weakness of considerable antiquity, and fault activity along it dates back to at least 1.7 Ga. Bookstrom (1981) notes that both Precambrian and Tertiary igneous and metamorphic rocks along the Colorado Mineral Belt exhibit significant enrichments in molybdenum, and suggests the existence of a Colorado molybdenum province.

The major molybdenum deposits are associated with a series of high-silica, alkali-rich rhyolite porphyries, emplaced between 33 and 17 Ma ago as composite stocks. Compositionally, these intrusions are distinct from the calc-alkaline intrusives associated with molybdenum-dominated variants of porphyry copper deposits in principal arc systems (Sillitoe 1980a). In addition, Climax-type molybdenum porphyries tend to contain substantially higher grades than arc-type molybdenum porphyries.

The generation of the alkali-rich rhyolitic igneous rocks with which Climax-type molybdenum deposits are associated in time and space (see Fig. 3.4) is apparently related in some manner to a transition stage between decreased convergence and the onset of true backarc rifting in an area which is now 1000 km or more inboard from the western continental margin (Fig. 3.5). W.H. White et al. (1981) envisage that this transition occurred in the Rocky Mountain region about 30 Ma ago, and involved steepening of the underlying slab and concomitant uprise of mafic asthenospheric material in the backarc region. Heat from these mafic magmas caused low-volume fractional melting in previously depleted portions of the lower crust to produce rhyolitic magmas enriched in lithophile elements. W.H. White et al. (1981)

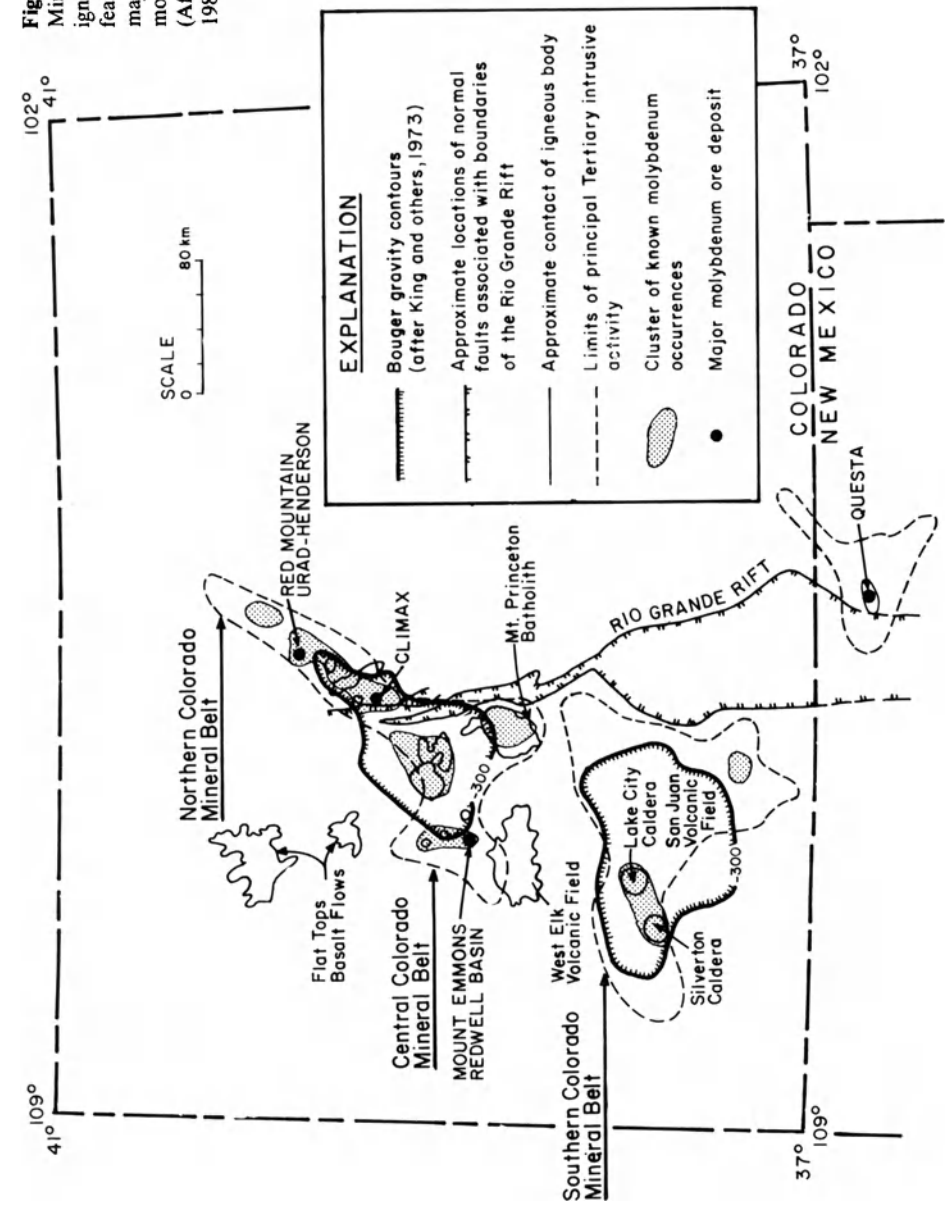

Fig. 3.4. Map of Colorado Mineral Belt showing major igneous and structural features, and location of major porphyry molybdenum deposits (After W.H. White et al. 1981)

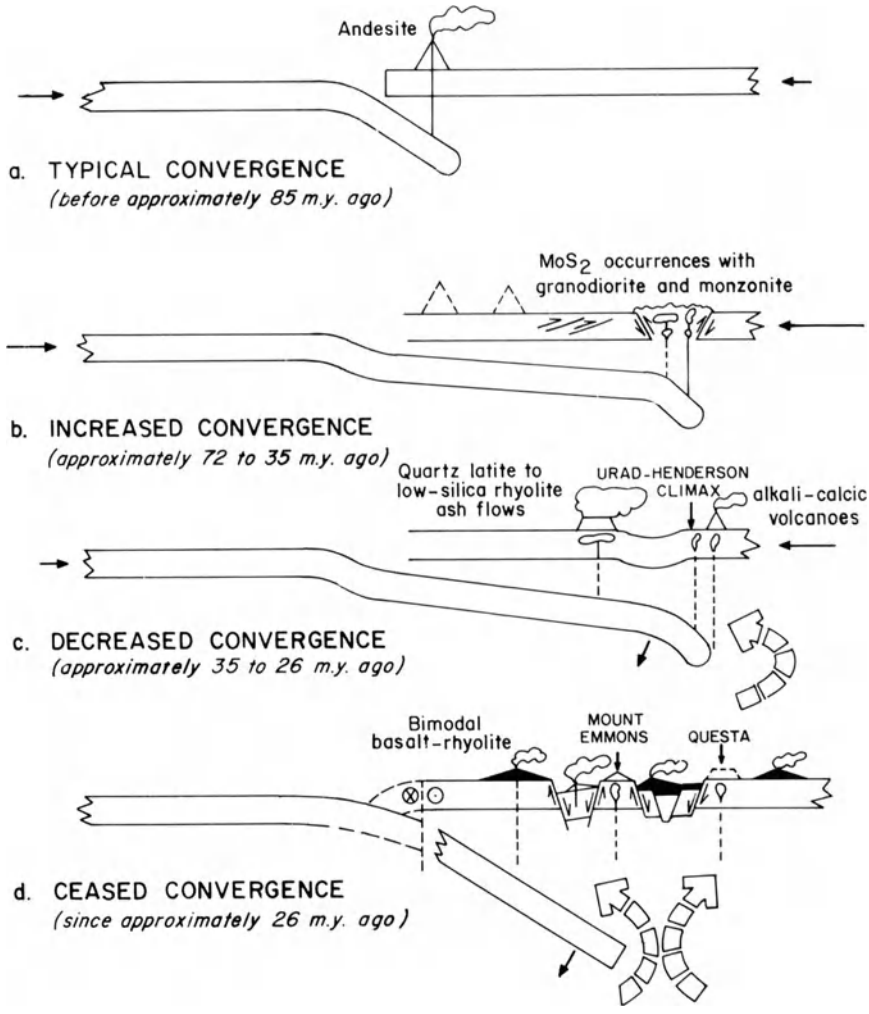

Fig. 3.5. Hypothetical plate tectonic cross-sections showing inferred changes in subduction, tectonism, and magmatism in the Colorado Rocky Mountain region in relation to the generation of porphyry molybdenum deposits (After Bookstrom 1981)

further postulate that repeated diapiric uprise of these magmas from the lower crust gave rise to the mineralized igneous complexes of Climax type.

The important porphyry molybdenum deposit of Questa, New Mexico formed 22 Ma ago at the intersection of the Rio Grande Rift and the northeast-trending Jemez lineament, locus of an earlier belt of calc-alkaline igneous activity (see Bookstrom 1981). The Mt. Emmons molybdenum porphyry system (17 Ma), formed within the Colorado Mineral Belt after the inception of rift-related basaltic volcanism.

3.2.1 Mineralization and Alteration Patterns

Climax-type molybdenum deposits are lithophile element-enriched deposits (tungsten, tin, uranium, niobium, tantalum) that contain essentially no copper. The orebodies consist of zones, typically in the form of inverted bowls, of intersecting stockwork veinlets of quartz and molybdenite. Mineralization is concentrated just above or within the uppermost portions of specific porphyry intrusions, and at both Climax and Urad-Henderson successive mineralization events are related to successive porphyry intrusive events (Fig. 3.6).

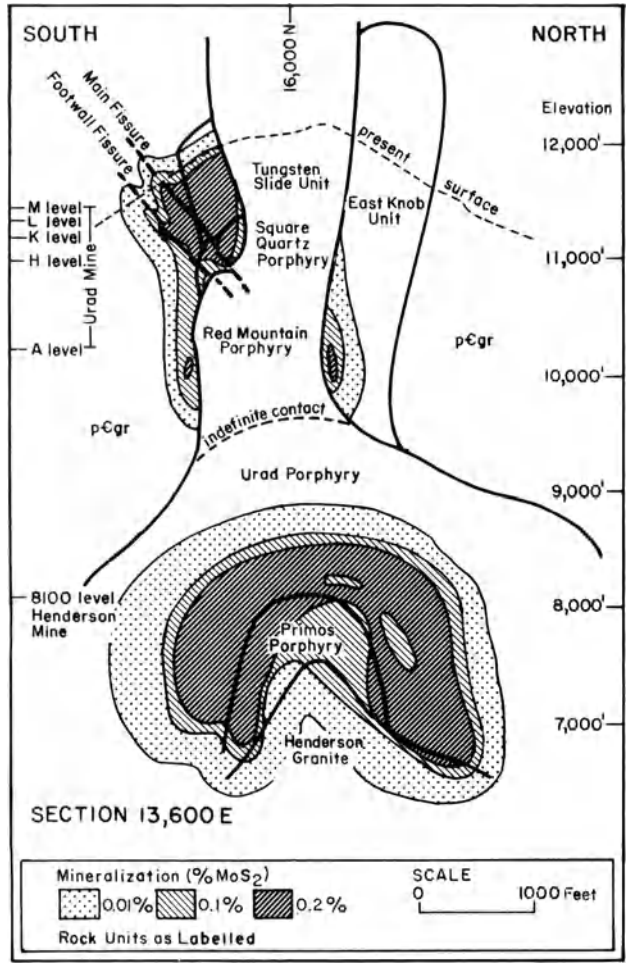

Fig. 3.6. Diagrammatic section showing the geologic relationships of the various intrusive units and their associated mineralization in the Urad-Henderson porphyry molybdenum district, Colorado (After Wallace et al. 1978)

In general, the molybdenite contained in the stockwork quartz veinlets is very fine-grained and intimately intergrown with quartz and lesser amounts of sericite, pyrite, and fluorite. In the deeper-seated mineralization of the Henderson orebody (see Fig. 3.6), the major proportion of the molybdenum is in veinlet form, but within the Henderson granite molybdenite occurs as clots and rosettes along veinlet walls and disseminated within greisen-type pods and segregations (Wallace et al. 1978).

Pyrite is the most common sulfide mineral in these deposits. It occurs predominantly above and peripheral to ore zones and may reach concentrations of 10 vol % locally. Where pyrite and molybdenite occur together, pyrite veinlets commonly cut molybdenite-bearing veinlets. Wallace et al. (1978) conclude that during the formation of the Henderson orebody, the molybdenite and pyrite were deposited simultaneously in their respective zones and the apparent age difference was caused by the innermost edge of the pyrite zone impinging on the outermost portion of the molybdenite zone during inward collapse of both zones. Other minor minerals associated with this group of deposits are mainly huebnerite, magnetite, hematite, sphalerite, galena, and chalcopyrite, but in all cases except at Climax, molybdenite was the only mineral recovered. At Climax, however, there was recovery of huebnerite, and lesser amounts of cassiterite and monazite, in addition to molybdenite and secondary molybdenum oxide minerals (Wallace et al. 1968).

Zonal patterns of hydrothermal alteration types are less pronounced in Climax-type molybdenum deposits, presumably because the multiple intrusion-mineralization events that characterize these deposits tend to obscure simple alteration zoning patterns. Alteration phases include quartz, potassium feldspar, sericite, and fluorite, accompanied locally by lesser amounts of clay minerals, rhodochrosite, biotite, chlorite, and epidote.

In the Henderson orebody, complexities due to multiple intrusion-mineralization events and shallow meteoric water circulation events are minimal, and here, MacKenzie (1970) was able to decipher the principal zones of alteration (Fig. 3.7). The major alteration event produced a central zone of potassium feldspar alteration, including a biotite subzone and a silicified zone, succeeded progressively outward by a quartz-topaz zone, a sericite-quartz-pyrite zone, an argillic zone, and a broad zone of propylitic alteration. This series of alteration events was followed by a much weaker alteration consisting of a greisen zone overlain by an argillic zone. This later event is thought to be related to the Henderson granite. The major alteration zoning at Henderson is thus analogous to that characterizing porphyry copper deposits.

Fluid inclusion studies of the Henderson deposit (Kamilli 1978; W.H. White et al. 1981) indicate a temperature range of 500–650°C during the quartz-molybdenite stage of mineralization to 250°C in the final stage. Three types of inclusions were found: liquid-rich inclusions containing 30–65 equiv. wt% NaCl and numerous additional daughter minerals; vapor-rich inclusions containing 5–20 equiv. wt% NaCl; and very low salinity (< 2 equiv. wt% NaCl) liquid-rich inclusions. Investigators have concluded that much of the intense

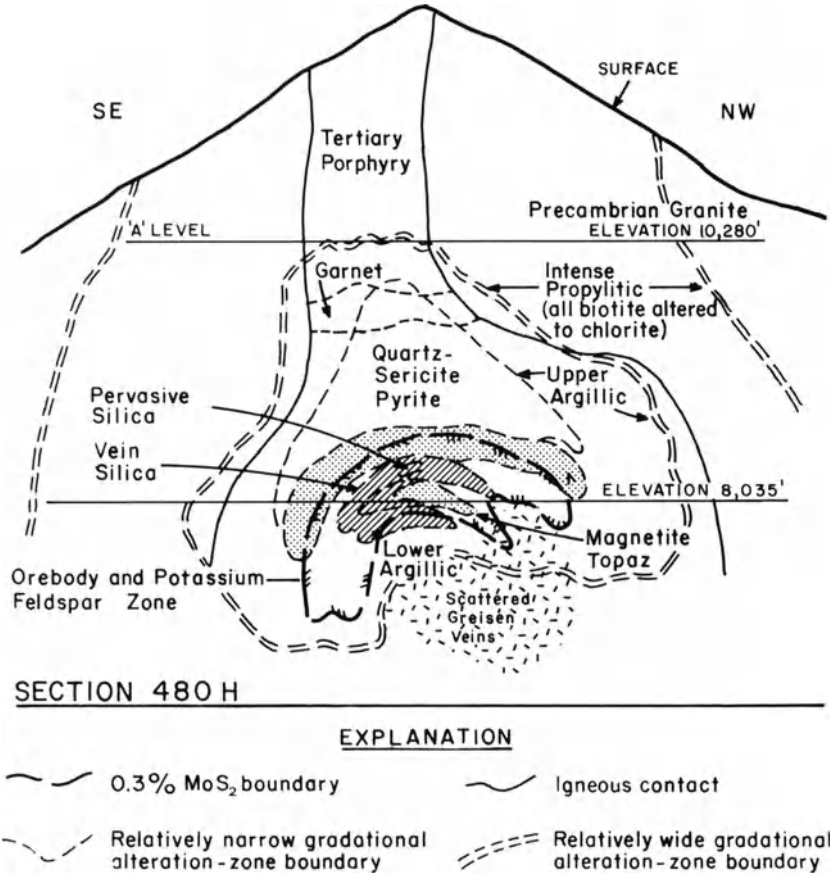

Fig. 3.7. Section through the Henderson deposit illustrating the spatial relationships of the alteration zones associated with development of the molybdenum porphyry orebody (After W.H. White et al. 1981)

fracturing was caused by the high vapor pressures of the evolving hydrothermal fluids, and that the average temperature of quartz-molybdenite mineralization was at least 500°C.

More recent studies of the fluid inclusion assemblages in minerals from the Henderson deposit (Carten et al. 1988) have indicated the evolution of two immiscible liquids in the apices of stocks, one Cl-rich and the other F-rich. The Cl-rich liquid can be extremely saline (62 equiv. wt% NaCl) and together with its associated Na, K, Fe, and Mn apparently evolved directly from the magma. The F-bearing aluminosilicate liquids are found in areas characterized by pegmatitic textures and inclusions containing them exhibit abundant mica-like daughter minerals. Carten et al. suggest that each liquid was responsible for different aspects of mineralization and alteration at Henderson, but that the molybdenum ores were formed from the F-rich liquids.

Stein and Hannah (1985) report lead, oxygen, and sulfur isotope data obtained from the Henderson system that convincingly demonstrate that the metals and sulfur were derived "in toto" from within the Tertiary age Henderson magmatic system. They also conclude that country rocks at the upper crustal level and meteoric water played no role in the ore-forming process.

3.2.2 Discussion and Suggestions for Exploration

Although Climax-type molybdenum deposits occur predominantly within a relatively limited area of the western United States and were emplaced during a time interval of approximately 20 million years, their economic importance justifies their designation as a distinctive metal deposit type. Furthermore, their association with an intrusive suite of alkali-rich, high-silica rhyolites, which can be related to the initiation and development of arc-related rifting is reasonably clear-cut. Whether similar deposits have been generated at other places and times during continental evolution is not clear, but some of the molybdenum porphyry deposits in China seem to be representative of this type (Sillitoe, pers. comm).

Westra and Keith (1981) reviewed the relationship between magma chemistry and porphyry molybdenum deposits, and demonstrated that a convincing interdependence between magma chemistry, degree of lithophile metal enrichment, and tectonic setting is exhibited by the three main subtypes of porphyry molybdenum deposits (Fig. 3.8). They concluded that the differences between Climax-type deposits and their calc-alkaline and alkalic counterparts result from initial magma chemistry and the subsequent evolution of the magmatic hydrothermal system. They also posit a subcrustal source for the major constituents in such systems, based on isotope considerations. This important contribution by Westra and Keith not only adds substantially to the understanding of porphyry molybdenum deposits but also convincingly demonstrates that when the empirical data base is sufficiently broad, as for western North America, the relationships between certain deposit types and coeval plate tectonic activity emerge with enhanced clarity.

The importance of the systematics detailed above to the exploration geologist is self-evident, and it is probably true to say that the impressive increase in molybdenum resources in North America during the past decade has in some measure resulted from the utilization of these systematics. On a more specific level, the recognition that many Climax-type molybdenum deposits contain a series of vertically stacked ore zones is critical in planning drilling programs on prospects, especially where there is evidence of multiple intrusive events. The search for blind molybdenum porphyries is more difficult, but attention to the occurrence of high-level, alkali-rich rhyolite intrusions or near-vent volcanics of similar composition, and careful evaluation of distal alteration zones is required. The recent discovery of three separate ore zones at Mt. Emmons (Fig. 3.9) provides an elegant example of the successful application of these principles (Thomas and Galey 1982). Here,

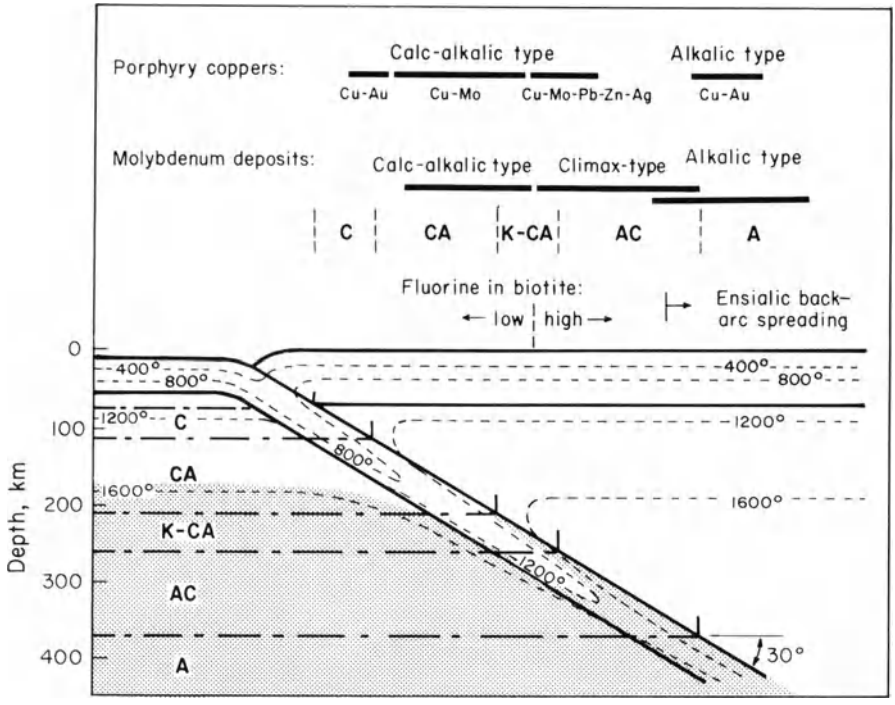

Fig. 3.8. The relationships of porphyry copper and porphyry molybdenum deposits to subduction regime and associated magma chemistry (After Westra and Keith 1981)

the presence of molybdenite in peripheral Pb-Ag veins and in breccia dikes is an important key to underlying molybdenum mineralization. The strong relationship between potassium and molybdenum enrichment emphasized by Westra and Keith (1981) is also of significance in the search for and evaluation of such deposits.

3.3 Additional Lithophile Suite Deposits in Arc-Related Rifts

Sillitoe (1981a) details a series of lithophile suite deposits of somewhat lesser importance than Climax-type Mo deposits that can be associated with arc-related rifting. These include the series of fluorite deposits in northeastern Mexico (Kesler 1977) and along the Rio Grande Rift in the United States (Van Alstine 1976) that, in general, exhibit a relationship with fluorine-rich rhyolite intrusions.

A varied group of lithophile element deposits are also associated with rhyolitic volcanics in arc-related rift settings. These include the numerous small tin deposits associated with the mid- to late-Tertiary rhyolitic ignimbrite

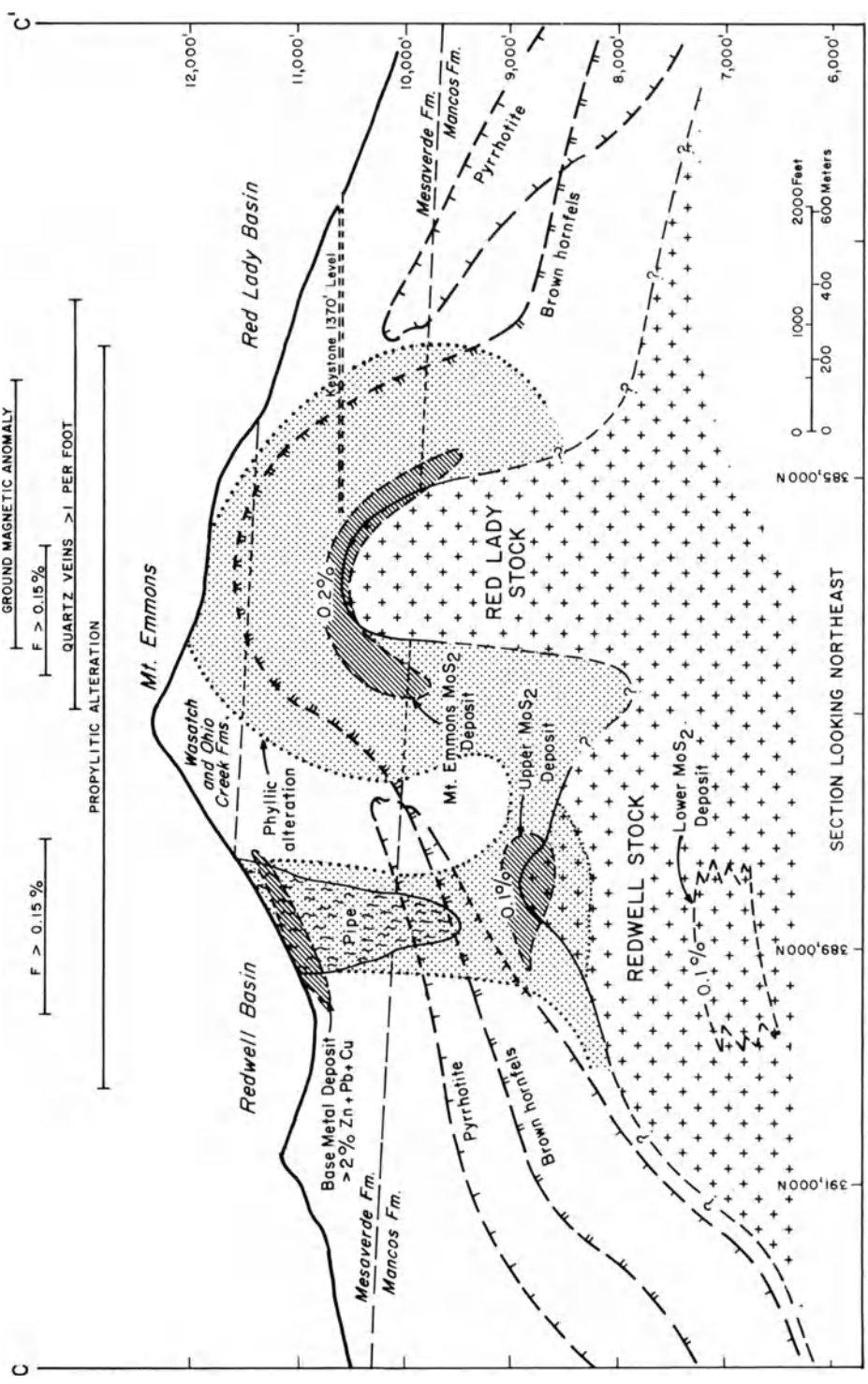

Fig. 3.9. Diagrammatic section showing the geologic relationships of the three porphyry molybdenite deposits of Mt. Emmons. Note that in the case of the Mt. Emmons orebody the present surface only intersects the uppermost edge of the phyllic alteration envelope. This emphasizes the importance of a full understanding of possible alteration envelope geometries in the search for blind porphyry deposits (After Thomas and Galey 1982)

province of west-central Mexico (Lee-Moreno 1980; Huspeni et al. 1984). Mineralization occurs as either cassiterite or wood tin in narrow fissure veins and volcanic breccias or as disseminations in tuffs, and a spatial relationship to volcanic centers is indicated.

An example of uranium and separate mercury mineralization in a caldera setting is provided by the Miocene age McDermitt district on the Nevada-Oregon border (Rytuba 1981; Fig. 3.10), where both the uranium and the mercury deposits occur in caldera-lake tuffs and sediments. Vein deposits of uranium accompanied by fluorite and molybdenum also occur at Marysvale, Utah, and a series of mid- to late-Tertiary beryllium deposits are known in the western United States, although the only one of consequence is that at Spor Mountain, Utah. Here, bertrandite occurs in a large stratabound lens in tuff and breccia associated with topaz rhyolite (Lindsey 1977).

The igneous rocks associated with this diverse group of deposits are almost invariably alkali-rich, high-silica intrusions or extrusions, and it seems clear

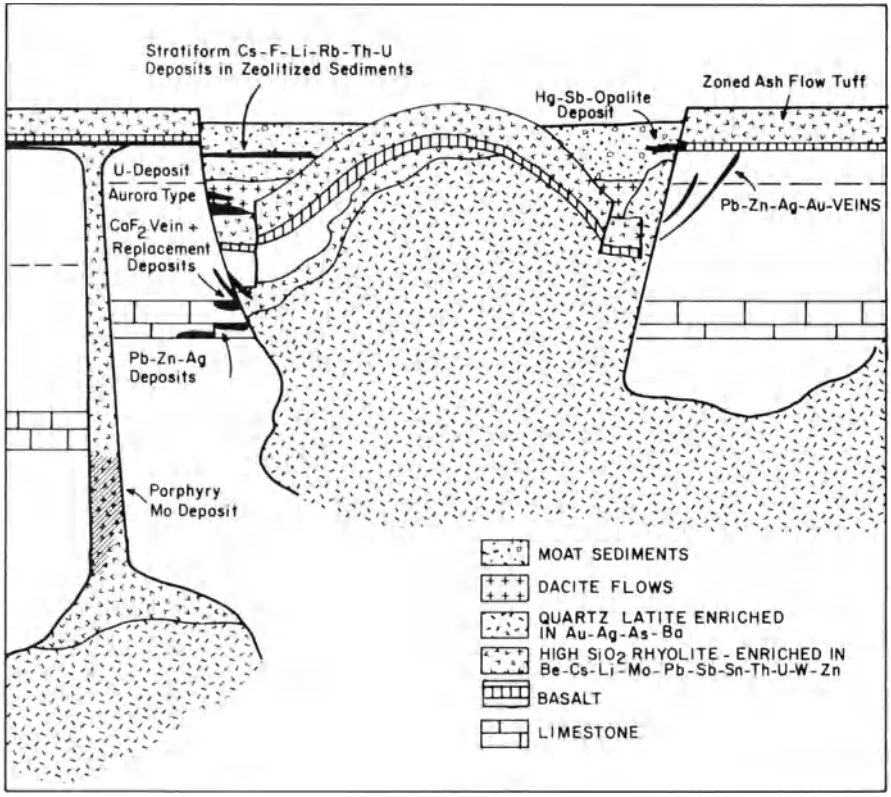

Fig. 3.10. The possible ore deposits that can occur in caldera environments related to high silica, rhyolitic volcanism (see also Sillitoe and Bonham 1984). Based mainly on the McDermit area, Nevada. It should be noted, however, that the McDermit caldera itself contains peralkaline volcanics and these never give rise to base metal deposits (After Rytuba 1981)

that the metals and fluorine involved originated from them, although in at least some instances, circulating meteoric water was probably involved in the ore-forming process. As in the case of Climax-type deposits, all the examples of this lithophile suite are from North America. Whether this area is unique in tectonic and/or lithogeochemical terms, or whether similar provinces elsewhere in the world have yet to be recognized, is unclear at this point in time.

3.4 Kuroko-Type Massive Sulfide Deposits

Polymetallic conformable lenses of massive sulfide ore exhibiting a close stratigraphic relationship to felsic volcanism represent an important and widespread type of metal deposit. The type examples occur within the so-called Miocene Green Tuff belt of Honshu and Hokkaido in Japan (Fig. 3.11), but metal production has been dominated by the cluster of deposits within the confines of the Hokuroku Basin. Essentially similar deposits have been found around the entire Pacific Rim and elsewhere, and in most terranes that are characterized by the presence of submarine felsic volcanics (Table 3.1).

All deposits exhibit a close time-space relationship to fragmental submarine volcanics of dacitic to rhyolitic composition, although in some instances volcanics only represent a small fraction of the total volcanic-sedimentary assemblage. In Japan, all the Kuroko deposits were formed during a relatively restricted period that marked the end stages of a major pulse of volcanic activity initiated in late Oligocene time. In the Hokuroku Basin, however, a distinct break in volcanism occurred between late-Oligocene andesitic volcanism (Monzen stage) and bimodal basalt-rhyolite volcanism that straddled the early Miocene–mid-Miocene boundary (Nishikurosawa stage). These and other tectonic, igneous and metallogenic events in the Hokuroku Basin during Miocene time are summarized in Fig. 3.12. Urabe (1987) notes that Kuroko mineralization in Japan, although not as restricted in time as previously thought (Ohmoto et al. 1983), coincided with a major shift in stress field, a peak in bimodal volcanic activity, and a maximum degree of subsidence.

These events coincided with the time at which the Pacific plate experienced a change of direction of motion, as recorded by the age of bending of the Hawaiian-Emperor seamount chain (~25 Ma; Jackson et al. 1972). A plate tectonic control of this volcanic pulse is thus indicated. In the Hokuroku district there is strong evidence for a period of rapid subsidence at the beginning of the middle Miocene (Fujii 1974; Sato et al. 1974), and this subsidence has been interpreted as due to caldera formation by some workers (e.g., Sillitoe 1980b). Whether the entire Hokuroku Basin is a single or several collapse-caldera structures is uncertain, but isopach mapping indicates a series of northeast-trending normal faults that were active during this middle Miocene period. As detailed by Sillitoe (1980b), Uyeda and Nishiwaki (1980), and Dewey (1980), certain island arcs can undergo periods of tension, typically

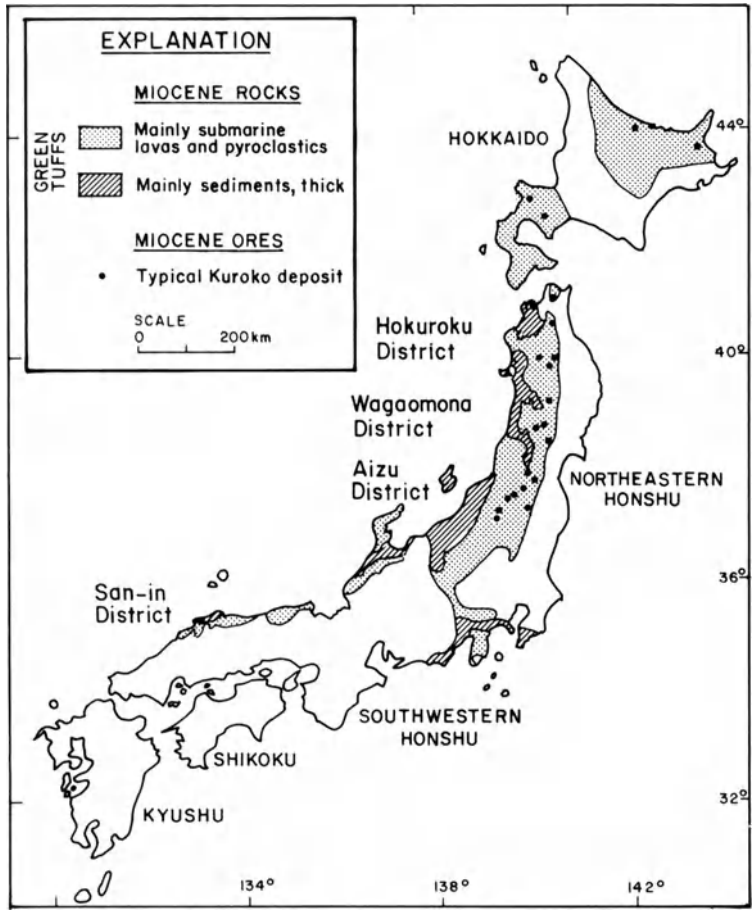

Fig. 3.11. The various tectonic, volcanic, and metallogenic events that occurred in the Hokuroku Basin in northern Hokkaido during mid- to late-Tertiary time (After Sato 1974)

associated with the opening of backarc basins (Vine and Smith 1981). Cathles et al. (1983) have suggested that the Green Tuff belt of Japan and its associated massive sulfide deposits are products of an abortive intraarc rifting episode and demonstrate that a linked system of rifts and transforms is capable of explaining the geographic extent of Green Tuff volcanism. The actual water depth that resulted from subsidence in the Hokuroku Basin is uncertain, and foraminiferal data (Guber and Merrill 1983; Matoba 1983) have not yielded unequivocal results. It can be estimated on the basis of fluid inclusion studies, however (see later), that water depths must have exceeded 1800 m at the time of Kuroko ore formation.

As studies of Kuroko-type and similar massive sulfide mineralization elsewhere become more detailed, evidence for subsidence just prior to ore formation becomes more widespread (Sillitoe 1982), and it is becoming clear

Table 3.1 Kuroko-type massive sulfide deposits (After Sillitoe 1982)

Deposit or district	Age	Metal Composition[a]	Ore associated volcanics	Petrologic affiliation	References
Undu Peninsula, Fiji	Late Miocene-early Pliocene	Zn,Cu	Dacite	Island-arc tholeiite and andesite	Colley and Greenbaum (1980)
Kuroko districts Japan	Mid-Miocene	Zn,Cu,Pb	Dacite, rhyolite	Calc-alkaline andesite	Sato (1974)
Pontid Belt, Turkey	Late Cretaceous	Cu,Zn	Dacite	Island arc tholeiite and andesite	Leitch (1981) Egin et al. (1979)
Sierra Madre del Sur Mexico	Early Creataceous	Zn,Pb,Cu	Rhyolite, dacite	Calc-alkaline	Lorinczi and Miranda (1978)
East Shasta, Calif.	Triassic	Cu,Zn	Rhyolite	Island-arc tholeiite? andesite	Albers and Robertson (1961)
West Shasta, Calif.	Mid-Devonian	Zn,Cu	Rhyolite	Island-arc tholeiite andesite	Kinkel et al. (1956) Barker et al. (1979)
Buchans Newfoundland Canada	Silurian	Zn,Pb,Cu	Dacite	Calc-alkaline basalt, dacite	Thurlow and Swanson (1981)
Avoca, southeast Ireland	Late Ordivician	Cu,Zn,Pb	Rhyolite	Calc-alkaline	Platt (1977) Stillman and Williams (1978)
		Precambrian examples[b]			
Jabal Sayid Saudi Arabia	Late Proterozoic	Cu,Zn,Pb	Rhyolite	Calc-alkaline	Sabir (1979) G.C. Brown (1980)
Prescott, Jerome and Bagdad, Ariz.	Middle-Proterozoic	Cu,Zn	Rhyolite	Calc-alkaline	Anderson and Guilbert (1979) Donnelly and Hahn (1981)
Noranda, Quebec Canada	Archean	Zn,Cu	Rhyolite	Island-arc tholeiite	Spence and de Rosen-Spence (1975)

[a] Metals are listed in order of decreasing abundance. All deposits also contain recoverable gold and silver values.
[b] See Chapter 4.

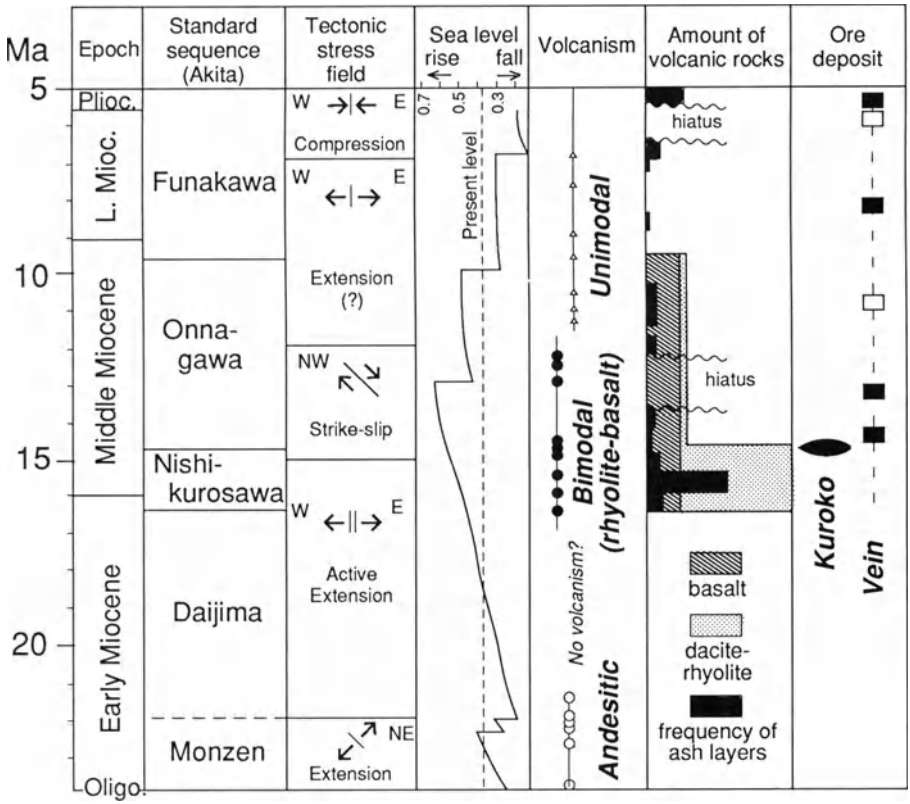

Fig. 3.12. Generalized comparative stratigraphic sections of Green Tuff areas that contain Kuroko-type metal deposits. Note restriction of the deposits to a narrow time interval during the middle Miocene (After Urabe 1987)

that subsidence is probably an important factor in the tectonomagmatic settings in which such massive sulfide ores form. The bimodal nature of the volcanism at the time of ore formation in the Hokuroku Basin (Urabe 1987) is also mirrored in many other massive sulfide districts (Sillitoe 1982), and can be interpreted as a signature of extensional tectonic regimes (Martin and Piwinskii 1972).

Investigations of the lithologic settings of the Kuroko deposits in the Hokuroku Basin at a more detailed level (Urabe 1987) indicate that virtually all deposits are underlain by lithic tuff breccia and/or rhyolite lava erupted from nearby volcanic centers. Urabe also demonstrates that Kuroko deposits can be divided in terms of the immediately overlying lithologies. Those overlain by pumice tuff tend to be large ($\approx 10^7$ tons) and have strong development of copper-rich yellow ore, those overlain by basalts tend to be somewhat smaller ($\sim 10^6$–10^7 tons) and have lesser development of yellow ore, and those overlain by mudstone are small ($\sim 10^5$–10^6 tons) and essentially lack development of yellow ore. Breccia dikes are mainly associated with the first

type, and they contain abundant fragments of granodiorite. These fragments attest to the presence of felsic plutons at depth.

Nozawa (1983) notes that granitic intrusive bodies occur sporadically throughout the Green Tuff terrane. The intrusions are mostly relatively small bodies of quartz diorite, tonalite, or granodiorite that are closely related to the volcanics they intrude, and in places they grade into granodiorite porphyries and quartz porphyries. These igneous rocks belong to the magnetite series (Ishihara 1978), and based on their H/D isotope systematics and Fe/(Fe + Mg) distribution between coexisting biotite and hornblende were apparently saturated with water during their late magmatic stages (Kuroda et al. 1983).

3.4.1 Mineralization and Alteration Patterns

Although individual Kuroko-type deposits exhibit considerable variability in terms of geometry and metal contents, a valid general model for such deposits has evolved (Fig. 3.13). Three basic ore types are recognized: a low-grade underlying stockwork (Keiko) ore, consisting of quartz veinlets containing pyrite and chalcopyrite; yellow (Oko) ore, consisting mainly of massive pyrite plus chalcopyrite; and black (Kuroko) ore, consisting of massive galena, sphalerite, and barite with variable amounts of chalcopyrite and pyrite. Overlying these lenses of massive sulfide locally are barite layers containing patchy sulfides, and in some instances a ferruginous chert layer is present on top of the sequence, although this is by no means a universal feature.

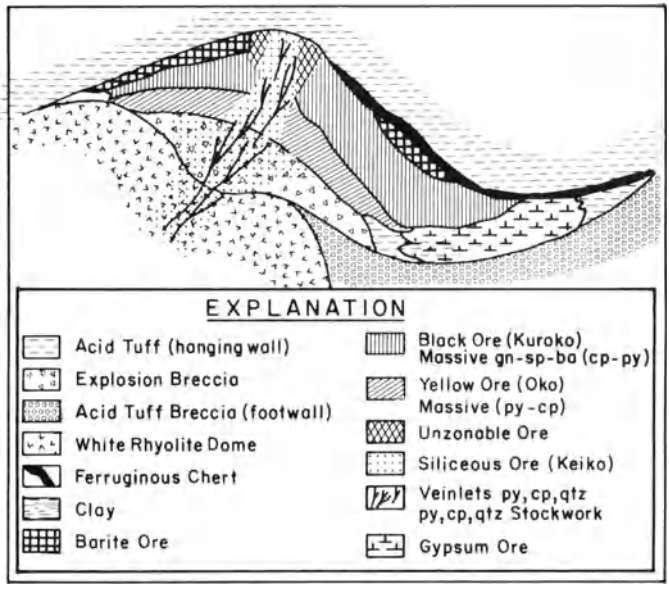

Fig. 3.13. Idealized section of a typical Kuroko deposit showing relationships between various ore types and associated geologic units (After Franklin et al. 1981)

Whereas mineral banding in these deposits is typically restricted to the uppermost or peripheral portions of the black ore, they are nonetheless grossly layered in nature. In general, grain size decreases upward through a deposit, and in much of the black ore the larger grains of major minerals do not exceed 200–300 microns in diameter (Shimazaki 1974). Minor minerals are usually an order of magnitude smaller. Within the lower portions of black ore lenses the mineral assemblage is typically just sphalerite-galena-chalcopyrite-pyrite-barite, but upwards there is increasing concentration of minor elements such as arsenic, antimony, gold, and silver, and this is reflected mainly in the presence of sulfosalt minerals, especially tetrahedrite-tennantite. Recently there has been increased interest in the distribution patterns of gold in massive sulfide deposits and it is now recognized that high gold contents can occur both in uppermost and distal portions of massive sulfide orebodies and in the copper-rich feeder zones below them (Large et al. 1987a).

Most ores are compact and massive, but bedded, brecciated, or colloform textures dominate locally, and graded bedding in black ore has even been observed in several localities. The average tenor of the ores mined in the Hokuroku district is approximately 2% Cu, 5% Zn, 1.5% Pb, 21% Fe, 12% Ba, 1.5 g/ton Au, and 95 g/ton Ag (Lambert and Sato 1974). Each of the major mines in this area is centered on a cluster of separate ore lenses (Fig. 3.14) that range in size from less than 0.1 million tons to about 10 million tons, and total ore tonnage of the district is estimated to be 90 million tons (Sangster 1980). The stratabound lenses are typically elongate, with sharp upper boundaries and more diffuse lower boundaries that grade downward through lower-grade stockworks into unmineralized footwall volcanics and tuffs (see Fig. 3.13).

Eldridge et al. (1983) have attempted, largely on the basis of ore microscopy, to revise previously accepted ideas regarding the paragenetic sequence by which Kuroko-type deposits form. They concluded that black ore forms first and that it is progressively replaced by yellow ore during thermally intensifying mineralization. While their empirical observations of localized replacement of sphalerite and other minerals by chalcopyrite do indicate a certain reworking of earlier stages of the paragenesis by later hydrothermal events, evidence of this on a larger scale is notably lacking. Yui and Ishitoya (1983), for example, show clear evidence of fragments of yellow ore enclosed within black ore, both at the macro- and microscale. Furthermore, at Woodlawn, N.S.W. (McKay and Hazeldene 1987), where open-pit mining allows clear observation of the relationship between the copper core and overlying bedded lead-zinc ores (Fig. 3.15), it can be demonstrated that the great bulk of massive sulfide deposition took place under conditions of decreasing temperature of ore fluids.

The alteration patterns associated with Kuroko ore lenses (Fig. 3.16) have been superimposed on a regional zeolite facies alteration that characterizes the Green Tuff formations in Japan. In general, the stockwork zone and the immediate environs of the ore lenses exhibit Mg-chlorite plus sericite alteration and local silicification. Surrounding this, and commonly extending well up into the overlying rocks (up to 200 m), is a zone of less intense alteration containing sericite, interstratified sericite-montmorillonite, and chlorite, with

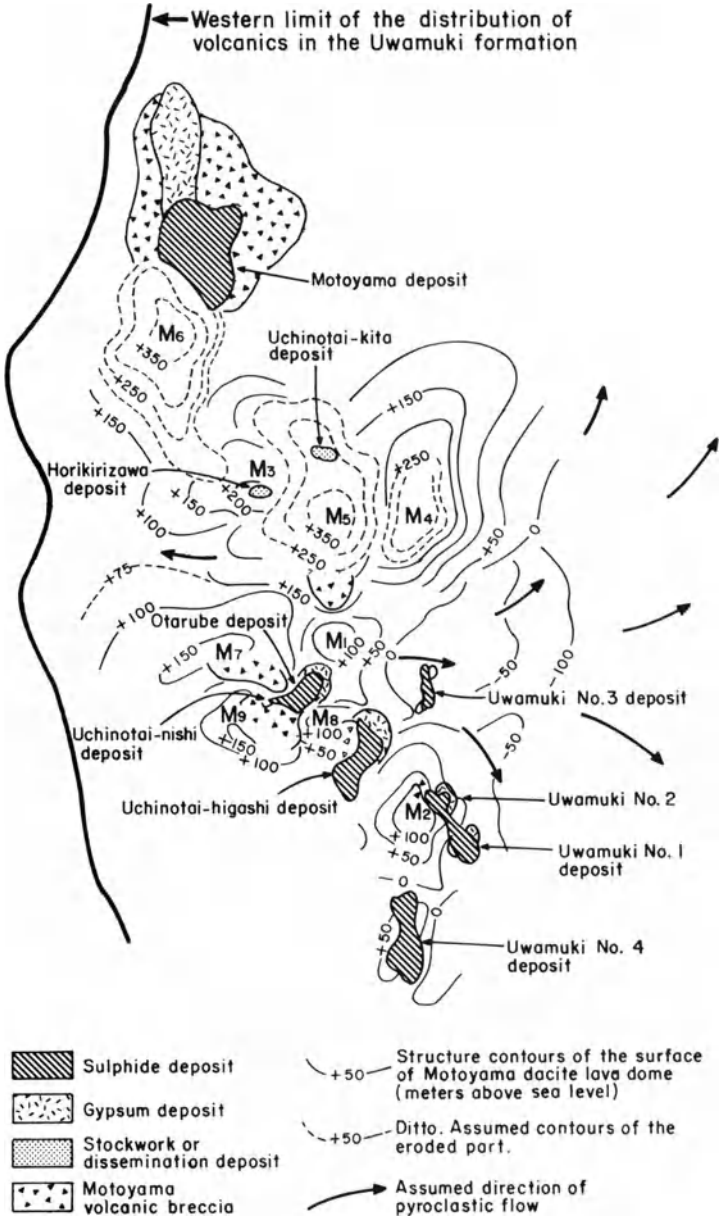

Fig. 3.14. Relationships between white rhyolite lava domes, massive sulfide lenses, and mineralized stockworks, Kosaka Mine, Hokuroku district, northeast Honshu. Note tendency of massive sulfide lenses to occur in clusters (After Urabe and Sato 1978)

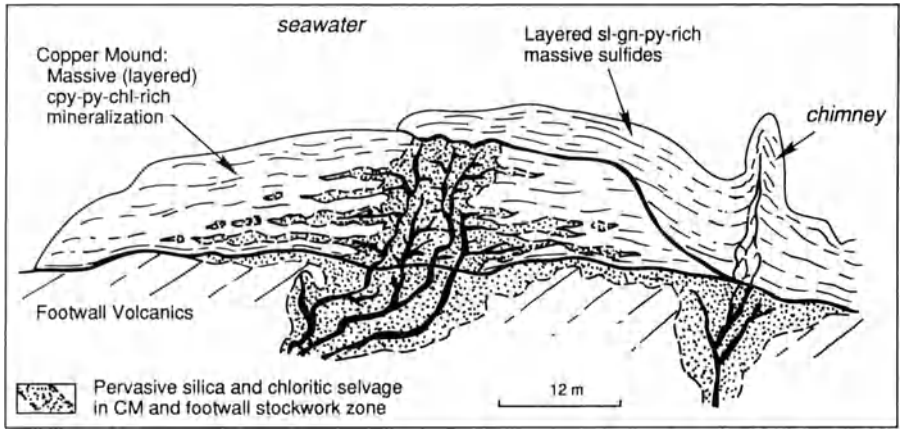

Fig. 3.15. Relationships between the copper ores (early mound sulfides) and zinc-lead ores (overlying layered sulfides) as discernible at the Woodlawn deposit, N.S.W., Australia (After McKay and Hazeldene 1987)

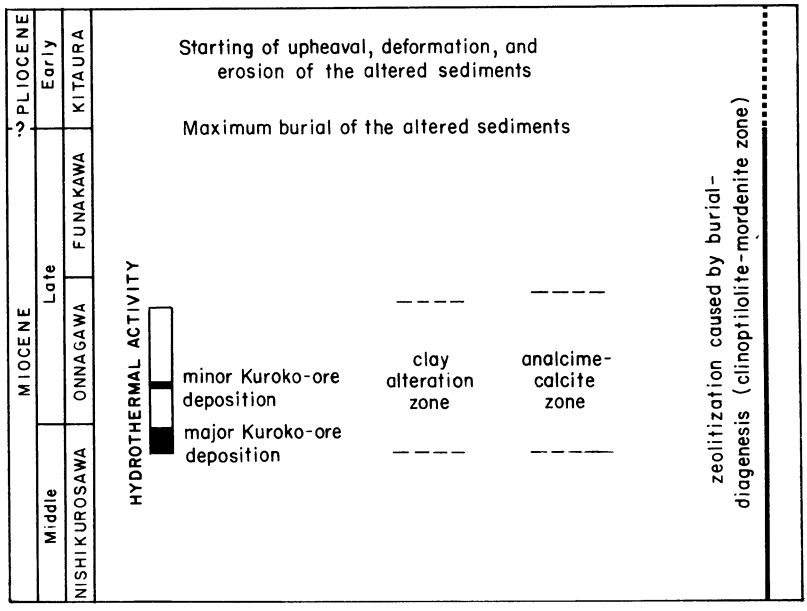

Fig. 3.16. Alteration of the volcanic section that hosts Kuroko deposits. Note that alteration can reach upwards a considerable distance about the ore lenses, indicating that hydrothermal activity must have continued for considerable time periods after the syngenetic formation of the ore deposits (After Iijima 1974)

some development of albite and potassium feldspar (Iijima 1974). The most distal alteration, which grades into the regional zeolite facies alteration, contains montmorillonite as the main clay mineral accompanied by lesser amounts of cristobalite and zeolites. The extension of alteration assemblages well into the hanging wall rocks indicates continued, or at least intermittent, hydrothermal activity for periods of up to 1 or 2 million years after cessation of ore deposition (Iijima 1974; see Fig. 3.16). In chemical terms, alteration represents strong Mg metasomatism in all zones, and K metasomatism in the footwall alteration zones. Calcium and especially sodium are removed during the alteration process except in the distal alteration above ore lenses where Na-fixation is commonly observed. The "white rhyolite" domes closely associated with many of the Kuroko-type deposits (Date and Tanimura 1974) appear to have originally been dacite, now intensely altered to quartz-sericite assemblages. Urabe et al. (1983) have demonstrated that the alteration halos around Kuroko and similar massive sulfide deposits are broad (2–4 km in diameter), and that the major control on outward zoning of alteration types is a decline in temperature and an increase in cation/H^+ ratios.

The preceding generalized comments on the mineralization and alteration patterns revealed by the massive sulfide deposits of the Hokuroku basin can be applied not only to other Kuroko-type ores in Japan, but to the great majority of Phanerozoic massive sulfide deposits generated in similar lithologic-tectonic settings. It should realized, however, that variations on the theme are not uncommon in individual cases, especially in terms of metal ratios and the presence or absence of associated sulfate bodies.

3.4.2 Fluid Inclusion and Stable Isotope Data

A number of fluid inclusion studies have been carried out on quartz, sphalerite, and barite from Kuroko-type deposits (e.g., Tokanaga and Honma 1974; Farr and Scott 1981; Pisutha-Arnond and Ohmoto 1983). These studies indicate that ore deposition occurred in the range 320–200°C. The highest temperatures are found in stockwork quartz, and temperatures progressively decrease upward into black ore zones (Fig. 3.17). Fluid inclusion salinities fall mainly in the range of 2.4 to 8.4 equiv. wt% NaCl, but some higher salinities have been reported. As in the case of temperatures, the salinities of fluid inclusions are higher (~ 5–8 equiv. wt% NaCl) in stockwork ore than in bedded ore.

Stable isotope studies of minerals and inclusion fluids in Kuroko-type deposits (Ohmoto and Rye 1974; Ishihara and Sasaki 1978; Hattori and Sakai 1979; Hattori and Muehlenbachs 1980; Pisutha-Arnond and Ohmoto 1983) indicate a major component of seawater in Kuroko ore fluids, but consistently negative δD values indicate the involvement of another fluid in the ore formation process. Several workers (e.g., Urabe and Sato 1978; Hattori and Muehlenbachs 1980; Farr and Scott 1981; Sawkins 1986a; Urabe 1987) have suggested that the isotope and salinity data are best explained in terms of involvement of certain amounts of magmatic fluid in addition to evolved

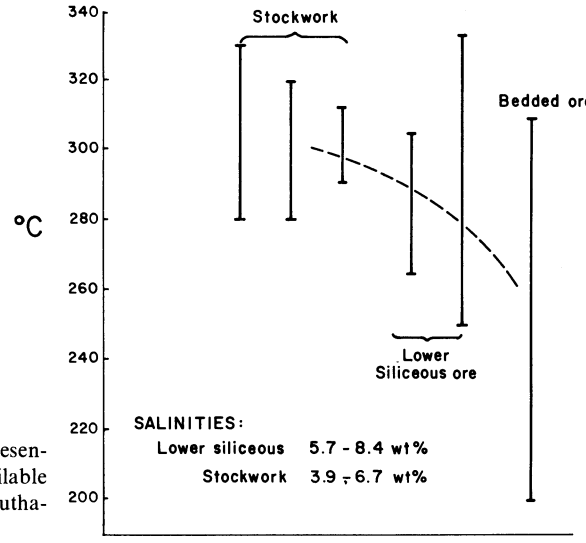

Fig. 3.17. Compilation of representative fluid inclusion data available for Kuroko deposits (see Pisutha-Arnond and Ohomot 1983)

seawater in Kuroko-type ore-generating systems. Ohmoto et al. (1983), however, have constructed a complex chemical model for the genesis of the deposits of the Hokuroku basin involving leaching of metals by evolved seawater fluids in thermally intensifying convection cells. Their attempts to accommodate certain critical aspects of the empirical data base, such as the δD values of inclusion fluids, are unconvincing. In contrast to their approach, Urabe (1987) demonstrates that the entire isotope data base available for these deposits (Fig. 3.18) can be satisfactorily accounted for by assuming a magmatic source for virtually all critical components, but recognizing the inevitable admixture of seawater fluids to the ore-generating system.

3.5 Paleozoic Volcanic-Hosted Massive Sulfide Deposits

3.5.1 Buchans Polymetallic Sulfide Deposit, Newfoundland

The important Buchans camp has produced almost 18 million tons of ore from a number of orebodies with an average grade of 14.6% Zn, 7.6% Pb, 1.34% Cu, 105 g/ton Ag, and 1.2 g/ton gold (Thurlow and Swanson 1981, 1987). On the basis of contained metal tonnage, the Buchans deposit is comparable with the Noranda and Hokuroku districts that contain numerous orebodies spread over much larger areas (Sangster 1980).

The complex assemblage of volcanic and sedimentary rocks known as the Buchans Group has been dated at 446 ± 13 Ma (Bell and Blenkinsop 1981). The ore-associated felsic volcanic rocks are in part comagmatic with the

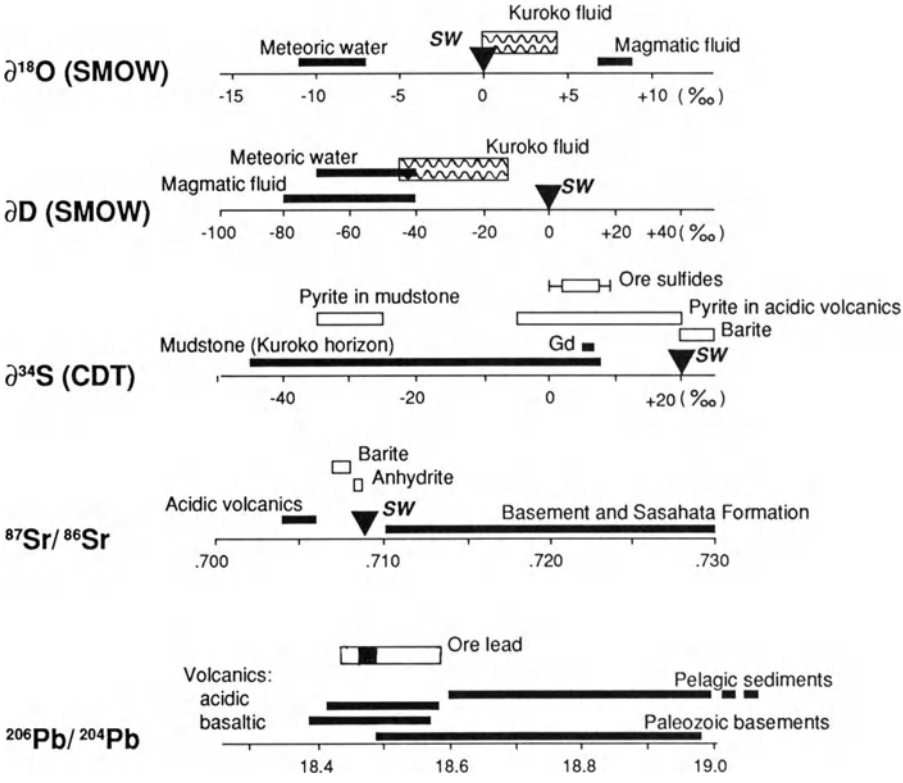

Fig. 3.18. Compilation of isotope data pertaining to the Kuroko massive sulfide deposits, in particular those from the Hokuroku Basin. Note that the data from virtually every system indicate a significant departure from seawater (*SW*) values. This is especially true for the H/D isotope ratios, a critical determinant of fluid origins (After Urabe 1987)

intrusive Feeder Granodiorite (Fig. 3.19). Due to structural complexities, the thickness of the Buchans Group is imprecisely known, but estimates indicate a probable thickness of 5 to 9 km (Thurlow and Swanson 1981; Kirkham 1987). A thick flysch sequence underlies the Buchans Group, whereas red sandstones and conglomerates of Carboniferous age unconformably overlie it.

Within the Buchans Group, the volcanic rocks range in composition from basalt to rhyolite, and despite a relative paucity of andesite, the volcanics exhibit typical calc-alkaline chemical trends (Thurlow et al. 1975). The lower portion of the sequence is composed predominantly of pillowed amygdaloidal basalts, whereas the upper portion contains a high proportion of felsic pyroclastics. Clastic sediments occur mainly in what must have been local basins within the felsic pyroclastic sequence. The major orebodies at Buchans occur near the top of the Lower Buchans Group within the Lucky Strike Ore Horizon Sequence (Fig. 3.20), which, prior to thrust faulting, was probably time equivalent to the Oriental Ore Horizon Sequence (Thurlow and Swanson

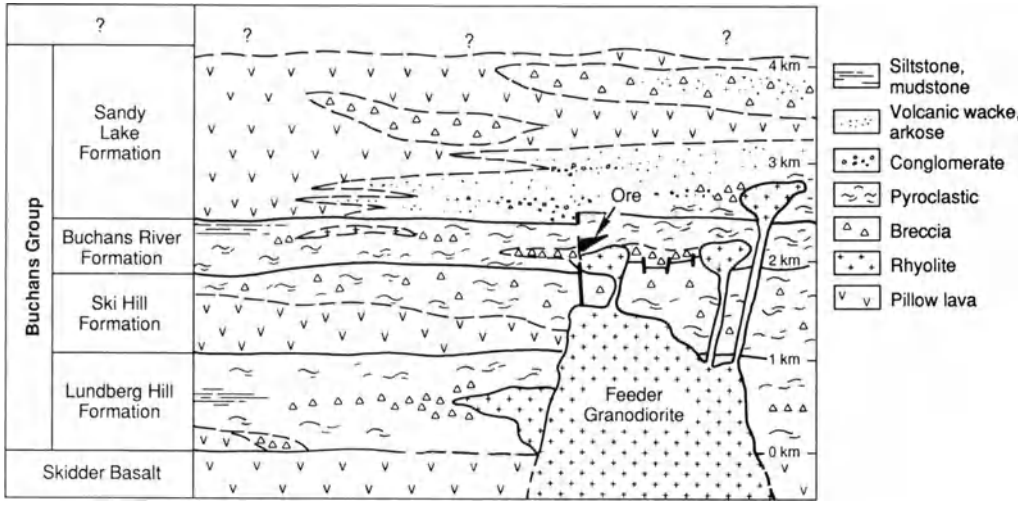

Fig. 3.19. Reconstructed cross-section showing the sequence of volcanic and volcaniclastic units and related intrusions that host the Buchans orebodies (After Thurlow and Swanson 1987)

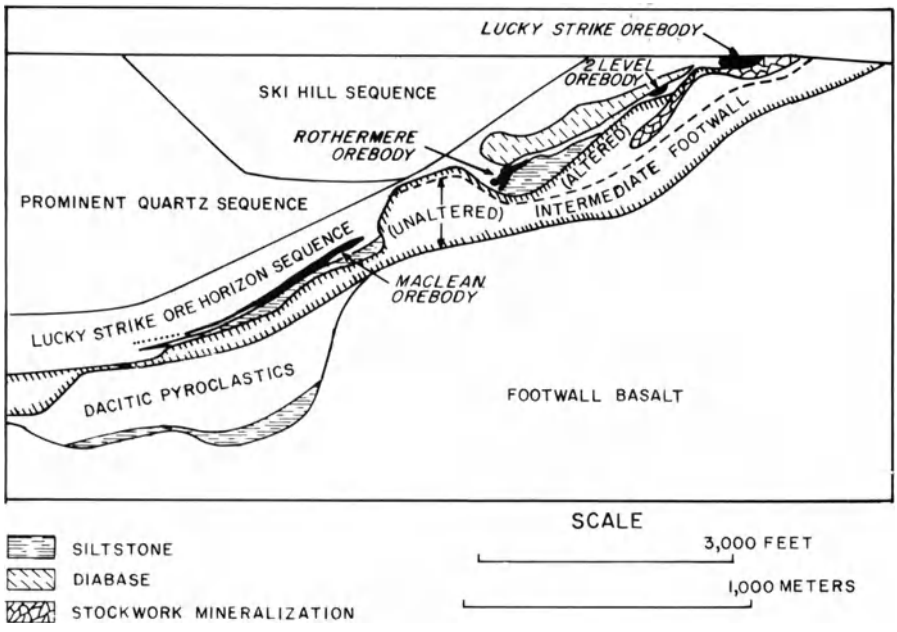

Fig. 3.20. Vertical section through the Buchans Mine area to illustrate the relationships between the in situ Lucky Strike orebody, the transported orebodies, and enclosing rock units (After Thurlow and Swanson 1981)

1987; see Fig. 3.19). Both these units and the intermediate-composition footwall rocks represent a marked change toward very localized litho-units of volcanics and sediments, as compared with the broad extent of the underlying footwall basalt and the footwall arkose to the east. Based on amygdule contents of basalts and the strongly pyroclastic nature of the felsic volcanism, Thurlow and Swanson (1981) suggest that water depths were relatively shallow during accumulation of the Buchans Group, and at the time of ore deposition, during initial accumulation of the Ore Horizon pyroclastics, a rugged subaqueous paleotopography is indicated (see also Kirkham and Thurlow 1987).

The metallization events at Buchans produced three types of ore: stockwork ore; in situ ore; and transported ore (Fig. 3.21), the last two types accounting for approximately 98% of production. Stockwork ore emplaced in intermediate-composition footwall rocks occurs below and adjacent to the Lucky Strike massive, in situ orebodies, and consists of a network of sulfide veins and veinlets cutting pervasively altered host rocks. The central portions of stockwork orebodies are characterized by silicification and/or chloritization, whereas the peripheral portions exhibit clay alteration (mainly illite, Henley and Thornley 1981). Pyrite, as veinlets and disseminations, occurs marginal to central zones in which the veins contain base metals and barite. Overall, the Buchans stockwork mineralization and alteration forms a blanket-like zone that does not exceed 100 m in thickness.

The Lucky Strike orebody is a thick lens of massive base metal sulfides that lacks well-developed banding and contains less than 10% pyrite. The fine-grained ore is crudely zoned with chalcopyrite-rich yellow ore lying mainly below predominantly lead-zinc-rich black ore. Typical ore consists of a fine-grained aggregate of sphalerite, galena, and barite, with lesser chalcopyrite, and minor tetrahedrite, bornite, and silver minerals such as argentite.

The Rothermere, Maclean, and other transported orebodies occur in a roughly linear array along a paleochannel trending northwest from the Lucky

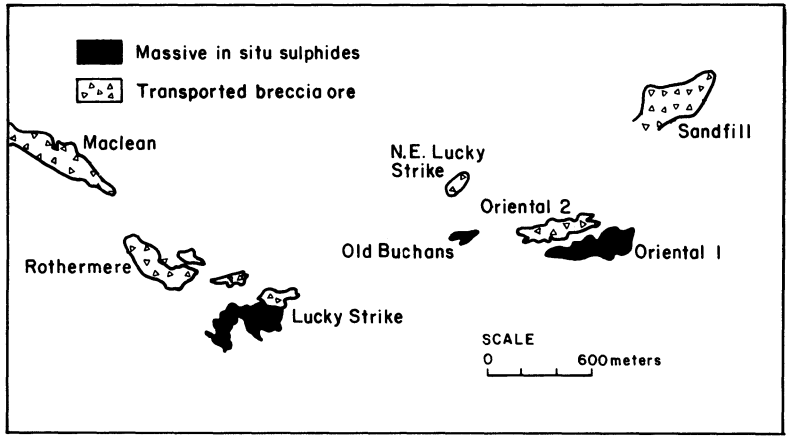

Fig. 3.21. Simplified plan illustrating the spatial relationships between in situ and transported ores (ore breccias) in the Buchans district (After P.N. Walker and Barbour 1981)

Strike orebody, and a similar line of transported orebodies trends northeastward from the Oriental 1 in situ orebody (Fig. 3.21). These transported orebodies consist of mechanical mixtures of sulfides and lithic fragments, including rounded granodiorite clasts (see Stewart 1987). Sharp contacts with the enclosing pyritic siltstones and dacitic tuffs are common, and locally, weak imbrication of tabular fragments is visible, indicating transport away from the Lucky Strike area (P.N. Walker and Barbour 1981). Detailed observations indicate that individual orebodies are in some instances the result of multiple downslope slumping events of massive sulfide ores following hydrothermal eruptions. It is of some interest that isolated base metal clasts have been observed in drillholes up to 6 km away from the nearest known in situ massive sulfide orebodies (Thurlow and Swanson 1981), and that some of these occur at stratigraphic levels for which no massive sulfide mineralization is known.

Paragenetic and stable isotope studies, concentrated mainly on stockwork mineralization (Kowalik et al. 1981), indicate that initial pervasive chloritization and pyritization of the rocks subjacent to the Lucky Strike orebody were followed by silicification and associated pyrite and chalcopyrite deposition. Subsequently, deposition of sphalerite and galena occurred, and the gangue mineralogy changed from quartz to barite and calcite. Stable isotope data for quartz-chlorite pairs indicate depositional temperatures in the range 243–371 °C and a range of 140–322 °C for galena-sphalerite pairs, and also indicate that temperatures decreased away from the major plumbing system. $\delta^{34}S$ data suggest that the sulfur in the deposits was predominantly of seawater origin, and, as such, similar to that in Japanese Kuroko deposits. $\delta^{18}O$ and δD data also indicate the hydrothermal fluids were mainly of seawater origin, but are permissive of a magmatic component of up to 15%.

The possibility of a significant magmatic contribution of lead and other base metals to the Buchans ore-generating system is supported by an analysis of lead budgets at Buchans, where transportation of at least 2.7×10^{12} g of lead was effected (Sawkins and Kowalik 1981). Extraction of this lead from the basalts that underlie the Buchans ores would involve a hydrothermal convection cell of unrealistic size (~ 600 km^3), whereas a magmatic-hydrothermal source for the bulk of the lead and other metals requires a magma body of only about 50 km^3. Such a model does not violate any aspect of the empirical data available for Buchans and most other Kuroko-type deposits (Fig. 3.22).

The similarities of the Buchans ores to those of the Japanese Kuroko province are strong, for close equivalence in stockwork ores, yellow ores, black ores, and bedded barites, as well as isotope characteristics, can be demonstrated. Minor disparities exist, however. The "white rhyolite" bodies present at Buchans do not exhibit the close spatial relationship to ore manifest in many Kuroko districts. Furthermore, gypsum is absent at Buchans, and the ores are both notably higher grade and less pyritic than average Kuroko ores. Finally, the mechanical redistribution of ores by hydrothermal disruption and slumping is far more prevalent at Buchans.

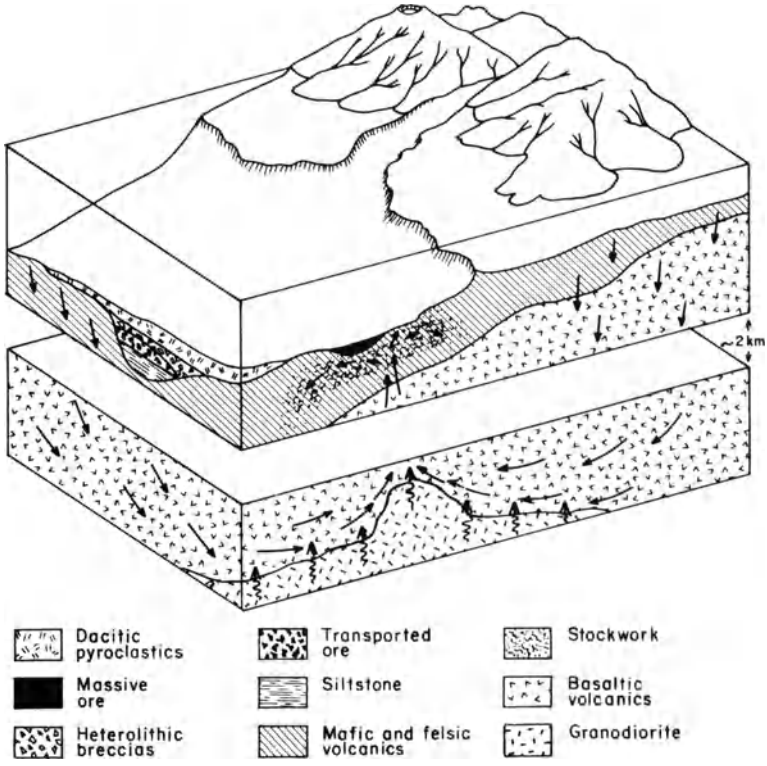

Fig. 3.22. Idealized reconstruction of the environment of ore formation at Buchans. Seawater was the dominant fluid in the convecting hydrothermal system (*solid arrows*), but a component of magmatic fluid is added from the crystallizing felsic magmatic system (*wavy arrows*) that provides the heat for seawater convection. Both the basalts and the magmatic system can be envisaged as sources for the metals in the Buchans ores, but the majority of lead is probably of magmatic derivation (After Sawkins and Kowalik 1981)

3.5.2 Rio Tinto Massive Sulfide Deposit, Spain

The Rio Tinto massive sulfide deposit is estimated to have originally contained more than 500 million metric tons of pyritite (D. Williams et al. 1975), and thus is probably the largest massive sulfide deposit known. The Iberian Pyrite Belt (Fig. 3.23) includes, in addition to Rio Tinto, a number of very large massive sulfide deposits and many smaller ones, and total current reserves of pyritite exceed 750 million metric tons (Instituto Geologico y Minero de España 1982). The majority of the massive sulfide ores are low in associated base metals, and were mined mainly as raw material for sulfuric acid production. Nevertheless, some of the ores are of polymetallic type (Cu + Zn + Pb), and, Neves Corvo, the last major deposit to be discovered in the Pyrite Belt, contains 40 million tons of ore grading 8% Cu as well as large Cu-Zn-bearing pyritite lenses of possible economic potential (Carvahlo 1988).

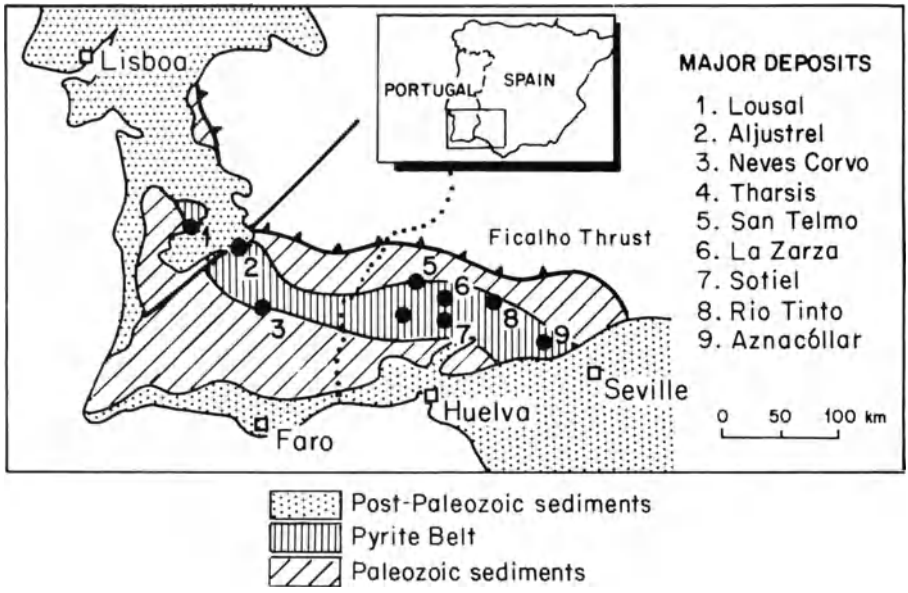

Fig. 3.23. Map of the Iberian Pyrite Belt showing the location of the major massive sulfide deposits (After Schütz et al. 1987)

The overall geologic setting of the Rio Tinto deposit and its environs (Rambaud Perez 1969; Garcia Palomero 1980, 1983) involves three major stratigraphic units: the critical Volcano-Sedimentary Complex that hosts all the Iberian pyritite ores, the underlying late Devonian flysch, and the overlying early Carboniferous Culm facies sedimentary rocks (Fig. 3.24). Petrochemical studies of the volcanic rocks have led Munha (1983) to conclude that they are related to the initial stages of ensialic backarc spreading.

In the vicinity of Rio Tinto, these units occur in a series of large amplitude, southward-verging folds. As little as 5 km to the north and east of the Rio Tinto mine is a complex of mafic and felsic intrusive rocks that are of broadly similar composition to the mafic and felsic volcanics of the Volcano-Sedimentary Complex (Schütz et al. 1987; Fig. 3.25).

The Volcano-Sedimentary Complex exhibits a great deal of lithologic variation throughout the Iberian Pyrite Belt, but in the vicinity of Rio Tinto consists mainly of a sequence of locally pillowed mafic volcanics overlain by felsic pyroclastics and rhyolite flows and flow domes, and their associated volcaniclastic sedimentary units, together with minor shales and exhalites. The latter are locally manganese-rich and have in the past supported significant manganese mining operations. Regional deformation has imparted a strong penetrative cleavage to almost all the less competent sedimentary and volcanic rocks.

Recent studies of the felsic volcanic units (Halsall and Sawkins 1989) indicate that some of the felsic pyroclastic units are welded ignimbrites, and as

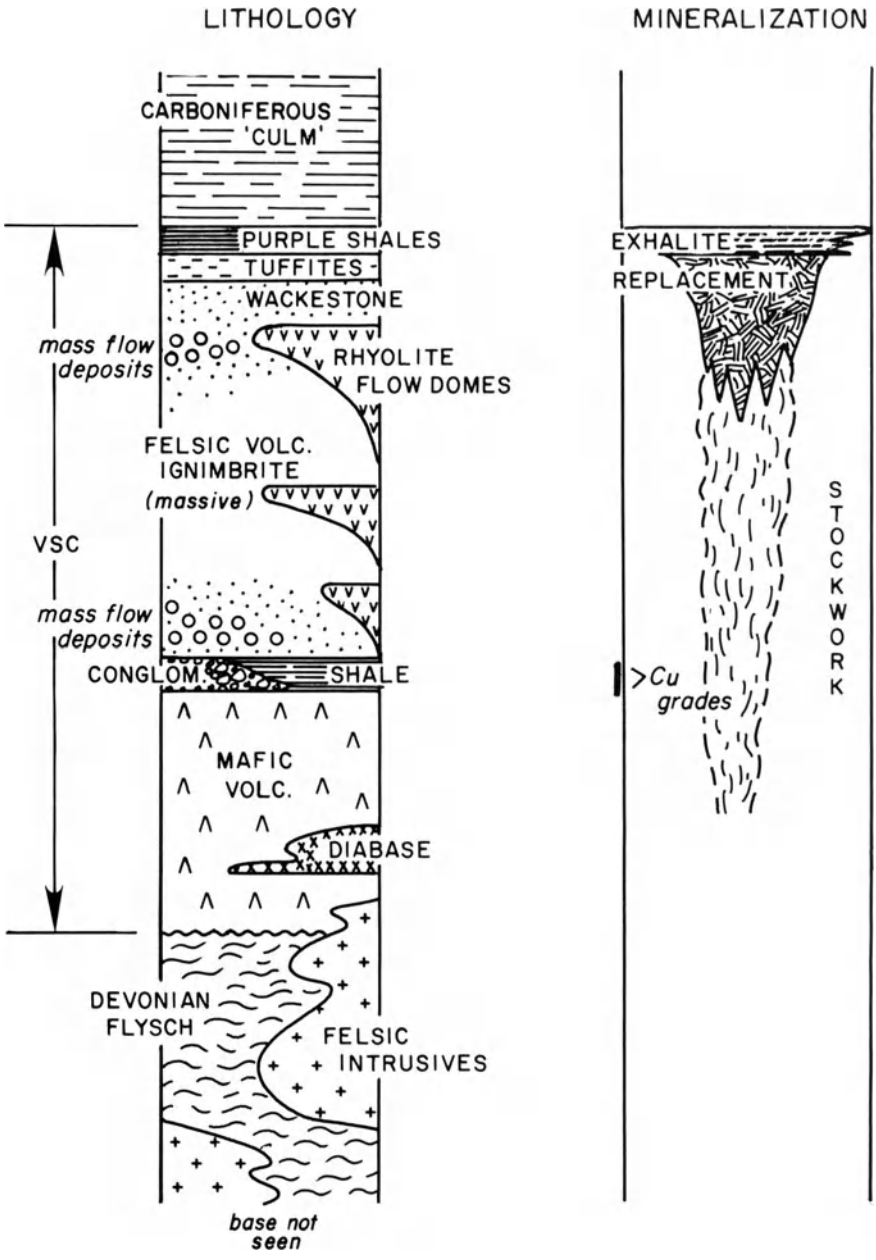

Fig. 3.24. Generalized lithologic sequence of the volcanic and sedimentary units in the Rio Tinto area. Also shown are intrusive units and the extent of massive sulfide and stockwork mineralization (based in part on work by R.H. Sillitoe and the author, and in part on Schütz et al. 1987). *VSC* Volcanic Sedimentary Complex

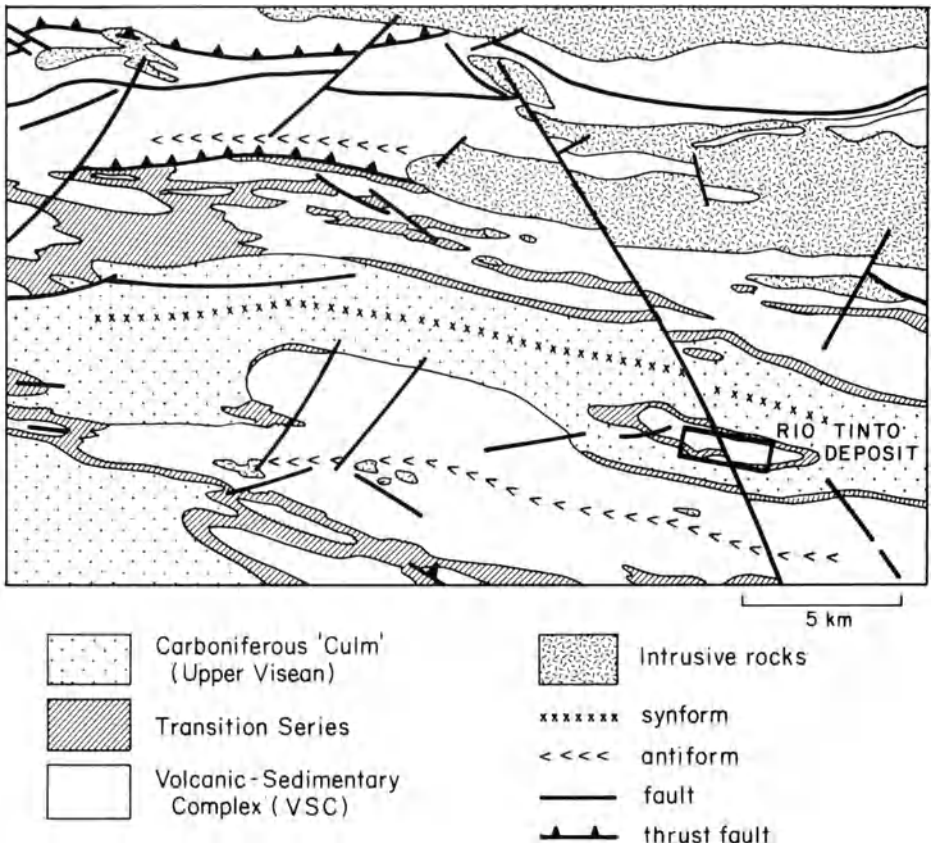

Fig. 3.25. Generalized map of the area surrounding and west of Rio Tinto. Note the major development of intrusive rocks to the north of the mine area. These consist mainly of trondjhemites, tonalites, and granodiorites that intrude only the lowermost portions of the Volcanic Sedimentary Complex and are comagmatic to the felsic volcanics (based on Instituto Geologia de España maps)

such must have formed under subaerial or shallow water conditions (Sparks and Wright 1979; Sheridan 1979). This is perhaps a surprising observation in that the world's largest known massive sulfide deposit lies almost directly above these welded volcanic units. The volcaniclastic rocks also contain a significant component of mass flow units consisting of rounded rhyolite fragments (~0.1 to 20 m) scattered through a sand-sized volcaniclastic matrix.

The pyrite-rich ores of Rio Tinto are of two basic types: bedded massive sulfide of exhalative origin, and vein-type stringer ore of replacement origin. These replacement ores have developed so strongly in some places, especially at the top of the stringer zone, that massive pyritite formed in this manner is not easy to distinguish from overlying exhalative pyritite (see Fig. 3.24).

Massive pyritite, of both exhalative and replacement origin, contains an average of 48 wt% S, and close to 1 wt% Cu. Bedded massive sulfides at the easternmost extremity of the system (Planes orebody) and at the western edge of the San Dionisio orebody in the west are of more polymetallic character and contain about 2% Zn and 1% Pb, in addition to approximately 1.5% Cu. The stringer ores below massive ores contain on average 13 wt% S and 1.6 wt% Cu where they can be categorized as copper-rich. Pyrite is virtually the sole non-silicate iron mineral, but very minor amounts of magnetite do occur locally in the deep parts of stringer zones. Sphalerite and galena account for the Zn and Pb in the ores, and the copper occurs as chalcopyrite and minor bornite.

Additional sulfide and sulfosalt phases occur only in trace amounts. Quartz is the sole introduced gangue mineral of consequence. The gold and silver contents of the massive sulfides are low, but they have been sufficiently upgraded during in situ oxidation of the sulfides that bulk mining and heap leaching of this material (1 g/ton Au equiv) is currently feasible. Reserves of this oxide ore are estimated at 100 million tons.

The felsic volcanics below the massive sulfides are extensively sericitized, but within stringer zones the felsic volcanics are locally so strongly chloritized that only the presence of scattered quartz phenocrysts distinguishes them from the underlying chloritized basalts.

Geochemical and isotope studies have failed as yet to provide major insights into the process of ore formation at Rio Tinto. Sulfur isotope measurements (Eastoe et al. 1986) indicate a range of values (−15 to + 12‰ $\delta^{34}S$), but the bulk of the sulfides lie within a few per mill of $\delta^{34}S = 5‰$. Munha et al. (1986) measured $\delta^{18}O$ and δD values for quartz-chlorite pairs in just a few samples from Rio Tinto and deduced that fluids of seawater origin operating at 230°C were responsible for ore formation. Unpublished results of $\delta^{18}O$ studies of quartz-magnetite pairs from deep within the San Dionisio stockwork indicate temperatures in excess of 350°C and fluids with $\delta^{18}O$ values of + 6‰ (Halsall and Sawkins 1989).

Field observations north of the Rio Tinto deposit by R.H. Sillitoe and the author strongly support the conclusions of Soler (1980) and Schütz et al. (1987) that the suite of gabbroic and tonalitic intrusions in that area are time equivalents of the mafic and felsic volcanics of the Volcanic-Sedimentary Complex. Some of these intrusions contain disseminated pyrite and veinlets of quartz-specularite-siderite. The sheer size and iron-rich, lead-poor nature of the Rio Tinto ores, coupled with the character of the subjacent lithosequence (thin volcanic units, and underlying thick graywackes, shales, and quartzites) render these intrusions an attractive source of metals from the Rio Tinto deposit, and the fluids that transported them. The preliminary oxygen isotope data cited above support this conclusion.

3.5.3 Massive Sulfide Deposits of the Bathurst-Newcastle District, New Brunswick, Canada

The Bathurst-Newcastle district embraces over 20 Zn-Pb-Cu-Ag massive sulfide deposits (Fig. 3.26), one of which, the Brunswick No. 12 deposit, contains over 100 million tons of ore grading 13% of combined zinc and lead (Luff 1977). All the deposits occur within rocks of the Tetagouche Group, a sequence of felsic and mafic volcanics and clastic metasedimentary rocks (Harley 1979). A good deal of uncertainty surrounds the precise age and regional structural setting of the Tetagouche Group due to paucity of fossils, poor exposure, and polyphase deformation. It appears, however, that a sedimentary unit consisting mainly of arenaceous sandstones and feldspathic

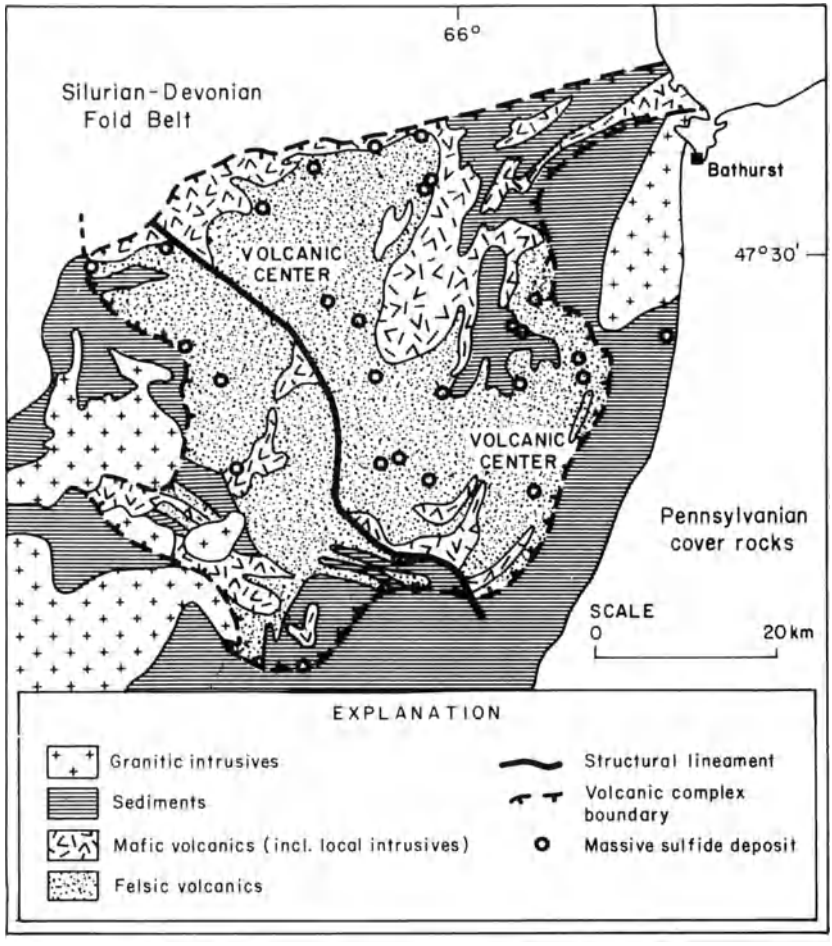

Fig. 3.26. Geology of the Bathurst-Newcastle mining district, northern New Brunswick showing locations of massive sulfide deposits and inferred volcanic centers (After Harley 1979)

wackes of early Ordovician age is succeeded upward by felsic volcanics, then basaltic volcanics, and finally dark slates and lithic wackes of mid-Ordovician age (see Harley 1979 and references therein). Whitehead and Goodfellow (1978) have studied the geochemistry of the Tetagouche volcanics and demonstrated that they are strongly bimodal in character. In addition, the basalts have both tholeiitic and alkaline affinities, and rocks of calc-alkaline andesitic composition are conspicuously absent. This lithosetting is comparable to that described in the previous section for the Rio Tinto and related ores of the Iberian Pyrite Belt.

Harley (1979) notes that, although all the massive sulfide deposits in the district exhibit a broad relationship to felsic volcanic rocks, two subtypes can be recognized. The largest deposits, such as Brunswick No. 12, Brunswick No. 6, and Orvan Brook, are associated regionally with sheet-like bodies of rhyolite porphyry but occur in intravolcanic sedimentary horizons (Davies et al. 1973). They also exhibit an association with oxide, silicate, and carbonate facies iron formation (Helmstaedt 1973) and tend to be laterally extensive. The other type of massive sulfide deposit occurs as smaller lenses and exhibits a close association with siliceous tuff breccias, and these deposits thus appear to be related to the presence of brecciated lava domes, a characteristic of Kuroko deposits.

The Orvan Brook deposit (Tupper 1969) is of some interest because it occurs as a steeply dipping thin sulfide lens (max. thickness 5 m) almost 2000 m long, lying either within a quartz sericite schist or at its contact with an overlying graphitic schist. Below the sericite schist is an iron-formation unit consisting of quartz-chlorite schist containing scattered bands of quartz-hematite and jasper-hematite-magnetite iron formation. The immediate setting of the deposit is thus one of sedimentary rocks, though metarhyolites are present a short distance downsection. The sulfide minerals consist predominantly of pyrite, lesser sphalerite and galena, and minor amounts of chalcopyrite, arsenopyrite, and tetrahedrite. The sulfide ore is massive, fine-grained, banded, and locally contorted. Zinc to lead ratios in the ores are approximately 2:1 and the combined Zn + Pb grade averages about 9% (Tupper 1969).

The New Brunswick No. 12 deposit is easily the largest massive sulfide orebody in the Newcastle-Bathurst district, and contains almost 100 million tons of lead-zinc ore grading 9.2% Zn, 3.8% Pb, 0.3% Cu, and 0.79 g/ton Ag. In addition, another 14 million tons of copper ore grading 1.1% Cu, 1.3% Zn, 0.4% Pb, and 0.30 g/ton Ag are known (Luff 1977). The ores occur within a sequence of argillites and other metasediments, including iron formation, that appear to have accumulated during a break in felsic volcanic activity (Fig. 3.27). These felsic volcanics are mainly crystal and siliceous metatuffs and are overlain by mafic volcanics, and thus the stratigraphic sequence exhibits strong similarities to that enclosing the Orvan Brook deposit discussed above.

Isoclinal folding and faulting have affected both the ores and their enclosing rocks, but, according to Luff (1977), both conformable massive sulfide lenses and subjacent stockwork zones can be distinguised. In addition,

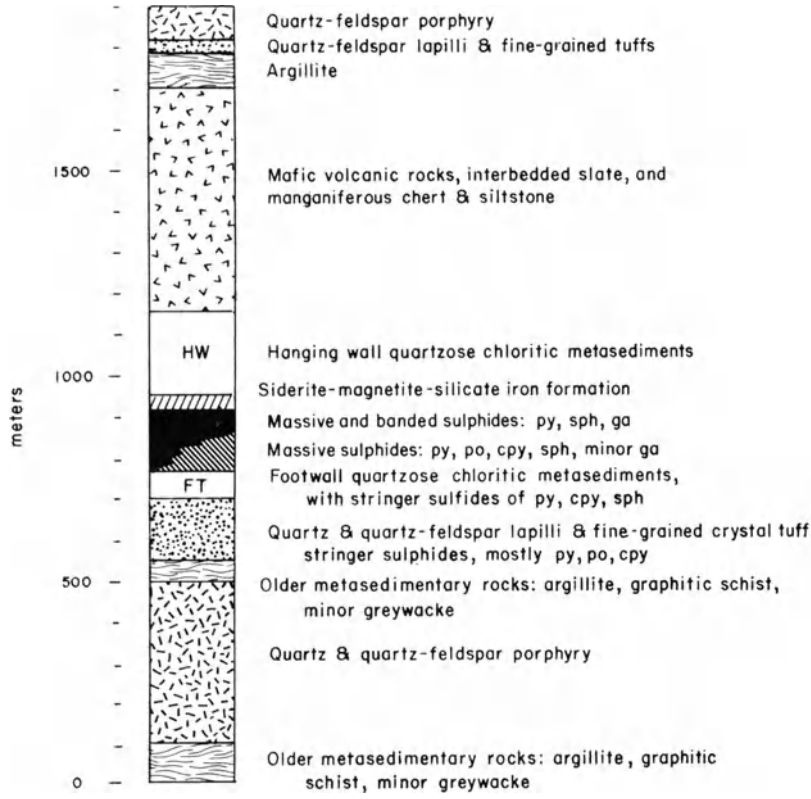

Fig. 3.27. Stratigraphic section of the Brunswick No. 12 area, New Brunswick. Note that although the volcanic rocks occur both down-section and up-section the massive sulfides are hosted by metasediments (After Franklin et al. 1981)

a pyrrhotite-pyrite pipe-like feature is present in the footwall and is thought to be the original site where venting of the ore fluids occurred. Van Staal and Williams (1984) claim that the shapes of orebodies are controlled by folding, despite their probable syngenetic origin. Four sulfide zones are recognized in the deposit, the largest of which is the main zone, a massive sulfide lens up to 1000 m long and 100 m thick. A number of zonal features are apparent in this lens. It is sandwiched between upper and lower pyrite units, and within it both pyrrhotite and chalcopyrite, and sphalerite and galena decrease upward. The quartz content, however, increases upward, from about 5% to as high as 20%, but the iron content of the sphalerite decreases upward through the lens.

Sulfur isotope studies of various ores in the district (Lusk and Crocket 1969; Lusk 1972) indicate that the sulfides in the southeastern portion are isotopically heavy (median $\delta^{34}S = 16‰$), whereas the ores in the central and northern areas are isotopically lighter (median $\delta^{34}S = 7‰$; Franklin et al. 1981). The isotope fractionation between individual sulfide minerals indicates

temperatures ranging from 317–357°C. Lusk and Crocket (1969) have suggested that these values represent metamorphic reequilibration temperatures, but, given the fine-grained nature of most of the ores in the district, these temperatures may approximate original depositional temperatures.

Harley (1979) has suggested that the distribution of Tetagouche felsic volcanic rocks can be interpreted in terms of a resurgent caldera complex developed within a continental setting characterized by extensional tectonics. More recently (van Staal 1987) a backarc setting for the Tetagouche volcanics has been suggested, based on petrochemical and structural data.

3.5.4 Discussion of Tectonic Environments

The Paleozoic massive sulfide deposits discussed in the preceding sections are characterized by settings marked by thick sequences of flyschoid clastic rocks and relatively thin sequences of bimodal volcanics. A similar setting is indicated for the Devonian-Mississippian Arctic massive sulfide district in northern Alaska (Hitzman et al. 1986) that contains the 36-million-ton Arctic deposit (Schmidt 1986, 1988). This deposit grades 4.0% Cu, 5.5% Zn, 1.0% Pb, 42 g/ton Ag, and 0.5 g/ton Au, but owing to its remote location is not economic at this time.

In all three of the districts cited above an ensialic (continental) rift environment has been suggested (Sawkins and Burke 1980; Sillitoe 1982; Schmidt 1986), but as noted earlier, Munha (1983) favored an early backarc rifting environment for the Iberian Pyrite Belt. Van Staal (1987) has suggested a similar setting for the Tetagouche Group volcanics in New Brunswick, and the Ambler district (Arctic deposit) in Alaska could well be equivalent in tectonic terms.

Sillitoe (1982, Table 1) notes that many massive sulfide deposits of more apparent continental settings exhibit felsic volcanics succeeded by mafic volcanics, and this relationship can also be seen in many of the Proterozoic massive sulfide ores of central and southern Finland (Huhtala 1979; Latvalahti 1979). This situation also pertains in the Hokuroku district of Japan and is elegantly explained by Urabe (1987) in terms of basaltic magma-induced crustal melting and later eruption of the mafic melts. Finally, the fact that these environments seem to undergo deformation, metamorphism, and intrusion relatively soon after formation supports that notion that they are fundamentally related to subduction regimes.

Clarification of the uncertainties regarding various types of extensional tectonic settings and their petrochemical and lithologic signatures will at best be a difficult matter, but new insights are being developed continually. For example, Tapponnier et al. (1982) have demonstrated from modeling studies that continental collision, such as that of southern Asia, can spawn large strike-slip faults that tend to develop rifts near their distal extremities, and that such rifts can develop into fully evolved marginal basins (see also Burke and Sengor 1986).

3.5.5 Discussion and Suggestions for Exploration

Despite all the research attention that Kuroko-type and related massive sulfide deposits have generated, some problems remain, especially regarding their limited stratigraphic distribution within volcanic piles, and the source of their contained metals. Urabe (1987) appears to have made a major contribution regarding the former problem by demonstrating that the preore felsic volcanics in the Hokuroko Basin are meta-aluminous, whereas the postore volcanics are more alkaline. Urabe (1985) also has demonstrated experimentally that partitioning of metals from a felsic melt to a hydrous phase is efficient for aluminous melts, but inhibited by alkalic melts. This finding, together with the evidence for the presence of felsic magmas at depth during the time ore deposition was occurring (see earlier), provides an explanation for the restricted timing of Kuroko ore generation. To the author's knowledge, similar investigations have not been carried out in other districts, but they would be predictably hampered by the invariably altered nature of the footwall rocks in massive sulfide districts.

The problem of the source of the metals in Kuroko-type deposits is considered an important matter. This author (Sawkins and Kowalik 1981; Sawkins 1982b, 1986a) has long been an advocate of a magmatic source for the metals in Kuroko-type deposits, but the support of many workers for the concept of an origin by rock leaching (e.g., Large 1977; MacGeehan and Maclean 1980; Ohmoto 1986) has unquestionably become the conventional wisdom. Enthusiasm for leaching models is based on several factors: the results of hydrothermal water-rock experimental studies, mineral solubility data, theoretical calculations, and the chemical and isotope results from numerous deposits which indicate that seawater becomes involved in seafloor metallization events. The results from studies of currently active spreading ridge geothermal systems and their ancient analogs in ophiolite complexes (see Chap. 5) appear to provide corroboratory information.

As was noted in the previous section, the full range of isotope parameters available for the deposits in the Hokuroku Basin (see Fig. 3.18) are compatible with a magmatic-hydrothermal model for metallogenesis. This model has been further reinforced by the realization that the average $\delta^{34}S$ value of sulfur in subduction-related magmas is about +6 and not close to zero (Ueda and Sakai 1984). The range of measured $\delta^{34}S$ values from Kuroko sulfides is close to this value. Furthermore, the compositions and the narrow range of lead isotopes throughout the Kuroko ore province (K. Sato and Sasaki 1973; T. Sato 1975) preclude the various pre-Tertiary basement rocks in the region as significant sources of lead. To circumvent this problem, proponents of a convective leaching model have suggested that the metals were obtained from the underlying crystallized intrusive systems that provided both the Miocene volcanics and the requisite heat to drive the seawater convection systems (Ohmoto 1978). In view of the consistent evidence noted earlier for negative δD values in the Kuroko ore fluids, and the occurrence of salinities significantly greater than those of seawater, a direct magmatic contribution of metals from

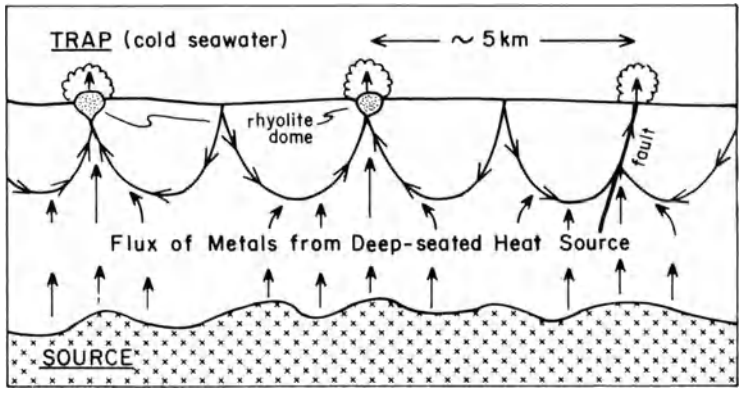

Fig. 3.28. Genetic model for Kuroko-type deposits favored by the author. The major source of metalliferous fluids is the underlying magmatic system, but the convecting fluids of seawater origin may be a factor in terms of focusing their discharge (After Sawkins 1986a)

underlying magmatic systems, perhaps with a minor addition of leached metals appears to represent a more viable genetic model (Sawkins 1982b, 1986a). The main significance of seawater convection systems in this model relates to their role in focusing the discharge of the diluted magmatic metalliferous fluids at specific points (Fig. 3.28). The rapid cooling of these discharging fluids by ambient seawater causes the precipitation of the metal sulfides (Janecky and Seyfried 1984).

To the exploration geologist, Kuroko-type orebodies present challenging targets because of their relatively small size and stratabound character. Their tendency to occur within restricted time-stratigraphic intervals in volcanic sequences is clearly important, as are their spacing characteristics, which are controlled by the typical dimensions of thermal convection cells in rocks (~ 5 km; see Sawkins 1980). The strong tendency toward magnesium enrichment and sodium depletion in footwall rocks near Kuroko-type orebodies has been carefully documented in Japan and is used as an aid in exploration (Date et al. 1983). Geophysical methods involving electrical potential, electromagnetics, and induced potential have all been used with success in locating massive sulfide orebodies, especially those of high iron sulfide content, and those that have been rotated into attitudes of steep dip.

3.6 Base and Precious Metal Vein Deposits

Examples of vein deposits that are emplaced in arc-related extensional settings include those in the Green Tuff districts of Japan (Lambert and Sato 1974; Shikazono and Tsunakawa 1982), and gold veins in what are probably arc-related rift terranes of Devonian age in New South Wales, Australia

(McIlveen 1974). One of the most important regions for vein deposits formed in a tectonic setting that could be regarded as a backarc extension is that of the western USA. For example, the broad development of caldera-type volcanism in the San Juan Mountains, Colorado during mid-Tertiary time suggests regional tension. Many of these caldera structures became hosts to important polymetallic and precious metal vein deposits. Despite the fact that the plate tectonic setting of the western USA cannot be viewed in terms of simple arc-related rifting (see Chap. 4), the vein deposits in the San Juan volcanic field will be discussed at this juncture.

3.6.1 Vein Deposits of the San Juan Volcanic Field

The volcanotectonic evolution of the San Juan region, with its array of caldera structures and associated mineral deposits (Fig. 3.29) has been worked out mainly by Steven and Lipman and their co-workers (see Steven and Eaton 1975 and references therein; Steven and Lipman 1976; Lipman et al. 1978 and

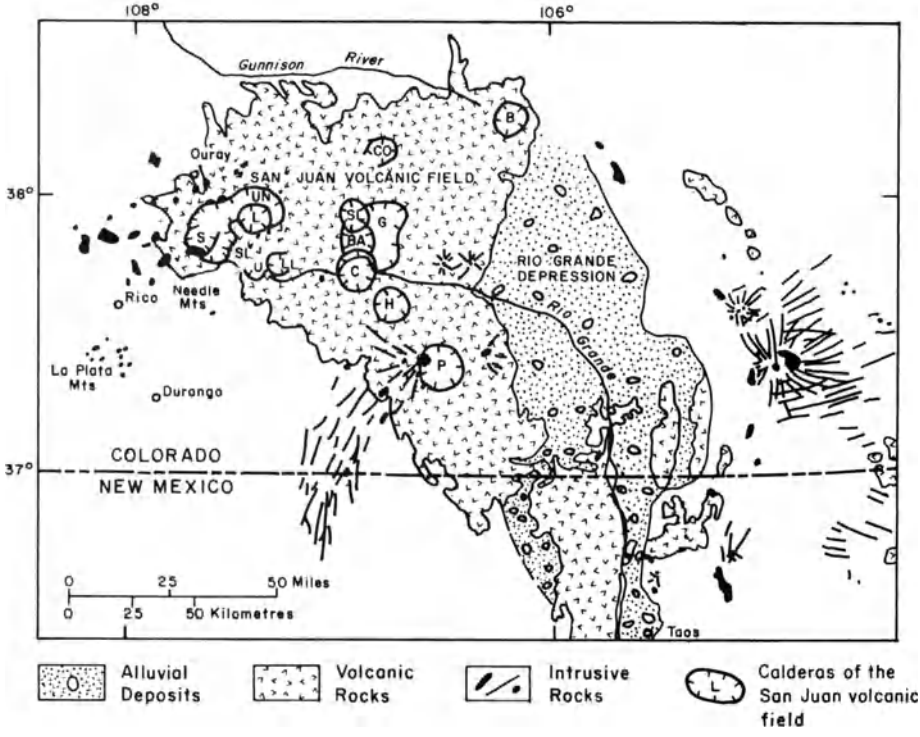

Fig. 3.29. Map of the San Juan volcanic field at the southwest end of Colorado Mineral Belt. Note that only some of the caldera systems are known to have mineralization associated with them. *B* Bonanza; *Ba* Bachelor; *C* Creede; *CO* Cochetopa; *G* La Garita; *H* Mt. Hope; *L* San Luis; *U* Ute Creek; *UN* Uncompahgre (After Lipman et al. 1976)

references therein). Of the 12 recognized calderas in the San Juan volcanic field, only 6 have significant metal deposits associated with them (see Fig. 3.29), and radiometric age studies (see later) indicate that most mineralizations distinctly postdate caldera formation. It is now realized (McKee 1979; Rytuba 1981) that the genetic connection between calderas and metal deposits has been much overemphasized, and that the main factor of importance is the throughgoing fracture systems that result from caldera development (Lipman et al. 1976).

Many studies of vein mineralization have been carried out in the San Juan region (e.g., Casadevall and Ohmoto 1977; Slack 1980), but the main focus has been on the silver-rich, base metal veins of the Creede district (Bethke et al. 1976; Barton et al. 1977; Bethke and Rye 1979; Robinson and Norman 1984), which are low-sulfidation, adularia-sericite type (see Chap. 2). The Creede vein system consists of a series of more or less parallel veins that occupy a north-south graben structure beyond the Creede caldera (Fig. 3.30). The Amethyst-OH system has been continuously mined for nearly 3 km, and the

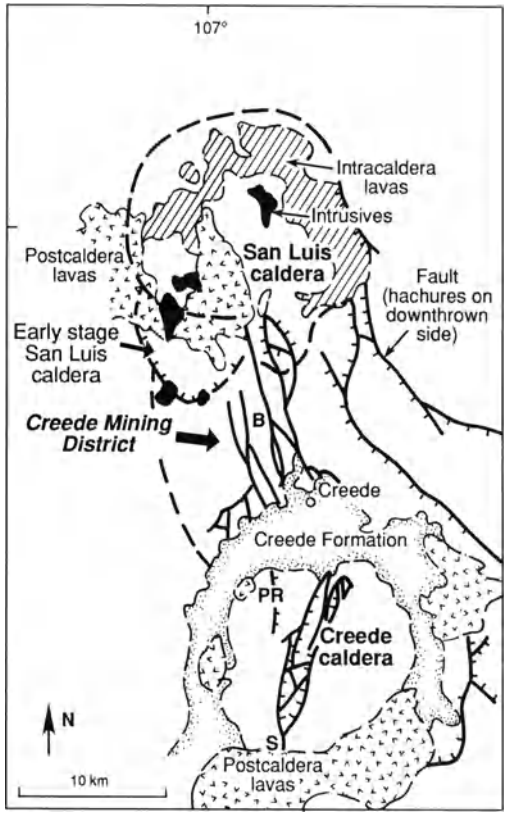

Fig. 3.30. Generalized geology of the Creede and San Luis calderas. Note that Creede mining district is localized by a set of normal faults that extend northwards from the Creede caldera rim (After Steven and Lipman 1976)

Bulldog system for over 2 km. Total silver production has been approximately 3.5×10^5 kg.

Extensive studies of these veins indicate that they are all part of a single ore-generating event that occurred in five identifiable stages. Metallization, however, was essentially restricted to stages two and four (Hayba et al. 1985). A strong zoning pattern was imposed on these mineralization stages during their development, with a higher temperature (OH) assemblage in the north and a lower temperature (Bulldog) assemblage in the south reflected in terms of mineralogy and fluid inclusion homogenization temperatures. The OH mineral assemblage is chlorite + hematite + quartz + adularia + galena + sphalerite + chalcopyrite + pyrite + fluorite + tetrahedrite, whereas the Bulldog assemblage is barite + rhodochrosite + quartz + adularia + galena + sphalerite + fluorite + tetrahedrite + silver sulfosalts + native silver. Another observation supportive of a north to south flow direction of the hydrothermal solutions is the greater intensity of hydrothermal leaching of vein minerals at the north end of the system.

Considerable attention has also been directed toward wall-rock alteration features, fluid inclusion assemblages, and the chemical and isotopec parameters of the ore fluids (see Hayba et al. 1985, and references therein). These results have led to a general model for the Creede hydrothermal system (Fig. 3.31) that involves a complex hydrologic scenario involving two distinct meteoric water sources and probable contributions from a postulated underlying magmatic heat source.

The importance of an underlying magmatic system in terms of a source for the sulfur, chlorine, and metals in the Creede ores and ore fluids has been downplayed, and most of the Creede investigators have favored the moat sediments of the Creede Formation (see Fig. 3.31) as the source of the chloride and some of the metals. Lead isotope data (Doe et al. 1979), however, indicate that the bulk of the lead in the Creede ores must have its ultimate source in the 1.4–1.7 Ga basement rocks that underlie the San Juan volcanic field. This radiogenic lead could have been incorporated in the Creede ores by leaching of lead directly from the Precambrian basement or sediments derived therefrom, or more probably by assimilation into Tertiary magmatic systems and subsequent addition to ores directly or via leaching from volcaniclastic materials. A Tertiary magmatic history for the Creede ore leads is in fact suggested by the latest lead isotope work on ash-flow tuffs from the central San Juan calderas (Matty et al. 1987). The critical point is that data from lead isotopes are at present equivocal in terms of a genetic model for the Creede deposit.

Whatever the full genetic history of the Creede system, the extrapolation of ore genesis concepts based on Creede to a general model for epithermal deposits must be viewed with caution. In particular, the presence of a thick sequence of intracaldera sediments, with which circulating groundwaters could interact and perhaps obtain elevated chlorine contents (Hayba 1987), is not a common situation and simply cannot be applied as a general model to polymetallic and precious-metal epithermal environments. Furthermore, the San Juan region must have been underlain by some large bodies of magma

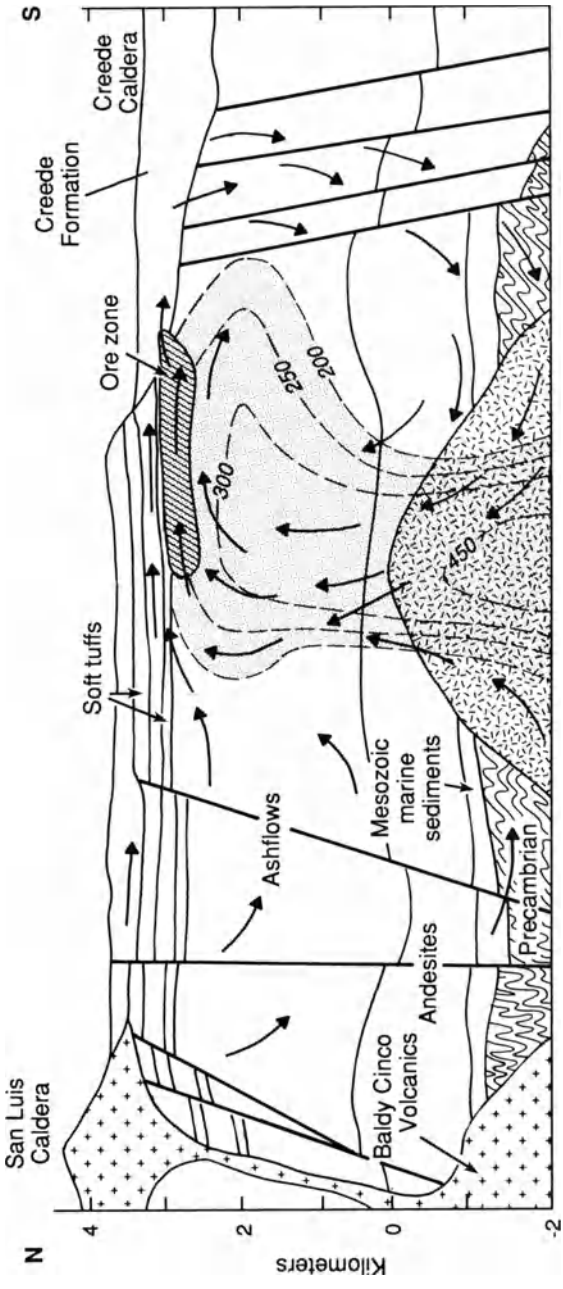

Fig. 3.31. North-south cross-section showing the hydrologic model proposed for the genesis of Creede vein mineralization on the basis of fluid inclusion and isotope data (After Hayba et al. 1985)

during mid-Tertiary time, and it would be surprising indeed if these contributed little more than heat to the spectrum of metal deposits that formed at Creede and elsewhere at the southern end of the Colorado Mineral Belt.

Recent studies of the Au-Cu-Ag deposits within the Summitville caldera (Stoffregen 1987) indicate that the mineralization, which occurs as a series of discontinuous zones in porphyritic quartz latite, is of high-sulfur type. The irregular pipes and lenticular pods of ore lie within a zone of intense quartz-alunite alteration, and have a limited vertical extent (200 m). Luzonite + covellite + native gold give way downward to chalcopyrite + tennantite with the ore minerals lining cavities in vuggy silica material or occupying microveinlets. Mineral assemblages indicate that very low pH values (~ 2) and relatively high fo_2 values were maintained during the intense quartz-alunite alteration. Stoffregen (1987) concludes that a change from a magmatic vapor-dominated system to a more reduced liquid-dominated system occurred between the alteration and metallization events.

3.6.2 Discussion

Despite the abundance of calderas in the San Juan volcanic field, the association of metal deposits with them is selective in both time and space. During early stages of caldera development, voluminous calc-alkaline volcanics were erupted, mostly as andesites and quartz latites that give K-Ar ages from 31.1 to 34.7 Ma (Lipman et al. 1970, 1976; Steven and Lipman 1976). These were followed by ash-flow sheets of more felsic composition (29.8–26.2 Ma), and finally after about 25 Ma, volcanism produced widespread basaltic lavas and local rhyolitic flows and tuffs.

In general terms, the ore deposits are related to the youngest, most differentiated intrusions in the caldera cycles. Lipman et al. (1976) have demonstrated that the earlier intrusions of more intermediate composition did generate hydrothermal convection systems, but that they produced only barren alteration and quartz-pyrite veins. Thus, the richest ores in the region, those associated with structures related to the Silverton caldera, formed 5 to 15 Ma after caldera collapse, and exhibit a time-space relationship to minor intrusions of quartz-bearing silicic porphyry. One exception to this is the base and precious metal mineralization associated with the relatively young Lake City caldera (Slack 1980), where the radiometric data indicate that some of the mineralization was closely associated in time with caldera formation 22.5 Ma ago.

The transition from compressional to extensional environments in this portion of the North America Cenozoic arc system was clearly a complex matter, but the very change from early, central-type volcanism to caldera formation is indicative of a relaxation of regional compression. Furthermore, the emplacement of the great bulk of the ores in the Colorado Mineral Belt subsequent to the initiation of bimodal basalt-rhyolite volcanism justifies their inclusion within the category of deposits related to arc-rifting environments.

Chapter 4 Additional Aspects of Arc-Related Metallogeny

In the foregoing chapters, the most important types of deposits found in largely post-Paleozoic, arc-related tectonic settings were examined. These younger arc terranes are clearly more tractable to tectonic analysis than their older counterparts, where a combination of deeper erosion levels and later orogenic events render plate reconstructions more tenuous. There are, however, many important metal deposits in older orogenic belts that must be included in any meaningful synthesis of the relationships of metal deposits to plate tectonics. Furthermore, there are a number of metal deposits in post-Paleozoic arc systems that do not fall into the tectonic subdivisions of arcs dealt with in Chapters 1, 2, and 3. This latter group will be considered prior to a discussion of the metallogeny of older arc-related metal deposits.

4.1 Metal Deposits Related to Forearc Felsic Magmatism

In modern convergent plate boundary environments, the arc-trench gap is an important area of sediment accumulation. Thick sequences of sparsely fossiliferous turbidites accumulate in this zone, and igneous rocks are typically restricted to slices of ophiolite that become tectonically incorporated in the sedimentary prisms during subduction-related imbricate thrusting along the inner trench wall. The deeper levels of these sequences in older arc systems are characterized by low temperature-high pressure metamorphism (blueschists).

The forearc terranes of southern Alaska, southwest Japan, and western Sumatra contain granitic intrusions emplaced between the magmatic arc and trench. The Sanak-Baranof belt (Hudson 1983), which extends 2000 km along the curvilinear southern margin of Alaska, is perhaps the prime example of this type of forearc magmatism. The plutons throughout the belt have intruded an upper Mesozoic-lower Tertiary accretionary prism that lies close to the present-day continental margin. The stocks consist mainly of biotite granodiorite and biotite granite, and many are elongate parallel to the regional structural trends of the strongly deformed host rocks. Age dating of these intrusive rocks (see Hudson 1983 and references therein) indicates emplacement ages of the range 47–51 Ma in the eastern segment and 58–60 Ma in the western segment.

The origin of such granitic magmas in areas generally characterized by low heat-flow is puzzling, but Marshak and Karig (1977) and Delong and Schwarz (1979) have suggested that the subduction of spreading ridges associated with triple junction plate configurations would cause sufficient local heating of the base of the forearc sedimentary pile to induce melting. Hudson et al. (1979)

report petrologic and strontium isotope data from granodioritic plutons in the Chugach Mountains of Alaska that strongly indicate an anatectic origin for the biotite tonalite, biotite, granodiorite, and granite intrusions there. In contradistinction to the petrogenetic model above, however, they suggest that cessation of accretionary offscraping of cold materials to the base of the sedimentary pile would allow temperatures to rise sufficiently to permit partial melting. Finally, Hollister and Crawford (1986) have suggested that melting at depth within arc systems is a major factor in facilitation of deformation and that some of the melts can intrude back up deformation surfaces during surge-like activity to reach sites within the accretionary prism.

No mineralization of consequence has been reported from these forearc intrusions in Alaska or from those in Sumatra, but the ilmenite-series Cenozoic plutons within the thick flysch-type sediments of the Shimanto Belt of southwest Japan have minor tin, tungsten, copper, and antimony deposits associated with them (Fig. 4.1) (Oba and Miyashisa 1977). In addition, Mitchell and Garson (1981, pp. 172–173) suggest that the early Devonian granites of the Southern Uplands of Scotland, emplaced within flysch-type sediments of late Ordovician to Silurian age, could represent Paleozoic examples of forearc magmatism. Minor uranium and copper mineralization is associated with this igneous suite.

Although this mineralization is of limited significance when compared with other facets of arc metallogeny, the recognition of forearc igneous suites and possible associated mineralization is important to a full understanding of arc systems. The only other metal deposits found in forearc terranes are those associated with slices of ophiolite that can become incorporated in the imbricate zones that characterize forearc outer belts. Because their presence results purely from tectonic processes, they are more appropriately related to the metallogeny of spreading ridge systems (see following chapter).

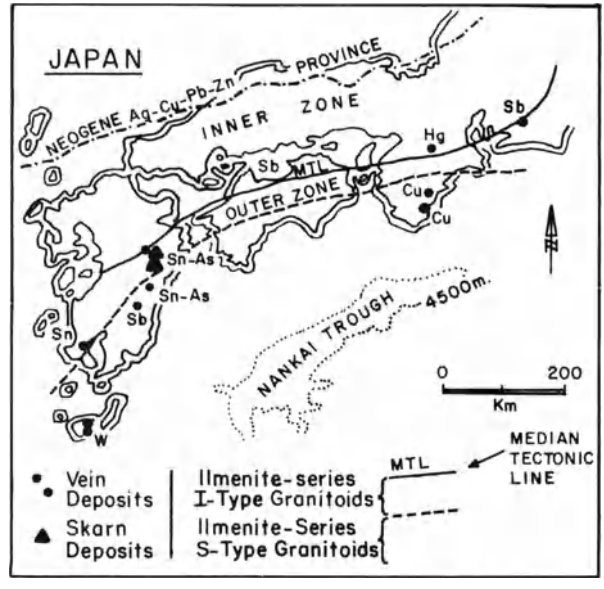

Fig. 4.1. Distribution of mid-Miocene vein and skarn deposits in Outer Zone of Japan. Note that granitoids are all ilmenite series, but include *S*-types (nearest trench) and *I*-types in discrete belts, and the roughly coeval magnetite-series Ag-Cu-Pb-Zn-belt to north of the Inner Zone (After Sillitoe 1981a)

4.2 Gold Deposits of a Complexly Evolving Continental Margin Arc-Rift-Transform System: Western USA

4.2.1 Gold Deposits of the Mother Lode System, California

The Mother Lode is the name given to a composite system of lode gold deposits that extends 195 km along the western foothills of the Sierra Nevada in central California (Fig. 4.2). Together with the Grass Valley and Alleghany districts to the north, it has produced close to 1000 tons of gold from ore that averaged close to 10 g/ton. The veins in the Grass Valley district occur mainly within granodiorite (Johnston 1940), but the Mother Lode is a complex system of quartz veins and mineralized rock associated with a steeply east-dipping major fault zones (Knopf 1929). The structural and stratigraphic details along this zone are still contentious (see Ernst 1981), but the Melones Fault Zone and adjacent structures form the locus of most of the gold lodes, especially in the southern segments (Dodge and Loyd 1984).

The quartz lodes form discontinuous lenticular bodies that are typically of short strike length but can exhibit rake lengths of over 2000 m. Furthermore, as noted by Knopf (1929), some ore shoots top out as much as 1000 m below the surface. The host rocks for the quartz lodes and lower-grade disseminated orebodies are primarily Jurassic greenstones and slates, but in places serpentinites occupy the fault zones and may host the gold mineralization (Clark 1969). At their margins the quartz lodes terminate abruptly, but at their ends the quartz splays out to form stringer zones. The wall rocks along the Mother Lode are heavily altered to sericite-carbonate assemblages in most places, and locally these carbonatized bodies are of sufficient size and gold content to comprise low-grade ore amenable to bulk mining. These are particularly common in the southern portions of the Mother Lode (Albers 1981). Several of these bulk-mineable gold deposits have been placed in production recently (see T.K. Smith et al. 1987; Bonham 1988) and they represent a total of over 50 million tons of ore averaging about 2 g/ton Au.

The gold in the orebodies occurs largely as native Au, but the gold telluride mineral petzite is present in some deposits. Gold-silver ratios range between 8 and 9 to 1. Sulfide contents of the ores are typically low and comprise mainly pyrite with minor amounts of arsenopyrite, sphalerite, galena, chalcopyrite, and tetrahedrite (Knopf 1929). Scheelite is common locally in the Grass Valley district (Johnston 1940). Quartz dominates the gangue assemblages, but locally ferroan dolomite, other carbonates, and sericite are present.

Recent age studies of the gold mineralization in several districts in the Foothills Metamorphic Belt, including the Mother Lode and Grass Valley, have focused on the Rb-Sr and K-Ar systematics of quartz-mica assemblages formed from ultramafic wall rocks adjacent to veins (Bohlke and Kistler 1986). The results indicate that mineralization ages throughout the Foothills Belt were concentrated between 115–120 Ma, significantly later than prograde metamorphism and penetrative deformation related to accretion of oceanic

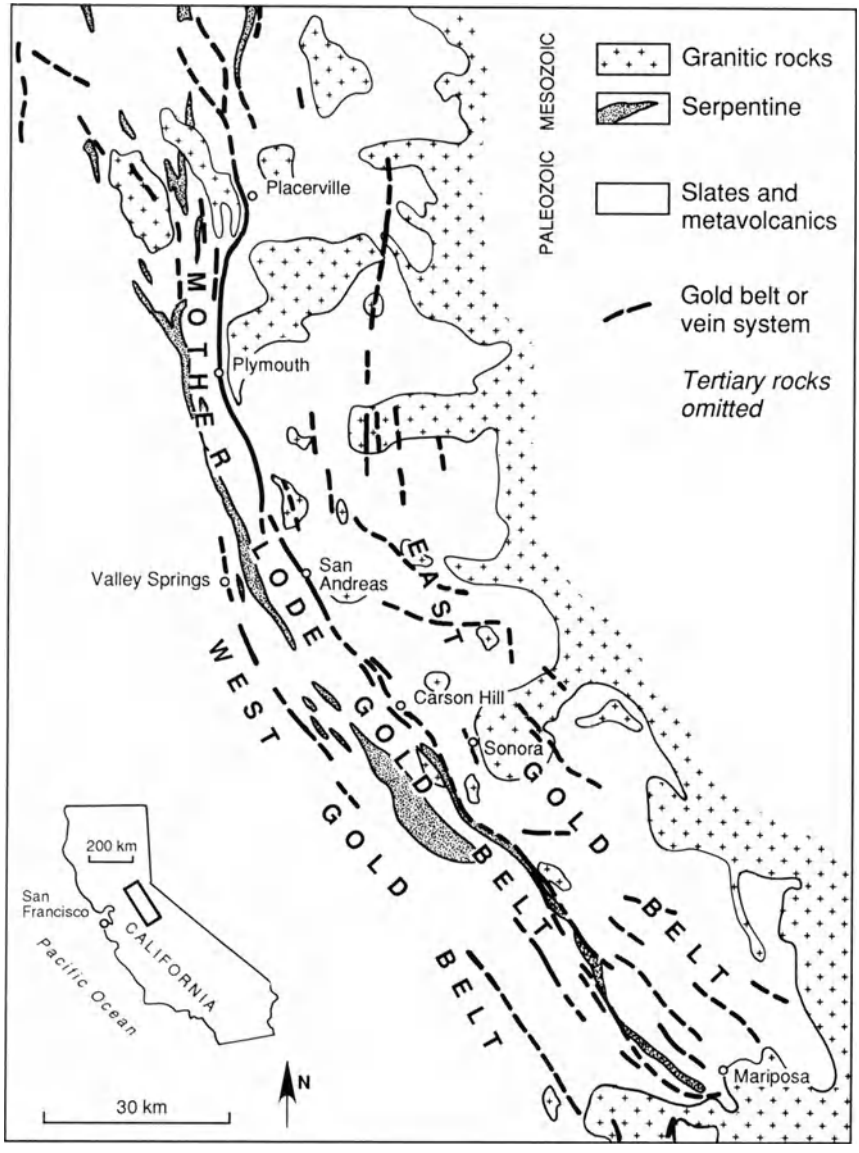

Fig. 4.2. Simplified map of the Mother Lode gold belt in California. Note the general parallelism of the Mother Lode and adjacent belts to the western edge of the Sierra Nevada batholith granitic rocks (After Clark 1969)

island arc terranes. Bohlke and Kistler (1986) suggest that the mineralization is related to fluids set in motion by deep-seated magmatic activity that reflects the resumption of subduction under North America after termination of the late Jurassic Nevadan collision event.

The model is based on the evidence from stable isotope and strontium isotope analyses of hydrothermal minerals, which indicate the presence of CO_2-rich, high $\delta^{18}O$ fluids of crustal origin during hydrothermal activity. Weir and Kerrick (1987), in their studies of a number of gold deposits along the southern portions of the Mother Lode, concluded that the fluids could have been either of metamorphic or magmatic origin. Both sets of authors find evidence for depositional temperatures in the 250–350°C range. These are similar to, but slightly lower than, the temperatures reported by Coveney (1981) based on fluid inclusion studies of quartz from the Oriental Mine, Allegheny district. Here, temperatures are indicated to be above 340°C for the major stage of quartz and gold introduction, under pressures ranging from 670 to 2500 bar.

Nesbitt et al. (1986) report mineralogic, fluid inclusion and stable isotope data from mesothermal gold deposits in the Canadian Cordillera that in many respects are similar to those for the Mother Lode of California. The Canadian gold deposits, like the Mother Lode, are also hosted in accreted terranes of oceanic or island arc origin (Gabrielse 1985) and similar mesothermal lode-gold deposits in the Juneau gold belt, Alaska, have comparable settings and isotope characteristics (Goldfarb et al. 1988). Given the overlap in their mineralogical and stable isotope characteristics with many lode-gold deposits of Archean age (Fig. 4.3), they provide strong support for the tectonic and genetic concepts suggested for Archean lode gold deposits associated with major fault structures (breaks) in greenstone belts (see later).

4.2.2 Gold and Silver Vein Deposits of the Great Basin

A large number of vein deposits carrying precious metals are scattered through the western USA, particularly within the Basin and Range Province (Silberman et al. 1976; Guild 1978; Silberman 1978). Although the precise mineralization ages of many of the smaller deposits is not known, the vast majority occur within late Cenozoic felsic volcanic rocks (Silberman et al. 1976), and the major deposits are arrayed along a northwesterly trend in western Nevada called the Walker Lane. This belt is thought to be a trans-current fault zone, and contains the Tonapah, Goldfield, and Comstock Lode deposits in addition to many smaller deposits and widespread alteration zones (Fig. 4.4). At current prices, the Tonapah and Goldfield deposits have each produced in excess of $1 billion worth of precious metals and the Comstock Lode well over $2 billion. These and numerous other deposits are essentially similar to epithermal precious metal deposits in principal arcs and, as in other arcs, both adularia-sericite and acid-sulfate types are present.

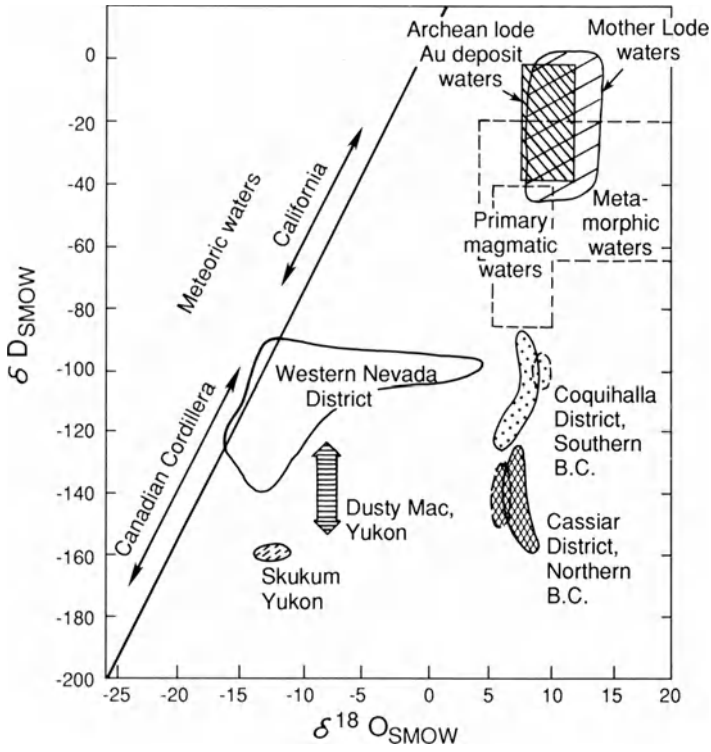

Fig. 4.3. δD vs $\delta^{18}O$ plot of the fluids associated with gold deposits in western North America (After Nesbitt et al. 1986). Such plots should be viewed with caution, however, because the meteoric fluids which they indicate as involved in gold mineralization may pertain more to the formation of gangue components and not to the introduction of the gold

The quartz veins in the Tonapah district contained ore-grade mineralization within a well-defined favorable zone (Fig. 4.5). The chief ore minerals are argentite, polybasite, and pyrargyrite. Silver/gold ratios are about 100:1 and the gold was present chiefly as electrum (Nolan 1933). Detailed observations of the hydrothermal alteration patterns at Tonapah are reported by Bonham and Garside (1979) who recognized a zonal arrangement of alteration facies. The innermost zone, adjacent to the quartz veins, consists of quartz, sericite, and adularia, plus disseminated pyrite. This K-silicate zone grades outward to an intermediate argillic zone that can be divided into an inner subzone of kaolinite-halloysite, plus some quartz and sericite, and an outer subzone characterized by montmorillonite, plus lesser kaolinite and sericite. Disseminated pyrite occurs in this intermediate zone, and both it and the inner zone appear bleached. The combined widths of these two zones on both sides of the veins can reach 40 m.

The inner and intermediate zones of hydrothermal alteration are set within a broad zone of propylitic alteration that decreases in intensity outward

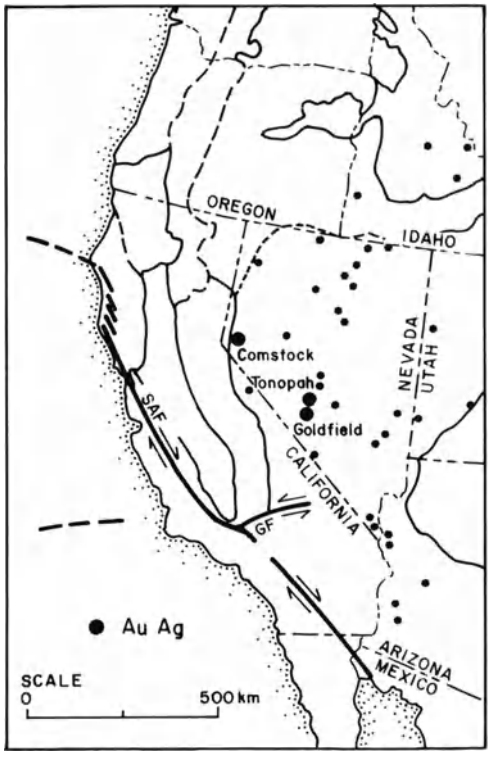

Fig. 4.4. Principal post-Laramide precious metal vein deposits of the Basin and Range, western United States. Note crude linear array (Walker Lane) of major deposits in western Nevada (After Guild 1978)

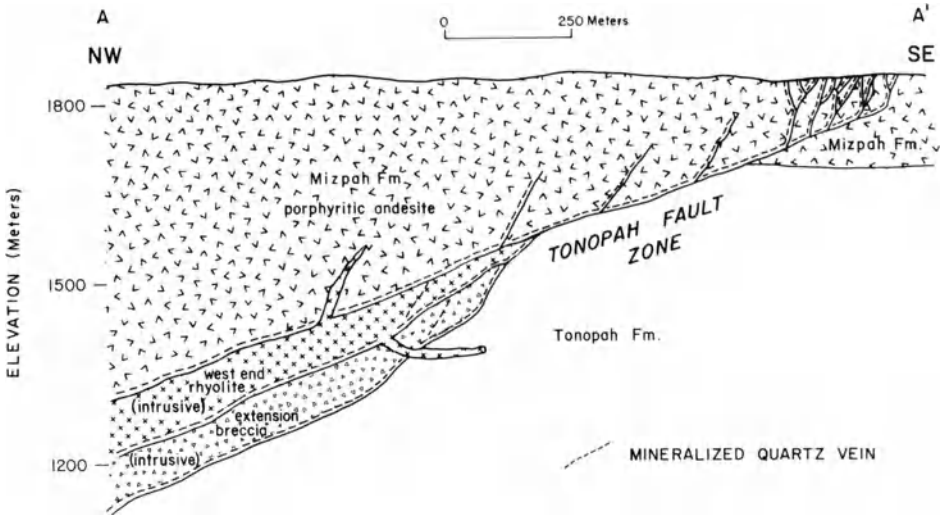

Fig. 4.5. Generalized cross-section through the main part of the Tonapah district, looking northeast. Note restriction of the mineralization to a limited part of the volcanic stratigraphic section (After Fahley 1981)

from the center of the district. Chlorite, calcite, albite, and hydrothermal K-feldspar are the main minerals developed, and the innermost portions of this propylitic zone contain disseminated pyrite. The altered rock is a greenish-gray color. Mineralized quartz veins toward the margins of the district pass upward into quartz and calcite stringer zones: pyrite is essentially the sole sulfide present in these vein tops and propylitic alteration extends upward from them for up to 200 m. Little silver or gold is present.

Isotope studies (H.P. Taylor 1973) indicate that large volumes of the volcanic host rocks at Tonapah are equilibrated with $\delta^{18}O$ and deuterium-depleted meteoric waters. Both the isotope data and increasing silver/gold ratios indicate a temperature zonation from about 300°C to lower values, outward from the center of the district. Thus, a convecting, meteoric water-dominated hydrothermal system powered by an underlying intrusive body seems to be clearly related to the formation of the Tonapah ores. The occurrence of high Mo in the veins, especially at depth, and the presence of high-SiO_2 rhyolitic domes suggest that this may be the top of a Climax-type Mo system (R.H. Sillitoe, per. comm.).

The Comstock Lode, at the northwestern end of the Walker Lane, is another adularia-sericite type deposit and one of the world's great bonanza-type epithermal precious metal deposits and since 1859 has produced 235 tons of gold and 5500 tons of silver (Bonham and Papke 1969). Over 95% of this production has come from the Comstock fault zone, and the remainder from the adjacent Silver City, Occidental, and Flowery vein systems. The high-grade orebodies (bonanzas) were distributed along 3.8 km of the Comstock structure and extended to a depth of over 900 m from the surface. The largest bonanza orebodies contained as much as 1.4 million tons grading 54 g/ton Au, and 850 g/ton Ag.

Recent age determinations on the igneous rocks in the area (Vikre et al. 1988) indicate that intermediate to felsic volcanic and intrusive activity occurred during a span of 10 million years, from 22–12 Ma. Spatially and temporally associated with the ores, which were deposited 13.7 Ma ago (Vikre et al. 1988), are the Kate Peak latite intrusions and domes. Vikre (1987) reports a complex array of vein assemblages, but apparently the ore minerals, electrum and acanthite, occur in the earliest assemblage together with quartz + pyrite + base metal sulfides + K-feldspar. This is cut by several later generations of quartz, while the last stage of vein filling is represented by calcite. Alteration minerals formed in the wall rocks adjacent to veins are quartz, sericite, pyrite, chlorite, and montmorillonite, whereas away from the veins a quartz + chlorite + albite + calcite + epidote + pyrite assemblage persists for tens of meters.

Vikre (1987) reports fluid inclusion temperature and salinity data from an extensive set of samples from the Comstock fault vein material, both within and outside orebodies. These indicate that bonanza ores were deposited in the temperature interval 250–275°C by fluids that ranged from < 2 to > 6 equiv. wt% NaCl. The temperature data also suggest a center of upwelling (temp. $>$ 280°C) below the Cedar Hill area, toward the north end of the mineralized

Comstock sector. This conclusion is also supported by mineral composition trends. Sampling problems made it impossible to isolate ore-stage fluids from fluid inclusions to permit definitive isotope measurement of the δD and $\delta^{18}O$ of the metallizing fluids, but the data reported by Vikre suggest that magmatic fluids played a significant role in the ore-forming events.

The major epithermal precious metal deposits of western Nevada are Miocene in age (Silberman et al. 1976) and, as noted above, occur predominantly within felsic volcanics. By Miocene time, extensional tectonic activity and related basalt or rhyolite and basalt volcanism was already well established farther east in the Basin and Range Province, but it appears that principal arc magmatism was withdrawing westward at that time toward its present position along the Cascades (Snyder et al. 1976; Fig. 4.6). Presumably this westward movement of principal arc magmatism was due to steepening of the underlying subducting slab, as has been suggested by geochronologic and petrologic studies in Arizona and northern Mexico (Keith 1978; Clark et al. 1982).

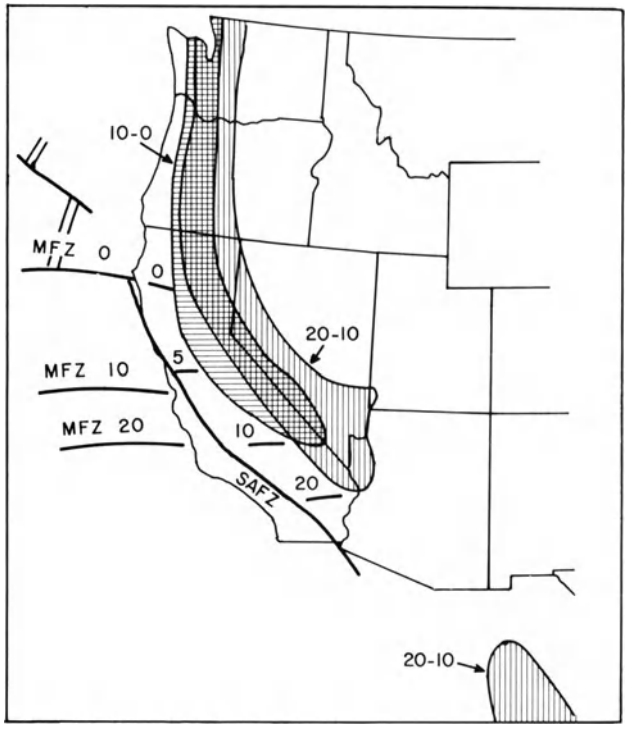

Fig. 4.6. The westward withdrawal of the zone of calc-alkaline volcanism during the late Cenozoic to its present position in the Cascades. *MFZ* Mendicino Fracture Zone; *SAFZ* San Andreas Fracture Zone. *Numbers* refer to age ranges (m.y.) of calc-alkaline volcanics (After Burchfield 1979)

4.2.3 Sediment-Hosted Gold Deposits of the Great Basin

Over 25 disseminated gold deposits hosted by sedimentary rocks and amenable to bulk mining techniques are now in production in the Great Basin (Bonham 1988). Some of these so-called sediment-hosted or Carlin-type deposits are concentrated along linear belts in north-central Nevada (Percival et al. 1988). The NW-trending Carlin zone is at least 60 km long but only 2 km wide.

Carlin-type deposits are characterized by host rocks consisting of thin-bedded, commonly carbonaceous, silty limestones or limy siltstones; by micron- to submicron-sized gold; and by anomalous arsenic (100–1000 ppm), antimony (10–50 ppm), mercury (1–30 ppm), thallium, molybdenum, and to some extent tungsten, values. Gold/silver ratios in Carlin-type deposits are typically 1:1 or greater, and the ores exhibit little, if any, enrichment in copper, zinc, and lead. Major introduction of silica, primarily in the form of jasperoid, is the most conspicuous feature of Carlin-type mineralization and represents an important guide to ore, especially when coupled with geochemical analysis for Carlin-type suites of trace elements. Barite is a characteristic gangue minerals and locally may be accompanied by fluorite.

The orebodies themselves exhibit a variety of geometries, such as tabular zones parallel to bedding, and pipes and vein-like forms cutting across bedding. High-angle faults of limited offset were important controls of ore-fluid plumbing, and orebody sites and shapes tend to be controlled by the intersection of such faults, either with favorable beds or other faults.

Detailed studies of the Carlin deposit (Radtke et al. 1980; Radtke 1985; Bakken and Einaudi 1986; Kuehn and Rose 1986) have provided a somewhat clearer understanding of this type of deposit, but much remains to be understood regarding precise metal and fluid sources. The Carlin ores occur primarily as tabular replacements of Paleozoic thin-bedded argillaceous to arenaceous beds rich in carbonate that are exposed in a window through the upper plate of the Roberts Mountain thrust (Fig. 4.7). Subsequent normal faulting has been extensive in the area and resulted in intense shattering of the lower plate carbonate-rich sediments. Larger Basin and Range faults have caused rotation of the sedimentary units but are almost certainly postmineralization in age.

Most of the orebodies at Carlin occur within the upper 250 m of sediments of the Roberts Mountain Formation. This formation is overlain by the Popovich Formation, which in turn is overlain and truncated by the Roberts Mountain thrust. Three ore zones, west, main, and east, have been delineated (see Fig. 4.7) and consist mainly of stratigraphically controlled, tabular zones adjacent to faults. The unoxidized hypogene ores are of various types, the major type consisting of rocks closely resembling unaltered host rocks, but where calcite has been removed and fine-grained pyrite and silica, together with gold, arsenic, thallium, antimony, and mercury have been introduced. Siliceous ore, on the other hand, contains large amounts of introduced

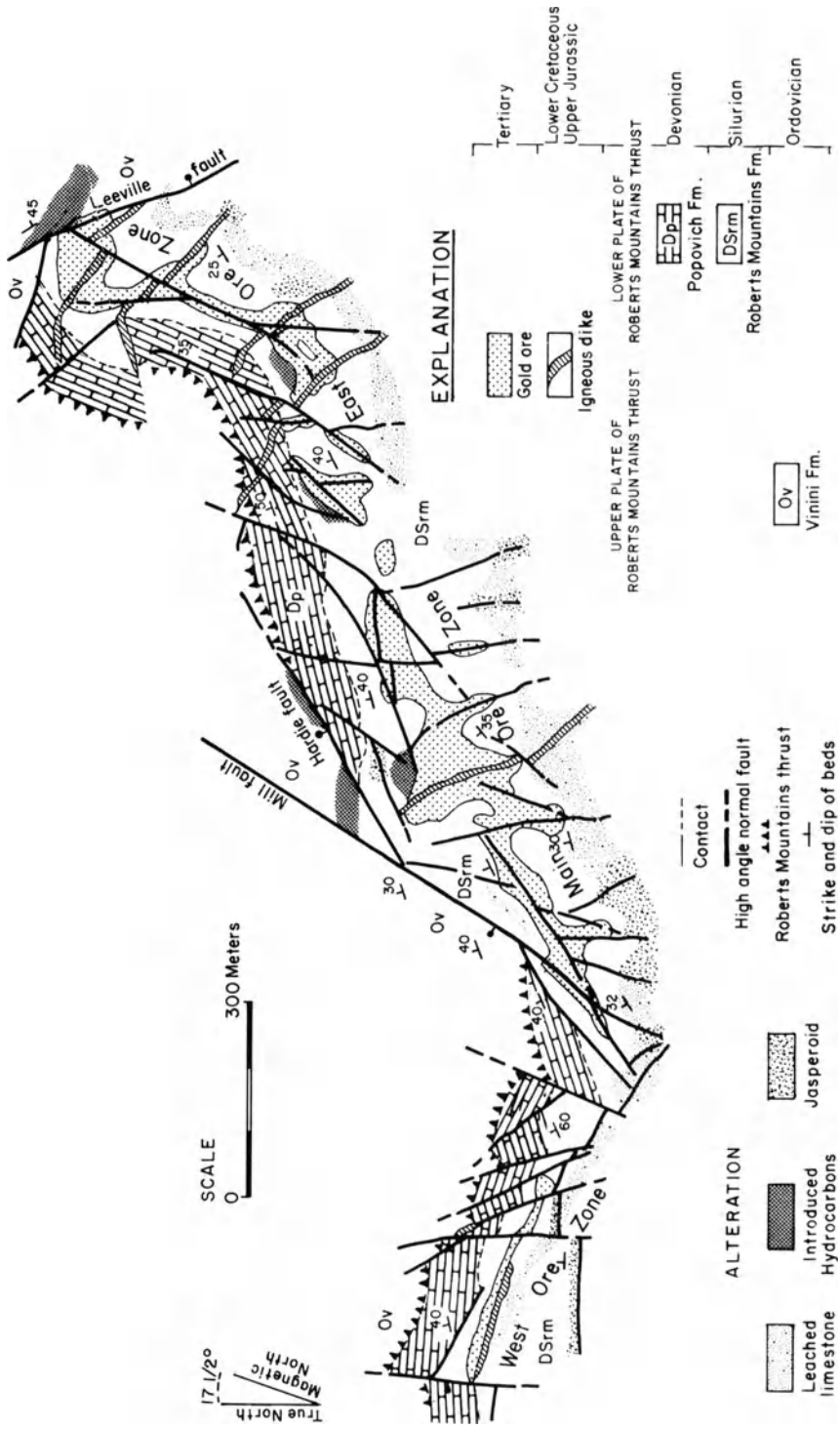

Fig. 4.7. Generalized geologic map of the Carlin gold deposit. Note the substantial development of normal faulting and its control of most of the ore bodies (After Radtke et al. 1980)

fine-grained silica and grades into jasperoid. Pyritic, carbonaceous, and arsenical ores represent variants of mineralization style.

In detail, the tenor of gold and its associated trace metals is highly variable. The gold occurs largely in association with arsenic, antimony, and mercury as fracture fillings and coatings on pyrite grains and to a lesser extent with organic carbon. The uppermost portions of orebodies have been subjected to varying intensities of acid leaching and are strongly altered and oxidized. The rocks in this zone consist mainly of fine-grained quartz and illite, with lesser kaolinite, sericite, and minor montmorillonite and limonite. Gold in this material occurs as tiny particles (up to 10 microns), contained either in quartz or associated with oxides or clay minerals.

Detailed studies of the nature and timing of wall-rock alteration at Carlin (Bakken and Einaudi 1986) have demonstrated five stages of increasing intensity of carbonate removal and jasperoid introduction. Optimum gold concentrations are associated with intermediate levels of alteration, apparently a reflection of permeability in the partially altered host rocks. Veinlets are not directly related to mineralization and apparently formed mainly in highly silicified areas at a relatively late stage.

Fluid inclusion studies of the Carlin ores (Kuehn and Rose 1986) indicate a complex sequence of fluid events, including the introduction of hydrocarbons by a saline brine containing abundant CH_4 and under relatively high (1 kbar) pressure conditions. These events, however, clearly predate the time of gold mineralization, which according to data obtained from later generations of fluid inclusions was effected by moderately reduced (pyrite stable) acidic, low salinity CO_2-bearing fluids at temperatures of less than 250° C.

Stable isotope data for hydrogen and oxygen indicate that the fluids involved in ore deposition were of meteoric origin (δD -140 to -160 ‰) but that they were highly exchanged with heavier $\delta^{18}O$ from the country rocks. In addition, $\delta^{18}O$ values increased substantially (from ~ 3 to 10 ‰) during the episode of late boiling indicated by the fluid inclusion data.

The range of $\delta^{34}S$ values from hydrothermal pyrites (4–16 ‰) is comparable to that obtained from diagenetic pyrite in the host rocks, suggesting a sedimentary origin for the sulfur in the deposit. Overall, the data available for the Carlin deposit suggest an ore-generating system consisting of a meteoric water convective cell that utilized the fault and fracture systems that characterize the area (Fig. 4.8). The driving mechanism was presumably an underlying Tertiary felsic magma body. Radtke et al. (1980) and Radtke (1985) suggest that the components of the ores were derived by leaching from the sedimentary country rocks within the deeper portions of the convection system.

As noted by Bonham (1988), Carlin-type deposits, despite distinctive host rock environments, display some provocative similarities to Archean lode gold deposits. These include alignment along major crustal "breaks" (see later), an elemental chemistry characterized by low base metals but elevated As, Sb, Hg, Th, W, and B, and H_2O-CO_2-rich ore-forming fluids of low salinity. In the previous section possible genetic similarities between the Mother Lode ores

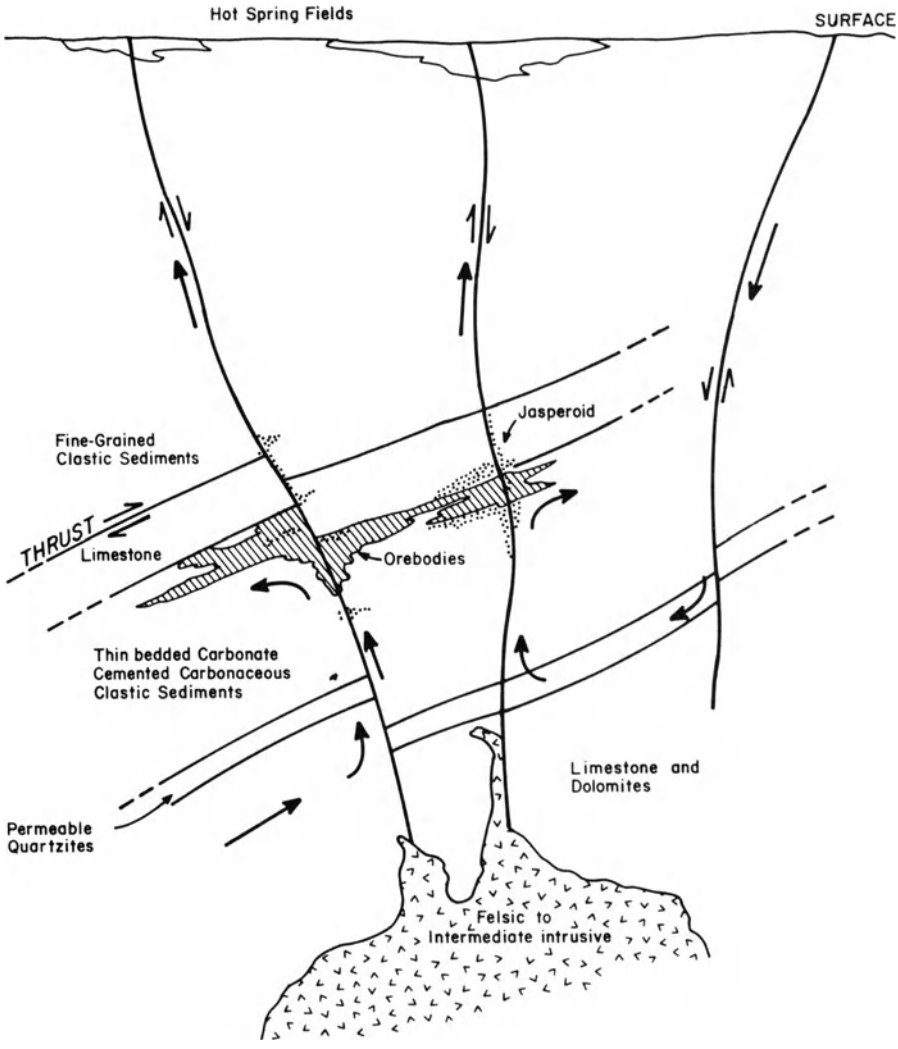

Fig. 4.8. Schematic cross-section of a disseminated replacement (Carlin-type) gold deposit (After Nelson and Giles 1985)

and Archean lode gold deposits were related to tectonic, geochemical, and isotope data suggestive of deep metamorphic-magmatic source environments. The linear "trends" of gold deposits in Nevada suggest control by major basement structures. These structures have also controlled intrusive events during Cretaceous and Tertiary time (Silberman et al. 1976). The stable isotope data reported by Rye (1985) for Carlin-type deposits seem to support deep metamorphic-magmatic sources. The observations above raise the intriguing possibility that Carlin-type deposits may represent the shallow-level (epithermal) equivalents of deeper-seated (mesothermal) lode gold systems.

4.2.4 Gold Deposits Related to Low-Angle Detachment Faults

In recent years, considerable exploration activity has been focused on a previously unrecognized class of disseminated gold deposit that occurs in metamorphic terranes in southeastern California and western Arizona. The deposits include the Mesquite mine (48 million tons, 1.7 g/ton), and the American Girl and Padre y Madre deposits in southeastern California that have announced reserves of 18 tons of gold between them (Bonham 1988).

The regional geology of this portion of the southwestern USA is characterized by metamorphic rocks ranging in age from Precambrian to late Mesozoic. These are overlain unconformably by Tertiary sedimentary and volcanic units. Regional-scale detachment faults are common, and they separate the metamorphic rocks of the lower plates from essentially unmetamorphosed sedimentary and volcanic units of the upper plates (Fig. 4.9). The metamorphic rocks of the lower plates show evidence of intense dynamothermal metamorphism and mylonitization at midcrustal levels during Mesozoic time and were intruded by a variety of plutonic rocks, ranging from diorite to peraluminous granite.

The gold in these deposits occurs in disseminated form in pyrite-bearing quartz veins and stockwork veinlets. Copper, lead, zinc, arsenic, and tungsten are the main associated metals, but of these only copper occurs in amounts of 1% or more. Studies of the Mesquite deposit (Willis and Holm 1987; Manske et al. 1987) indicate that the gold occurs in quartz veinlets, siliceous breccia, and ankerite-dolomite veinlets and that adularia, epidote, and sericite are the principal alteration minerals. The fine-grained gold is associated with pyrite, and minor amounts of molybdenite, base metal sulfides, and tellurides also occur in the ore. Fluid inclusion studies indicate low temperature (215–230° C), low salinity ore fluids with a moderate CO_2 content. Studies by Guthrie et al. (1987) on the American Girl and Padre y Madre deposits indicate essentially similar conditions during mineralization. Genetic models for this intriguing new type of bulk-mineable gold deposit remain to be worked out, but it seems clear that the detachment structures are an integral part of the story, primarily through providing structural control of fluid pathways.

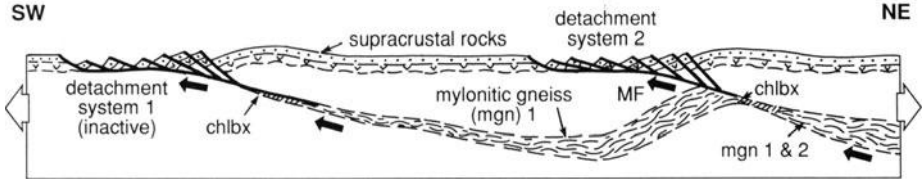

Fig. 4.9. Diagrammatic cross-section to illustrate the principal features of major detachment-type faults. Gold mineralization occurs locally within the chloritic breccias of these faults and in normal fault structures above (After Wernicke and Burchfield 1982)

4.2.5 Additional Gold Deposits of the Great Basin

Two additional types of gold deposits occur within the gold-rich metallogenic province that appears to coincide with the Great Basin. These are gold-bearing skarns (see Chap. 1) and volcanic-hosted, hot-springs-type deposits (Bonham 1988). Two actively producing examples of the former occur in north-central Nevada (Bonham 1988). At the Fortitude deposit in the Battle Mountain district (Wotruba et al. 1988), skarn formation took place in Pennsylvanian and Permian limestones adjacent to a granodiorite porphyry of Eocene age. The gold mineralization occurs in an actinolite-tremolite-chlorite-calcite-quartz-sulfide assemblage that overprints prograde garnet-diopside-epidote skarns, and aggregates 14.5 million tons grading 5 g/ton Au and 20 g/ton Ag. The gold occurs as electrum and is associated with pyrrhotite, pyrite, chalcopyrite, arsenopyrite, sphalerite, and galena. Potential for the discovery of additional skarn-type gold deposits in the Great Basin appears to be considerable.

We have dealt with the various types of volcanic-hosted vein deposits of precious metals in Chapters 1 and 2 and earlier in this section certain major vein deposits of gold in the Great Basin. However, relatively new targets in gold exploration are disseminated, bulk-mineable gold deposits which represent the uppermost, near-surface portions of epithermal systems (Fig. 4.10). These deposits have been termed hot-spring-type deposits (Nelson and Giles 1985), and examples are provided by Hasbrouck Mountain and Sulfur (Silberman 1982), and Round Mountain (178 million tons at 1.2 g/ton; Tingley and Berger 1985) in Nevada. Important additional examples of such deposits in other parts of the world are the Cinola deposit in British Columbia (Kimbach et al. 1981) and the Pueblo Viejo deposit in the Dominican Republic (Russell et al. 1981), both of which contain major amounts of recoverable gold.

As noted by Bonham (1988), considerable variation in the details of this type of deposit is apparent, but common features can be recognized (Fig. 4.10). These features include enrichment in Hg, Sb, As, and Tl, intense alteration leading to kaolinite + silica + alunite assemblages, the dumping of large amounts of silica as chalcedony and opal, and the formation of hydrothermal eruption breccias. The fluids involved were of low salinity, near neutral in pH, and contained small but significant amounts of CO_2 and H_2S. As such, they closely resemble the fluids found in certain modern geothermal systems, such as those in the Taupo Volcanic Zone, New Zealand (see Chap. 3) and in adularia-sericite type epithermal deposits. Although the fluids in these systems are probably of overwhelmingly meteoric origin, it is clear that the gold and the sulfur, which is considered critical to gold transport, are inherent to the magmatic evolution of each volcanic edifice (Sillitoe and Bonham 1984), and in a number of cases, ore generation may represent redistribution of precious metals from underlying, more complex mineralization (Sillitoe in press).

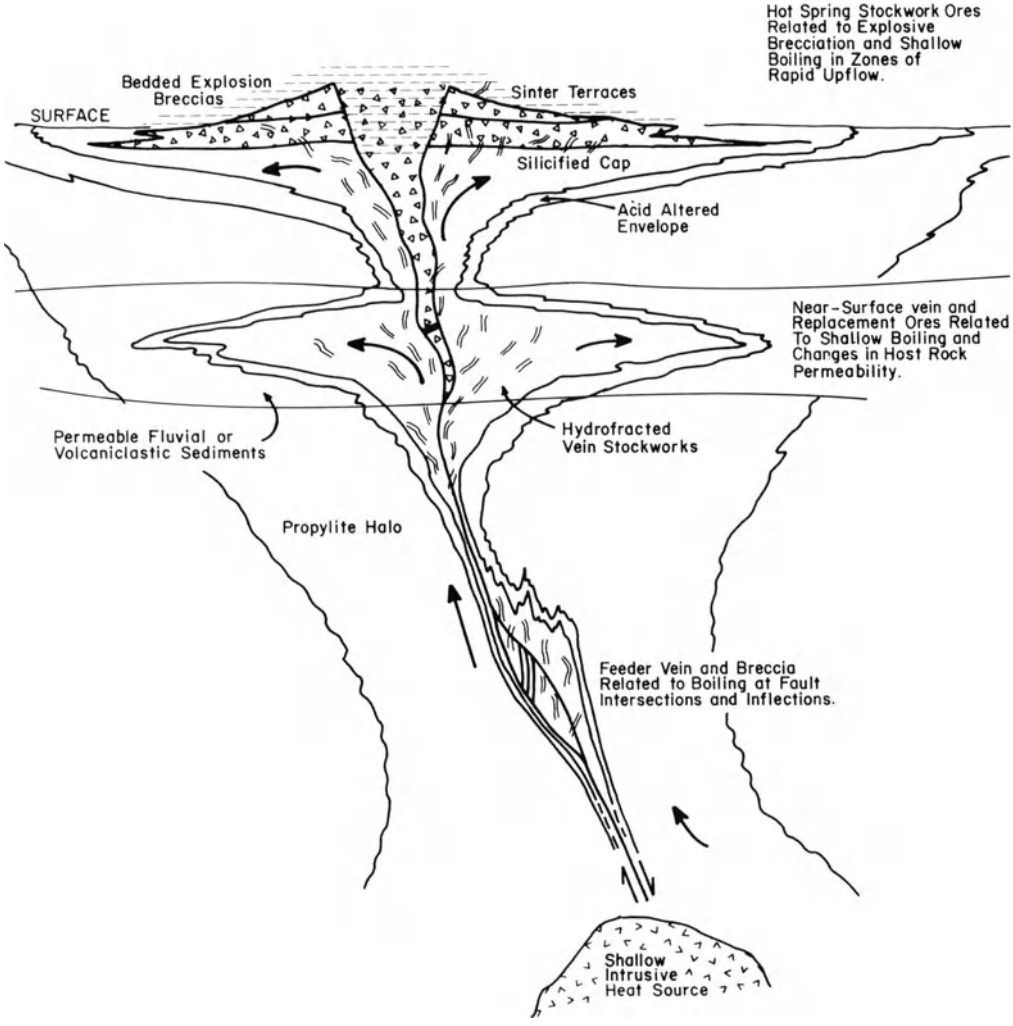

Fig. 4.10. Schematic cross-section of a hot-spring-type gold deposit. Note importance of either hydrofracture or explosive brecciation in the creation of near-surface bulk tonnage gold ores (After Nelson and Giles 1985)

4.2.6 Gold Mineralization Associated with Transform Faults

The sole, well-established example of this type of gold deposit in the western USA is McLaughlin in northern California with initial ore reserves of 17.5 million tons grading 5.2 g/ton. This important gold deposit was discovered as a result of reinvestigation of an old mercury mine in the area by geologists cognizant of the possible relationship between mercury and shallow-level gold mineralization.

The late Cenozoic geologic history of this area is dominated by transform faulting and volcanism. The Clear Lake volcanics (Hearn et al. 1982) represent the northernmost and youngest (0.01 to 2.1 Ma) group of a series of late Cenozoic extrusive igneous rocks that are strung out along the central Coast Ranges of California. All of these volcanic rocks exhibit a spatial association with the San Andreas transform and associated faults to the east, and a general northward younging (23.5 to 0.01 Ma) of volcanism is apparent (Fig. 4.11; see Hearn et al. 1982 and references therein). Although these volcanics range in composition from basalt to rhyolite and are essentially of calc-alkaline type, they exhibit complex strontium isotope variations suggestive of multiple magma sources in the upper mantle and lower crust (Futa et al. 1982).

The northward migration of volcanism referred to above has led to the suggestion of a hotspot control of igneous activity (Hearn et al. 1982), but

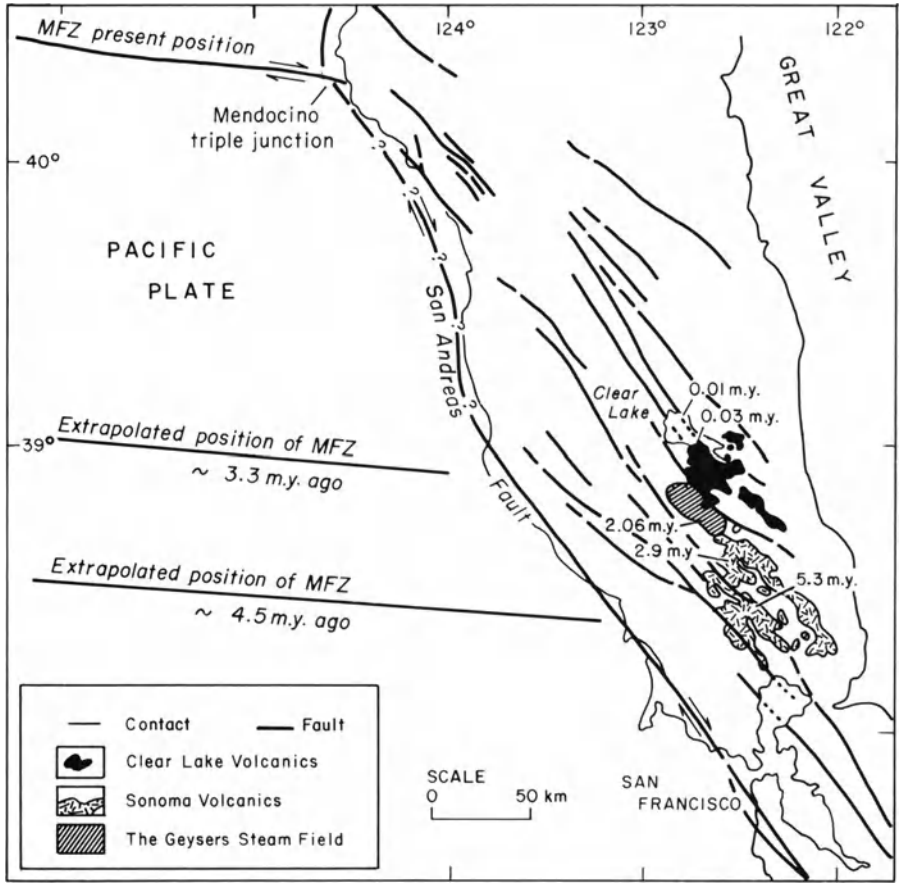

Fig. 4.11. Major faults in northern California associated with the San Andreas transform system. Also shown are the northward younging series of lava fields associated with the system (After McLaughlin 1981)

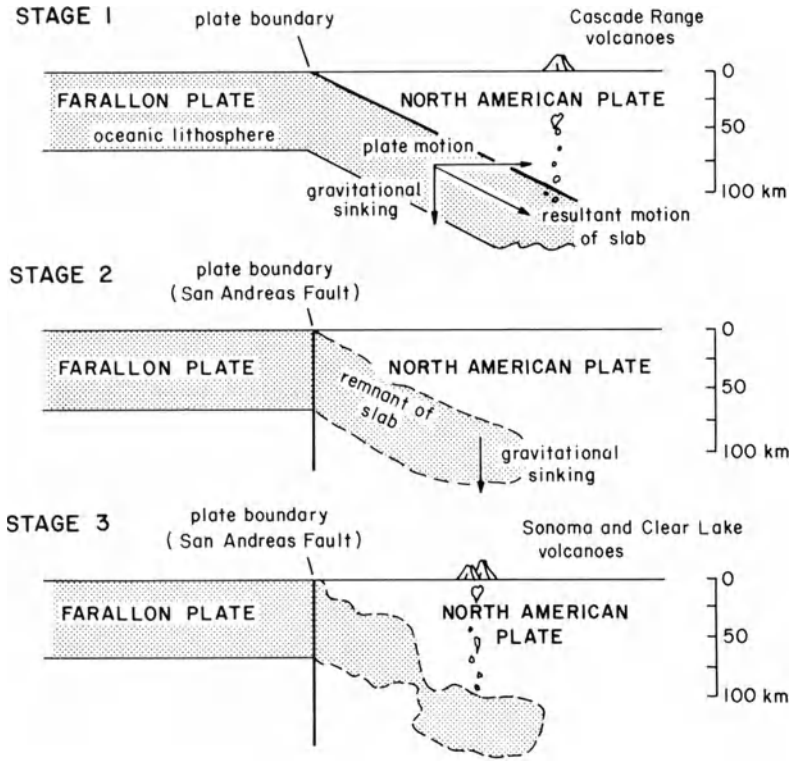

Fig. 4.12. Conceptual model of Isherwood explaining the origin of the Clear Lake volcanics, northern California (After Isherwood 1982)

Isherwood (1982) sees the main control of magmatism as downward settling of a subducted slab after its detachment from the Farallon Plate by the San Andreas transform (Fig. 4.12). Whatever the ultimate triggering mechanism for the magmatism, its association with transform faulting is clear, as is the relation of the mercury and gold deposits to this magmatism. The gold mineralization that forms the important McLaughlin deposit appears to be of typical hotspring type, and additional examples of disseminated gold mineralization may well occur along leaky transforms elsewhere. Geophysical studies (Isherwood 1982) indicate that magma bodies are still present under the Clear Lake volcanic field and heat from these is responsible for the Geysers system, a major geothermal energy resource.

4.2.7 Discussion

The multiplicity of precious-metal deposit types associated with arc-related volcanism in the western USA, as discussed in the foregoing sections, is illustrative of the variability that should be expected elsewhere. Such deposits,

containing just a few ppm gold, are not easy to find in the complex geology of accreted volcanic arcs unless exploration programs are specifically targeted toward them. However, as more about their character and setting is learned, it seems probable that additional examples will be found, perhaps in the young island arc systems of the western Pacific or in the Andes.

Firm exploration guides for all of these deposit types have yet to emerge, but an understanding of depth-related changes in the character of mineralization and alteration is important to exploration strategy. In shallow systems the presence of considerable fine-grained silica, argillic alteration, and hydrothermal breccias are certainly positive indications. If such areas are also characterized by anomalous amounts of arsenic, antimony, or mercury, further careful work, and perhaps shallow drilling are justified.

4.3 Paleozoic and Older Porphyry Copper Deposits

In discussions of the epigenetic metal deposits of principal arc and backarc regions in previous chapters, it was emphasized that such deposits are emplaced within a few kilometers of the earth's surface and are thus particularly prone to erosion, especially in continental margin arc systems that tend to stand high with respect to sea level. It follows that deposits of this type should be increasingly less common in progressively older arc systems. This is, in fact, the case. Porphyry copper deposits, for example, are predominantly of post-Paleozoic age and Cenozoic deposits are considerably more common than Mesozoic deposits. Notable examples of Mesozoic porphyry copper deposits include Bisbee (198 Ma), Ely (115 Ma), and Yerington (approx. 140 Ma) in the western USA (Titley and Beane 1981), and a number of major porphyry copper deposits of western Canada that fall within the 140–200 Ma age range (Ney and Hollister 1976). The large Mocoa porphyry copper deposit in Colombia also has an age of close to 200 Ma (Sillitoe et al. 1984).

In contrast, the major belts of porphyry copper deposits in Russia are Paleozoic in age (Fig. 4.13). Laznicka (1976) has demonstrated that most of these deposits can be related to either island-arc or Andean-margin geotectonic settings, implying that these deposits for some reason did not suffer uplift and erosion subsequent to their formation. Similarly, several porphyry-type copper-molybdenum deposits in eastern Queensland, Australia range in age from Silurian to early Cretaceous. Horton (1978) has demonstrated that four periods of mineralization – Siluro-Devonian, Permo-Carboniferous, Permo-Triassic, and early Cretaceous, can be recognized within this portion of the Tasman Orogenic Zone. The deposits occur mainly within discrete northwest-trending narrow belts up to 400 km long. Unfortunately, the grades of these Queensland deposits are mostly low and none currently support mining.

Hollister et al. (1974) report on porphyry copper and molybdenum occurrences of the Appalachian orogen of eastern North America that extend from Maine to Newfoundland. Within this belt there is a general shift with age

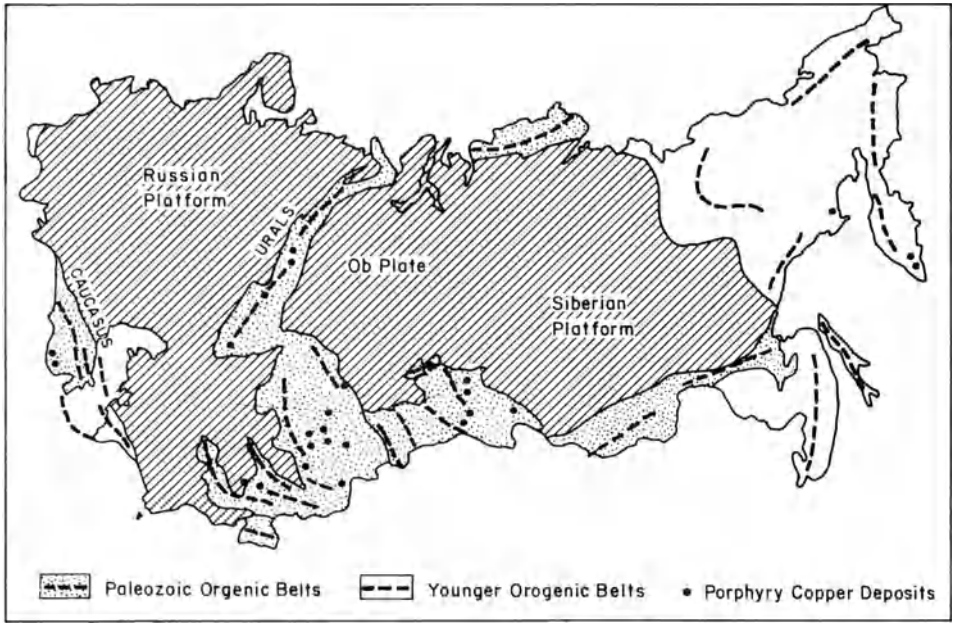

Fig. 4.13. Phanerozoic orogenic belts in the USSR, showing location of porphyry copper deposits (After Laznicka 1976)

from earlier porphyry copper mineralization (Cambrian-Ordovician) to later porphyry molybdenum mineralization rich in lithophile elements (Devonian). Hollister et al. (1974) conclude that these Appalachian porphyry systems generally resemble their Tertiary counterparts, but believe they were emplaced at somewhat deeper crustal levels. Deeper emplacement level is indicated by the relatively high Mo/Cu ratios in the deposits, and a predominance of equigranular rather than porphyritic textures in associated, typically quartz monozonitic, intrusions.

Porphyry copper-type mineralization in Precambrian terranes is not common, but examples have been reported from the Canadian Shield (Kirkham 1972; Franklin and Thorpe 1982), from Brazil (S.V. Richardson et al. 1986), Africa (Wakefield 1978), and from Australia (Barley 1982; de Laeter and Martyn 1986). At the Haib deposit in southern Namibia essentially unmetamorphosed porphyry copper-type mineralization occurs within a 2 Ga calc-alkaline terrane of typical volcano-plutonic arc character (Reid 1977; Reid et al. 1987). Probably the most important example of Precambrian porphyry copper-gold mineralization is that at McIntyre, Ontario (Fig. 4.14). Here, 35 million tons of copper-gold ore grading 0.67% Cu and 0.59 g/ton Au have been mined from the Pearl Lake porphyry (Burrows and Spooner 1986; Mason and Melnik 1986). In addition, the Don Ruyon mine near Noranda, Quebec, contains copper-molybdenum mineralization as disseminations and fracture fillings in trondhjemitic intrusions, and is operated as a source of

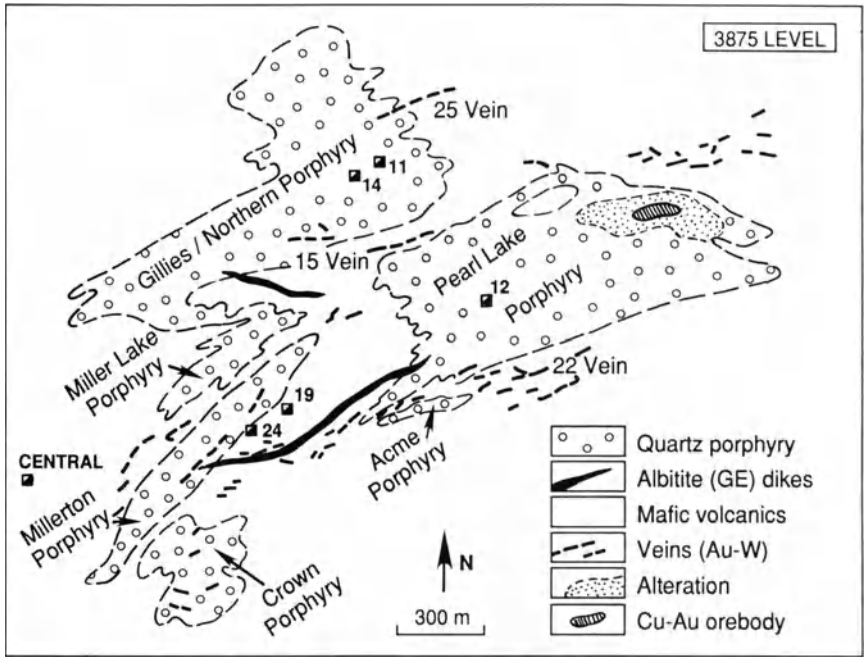

Fig. 4.14. Map of 3875 foot level of the Hollinger-McIntyre gold district, Ontario, showing the copper-gold disseminated mineralization and some of the surrounding gold vein deposits (After Burrows and Spooner 1986)

cupriferous siliceous flux for the Noranda smelter (Goldie et al. 1979). Later metamorphism has overprinted any original hydrothermal alteration patterns at Don Ruyon, but they are still mappable at McIntyre.

Although these older examples of porphyry-type mineralization do not tend to match the tonnage and grade characteristics of top-rank continental margin Tertiary deposits, occurrences such as Kounrad, USSR (Paleozoic) indicate that major porphyry copper metallogenesis was not confined to the latter portions of Phanerozoic time. As stated earlier, the marked decrease in porphyry copper deposits in older arcs is best explained in terms of erosion of the upper portions of these arcs. The same considerations apply equally to the other major types of epigenetic arc-related deposits such as skarns, limestone replacement deposits and, in particular, epithermal vein deposits.

4.4 Massive Sulfide Deposits in Greenstone Belts

In contradistinction to epigenetic arc-related deposits, massive sulfide deposits associated with arc and backarc volcanism are distributed throughout geologic time. This is especially true if one accepts the proposition that greenstone belts

represent Precambrian analogues of backarc or intra-arc basins. Many workers (e.g., Tarney et al. 1976; Tarney and Windley 1981) see evidence for rifting in the environment on which Archean greenstone belts formed, but it should be emphasized that the backarc model for greenstone belt development involves just that. It also allows for the possibility that such volcanic and sedimentary sequences could have formed entirely in oceanic environments, such as certain western Pacific arc systems, or could have formed adjacent to and partially overlapping older continental type crust. Furthermore, the concepts of accretionary tectonics that have been worked out for the Mesozoic and Cenozoic terranes of western North America are being increasingly applied to models of continental growth for greenstone-granite terranes of Archean, early Proterozoic, and late Proterozoic time (Hoffman 1988). This general model is steadily gaining broader and broader acceptance in that it seems capable of explaining many of the tectonic, petrologic, and metallogenic features of large parts of Precambrian continental crust in uniformitarian terms. The nonuniformitarian aspects of the early earth, such as higher mantle heat production, are nonetheless also accommodated in terms of the more rapid accretion and destruction of numerous small plates, a feature that is indicated by the less pronounced linearity of greenstone belts.

Greenstone belts vary in size from small infolded remnants of volcanics and sediments just a few tens of km^2 in area to the 94 000 km^2 areal extent of the Abitibi greenstone belt (Fig. 4.15). The Abitibi belt contains 11 discrete eruptive centers, and although felsic volcanic rocks account for only 3.6% of the

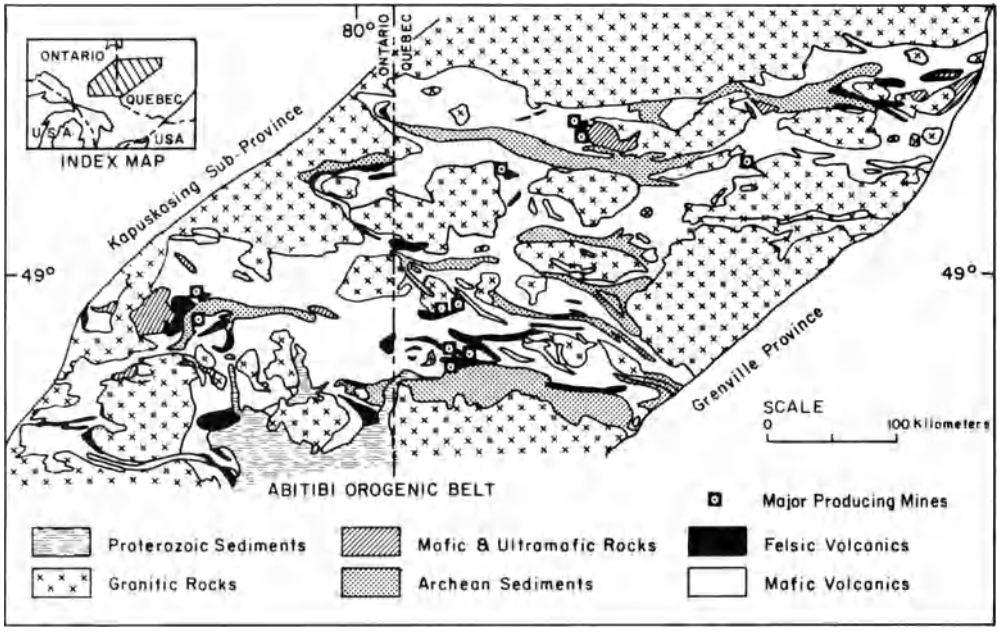

Fig. 4.15. Generalized geology of the Abitibi greenstone belt

area (Goodwin and Ridler 1970); virtually all the known massive sulfide deposits are spatially associated with these felsic rocks. Recently, Lesher et al. (1986) have demonstrated that the felsic volcanics can be further subdivided on the basis of REE patterns into ore and nonore-associated types. This trace element discriminant seems to have application to all volcanic-hosted massive sulfide deposits (see later) and has considerable potential in terms of exploration strategy. Copper- and zinc-bearing massive sulfide deposits are an important facet of greenstone belt metallogeny (see Table 3.1) and in a number of respects form an intermediate type between the Kuroko-type deposits discussed in Chapter 3, and the Cyprus-type deposits that will be described in Chapter 5.

The volume of literature that has been generated on the massive sulfide deposits of the Canadian Shield is awesome (see Franklin et al. 1981; Franklin and Thorpe 1982; Lydon 1988), but the deposits of the Noranda camp have been particularly well studied and serve as useful examples of massive sulfide metallogenesis in greenstone belts. As in the case of the Kuroko province of Japan, there is a strong tendency for deposits to be concentrated at particular volcanostratigraphic levels marked by felsic volcanism (Fig. 4.16). This tendency, however, is not as marked as that in Japan. At Noranda, the multicyclic andesite to rhyolite volcanic sequence containing the massive sulfide deposits is underlain and intruded by the Flavrian tonalite-trondhjemite pluton (Goldie 1979), whose age (2710 Ma; Krogh and Davis 1971) and composition suggest that it is comagmatic with the felsic volcanic rocks.

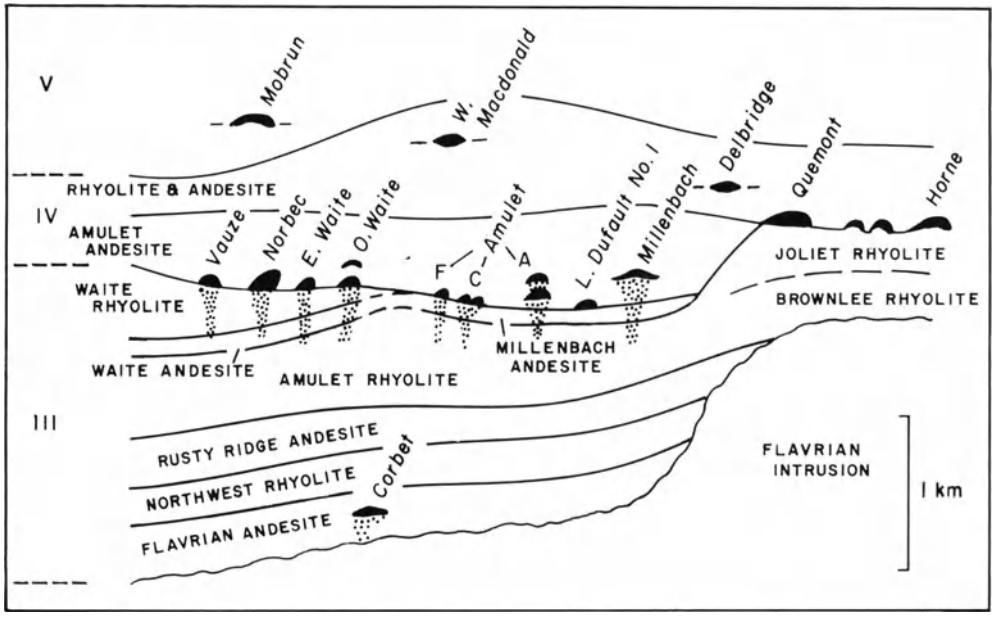

Fig. 4.16. Sequence of volcanic units in the Noranda district showing main massive sulfide deposits. Note tendency of deposits to concentrate strongly at specific stratigraphic intervals (After Franklin et al. 1981)

Well-developed alteration pipes containing stringer copper zones, in some instances of ore grade, underlie most of the deposits, and in many cases these have been controlled by synvolcanic fractures (Scott 1980). Although some orebodies occur within mafic volcanic rocks, most are close to small domes of massive rhyolite (Franklin et al. 1981), and this situation is particularly well displayed by the Millenbach deposit (Fig. 4.17). Another noteworthy aspect of the majority of deposits in the Noranda camp, and for that matter in greenstone belt massive sulfides in general, is that orebodies tend to occur at stratigraphic levels where the presence of tuff and chert layers indicate a break

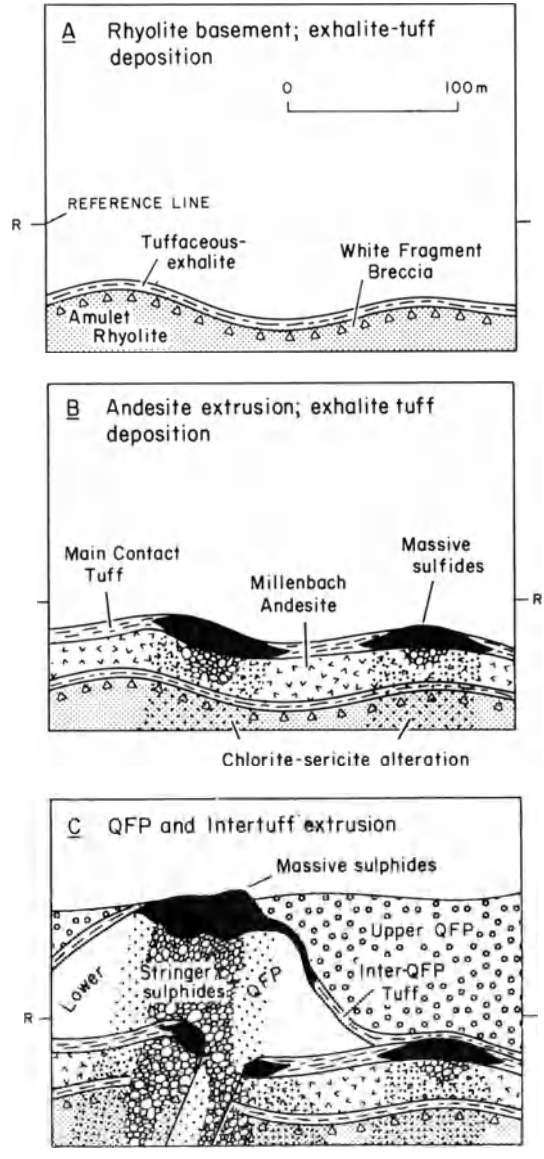

Fig. 4.17A-C. Cross-sections showing sequence of events related to formation of a massive sulfide lens in the Millenbach Mine, Noranda district. *QFP* = quartz feldspar porphyry (Riverin and Hodgson 1980)

in volcanic activity. This is similar to the situation in the Hokuroku Basin in northern Honshu, where thin mudstone accumulated at the level of massive sulfide emplacement.

4.4.1 The Kidd Creek Massive Sulfide Deposit, Ontario

The Kidd Creek mine, which probably contains over 100 million tons of ore, is one of the largest volcanic-hosted massive sulfide deposits known. Since its discovery in 1963 until 1985, it produced 68 million tons of ore grading 7.6% Zn, 1.9% Cu, 0.3% Pb, and 16 g/ton Ag.

The Kidd Creek deposit lies north of Timmins in the western portion of the Abitibi greenstone belt, within a sequence of steeply dipping, overturned mafic and felsic volcanic rocks (Fig. 4.18), which in the mine area has been precisely dated at 2717 Ma (Nunes and Pyke 1980). The Kidd Creek orebodies occur within the uppermost portion of a group of felsic rocks consisting of rhyolitic tuffs and breccias and massive rhyolite, some of which appears to be intrusive (R. R. Walker et al. 1975). A series of carbonaceous rocks that include argillites, cherts, and heterogeneous volcaniclastics occurs at the level of sulfide mineralization, whereas stratigraphically above it are a series of basaltic and andesitic flows and some large masses of metadiabase. Below the rhyolitic rocks are altered ultramafic rocks.

The pervasive lower and middle greenschist metamorphism present in the area makes recognition of alteration associated with mineralization difficult, but the alteration or meta-alteration minerals include sericite, chlorite, quartz, carbonate, biotite, talc, tourmaline, albite, and fluorite (R.R. Walker et al. 1975). Structurally, the area is complex with folding at all scales, and shearing controlled in part by stratigraphy. The felsic carbonaceous rocks are also characterized by strong schistosity of variable orientation.

Dating of the Kidd Creek mineralization event has been attempted using both Sm-Nd and Rb-Sr techniques (Mass et al. 1986). A Sm-Nd isochron was obtained for altered felsic volcanics, which exhibited a large range of Sm/Nd ratios, and an age of 2674 $\pm$ 40 Ma is indicated for mineralization and hydrothermal alteration. Both altered and distal felsic volcanic rocks give a younger Rb-Sr age of 2576 $\pm$ 26 Ma, which is almost certainly related to later hydrothermal events that accompanied regional metamorphism.

The Kidd Creek ores are more or less typical of the massive sulfide deposits in the Abitibi greenstone belt. Below the massive ores, are copper-rich (av. 2.5% Cu) stringer ores which ramify through silicified rhyolitic pyroclastics. The massive ores consist of both homogeneous massive sulfides and complex sulfide mixtures, whereas the banded varieties contain pyrite-sphalerite, sphalerite-chalcopyrite, or pyrite-sphalerite-chalcopyrite. Bedded ores are present within the carbonaceous horizon, as laminated or thinly bedded sulfidic sediments containing numerous primary sedimentation features. Finally, breccia ore is present and consists of fragments of pyrite and sphalerite mixed with fragments of volcanic and sedimentary rocks; R.R. Walker et

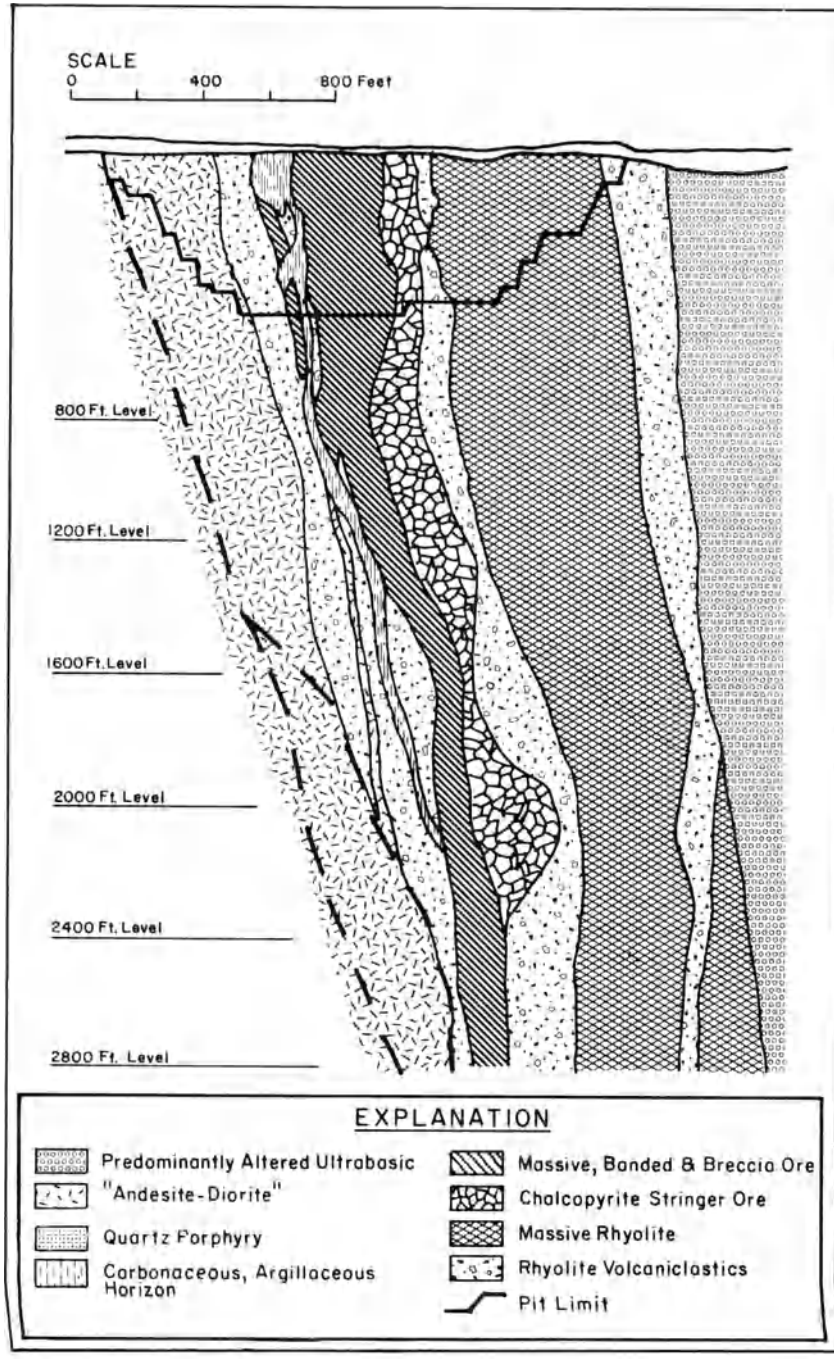

Fig. 4.18. Geologic cross-section of the Kidd Creek deposit. Stratigraphic tops are to the *left* (After R.R. Walker et al. 1975)

al. (1975) reported sulfide fragments up to 10 m across in these breccia ores. The pyrite content of Kidd Creek ores is somewhat variable, but in the ore mined has averaged about 40% by volume.

Overall, the geologic relationships at Kidd Creek suggest that ores formed within a felsic volcanic center by submarine hot-spring activity during a lull in explosive volcanism. Beaty et al. (1988a) have obtained $\delta^{18}O$ data from the altered rocks that constitute the footwall to the Kidd Creek orebodies, and calculate the $\delta^{18}O$ of the ore fluids to have ranged from 6–9‰. These values are distinct from the values obtained from most massive sulfide deposits (e.g., Beaty and Taylor 1982), but they are evidence for a major magmatic component in certain fluids responsible for this giant, base metal-rich massive sulfide deposit. Beaty et al. (1988a), however, attempt to explain the values in terms of evaporation of Archean seawater.

4.4.2 Discussion and Suggestions for Exploration

Massive sulfide deposits are not limited to Archean greenstone belts and occur in early Proterozoic greenstone belts in several places in North America. Notable examples include the Crandon deposit, Wisconsin (61 million tons averaging 1.1% Cu, 5.6% Zn, 0.5% Pb, 37 g/ton Ag, and 1 g/ton Au; Lambe and Rowe 1987), the Flin Flon and Snow Lake camps in Manitoba (Gaskarth and Parslow 1987), and the United Verde deposit, Jerome, Arizona (> 33 million tons of 4.8% Cu, 48 g/ton Ag, and 1.2 g/ton Au; Vance and Condie 1987 and references therein). In all three cases massive sulfide deposition took place about 1.8 Ga, during periods of subduction-related volcanism that preceded major continental accretion events (Hoffman 1988).

The essential similarities between Phanerozoic volcanic-hosted massive sulfide deposits and those present in greenstone belts are now clearly recognized, despite the inevitable metamorphic overprinting of the latter. Thus Hodgson and Lydon (1977) have attempted to apply the insights garnered from the Kuroko ores and modern geothermal systems to the formulation of conceptual models for the Precambrian deposits. As a result, they emphasize the importance of resurgent caldera structures, contemporaneous faulting, and the sealing of hydrothermal convective systems prior to exhalative events.

The main uncertainty regarding the genesis of Precambrian volcanic-hosted massive sulfide ores, as with their younger analogs, relates to the origin of the ore metals, a point discussed in some detail by Franklin et al. (1981). Fox (1979) has noted that, although most volcanic-hosted massive sulfides occur in association with dacitic to rhyolitic volcanics, petrochemical data indicate that these and their associated more mafic rocks can be categorized as either belonging to tholeiitic (high-iron) or calc-alkaline (low-iron) suites. The massive sulfide ores in tholeiitic sequences tend to be Zn-Cu types with abundant, associated iron sulfides, whereas those in calc-alkaline sequences tend to be Pb-Zn-Cu types that include relatively iron-poor, sphalerite-rich ores.

Despite these differences, certain common denominators seem to be emerging with respect to the tectonic and petrochemical settings of massive sulfide generation throughout the geologic record. Most massive sulfide deposits are closely associated in both time and space with bimodal basalt-dacite or basalt-rhyolite suites, the felsic parts of which were generated from high-level, strongly fractionated magma bodies. This latter feature is consistently reflected in the REE patterns (Fig. 4.19) of ore-associated felsic volcanics (Lesher et al. 1986, and references therein). It thus appears that intrusions associated with massive sulfide generation must be considered to play a far more crucial role in ore genesis than as mere passive heat engines that drive hydrothermal convection (see Urabe 1987). These same REE patterns hold considerable promise in terms of exploration strategy, at least for delineation of the levels within a volcanic pile that have the maximum potential for hosting massive sulfide deposits.

The large majority of the over 100 significant volcanic-hosted massive sulfide orebodies found in the Canadian Shield in the last 65 years were first located by geophysics, typically involving airborne electromagnetic surveys (Boldy 1981). The effective depth of penetration of most geophysical techniques used in massive sulfide exploration is less than 300 m, however, and because diamond drilling can reach considerably deeper, there is considerable scope for the application of geochemical techniques and geological inference in the search for deeper orebodies, especially in established massive sulfide districts.

Mercury leakage haloes can in some cases be identified up to 700 m above orebodies (Boldy 1981), and attention has been focused on the petrochemistry of the volcanics themselves and their altered equivalents, in attempts to follow favorable stratigraphic intervals that could host ore (e.g., Marcotte and David 1981). The great majority of known massive sulfide deposits in greenstone belts of the Superior Province contain stringer zones (in some cases of ore grade) stratigraphically below them. However, MacGeehan et al. (1981) have demonstrated that the ore lenses of the Norita Mine in the Matagami district,

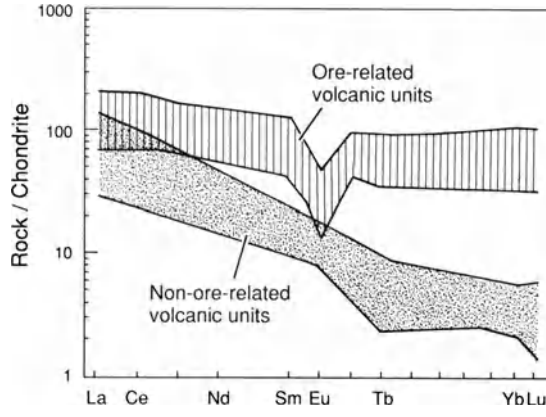

Fig. 4.19. Plot of REE (slope) patterns obtained from Archean felsic volcanics that are barren of massive sulfide mineralization and REE patterns (flat) obtained from felsic volcanics that host important massive sulfide deposits (After Lesher et al. 1986). Note clear difference between the two data sets

Quebec, are of distal type and their location was controlled by submarine paleotopography. Such ores may be more common in greenstone belts than currently indicated, but their location would require careful attention to the geometry of rock units at favorable horizons prior to deformation.

4.5 Gold Deposits in Greenstone Belts

Late Archean greenstone belts host a major portion of the world's nonplacer gold resources and were almost certainly the source of the gold in the preeminent paleoplacer gold deposits of the Witwatersrand Basin (see Chap. 8). A great deal of attention is being focused on the gold metallogeny of greenstone belts, both by exploration geologists and by the research community. Ideas about the main types of greenstone-hosted gold deposits and their genesis are still in a state of flux at this writing, but some patterns are now emerging that will be important in understanding the spectrum of greenstone-hosted gold deposits, their fundamental tectonic controls, their relationship to Phanerozoic gold metallogeny, and eventually their genesis.

With these concepts will inevitably come some key insights in terms of exploration strategy, especially regarding the timing of gold mineralization with respect to the geologic history of the surrounding host rocks. This is a nontrivial problem because many of the textural and structural features of gold deposits in metamorphosed host rock can be interpreted in different ways, depending on the conceptual bias of the individual. There is, for example, strong support among many experienced workers on greenstone-hosted gold deposits for an all-embracing structural model for gold ore genesis (Colvine et al. 1988). Although postmetamorphic, structurally controlled, gold-quartz vein deposits are probably the most numerous and most productive deposits in greenstone belts, other types of gold deposits account for close to 40% of recoverable gold in greenstone belts (Bache 1987) and cannot be ignored.

4.5.1 Gold Ores of Probable Exhalative Origin: Homestake-Type Deposits

A number of gold deposits in greenstone belts exhibit an extremely marked stratiform character that is quite distinct from the crosscutting vein aspect of lode gold deposits (Table 4.1). In addition, the majority of these stratiform deposits occur within siliceous iron-rich rocks consisting of lean, cherty, carbonate, or silicate iron formation or their metamorphosed equivalents. Although the concept of significant gold ore of exhalative origin is rejected by some groups (Colvine et al. 1988, and references therein), a great deal of empirical data can be gathered from volcanic terranes of all ages in support of the reality of such processes (Hutchinson and Burlington 1984). Not the least of these is the observation that geothermal systems in the Taupo Volcanic Zone, New Zealand, are currently delivering gold, arsenic, and antimony to surficial sinters (Krupp and Seward 1987). Should such processes occur in a

Table 4.1 Major iron formation-hosted gold deposits of probable exhalative type

Deposit	Locality	Contained Au(tons)	Host rocks[a]	Sulfides[a]	Metamorphic grade	Reference
Homestake	S. Dakota, USA	1100	Cherty carbonate I.F.	Aspy, py, pyrr	Biotite-staurolite	Rye and Rye (1974)
Lupin	N.W.T., Canada	~56	Sulfide I.F.	Aspy, pyrr	Amphibolite	Sassos (1986)
Morro, Velho	Minas Gerais, Brazil	370	Carbonate I.F.	Aspy, py, pyrr	Amphibolite	Gair (1962)
Geita	Northern Tanzania	~28	Oxide I.F. locally sulfidic	Py, pyrr	Greenschist	Van Straaten (1984)
Vubachikwe	Gwanda, Zimbabwe	36	Sulfidic iron formation	Aspy, pyrr	Amphibolite	Fripp (1976) Saager et al. (1987)
Hutti	Southern India	~25	Chlorite schist, sulfides	Aspy, pyrr, py	'Epidote-amphibolite	Naganna (1987)
Kolar	Southern India	805	Iron-rich amphibolites, iron formation	Aspy, pyrr, py	Amphibolite Amphibolite	J.V. Hamilton and Hodgson (1986) Lewis (1965)
Hill 50	Mt. Magnet, W. Aust.	40	Jaspilite (siliceous I.F.)	Pyrr		

[a]I.F. = iron formation, aspy = arsenopyrite, py = pyrite, pyrr = pyrrhotite

marine environment, siliceous gold-rich units of stratiform geometry could result.

Examples interpreted as exhalite-type gold ores are numerous, and most cannot be discounted as incorrectly identified bedding-parallel, shear zone-type mineralization. For example, the studies of Roobol and Hackett (1987) on paleovolcanic facies in little metamorphosed greenstone belts of late Proterozoic age in the Arabian Shield indicate an association of gold with distal facies exhalites. Similar relationships were deduced by Worthington and Kiff (1970), Mangan et al. (1984), and Duke and Hodder (1987) for gold deposits in iron-rich exhalites in the central Appalachians.

Ridler (1970) was one of the first to recognize the association of certain Archean gold deposits in Canada with carbonate iron formations. Strong supporting evidence for this concept of exhalative gold came from studies of the Homestake gold deposits by Rye and Rye (1974), and subsequently Sawkins and Rye (1974) applied the term Homestake-type deposits to gold ores of this type and suggested that their occurrence was worldwide, and included certain major deposits such as Morro Velho, Brazil (Gair 1962) and the Kolar goldfield, India. The Kolar goldfield has been subject to alternate genetic models (Narayanaswami et al. 1960; J.V. Hamilton and Hodgson 1986) but the fidelity with which the gold lodes follow lithologic units for many kilometers is strongly suggestive of a predeformation (syngenetic) timing for gold mineralization. Similar arguments can be applied to the stratiform gold deposits of the nearby Hutti and Ramagirl schist belts (Naganna 1987), and additional deposits in southern Africa (Potgieter and de Villiers 1986).

Another prime example of this type of gold deposit is the Lupin mine located in the North West Territories of Canada, just 80 km below the Arctic Circle (Sassos 1986). Ore reserves are given as 3 million tons grading 10 g/ton, but it is considered almost certain that at least twice that amount of gold ore exists in the deposit. The gold orebodies are hosted by amphibolite grade, sulfide-rich iron formation overlain by phyllites (mudstones) and underlain by quartzites (graywackes) which form part of the Archean metasedimentary Contwoyto Formation of the Yellowknife Supergroup (Tremblay 1976). The iron formation and its enclosing units have been deformed into a series of large vertically plunging antiforms and synforms (Fig. 4.20). The ore zones consist of multiple, interbedded, sulfide-rich and sulfide-poor horizons ranging in thickness from a few centimeters to almost 2 m, and the gold is associated with pyrrhotite and to a lesser extent arsenopyrite/loellingite grains. Late-stage quartz veins make up about 15% of the ore zones, but are considered to be unrelated to initial gold introduction.

4.5.2 The Homestake Gold Mine, South Dakota

The Homestake mine has produced over 1000 tons of gold since it began production in 1877. The Precambrian metasediments that host the deposit occur in the northern extremity of the Black Hills dome, a window of Precambrian rocks surrounded by Phanerozoic sediments. The small areal

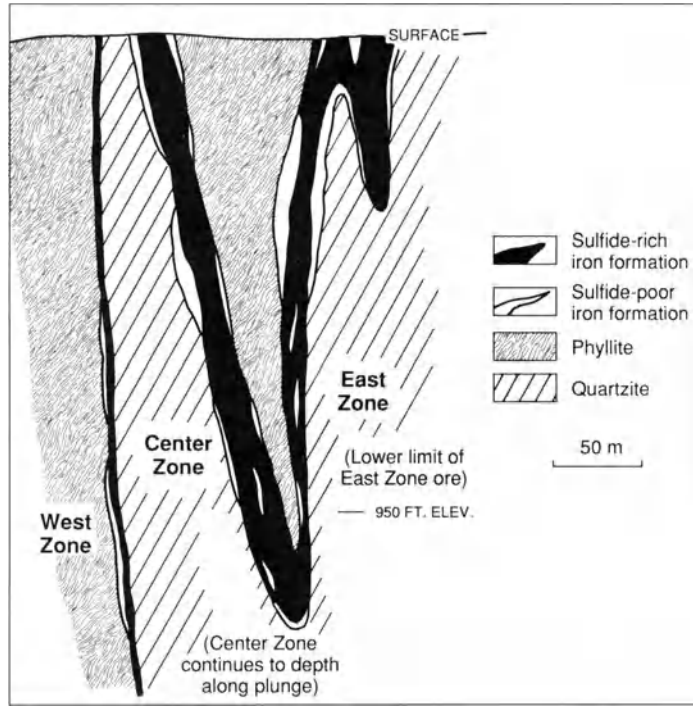

Fig. 4.20. Sectional view of the Lupin gold district, Northwest Territories, Canada. Gold ore occurs only in the sulfide-rich iron formation, and apart from some minor quartz-filled tension gashes evidence for hydrothermal activity is lacking (After Strachan and Moffett 1985)

extent of this window does not readily permit the assignment of the exposed units to a greenstone belt environment, but the ores bear a striking similarity to other Homestake-type deposits, virtually all of which do occur within greenstone belt terranes.

The orebodies are restricted to the Homestake Formation, a thin (< 100 m), auriferous, quartz-sideroplessite schist unit within a thick sequence of metasedimentary and minor metabasaltic rocks (Fig. 4.21; Slaughter 1968). It is noteworthy, however, that where lithologies similar to the Homestake Formation occur higher in the section (Flagrock Formation), they are gold-bearing. The Poorman Formation, which underlies the Homestake Formation, is a graphitic, ankeritic carbonate unit containing minor amounts of phyllite and recrystallized chert. Its base is not exposed and it is thus of unknown thickness. The Ellison Formation, overlying the Homestake Formation, consists mainly of dark phyllite, but contains many lenses of graphitic quartzite. Some mafic amphibolites occur locally within the Poorman Formation and probably represent metamorphosed basalts. Similar rocks are present higher in the section within the Flagrock Formation.

The package of rocks that hosts the gold deposits has been metamorphosed and deformed into a set of complex folds plunging 10° to 45° to the southeast, with axial planes dipping to the east. In the extreme northeast,

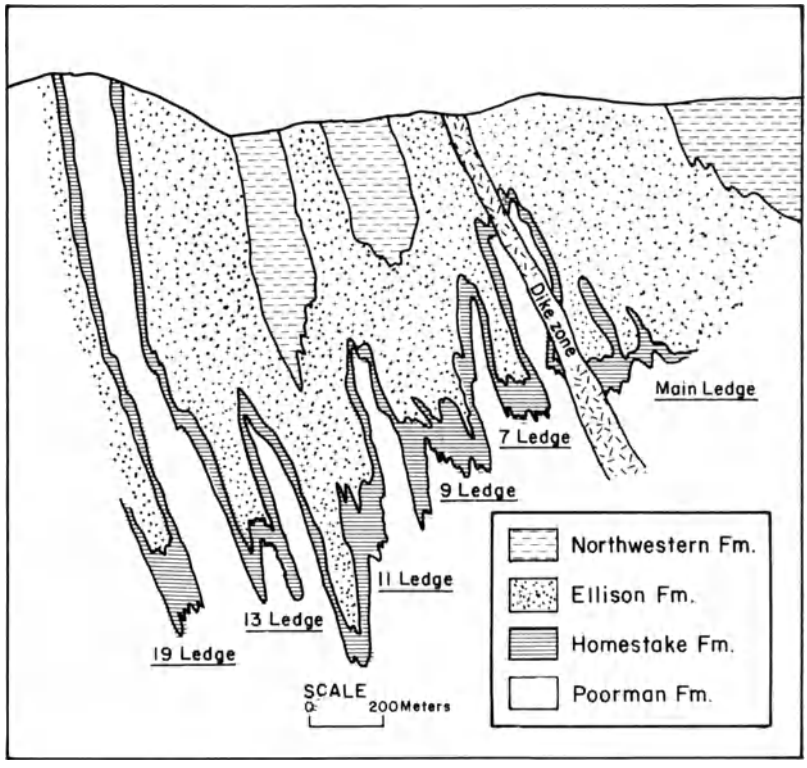

Fig. 4.21. Generalized cross-section of the Homestake Mine showing relation of major orebodies to areas of Homestake Formation thickened by folding (After Rye and Rye 1974)

metamorphism reaches staurolite grade but decreases to biotite grade over a distance of about 6 km toward the southwest. The entire section is intruded by early Tertiary dikes, sills, and stocks of granitic, monzonitic, phonolitic, and syenitic porphyry. Some of these felsic dikes cut through the center of the mine area.

The Homestake orebodies are elongate, steeply plunging, spindle-shaped zones that appear to be localized, at least in part, by dilatant zones formed by superposition of F_1 and F_2 fold structures. This is suggestive of some remobilization of gold during deformation. The orebodies consist essentially of quartz, chlorite, and ankerite in various proportions, accompanied by pyrrhotite and arsenopyrite. The quartz occurs as both metamorphic segregations, which form irregular masses or short veins, and recrystallized chert. Most of the chlorite appears to have formed at the expense of cummingtonite or sideroplessite in the metasedimentary wall rocks. Arsenopyrite, commonly as euhedral crystals, is typically developed in the chlorite adjacent to quartz segregations, whereas pyrrhotite occurs with ankerite clots, and in more broadly disseminated form. The sulfide content of nonore Homestake Formation is about 2%, but it can reach 8% within orebodies.

The genesis of the Homestake ores was obscured for a long time by the presence of small amounts of unequivocal Tertiary gold mineralization associated with igneous rocks of the same age. Furthermore, Lindgren (1933) had designated the Homestake ores as a type example of his class of hypothermal replacement ore. The stable isotope studies of Rye and Rye (1974), however, demonstrated convincingly that the sulfide sulfur and the oxygen in quartz from those in the orebodies were indigenous to the Homestake Formation and distinct from Tertiary mineralization. In addition, they found that $\delta^{34}S$ values of sulfides tended to decrease from fold limbs to dilatant areas in fold hinges where sulfides are now more concentrated in ore zones (Fig. 4.22). These results all indicate that the components of the Homestake ores, including the gold, were original (syngenetic) constituents of the Homestake Formation, but they were redistributed and concentrated to some extent during folding and metamorphism. This concept is in agreement with that proposed earlier by Ridler (1970) for certain gold ores in the Abitibi greenstone belt, and later by Fripp (1976) for conformable gold ore zones in greenstone belts of Zimbabwe.

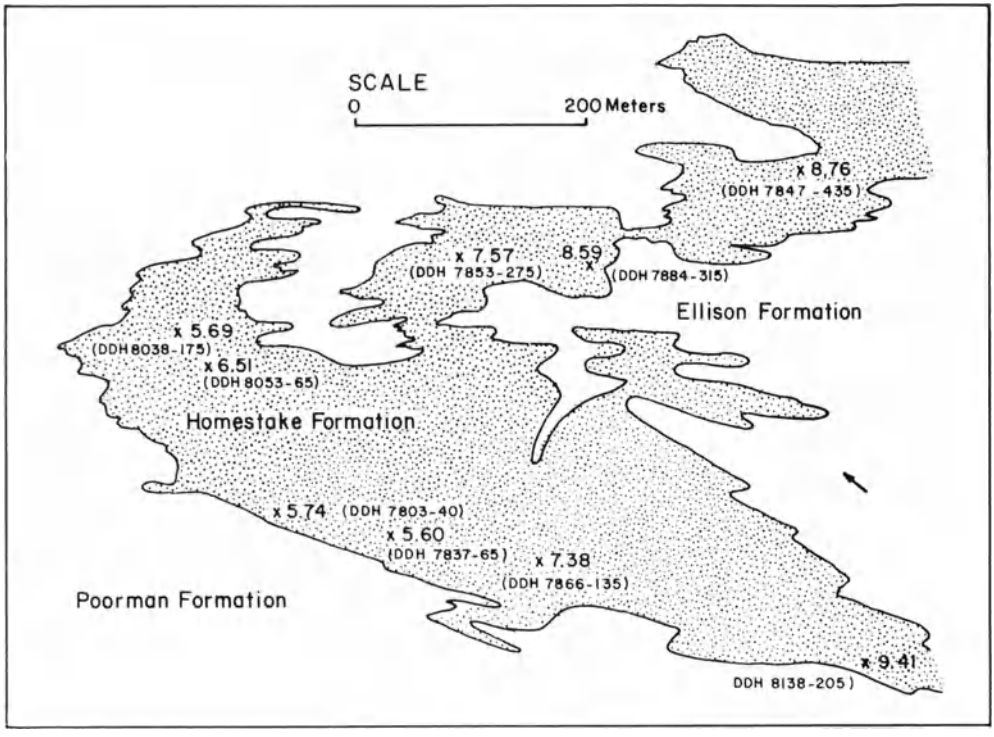

Fig. 4.22. ^{34}S values of sulfides at the 5900 level of the number 13 ledge orebody, Homestake Mine. Note progressive reduction of ^{34}S values as the nose of the fold structure is approached from each limb (After Rye and Rye 1974)

4.5.3 Pre-Metamorphic Stratiform Gold Ores: The Hemlo Deposit, Ontario

The Homestake-type deposits referred to in previous sections, if correctly assigned in terms of the timing of gold mineralization, will obviously be affected by all subsequent metamorphic and deformational events. Similar considerations would apply to any gold deposit that formed during the original stages of volcanoplutonic arc development. Thus, the genesis of any porphyry- and epithermal-type gold deposits analogous to those in modern arc systems would be rendered obscure by metamorphic and deformational overprinting. In rocks where competency differences can be created and/or enhanced by alteration effects, interpretations of empirical field and textural relationships are hazardous at best. An excellent example of this problem is provided by contrasting views of timing of mineralization vis-à-vis deformation at the huge Hollinger-McIntyre gold camp (> 1000 tons contained Au), in Ontario (see Burrows and Spooner 1986; Wood et al. 1986; Mason and Melnik 1986).

Despite these caveats, the important Hemlo gold camp in western Ontario, and certain other similar deposits elsewhere in the world, appear to represent valid examples of metamorphosed, shallow-level epigenetic mineralization in greenstone belts. Since its discovery in 1981 it was clear that the Hemlo gold deposit was both important (estimated > 80 million tons averaging 7.2 g/ton Au) and atypical in terms of greenstone-hosted lode gold deposits (D.C. Harris 1986; Burk et al. 1986; Kuhns et al. 1986; Kuhns 1986; Valliant and Bradbrook 1986; Walford et al. 1986). The deposit is distinctive in terms of its predominantly sedimentary host rocks, its conformable geometry, its relationship to bedded barite, and its suite of associated minerals such as molybdenite, native arsenic, cinnabar, and stibnite.

The regional geologic setting of the Hemlo gold deposit and the lithologic sequence hosting the orebodies are illustrated in Fig. 4.23A,B. The stratiform orebody occurs within amphibolite facies metasedimentary-metavolcanic schists and granofels of the Archean Hemlo-Heron Bay greenstone belt (Muir 1985). The gold mineralization is located in the vicinity of a facies change from volcaniclastic rocks in the west to clastic rocks in the east. The main ore zone (see Fig. 4.23B) lies at the contact between a footwall muscovite-quartz-feldspar schist and overlying units that vary from biotite-quartz-hornblende-feldspar schist (meta-tuff?) to quartz-biotite schist, some containing kyanite/sillimanite others containing feldspar (Kuhns et al. 1986). In detail, the ore zone exhibits considerable complexity, both in terms of mineralogy and textures. This is the result of metamorphic and deformational overprinting of a zone characterized by strong variations in competency due to the presence of a sedimentary barite layer, phyllosilicate alteration assemblages, and a porphyry unit. In addition, later postpeak metamorphism and postore shearing developed which coincide with the main ore zone in some places but not in others (Kuhns 1988).

Detailed studies of the lithogeochemistry of the ore zone and flanking units on the Golden Giant property which represents the central portions of the Hemlo main ore zone (Kuhns 1986) indicate the presence of an asymmetric

alteration envelope (Fig. 4.24). The main chemical changes associated with this alteration involved strong K-enrichment and strong depletion of Na, Ca, Mg, and Mn, and are zoned to suggest a proximal meta-potassic alteration (microcline) flanked by a meta-phyllic facies (quartz-muscovite schists), and distal meta-argillic alteration facies (kyanite-sillimanite schists). Kuhns et al. (1986) have noted that, despite complexities involving overprinting of the original regional metamorphism by contact metamorphism from the adjacent Cedar Creek pluton and still later shearing events, the ores exhibit little retrograde metamorphism and must have been emplaced prior to peak metamorphism. These observations, coupled with evidence for a large fold structure at Hemlo that repeats the auriferous pyritic "Sucker zone" (see Fig. 4.23B) in the stratigraphic hanging wall sequence, all indicate that gold mineralization was an early feature.

The critical empirical relationships that have emerged from studies of the Hemlo ores and their host rocks can be summarized as follows:

1. The ores occur at the boundary of a deformed porphyry and overlying volcaniclastic units.
2. The elemental composition of the Hemlo ores is suggestive of epithermal mineralization.
3. The alteration assemblages associated with the main ore zone suggest a zoned sequence varying from high K^+ to high H^+ activity outward from the ore zone.
4. The ores and the alteration assemblages have undergone the full gamut of regional, contact, and shear zone metamorphism but exhibit only limited evidence of retrograde metamorphism.

All the above features suggest mineralization of epigenetic type, perhaps akin to some of that occurring at the present time in the Taupo Volcanic Zone, New Zealand. The epigenetic model for ore formation at Hemlo is further supported by the close similarities between the Hemlo deposits and those at Shamva, in Zimbabwe (Foster et al. 1986a). The Shamva deposit has yielded nearly 60 tons of gold from stratiform pyritic zones in volcaniclastic sediments and is characterized by strong enrichment in Mo, As, and K. It has, however, undergone considerably less damage from deformation and metamorphism, and a genetic model involving epithermal mineralization of tuffaceous sediments is indicated by the geologic relationships. A similar model can be applied to the important (> 100 tons Au) stratiform Big Bell deposit in Western Australia (Chown et al. 1984).

4.5.4 Post-Metamorphic Quartz-Rich Vein Ores: The Sigma Mine, Quebec

Crosscutting quartz-rich veins represent the most important type of greenstone-hosted gold deposits, and it is into this category that two of the world's giant nonplacer gold deposits fall: the Golden Mile camp, Kalgoorlie, and the Porcupine camp (Hollinger-McIntyre), Ontario, both of which have produced

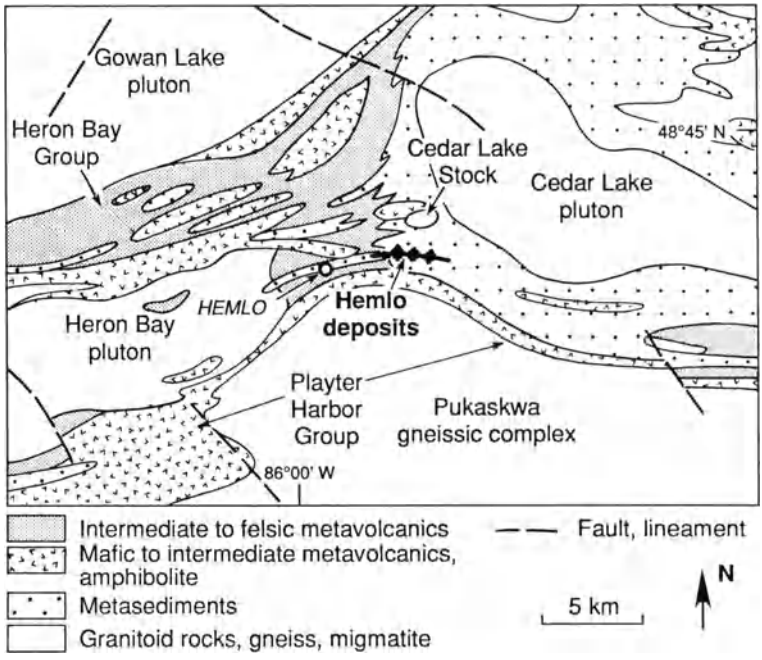

Fig. 4.23A. Map of the area surrounding the Hemlo gold deposits, Ontario, Canada. Note the position of the deposits in the relatively narrow corridor between the Pukaskwa gneiss complex and the Cedar Lake pluton. **B** Cross-section of the orebody and surrounding units as present on the Golden Giant (Noranda) portion of the Hemlo deposit (After Kuhns 1988)

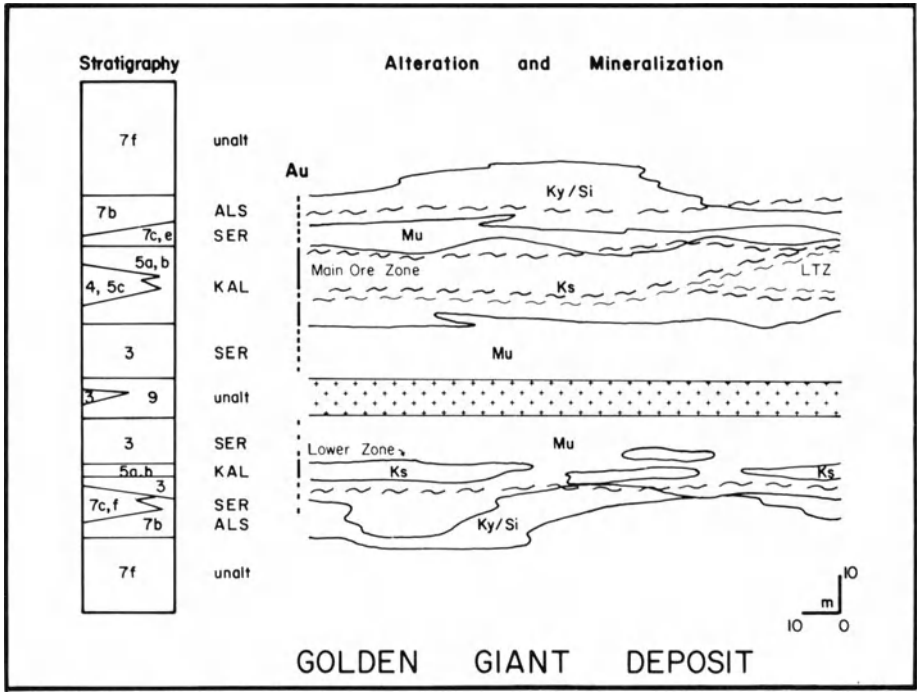

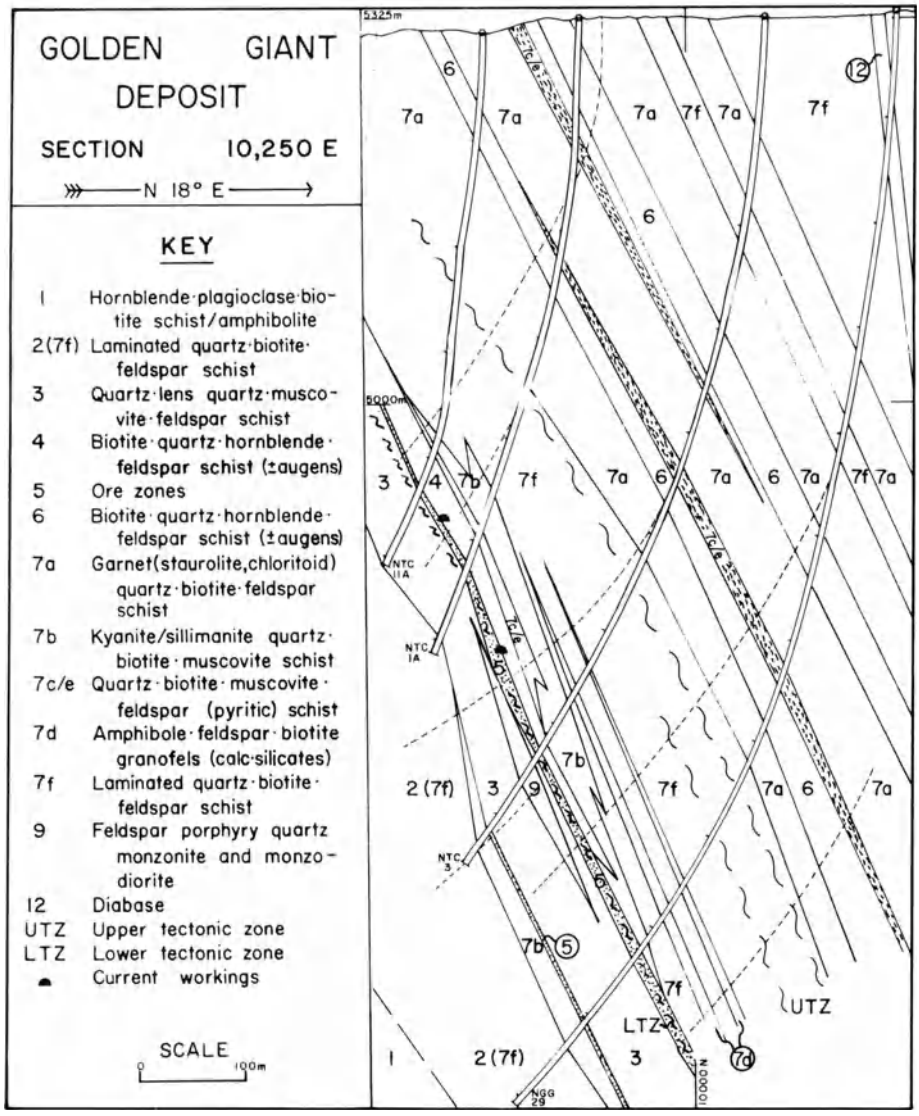

Fig. 4.23B.

Fig. 4.24. The mineralization and alteration relationships present in the Golden Giant portion of the Hemlo gold deposit. Stratigraphy as in Fig. 4.23B (*ALS* aluminosilicate; *SER* sericitic; *KAL* potassic; *Ky* Kyanite; *Si* sillimanite; *Mu* muscovite; *Ks* potassium feldspar) (After Kuhns 1988)

in excess of 1000 tons of gold (see Boulter et al. 1987 and references therein; Wood et al. 1986 and references therein). In regional terms the most important aspect of these, and many other mesothermal, greenstone-hosted, vein deposits, is their spatial relationship to major faults, shear zones or "breaks" (Colvine et al. 1988; Hodgson 1986; Mueller and Harris 1987). These major breaks (Fig. 4.25) are long-lived, but relatively late features which appear to have been active mainly during Archean terrane accretion events. In the case of the important Norseman-Wiluna Belt, which contains most of the gold deposits of the Yilgarn Block in Western Australia including the giant Kalgoorlie district (Fig. 4.26), L.B. Harris (1987) sees evidence for the former presence of major sinstral and dextral transcurrent shear zones. It is in certain second- and lower-order structures associated with these major structural discontinuities that the gold-quartz deposits are localized.

The Sigma deposit, in the Val d'Or camp, Quebec, occurs less than 10 km north of the Larder Lake-Cadillac Break (see Fig. 4.25) and has produced 90 tons of gold since 1937. The country rocks here are mainly steeply dipping massive and pillowed andesites of the Upper Malartic Group, intruded prior to folding by a body of porphyritic diorite (Robert and Brown 1986a). Feldspar porphyry dikes intruded this sequence and are undeformed. All these rocks were subjected to regional metamorphism of greenschist facies, but a transition to lower amphibolite facies is indicated at the deepest levels of the mine (Fig. 4.27).

The dominant structural features in the mine area are sets of E-W-trending, steeply dipping shear zones (see Fig. 4.27), but the block of mineralized ground is also bounded by N-S shears. The final structural event was the development of postore, subvertical, normal faulting (Robert and Brown

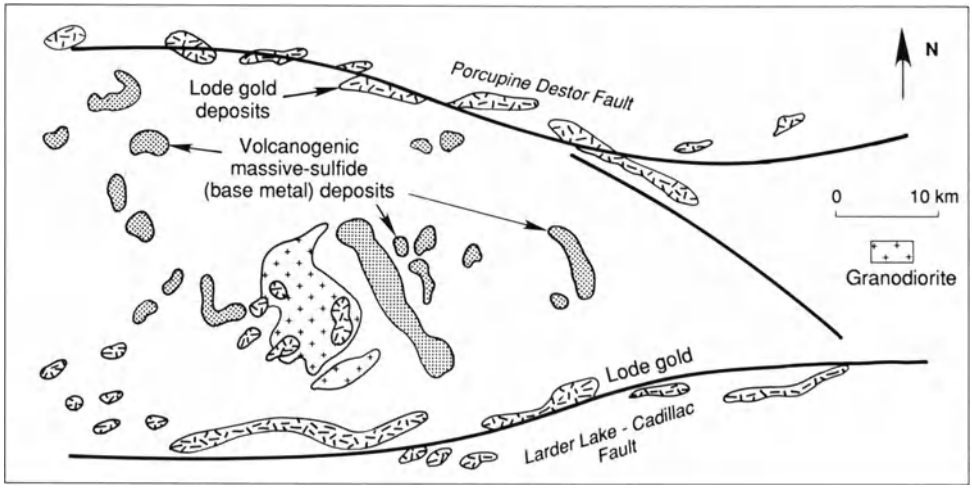

Fig. 4.25. Sketch map of part of the southern portion of the Abitibi greenstone belt (see Fig. 4.15) to illustrate the strong spatial relationship of lode gold deposits to the major "breaks" in that area, the Porcupine-Destor Fault, and the Larder Lake-Cadillac Fault (After Cathles 1986)

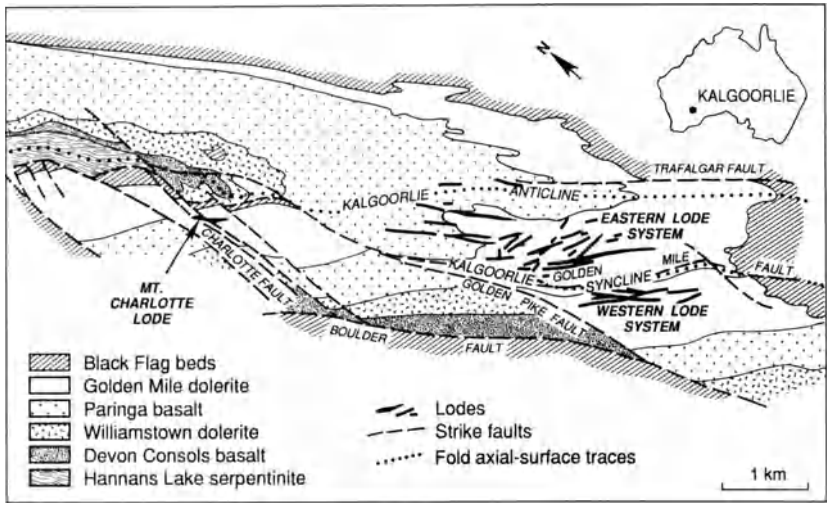

Fig. 4.26. Lode gold deposits of the Kalgoorlie district, an area that has produced over 1000 tons of gold. The major production came from the Golden Mile area that encompasses the Eastern and Western Lode systems. Note the strong transcurrent sense of the major faults (After Boulter et al. 1987)

1986a). Three sets of gold-bearing veins are present in the mine: subvertical veins that exhibit evidence of deformation; extensive subhorizontal ("flat") veins that exhibit little evidence of deformation; and stringer veins in the porphyry dikes that are similar in texture to the flat veins (Fig. 4.28).

The mineralized veins consist of quartz and lesser tourmaline, and minor amounts of carbonates, pyrite, chlorite (biotite at depth), and scheelite. The gold occurs as both the native metal and as gold tellurides, both of which were introduced into fractures and grain boundaries of recrystallized vein minerals during a post veinformation episode of deformation (Robert and Brown 1986b). The final siting of the gold is thus a very late event. Alteration adjacent to the veins consists of an outer cryptic chlorite-carbonate-white mica assemblage and an inner zone of alteration consisting of carbonates and white mica succeeded inward by carbonates and albite at the vein boundary (Robert and Brown 1986b).

Fluid inclusion studies of the quartz in the Sigma veins (Robert and Kelley 1987) demonstrated that all the inclusions present are of secondary type. Investigation of these assemblages indicated three parts: (1) a group of H_2O-NaCl inclusions with 25–34 wt% NaCl, (2) a group of CO_2-rich inclusions containing lesser H_2O and CH_2, and (3) a group of low-salinity H_2O-CO_2 inclusions ($<$ 10 wt% NaCl, CO_2 mainly 15–30 mol%). Temperature studies on this latter group revealed trapping in the range 285–395°C. Robert and Kelly (1987) deduce that types 1 and 2 resulted from unmixing of type 3 fluids, and that strong pressure fluctuations occurred at the time of inclusion trapping.

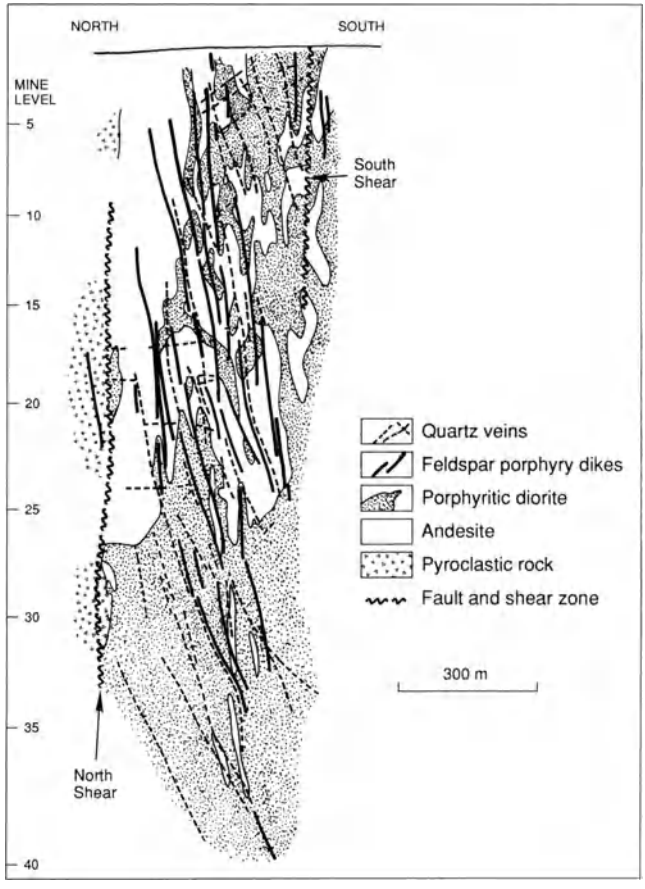

Fig. 4.27. Simplified cross-section of the vein structures present in the Sigma mine, Quebec, Canada. Note restriction of veins to the zone bounded by the South and North Shears (Robert and Brown 1986)

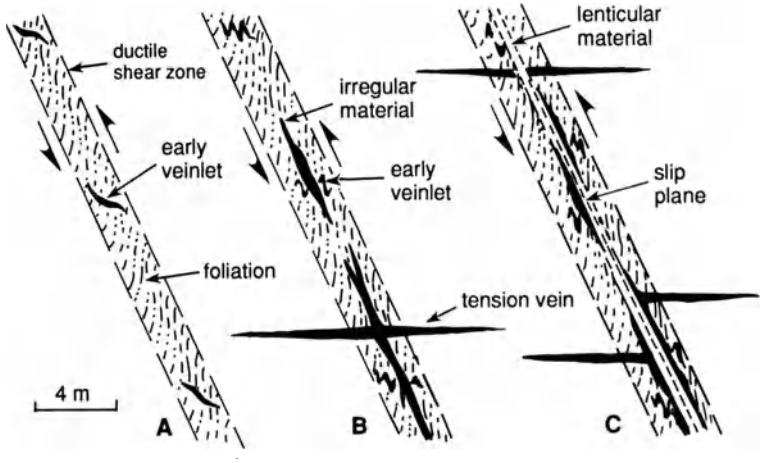

Fig. 4.28. Schematic illustration of progressive vein development in relation to shearing at the Sigma Mine, Quebec, Canada (After Robert and Brown 1986a)

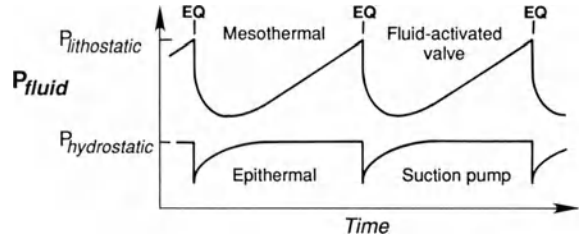

Fig. 4.29. The contrasting behavior of fluids at high pressures (mesothermal) and low pressures (epithermal) after earthquake (*EQ*) events. Note that a pressure decrease following a seismic event is more profound and longer lived under mesothermal conditions than under epithermal conditions (After Sibson et al. 1988)

Sibson et al. (1988) have noted that many of the mesothermal gold-quartz deposits in greenstone terranes are localized along high-angle reverse or reverse-oblique shear zones. Deposits emplaced and deformed in such zones typically contain structures formed in both ductile and brittle mode, such as shear veins, and local extension features, respectively (see Fig. 4.28). Sibson et al. (1988), citing textural and metamorphic evidence, infer that these gold systems formed near the base of the seismogenic zone (~ 10 km), where the transition from ductile to brittle deformation styles occurs. An important facet of the model involves the reverse faults acting as valves in which fluid pressures repeatedly vary from supralithostatic to hydrostatic (Fig. 4.29). The source of the fluids involved could be either from metamorphic dewatering, deep-seated magmatism, or a combination of both.

The late timing of most such greenstone-hosted, gold-quartz vein deposits, in relation to the major episodes of regional metamorphism, suggest that a simple metamorphogenic model (e.g., Phillips et al. 1987) may not be adequate to explain gold ore genesis. The common presence of apparently vein-contemporaneous porphyry intrusions in the major fault zones near gold-quartz vein deposits has been noted by many workers (e.g., Cherry 1983; Rock et al. 1987). The alkalic character of many of these porphyries has led to suggestions of genetic connections between lamprophyric intrusions and gold-quartz vein deposits (Rock and Groves 1988; Wyman and Kerrich 1988). Thus, magmatism may play a role in the genesis of these deposits. It is noteworthy, for example, that the association of gold tellurides with alkalic magmatism seen in Phanerozoic backarc environments (see Chap. 2) seems to be mirrored by the gold telluride-syenite association in the Kirkland Lake camp (Hodgson 1986).

4.5.5 Discussion and Suggestions for Exploration

The preceding sections provide ample evidence that greenstone belts contain several types of gold deposits that are distinctive in terms of their environments of deposition and their emplacement timing vis-à-vis the depositional and deformational history of the rocks that enclose them. In view of this, attempts to place all greenstone-hosted gold deposits into a single, comprehensive

genetic model (e.g., Colvine et al. 1988; Phillips et al. 1984) are unlikely to illuminate problems of gold metallogenesis. The timing of gold mineralization relative to the other events recorded in the rocks continues to be a point of contention. For example, even the late vein-type deposits tend to exhibit deformational textures, indicating that they formed mostly prior to cessation of movement on the structures that host them. Thus, the textures and microstructures displayed in mesothermal vein deposits tend to converge in appearance with the metamorphogenic quartz segregation veins developed in deposits initially mineralized prior to deformation and metamorphism. This is a nontrivial problem because, depending upon personal bias, the same textural relationships can be used to support diametrically opposed conclusions regarding the timing of gold mineralization.

In quantitative terms, postmetamorphic, gold-quartz vein deposits have been the most productive, but it is worth noting that the gold production from massive sulfide deposits and Homestake-type deposits ($>$ 4000 tons) represents about 40% of the total gold inventory of greenstone belts (Bache 1987). Furthermore, most of the research activity in recent years has been focused on gold-quartz vein ores. The fundamental similarities between western Pacific island arcs and Archean greenstone belts may also be mirrored in terms of their gold metallogeny. Thus the search for metamorphosed and sheared up gold-rich porphyry and epithermal systems in greenstone belts may prove to be a fruitful one. Furthermore, such systems may represent the original source of gold in some (? many) much later lode gold deposits.

Not only do the various types of gold deposit have a tendency to converge in terms of their textural aspects, they also display broad similarities in certain aspects of their geochemistry. Thus, Kerrich (1983) was able to demonstrate that both the lode gold-quartz deposits and auriferous chemical sediments in the Abitibi greenstone belt are enriched in Au, Ag, B, W, (+ Se, Te, Bi, Pd) by three to four orders of magnitude, whereas the more abundant and soluble base metals exhibit either little enrichment or an actual depletion relative to average crustal abundances (Fig. 4.30). This indicates that the fundamental chemistry of gold transport in exhalative, epithermal, and mesothermal environments of greenstone belts must have been distinctive from that responsible for base metal-rich deposits.

Numerous fluid inclusion studies have now been carried out on Archean lode gold deposits (T.J. Smith et al. 1984; Ho et al. 1985; Robert and Kelly 1987; Brown and Lamb 1986; Wood et al. 1986), and although major uncertainties remain regarding the problem of survival of primary inclusions in such environments, the results indicate CO_2-rich, low-salinity fluids were present in the structures. Similar fluid chemistries have been observed in studies of inclusions in quartz from the Mother Lode (Weir and Kerrick 1987). Furthermore, this fluid composition is similar in important respects to the high-CO_2, low-salinity geothermal waters responsible for current gold transport in the Taupo Volcanic Zone, New Zealand (Henley and Hoffman 1987). Thus, an explanation for the contrasting metal composition between greenstone-hosted massive sulfide deposits and gold deposits may lie mainly

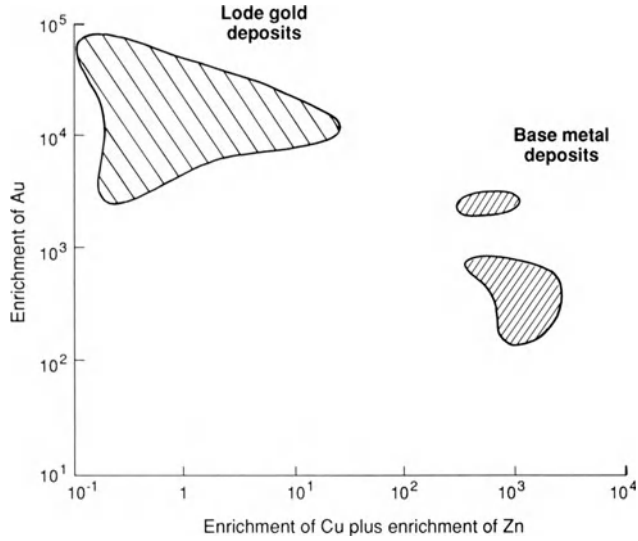

Fig. 4.30. Plot illustrating the profound difference in the content of base metals between lode gold deposits and massive sulfide deposits in the Superior Province of the Canadian Shield. Note that although some of the base metal deposits can achieve high levels of gold enrichment, many lode gold deposits are actually depleted with respect to average crustal abundances of copper plus zinc (After Kerrich 1983)

in variations in the chloride and CO_2 chemistry of their respective ore fluids (Cathles 1986).

One of the intriguing problems related to greenstone-hosted gold deposits is their strong concentration in late Archean greenstone belts. It is estimated by Colvine et al. (1984) that 65% of the world's mined gold was introduced into the developing Archean crust, much during the closing stages of the Archean. Although explanations for this phenomenon have remained elusive, it is noteworthy that the four major types of gold deposits found in Archean greenstone belts, i.e., exhalative, epithermal, mesothermal quartz vein, and porphyry type, all have analogs in Phanerozoic terranes of equivalent tectonic setting.

Many of the concepts outlined in this section on greenstone-hosted gold deposits have considerable exploration utility. The association of stratiform gold deposits with lean-banded iron formations, although deemphasized by many, is important, and at least 3000 tons of recoverable gold have been found in this lithologic environment (Bache 1987). This suggests that iron formations and related chemical exhalites represent worthwhile targets for gold exploration, irrespective of the genetic model favored for such deposits. Furthermore, both oxide and sulfide facies iron formations can be sought initially by regional airborne geophysical surveys.

One important characteristic of these Homestake-type gold deposits is their stratigraphic continuity, although the mineralized zone typically contains a series of discrete orebodies. Thus, the Morro Velho mine in Brazil and

the Champion mine in the Kolar goldfield have produced considerable amounts of gold, and are among the deepest metal mines in the world.

Recent studies of mineralized vent systems and associated silicification of sedimentary and volcanic rocks in the southern part of the Barberton greenstone belt (de Wit et al. 1982) have documented startling similarities of certain structures in these 3.3 Ga old rocks to features of modern hot-spring systems. Significant amounts of gold are present locally in these ancient silicified structures, and they appear to have fundamental similarities to some Tertiary hot-spring-type gold deposits.

Recognition of the hot-spring-related, essentially stratabound nature of Homestake-type gold ores and their tendency to occur within siliceous, sulfide-bearing, carbonate iron formation provides an initial guide for exploration. In many of the known deposits, strong deformation and recrystallization during metamorphism have reconcentrated and coarsened the gold, thereby aiding its recognition. It seems possible, therefore, that some chemical sediments in less deformed and metamorphosed greenstone belts may contain substantial reserves of fine-grained, essentially unrecognizable, gold ore. No examples of such deposits are known, and it would require carefully conceived exploration programs to find them. Clearly, carbonate iron formations should be the primary lithology sought, but interflow sediments and certain tuffs also deserve attention. In geochemical terms, arsenic is the best pathfinder element.

Hemlo-type gold deposits represent a relatively new and challenging target for gold exploration, largely because of their disseminated stratiform nature. However, they tend to be of large size and the three known examples account for close to 1000 tons of recoverable gold. Despite arguments that have been made for the structural control of Hemlo-type deposits (Hugon 1986), the fact remains that for both Hemlo- and Homestake-type gold deposits, the explorationist who bases his program on a stratigraphic as opposed to a structural approach will undoubtedly enjoy more success.

The gold-quartz vein deposits are best sought in the vicinity of major Precambrian fault/shear zones (e.g., Mueller and Harris 1987), but it needs to be emphasized that a great many such structural discontinuities in ancient cratons exhibit no evidence of economic gold mineralization (Southwick and Sims 1980). If these mesothermal deposits formed within 1–2 km of the base of the seismogenic zone, as Sibson et al. (1988) suggest, then brittle fault zones representative of shallower levels within the seismogenic zone may contain blind gold-quartz ores at depth. To the best of the author's knowledge, discoveries of this type have yet to be made in Archean greenstone belts, but many of the ore shoots along the northern portions of the Mother Lode were blind and extended from below surface to depths of over 1500 m (Knopf 1929; Clark 1969).

4.6 Additional Aspects of Greenstone Belt Metallogeny

It is noteworthy that massive sulfide deposits are rare in pre-3 Ga-old greenstone belts. However, a series of baritic lenses containing zinc, lead, and minor copper have been reported from a greenstone belt in the Pilbara craton of western Australia (Sangster and Brook 1977). Their composition and spatial association to rhyolite domes indicate a very strong similarity to Kuroko-type deposits. Model lead ages suggest an age of 3.5 Ga for these small, but intriguing deposits. The Murchison Range greenstone belt in southern Africa (Muff 1978) contains a line of subeconomic, copper-zinc occurrences in massive pyrite-pyrrhotite lenses reminiscent of Noranda-type deposits (Fig. 4.31), but it is more renowned as a major world source of antimony. The antimony deposits occur along a zone of cherty carbonate, quartzite, and schist rocks within the upper sedimentary portion of the greenstone belt. The ores are considered by Muff (1978) to be of exhalative origin.

In 1966, the Kambalda nickel deposits were discovered in western Australia. This discovery led to an intense exploration effort for nickel sulfide deposits in the Archean greenstone belts of the Yilgarn block, and by 1979 over 50 nickel sulfide deposits had been discovered in this area, making it the third largest producing region of sulfide nickel in the world (Ross and Travis 1981). Recently (see Econ. Geol., vol. 76, no. 6), a great deal of information on the geology and geochemistry of these Australian nickel ores and their host rock has become available.

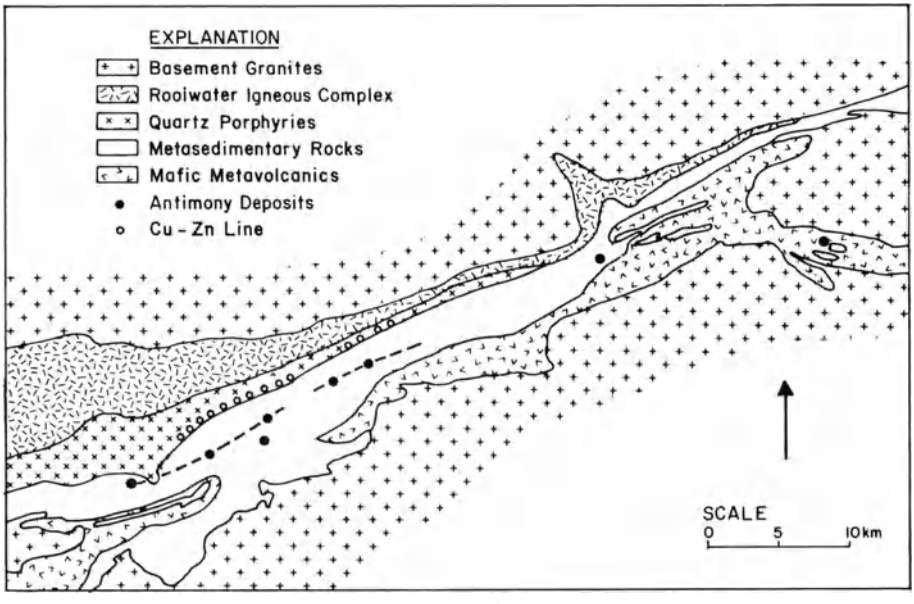

Fig. 4.31. Map of central portion of the Murchison greenstone belt, South Africa, showing linear array of antimony deposits and line of copper-zinc massive sulfide occurrences (After Muff 1978)

An excellent review of these nickel sulfide ores has been presented by Marston et al. (1981), and the following details are summarized from their contribution. The nickel deposits are strongly concentrated in the eastern part of the Archean Yilgarn block and occur almost entirely within greenstone belts. Two principal types of nickel deposits are found: those associated with intrusive dunites cluster mainly in the north, and those associated with volcanic peridotites are encountered mainly in the south (Fig. 4.32).

The nickel deposits associated with dunitic intrusives tend to be larger but lower grade than those within ultramafic volcanics (e.g., Mt. Keith: 290 million tons, 0.6% Ni). Their dunitic host rocks occur mainly as lenses of magnesium-rich peridotite that were emplaced as sills or dike-like bodies. The "magmas" are thought to have consisted of olivine-sulfide mush and probably represent the residue after eruption of komatiitic lavas at the surface. The nickel sulfides typically occur near the centers or at the margins of the thickest parts of the intrusive lenses (Fig. 4.33), and within the mineralized zones low-grade iron and nickel sulfides are abundant and enclose small higher-grade areas of more massive ore. Ni/Cu ratios in these ores range from 19 to 70, and Ni/Co ratios from 30 to 70.

The smaller, higher-grade, volcanic-associated ores ($<$ 5 million tons, 2–4% Ni) occur at or near the bases of volcanic flows of ultramafic komatiite, which are locally present within metabasalt sequences low in the greenstone stratigraphic sequences. The nickel deposits of this type are concentrated in the

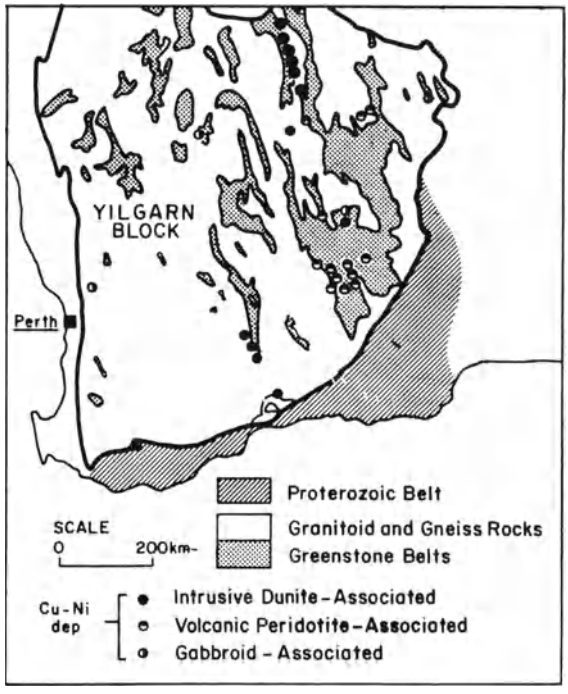

Fig. 4.32. Map of the Archean Yilgarn Block showing locations of major western Australian nickel deposits.

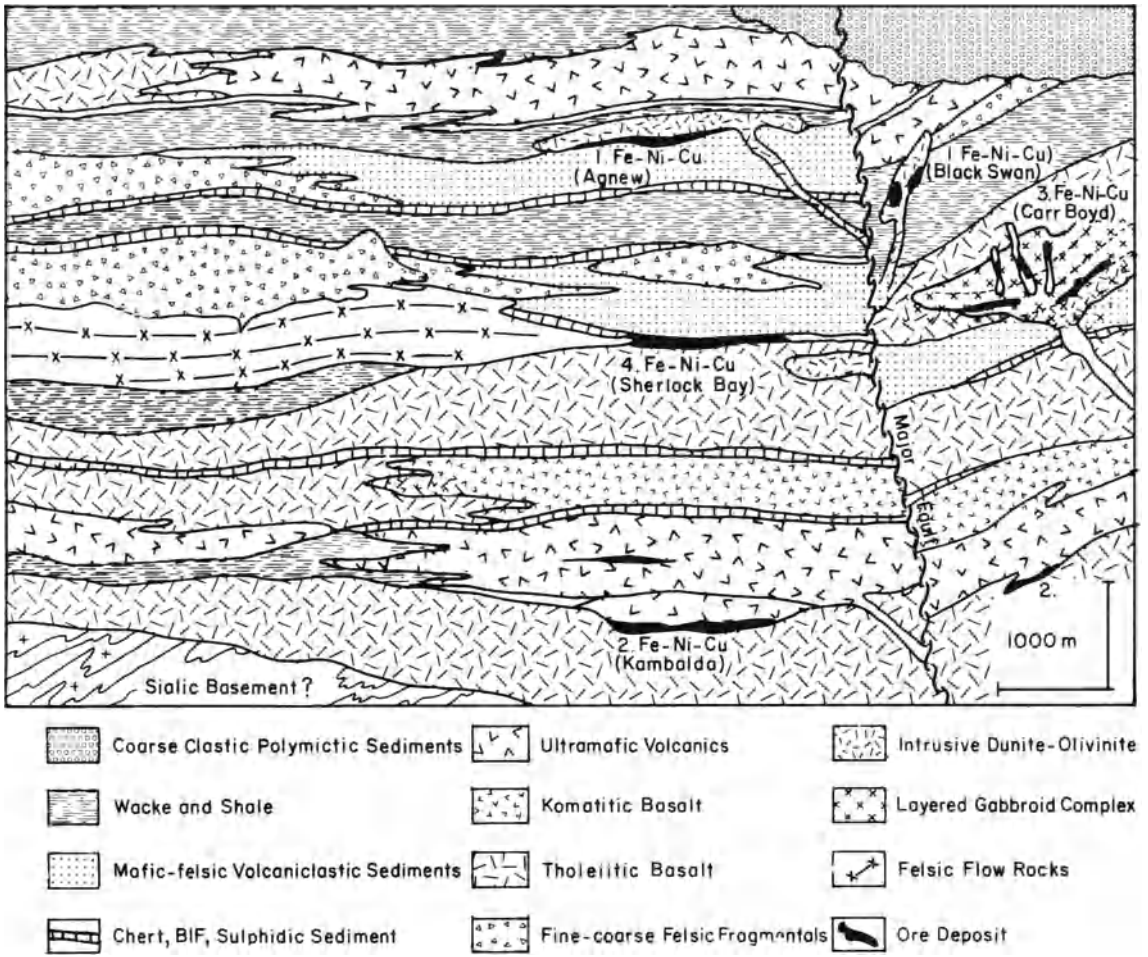

Fig. 4.33. Schematic cross-section showing stratigraphic relationships of western Australian nickel deposits (After Marston et al. 1981)

Kambalda-Norseman zone of the Wiluna greenstone belt, which contains 87% of the volcanic-associated deposits. The mineralization occurs in the lowermost zones of thicker flows, at or near the bases of the peridotite lava sequences and tends to occupy original depressions in the surfaces over which the host flows were erupted (see Fig. 4.33). The ores consist of thin, discontinuous, massive sulfides overlain by thicker, continuous, and more extensive zones of matrix and disseminated sulfides. The sulfide fraction of these volcanic ores contains 5 to 23% Ni and exhibits Ni/Cu ratios of 10 to 16 and Ni/Co ratios of 40 to 65. The sulfides are thought to have segregated from the host magmas by a combination of gravitational settling and flow differentiation and to have been subjected to a certain amount of physical modification during later metamorphism. In certain cases, however, assimilation of sulfide-rich iron formation appears to have provided some of the sulfur in the ores (e.g., Windarra deposits; Groves et al. 1979). Some minor nickel deposits associated with gabbroid intrusions have also been discovered in the Yilgarn block, and rare examples of sediment-hosted conformable and vein-type deposits rich in arsenic are also known.

The volcanic peridotite nickel deposits of western Australia have analogs in greenstone belts in Canada (Green and Naldrett 1981). In both areas the deposits occur within 2.7 Ga old greenstone belts, but the older ($>$ 3 Ga) greenstone belts of southern Africa do not appear to contain such deposits, despite considerable exploration activity. The tectonic situations that generate these high-magnesium magmas are not known, but a high degree of partial melting of the mantle must have been involved to produce them. It seems likely that the tectonic conditions during the early stages of greenstone belt formation (subduction?) caused perturbations in the asthenosphere and generation of these melts, but this situation still does not explain the restriction of nickel sulfide deposits to late-Archean greenstone belts and their strong concentration within a single greenstone belt in the Yilgarn block of western Australia.

4.7 Overview of Arc-Related Metallogeny

In the foregoing chapters we have seen that the spectrum of metal deposit types generated in arc systems is a broad one but that each deposit type can be keyed to one of the specific tectonic subdomains within subduction-related volcanoplutonic settings. Thus, as arcs evolve through tensional, neutral, and compressional modes (Dewey 1980; Uyeda and Nishiwaki 1980; Jarrard 1986) different deposit types will tend to form.

4.7.1 Relation of Arc Metallogeny to Subduction Style

The most fundamental process operative at convergent plate margins is the subduction of oceanic lithosphere, and therefore, as argued cogently by

Sillitoe (1981a), it is logical to seek an explanation for variations in arc metallogeny in terms of variations of both the subducted materials, the style of subduction, and the stress regime in the overriding plate (Dewey 1980). Thus, principal arcs, with their characteristic Cu, Fe, Mo, Au (± Ag) metal suite, form as linear belts above steep- to moderate-dipping Benioff zones (Fig. 4.34a) either in oceanic or near-trench Cordilleran settings. Such ores appear to be essentially restricted in time and space to the emplacement of shallow-level, I-type, magnetite-series granitoids (Takahashi et al. 1980).

An increase of the relative convergence vectors along Cordilleran margins results in a decrease of subduction angle, and it is under these conditions that the inner arc suite of silver-lead-zinc (± copper) deposits are generated (Sillitoe 1981b; Clark et al. 1982). However, as noted earlier (see Chap. 2) the

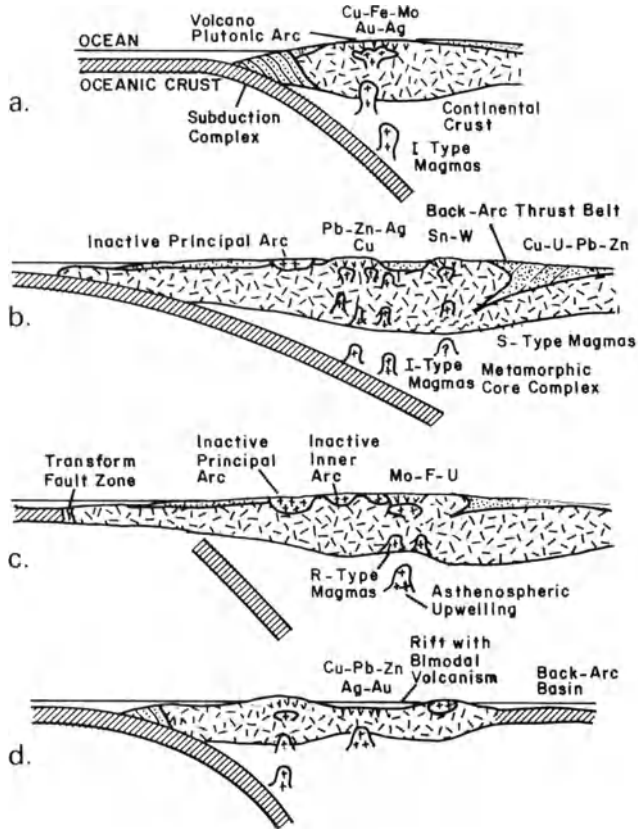

Fig. 4.34a-d. Schematized relationships between styles of subduction and arc metallogeny. **a** Moderate to steep subduction with emplacement of Cu-Fe-Mo-Au-Ag deposits in principal arc; neutral stress regime. **b** Shallow subduction with emplacement of Pb-Zn-Ag-Cu deposits and Sn-W-U in inner-arc belts; compressional regime. **c** Rapid steepening of detached, freely sinking slab due to transition from subduction to transform margin, with emplacement of lithophile element-type deposits; extensional regime. **d** Steep subduction and commencement of intra-arc rifting with emplacement of Kuroko-type deposits in a submarine setting; extensional regime (after Sillitoe 1981a)

demarcation of the boundary between principal arc and backarc regimes is difficult, especially in complex Cordilleran systems such as that of the western USA, where migration of the principal arc has occurred in response to repeated subduction angle changes, and the whole tectonic assemblage has been telescoped by accretion.

The generation of belts of tin-tungsten deposits on the innermost sides of backarc terranes appears to involve deeply penetrating, shallow subduction that is somehow capable of generating S-type magmas (Sillitoe 1981a), perhaps in connection with the formation of metamorphic core complexes (Armstrong 1982) and/or the development of back-arc thrust belts (see Fig. 4.34b). The fact that tin-tungsten deposits of this type occur only within restricted segments of Cordilleran arcs (e.g., Bolivia, northern British Columbia-Yukon) is puzzling for igneous rocks with certain S-type characteristics, but apparently lacking such mineralization, are now being found in a belt stretching from Idaho to Baja California (Miller and Bradfish 1980; A.R.J. White et al. 1986).

The high-silica rhyolites and associated Climax-type porphyry molybdenum deposits that were generated after 30 Ma ago in the western USA appear to relate to abrupt slowing and cessation of subduction in the eastern portions of the western USA, as discussed by W.H. White et al. (1981) (see Fig. 4.34c). These changes in the east were accompanied by the gradual withdrawal of calc-alkaline volcanism across the Great Basin to its present position in the Cascades (Eaton 1982). Wells and Heller (1988) have analyzed the tectonic rotation of the Pacific Northwest that is convincingly indicated by paleomagnetic data, and concluded that dextral shear related to oblique subduction has been the main contributor to this. This rotation in turn provides an explanation for the well-documented extension and related magmatism that control metallogenesis throughout the region.

The development of volcanic-hosted massive sulfide deposits in arc systems is closely associated with rifting events above relatively steeply dipping Benioff zones, which tend to develop caldera-style submarine volcanism (Sillitoe 1980c, 1982) (Fig. 4.34d). The absence of lithophile-element deposits in ensimatic arcs characterized by extension is presumably related to the limited crustal thickness of such arcs and their lack of material suitable for partial melting and generation of S-type magma (Sillitoe 1981a). The segmentation of arc systems and its influence on along-arc variations in magmatism and metallogeny, as noted by Sillitoe (1974a), is presumably also controlled by segmentation of the subducting plate (Dewey 1980).

In the preceding chapters, an important role has been assumed for magmas in the genesis of arc-hosted deposits, a concept that runs counter to the conventional wisdom for many workers. However, despite the role of nonmagmatic fluids in ore deposits formed in very shallow or exhalative environments, it is becoming increasingly apparent that actual metallogenesis is invariably tied either directly to magmatic-hydrothermal events or to the reworking of previously deposited magmatic-hydrothermal protores (cf. Butte vein ores, Montana; Chap. 1). Leaching of metals from wall rocks by non-

magmatic fluids undoutedly occurs to some extent, and minor mineralization can presumably result. However, in nearly every case where adequate data for a world class, arc-hosted metal deposit are available, a magmatic-hydrothermal origin can be postulated. One of the most compelling general relationships supportive of the foregoing conclusion is the consistent association of specific ore compositional types with specific composition and/or oxidation state of time- and space-related igneous rocks (see Ishihara 1981; Keith and Swan 1987; foregoing Chapters of this book). Thus, the metal deposits that characterize arc systems form an essentially coherent spectrum in relation to the magmatic hearths that generate them (Fig. 4.35).

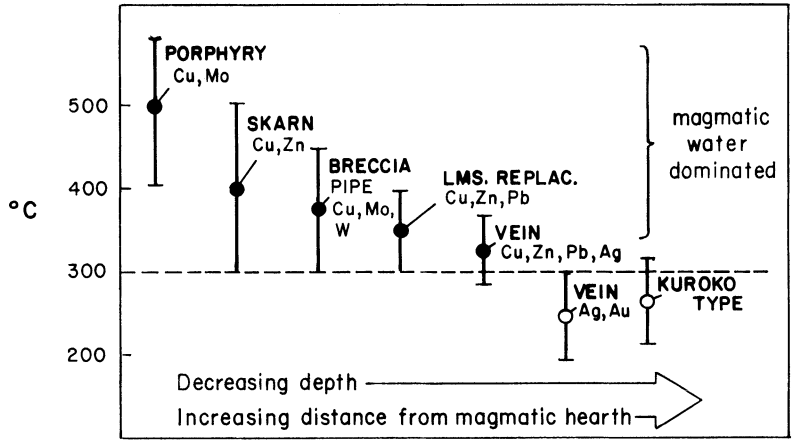

Fig. 4.35. Generalized temperature-deposit type relationships for the major hydrothermal ore types found in arc systems emphasizing the essential coherence of arc metallogeny despite variations in the metal content of individual deposits

Part II
Divergent Plate Boundary Environments

Chapter 5 Metallogeny of Oceanic-Type Crust

5.1 Introduction

The volumes of magma generated per year along the current > 50 000-km-long system of oceanic spreading ridges are estimated to exceed that of the remainder of the earth by about one order of magnitude (Menard 1967). Oceanic crust and lithosphere are mainly formed at so-called midocean ridge systems, but essentially similar oceanic crust is also generated during the earlier stages of continental separation (e.g., Red Sea), and during the formation of marginal basins behind some subduction-related arc systems (Karig 1971). Pearce et al. (1984) have also suggested, based on geologic observation and geochemical data, that many well-preserved ophiolite complexes formed directly above subduction zones, prior to mature arc construction.

The nature of oceanic crust and underlying mantle material was little known until the realization that certain mafic-ultramafic complexes (ophiolites) embedded in many of the younger orogenic belts of the world exhibit thicknesses, and seismic and petrologic features that appeared to match those known from oceanic areas (Coleman 1977). The ophiolite model for the crust of the deep ocean basins needs to be approached with some caution, however, because it has become apparent that most major ophiolite complexes represent either forearc limbs of island arc complexes (Gealey 1980; Casey and Dewey 1984), marginal basin material (Harper 1980; Hawkins 1980), or former oceanic crust adjacent to fracture zones (Karson and Dewey 1978). Emplacement of major ophiolite complexes has typically involved an arc-continent collision event, and under normal conditions of subduction only thin slivers of ophiolite material tend to be incorporated in imbricate, forearc melange terranes (Gealey 1980). Oblique subduction typically gives way to translation motion (transpressive margins) in which slivers of oceanic material are also plastered along a continental margin (California, Pakistan). Continent-continent collision events can result in the trapping within the suture zone of oceanic crustal materials, but tectonism is typically severe and the ophiolitic sequences become dismembered to an extent that little more than their mafic-ultramafic, ensimatic character is apparent.

Considerable research effort has been focused in recent years on the petrology and petrochemistry of ophiolite complexes (see Panayiotou 1980, Proceedings of International Ophiolite Symposium, Cyprus 1979). However, Fox et al. (1980) emphasize that, although a generally acceptable model of

oceanic crust via ophiolite studies is at hand, there are many puzzling first-order variations in the structure, thickness, and composition of ophiolite complexes. For example, the ophiolite complexes of the western Tethyan area (Italy to Turkey) are distinctive in regard to some aspects of their trace element geochemistry compared to those of eastern Tethyan regions, which in turn exhibit certain differences from typical midocean ridge basalts (MORB) (Pearce 1980). The lavas of the complete ophiolite complexes in this area (Troodos Massif, Semail Nappe; Fig. 5.1) are strongly depleted in Cr and contain much lower Ce/Sr ratios than MORB. These and other trace element data repeatedly suggest that the lavas and their associated ophiolitic units formed in marginal basins above active subduction systems. Detailed petrologic studies of the Troodos Complex volcanics (Thy et al. 1985) and sheeted dikes (Baragar et al. 1988) have demonstrated that the magmatism has a distinctive, but subtle, calc-alkaline flavor that is a manifestation of the former presence of an underlying subducting slab. Thus, Thy et al. (1985) and Thy (1987) find evidence for relatively high water contents in Troodos magmas, and Baragar et al. (1988) report rocks as felsic as dacites among the dikes of the sheeted complex. Similar conclusions have been reached regarding the late phases of volcanism in the Semail ophiolite (Alabaster et al. 1982) where the central volcanic complexes contain lavas of dacitic composition. Late gabbroic dikes that crosscut the upper mantle and layered gabbro of the Semail crustal unit clearly postdate the main ophiolite construction (Vetter and Stakes 1988). These contain clinopyroxene, orthopyroxene, plagioclase, and brown hornblende phases reminiscent of island arc intrusions. At this stage of geologic knowledge, the magmatism and related hydrothermal activity currently occurring at midocean ridges must be considered as similar in most respects, but by no means identical, to that manifest in fossil form in ophiolite complexes.

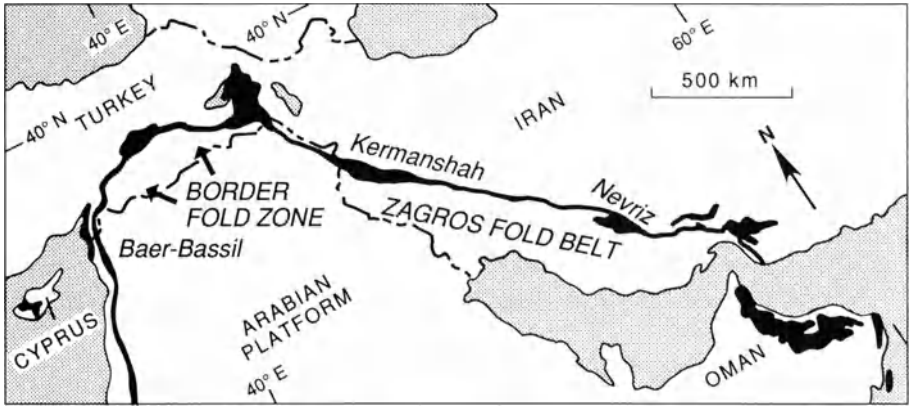

Fig. 5.1. Map of the distribution of ophiolites between the eastern Mediterranean and the Indian Ocean (After Mukasa and Ludden 1987)

Ophiolite complexes are now known to have a wide distribution in time and space. In addition to the well-studied ophiolites of the Tethyan and North American Cordilleran regions, similar complexes have been documented in the late Proterozoic terranes of Morocco (Leblanc 1981) and those of the Arabian-Nubian Shield (Vail 1985; Pallister et al. 1987). Much older ophiolite complexes have also been reported, for example from the early Proterozoic Cape Smith belt in northern Labrador (St-Onge et al. 1988) and from the Wisconsin terrane, north-central USA, of similar age (Schulz and Laberge 1986). Archean ophiolitic sequences are postulated in Wyoming (Harper 1986), in the Yellowknife belt of northern Canada (Helmstaedt and Padgham 1986), and even in the 3.5 Ga terrane of the Barberton greenstone belt in southern Africa (de Wit et al. 1987). Acceptance of these very old sequences as ancient oceanic crust is by no means unanimous, but few would refute the presence of ophiolite complexes in the late Proterozoic terranes of northern Africa and Arabia.

5.2 Processes Operating at Modern Spreading Centers

As newly formed oceanic lithosphere moves away from midocean ridges it cools, thickens, and decreases in elevation, attaining normal oceanic depths after a time interval of approximately 50 Ma. Slow-spreading ridge systems, such as the mid-Atlantic Ridge, are characterized by steep topography, whereas the fast-spreading East Pacific Rise is a much broader, but has topographically smoother feature (see Fig. 4, Introduction). The elevation of oceanic ridge systems reflects their underlying thermal structure, and the steeper topography of slow-spreading ridges is probably related to the longer residence time of newly formed crust over the area of magma chambers.

The mechanisms of magma generation and crystallization during formation of oceanic lithosphere are also somewhat contentious, but recent models proposed by Duncan and Green (1980) and Dick (1982; Fig. 5.2) appear capable of explaining many of the subtleties of ophiolite petrology. It is noteworthy that bodies of plagiogranite are observed in many ophiolite complexes, and small volumes of rhyolite are generated in Iceland and have been recorded, albeit rarely, from oceanic ridge samples (Melson et al. 1976). The significance of such felsic igneous rocks in this setting is not fully understood, but their presence indicates that considerable degrees of igneous fractionation can occur in oceanic settings.

The observation that the empirical heat-flow patterns associated with spreading ridge systems were markedly disparate from those predicted by theoretical considerations (Lister 1972, 1980; Sclater et al. 1974; Wolery and Sleep 1976; Fig. 5.3) led to a search for evidence of convective hydrothermal activity, and eventually the actual sites at which thermal springs were debouching on the seafloor were discovered (Corliss et al. 1979).

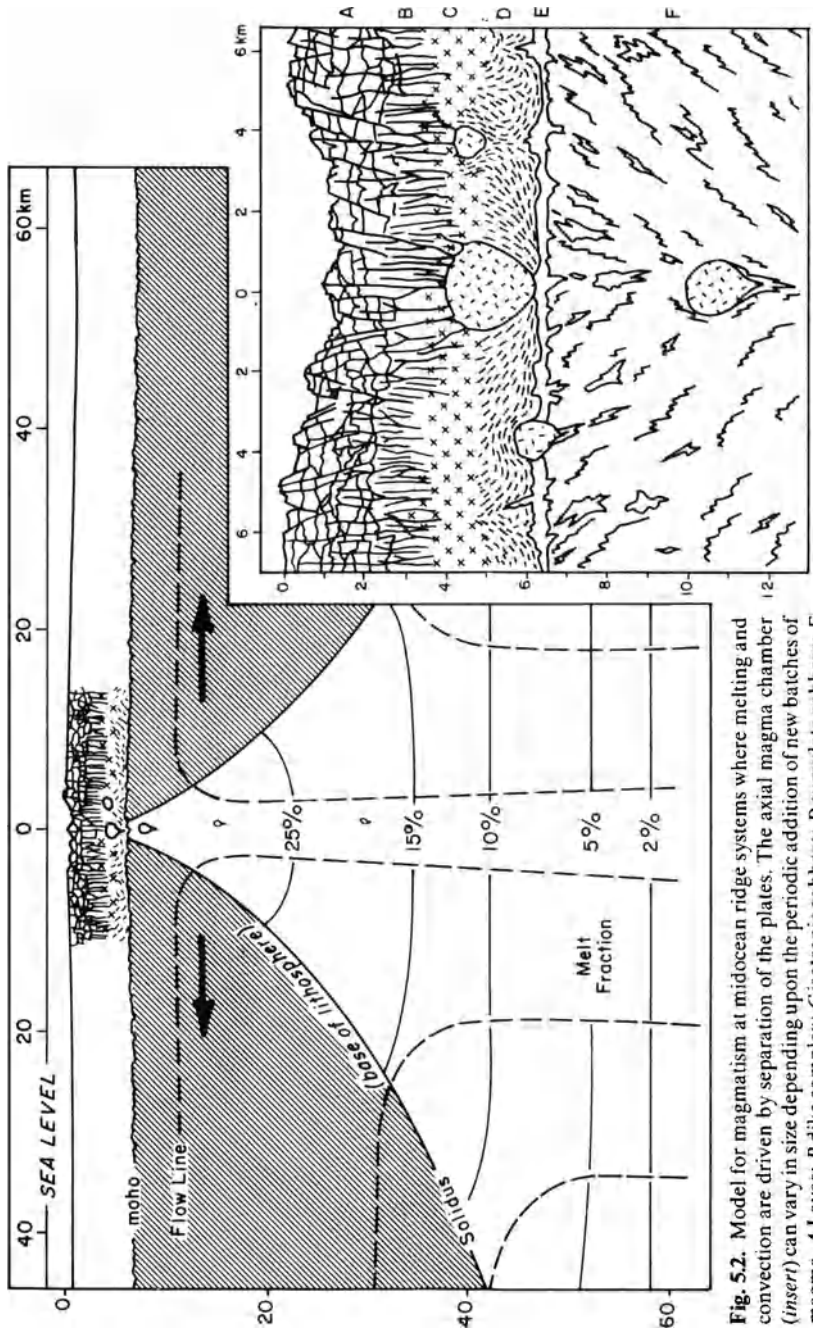

Fig. 5.2. Model for magmatism at midocean ridge systems where melting and convection are driven by separation of the plates. The axial magma chamber (*insert*) can vary in size depending upon the periodic addition of new batches of magma. *A* Lavas; *B* dike complex; *C* isotropic gabbros; *D* cumulate gabbros; *E* Moho zone; *F* peridotite (After Dick 1982)

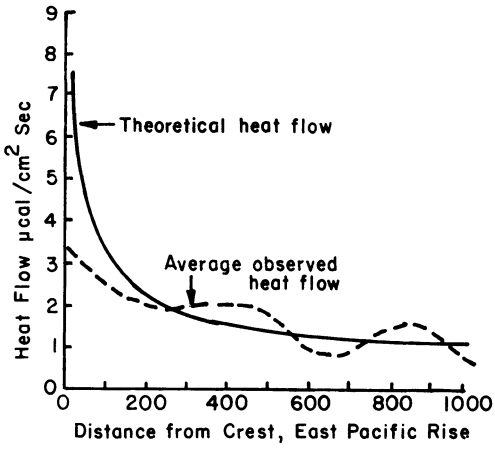

Fig. 5.3. Theoretical and average observed heat flow-distance curves for the Pacific Ocean. Similar relations are also found in the Atlantic and Indian Oceans (After McKenzie 1967)

Since that time there has been a major research effort to both discover additional sites of current seafloor hydrothermal activity and to understand the geologic settings and geochemistry of the hydrothermal systems. As a result, a whole series of vent sites has been discovered in the eastern Pacific (Fig. 5.4); others are known on the mid-Atlantic Ridge, and it is clear that high temperature, sulfide-depositing exhalations are a normal accompaniment to seafloor spreading activity. Fehn and Cathles (1986) note, however, that the high-temperature, primary convection cells responsible for black smoker activity and sulfide chimney formation are restricted to the immediate axial zone of the spreading system. The larger, lower-temperature ($< 200°C$) secondary cells are estimated to account for 80% of the heat loss from ridges and these cells actually move with the newly created oceanic crust and lithosphere. The transition zone between the primary and secondary convection cells lies at distances of from 5–25 km from the ridge crest.

Studies of the distribution of high-temperature vent sites along the East Pacific Rise have led to the realization that they occur where ridges attain their highest elevations (Ballard and Francheteau 1982), and that this in turn is related to inflation of the ridge by active magma bodies (Karson and Elthon 1987). At points where major transform faults cross ridges, elevations are lower, magmatic activity is more restricted, and high-temperature vents are unknown (Fig. 5.5). Backer and Lange (1987) claim that a sequence of events from magmatic inflation, to collapse and rifting can be postulated, and that maximum hydrothermal activity is associated with the latter.

The limiting factor in the generation of high-temperature, sulfide-depositing vents is the amount of heat available from ridge-related magmatic processes (Sleep et al. 1983; Mottl 1983), and it seems clear that to attain the temperatures necessary for sulfide exhalative activity ($> 350°C$), convection must occur parallel to the ridge axis (Fig. 5.6). Also limited by the same constraints are the volumes of oceanic crust that can undergo hydrothermal alteration and the amounts of metal sulfides that can be produced. Lister

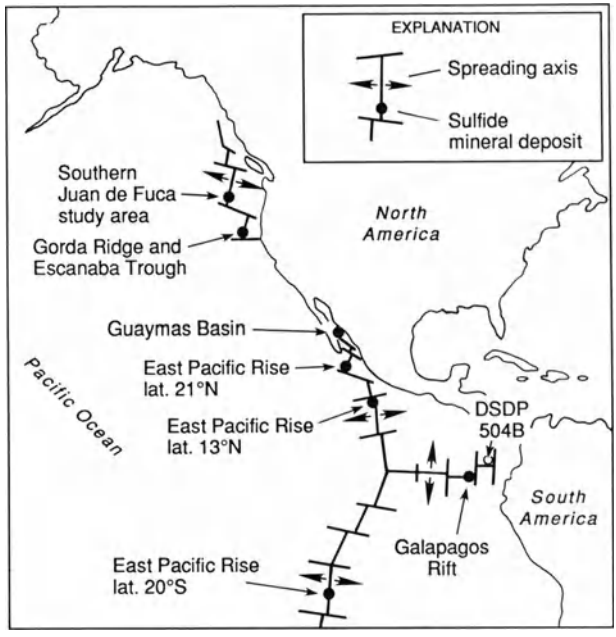

Fig. 5.4. Map of the eastern Pacific showing sites at which accumulations of seafloor sulfides related to modern vent sites have been found (After Shanks and Seyfried 1987)

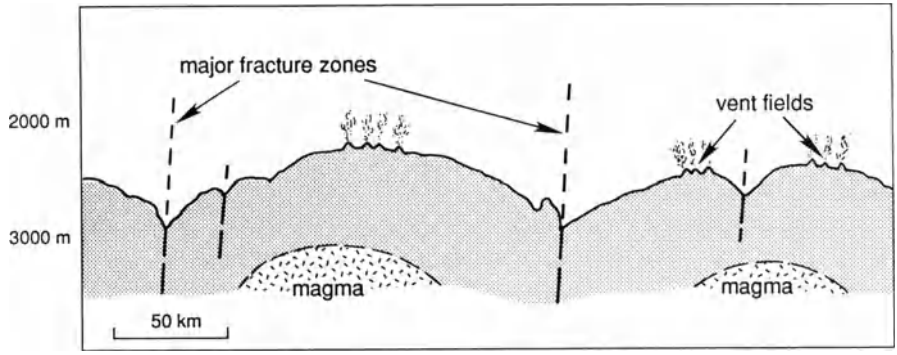

Fig. 5.5. Generalized longitudinal profile of a spreading ridge system illustrating the relationships between topography, fracture zones, and vent sites (author's sketch based on data in Ballard and Francheteau 1982)

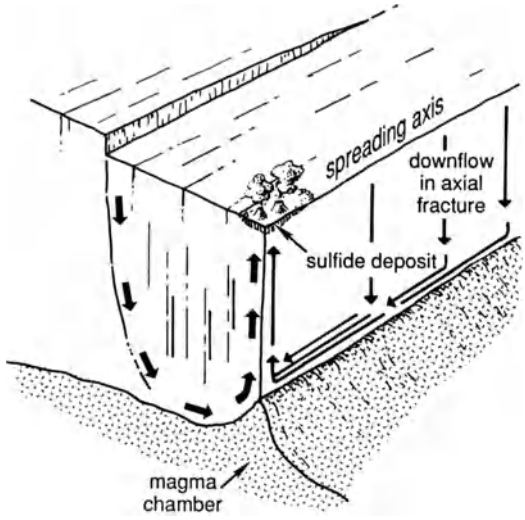

Fig. 5.6. Diagram illustrating the concept of circulation of fluids of seawater origin at spreading ridge systems (After Cann et al. 1985)

(1983) has demonstrated that the physical conditions for water-rock interaction at high temperatures and low water-rock ratios will occur close to the boundary of the axial magma chamber. A large body of both experimental and theoretical work is now at hand (Seyfried 1987, and references therein) that reinforces the conceptual model for hydrothermal convective activity outlined above, and places constraints on the chemical processes involved. Critical to the solubility of heavy and base metals is the mechanism of H^+ production.

At temperatures in excess of 350°C, metasomatic reactions involving Ca fixation and epidote-clinozoisite formation will generate low pH fluids at virtually all water-rock mass ratios and will be especially effective at low pressures (Seyfried and Janecky 1985; Hemley et al. 1986). The experimental data, for example, can be used to constrain the 21° N, East Pacific Rise end-member fluids to 395 ± 10°C and pressures from 330 to approximately 400 bar (Seyfried 1987). At temperatures < 350°C, and at virtually all pressures, Ca-titration reactions are unable to generate sufficient acidity to mobilize metals. Mg-fixation, however, can generate an acidic, metal-rich fluid at relatively low temperatures, provided dissolved Mg concentrations approach seawater values. This is only possible for so-called seawater-dominated systems (Seyfried and Mottl 1982) which may characterize off-ridge hydrothermal activity leading to Fe-Mn oxide accumulations from low-temperature submarine discharges.

5.2.1 Known Sites of Modern Seafloor Sulfide Accumulations

The rate at which new examples of seafloor spreading-related sites of sulfide exhalation have been found over the past few years virtually guarantees that this section will seem dated by the time this book comes off the presses.

Nevertheless, a review of known current seafloor sulfide systems and their variability is deemed appropriate at this point.

The large majority of seafloor sulfide systems has been discovered in the axial graben-like portions of spreading ridges, but similar activity is now known to occur in sites such as the caldera of Axial seamount on the Juan de Fuca Ridge (Hannington and Scott 1988), on Green seamount west of the East Pacific Rise at latitude 21° N (Lonsdale et al. 1982), and on Palinuro seamount in the Tyrrhenian Sea (Minniti and Bonavia 1984). Hekinian and Fouquet (1985) report a large massive sulfide deposit on the flank of a seamount east of the East Pacific Rise at 13° N. Since the amounts of sulfide material that can be produced at any one site are constrained by the availability of thermal energy to drive convection, seamounts are of some interest in terms of the potentially larger magma volumes associated with them (see later).

Direct observations and sampling of the hydrothermal activity at 21° N on the East Pacific Rise have generated considerable research activity (Macdonald et al. 1980; Edmond et al. 1982). Some warm springs sampled from the Galapagos Ridge apparently represent high-intensity systems that have undergone near-surface cooling by admixture with shallow convecting seawater. Certain aspects of their chemistry, however, indicate an original high-temperature, low water-rock interaction with deeper levels of oceanic crust (Edmond et al. 1979, 1982). Mottl (1983) demonstrates that the rate of heat loss from underlying magmatic systems achieved by the high-temperature discharges is such that both they, and the magmatism that drives them, may be episodic in nature. The amount of deep-seated water, carbon dioxide, and other volatile components in these high-temperature discharges is as yet unknown, but may not be negligible.

The high-intensity discharges at 21° N on the East Pacific Rise (East Pacific Rise Study Group, 1981) are of two types, termed black and white smokers. The black smokers represent dicharges that upon entry into ambient seawater produce clouds of pyrrhotite particles. Samples of the columnar vent structures themselves indicate that they are composed of sulfides that exhibit surficial oxidation to ochreous iron oxides. Two main types of sulfide "ore" are present: a zinc-rich material containing about 25% Zn and an iron-rich material with 20–40% Fe and $<$ 1–6% Cu. Additional metals present in minor amounts are Co, Pb, Ag, and Cd. The distribution of gold in seafloor sulfides has been studied by Hannington et al. (1986). The white smokers contain little sulfide material, and the precipitate formed on the admixture with seawater is predominantly barite.

Hydrothermal activity with formation of iron, zinc, and copper sulfide mounds scattered over an area 7 km long and 2 km wide has recently been discovered in the Guaymas Basin, Gulf of California (Lonsdale et al. 1980; Scott et al. 1983). Although the Gulf of California primarily represents a transform plate boundary, it contains a number of short seafloor spreading centers that link en echelon transform faults (Fig. 5.7). The Guaymas Basin is underlain by one such actively spreading segment, but because of relatively high sedimentation rates, the Basin contains considerable sediment fill and the

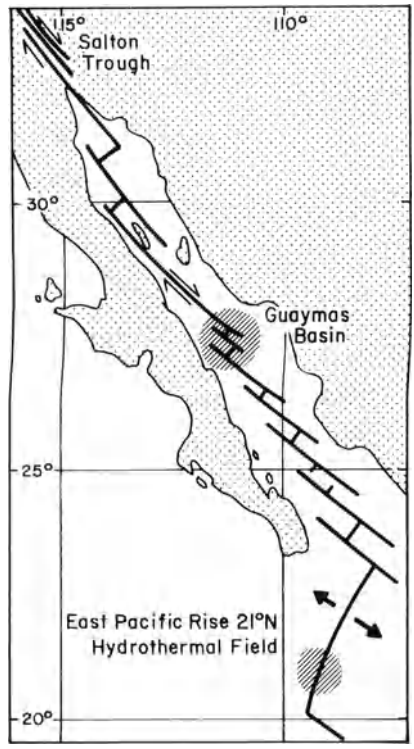

Fig. 5.7. Location of the Guaymas Basin above two short segments of spreading in the Gulf of California. The hydrothermal activity and sulfide deposits occur in the northern trough at depths of approximately 2000 m. Note positions of the 21° N hydrothermal field and position of Salton Trough along this same plate boundary system (After Lonsdale et al. 1980)

sulfides are accumulating in a sedimentary environment well above oceanic basement. Scott et al. (1983) have suggested that this situation may well be representative of that in which the sediment-hosted, Cu-Zn Besshi-type deposits formed (see Chap. 8).

Recently, contemporary hydrothermal activity and base metal sulfide accumulations have also been discovered on the Galapagos ridge (Cu) and the Juan de Fuca Ridge (Zn) (Normark et al. 1983). Together with the East Pacific Rise activity, these occurrences are of major interest, not only in terms of providing actualistic examples of processes of "ore" formation, but also because data gained from these systems have an impact on the resolution of problems as diverse as the formation of oceanic crust, its subsequent metamorphism, the chemistry of seawater, and the global magnesium flux (Mottl 1983). Study of these systems has also allowed for a particularly intriguing marriage of the empirical, experimental, and theoretical approaches to the solution of geologic problems. Active circulation of metalliferous brines and recent precipitation of economically interesting sulfide layers within a marine environment are also known from the axial portions of the Red Sea (Degens and Ross 1969). These will be discussed in a later chapter.

Given the variability of seafloor environments known to be producing sulfide-depositing hydrothermal activity (see Fig. 5.4) it is in fact surprising

that they exhibit basic similarities in the temperature and chemistry of their "end-member" fluids (Table 5.1). It is noteworthy, however, that the base metal concentrations in these fluids are very low compared to those in magmatic-hydrothermal fluids of approximately similar temperature (Sawkins and Scherkenbach 1981). This finding could indicate either that the high-temperature fluids only attain metal contents of several ppm, or that significant deposition of metals takes place in shallow fracture systems prior to exhalation. Some variations in the fluids from different vent areas are puzzling, however, in particular their chlorine contents, which range from less than seawater values to twice that of seawater (Table 5.2). Fluid inclusion studies of quartz from sulfide-bearing breccias recovered from the mid-Atlantic Ridge at 23.6° N indicate salinities of almost three times seawater (Delaney et al. 1988), and fluid inclusions in augite, epidote, plagioclase, and apatite in altered gabbros from the same area exhibited salinities of up to 50 wt% NaCl and temperatures in excess of 700°C (Vanko 1986; Kelley and Delaney 1987; Stakes and Vanko 1986). These high-temperature, high-salinity fluids may well be of magmatic origin and indicate that modern seafloor hydrothermal systems are probably more complex than current models indicate.

The alteration reactions that occur in both the high temperature axial convection cells and the lower temperature off-axis cells (Alt et al. 1986) represent one of the fundamental geochemical processes occurring on the planet earth and at current rates, a volume of fluid equivalent to that in the

Table 5.1. Calculated[a] end-member compositions of eastern Pacific vent waters compared to the composition of seawater (Scott 1985)

	Locations of vent fields						
	21°N	13°N (A)	13°N (B)	Explorer	Axial	Guaymas	Seawater
T,°C	350	368	--	(617)	300	315	2
pH	3.5	3.4	3.9	5.0	--	5.9	7.8
Cl (ppt)	18.26	31.83	26.15	20.36	--	21.25	19.18
ppm							
H_2S	252	157	164	60	224	162	0
SiO_2	1050	1253	1396	610	1139	735	10
Ca	647	2796	2072	1720	1152	1252	408
Ba	2	5	4	1	3	4	0
Sr	7	21	15	12	9	18	8
K	939	1290	1180	1815	--	1671	383
Mn	49	88	47	15079	30	9	0
Fe	80	663	82	15	3	4	0
Cu	2	--	--	0	--	0.04	0
Zn	5	--	--	0.05	--	0.7	0
ppb							
Ag	3	--	--	--	--	9	0
Pb	54	--	--	--	—	75	0

[a] End-member calculated for Mg = 0.

Table 5.2. Chlorinity as a fraction of seawater (sw) value for several vent sites in the eastern Pacific (chlorinity of sw = 540 mmol/kg) (Scott 1985)

Sites	T, °C	Chlorinity
10°57′ N EPR[a]	347	0.6 × sw
Endeavour	380	0.8 × sw
21°N EPR	350	sw
Explorer	291	1.1 × sw
Guaymas	315	1.2 × sw
11°15′ N EPR	--	1.3 × sw
12°50′ N EPR	381	1.4 × sw
S. Juan de Fuca	--	2 × sw

[a] EPR = East Pacific Rise

world oceans is cycled through young oceanic crust along ridges every 5–11 Ma (Wolery and Sleep 1976). Estimates of the degree and volume of oceanic crust altered and hydrated by these processes of convective circulation come mainly from the heat budgets available to drive convection and can only be approximate (Morton and Sleep 1985). However, this alteration can be viewed as a critical first step in the series of events that lead to the production of volcanoplutonic arcs and their associated metal deposits.

5.2.2 Economic Potential of Submarine Metal Concentrations

The discovery of hydrothermal systems actively transporting and depositing base metal sulfides on the ocean floor has understandably fired the imagination of economic geologists, both in terms of the formulation of models for ore genesis and as potential targets for mining operations. However, given the difficulties of sampling seafloor sulfide deposits, let alone actually estimating their volume and average grade, most of the evaluations of their potential must be viewed with caution.

For example, many of the recovered samples exhibit zinc contents that are much higher than the average amounts found in analogous, land-based deposits. This finding is probably a function of the sampling of sulfide chimneys where zinc sulfides tend to concentrate relative to sulfides of iron and copper. Thus, the estimates of Bischoff et al. (1983) for average grades of massive sulfide deposits at 21° N and along the Juan de Fuca ridge are improbable.

Limit estimates of the tonnage potential of vent clusters is on somewhat firmer ground because the volume of hydrothermal fluid that can be convected at high enough temperatures to effect metal transport is constrained by magmatic heat budgets. These estimates can be approximated with reasonable accuracy (Converse et al. 1984). Scott (1987) estimates that, apart from the Red Sea sulfide deposits (see Chap. 8), virtually all modern seafloor deposits will be of the order of 1000 tons and that accumulations of more than 1 million tons

will only occur where clusters of vents are present, or perhaps in association with the larger magmatic systems represented by seamounts.

Another very real problem in terms of the potential of modern seafloor sulfides is their tendency to undergo oxidation and dissolution. It is thus only under conditions of burial and removal from oxidized ocean-bottom waters that deposits can be preserved. This process undoubtedly happens in many instances, but it effectively removes these deposits from the likelihood of either discovery or economic exploitation on the ocean floor.

The oxidation and dissolution of seafloor sulfide deposits presumably contributes to the metals available for incorporation into ocean-floor manganese nodules. The economic potential of these must be considered greater and more immediate than that of sulfide deposits (Horn et al. 1973; McKelvey 1986; Siapno 1987). The ferromanganese nodules, which are of hydrogenous origin, have Fe/Mn ratios on the order of 1, and much higher contents of trace metals (Ni, Co, Cu, and Zn) than the iron and manganese encrustations on pillow basalts caused by deposition from off-axial convection cells. Furthermore, considerable areas of the Pacific Ocean floor are covered with nodules containing sufficient quantities of nickel, copper, and other metals in addition to iron and manganese, to make them of economic interest (Cronan 1987).

Ferromanganese crusts on seamounts in the central Pacific have also been investigated recently (Mangini et al. 1987), and although the crust thicknesses are only between 0.5 and 10 cm, they occur in much shallower water (1000–2000 m) than nodule fields and contain significantly greater amounts of cobalt (av. 0.9%) than abyssal manganese nodules.

5.3 Ophiolite-Hosted Massive Sulfide Deposits

As noted earlier, knowledge of the internal constitution of oceanic crust has been obtained in large measure from the study of ophiolite complexes. The fact that ophiolite complexes contain massive sulfide deposits that bear close similarities to the sulfide material that collects at the base of and below black smoker chimneys at modern vent sites has stimulated considerable research activity focused on these deposits and the lithologic environments in which they are found.

5.3.1 Massive Sulfide Deposits of the Troodos Ophiolite, Cyprus

The precise tectonics of emplacement of the Troodos ophiolite massif is still a somewhat contentious subject (e.g., Bortolotti et al. 1976; Robertson 1977; Gealey 1980), but there is little doubt that this sequence of mafic and ultramafic igneous rocks and overlying pelagic sediments (Fig. 5.8) was originally formed at a submarine spreading center during late Cretaceous time. Recent dating of plagiogranites within the complex has indicated their emplacement at close to 90 Ma (Mukasa and Ludden 1987).

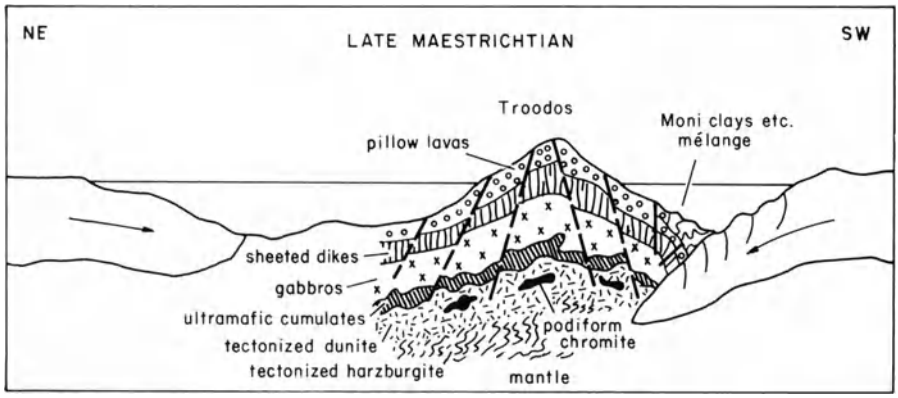

Fig. 5.8. Schematic cross-section explaining the uplift of the Troodos ophiolite complex to its present position (After Searle and Panayiotou 1980)

Petrologic studies of Troodos volcanics and intrusions (Thy et al. 1985; Thy 1987; Baragal et al. 1988) indicate that some facets of Troodos magmatism are water-rich and have calc-alkaline character (see above). This implies the presence of an underlying subduction zone, which in turn suggests that the seafloor spreading episode that formed the Troodos complex must have occurred in a narrow (young) backarc basin. However, the lack of volcaniclastic material overlying the pelagic ferromanganoan sediments and chalks of layer 1 indicate that the arc did not involve subaerial volcanism (Pearce et al. 1984).

The Troodos Massif proper forms an elongate domal uplift in which a plutonic core complex consisting of gabbros, lesser plagiogranites, and ultramafic rocks is surrounded by roughly concentric zones of sheeted dike complex and pillow lavas (Fig. 5.9). The complex is cut by numerous normal faults that trend mainly north-south, and a major east-west structure, the Arakapas Fault, that exposes additional plutonic igneous rocks on its south side (Searle and Panayiotou 1980). For a review of the geology of the Troodos massif, see Gass (1980 and references therein).

Structural studies of anomalous areas (Solea graben) in the upper parts of the Troodos complex (Varga and Moores 1985) have demonstrated listric faulting related to shallow detachment zones. Paleomagnetic studies (Allerton and Vine 1987) have confirmed this and indicate that parts of the dike and pillow lava sequence have been rotated up to 78° by listric faulting.

The massive sulfide deposits and related stockwork ores of the Troodos complex all lie within the pillow lava sequence (see Fig. 5.10). Over 90 deposits are known, but most are small (< 100 000 tons), and only 6 exceed 1 million tons in size. Of these, the most noteworthy are the Mavrovouni, Limni, and Skouriotissa deposits which together account for over 90% of the past production of sulfide ore in Cyprus (Table 5.3). In a number of instances, groups of small (< 1 million tons) deposits occur in relatively close proximity to one another (Adamides 1980; Fig. 5.11). A typical deposit consists of a zone of massive pyrite, containing variable amounts of marcasite and lesser chal-

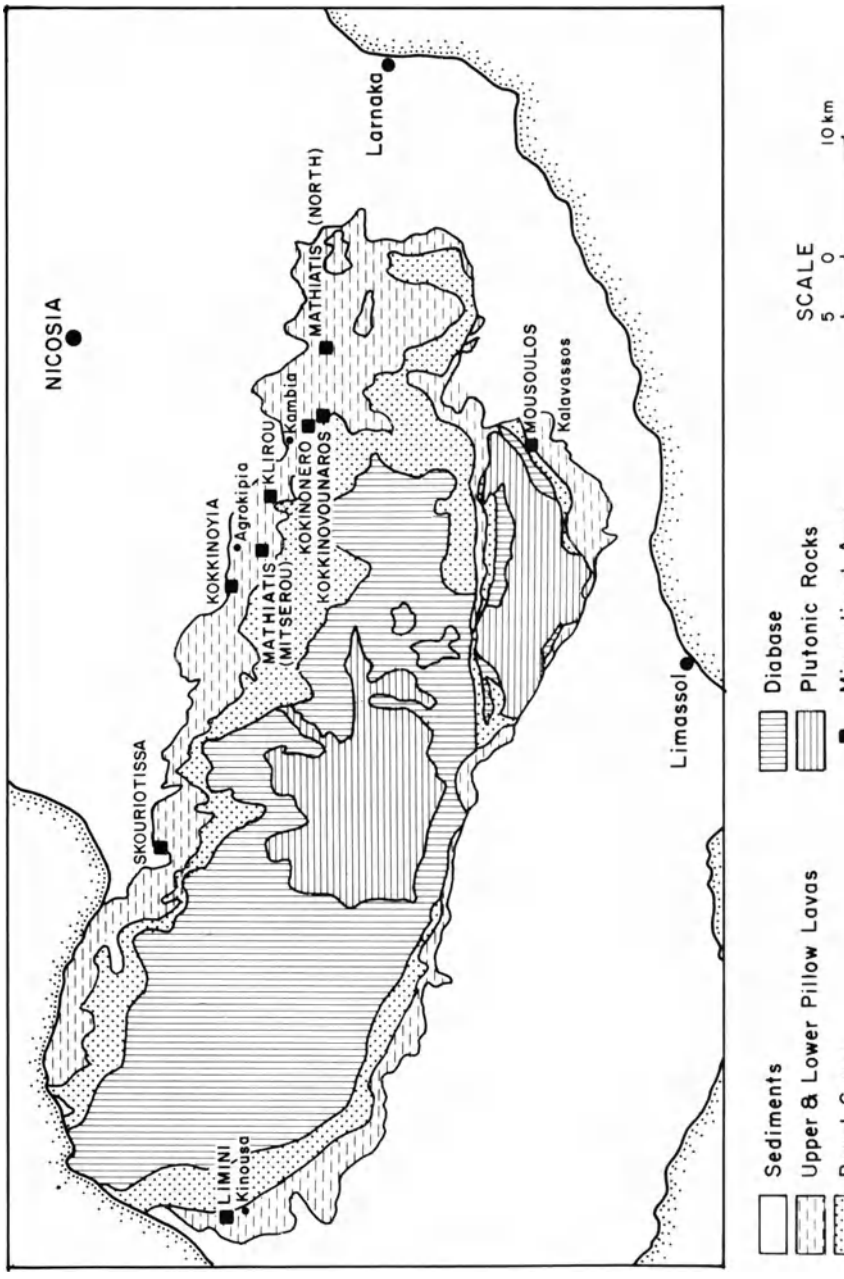

Fig. 5.9. Map of the Troodos complex showing crude annular structure with plutonic ultramafic rocks in central regions, and restriction of massive sulfide deposits to pillow lavas (After Maliotis and Khan 1980)

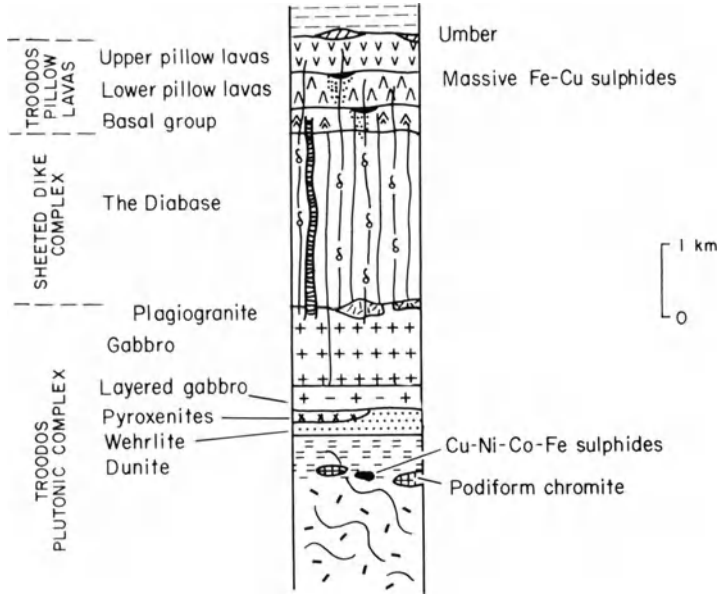

Fig. 5.10. Lithostratigraphic section of the Troodos Ophiolite (Searle and Panayiotou 1980)

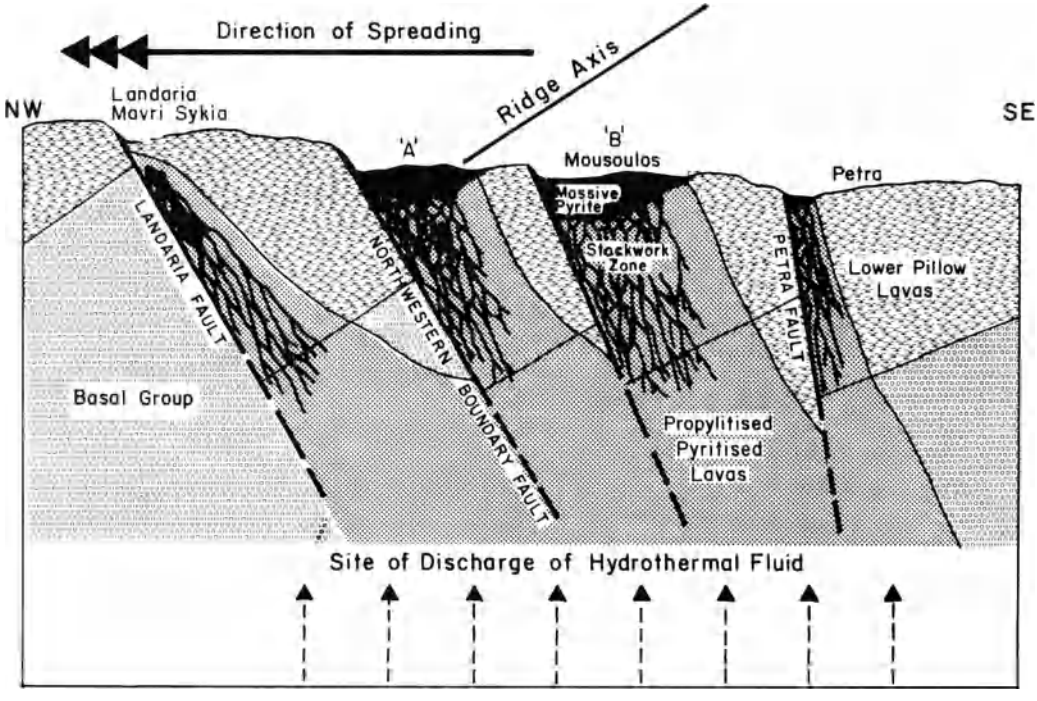

Fig. 5.11. The environment of formation of the Kalavasos ore deposits (After Adamides 1980)

Table 5.3. Size and grade for selected Cyprus-type massive sulfide deposits in Cyprus, Oman, Newfoundland, and Norway[a]

Deposit	Tonnage	Cu(%)	Zn(%)	Contained Cu (tons × 10^3)
		Cyprus		
Skouriotissa	6 000 000	2.2	--	132
Mavrovouni	15 000 000	4.0	0.5	600
North Mathiati	2 800 000	0.2	--	< 10
Apliki	1 650 000	1.8	--	29
Kalavasos A	1 000 000	0.25-2.5	0.7	< 10
Sha	350 000	0.5-1.2	--	15
Klirou East	420 000	1.1	1.4	< 10
Kinousa underground	300 000	2.4	3.4	< 10
Limni	16 000 000	1.0		160
		Oman		
Lasail	8 000 000	2.3	0.2	184
Bayda	750 000	2.7	1.3	20
Aarja	3 170 000	1.7	0.8	54
		Newfoundland		
York Harbor	332 000	1.9	4.7	< 10
Tilt Cove	9 000 000	1-12	--	180
Betts Cove	130 682	2-10	--	< 10
Little Bay	3 400 000	0.8-2.0	--	51
Miles Cove	200 000	1.45	--	< 10
Whalesback	4 181 708	0.85-1.1	--	42
		Norway		
Lokken	25 000 000	2.1	1.9	525

[a] Note that over half the contained copper in this list is in just two deposits and over 70% in just four deposits (Koski 1987 with additions by author).

copyrite and sphalerite, sandwiched between an overlying ochre horizon and a basal siliceous ore zone (Constantinou 1980). Below this are stringer zones consisting mainly of quartz and quartz-sulfide veins cutting chloritized basalt. Disseminated sulfides are also present in the altered pillow lavas. The ochre horizons consist of quartz and goethite with lesser illite and jarosite, and have been interpreted to result from submarine oxidative weathering of sulfide ore exposed to seawater (Constantinou and Govett 1972).

The massive sulfide ores typically consist of porous blocks of iron sulfides set in a friable sulfide matrix (Constantinou 1976). This conglomeratic texture is more pronounced in the lower portions of orebodies and is thought to have resulted from intense leaching of the sulfides, presumably due to passage of later fluids. The copper contents of massive ores are usually from 1 to 6%, with zinc contents somewhat lower. However, substantial amounts of zinc (approaching 10%) are present in certain orebodies (Bear 1963).

Chemical, fluid inclusion, and isotope studies have all tended to support the concept that the fluid responsible for the formation of these deposits was predominantly or solely seawater that had circulated deep into the newly formed oceanic crust. For example, fluid inclusion data from stringer zone quartz indicates temperatures of close to 350°C with salinities equivalent to that of seawater (Spooner and Bray 1977). Similarly, studies of strontium (Chapman and Spooner 1977) and stable isotopes (Heaton and Sheppard 1977) in the stringer zones and the adjacent altered rocks have tended to confirm the seawater origin of the fluids imprinted on these altered conduits.

Zones of intense alteration near the base of the sheeted dike complex occur in places. These zones are characterized by rocks consisting almost solely of quartz and epidote (so-called epidosite) which have had all their original content of base metals completely leached (C.J. Richardson et al. 1987). Although these zones appear to be volumetrically limited, they provide empirical evidence for the loss of base metals from precisely those parts of the crust where leaching should occur, according to models based on modern spreading systems (see Fig. 5.6).

5.3.2 Massive Sulfide Deposits of the Semail Ophiolite, Oman

The Semail ophiolite is a large, well-exposed ophiolite sheet that was formed at the same time as the Troodos complex (Tilton et al. 1981), and emplaced during the same Tethyan collision event. Here, as at Troodos, there are no arc-type volcaniclastic units overlying the ophiolite section and the metalliferous ambers that cap it, and on this and petrologic grounds (Pallister 1984) it can be designated as a suprasubduction zone ophiolite (see Pearce et al. 1984).

Although the Semail ophiolite nappe has the sequence of a typical ophiolite, the volcanic stratigraphy indicates a complex magmatic history (Alabaster et al. 1982) manifest by the presence of a series of volcanic centers strung out along the uppermost part of the ophiolite (Fig. 5.12). These volcanic centers (Lasail and Alley Units), which overlie the more typical nonvesicular aphyric basaltic pillow lavas (Geotimes Unit), are atypical of ophiolites in that they contain significant amounts of intermediate and even felsic volcanics apparently fed from intrusions emplaced discordantly into the sheeted dike complex (Alabaster and Pearce 1985; Vetter and Stakes 1988). Between these centers only minor evidence of localized hydrothermal activity is present, and no major sulfide lenses have been found. The large massive sulfide deposits in the Semail ophiolite are all associated with the volcanic centers (see Fig. 5.12).

Studies of the massive sulfide ores at Lasail (9 million tons grading 2.4% Cu), Aarja (3.3 m.t.), and Bayda (0.8 m.t.) (Ixer et al. 1984) indicate that the deposits occur at the top of the Geotimes pillow basalt unit, but they are overlain by units of the submarine volcanic centers. The Lasail orebody consists of a saucer-shaped lens that reaches a thickness of 50 m, and has been

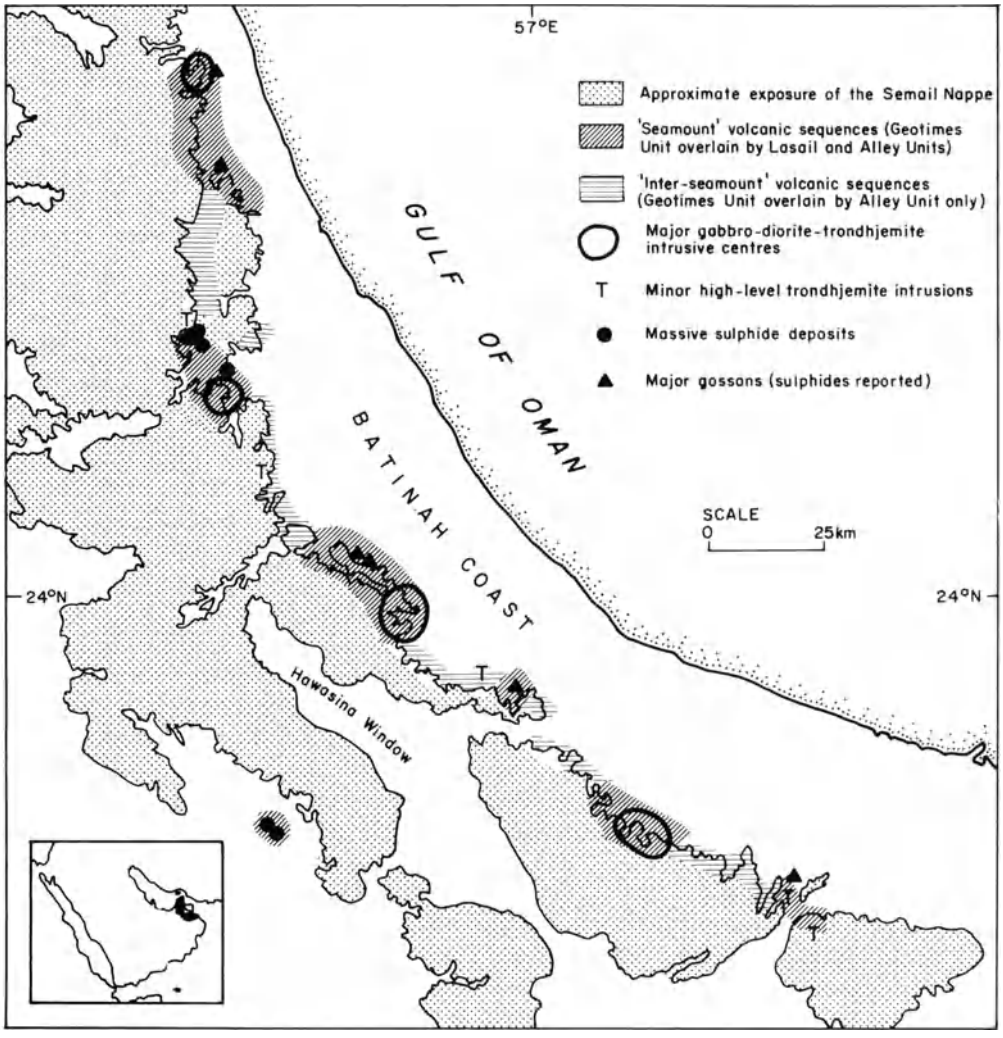

Fig. 5.12. Map of the Semail Nappe Ophiolite showing "seamount" volcanic sequences. Note that massive sulfide deposits are mainly associated with these more felsic volcanics (After Alabaster et al. 1980)

traced down-dip for 200 m. The pyritic massive sulfides contain thin bands (1 cm thick) of chalcopyrite-rich, magnetite-rich, and magnetite + hematite (± chalcopyrite)-rich material. Sphalerite and bornite are late-stage phases, and the lens is capped by a hematite-quartz layer. Gangue within the massive sulfides consists of patchy quartz (commonly chalcedonic), and lesser carbonates, and chlorite. Below the ore lens a stockwork consisting of veins containing quartz + chlorite + jasper + pyrite is present in the underlying basalts and epidote + quartz assemblages occur at the gabbro boundary.

The Aarja and Bayda deposits lie approximately 8 km to the north and are similar in many respects. However, the Aarja orebody, which consists of a cigar-shaped lens 75 m long, contains three major ore types consisting of mixed pyrite-chalcopyrite-bornite, banded pyrite-chalcopyrite-bornite, and a sphalerite-rich type with pyrite, chalcopyrite, and traces of tennantite and galena. In the dikes below the level of mineralization, epidote and jasper are present.

The distribution patterns of the massive sulfide bodies within the Semail ophiolite imply that ore generation was not related to the normal processes of seafloor spreading. Alabaster and Pearce (1985) conclude that it was the subseamount magma chambers that provided the thermal energy and the intrusive pressure-induced fracture systems favorable for ore genesis. It seems reasonable to ask whether these felsic magmatic systems did not also supply a significant amount of the metals now present in the ores.

5.3.3 The Turner Albright Massive Sulfide Deposit, Josephine Ophiolite, Oregon

The Turner Albright deposit consists of a series of massive sulfide pods which have been shown to contain about 3.3 million tons of ore with an average grade of 1.5% Cu, 3.3% Zn, 0.4 opt. Ag, and 2.8 g/ton Au (Kuhns and Baitis 1987). The ore lenses lie within the basal pillow lava sequence of the Josephine ophiolite, a marginal basin type accreted terrane formed 157 Ma ago, and emplaced during the Nevadan orogeny (Saleeby et al. 1982).

The ophiolite contains the typical sequence of litho-units from peridotite, through gabbros and sheeted dikes to pillow basalts, and is overlain by a thick flysch unit called the Galice Formation (Harper 1984). The ore lenses occur at three levels within the pillow lava sequence, but the Main Upper Zone and Main Lower Zone may be equivalent (Fig. 5.13). The uppermost lenses are small but of high grade. The ophiolitic stratigraphy, including the massive sulfides, has been somewhat disrupted by normal faulting, and from the distribution of sulfide mineralized breccias and the lithologies present as clasts in these breccias it appears that sulfide deposition and at least some of the fault activity were contemporaneous (Zierenberg et al. 1987).

Massive sulfides dominate the ore types at Turner Albright, and they typically pass downward into semimassive and then disseminated sulfides, presumably representative of feeder zones. Much of the massive and semimassive sulfide material (Fig. 5.14) appears to have formed below the seafloor and to have replaced olivine basalt hyaloclastites (Zierenberg et al. 1987). Fine-grained pyrite constitutes the great bulk of the sulfides and is followed by sphalerite, chalcopyrite, marcasite, and accessory sulfides in order of abundance. The deposit is noteworthy in terms of its relatively high gold content, which occurs as small ($< 30\ \mu$) blebs within sulfide minerals (Kuhns and Baitis 1987).

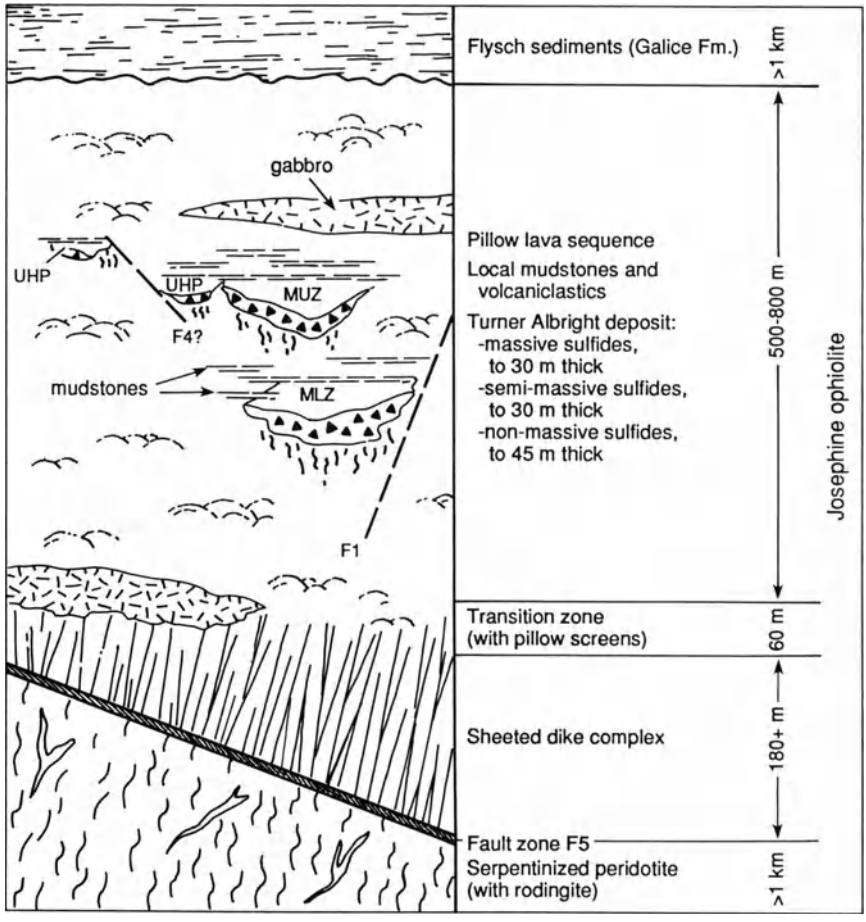

Fig. 5.13. Cross-section showing the position of the massive sulfide lenses that comprise the Turner Albright deposit in the Josephine ophiolite, Oregon. *UHP* Upper high-grade pods; *MUZ* Main upper zone; *MLZ* Main lower zone (After Kuhns and Baitis 1987)

Isotope studies of the sulfide ores have indicated an average $\delta^{34}S$ value of 4.7‰ for sulfide minerals, and from results of $\delta^{18}O$ measurements Zierenberg et al. (1988) conclude that the ore fluids were evolved seawater slightly enriched in $\delta^{18}O$. The interpretation of the $\delta^{18}O$ values of the fluids in this and many similar studies is dependent on values assigned for temperatures, which are not known, and it is possible that some of the fluids were more enriched in $\delta^{18}O$.

5.3.4 Massive Sulfide Deposits of the Norwegian Caledonides

A discontinuous belt of massive sulfide deposits extends for approximately 1500 km along the western edge of Scandinavia (Vokes 1976). They occur

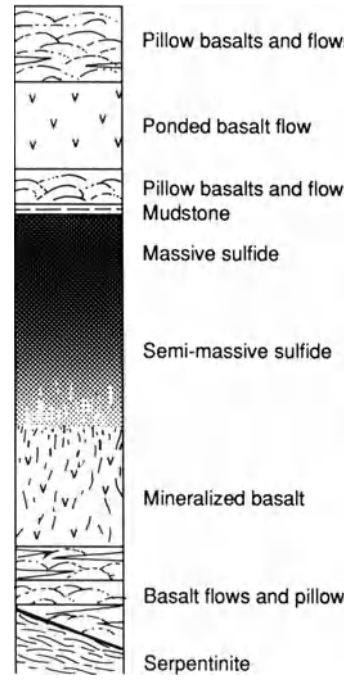

Fig. 5.14. Diagrammatic section illustrating the progressive change from massive to semimassive to stockwork mineralization downward through orebodies at the Turner Albright deposit (After Zierenberg et al. 1988)

within a series of strongly deformed allochthonous sheets composed primarily of Ordovician metavolcanics and metasediments. Major clusters of deposits occur in the Trondheim, Grong, and Sulitjelma areas, but a number of other districts can be delineated (Fig. 5.15). It is now recognized that many of the mafic volcanic and plutonic rocks in these thrust sheets are parts of dismembered and fragmented ophiolite complexes (Sturt et al. 1984). Furthermore, two periods of ophiolite generation have been recognized, one involving largely MORB-type chemistry that was generated in early Cambrian time, and one apparently representative of a restricted marginal basin setting generated in mid-Ordovician time (Gale and Roberts 1974; Furnes et al. 1980; Gale and Pearce 1982). A number of the massive sulfide deposits are associated with this latter group of ophiolitic rocks. Individual massive sulfide deposits vary in size from less than 1 million to 25 million tons, and virtually all fall along the Cu-Zn tie line on a Cu-Zn-Pb compositional plot.

The largest known massive sulfide deposit in the Scandinavian Caledonides is that at Lokken, southwest of Trondheim. Here, approximately 25 million tons of massive sulfide ore grading 2.1% Cu, 1.9% Zn, 19 g/ton Ag, and 0.29 g/ton Au occur within a sequence consisting primarily of little-metamorphosed basaltic pillow lavas. The deposit has a lensoid shape and is stratigraphically underlain by hydrothermally altered quartz-albite rock containing stringer sulfides. Above the massive sulfide lens (Fig. 5.16) is a layer of sulfidic black chert, and the overlying thin-bedded volcanics contain several horizons of quartz-magnetite-stilpnomelane rock interbedded with fine-

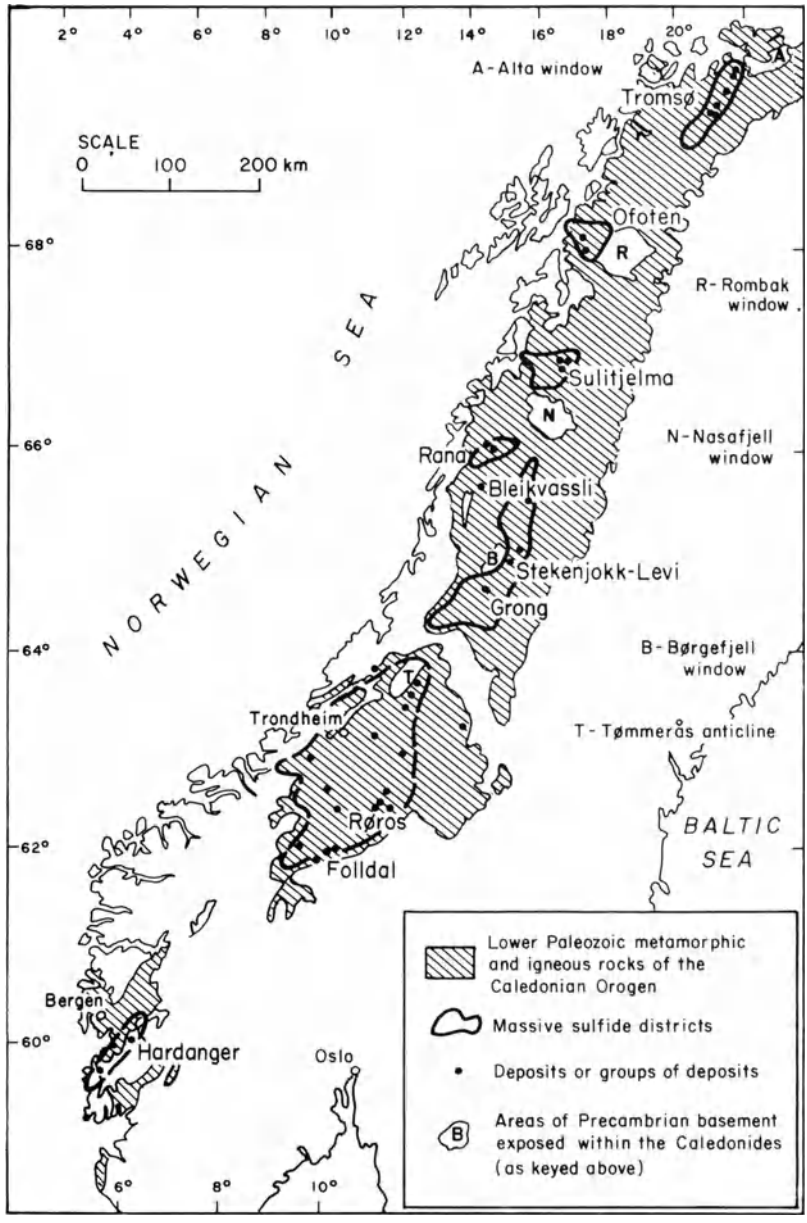

Fig. 5.15. Generalized map of Norwegian Caledonides showing location of major massive sulfide districts

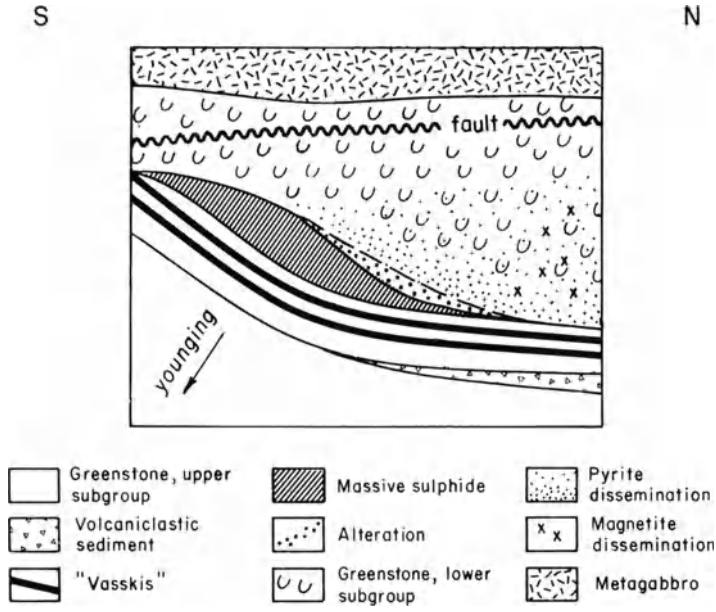

Fig. 5.16. Generalized cross-section of the Lokken orebody ("*Vasskis*" = pyritic chert). It is now believed by many that the basaltic rocks that host this deposit are part of a disrupted ophiolite complex. If this is correct then Lokken must be considered as a Cyprus-type deposit (After Franklin et al. 1981)

grained pyritic layers (Grammelvedt 1979). Apart from its size, the Lokken deposit is typical of many Caledonian massive sulfide deposits, although some have undergone considerably higher-rank metamorphism (Vokes 1968).

A few of the deposits (e.g., Stekenjokk orebody; Zachrisson 1982) are definitely associated with a localized felsic volcanics, but this situation is probably analogous to that in the Semail ophiolite discussed above. The two massive sulfide deposits in the Caledonian province that contain significant amounts of lead, Bleikvassli and Mofjell in the Rana district, are atypical. They occur within high-grade metagneisses and schists and have been reported to be of Proterozoic age (Frietsch et al. 1979, p. 995).

5.3.5 Additional Examples of Cyprus-Type Massive Sulfide Deposits

In many parts of the world where ophiolite complexes with their uppermost portions still intact are known, massive sulfide deposits similar to those of the Troodos massif have been discovered (Sillitoe 1972b; Franklin et al. 1981). This is the case particularly in the Ordovician ophiolite complexes of northeastern Newfoundland (e.g., Upadhyay and Strong 1973; Duke and Hutchinson 1974; Strong and Saunders 1988), where in the Betts Cove area, for example, massive sulfide deposits occur within the lowermost pillow lavas

overlying a sheeted dike complex. The largest deposit, Tilt Cove, contained 9 million tons grading 3% Cu and lesser Zn (Strong and Saunders 1988). Most of the deposits in Newfoundland ophiolites are spatially associated with chloritized fault zones and occur close to the bases of pillow lava sequences.

The group of massive sulfide deposits in the Rambler area, northeastern Newfoundland, consist of iron sulfide-rich lenses containing copper and zinc sulfides and, in the case of the Ming deposit, significant precious metal values (Tuach and Kennedy 1978). Although the tonnage of known massive sulfide ore in the area aggregates to less than 5 million tons, their lithologic setting is of some interest. The ore lenses exhibit a spatial relationship to a small center of felsic pyroclastic volcanism that overlies a pile of mafic and komatiitic pillow lavas, thought to be of early Ordovician age (Fig. 5.17). This lithologic setting appears similar to that described for the volcanic centers of the Semail ophiolite in Oman.

Additional examples of Cyprus-type deposits are known along much of the Tethyan suture zone, in particular in the Mesozoic ophiolites of Italy (Zuffardi 1977), the ophiolite zones of Turkey, the Sevano-Alceron zone of the USSR, and the Zagros Ranges of Iran (Jankovic 1980). A large number of massive sulfide deposits are known along the length of the Uralian suture in the USSR (W. Hamilton 1970). At least some of these appear to have typical ophiolitic associations, although others are associated with calc-alkaline volcanic sequences (Gealey 1980). The orebodies themselves are cupriferous

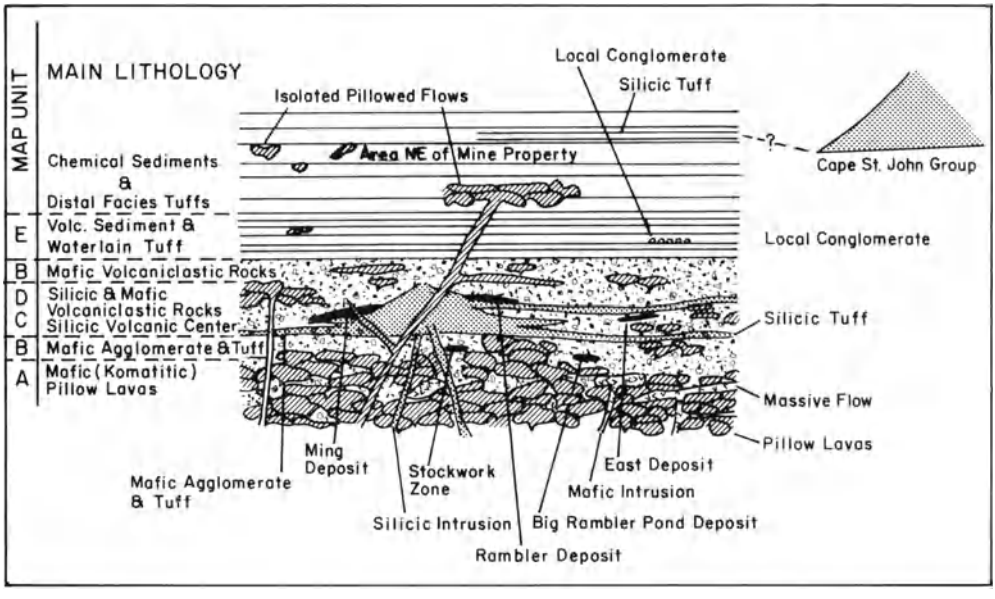

Fig. 5.17. Diagrammatic interpretation of the distribution of sulfide deposits in the Rambler area. All deposits are either associated with the silicic volcanic center or occur within mafic volcanics at the same stratigraphic level (After Tuach and Kennedy 1978)

pyrite lenses that commonly overlie sulfide disseminations in silicified altered footwall rocks (Smirnov 1970).

In the Philippines, especially on Balabac Island (John 1963) and in the Zambales Range of southwestern Luzon, a number of cupriferous massive sulfide deposits within mafic pillow lava sequences are known. The spatial association of these volcanics with ultramafic rocks, gabbros, and trondhjemite in many areas suggests that they constitute parts of ophiolite complexes, and thus the massive sulfides within them may be Cyprus-type deposits.

The recognition of Cyprus-type deposits, and for that matter ophiolite complexes themselves, in metamorphic terranes is not an easy matter. In such situations, recourse can and is generally made to patterns of immobile trace elements in the associated mafic rocks. It was on this basis that Grenne et al. (1980) originally suggested that the massive sulfide deposits of the Trondheim area (see earlier) were of Cyprus-type.

5.3.6 Discussion

The broad similarities between oceanic-type crust and ophiolite complexes, and between modern ocean ridge hydrothermal activity and Cyprus-type massive sulfide deposits, are without doubt impressive, but some intriguing problems remain. It is clear that the processes that create oceanic crust are fundamentally similar to those that created ophiolite complexes, but it is equally clear that most, perhaps all, ophiolites that contain economic massive sulfide deposits were formed in suprasubduction zone settings.

One significant difference between oceanic crust formed at oceanic (as opposed to backarc) spreading sites appears to be the thicknesses involved. Based on a great deal of seismic data, the crust below the present-day ocean basins is 8 km thick, whereas the thickness of the "crustal" portions of ophiolite complexes is typically significantly less. This may well relate to the particular tectonic conditions required to allow the incorporation of large allochthonous crustal segments into the fabric of the continental crust. Thus, backarc and suprasubduction zone, thin (? young) oceanic crust seems relatively prone to incorporation into the continental crust, whereas the type of crust being formed along most segments of the East Pacific Rise is slated for subduction only.

One key question that arises from the foregoing discussion is "Is the presence of an underlying subduction zone critical to the formation of large ($>$ 1 million ton) Cyprus-type deposits?" The geologic evidence would suggest that the answer must be yes, but many involved in marine geochemical research would take the opposite view, emphasizing that the generation of viable metal deposits can be viewed merely as a matter of adequate heat sources and plumbing systems. However, there are some real problems with the generation of larger massive sulfide deposits in tectonomagmatic environments represented by the East Pacific Rise. These problems center on the heat budgets and the enormous efficiency of axial convection systems in terms

of heat removal (Morton and Sleep 1985). Lister's (1972) analysis of this problem suggests that insufficient time would be available to produce a major deposit before the supply of magmatic heat was used up. To these problems must be added the observational evidence that the most vigorous seafloor exhalative systems disperse their metalliferous fluids over wide areas and thus the actual efficiency of metal sulfide fixation is low.

The evidence for the involvement of seawater-type fluids in modern axial sulfide exhalative systems is overwhelming, but the evidence that these are the *sole* fluids involved in the full scenario of ophiolite mineralization is markedly less robust (Stakes 1989), despite wide acceptance of this concept by the marine geochemical community. In fact, the geologic evidence seems to point to the conclusion that large (and therefore economic) massive sulfide deposits require tectonomagmatic settings involving subduction and felsic magmatism. If this indication is correct, then many of the caveats that must be applied to genetic models for Kuroko-type deposits (Chap. 3) may well also apply to Cyprus-type deposits. Furthermore, the compositional spectrum from Cyprus-type deposits, through Archean and Proterozoic volcanic-hosted massive sulfide deposits to Kuroko-type deposits (i.e., progressive increase in lead content), may mirror the increasing maturity of the arc systems to which they are related.

These considerations have their practical consequences in terms of exploration strategy. The geochemical fingerprinting of certain ophiolite complexes as arc-related or not, could be a critical first step in the assessment of the ore deposit potential of a particular ophiolitic suite. Based on the Semail ophiolite, central volcanic complexes containing felsic rocks would have greater potential than areas lacking these. Few other guides come readily to mind, especially in that massive sulfide deposits are known to occur at all levels within ophiolite pillow lava sequences.

In many Newfoundland ophiolites, the massive sulfides occur near the base of the pillow lavas, in Troodos most orebodies occur at the boundary between the lower and upper pillow lavas (Constantinou 1980), and in the Semail ophiolite the major ores are at the base of local volcanic centers superimposed on the pillow lava sequences. In Cyprus a variety of geophysical techniques, including IP and resistivity (Maliotis and Khan 1980), have been used to locate subsurface massive sulfide lenses, but with respect to interpretation of geophysical data in general, it is important to remember that most deposits are relatively small ($<$ 1 million tons; see Adamides 1980).

The spacing of deposits within ophiolite complexes is a possible aid to exploration, and Solomon (1976) has observed that they exhibit spacing-size relationships that are probably related to the size of the convective systems whose fossil discharge points they now mark. Modern subaerial hydrothermal convective systems, such as those in the Taupo Volcanic Zone, New Zealand tend to exhibit diameters of approximately 5 km, and this dimension is reflected in a crude manner in the spacing of Cyprus deposits and deposit clusters.

The alteration of oceanic crust by hydrothermal activity and the formation of metal deposits in layer-2 pillow lavas and of metalliferous sediments above

them do not represent any net increase in the metal budget of oceanic crust, merely a redistribution thereof. Nevertheless, this could be important in terms of arc metallogeny, given the recent evidence for the involvement of sediments and slab components in the genesis of arc magmas (see Chap. 4).

What is probably most important in terms of arc metallogeny is the extent to which water, and perhaps marine sulfur and chlorine, is fixed in oceanic crust during ridge-related hydrothermal processes. The subduction of relatively highly altered oceanic crust may thus be a more fundamental factor in generating arc systems that become well endowed with metal deposits.

5.4 Chromite Deposits in Ophiolite Complexes

World chromite consumption has doubled in each of the last two decades, and is now more than 12 million tons per annum. Although about 97% of world chromite reserves occur in large, nonophiolitic, layered mafic and ultramafic intrusions (see Chap. 6), over half of current world production comes from chromite deposits hosted by ophiolite complexes. Due to their tendency to form lensoid bodies, such deposits have been termed podiform chromite ores (Thayer 1964).

Although podiform deposits are restricted in their occurrence to ophiolite complexes (Fig. 5.18), only some contain podiform chromite ores, and the chromite grains are typically of different composition to the ubiquitous host rock spinels (Dupuy et al. 1981). Podiform chromite deposits occur as tabular, elongate, or irregular masses that invariably exhibit evidence of some degree of metamorphic deformation (Thayer 1969; Christiansen 1986). Important examples of these deposits are known from Yugoslavia, Greece, Turkey, Iran, and Pakistan along the Alpine-Himalayan collision belt, and from the Philippines, and New Caledonia in the western Pacific (Coleman 1977; Stowe 1987a and references therein). The ophiolite belts in Cuba also contain important deposits (Thayer 1942), as do those of the Urals (Smirnov 1977; Kravchenko 1986).

The late Precambrian ophiolites in the Arabian-Nubian Shield contain only minor examples of podiform chromites, but the early Proterozoic ophiolite belts of Brazil are now significant producers (Stowe 1987a).

Ultramafic rocks are typically of either lherzolitic or harzburgitic type (Stowe 1987a), but it is the latter that are the predominant type of subMoho material in ophiolite complexes, and it is only in harzburgite lithologies that podiform chromite deposits are found. These rocks invariably exhibit tectonite fabrics, in some instances of considerable complexity (Coleman 1977; Stowe 1987b), but despite this, evidence for gravitational accumulation of chromite grains within local Mg-rich (dunitic) melts is indicated in some deposits (Burgath and Weiser 1980; A.C. Brown 1980). Chromite concentrations in the large Orhaneli ophiolite massif, Turkey, for example, exhibit well-defined layering (Tankut 1980).

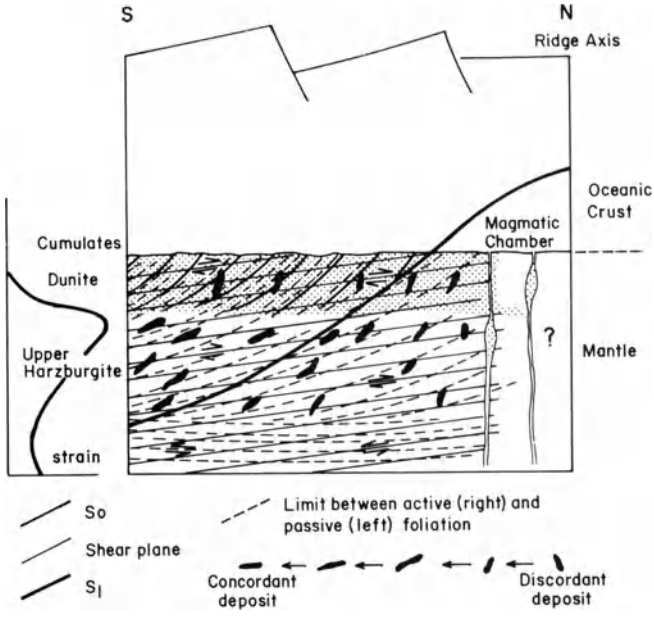

Fig. 5.18. Sketch illustrating one concept of the genesis and evolution of podiform chromite ores in the uppermost oceanic mantle beneath an active spreading ridge (After Lago et al. 1982)

5.4.1 Chromite Deposits of the Zhob Valley Ophiolite Complex, Pakistan

The Zhob Valley ultramafic suite occurs as part of a larger multiple series of tectonic klippe separated from underlying Cretaceous and Jurassic sediments by melange units (Ahmad and Bilgrami 1987). The rocks that host the podiform chromite orebodies are ultramafic tectonites that consist of harzburgite (70%) and dunite, or their serpentinized equivalents. On the basis of stratigraphic control from under- and overlying sedimentary units, the age of the Zhob Valley ophiolite is Paleocene to early Eocene (Ahmad and Bilgrami 1987).

The Zhob Valley, which is the principal chromite producing area of Pakistan, contains podiform chromite deposits of extremely varied shape and form. Most orebodies are relatively small and average about 5000 tons, whereas the largest known orebody attains a size os about 100 000 tons. Ahmad and Bilgrami (1987) make the following generalizations regarding the deposits.

1. The chromite deposits occur within a transgressive dunite unit that cuts obliquely across the layering of the host rocks. They consist of banded material that may be massive or disseminated, and in cases where tectonism is not too intense, the orebodies can be observed to grade outward from massive to banded ore to dunite. Massive orebodies tend to be highly deformed and have faulted contacts.

2. Cigar-shaped orebodies occur locally in intensely serpentized dunite. These have sheared contacts and are of larger average size.
3. Dike-like orebodies are confined mainly to the upper portion of the transgressive dunite, and lie a few 100 m below the gabbro portion of the ophiolite.

Approximately 1.5 million tons of chromite have been produced in this area and an equivalent amount is estimated to be available for future production.

5.4.2 The Chromite Deposits of the Vourinos Complex, Greece

The Vourinos Complex forms part of a broad band of Tethyan ophiolites that runs from the Alps through the Balkan Peninsula to Turkey and beyond. It is emplaced in crystalline Jurassic limestones and exhibits a full suite of ophiolitic rock types from pelagic sediments down through pillow lavas, dikes, gabbros, and ultramafics (Moores 1969).

In the northern part of the complex a cluster of podiform chromite deposits occur at Voidolakkos, within a dunitic host rock that crosscuts the ambient harzburgites (Zachos 1969). The orebodies are present as steeply dipping pipes of massive chromite that appear to have segregated from a mushroom-shaped intrusion of chromite-bearing dunite. Lineation and foliation within the ores and surrounding dunite are also steep and differ from that of the harzburgites. Individual orebodies tend to be small ($< 10\,000$ tons), but the chromite contains 40–50% Cr_2O_3 and is low in alumina and iron. As such it represents good metallurgical grade ore.

Distinct from this mineralization are the schleiren-type podiform ores of the Xerolivado area in the southern part of the complex (Zachos 1969). Here again dunite and serpentinized dunite form the immediate host rocks, and orebodies are mainly steeply dipping and in some cases attain vertical extents of 100–150 m and range up to 15 m in thickness. Strike lengths of the orebodies are difficult to determine due to faulting. As at Voidolakkos, geologic relationships indicate a late intrusion of chromite-rich dunite from which the deposits formed. These chromite ores of the Vourinos complex are typical of podiform deposits and, given the effects of later deformation, would seem to support the genetic model of Lago et al. (1982) (see later).

5.4.3 The Chromite Deposits of Selukwe, Zimbabwe

The chromite deposits of Selukwe (now Shurugwi), Zimbabwe have produced $>$ 12 million tons of high-grade ore. The chromite orebodies occur within a serpentinized ultramafic complex that was emplaced into magnesium-rich greenstones and subsequently involved in major recumbent fold and thrust structures (Stowe 1987c). A minimum age of 3.4 Ga is indicated for the sequence because granites intrusive into it have given radiometric ages in this range (Stagman 1978).

The Selukwe ultramafic complex, which attains thicknesses of up to 1 km, is everywhere in fault contact with the surrounding early Archean greenstones, and the actual thrust zones are marked by silicified serpentinite, quartz breccia, or chlorite-carbonate and fuchsite-carbonate phyllonites (Cotterill 1969; Stowe 1984, 1987c). The chromite orebodies occur in the form of elongated lenses or pods, and are typically surrounded by highly altered material consisting of serpentinite or talc-carbonate rock. This appears to have been dunitic in composition prior to alteration. The largest ore lenses attain dimensions of 25 × 12 × 1000 m, but most average about half this size. The massive ores consist of densely packed aggregates of chromite crystals, and the chromitite bodies they form tend to concentrate along certain specific levels within the ultramafic sheets. The banded ores, which are subeconomic, consist of finer-grained chromite in centimeter-scale cumulate layers, some of which have been traced for distances of tens of meters (Stowe 1987c). Chemically the chromites are characterized by their high chromium contents, and they exhibit a range of Mg/Fe ratios representative of both podiform and stratiform (see Chap. 6) chromites. However, the Selukwe chromites are most similar in their chemistry to chromites from the podiform deposits of the large Orhaneli ophiolite massif in Turkey which also exhibit well-defined layering (Tankut 1980).

The Selukwe chromite ores are of particular interest for they are hosted by a layered, ultramafic complex that was most probably formed within early Archean oceanic crust. Not only are the rocks ophiolitic in composition, they contain podiform chromite deposits that elsewhere are only known to exist in ophiolite complexes. The cumulate features seem to suggest formation in large magmatic systems within a thicker Archean ocean crust (see Sleep and Windley 1982). The deposits thus provide an example of ores providing clues to their tectonic setting (Guilbert 1981).

5.4.4 Discussion

Genetic models for the formation of podiform chromite deposits must provide explanations for their geometry, association with envelopes of dunite, and the tectonized nature of the ambient harzburgite in which they occur. The deformation of the orebodies (see Fig. 5.18) and the harzburgites is explicable in terms of the subcrustal environments below spreading ridge systems where solid state ductile movement predominates. However, the gravitational accumulation of chromite grains within local dunitic melts indicated for a great many of these deposits is less easy to explain.

Lago et al. (1982) have suggested that podiform chromite concentrations form within convecting dike-like bodies of basalt magma that crosscut harzburgite within peridotite diapirs (Fig. 5.19). Collapse of the accumulated chromite grains and nodules formed along one side of the magma chamber would produce brecciated, massive, or irregularly layered ore. Subsequent deformation during shearing of the enclosing dunite and more pervasive

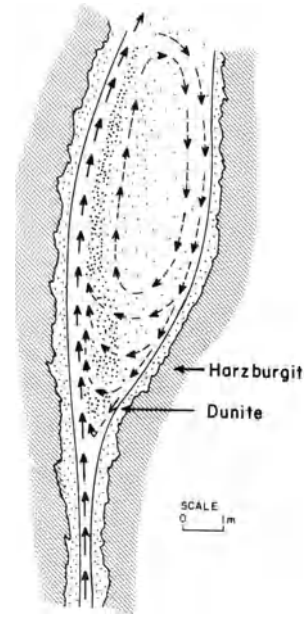

Fig. 5.19. Schematic model of podiform chromite development in a cavity along magma dikes in a tectonic harzburgite (Lago et al. 1982)

harzburgite would produce the wide variety of stretched and deformed shapes that podiform chromite bodies tend to exhibit. Whether the above scenario is adequate to explain all features of podiform chromite bodies, including observed variations in Cr and Al contents of the chromite grains (A.C. Brown 1980), remains to be seen. Dickey (1975) envisages the formation of podiform chromite bodies in the lowermost layer of cumulate activity during the formation of new oceanic lithosphere and the subsequent gravitational settling of these dense chromite-dunite autoliths into underlying harzburgite, itself a crystal mush (Fig. 5.20). This would explain the tendency of podiform chromite ores to occur within the uppermost portions of the harzburgite domains in ophiolite complexes (Cassard et al. 1981). Recently, Nicolas and Violette (1982) have suggested that spreading at ocean ridge systems may be of either horizontal or diapiric type. The former (Table Mountain type) is less favorable to generation of economic chromite deposits than the latter (Acoje type), which is characterized by inhomogeneous plastic flow patterns, deformed paleoMoho, and large-scale folds (Fig. 5.21).

5.5 Additional Minor Mineralization in Ophiolite Complexes

Cyprus-type massive sulfide deposits and podiform chromite deposits are the only hypogene metal concentrations of any significant economic consequence in ophiolite complexes, but important concentrations of nickel in the form of garnierite, a hydrated magnesium nickel silicate, tend to form in the lower soil

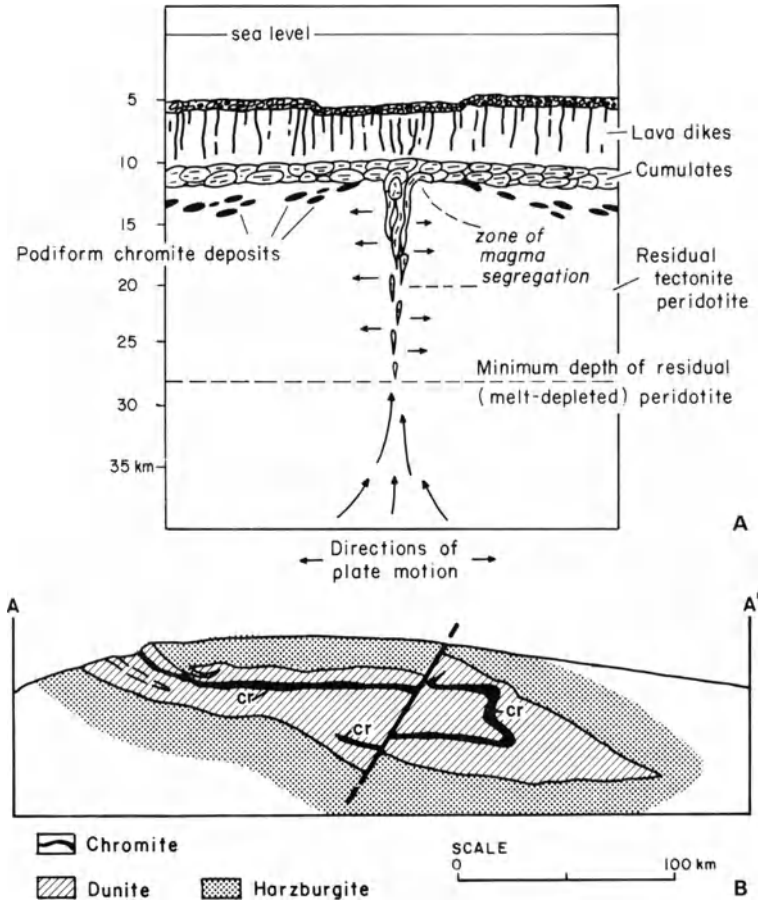

Fig. 5.20A. Dickey's model for the origin of podiform chromite ores. The ores and their associated dunite envelopes are seen as cumulates formed at the base of layer 3 of the oceanic crust, which subsequently sink into the underlying harzburgite of the uppermost mantle (After Dickey 1975). **B** Geologic cross-section of a chromite ore lens in the Vourinos Complex, Greece. Note isoclinal folding and thickening of chromitite and dunite along axis of fold (After Moores 1969)

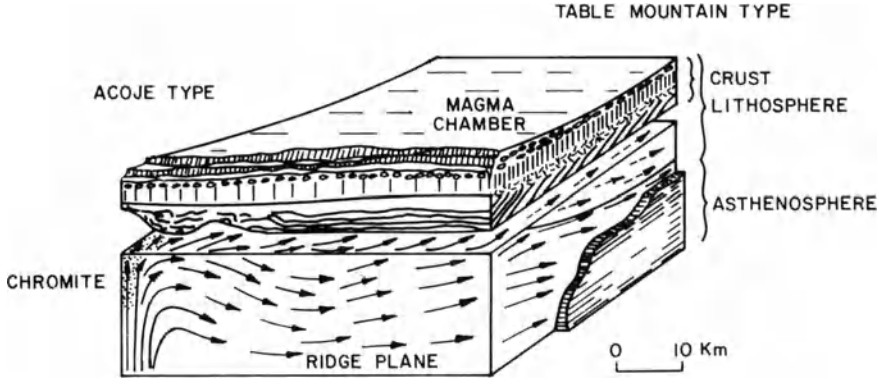

horizons above ophiolitic ultramafic masses subjected to tropical weathering. Such lateritic nickel deposits have been extensively mined in New Caledonia and the Dominican Republic, and similar deposits are known in Cuba, Colombia, and Brazil.

Minor hypogene mineralization containing mainly copper and nickel sulfides has been described from ultramafic rocks at Acoje in the Zambales ophiolite complex, in southwestern Luzon, Philippines (Bryner 1969), in gabbroic rocks of the Semail ophiolite, Oman (Hassan and Al-Sulaimi 1979), and in the Limmasol Forest area of the Troodos ophiolite (Panayiolou 1980). In this latter case, veins, massive pods, and disseminations of Cu, Ni, Co, and Fe sulfides and arsenides occur within serpentinized harzburgite along fault zones. Although these deposits were probably worked on a small scale by the ancients, recent investigations have failed to establish their economic viability.

Gold occurs in economic concentrations in some ophiolites, but is typically associated with highly altered, silicified, and carbonatized serpentinites. These are commonly found at the edges of fault-bounded blocks of ultramafic ophiolite and have been termed listwaenites by Russian geologists (Buisson and Leblanc 1986, and references therein). Typically these green-gray rocks consist of Mg-Fe-Ca carbonates and quartz, with lesser serpentine, talc, Mg-chlorite, fuchsite, and iron oxide and Fe-Cu-Ni sulfide minerals. The listwaenite lenses occur at tectonic contacts and grade laterally into serpentinized ultramafic rocks through a talc-carbonate zone (Fig. 5.22). The actual gold mineralization, which exhibits notable similarities to that found in Archean carbonatized ultramafic rocks and in parts of the Mother Lode (Pearton 1982; Pearton and Viljoen 1986), tends to be rather erratically distributed, but is most closely associated with pyrite and arsenide-rich zones, especially those with elevated cobalt contents. Gold is also found in late quartz veins.

Gold deposits of this type have been described from the northern Caucasus, USSR (Ploshko 1963), the Voltri ophiolite, Liguria, Italy (Zuffardi 1977; Pipino 1980), the ophiolites of the Arabian Shield (Pallister et al. 1987), and the Bou Azzer ophiolite, Morocco (Leblanc and Billaud 1982). In all these cases it appears that the alteration of the ultramafic rocks and the concentration of the gold was related to the time of tectonic emplacement of the ophiolite or to later events and not its initial formation (Gresens et al. 1982). In this sense these gold deposits more properly belong in Chapter 9 which deals with metal deposits related to collision environments.

Fig. 5.21. Model for accumulation of chromite ores based on relationships observed mainly in the Zambales Ophiolite, Philippines. *Full arrows*, flow lines in asthenosphere; *dashed arrows*, fossil flow lines in lithosphere; *thick lines*, chromitite layers in cumulate gabbros (Nicolas and Violette 1982). See text for further details

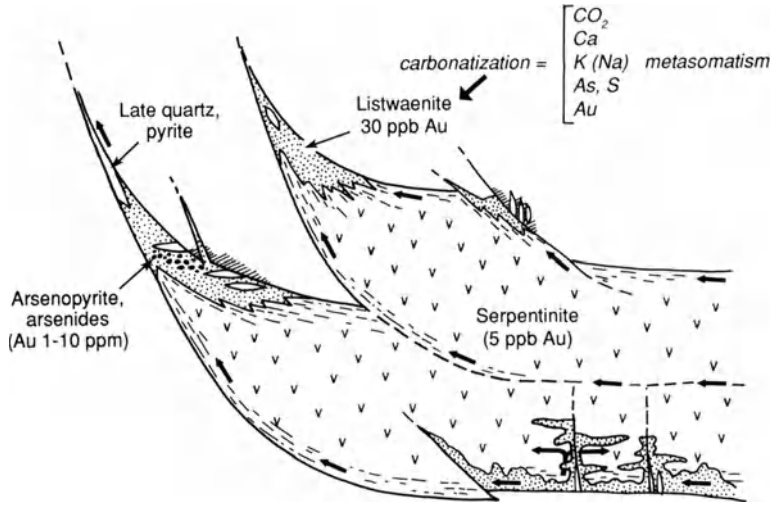

Fig. 5.22. The progressive enrichment of gold as a function of alteration of serpentinite bodies (After Buisson and Leblanc 1986)

Although beyond the province of this volume, mention can be made of the important nonmetallic mineral resources present in some ophiolite complexes. These include major deposits of magnesite, talc, and chrysotile asbestos. Economic concentrations of these minerals tend to develop within the highly serpentinized portions of ultramafic ophiolite complexes, and deposits of this type have been worked in the Mediterranean area and elsewhere. Two particularly important asbestos deposits of ophiolitic affinity in North America are those at Thetford, Quebec (Laurent 1980) and Coalinga, California (Mumpton and Thompson 1975).

Chapter 6 Intracontinental Hotspots, Anorogenic Magmatism, and Associated Metal Deposits

It is probably safe to say that the tectonics of plate interiors (see Geodynamics Series vol. 1, 1980, Am. Geophys. Un.) are less well understood than those of plate margins. In particular, there is much to learn about the forces responsible for the creation of broad intracontinental basins and plateau uplifts (Crough 1979, 1983). The latter are of interest at this juncture because they are connected with thermal perturbations of the underlying mantle (McGetchin et al. 1980). In fact, it has been argued by Thiessen et al. (1979) that the pronounced basin and swell nature of the African continent is related to down- and upwelling mantle currents, the latter marked in many instances by surface manifestations of igneous activity.

More recently, explanations for certain manifestations of intracontinental tectonic activity are being sought in tectonic interactions at, in some cases distant, plate boundaries. Thus, for example, the concept of impact-related rifting has been expanded, and some workers would even claim that the large majority of continental rift events are initiated in this way (Tapponier et al. 1982). In addition, it has been noted that the sites of many anorogenic igneous complexes can be related to major lines of weakness that later control the geometry of oceanic transform faults (Sykes 1978; Black et al. 1985).

Even before the formulation of an integrated theory of plate tectonics, J.T. Wilson (1963, 1965) had suggested that linear volcanic chains in the oceans were related to movement of oceanic lithosphere over mantle hotspots. Almost a decade later, Morgan (1972) proposed that hotspots were the crustal manifestations of rising mantle plumes. Despite their conjectural aspect, it is becoming increasingly clear that mantle plumes, or at least areas of anomalously hot mantle, are a fundamental aspect of the lithosphere-asthenosphere interactions that in a broad sense comprise plate tectonics. In continental settings, the manifestations of an underlying hotspots on the upper crust depend critically on the rates of relative motion between the asthenospheric source of the hotspot and the overlying continental lithosphere (Burke 1977). Where continental lithosphere drifts across a potent hotspot, lines of basaltic volcanoes will be formed that mark its passage. Such appears to be the case with respect to the basaltic lavas of Cenozoic age in eastern Australia (Wellman and McDougall 1974). A similar explanation has been proposed by R.B. Smith and Christiansen (1980) to explain the basaltic and rhyolitic magmatism of the Snake River Plain and Yellowstone areas.

Where the relative motions of hotspots and overlying continental crust are negligible or very small, mantle hotspots impinge more substantially on

overlying continental areas and appear capable in specific instances of generating an array of igneous rocks. These can include basalts, peralkaline mafic rocks, and carbonatites, and peralkaline and peraluminous felsic suites. Studies of the initial $^{87}Sr/^{86}Sr$ ratios of these igneous rocks indicate that some are of direct mantle derivation, whereas others are of largely crustal anatectic origin. Caution is required in the interpretation of the initial strontinum data, however, because at least some hotspots appear to be related to patches of mantle with an enhanced budget of heat-producing elements such as rubidium and uranium (D.L. Anderson 1975). In addition, the strontium isotope systems of hotspot magmas can be disturbed by interaction with meteoric waters (Bonin et al. 1979).

Mohr (1982) has questioned the widely accepted notion that broad domal uplifts are the precursors to rifting events (Burke and Whiteman 1973), and demonstrated that the major updoming in the East African rift system occurred only subsequent to the initiation of rifting. As is so commonly the case, modern studies of rifting environments and their relationship to hotspot activity, both past and present, are revealing far more variability and intricacy than envisaged originally. Despite these complexities, there are certain types of metal deposits that exhibit a clear relationship to hotspot activity and others for which such an association can be reasonably suggested.

6.1 Tin Deposits Associated with Anorogenic Granites

A clear association of certain tin districts, especially in Africa, and granitic rocks emplaced in stable, intracratonic environments is evident (Sillitoe 1974b; Bowden 1985). Burke and Dewey (1973) explain the generation of such granites in terms of underlying mantle plume activity. In Nigeria and Niger in West Africa several groups of granitic ring complexes in a crude north-south array are known (Turner and Webb 1974; Imeokparia 1985; Olade 1985; Fig. 6.1), although it needs to be emphasized that those at the northern extremity of the belt in Niger are considerably older (mid-Paleozoic) than the Jurassic complexes of the Jos Plateau at its southern extremity. Although many of the intrusions in this diachronous belt of granites exhibit some evidence of tin mineralization, the major tin deposits occur within the Jos Plateau.

In the Jos Plateau region over 40 granitic ring complexes intrude the surrounding Precambrian igneous and metamorphic country rocks, and in some cases cut local felsic volcanics and minor basalts (McLeod et al. 1971; Bowden and Kinnaird 1978; Bowden 1985). Peralkaline albite-riebeckite granites are a major rock type in these complexes, but the tin mineralization is associated with some of the less alkaline biotite granites (Bowden 1982; Olade 1985). Within these latter intrusions, cassiterite and tantalite occur both as disseminated grains, and within greisen zones and quartz veins containing pyrite and base metal sulfides. Mineralization occurs most commonly along horizontal roof sections of biotite granites, which were probably emplaced at depths of less than 1 km below the original surface.

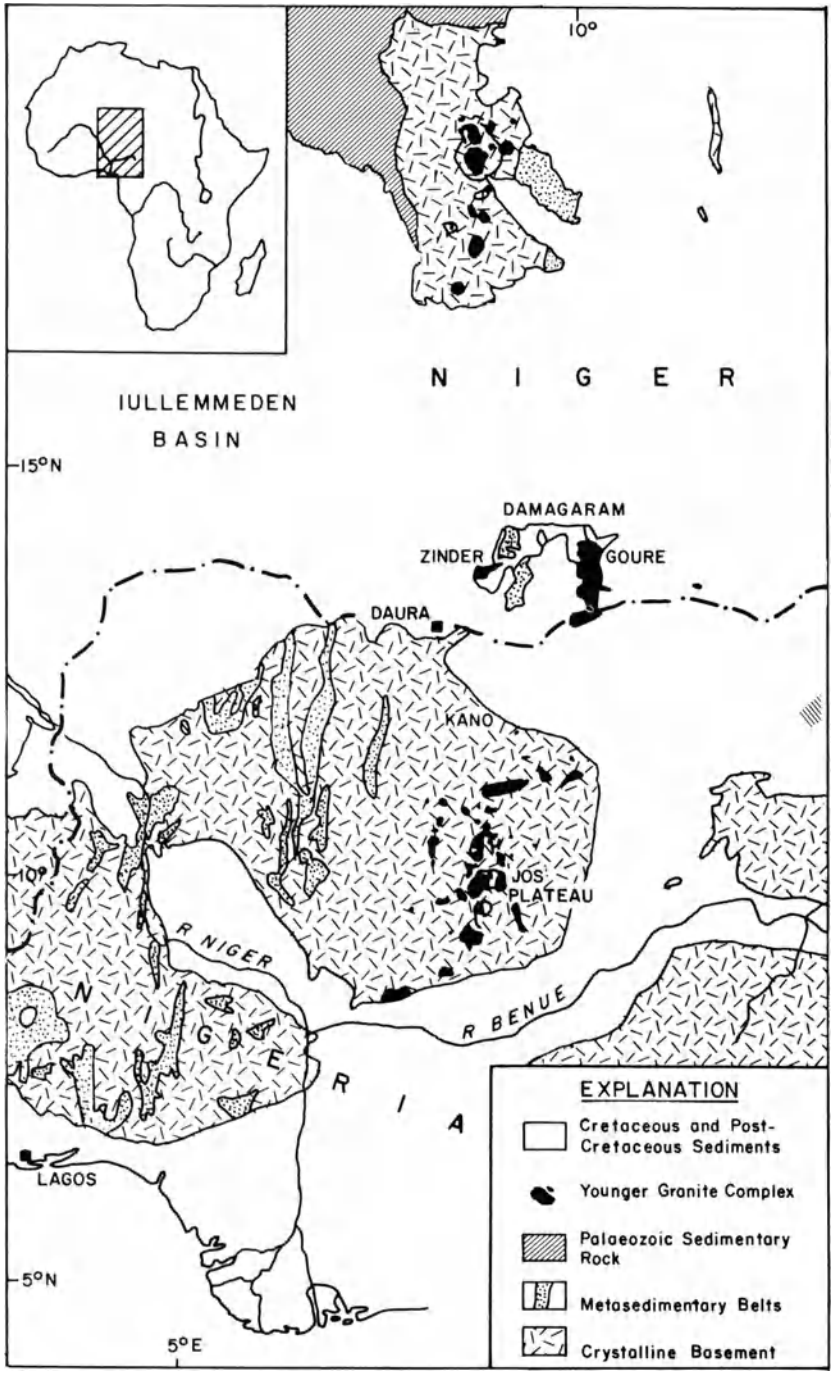

Fig. 6.1. Map of Nigerian anorogenic granites. Note north-south array of alkaline granitic complexes (After Turner and Webb 1974)

Olade (1985) notes that the disseminated cassiterite in the roof portions of certain biotite granites can represent an important tin resource. For example, the Odegi Granite, which is decomposed to depths of 50 m, contains 0.06% Sn over an area of 1 km^2, equivalent to 600 tons of tin per vertical meter. In some areas greisen and quartz veins are the main sites of tin mineralization. Kinnaird (1985) has summarized much of the information available for the various styles of mineralization associated with the Nigerian tin granites (Fig. 6.2). An initial Na metasomatism, locally associated with niobium introduction (as pyrochlore or columbite), is followed by potassium metasomatism, and some cassiterite introduction in the biotite granites. Subsequent H^+ metasomatism results in greisenization with introduction of monazite, zircon, and ilmenite followed by cassiterite and lesser wolframite, rutile, and other phases. This stage is followed in turn by large-scale introduction of quartz, accompanied by more cassiterite, major amounts of sphalerite, and subordinate chalcopyrite and galena. Wall-rock alteration at this stage involved development of chlorite and clay minerals adjacent to vein structures.

Fluid inclusion studies (Kinnaird 1985) have demonstrated that the initial fluids were highly saline, and high in temperature (380–550°C). Later vein mineralization occurred at temperatures of 300–380°C from fluids with salinities ranging up to 15 equiv. wt% NaCl, and during the final stages of hydrothermal activity temperatures fell below 300°C, and salinities were < 10 equiv. wt% NaCl. Evidence for CO_2 loss and boiling is also present in the fluid inclusion assemblages.

The cassiterite deposits of Rondonia, western Brazil, exhibit very strong similarities to those of the Jos Plateau, as noted by Kloosterman (1969). This important tin province is associated with a broad, approximately northeast-southwest trending, 250-km-long zone that contains 18 single or multiple alkali granite complexes that cut sharply across older basement complex rocks (Fig. 6.3). The largest individual ring complexes attain diameters of > 20 km. Priem et al. (1971) have reported a rubidium-strontium isotope age of close to 1000 Ma for these intrusives and, based on high initial strontium isotope ratios ($>$ 0.720), concluded that they were of crustal anatectic origin. It was also noted by Sawkins (1976b) that the Rondonia granites coincide with a major and widespread episode of hotspot activity that affected many continental areas about 1 billion years ago.

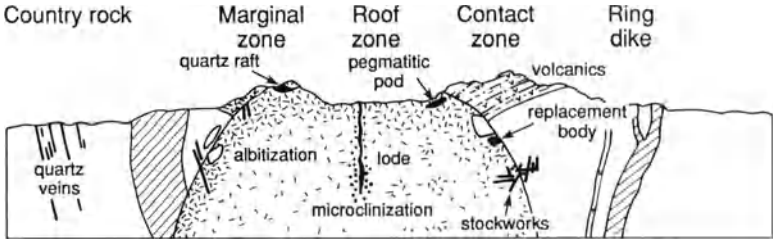

Fig. 6.2. Diagrammatic section illustrating the main type of bed-rock tin deposits associated with the Jos Plateau granites (After Kinnaird 1985)

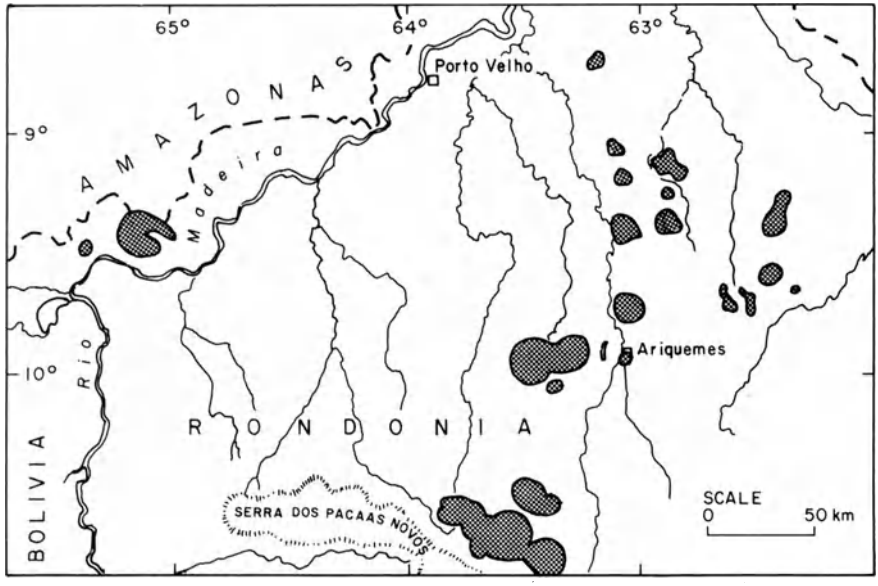

Fig. 6.3. The late Proterozoic anorogenic granites of the Rondonia Province, western Brazil. Note circular shape and considerable dimensions of many of these tin-bearing intrusive complexes (After Kloosterman 1969)

Detailed descriptions of the Rondonia mineralization are not available to the author, but according to Kloosterman (1969), both quartz-cassiterite and quartz-cassiterite-wolframite veins, and greisen bodies cut by quartz veinlets are present in many of the mineralized areas. The most common type of greisen contains quartz and green mica, with or without topaz. In both the Jos Plateau and Rondonia districts the predominant method of cassiterite recovery consists of removal and washing of cassiterite concentrated in saprolite or within gravels overlying decomposed bed rock. These gravels exhibit little evidence of having been transported more than a few tens of meters. Clearly, in both the Jos Plateau and Rondonia, concentration of cassiterite by tropical weathering processes is an important factor in the economics of tin recovery, but unfortunately, under such circumstances, the details of hypogene mineralization tend to be sketchy. Additional examples of tin mineralization associated with Phanerozoic anorogenic granites of postulated hotspot origin include a number of minor occurrences scattered across northern Africa and in Transbaikala-Mongolia (Sillitoe 1974b).

Anorogenic hotspot-related magmatism in the form of Rapakivi granites of Proterozoic age (1400–1750 Ma) is extensively developed across much of the North Atlantic Shield that stretches from western North America to the Black Sea (Bridgewater and Windley 1973). In southern Finland, where these unusual granitic rocks are present as four large batholiths, a number of tin-polymetallic veins and greisens are known (Haapala 1985). Fluid inclusion

studies of the greisen veins associated with the Eurajoki stock (Fig. 6.4) indicate deposition of cassiterite from fluids of 260–390°C, and 3.17 wt% alkali chlorides, whereas beryl deposition occurred from fluids of 360–410°C, and 11–17 wt% alkali chloride compositions.

A series of tin deposits are also associated with the Proterozoic Bushveld granites in South Africa (Hunter 1973; Fig. 6.5). These granites are considered to have resulted from crustal melting triggered by the emplacement of the huge Bushveld Igneous Complex. Whether the emplacement of this suite of igneous rocks was related to a meteorite impact event, as suggested by Rhodes (1975), or is a manifestation of a mantle hotspot, large-scale melting of the subjacent mantle is indicated by its mere size. The Bushveld tin deposits had yielded almost 70 000 tons of tin metal by 1971 (Lenthall 1974). The tin ores occur either as pipes or sheet-like disseminations in coarse-grained porphyritic

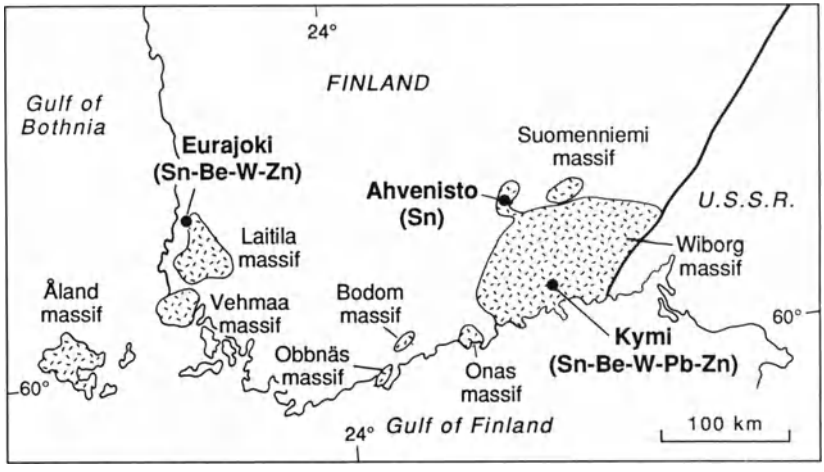

Fig. 6.4. Map showing distribution of the Rapakivi granites and associated ore deposits in Finland (After Imeokparia 1985)

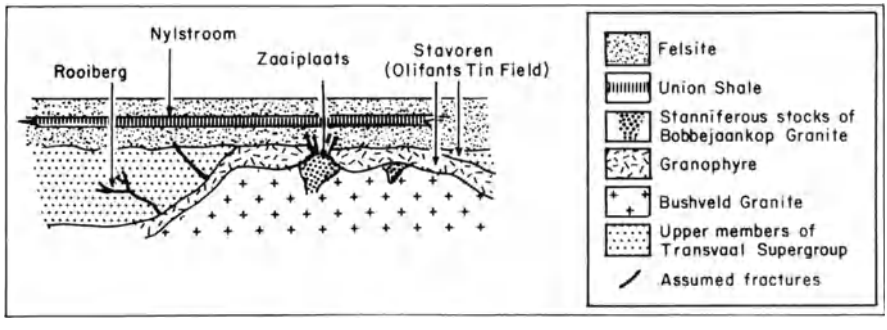

Fig. 6.5. Schematic cross-section showing relationships of certain tin deposits to the Bushveld Granite and associated intrusive units (After Hunter 1974)

granites, or as fissure veins, breccia zones, or replacements in the granites or their volcanic and sedimentary roof rocks (see Fig. 6.5; Hunter 1973; Crocker 1986; Rozendaal et al. 1986). Associated minerals include sericite, quartz, fluorite, chlorite, and tourmaline.

It is probable that certain tin deposits of the USSR may be of hotspot-related type, but the available descriptions (see Smirnov 1977) do not provide adequate details on which to base any meaningful speculations. One possible exception is the Kitelya deposit (Materikov 1977) which is confined to the contact zone of the Salma massif consisting of late Proterozoic rapakivi granites.

Finally, tin mineralization, albeit minor, is associated with a group of Proterozoic granite complexes in the St. Francois terrane, Missouri, that have been ascribed to mantle hotspot activity (G.R. Lowell 1976). Kisvarsanyi (1980) has accumulated the available surface and subsurface data and demonstrated that granitic magmatism and coeval felsic volcanism occurred in relation to ring fracturing and cauldron subsidence approximately 1.5 Ga ago. The last phase of magmatic activity involved emplacement of two-mica microcline granites and albite granites as central plutons in resurgent cauldrons. Many of these exhibit strong enrichment in Sn, W, Nb, U, and rare earth elements.

Virtually all of the intrusive bodies described in the preceding sections are A-type granitic rocks that are considered to be key indicators of anorogenic magmatism (Collins et al. 1982). A general consensus is emerging that they are, at least in part, the products of partial melting of felsic granulites in the lower mantle (J.L. Anderson 1983). This conclusion has come from consideration of isotope data (Sr/Sr and Nd/Sm) obtained from various complexes (see Bowden 1985). These data indicate both mantle and crustal signatures in the granitic rocks, but it is clear that the initial magmatism required for lower crustal melting must be transferred from the upper mantle by melts of mafic composition (Whalen et al. 1987). It is this very magmatism, which develops with no apparent relationship to orogenesis, that provides support for the concept of sublithospheric hotspots. Most workers have assumed a crustal origin for the tin, but Sillitoe (1974b) suggested that the tin may be, at least in part, of mantle origin. He also noted the linear arrays exhibited by the host granites, and suggested that this could have implications in terms of exploration strategy.

6.2 Iron-Titanium Deposits Associated with Anorthosites

The origin of anorthosite bodies of massif type has long represented an intriguing problem to petrologists (Wiebe 1980). Not only are these igneous rocks highly distinctive in terms of their composition, but they exhibit a relatively limited time control (1600–1000 Ma), and most occur within two linear belts on pre-Permian drift reconstructions: one in the southern

hemisphere and one extending across North America through Scandinavia to the USSR (Herz 1969). The major concentration of massif-type anorthosites in North America is within the Grenville province (J.M. Moore et al. 1986), a belt of locally intense metamorphism and tectonothermal reactivation (Fig. 6.6), that has been compared to the collision belt of the western Himalayas (Burke and Dewey 1973; Windley 1983). Many of the anorthosite massifs have been involved in the high-grade metamorphic events, but those of the Nain Province, Labrador (see Fig. 6.6) are virtually unaffected by postemplacement metamorphism and deformation (Emslie, 1978a,b). Dating studies (Easton 1986) demonstrate that most of the anorthosite massifs were emplaced between 1.4 and 1.5 Ga, well prior to the period of peak metamorphism in the Grenville belt, which occurred between 1.0 and 1.1 Ga. Thus, the continental collision model, although applicable to Grenville orogenesis, cannot also explain anorthosite formation, as suggested originally by Dewey and Burke (1973).

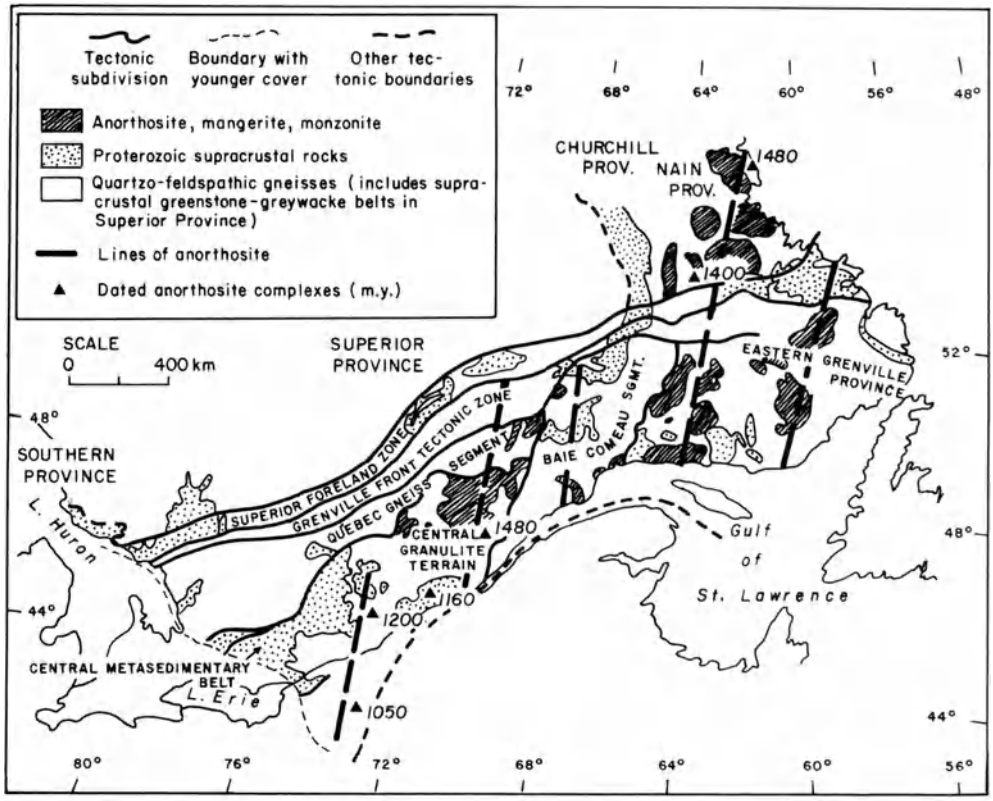

Fig. 6.6. Map of the Grenville province and adjacent areas showing anorthosites and related rocks. Note that anorthosite complexes are not restricted to the Grenville orogen, but also occur in anorogenic settings in the Nain province to the northeast (After Wynne-Edwards 1976)

Some of the anorthosite massifs in the southern portions of the Grenville Belt appear to have younger emplacement ages of close to 1.3 Ga (McLelland and Isachsen 1986), but still prior to deposition of the Grenville Supergroup (Roy et al. 1986). The central point is that massif anorthosites appear to have been emplaced primarily in an anorogenic setting (Bridgewater et al. 1974; McLelland 1986), and may have been precursors to crustal attenuation and rifting. Paleomagnetic reconstructions indicate the presence of a Proterozoic supercontinent at that time (e.g., Piper 1982), and thus the broad development of hotspot activity during this period, and the widespread tensional and rifting events that followed (Sawkins 1976a) may represent a prolonged series of attempts by the subcontinental mantle to rid itself of excess heat.

Certain anorthosite bodies of the Grenville Province and others in southern Norway have important iron-titanium ores associated with them (Gross 1967; Bugge 1978; Korneliussen and Robins 1985). Disseminated iron and iron-titanium oxides are a common feature of anorthosite bodies, but in some instances lenses or irregular bodies of massive ilmenite are present. Those at Allard Lake, Quebec (Hammond 1952), and in the Egersund anorthosite complex in southern Norway are the largest known. The Tellness deposit in the Egersund district, for example, contains over 300 million tons of ore grading 18% TiO_2 and production of ilmenite concentrate amounts to $>$ 800 000 tons per year (Bugge 1978). Lesser amounts of magnetite concentrate containing 0.6% V_2O_5 are also produced, as well as relatively minor amounts of nickel, copper, and cobalt sulfides. The Lac Tio deposit, Quebec contains in excess of 125 million tons averaging 32% TiO_2 and 36% Fe.

Within the Grenville Province, the iron-titanium deposits vary according to specific rock-type association and regional distribution (Fig. 6.7). Thus, ilmenite deposits, essentially devoid of magnetite, are associated with anorthosites, whereas gabbroic anorthosites tend to have deposits of titaniferous magnetite associated with them (Gross 1967). In addition, the major ilmenite deposits are concentrated in the southeast of the Grenville belt, whereas those deposits in the central and western parts of the belt contain titaniferous magnetite and, in general, exhibit significantly higher Fe:Ti ratios (Gross 1967).

The Kunene anorthosite suite (Simpson 1970; Vermaak 1981) occupies an area of $>$ 17 000 km^2 in southwestern Angola and northernmost Namibia and may be as much as 14 km thick. Unfortunately, this huge anorthosite complex is poorly exposed and has been mapped in detail only locally. It intruded early Proterozoic metamorphic rocks and is thought to have been emplaced approximately 1.5 Ga ago, although the isotope age data are somewhat variable (Vermaak 1981). The complex consists of more than 70% anorthosite and has a minor ultramafic border facies. Granitic rocks made up the rest of the suite. Titaniferous magnetite bodies containing on average 49.5% Fe and 18.7% TiO_2 are scattered through the north-central parts of the complex. It is not known at present whether these oxide bodies occur mainly in layered or plug-like form, but they appear to be typical of the iron-titanium oxide segregations known from the Grenville terranes.

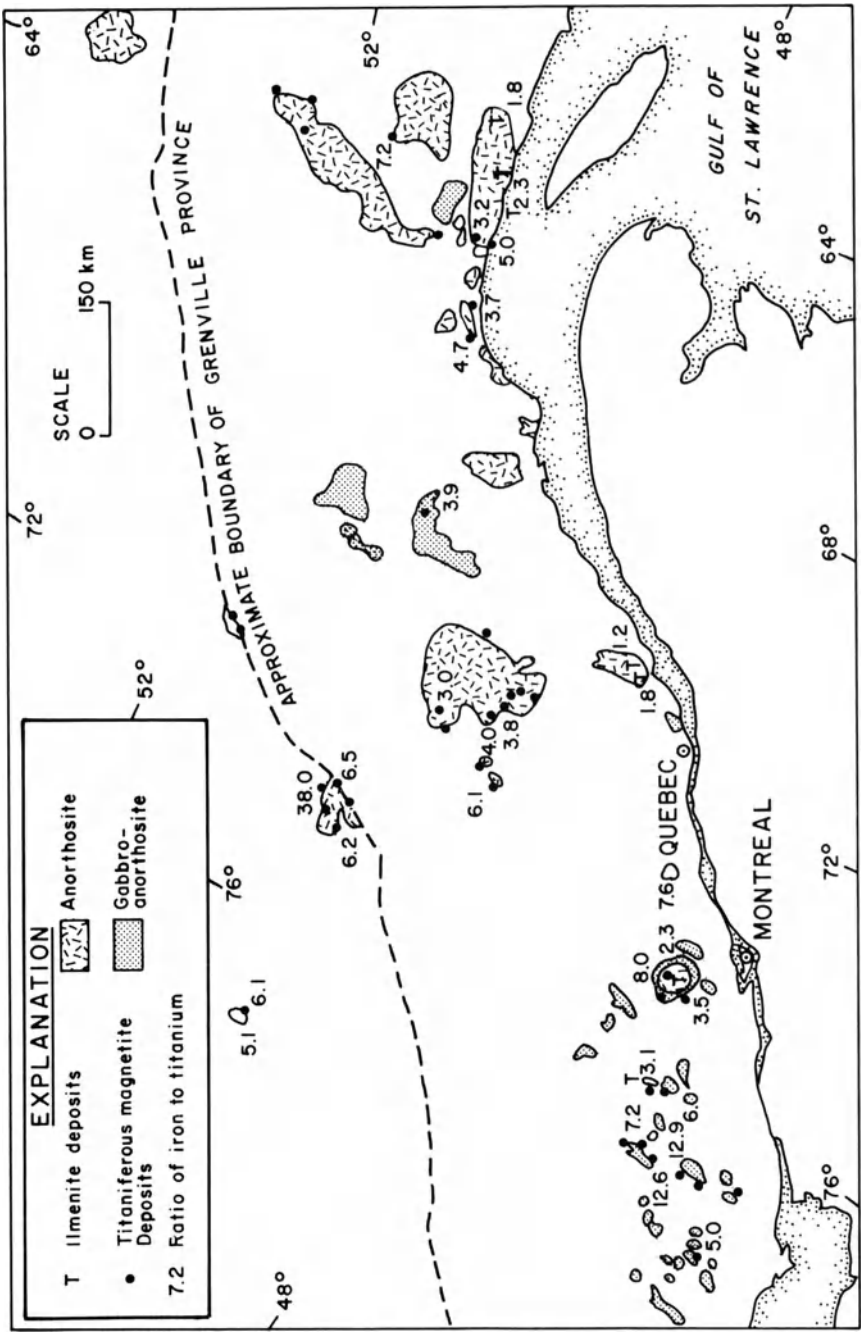

Fig. 6.7. Iron/titanium ratios of titaniferous magnetite and ilmenite deposits of the Grenville province (After Gross 1967)

The general relationship of these iron-titanium ores to their anorthositic host rocks suggests that they represent immiscible oxide segregations (Hargraves 1962), and there is little evidence of concentration of oxides by gravity settling of early crystallized phases in a silicate melt.

6.3 Hotspot-Related Layered Mafic Complexes and Associated Ores

Layered mafic complexes of basaltic composition are commonly emplaced in association with rifting events (Sawkins 1976b, 1982a) and can be considered as intrusive equivalents of tension-related flood basalts such as the Siberian Traps, Parana Basalts, and Deccan Traps. However, at least two important ore-bearing, layered mafic intrusive bodies, the Bushveld Complex and the Sudbury Norite, were emplaced in anorogenic environments where no prior or subsequent rifting occurred; therefore, it is perhaps appropriate to relate them to the presence of underlying mantle hotspots. A meteorite impact origin has been suggested for both the Sudbury and Bushveld complexes (French 1970; Rhodes 1975), but the scale of magmatism in each case, especially the latter, indicates that any impacts that may have occurred served only to trigger the rise of basaltic magma from underlying mantle that was already in a thermally perturbed or hotspot mode.

Interest in the economic aspects of layered mafic complexes has increased in recent years with the rise of platinum metal prices. Intrusive bodies of this type are of overwhelming importance in terms of world platinum production and reserves (Macdonald 1987; Naldrett et al. 1987). Approximately 80% of these reserves reside in the Bushveld Complex, South Africa, but significant additional reserves have been found in the Stillwater Complex, Montana, USA, and in a northern satellite to the Bushveld Complex in Botswana.

6.3.1 The Geology and Ores of the Bushveld Igneous Complex, South Africa

The Bushveld Complex (Fig. 6.8) represents a major storehouse of minerals and contains the world's largest deposits of chromite, platinoid minerals and vanadiferous magnetite (Willemse 1964, 1969; Von Gruenewaldt 1979; Vermaak and von Gruenewaldt 1986). The layered mafic portion of the Bushveld Complex represents a huge irregular lopolith that crops out over, or underlies, an area of 67 000 km^2. It is now recognized that the Complex consists of four major divisions, or compartments: the far western, western, eastern, and Potgietersrust lobes. A fifth lobe appears to be present to the northwest but is concealed below Kalahari sands. Each developed from the same magma source and exhibits the same sequence of layered igneous units, so it is assumed that the five were interconnected, at least for part of the time, during their

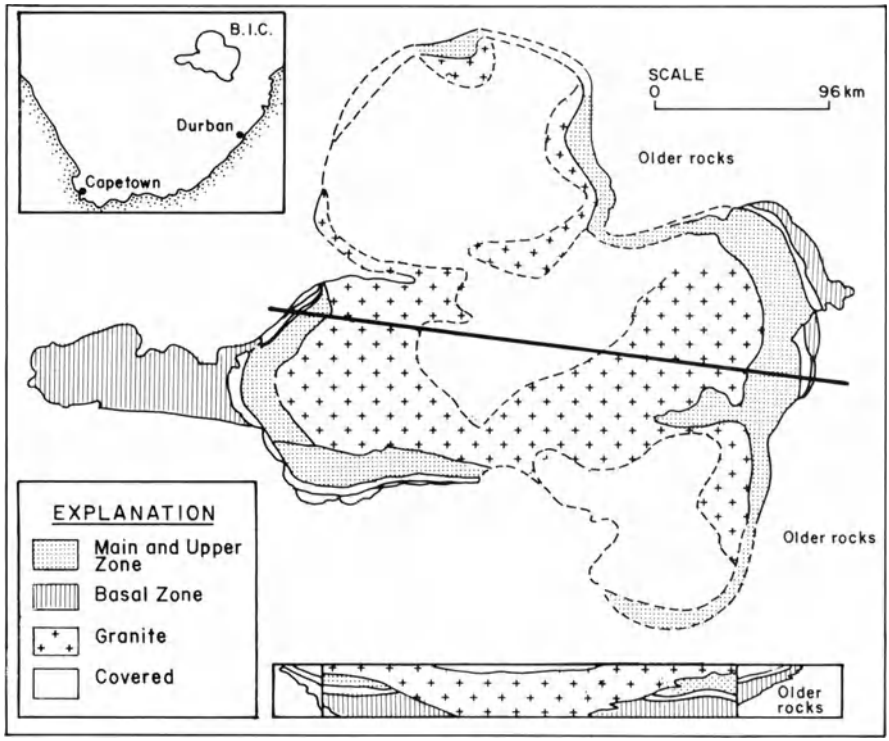

Fig. 6.8. Simplified map and cross-section of the Bushveld Igneous Complex. The extensive granitic rocks probably represent, in large part, melted crustal material, and are distinct from the mafic rocks, which have the average composition of basalt (sketch by author)

crystallization histories. Each lobe, however, has distinctive features when the finer details of their respective igneous stratigraphies are considered.

The Complex in its central portions has a thickness of about 8 km and has been divided into a series of zones, each representing a distinctive phase in the evolution of the Complex (Fig. 6.9). The marginal rocks and sills of the Complex transgress the Transvaal Sequence (~ 2.2 Ga) and have been little studied except in the Potgietersrust Lobe where the transgressive Platreef, a coarse-grained, platiniferous, feldspathic orthopyroxenite occurs (Barton et al. 1986). The Basal Zone consists primarily of ultramafic rocks and is not important in terms of mineral deposits, although in the Potgietersrust Lobe chromitite layers similar to those in the Great Dyke of Zimbabwe are known.

At the top of the Basal Zone lies the Main Chromite Seam. This unit marks the base of the Critical Zone, an interval of strongly layered rocks that contains the most important reserves of platinum group metals and chromite ores in the world. The interlayered rocks consist of pyroxenite, norite, and anorthosite, together with seams of chromitite. These layers have been separated into Lower, Middle, and Upper Group chromitites. The major commercial

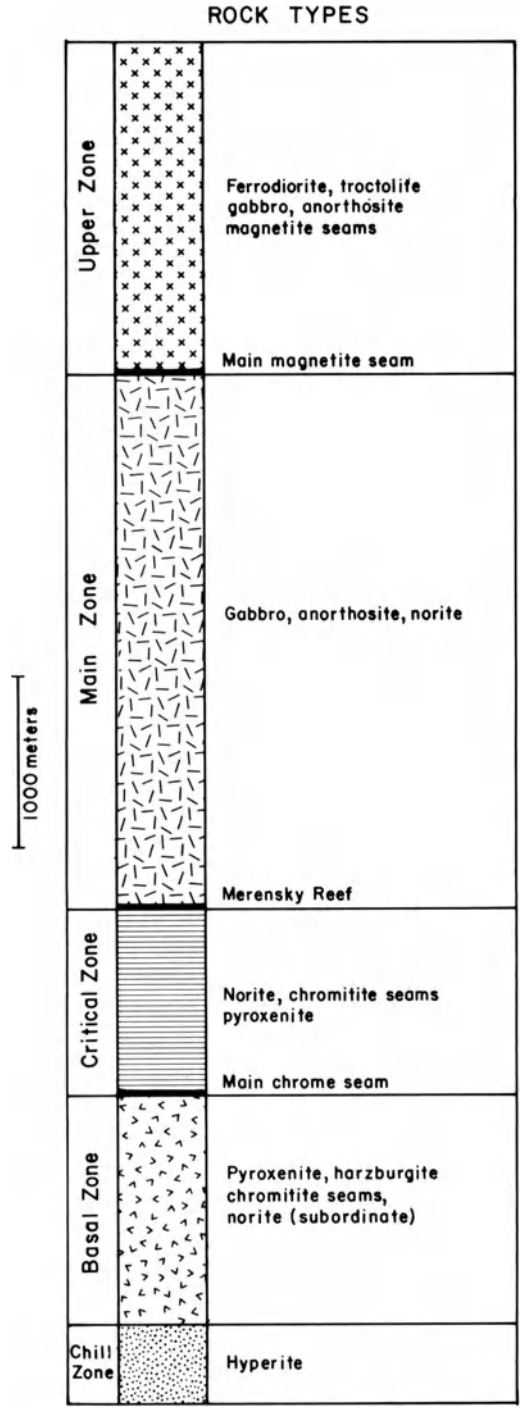

Fig. 6.9. Generalized cross-section of the eastern portion of the Bushveld Igneous Complex, showing main subdivisions of the mafic rocks, their constituent lithologies, and the main concentrations of chromite, platinum (Merensky Reef), and magnetite (Simplified from Willemse 1969)

chromitite layers occur in the western and eastern lobes of the Bushveld Complex (Hatton and Von Gruenewaldt 1987), and the chromite reserves of the eastern lobe are thought to aggregate more than 1 billion tons. Cumulate layering of pyroxene, olivine, plagioclase, and chromite has produced the various litho-units in the Critical Zone (Cameron 1980).

Lower Group chromitites occur in up to seven layers (LG 1–7). Of these the LG 6 chromitite horizon, which averages 0.8 m thick, is the most important in economic terms. The Middle Group chromitites consist of four distinguishable units, some of which are multiple in places. Lateral thickness changes can be quite marked in this group, and various units are exploited where thicknesses and accessibility are favorable. The Upper Group consists in most localities of just two layers, of which UG 2 is of major importance as a source of platinum group metals (Hiemstra 1985).

At the top of the Critical Zone is the famous Merensky Reef, originally the sole source of stratiform platinoids in the Complex but now exceeded in importance by the UG 2 platinoid resource, and almost matched by the Platreef deposits of the eastern Bushveld lobe (see Macdonald 1987). The Merensky Reef (Fig. 6.10) is a distinctive interval that is typically sandwiched between two thin chromitite seems and consists of sulfide-bearing pyroxenite or pegmatitic pyroxenite. The small amounts of nonsilicate minerals in the Reef include the oxides chromite, magnetite, ilmenite, cassiterite, and rutile, and the sulfides pentlandite, pyrrhotite, chalcopyrite, pyrite, cubanite, mackinawite, and valleriite. The platinum minerals are mainly sulfides, the arsenide sperrylite, and ferroplatinum (Cousins 1969).

One of the most important new developments in terms of understanding the mechanism of concentration of platinum metals in the Merensky Reef has

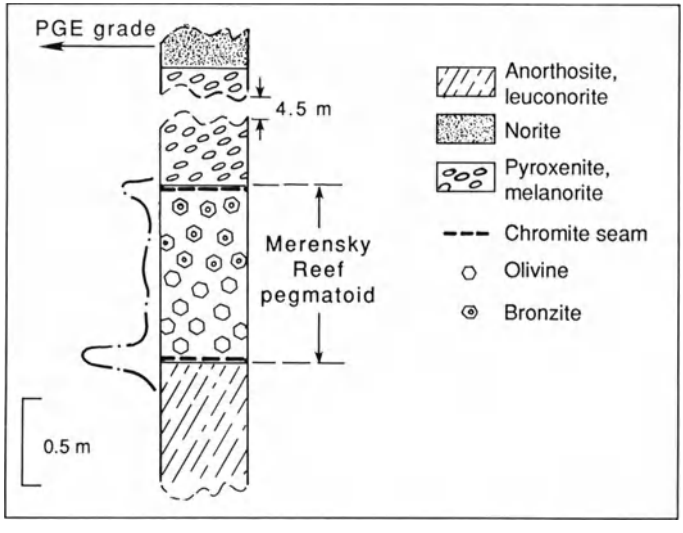

Fig. 6.10. Stratigraphy in the vicinity of the Merensky Reef, Bushveld Igneous Complex. Note distribution of platinum group elements relative to the Reef (After Naldrett 1981a)

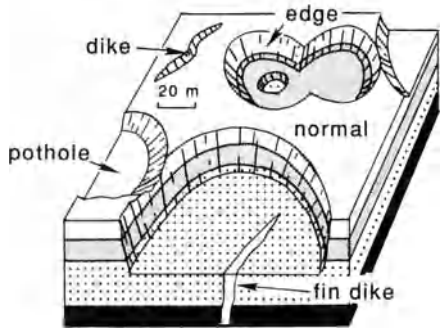

Fig. 6.11. Pothole structures at the level of the Merensky Reef (After Buntin et al. 1985)

been the demonstration by Ballhaus and Stumpfl (1985, 1986) that the Reef was in some way related to the presence of chloride-rich aqueous fluids. It also became recognized that the unusual pothole-like structures in the Merensky Reef (Fig. 6.11) were also somehow volatile-related (Buntin et al. 1985), although Naldrett et al. (1987) point out that the fundamental petrochemistry of each of the units in the upper parts of the Critical Zone, including the Merensky Reef, indicates control by magmatic differentiation processes. This argues in turn for an origin of the platinoid enrichments that relates to some facet of magmatic change (i.e., mixing) rather than an emplacement of platinum group metals by passage of aqueous fluids. A resolution to these problems awaits further work, but the structure of the potholes and the concentration of hydrous minerals and graphite in them clearly indicate an increased activity of water at the time the Merensky Reef formed.

The Main Zone of the Complex is about 3000 m thick and consists of noritic rocks toward its base and gabbroic rocks in its upper parts. Due to the limited economic significance of this zone and its somewhat monotonous character, it has received relatively little attention from geologists. The Upper Zone is separated from the Main Zone by a unit termed the Main Magnetite Seam (see Fig. 6.9), and consists of about 1600 m of gabbros and ferrodiorites interlayered with thinner units of anorthosite, troctolite, and magnetite. Up to 20 seams of magnetite containing significant amounts of vanadium occur within this unit, but only a few of the major seams are of economic importance (Cawthorn and Molyneux 1986).

A series of pipe-like pegmatoid bodies of various types occur at different levels within the complex, and some of them host ore deposits (Viljoen and Scoon 1985). The most significant are three pipe-like bodies of hortonolite dunite within the Critical Zone that have been mined for platinoids (Willemse 1969; Schiffries 1982). At higher levels within the complex, pipes of massive magnetite occur, but they have not been exploited, mainly because their content of vanadium is relatively low ($< 1\%\ V_2O_5$).

Rb/Sr dating studies indicate that the Bushveld Complex was emplaced close to 2.05 Ga ago (J. Hamilton 1977). More recent strontium isotope studies, coupled with extensive field investigations of the well-exposed eastern lobe of

the Complex (Harmer and Sharpe 1985), indicate that two magma types, one pyroxenitic and one gabbroic, were involved in formation of the Bushveld Complex, and that initial strontium isotope ratios increase progressively upward from 0.704 to 0.708. Furthermore, these changes cannot be related convincingly to the effects of crustal contamination, but appear to reflect the mixing of two magmas from distinctive mantle sources. A thermally agitated, or hotspot, condition in the mantle source regions is clearly indicated.

6.3.2 The Platinum Deposits of the Stillwater Complex, Montana

The Stillwater Complex is a layered mafic-ultramafic intrusion with a thickness of about 6000 m that exhibits similarities to the Bushveld in bulk composition, internal form and structure, mineralogy, and texture (Hess 1960; (Fig. 6.12). A rather precise Sm-Nd age of 2.701 Ga has been obtained for the Stillwater Complex by DePaolo and Wasserberg (1979), and although the tectonic setting into which the Stillwater Complex was emplaced during Archean time has been obscured by later events, it may well represent a manifestation of hotspot activity in an anorogenic setting.

The major tilting of the Complex which accounts for its present outcrop patterns did not occur until Laramide time. The lowermost portions consist of a thin noritic Basal Zone and an Ultramafic Zone 1200 to 2000 m thick,

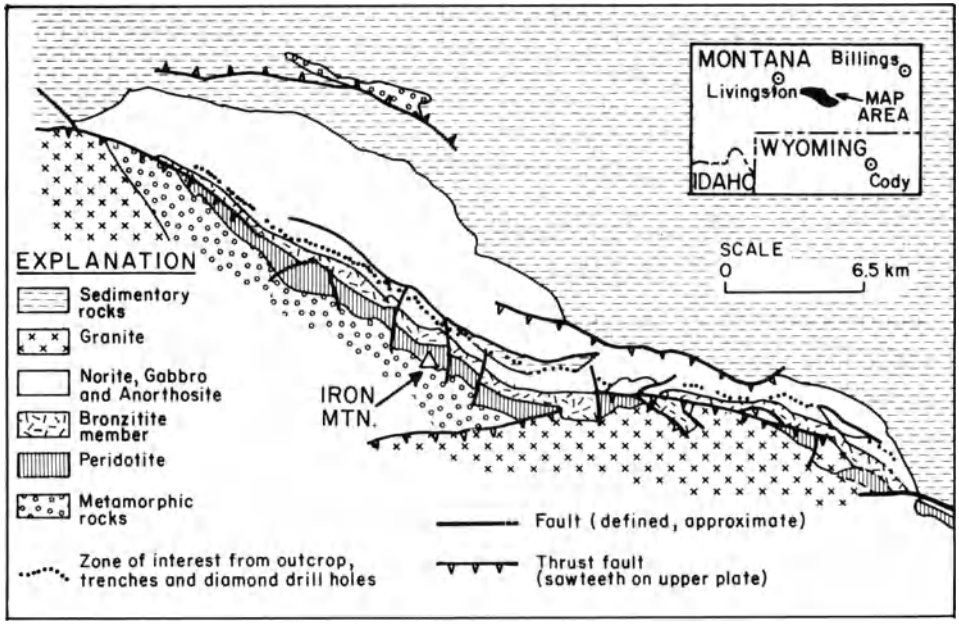

Fig. 6.12. Geologic map of the Stillwater Complex showing position of platinum-rich horizon near base of Banded and Upper Zone (After Conn 1979)

comprising a succession of layers of bronzitite, harzburgite, and chromitite (McCallum et al. 1980). Above this are the Banded and Upper Zones, consisting of layers of norite, anorthosite, troctolite, and gabbro, but the contact between the Ultramafic Zone and these overlying units is not well defined (W.R. Jones et al. 1960). The Ultramafic Zone can be divided into two subzones of roughly equal thickness: an upper subzone of bronzitite and a lower subzone consisting primarily of interlayered harzburgite and chromitite. The chromitites typically contain a lower massive chromitite layer overlain by a series of alternating chromite- and olivine-rich layers of cumulate origin (Jackson 1969), and some of the massive chromitite layers attain thicknesses in excess of 1 m and can be traced laterally for thousands of meters. Mining of some of these horizons has produced over 5 million tons of ore.

Exploration for platinoid concentrations in the Stillwater Complex was based on the model of the Merensky Reef in the Bushveld Complex. This approach was successful (Conn 1979; Macdonald 1987), and a platiniferous zone, the J-M Reef with many similarities to the Merensky Reef has been traced for 40 km along the igneous layering. Ore reserves of 49 million tons grading 22 g/ton PGE have been announced for just one sector of the J-M Reef, but the potential for major additional reserves is obviously considerable.

The J-M Reef is less strictly constrained by stratigraphy than the Merensky Reef and consists of four, somewhat irregular zones that occur on or close to the contact between gabbronorite and the lowest olivine-bearing rock within the Banded Zone (Fig. 6.13). However, other similarities to the Merensky Reef are notable. For example, in both Reefs the PGE occur in sulfides that lie at or near the base of a cyclic unit marked by the appearance of high-temperature cumulus phases and reversals of mineral composition trends. Both are characterized by pegmatoidal facies and pothole structures, and both occur at a stratigraphic level approximately 500 m above the level in each Complex where plagioclase first becomes a cumulus phase.

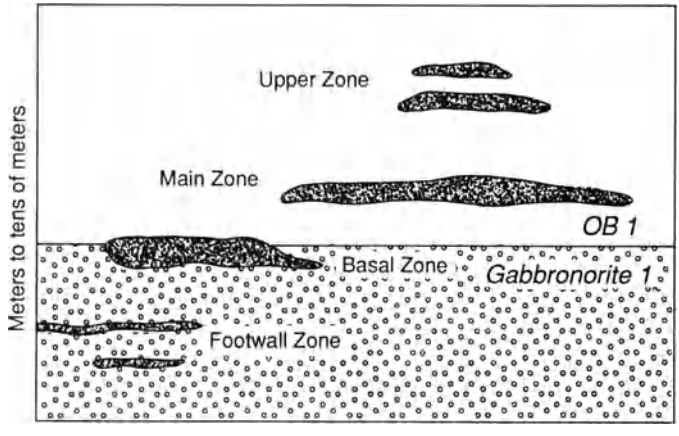

Fig. 6.13. Sketch illustrating the zones of PGE mineralization associated with the J-M Reef, Stillwater Igneous Complex (After Raedeke and Vian 1986)

Platinum group metal mineralization seems to be related in some manner, as in the case of the Merensky Reef, to the presence of a chloride-rich aqueous phase (Boudreau 1988), but in both Complexes the extent to which transport of PGE occurred through the agency of volatiles is unclear (see Naldrett et al. 1987).

6.3.3 The Copper-Nickel Ores of the Sudbury Irruptive, Ontario, Canada

The sulfide ores associated with the Sudbury Complex represent the world's greatest source of nickel (Naldrett 1981a,b), and mining of these ores has produced over 6 million tons of nickel, equivalent amounts of copper, and a significant quantity of platinum group elements, gold, and silver. The Sudbury Structure occurs as a roughly elliptical ring (~ 50 × 25 km) of igneous rocks surrounding a basin containing pyroclastic rocks and sediments (Pye et al. 1984). The igneous rocks that make up the Sudbury Complex (Fig. 6.14) were intruded between the overlying bedded rocks and the surrounding basement rocks 1.85 Ga ago (Krogh et al. 1984).

Naldrett and Hewins (1984) divide the intrusive rocks of the main mass of the Complex into a lower zone consisting of mafic norite, quartz-rich norite, South Range norite, and felsic norite, a middle zone consisting of quartz gabbro, and an upper zone consisting of granophyre. The units apparently underwent rapid consolidation in a funnel-shaped body from a magma subjected to both fractionation and contamination. The economically important sublayer rocks (Naldrett et al. 1984) are predominantly fine- to medium-grained noritic to gabbroic units present as discontinuous lenses at

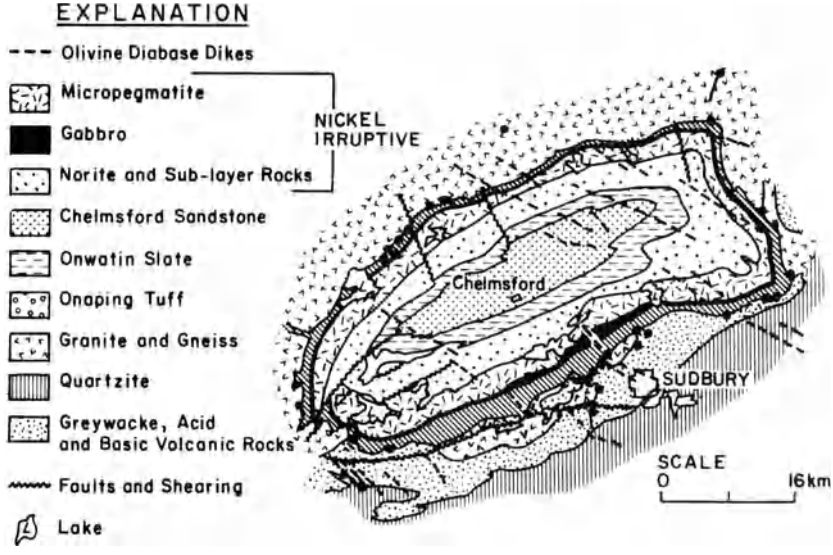

Fig. 6.14. Geologic map of Sudbury Irruptive showing location of nickel deposits (After Naldrett 1981)

the base of the main mass or in the form of dike-like offshoots extending into the country rocks.

The country rocks consist of an Archean granite-greenstone terrane to the north and Proterozoic metasediments and intrusive rocks to the south of the Complex. Within these country rocks a series of structures related to the emplacement of the Complex have been developed. These include large ring fractures, shatter cones and associated planar and kink features, the Sudbury Breccia, and a zone of contact metamorphism up to 1.2 km wide. The Sudbury Breccia is found all around the Complex and consists of in situ broken rock in a pulverized matrix of the same material (Dressler 1984) that was in place at the time of the main intrusive event.

The copper-nickel sulfide ores are not within the basal zone of the main norite as was originally supposed but are associated with a series of sublayer intrusions along the basal zone, and dike-like bodies radiating outward from it (Souch, Podolsky and Geological Staff 1969; Naldrett et al. 1972; Pattison 1979; Naldrett 1984). Relationships between the sublayer intrusions, leucocratic breccias, and sulfide accumulations are complex and puzzling in detail, and the timing of the various intrusive events is still a matter of contention. Many orebodies occur within depressions or embayments within the floor of the Complex, and at such sites a sequence of massive sulfides containing mafic inclusions is typically succeeded upward by sulfides containing inclusions, and disseminated sulfides (Fig. 6.15). Significant orebodies also occur in the dike-like offshoots within the underlying basement rocks. Sudbury ores consist of varied proportions of pyrrhotite, pentlandite, and chalcopyrite accompanied by lesser amounts of pyrite, cubanite, and millerite. Many orebodies exhibit an increase in Cu/Cu + Ni ratios toward the footwall and some exhibit marked increases in Cu + Ni/Fe in the same direction (Naldrett and Kullerud 1967; Naldrett 1984).

The suggestions by Dietz (1964) and French (1970) that the Sudbury Structure was related to a meteorite impact have gained wide, although by no means universal (see Muir 1984), acceptance. The structure clearly exhibits a wide spectrum of shock-related features, but the intrusive rocks and the

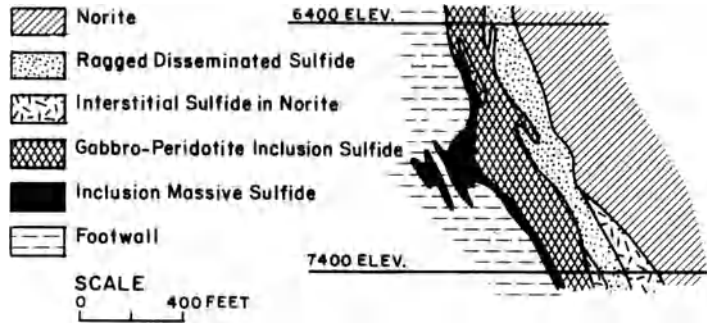

Fig. 6.15. Detailed section through the Creighton ore zone, Sudbury, showing relationships of massive and disseminated ores (After Souch 1969)

copper-nickel ores of the Complex are equally clearly of dominantly mantle provenance. However, the scenario of meteorite impact resulting in large-scale mantle melting appears to be an oversimplification, given the regional structural setting of the Sudbury Structure. Card et al. (1984), for example, demonstrate that the Sudbury Structure is spatially associated with a number of geological features of regional extent, including a linear zone of dense rocks indicated by geophysical data that passes right through the Structure. Overall, the data available seem to suggest that it was the impact of a meteorite coupled with mantle hotspot activity in the region of the impact site that gave rise to this unique feature.

6.3.4 Discussion

A number of other major mafic intrusive bodies are known, some of which contain metal deposits, but most of these can be more appropriately related to rifting events (see next chapter) as opposed to mere hotspot activity. The very large Dufek intrusion in Antarctica (Ford 1975) may represent another example of a hotspot-related mafic intrusion, but its precise setting and ore potential are unknown. The three important mineralized complexes described above have been singled out as hotspot related because no evidence exists in each case that a rifting phase developed. Their suggested relationship to hotspot activity is admittedly speculative, but it is noteworthy that the mafic rocks of each are characterized by relatively high initial strontium isotope ratios, not all of which can be explained by crustal contamination. This evidence suggests the local presence of mantle unusually enriched in incompatible elements. The postulated hotspot activity that gave rise to them may thus represent some combination of structural or impact triggering mechanisms and anomalous conditions in the underlying mantle.

6.4 Metal Deposits Related to Carbonatites

Carbonatites, and their not too distant relatives kimberlites, represent a miniscule fraction of the total volume of igneous rocks, but they are of interest on a number of counts. Many, together with their associated alkaline rocks, exhibit a broad spatial relationship to areas of hotspot-induced rifting (LeBas 1977; Bailey 1980; Bowden 1985). Furthermore, Herz (1977) has related Brazilian carbonatites and their associated igneous rocks to the events preceding and accompanying creation of the South Atlantic Ocean. The older (Paleozoic) carbonatites and alkaline massifs of the Kola Peninsula (Fig. 6.16) also appear to represent direct products of hotspot activity (Mitchell and Garson 1981). Despite their limited volume, carbonatites and their associated mafic alkaline rocks are widely scattered on most continents and embrace an age span of from 2 Ga ago until the present.

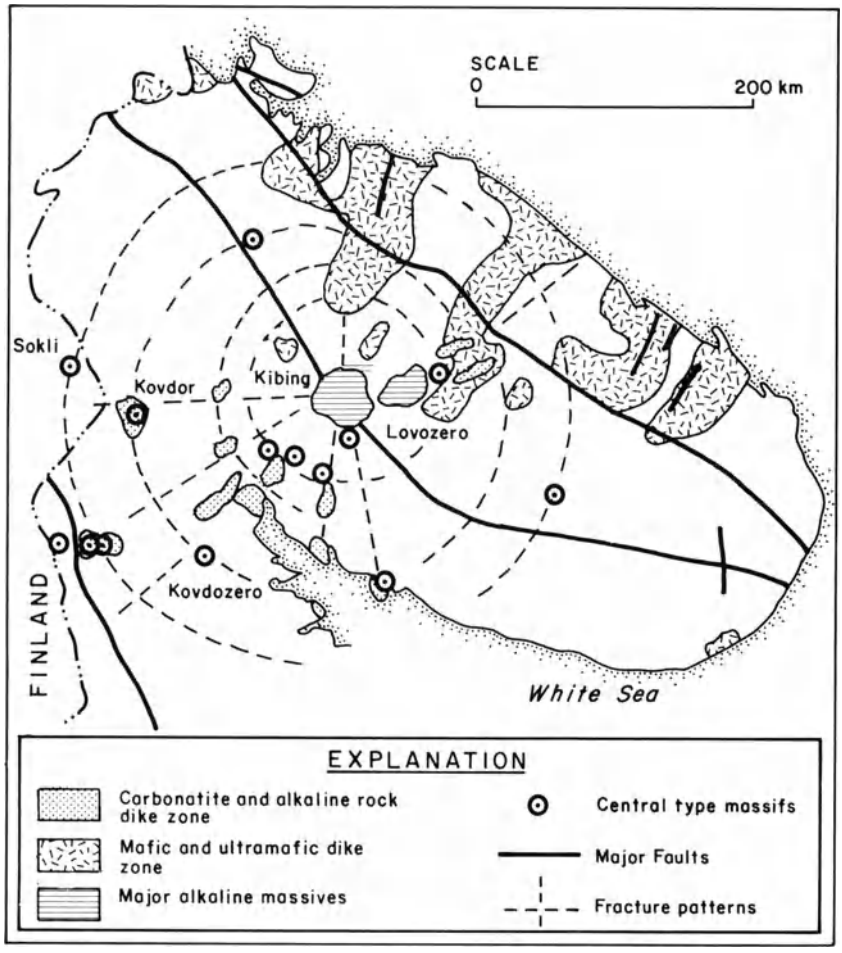

Fig. 6.16. Geologic map of main alkaline and mafic complexes, and structures of the Kola Peninsula, USSR (After Belyayev and Uvad'yev 1978)

Numerous metals, other elements, and nonmetallic minerals are enriched and locally concentrated in carbonatites (Semenov 1974; Verwoerd 1986). These include niobium, iron, titanium, copper, rare earth elements, apatite, fluorite, and vermiculite. However, only a few carbonatite complexes contain significant deposits of the more conventional metals, notably the Kovdor alkalic/ultramafic complex in the Kola Peninsula and the Palabora Complex in South Africa. The Kovdor complex contains relatively small amounts of carbonatite, but iron ore reserves of about 700 million tons and apatite reserves of 110 million tons are being actively mined from it (Northolt 1979).

The Palabora carbonatite in South Africa contains 300 million tons of copper ore grading 0.69% Cu, in addition to important economic deposits of

apatite and vermiculite (Palabora Mining Company Ltd Staff 1976; Fourie and de Jager 1986). The Palabora igneous complex consists primarily of a large, irregularly elongate body of micaceous pyroxenite (~ × 2.5 km) intruded in its central portion of various phases of carbonatite (Fig. 6.17). The disseminated copper mineralization is associated with the last phase of an irregular dike-like carbonate intrusion and occurs also as numerous veinlets

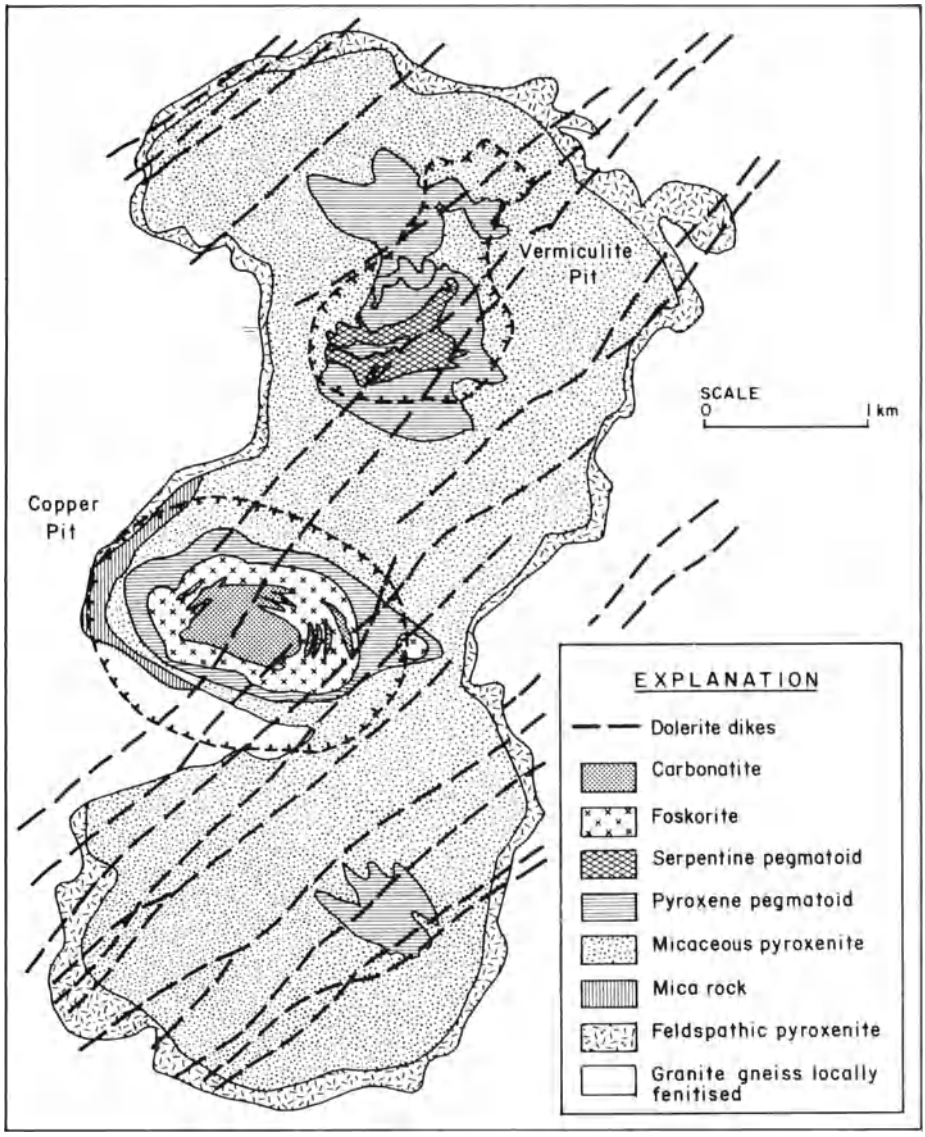

Fig. 6.17. Generalized geologic map of the Palabora Igneous Complex. The disseminated copper ores are mined by open-pit methods from the Loolekop carbonatite area (After Palabora Mining Company Staff 1976)

within the surrounding carbonatites and pyroxenites. Chalcopyrite and bornite are the major sulfide minerals in the orebody, but some cubanite, pyrrhotite and various nickel, cobalt, copper, lead, and zinc sulfides occur in very small amounts, Valleriite, an interlayered copper-iron sulfide and magnesium-aluminum hydroxide mineral, was formed as a late-stage phase, mainly along broad shear zones cutting the orebody. It replaces all other ore and gangue minerals, and its presence is detrimental to efficient copper recovery in the concentrator.

Aldous (1986) has studied fluid inclusions in pyroxenes from a pyroxenite diatreme marginal to the Palabora Complex. Primary fluid inclusions along growth zones in the pyroxenes contain daughter minerals of pyroxene, K-feldspar, apatite, sylvite, and chalcopyrite in addition to other phases. The data indicate the existence of water-rich, copper-bearing potassic melts from which both the pyroxenites themselves and the copper mineralization at Palabora developed.

The age of the Palabora complex is essentially the same as that of the Bushveld Igneous Complex (2030 ± 18 Ma; Eriksson 1984), and thus it can be viewed as a manifestation of the same episode of hotspot activity that gave rise to the Bushveld. The Bukusu carbonatite complex in Uganda contains small amounts of chalcopyrite (Baldock 1969), but the Palabora deposit is unique as a major carbonatite-related copper resource. It should be emphasized that this deposit, although of disseminated type, is quite distinct from porphyry copper deposits in terms of its tectonic setting, igneous rock associations, and ore fluid chemistry.

6.5 The Olympic Dam Cu-U-Au Deposit, South Australia

The Olympic Dam deposit (Roberts and Hudson 1983) is located on the Stuart Shelf west of the Adelaide Geosyncline (Fig. 6.18). It was discovered beneath a concealing, younger sequence of 350 m of late Proterozoic and Cambrian, flat-lying sedimentary rocks. The basement to these cover rocks at Olympic Dam consists of a red K-feldspar granite within which a huge oval-shaped breccia complex has developed. This array of breccias occupies an area of 4 × 7 km, and extends downward from the unconformity for at least 2 000 m. Granite breccia forms an annulus between the surrounding granite and polymict, hematite-rich, bedded, and intrusive breccias in the more central portions of the complex (Fig. 6.19).

The granite appears to be a typical anorogenic intrusion, based on its approximate age (1.6 Ga; Mortimer et al. 1988), composition (> 90% K-feldspar plus quartz), and suggested relationship to the extensive flat-lying Gawler Range Volcanics to the east (Wyborn et al. 1987). On this basis, and the very restricted area of the graben envisaged by Roberts and Hudson (1983) the breccia complex is interpreted by the author as having a pyroclastic, as opposed to sedimentary, origin. Locally, bedding does occur within the breccias, but it is localized in development (pers. observ.) and could easily have

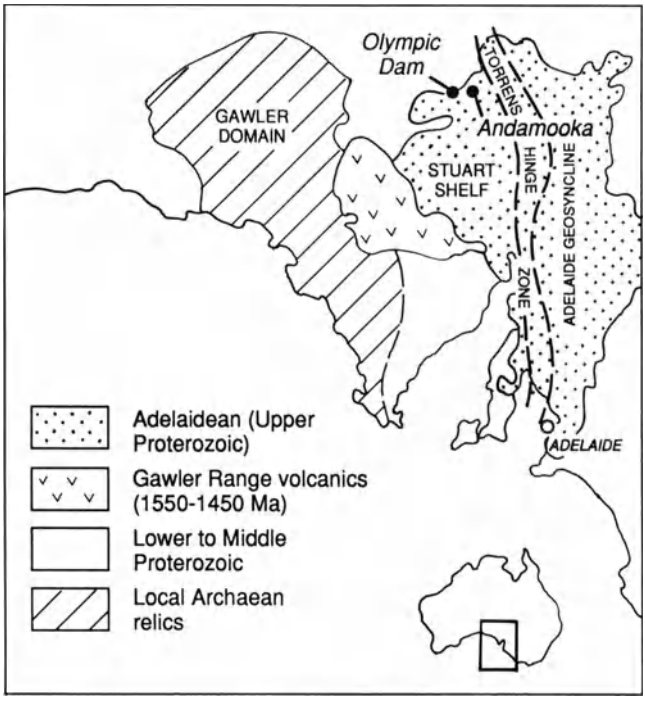

Fig. 6.18. Map illustrating location of the Olympic Dam deposit and its relationship to the surrounding terranes (After Lambert et al. 1987)

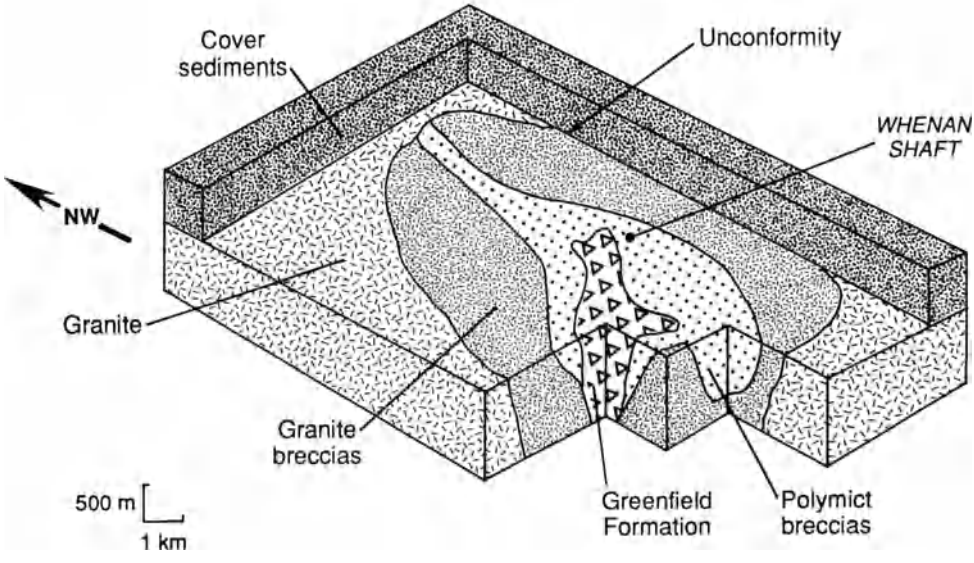

Fig. 6.19. The form of the various breccia bodies present at Olympic Dam. The most recent work has demonstrated that these breccias are transitional to one another (After Western Mining Company information handout)

developed in a diatreme. Clasts in the outer breccias consist only of the surrounding granite, but inward heterolithic breccias containing hematite, and/or felsic and mafic volcanic fragments in addition to granite clasts, occur. Clasts typically vary from 1 to 3 cm in diameter but can attain sizes of 12 m. The matrix to the breccias consists of the same material but of much finer grain size.

Mineralization within the various crosscutting and bedded breccias is developed over an area of approximately 3 × 5 km, and includes reserves of 2000 million tons grading 1.6% Cu, 0.06% U_3O_8, 0.6 g/ton Au, and 3.5 g/ton Ag. The highest grade mineralization is found in the breccias of most varied lithology. The copper minerals comprise chalcopyrite, bornite, and chalcocite, occurring either as clastic fragments in the breccia matrices or as replacements and open-space fillings. Zoning of the copper minerals is prominent and involves changes from chalcopyrite + pyrite → chalcopyrite → bornite + chalcopyrite → bornite → digenite + bornite → chalcocite + bornite upward through the breccia sequence. Uranium is present as uraninite accompanied by lesser amounts of coffinite and minor brannerite. The rare earth element-bearing minerals bastnaesite and florencite also occur in the ore and are a potentially economic source of cerium and lanthanum. The breccias are also cut locally by thin veins containing fluorite, barite, and siderite.

Alteration of the breccias is variable in intensity, but hematite, chlorite, and sericite are pervasive, especially in the breccias with a high content of granite fragments. Locally, intense hematite and chlorite alteration is present, especially in the central parts of the breccia column.

Further studies of this huge deposit are in progress, but it has few known analogs elsewhere in the world. One deposit that exhibits certain similarities to Olympic Dam is the Vergenoeg hematite-fluorite breccia pipe, one of a series of fluorite-hematite deposits genetically related to the Bushveld granites (Crocker 1985). The Vergenoeg breccia pipe extends downwards for 700 m through rhyolite host rocks and contains small amounts of iron and copper sulfides as well as rare earth element-bearing minerals similar to those found at Olympic Dam.

Despite the many uncertainties relating to the genesis of the Olympic Dam deposit, at this time it does seem to have developed in an anorogenic environment characterized by alkali granite magmatism. On this basis, a hotspot-related setting is considered appropriate for this important deposit.

6.6 Afterword

The various deposits and their associated igneous rocks that have been suggested as having a relationship to mantle hotspot activity in this chapter are indeed diverse, and it could be argued that this diversity seriously impairs the credibility of much of the foregoing argument. However, the precise manifestation of mantle hotspot activity on overlying crust will surely depend on a number of parameters. For example, some hotspots may represent mantle

plumes (Morgan 1972), whereas others may be generated by a surfeit of heat-producing elements within a particular patch of subcontinental mantle (D.L. Anderson 1975). Other factors, such as supercontinental assemblies and distance from spreading ridges (Sawkins 1976a), longevity and intensity of hotspot activity, and access routes to the surface can all vary in individual cases. When all these possible variables are acknowledged, it is less surprising that the final manifestations of hotspot activity display considerable heterogeneity.

Chapter 7 Metal Deposits Associated with the Early Stages of Continental Rifting

7.1 General Considerations

As noted in previous chapters, rifting activity in oceanic and arc environments can be associated with the generation of certain types of metal deposits, but in this chapter metal deposits that tend to form in continental rift settings will be considered. As stated so aptly by Mohr (1982), "sufficient unto rift valleys are the existing models thereof." Mohr stresses the complexity and variability of rift systems and the need to reexamine some the notions regarding rifting that have become entrenched in the minds of many workers. He demonstrates, for example, that the stratigraphic record, where legible, does not always support the notion of prior updoming, and the development of suites of exotic alkaline rocks is not a universal feature of rift development.

The plethora of rifting models that have been proposed are perhaps an indication that extensional tectonics and rifting in continental environments can be manifest in a variety of ways. McKenzie (1978), for example, has suggested that formation of all large sedimentary basins must involve some degree of crustal thinning and therefore necessitate tensional tectonics.

Burke et al. (1981) provide an excellent brief summary of continental rifts and stress that they are both more common than previously recognized and can develop in a variety of tectonic settings. Four basic types of rifts are recognized: (1) rifts formed by continental rupture, (2) failed rifts at Atlantic-type margins, (3) aulacogens, and (4) impactogens. Given the continuum of plate tectonic processes, the first three of these rift types represent variations on a single theme, and due to either Wilson Cycle or ensialic collision events (see Chap. 9), most rift sequences developed by continental rupture eventually become enmeshed in orogenic belts and may be difficult to recognize. Aulacogens, defined originally by Shatski (1947), are rifts striking into foldbelts but must have originally been failed rifts at Atlantic-type margins (Burke 1977). Impactogens also strike into foldbelts, but they differ from aulacogens in that they form as a consequence of a collision event, rather than during initial rifting that is eventually followed by collision (Sengor et al.1978).

An important additional type of rift system is that formed as a result of collision events, but this type, unlike impactogens, develops at considerable distances from the collisional orogen. Tapponnier et al.(1982 and references therein) demonstrate that this concept explains much of the rifting in eastern Asia, including the Baikal Rift, Siberia, and the Shansi Basin, China, in addition to major transform faults such as the Altyn Tagh and Red River

systems. The realization that intracontinental plate stresses may have their sources at distant plate boundaries, and not solely in the underlying asthenosphere, is important to an understanding of the full spectrum of rift processes.

Rosendahl (1987) demonstrates that the predominant style of rifting throughout the East African Rift System involves half-graben geometries, commonly as a sequence of linked, but opposing units. The concept of alternating, opposing half-grabens is combined with that of low-angle detachment faulting by Bosworth (1987) to explain the major features of the Gregory Rift, including the siting of very large off-axis volcanic centers such as Mt. Elgon and Mt. Kenya (see Fig. 7, Introduction). The whole idea of one-sided rift faults, combined with ductile extension at midcrustal levels, is being increasingly applied to an understanding of passive continental margins (see Barangazi and Brown 1986; Mathews and Smith 1987), most of which were initiated by continental rifting.

The whole question of volcanism in rift systems, its intensity and petrochemistry, is as yet little understood, but some rift systems are notably "dry" and others contain huge volumes of volcanic rocks (Mohr 1982; Rosendahl 1987). These variations must reflect most directly the thermal state and degree of involvement of the underlying asthenosphere in the rifting process (Fig. 7.1). In the case of the Midcontinent rift system in the USA (Van Schmus and Hinze 1985), volcanism played a major role, and recent geophysical studies (Behrendt et al. 1988) have indicated thicknesses of rift fill below Lake

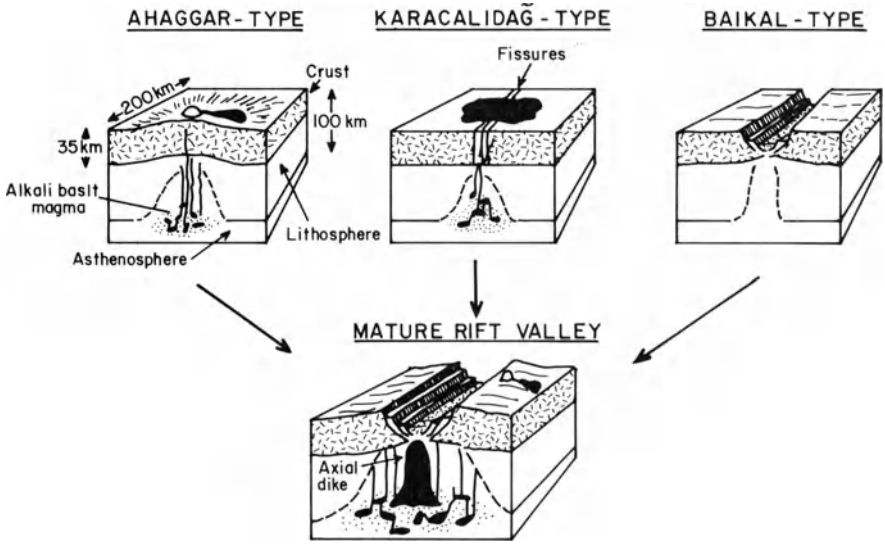

Fig. 7.1. Sketches illustrating how a mature rift valley may evolve from three different origins. In the *Ahaggar*-type, the mantle is active and uplift and volcanism precede rifting. In the *Baikal* type, the mantle is passive and rifting is not preceded by doming or volcanism. The *Karacalidag*-type is more complex with fissure formation and magmatism prior to major down-faulting (After Burke et al. 1981)

Superior of up to 30 km, at least half of which is apparently mafic volcanics. The Midcontinent rift system represents a rare example of an untectonized Proterozoic rift, and Chase and Gilmer (1973) have presented a plate tectonic model for its form and origin involving rotation about a pole in the southwestern USA and transform fault offsets.

Dewey and Burkey (1974) have emphasized that continental rifting is a necessary initial step in the operation of Wilson Cycles, but whether all the ancient orogenic belts that now lie in continental interiors are the products of Wilson Cycle tectonics, or whether the concept of ensialic orogeny has validity, is a matter of considerable debate (Kroner 1977a; Martin and Porada 1978; see Chap. 9). If a supercontinent did exist for a significant portion of Proterozoic time, as argued by Piper (1982), then the operation of Wilson Cycle tectonics involving large ocean basins during that period becomes problematic. However, many of the orogenic belts now locked into the fabric of the continents, whatever their precise evolutionary histories, were demonstrably initiated by continental rifting events and thus represent viable terranes for exploration for rift-related metal deposits.

The difficulty inherent in any meaningful attempt to relate metal deposits to rifting environments through much of earth history lies in the recognition of such environments in terranes where much of the critical evidence is obscured by later tectonic events (Sawkins 1986b). Furthermore, concepts of rifting have to be viewed in a broader context than merely the development of half-graben, graben, and eventually parallel-sided rift valleys, and they should include all environments resulting from attenuation of continental crust. On the other side of the coin, it is all too tempting in some cases to interpret certain lithologic sequences in terms of rifting where the available evidence does not warrant this conclusion. An understanding of the spectrum of rift-related metal deposits can help in this regard, for it has become abundantly clear that metallogenesis is an important facet of rifting activity (Russell 1968; Vokes 1973; Sawkins 1976b, 1982a, 1986b). Thus, the presence of a metal deposit similar to others of clear rift association justifies the search for additional evidence of rifting within the surrounding terrane.

This text divides continental rift-related deposits into those that tend to be formed during the early stages of rifting and those formed during the more advanced stages of rifting; the former are addressed in this chapter. The division is somewhat arbitrary, especially when dealing with older deposits, but in general the basins formed by rifting or tensional events tend to evolve from an initial terrestrial sedimentation stage through a shallow marine to a deeper marine stage. The transition from shallow marine to deeper marine roughly coincides with a break in the spectrum of metal deposits associated with rifting environments.

7.2 Hydrothermal Copper Deposits

Copper deposits of clear epigenetic hydrothermal origin are relatively rare in continental rift environments, but they do represent a recognizable facet of rift-related metallogeny. Examples of minor hydrothermal copper mineralization are known from the Zambian copper belt (Darnley 1960) and the Coppermine River area, Canada (Kindle 1972), and more substantial deposits occur within the Keweenawan rift province (Robertson 1975; Norman 1978; Norman and Sawkins 1985) and in the Messina district, South Africa (Sawkins 1977; Bahnemann 1986). These rift-related copper deposits differ significantly from those in arc systems not only in their tectonic setting, but also in terms of their mineralogy and associated host-rock alteration.

7.2.1 The Messina Copper Deposits, South Africa

The breccia pipe and replacement copper deposits that are mined in the vicinity of Messina have to date produced over 300 000 tons of copper metal from ores that, on average, grade close to 3% Cu. The district lies within the third (failed) arm of Lower Limpopo triple junction of Burke and Dewey (1973) (Fig. 7.2). The deposits occur in a linear array along the Messina Fault that cuts across high-grade metamorphic rocks of the Limpopo mobile belt. These metamorphic rocks form a horst block within the broader confines of the Limpopo rift structure.

The geology of the Messina copper deposits has been described by Bahnemann (1986). Alteration studies were carried out by Jacobsen and McCarthy (1976), and fluid inclusion and isotope studies by Sawkins (1977) and Sawkins and Rye (1979). During the rifting and igneous events that signaled the breakup of Gondwanaland, voluminous basalts and lesser rhyolites were erupted along the Sabi and Lebombo Monoclines (see Fig. 7.2) and probably covered the entire area of the Limpopo rift. In addition, a line of ring complexes of bimodal character, known as the Nuanetsi igneous province, was emplaced along a northeast-southwest trend (Cox et al. 1965). An age range for these igneous rocks of approximately 210 to 170 Ma is indicated by rubidium-strontium data (Manton 1968).

The orebodies of Messina form a linear array, as noted earlier, and occur as either replacement bodies (Artonvilla Mine) or within large breccia pipes (Fig. 7.3). The three replacement orebodies in the Artonvilla area occur as elongate pipes confined to mafic units in a sequence comprising cordierite and pyroxene-garnet granulites. They exhibit structural control by minor warps on the flank of a steeply plunging F_1 fold. Early stage hydrothermal activity caused silica dissolution and formation of a central core of albite surrounded by a sericite envelope, and was followed by intense chloritization, and formation of epidote, copper sulfides, iron oxides, and quartz. As noted by Jacobson and McCarthy (1976), the orebodies exhibit an unusual concentric zoning with chalcocite in the central, most altered zone, and succeeded

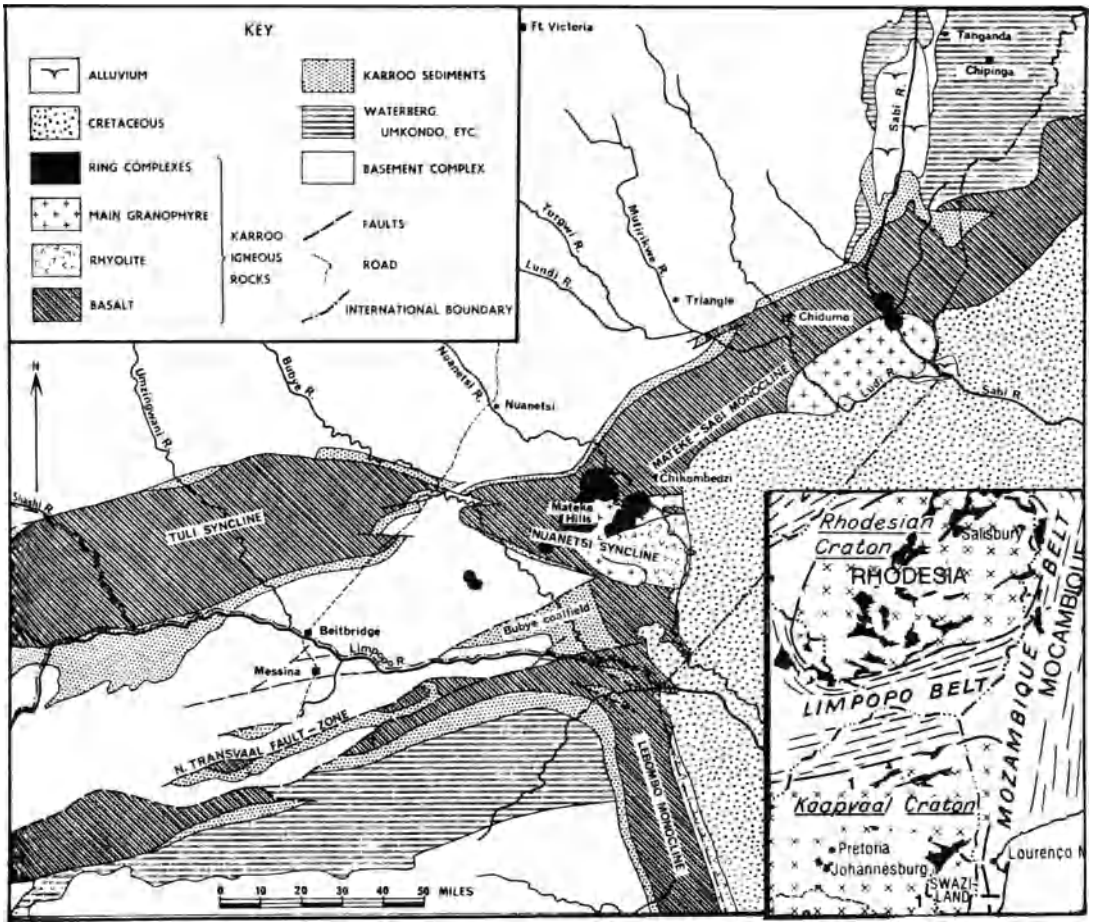

Fig. 7.2. Map of Lower Limpopo triple junction showing Lebombo and Mateke-Sabi Monoclines and the Messina horst within the third (failed) rift arm (After Sawkins 1977)

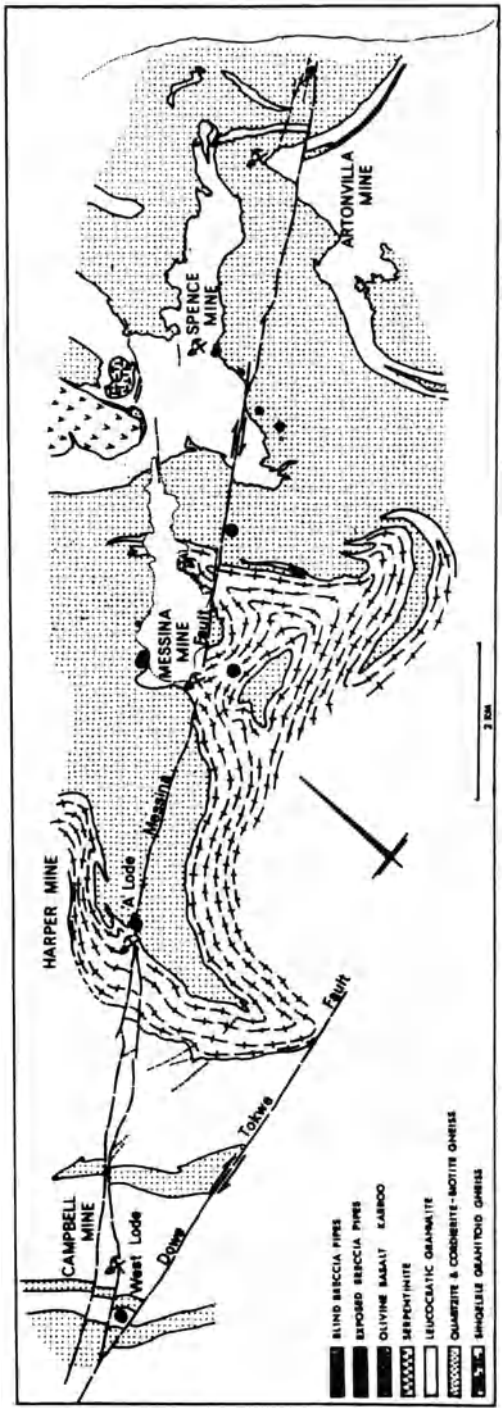

Fig. 7.3. The Messina copper district showing the position of the various breccia pipe and replacement (Artonvilla Mine) deposits. Note position of orebodies along or adjacent to Messina Fault (After Sawkins 1977)

outwards by bornite and then chalcopyrite. Pyrite is minor and occurs mainly around the margins of orebodies.

The breccia orebodies occupy the uppermost portions of large breccia pipes, most of which terminate prior to reaching the surface (Fig. 7.4). Downward movement of fragments can be demonstrated by comparison of the lithologies of some blocks with those in the surrounding rocks. In general, the breccia fragments are little altered, but pink albite and quartz, accompanied by lesser epidote, clinozoisite, chlorite, and copper sulfides, occupy the interstices between fragments. Where filling was incomplete, zoned quartz crystals locally containing occluded specularite, epidote, and copper sulfides are developed. Deposition was terminated by local formation of calcite. The copper sulfides within the pipes are zoned, with chalcopyrite present in the uppermost parts and bornite at deeper level.

Fluid inclusion and stable isotope studies (Sawkins and Rye 1979) have demonstrated that mineralization was effected by low-temperature aqueous fluids (130–210° C) with salinities that varied from 1 to approximately 26 equiv. wt% NaCl. $\delta^{18}O$ values of the aqueous fluids (calculated from $\delta^{18}O_{qtz}$ values and fluid inclusion temperature data) indicate they ranged from –0.4 to –8.4, whereas δD values obtained directly from inclusion fluids ranged from –39 to –56. These numbers suggest the ore fluids were relatively unexchanged meteoric water.

Sawkins and Rye (1979) suggested a genetic model for the Messina orebodies that envisages the leaching of copper from overlying copper-rich rift basalts (see Sawkins 1976b) by meteoric fluids, some of which attained high salinities by evaporative concentration of rift valley playa lakes. These fluids were involved in convective geothermal systems in and close to the Messina Fault system. The high heat flow typical of active rift systems was important in providing the thermal energy to drive the convection. This scenario is perhaps an unusual one for the genesis of copper deposits, but it is supported by the unusual temperature, salinity, and stable isotope data available, and the mineralogic and alteration relationships. The breccia pipes are seen as solution collapse features formed by dissolution of host rocks by initial circulation of convecting alkaline meteoric waters. There is excellent evidence for host-rock dissolution in the cavernous, but nonbrecciated Artonvilla orebodies. Here, apparently volume reduction was insufficient to induce collapse and brecciation.

7.2.2 Discussion

The copper-bearing breccia pipes of the Tribag mine, Ontario (Blecha 1965) were formed by higher temperature, more saline fluids and appear to be more closely related to the emplacement of felsic magma at an important structural intersection within the Keweenawan province (Norman and Sawkins 1985). They also have zones of disseminated molybdenite associated with them and thus may be transitional to rift-related stockwork molybdenum deposits.

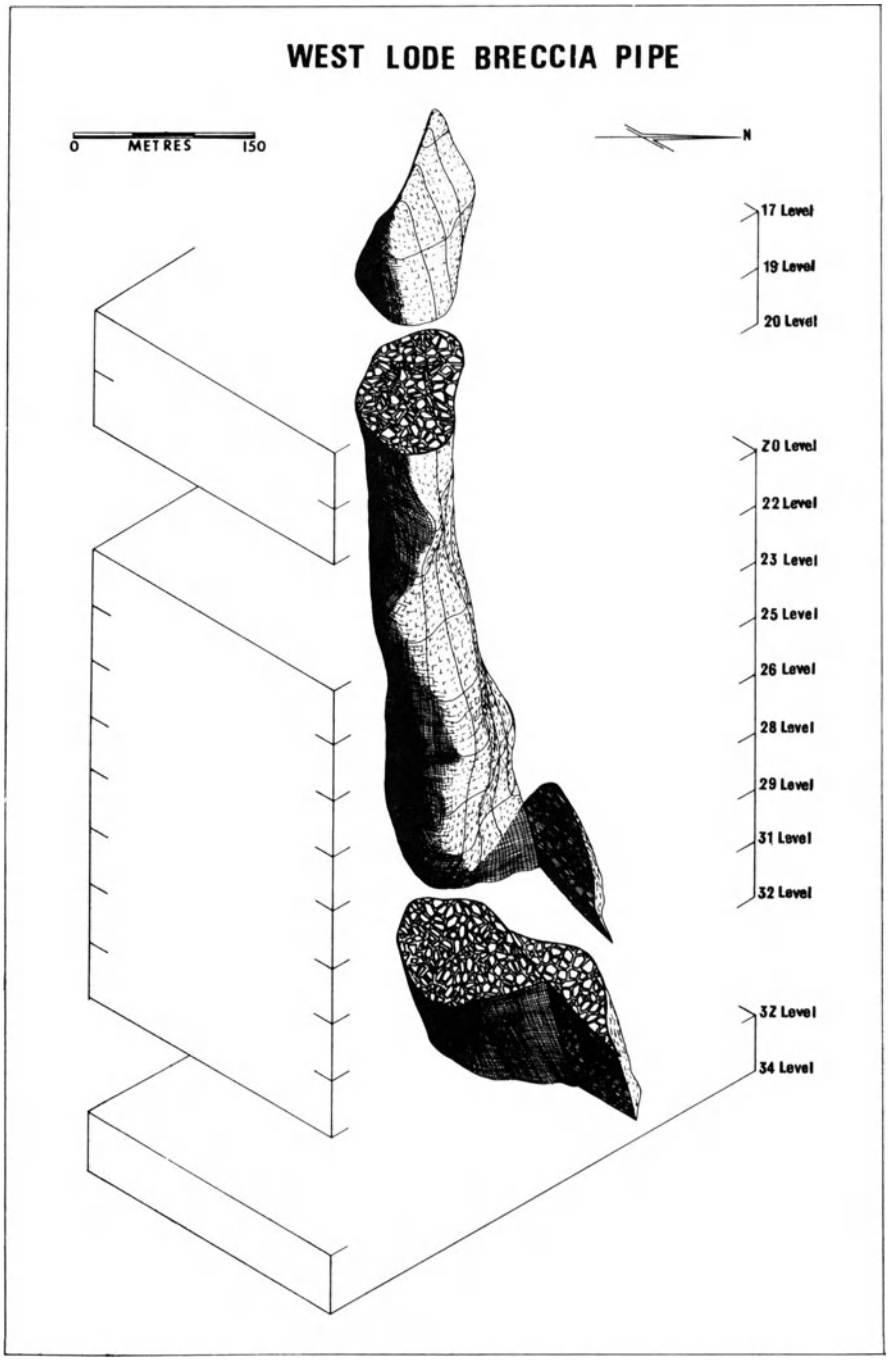

Fig. 7.4. Diagram showing shape of the West Lode breccia pipe. Note upward termination of the pipe, suggesting formation by a solution collapse rather than an explosive mechanism (After Jacobsen et al. 1976)

The association of hydrothermal copper deposits with rift environments is a relatively limited one, but the fact that several of the important Messina orebodies are blind upward suggests that important copper deposits of this type may await discovery in other rift terranes.

7.3 Rift-Related Molybdenum Deposits

It has been demonstrated in Chapter 3 that Climax-type molybdenum deposits can be related to rifting events on the innermost side of the North American convergent plate boundary. The Oslo Rift in Norway has long been known to contain vein-type molybdenum mineralization (Ihlen and Vokes 1977), and the presence of porphyry-type molybdenum mineralization has been recognized (Geyti and Schoenwandt 1979). Occurrences of generally weak molybdenum mineralization are widespread in the Oslo Rift and are almost exclusively associated with subalkaline granitic intrusives (Fig. 7.5), but the porphyry-type mineralization is restricted to isolated stocks, some of which may be controlled by ring structures within batholithic intrusions.

At the Bordvika occurrence within the Glitrevann cauldron, two quartz-feldspar-porphyries and an aplitic granite occupy the central parts of the cauldron and the porphyries have recently been recognized as ignimbrite units (R.H. Sillitoe, pers. comm.). Broad areas of hydrothermal alteration are developed along the shores of the Glitrevann Lake at the northern extremity of these porphyry and aplite bodies, and these areas involve four alteration types: (1) K-feldspar alteration as a stockwork of millimeter wide veins, (2) sericitic alteration as selvages along veins containing quartz-sericite-pyrite and as pervasive host-rock alteration, (3) argillic alteration in the form of intense replacement of feldspar phenocrysts by clay minerals, and (4) propylitic alteration in the form of veinlets and cavity fillings of chlorite plus calcite accompanied locally by epidote and/or fluorite. The K-feldspar alteration is only known from one locality, and the sericitic alteration is the most prominent and widespread type of alteration. The propylitic zone is difficult to map but, as with most porphyry-type mineralization, represents the distal facies of alteration.

Molybdenite occurs as both veinlet fillings and disseminations within the areas of K-feldspar and sericitic alteration, in some samples attaining grades of 0.5% Mo. Whether these molybdenum occurrences within the Oslo Rift will ever support viable bulk mining operations remains to be seen, but their presence does indicate that the porphyry molybdenum potential of subvolcanic granitic complexes within continental rift systems elsewhere in the world should not be overlooked. The Malmbjerg porphyry molybdenum occurrence in central East Greenland represents a good example of such mineralization and contains approximately 200 million tons grading 0.25 MoS_2 (Nielsen 1976). The mineralization occurs within and adjacent to a Tertiary alkali granite associated with syenites that form part of the East Greenland igneous province associated with Atlantic rifting. Were this deposit less isolated, it

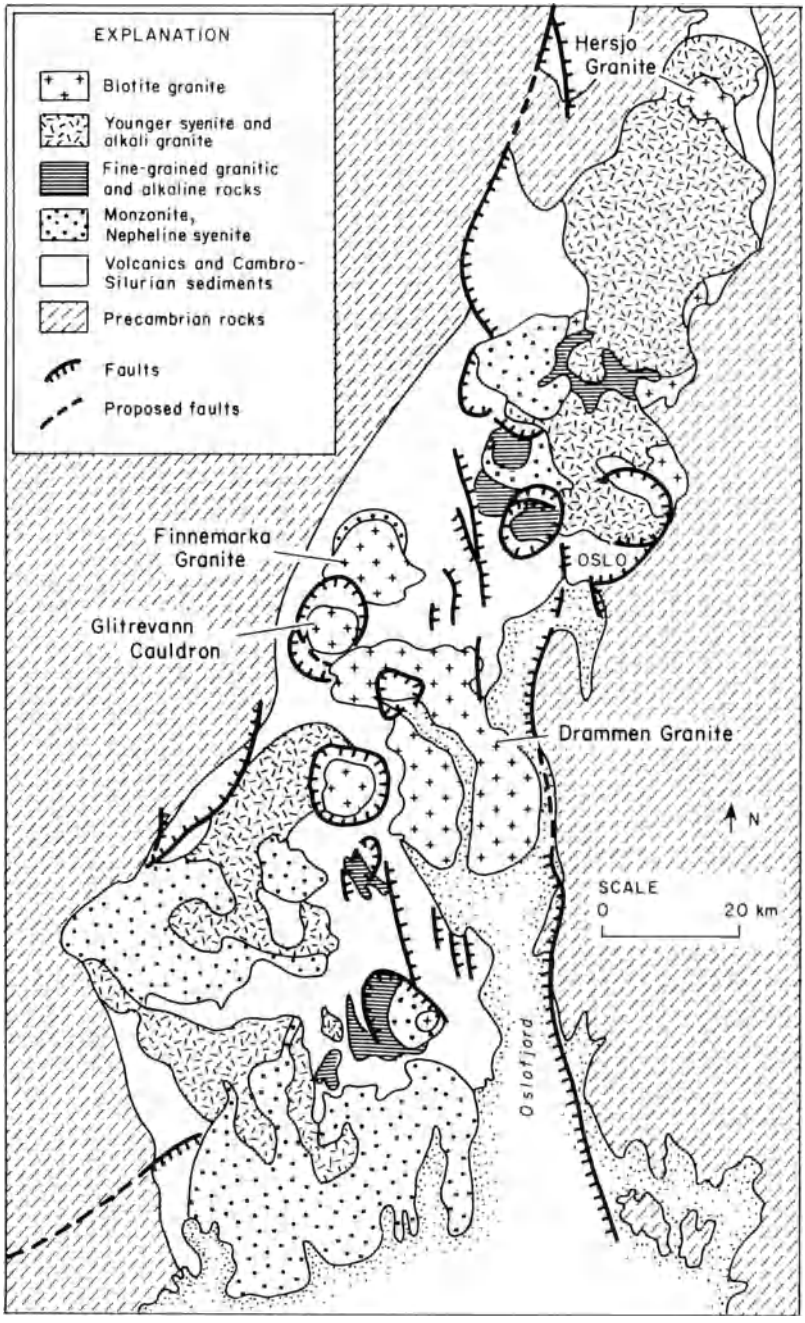

Fig. 7.5. Simplified map of the Oslo Graben showing major granitic intrusives and cauldron complexes. Disseminated molybdenum mineralization is mainly associated with the biotite granites, especially those in the Glitrevann cauldron (After Gaut 1981)

would represent an important source of molybdenum. Similar mineralization of Cambrian age has been discovered in southernmost Namibia (Bernasconi 1981).

7.4 Rift-Related Stratiform Copper Deposits

Stratiform copper deposits represent a well-defined ore type and are second only to porphyry copper deposits in terms of global resources of this metal (Gustafson and Williams 1981). The late Proterozoic sedimentary units of the Lower Roan in Zambia and Zaire, for example, contain an estimated 150 million tons of recoverable copper metal and an additional 8 million tons of cobalt. Stratiform copper deposits also tend to contain higher-grade hypogene ores than those of typical porphyry copper deposits. In contrast to sediment-hosted massive sulfide deposits (see Chap. 8), stratiform copper deposits are disseminated rather than massive in character, occur in sediments of distinctive paleoenvironmental setting, tend to have characteristic mineralogy and zoning patterns, and contain relatively insignificant amounts of associated lead and zinc sulfides. Stratiform copper deposits occur in all the continents and encompass an age range from 2.0 Ga to Miocene (Table 7.1). There is, however, a significant concentration of deposits in Upper Proterozoic lithologic sequences (Rowlands 1980; Sawkins 1983, 1986b).

7.4.1 Lithologic Setting

Most of the major deposits of this type, such as those of the Zambian copper belt (Mendelsohn 1961), the Kupferschiefer (Rentzsch 1974), and at Lubin, Poland (Konstantynowicz 1973; Jowett et al. 1987a), occur within the first marine transgressive unit laid down after a period of red-bed sedimentation (see also Maiden et al. 1984). In other deposits, exemplified by Udokan, U.S.S.R. (Samanov and Pozharisky 1977) and Dzhezkazgan, U.S.S.R. (Bogdanov 1986) the lithologic settings are more varied, but the deposits occur in shales, sandstones or dolomitic units, typically of drab color, within red-bed sequences.

In many instances there is evidence for the former presence of evaporites in the immediate section (Gustafson and Williams 1981) and, in the case of the Zambian deposits and the Kupferschiefer, carbonate units are present up-section. In other cases, such as the stratiform copper deposits in the Adelaide Geosyncline, marine lithologies characteristic of the more advanced stages of rifting are developed up-section (Von der Borch 1980; Lambert et al. 1986).

The general lithoenvironments in which stratiform copper deposits occur are typical of the early stages of rifting, either in continental interiors (Raybould 1978; Sawkins 1986b) or foreland basins (Jowett and Jarvis 1984). Rifting near continental margins is also important locally, and the relation of

Table 7.1. Stratiform Copper Deposits

Deposit or District	Age	Host rocks	Lithology	Rifting	Reference
Basal Cretaceous, Angola	Cretaceous	Cuvo-formation	Mudstone and siltstone	Association with South Atlantic rifting	Van Eden (1978)
Mansfeld copper deposits, Central Europe	Permian	Kupferschiefer	Black shale	Basin and range type faulting, basalt-rhyolite (see reference)	Lorenz and Nicholls (1976)
Aynak copper deposits, northeastern Afghanistan	Infracambrian	?	Metasandstone metadolomite	Association with formation of Tethys Ocean	Sillitoe (1980d)
White Pine, Michigan, U.S.A.	1.0 b.y.	Nonesuch Shale	Gray-maroon shale	Keweenawan basaltic magmatism	White (1968)
Spar Lake, Montana U.S.A.	Late Proterozoic	Revett Formation	White quartzite and siltite	Thick sedimentary sequence, basaltic magmatism	Harrison (1972, 1974)
Seal Lake, Labrador, Canada	Late Proterozoic	Adeline Island Formation	Gray-green shales	Thick clastics, associated basalts	Gandhi and Brown (1975)
Coppermine River N.W.T. Canada	Late Proterozoic	Rae Group	Gray-green glauconitic sandstone	Thick clastics, associated basalts	Kindle (1972)
Redstone Copper Belt N.W.T. Canada	Late Proterozoic	Redstone River Formation	Siltstones and carbonates	Normal faulting, associated basalts	Eisbacher (1977)
Zambian Copper Belt Central Africa	Late Proterozoic	Ore shale, Lower Roan Formation	Argillite and impure dolomite	Sediment thickness changes, time equiv. Bukoban basalts	Mendelsohn (1961)
Witvlei and Klein Aus mines, Namibia	Late Proterozoic	Wituki Formation, Nosib group	Greenish-grey argillite	Thick clastics, underlying basalts	Toens (1975)
Adelaidean copper province, South Australia	Late Proterozoic	Lower Willouran, Adelaidean System	Dolo-siltstones carbonaceous dolo-arenites	Thick clastics underlying basalts	Rowlands (1974)
Kilembe Mine Uganda	Early Proterozoic	Kilembe Series	Meta-siltites	Thick meta-clastics, underlying metabasalts	Davis (1967)
Udokan, U.S.S.R.	Early Proterozoic	Udokan Series	Siltstones, sandstones	Thick clastics	Samanov and Pozharisky (1977)

Miocene rift development and stratiform copper mineralization is particularly clear at the Boleo deposit in Baja California (I.F. Wilson 1955). Igneous rocks, where present in these rift-related sequences, are invariably basaltic in composition and in some instances, especially in the Keweenawan area, underlie the sedimentary section in which the stratiform deposits are hosted (Norman 1978). In fact, in virtually all known cases, some evidence of basaltic magmatism is present within or near the basins in which stratiform copper deposits occur (see Annels and Simmonds 1984; Jowett et al. 1987a).

7.4.2 Mineralization

As stated earlier, a characteristic feature of stratiform copper deposits is the disseminated nature of the mineralization. Another characteristic feature is the high copper: iron ratios in the ores, and in many deposits, chalcocite and bornite are the predominant ore minerals, whereas pyrite + chalcopyrite assemblages are typically minor and occur at the fringes of the orebodies. In fact, the distribution of copper and iron sulfide minerals in stratiform copper deposits in many cases exhibits well-defined zonal characteristics. At the White Pine Mine, Michigan (A.C. Brown 1971), and in the Kupferschiefer of the Mansfield district (Rentzsch 1974; Jowett 1986), an upward and/or outward zoning of copper minerals from chalcocite, and even native copper, to digenite, bornite, and finally chalcopyrite is manifest (Fig. 7.6). Above the chalcopyrite zone, any lead, zinc, and cadmium present in the systems tend to occur together with syngenetic pyrite in the reduced shale host rocks (A.C. Brown 1980, 1984).

In other deposits, especially those of the Zambian copper belt, somewhat similar zoning patterns are found, but here the transition from chalcocite to bornite to chalcopyrite has been interpreted in terms of syngenetic zoning out-ward from paleoshorelines. In detail, however, mineralogic zoning in many Zambian orebodies is complex and not easily understood solely in terms of paleoshorelines (Garlick and Fleischer 1972). Certain stratiform copper deposits tend to contain notable amounts of silver and cobalt in their ores, and the silver exhibits a close correlation with copper minerals rather than with galena, which is present in both the Kupferschiefer and Dzhezkazgan ores. Cobalt is particularly important in the central African stratiform copper deposits of Zambia and Zaire, and this region represents a major world source of that metal (Annels and Simmonds 1984).

7.4.3 Ores of the Zambian Copper Belt

The Zambian copper belt and the related deposits of neighboring Zaire represent an extraordinary concentration of copper metal in this portion of the African continent. In Zambia, well over 1.5 billion tons of ore, containing on average approximately 3% Cu and locally significant cobalt, have been discovered, and there are also major amounts of subeconomic copper miner-

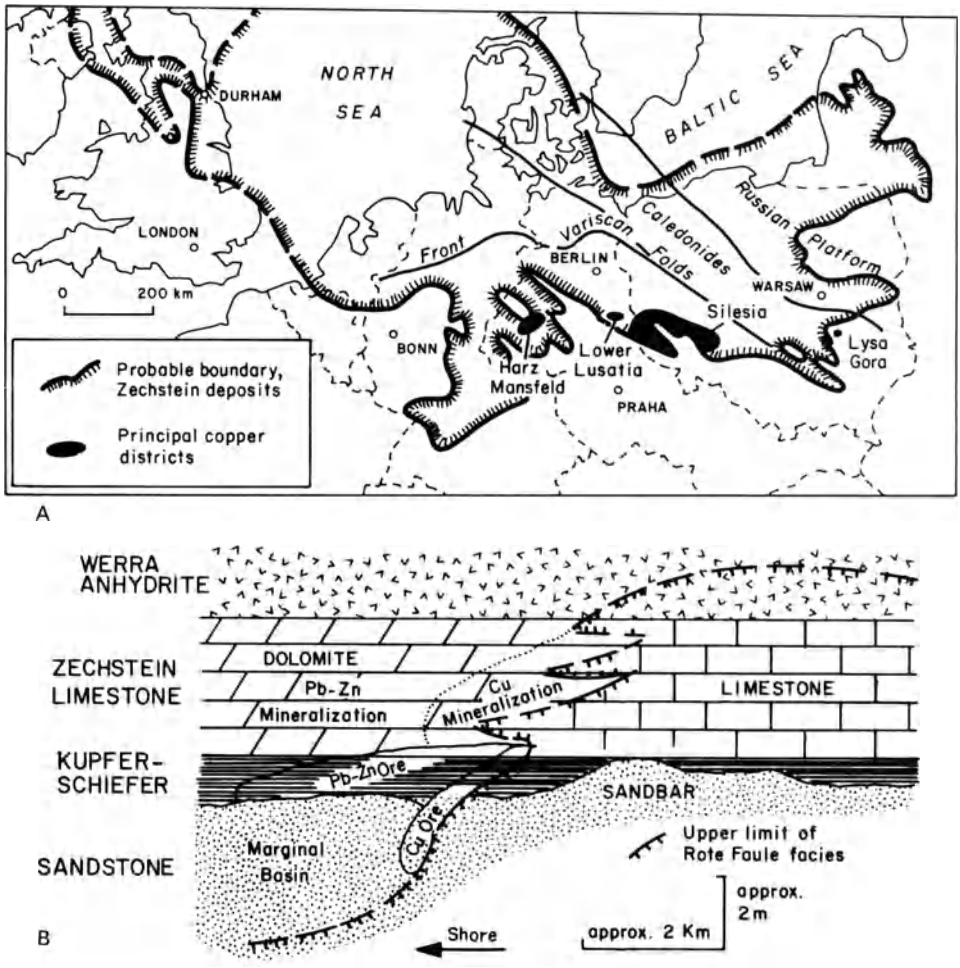

Fig. 7.6A. Map of the present extent of the marine Zechstein deposits in western and central Europe showing position of the principal known copper districts (After Rentzsch 1974). **B** Generalized cross-section to illustrate transgressive metal sulfide zoning within and adjacent to the Kupferschiefer. Note extreme vertical exaggeration of section (After Rentzsch 1974)

alization known in the area. Orebodies are of tabular shape and typically about 2000 m long and tens of meters thick. Host rocks for the disseminated ores are of two types, shales and arenites, with about 60% of the ores occurring in shales.

The ores occur predominantly within the Lower Roan sedimentary rocks of the Katanga Supergroup and are arrayed in two roughly linear belts separated by the Kafue anticline along the southeastern extremity of the Lufilian arc (Fig. 7.7). To the west, this foldbelt swings westward and probably connects with the Damarides of Namibia where smaller stratiform deposits in

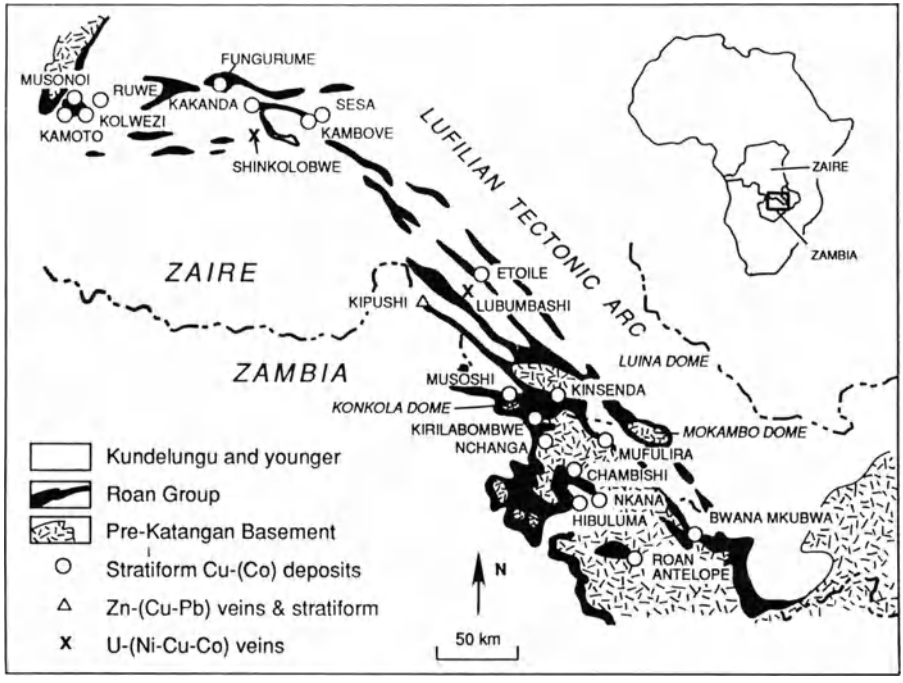

Fig. 7.7. Map of the Lufilian Arc showing location of major copper and other deposits in Zambia and Zaire (After Richards et al. 1988)

rift-related sedimentary sequences of similar age occur (Ruxton and Clemmey 1986; Borg 1988). These Katangan sedimentary sequences are preserved in synclines and basins formed by northward-directed compressive forces between the Kibaran massif to the west and the Bangwenlu massif to the northeast. The development of crossfolds produced a series of roughly equant domes and basins in the region. Metamorphism decreases in intensity toward the northeast, and the epidote-amphibolite isograd slices at a low angle across the southwestern line of copper deposits.

The Katangan sedimentary successions are separated from the basement schists, arenites, and granites by a major unconformity (Mendelsohn 1961; Annels 1984; Fig. 7.8). The lowermost units above the unconformity consist of conglomerates, talus scree, and presumed aeolian sandstones, and their distribution and textures attest to a rugged, probably fault-controlled, basement topography. Subsequently, shallow marine and littoral deposits and local algal bioherms formed as a northeastward-directed marine transgression occurred. These pass upward into sandstones and shales, and most of the former contain carbonate and sulfate minerals. Broadly speaking, the Lower Roan clastics are overlain by Upper Roan dolomites and dolomitic argillites containing some anhydrite beds, and in some areas, these Upper Roan units have been invaded by massive gabbro sills (Annels and Simmonds 1984). Up-section are dolomite

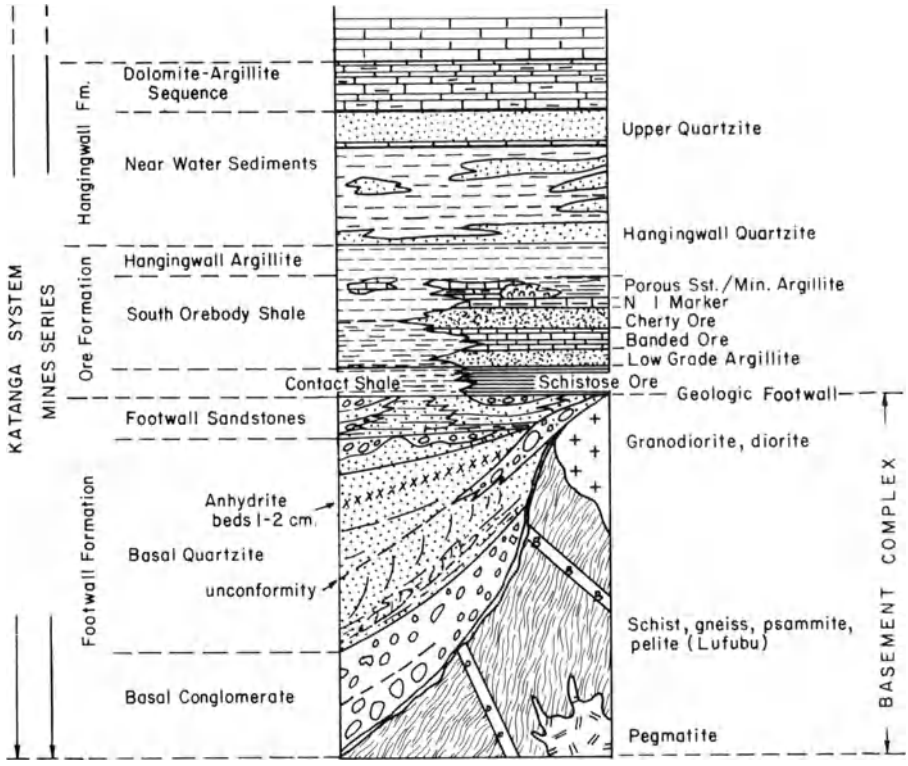

Fig. 7.8. Idealized stratigraphic column for the Lower Roan sedimentary rocks in the Kitwe area, Zambia. The stratiform copper mineralization in this area is restricted to the shaly and carbonate units of the Ore Formation (After Clemmey 1974)

and carbonaceous and pyritic shale, a diamictite of probable glacial origin, limestones and dolomites, and finally pyritic shales grading upward into massive arenites.

Although evidence for synsedimentary faulting has yet to be unequivocally demonstrated, the succession is typical of a magmatically "dry" continental rift system. It is of some significance, in terms of the possible origin of the copper, that at the time the Lower Roan sediments were accumulating (~ 1.0 Ga, Cahen et al. 1971, 1984), the copper-rich Bukoban basalts and associated sediments were probably undergoing erosion in southern Tanzania (J.F. Harris 1961; Cahen 1970). These basalts and sediments contain abundant evidence of copper mineralization and originally were probably considerably more extensive than their present area of outcrop. Some authors (e.g., Pienaar 1961; Wakefield 1978; Annels 1984) have noted, however, the copper-rich nature of the basement rocks and have suggested them as the source of the copper in the Katangan sediments.

The orebodies of the Roan Antelope mine (Fig. 7.9) are typical of copper mineralization hosted in shales. The Ore Shale unit here varies in thickness from 17–55 m. It is not uniformly mineralized, but in some localities the lowermost two-thirds of the Ore Shale contains disseminated chalcocite and bornite, whereas in some others two separate orebodies, the Lower and Upper Orebodies, are separated by barren pyritic shales. These orebodies extend for many kilometers and exhibit sulfide mineral zoning patterns that have been interpreted in terms of transgressive and regressive events superimposed on a basic shoreline control (Fig. 7.10). The cobalt resources of the Zambian copper belt lie exclusively within shale-hosted orebodies of this type (Annels and Simmonds 1984).

The Mufulira ores provide good examples of sandstone-hosted mineralization. Here, three main orebodies. A, B, and C, occur in a sandstone unit 30 to 80 m thick (Fig. 7.11). These host sandstones contain quartz and feldspar, and each appears to represent an initial high energy sedimentation event followed by quieter conditions. Margins of orebodies are controlled by changes in sediment type (upward), and by changes from clean mineralized arenites to dirty barren ones (laterally).

The mineralogic zoning patterns in these sandstone ores are distinct from those of shale ores, and basement topography apparently exerted a significant control on the sites of orebody development. Sandstones containing only pyrite occur over paleohighs, whereas the richest orebodies occur on the flanks

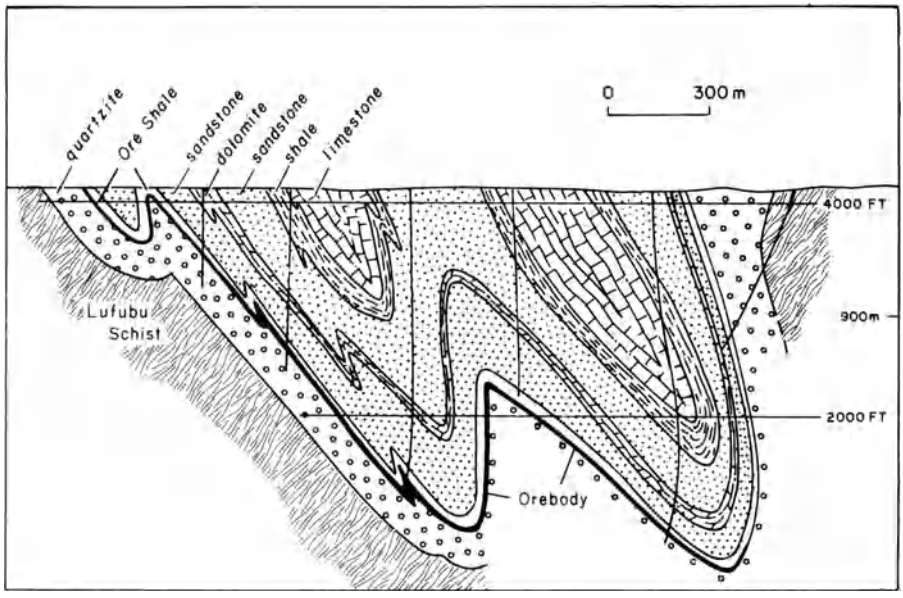

Fig. 7.9. Section through part of the Roan extension orebody showing marked restriction of mineralization to the lower portions of the ore shale and its considerable extent (After Fleischer et al. 1976)

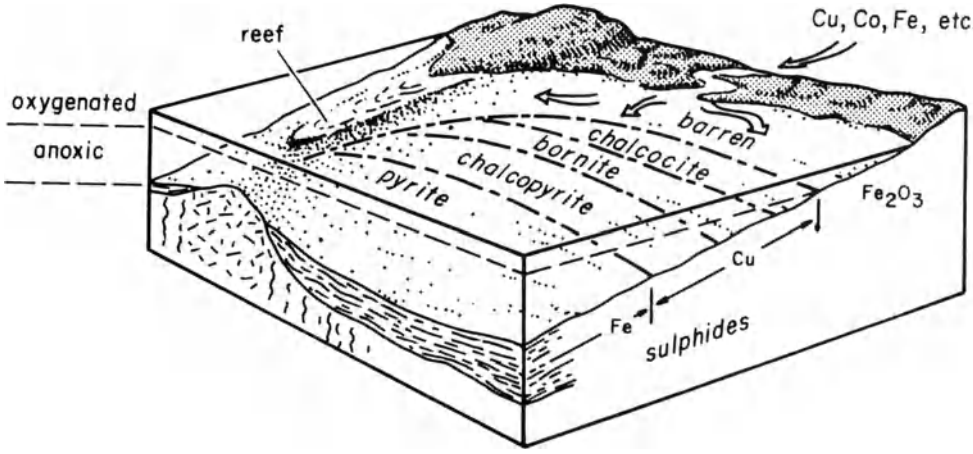

Fig. 7.10. Block diagram showing one suggested explanation for the mineralogic and metal zoning patterns observed in shale-hosted Zambian copper deposits (After Fleischer et al. 1976)

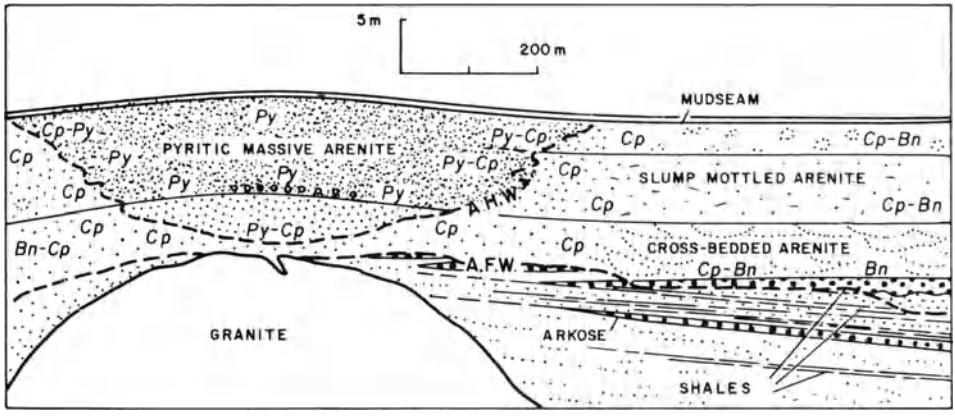

Fig. 7.11. Cross-section through the Mufulira west ores. Note that the mineralogic zoning patterns of sulfides in these sandstone-hosted ores are essentially the reverse of those observed in shale-hosted Zambian deposits. *A.H.W.* and *A.F.W.* refer to assay hanging wall and assay footwall, respectively (Fleischer et al. 1976)

of these highs (see Fig. 7.11). Clearly, such zoning patterns cannot be explained in terms of the same shoreline control claimed for the shale-hosted ores.

The important ores of the Shaba Province of Zaire occur in the northwestern extremity of the Katangan belt and farther west in the essentially similar rocks of the Mines Series (see Fig. 7.7). Cahen (1970) has demonstrated that deposition of these sedimentary rocks probably occurred close to 1 Ga ago. The Mines Series is dominated by dolomitic units, however, and this relationship led earlier workers to correlate it with Upper Roan units in

Zambia. Stratiform copper ores, containing significant cobalt, occur in siliceous dolomites (Francois 1974), but in addition important uranium-copper-cobalt-nickel ores (e.g., Shinkolobwe) occur in vein-type ores in faulted and brecciated areas. It seems possible that these ores represent remobilization of originally stratiform metal concentrations (Cahen et al. 1971; Richards et al. 1988).

7.4.4 Copper Ores of the Kupferschiefer, Lubin, Poland

The copper deposits of the Lubin area of Lower Silesia, Poland represent one of the major world resources of that metal and are reported to contain 10 tons of ore grading 1.5–2% Cu, 30 g/ton Ag and recoverable amounts of lead and zinc (Jowett et al. 1987a and references therein). Depending on host lithologies, stope heights range from 2 to 10 m. The exploration for and development of these huge deposits have provided a particularly clear picture of tectonically controlled sedimentation and the subsequent development of a major ore-generating system.

During the early Permian (~ 280 Ma), strong extensional tectonic movements in Central Europe resulted in the formation of linear rift basins and the local development of abundant bimodal volcanics. Jowett and Jarvis (1984) have noted that this combination of extensional tectonism, bimodal volcanism, and clastic sedimentation closely parallels that of the Basin and Range province of the western USA during mid- to late-Tertiary time. In the Fore-Sudetic monocline (Fig. 7.12), 1500 m of alkaline felsic volcanics and basalt accumulated during this phase of Lower Rotliegendes basin filling. Elsewhere volcanic rocks are more restricted and the rift basins were initially filled with coarse alluvial fan and braided stream deposits and minor aeolian and saline lake units. Upper Rotliegendes sedimentation was characterized by finer-grained sediments, with eolian and saline lake environments becoming more predominant.

The widespread transgression that initiated the Zechstein basin resulted in a reworking of the uppermost Rotliegendes and formation of the Weisliegendes sandstones. The overlying Zechstein formations consist of four to five cycles in each of which coaly carbonate-rich shales are succeeded by shallow marine carbonates and then thick evaporites. These Zechstein cyclic units extend through much of northwest Europe and indicate a far more stable tectonic environment than that of the preceding Rotliegendes. They do, however, tend to be thicker over Rotliegendes basins and thinner over former highs. The Kupferschiefer is the first distinctly marine unit of the lowermost cycle, and on the basis of delicately preserved land plants, it is thought to represent a shallow marine (lagoonal) environment. Two aspects of the basal Zechstein were critical to the ore-generating system that followed: a reduced pyritic rock was present immediately above the Rotliegendes sequence, and the thick overlying evaporites could act as cap rocks and permit geopressuring of the hydrologic systems that developed.

Fig. 7.12A

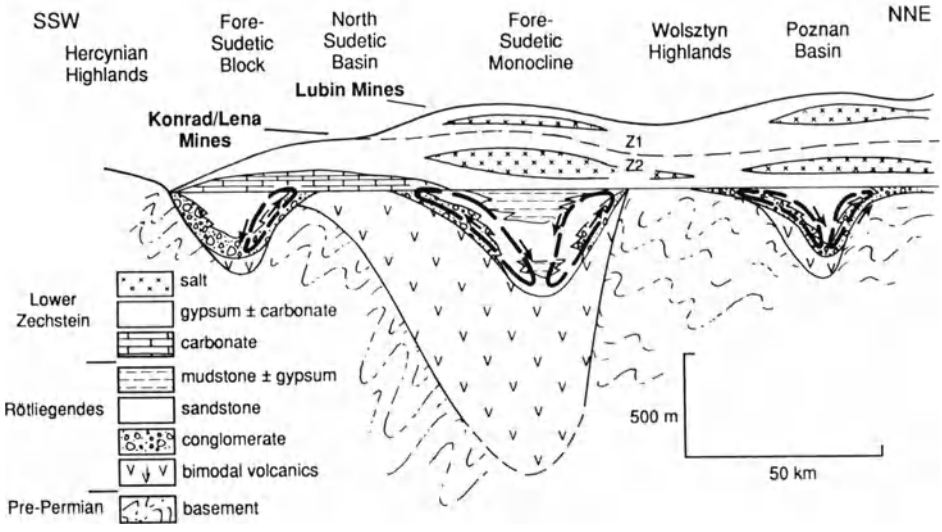

Fig. 7.12B

Fig. 7.12A. Map showing location of the Lubin mining district on the northeast flank of the Fore-Sudetic block. Note also the location of the Konrad and Lena districts that occur in a similar position at the edge of the North Sudetic basin (After Jowett 1986). **B** Interpretive cross-section illustrating movement of basinal fluids up toward the flanks of adjoining structural highs. Note that the largest copper deposits (Lubin district) coincide with the presence of a thick underlying section of bimodal volcanics (After Jowett 1986)

The most important feature of the Lubin copper deposits, both in terms of understanding their genesis and exploration strategy, is the mineralogic and metal zoning patterns that have developed. The copper and surrounding lead and zinc zones formed adjacent to areas where strong oxidation and hematization of the basal Zechstein units has occurred (Fig. 7.13). These irregular, oval zones are called Rote Faule and together with their surrounding copper zones only occur over buried basement highs that lie adjacent to basins containg abundant volcanics and/or volcanic detritus (see Fig. 7.12). The Rote Faule developed in a number of different lithoenvironments, suggesting that their control is hydrologic rather than lithologic. They demonstrate no relation to large Alpine-age faults but do seem to have been controlled in part by minor growth faults that were active during Zechstein sedimentation.

Jowett et al. (1987a) note that the Rote Faule can be subdivided into two facies, one in which the oxidation of original sulfides is only partial and an underlying facies in which oxidation is complete. Paleomagnetic study of the Rote Faule (Jowett et al. 1987b) has indicated a mid-Triassic pole position for the chemical remanent magnetization, indicating that mineralization must have occurred approximately 240 Ma ago, about 20 Ma after deposition of the Kupferschiefer host rocks.

The sulfide mineralization that is zoned outward from Rote Faule zones is developed in sandstones immediately below the Kupferschiefer, within the Kupferschiefer or in the carbonate rocks that overlie it (see Fig. 7.6). Jowett (1986, 1987) has demonstrated that the ore-generating system that formed the Lubin and related deposits was probably set in motion by a second phase of rift activity during Triassic time, a phase that caused convective overturn of the Na-Ca-Cl brines within the Rotliegendes. The observed hematite-chalcocite-bornite-chalcopyrite-galena-sphalerite-pyrite zoning sequence is the predictable result of a brine, initially in equilibrium with hematite and sulfate, equilibrating with a reduced sulfur-rich rock (see also Sverjensky 1987). Under such conditions no pH or temperature control of the ore depositional process is required.

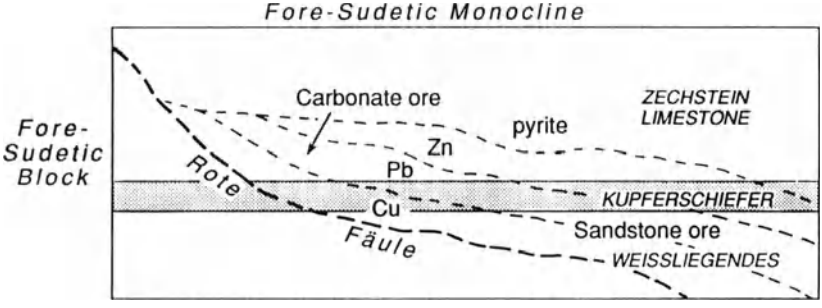

Fig. 7.13. The relationship between oxidized Kupferschiefer and enclosing units (Rote Faule) and the sequence of dominant metals in ores formed adjacent to these oxidation fronts (After Jowett 1986)

7.4.5 Discussion and Suggestions for Exploration

Although concrete evidence for rifting during the accumulation of the Katangan sedimentary successions in Zambia and Zaire is not available, many of the analogous stratiform copper deposits listed in Table 7.1 have clearly formed in environments controlled by rifting (Sawkins 1976b, 1986b). The Adelaide Geosyncline, for example, has been shown to have strong parallels to post-Permian rifts in terms of its tectonic evolution (von der Borch 1980), and the stratiform copper deposits of the Kupferschiefer and the Dzhezkazgan region, USSR, that are related to Permian rifting events, are essentially similar to stratiform copper deposits of Proterozoic age. Small stratiform copper deposits also tend to occur in red-beds deposited in nonrift settings (e.g., Creta, Oklahoma; Ripley et al. 1980) or in intraarc rifts (e.g., Corocoro, Bolivia; Ljunggren and Meyer 1964), but these deposits are of little consequence in comparison to continental rift-related examples.

The reason that rift environments are so favorable for the generation of stratiform copper deposits appears to stem from the coincidence of four features that tend to be common to rifting environments: (1) the copper-rich nature of rift basalts, (2) the presence of abrupt Eh boundaries in rift sedimentary environments, (3) the operation of tensional faulting during rift sedimentation, and (4) the enhanced heat-flow characteristic of rift environments. Thus, not only are suitable copper sources and traps available, but permeability factors, both in terms of the sediments and the structures, are such that the copper can readily migrate from sources to traps. The enhanced heat-flow can be expected to promote both the leaching of the copper and the migration of the fluids that transport it (Fig. 7.14).

Sverjensky (1987) has provided a fifth and possibly critical reason for the association of stratiform copper deposits and rift environments: the presence of evaporites in most copper-bearing rift sedimentary sequences (see Renfro 1974). He demonstrates that the passage of connate fluids, such as oil field brines, through red-bed sequences containing evaporites will produce oxidized fluids capable of transporting considerable quantities of base metals,

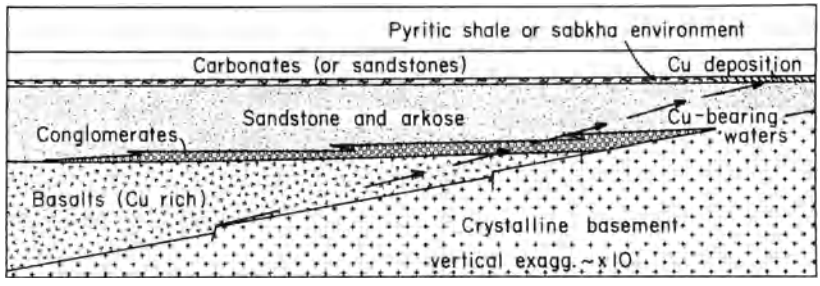

Fig. 7.14. Conceptual model linking copper-rich rift basalts and the formation of stratiform copper deposits. The basal source rocks may lie below the host rocks of the copper ores (White Pine) or could be exposed nearby (Zambian copper belt) (sketch by author)

especially copper. Thus, once high oxidation levels have been attained in the brines, chemical reactions with clastic mineral grains, during brine migration through aquifers, will generate metal-bearing fluids. These same ore fluids will readily deposit their metals on encountering sediments containing organic matter and/or diagenetic pyrite. This geochemical model for metal solution, transport, and deposition fits the empirical data base remarkably well, including the transgressive sulfide mineral zoning patterns present at White Pine, Michigan, and in the Kupferschiefer deposits of Europe (see Fig. 7.6B). These patterns provide eloquent evidence for an epigenetic-diagenetic timing for copper mineralization.

The common separation of copper from lead and zinc in these processes of ore genesis is puzzling, but this separation may well reflect the ready availability of copper from rift basalts (Sawkins 1976a, 1982a). In this regard, it is pertinent that Jowett et al. (1987a) note the restriction of major copper ores in the Kupferschiefer deposits of Poland to the flanks of those Rotliegendes basins that contain thick accumulations of volcanic detritus (Fig. 7.12).

Another interesting aspect of stratiform copper deposits is the strong concentration of this type of mineralization in late Proterozoic sedimentary sequences (see Table 7.1). The prime cause of this concentration appears to be a function of the widespread rifting events that occurred about 1 billion years ago (Sawkins 1976a; Young 1984). However, it may also reflect the amount of sulfate available from seawater for incorporation in evaporites, as the earth's atmosphere evolved. The approximately 2 Ga age of the very large Udokan stratiform copper deposits of the north Transbaikal area, USSR (Fig. 7.15; Kratz and Mitrofanov 1980; Bogdanov 1986) does suggest that sulfates capable of oxidizing potential ore fluids must have been present in these early Proterozoic rift sequences.

In terms of exploration, two major points can be extracted from the data base. First, stratiform copper mineralization is a relatively common feature of early rift sedimentary sequences, and second, the first reduced sedimentary unit above an oxidized clastic sequence overlying the basement tends to host

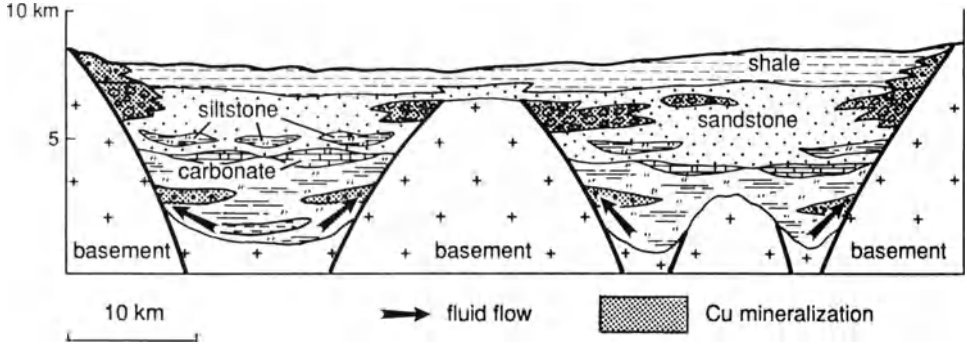

Fig. 7.15. Diagrammatic cross-section illustrating the tectonic and stratigraphic setting of sediment-hosted copper deposits in the Kodar-Udokan zone, USSR (After Bogdanov 1986)

such mineralization. In addition, the early sedimentary sequences of late Proterozoic rift environments should be carefully prospected for stratiform copper deposits. In areas where outcrops are sparse, such as the Zambian Copper Belt, applied geochemical techniques involving soil, and in some instances geobotanical, samples have been used with considerable success in locating mineralized horizons (Ellis and MacGregor 1967).

7.5 Rift-Related Magmatic Copper-Nickel Deposits

As discussed in Chapter 6, certain large, layered mafic intrusions can be related to subcontinental mantle hotspots. Other mafic intrusions, however, provide evidence of emplacement during rifting events, and some important copper-nickel deposits occur within such complexes. As Naldrett (1981a & b) and Naldrett and MacDonald (1980) have pointed out, the two most significant examples of such magmatic copper-nickel ores are those of the Noril'sk-Talnakh region of the USSR (Glaskovsky et al. 1977; Distler et al. 1986) and the mineralization associated with the Duluth Complex, Minnesota, USA (Weiblen and Morey 1980; Foose and Weiblen 1986). A rift-related origin is also indicated for the mafic and ultramafic intrusions and associated copper-nickel mineralization of the Pechanga Belt of the Kola Peninsula, USSR (Glaskovsky et al. 1977).

A rift setting for the important copper-nickel deposits of the Thompson Belt, Manitoba, Canada (Peredery 1982), the copper-nickel mineralization of the Ungava Belt, Canada (Barnes et al. 1982), and the ores of the Limpopo Belt, Botswana (Gordon 1973; Gallon 1986) is more tenuous. However, the Ungava Belt represents a thick pile of basaltic volcanics and minor sediments between the Churchill Province gneisses to the north and the Superior Province gneisses to the south, thus a rifting environment seems probable (Hynes and Francis 1982). A series of ultramafic komatiitic intrusions has invaded this sequence and many of these contain disseminated ore-grade copper-nickel sulfides along their basal contacts (Barnes et al. 1982).

The copper-nickel deposits of both the Thompson and Limpopo Belts occur within linear high-grade orogenic belts, and thus original tectonic environments are obscure. It is noteworthy, however, that in both areas emplacement of the ore-bearing mafic intrusions was restricted to sedimentary cover rocks. In the case of the Thompson Belt, this occurred at 2.0 ± 0.1 Ga, based on Rb/Sr isotope studies (Brooks and Thayer 1981). Such patterns of cover rock sedimentation and subsequent major tectonism and metamorphism involving remobilization of crystalline basement rocks are thought to be a common feature of rifting-initiated intracratonic orogenic belts (Sawkins 1982a, 1986b).

7.5.1 Copper-Nickel Deposits of the Noril'sk-Talnakh Region, USSR

Clearer and more important examples of rift-related magmatic copper-nickel deposits are those of the Noril'sk-Talnakh region in the northwest corner of the Siberian Shield. Here the mafic host rocks are related to the extensive intracratonic igneous events that produced the Siberian Traps, a late Permian to Triassic effusion of flood basalts. The mafic host intrusions were emplaced along a north-northeast trending zone of active block faulting adjacent to the deep Yenisei and Khatanga Troughs, to the west and north, respectively (Glaskovsky et al. 1977). Both these troughs contain about 10000 m of sedimentary fill and are underlain by thinned continental crust (Tamrazyn 1971).

The ore-bearing intrusions, many of which are associated with the Noril'sk-Kharadakh Fault (Fig. 7.16), typically consist of differentiated picrite and picrite dolerite grading upward to slightly more felsic compositions. They are sill-like in form and attain lengths of 12 km and thicknesses of 30–350 m. The copper-nickel-platinoid mineralization occurs in relatively persistent ore horizons, and consists of disseminated and massive accumulations of pyrrhotite, pentlandite, and chalcopyrite in the lower portions of these mafic intrusions. Sulfide disseminations and veins are also present locally in footwall rocks. The ores in the Noril'sk area are lower in grade than at Talnakh and mining operations are now concentrated in this latter area.

The sedimentary country rocks in the region are Carboniferous and Permian continental sediments and coal measures underlain by Devonian and Carboniferous limestones and evaporites. The evaporites are thought to have played an important role in ore formation in terms of providing a source of sulfur for the mafic magmas (Naldrett 1981b). This notion is strongly supported by $\delta^{34}S$ data on ore sulfides which indicate values of +7 or greater (Godlevskii and Grinenko 1969; Kovalenko et al. 1975). The incorporation of sulfur from sedimentary sources has also been demonstrated as a factor in the development of copper-nickel mineralization near the base of the Duluth Complex, Minnesota (Mainwaring and Naldrett 1977; Ripley 1986).

7.5.2 Discussion

The geologic settings of the copper-nickel deposits of the Thompson Belt, Manitoba and the Limpopo Belt, southern Africa appear vastly different from those of the Noril'sk-Talnakh, USSR and Duluth, Minnesota areas. The major differences, however, may be essentially due to differences in their histories subsequent to the rifting environments in which they formed.

It is perhaps interesting that the proportion of mafic metaigneous rocks in high-grade orogenic terranes such as the Thompson and Limpopo Belts is relatively small. Furthermore, as far as can be determined, no extensive terranes of high-grade mafic rocks have been described. This in turn suggests that magmatically "wet" intracontinental rifts (e.g., Keweenawan Rift, northcentral USA) have less tendency to develop at a later stage into high-

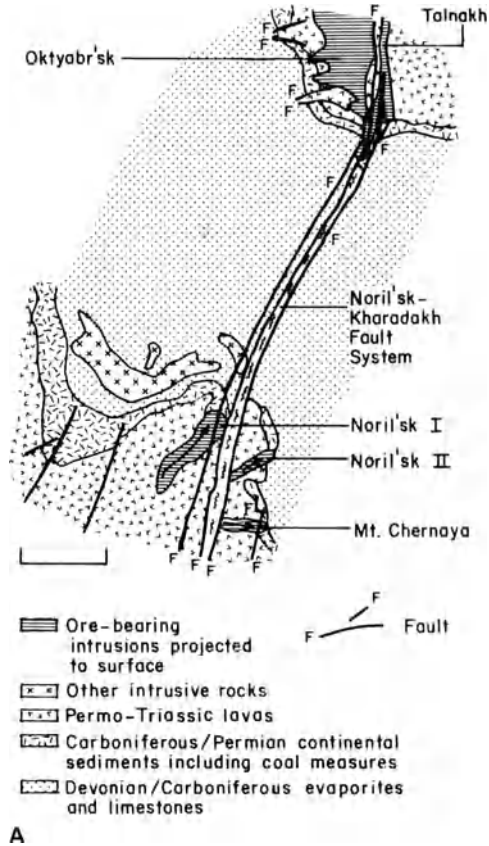

A

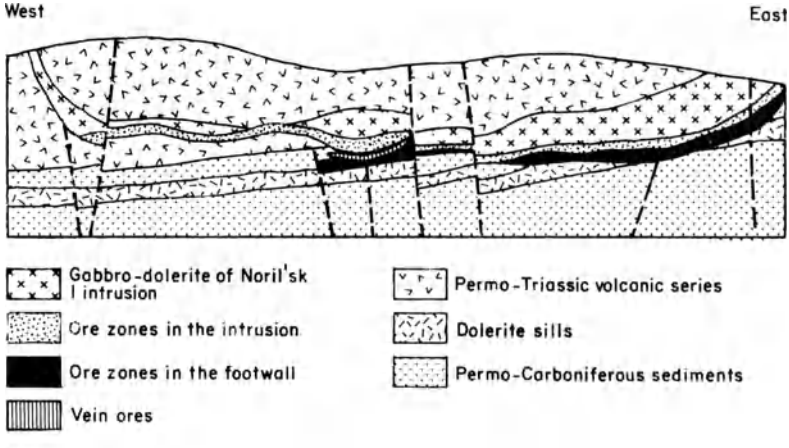

B

Fig. 7.16A. Schematic geology of the Noril'sh-Talnakh nickel districts, USSR (Naldrett and MacDonald 1980). **B** Cross-section through the Noril'sk I deposit (After Glaskovsky et al. 1977)

grade metamorphic belts than magmatically "dry" rifts. This observation may be invalid due to erosional factors, but the possibility that large-scale basaltic magmatism somehow defuses later orogenic activity perhaps merits further investigation.

The tendency of sulfur-rich sedimentary rocks such as evaporites to form in rift environments is well established, as is the tendency for basaltic magmatism. It thus seems possible that additional situations where the juxtaposition of these two elements has occurred in a rift setting (e.g., Noril'sk-Talnakh) may await the attention of the exploration geologist. The Great Dyke, Zimbabwe (Vail 1977; Fig. 7.17) is not noted for its copper-nickel mineralization but deserves mention at this juncture as the oldest (2.6 Ga) known example of a failed continental rift system. It is, however, the host for important stratiform chromite and platinum deposits (Bichan 1969).

7.6 Additional Deposits Related to the Early Stages of Continental Rifting

7.6.1 Late Archean/Early Proterozoic Uraniferous Conglomerates

The important uranium deposits of the Elliot Lake area, Ontario, Canada, lie within the lower portion of the Huronian Supergroup (Frarey and Roscoe 1970; Young 1973). This thick sequence of early Proterozoic clastic rocks exhibits clear evidence of having been deposited in an east-west-trending rift basin. Not only was it initiated by basalt and rhyolite volcanics, but a series of east-west faults controlled the clastic sedimentation, which is clearly derived from the Archean Superior Province to the north. The bimodal volcanism, great thickness, and contemporaneous normal faulting all support the concept that sedimentation was controlled by rifting events.

Much the same setting may have existed during the accumulation of the 16-km thickness of felsic and mafic volcanics, and clastic sediments present in the Witwatersrand Basin in South Africa. Pretorius (1975) has interpreted the Witwatersrand succession as having formed in a yoked basin that was fault-controlled along its northern margin (Fig. 7.18), and van Biljon (1980) has presented a rather speculative tectonic model for the Witwatersrand Basin involving an embayment along a continental margin.

More recent attempts to understand the tectonic setting of the Witwatersrand Basin have led Burke et al. (1986) to suggest that it represents rifting in a foreland basin environment and that the overlying Ventersdorp volcanics formed in a rift system related to collision between the Kaapvaal and Zimbabwe Cratons. Clendenin et al. (1988) have suggested a three-stage rift model that is based on stratigraphic analysis, but it also calls on stresses generated by oblique collision between the Kaapvaal and Zimbabwe Cratons.

In addition to uranium, the conglomerates and carbon seams of the Witwatersrand system represent the source of most of the world's gold

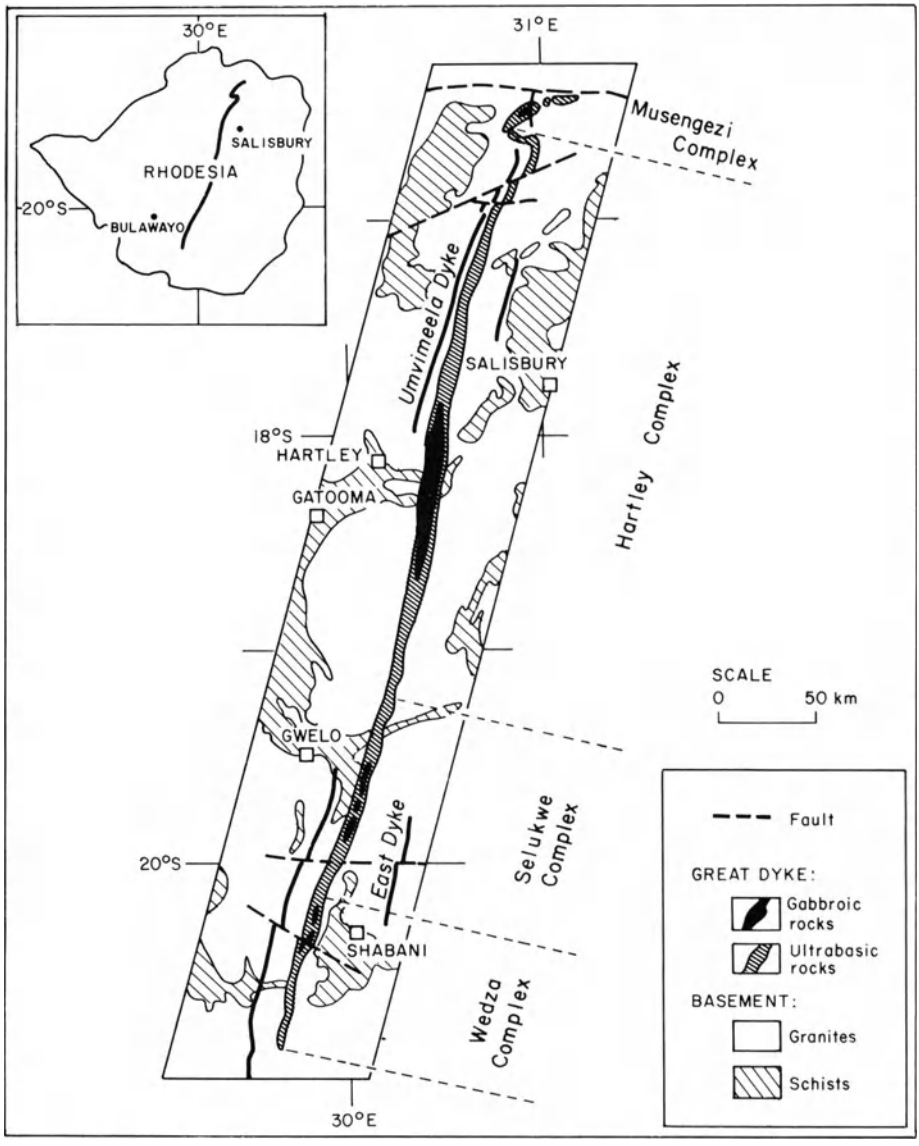

Fig. 7.17. Generalized map of the Great Dyke, Zimbabwe (Bichan 1969)

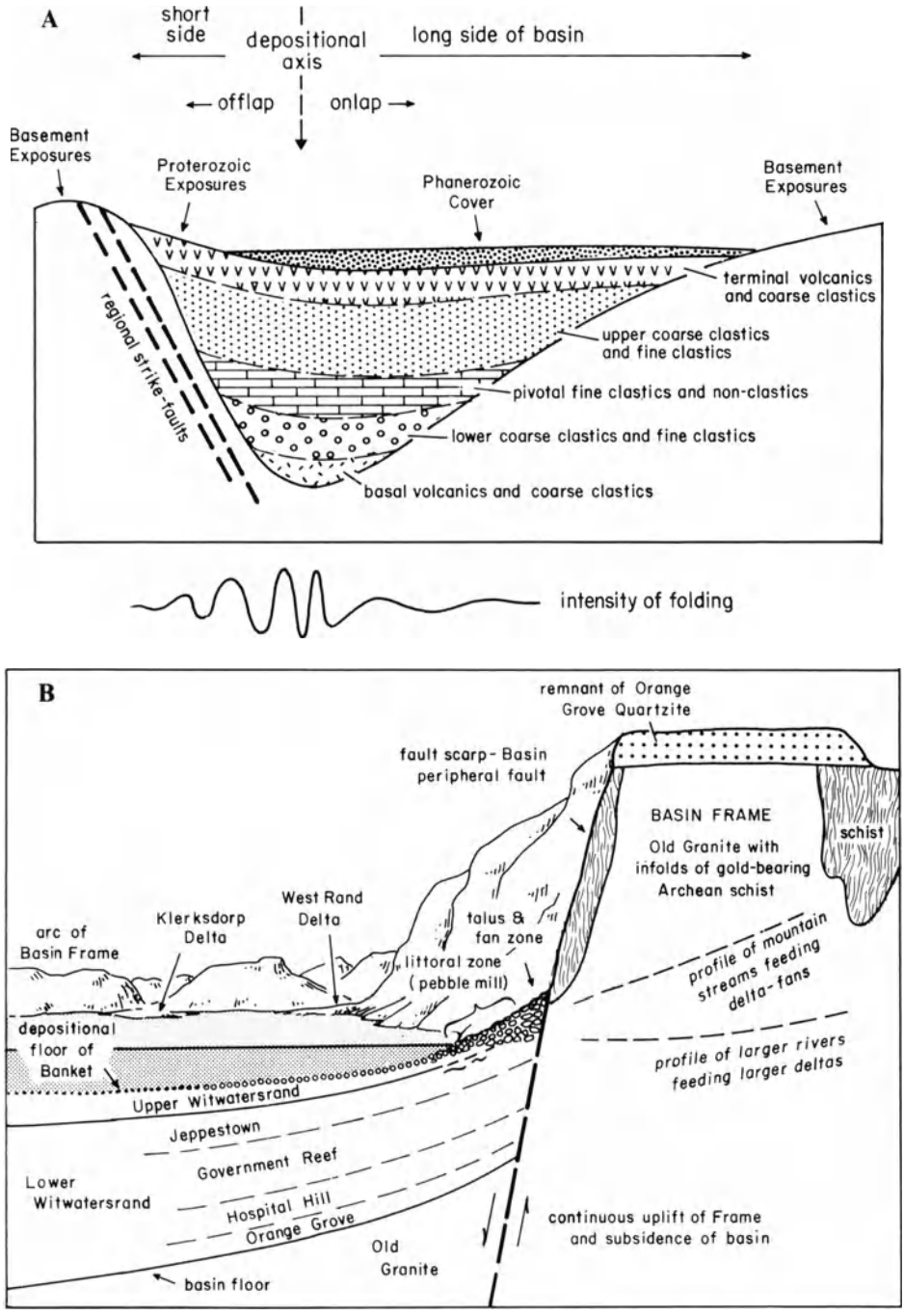

Fig. 7.18A. General concept of a one-sided rift basin, as developed during Proterozoic time on the Southern African Craton. Note gross mirror-image aspect to the stratigraphic succession (After Pretorius 1981a). **B** Concept of the rift basin shown in **A** applied to the depositional framework of the gold-bearing placers of the Witwatersrand Supergroup (After Brock and Pretorius 1964)

(Pretorius 1986 and references therein), and as Pretorius (1981b) has pointed out, if Western world gold production is to be sustained, it is imperative that other major examples of Witwatersrand-type gold deposits be discovered.

7.6.2 The Five-Element (Ag-Ni-Co-As-Bi) Vein Association

Five-element veins have been the focus of considerable study (Andrews 1986), but more importantly they have been a major source of silver in some districts. Kissin (1988) notes that all the scattered five-element vein districts in North America and Europe can be related to areas and times of extensional tectonics. In addition, studies of the Thunder Bay district in Ontario, Canada (Franklin et al. 1986) indicate that lead, sulfur, carbon, hydrogen, and oxygen isotope systems all point to nonmagmatic sources for the ore fluids. Despite this indication, fluid inclusion temperatures from some deposits are relatively high (Franklin et al. 1986), suggesting that heating of these fluids by rift-related mafic intrusives may be a factor in their evolution and eventual metal chemistry.

7.6.3 Magmatic Copper Deposits in High-Grade Metamorphic Terranes

An interesting but puzzling aspect of the metallogeny of high-grade metamorphic terranes is the copper deposits of the O'Kiep district, Namaqualand. Here, past production and reserves of copper sulfides contained in mafic rocks scattered through the high-grade gneisses of the area total 84 million tons of 2.1% Cu (Lombaard and Schreuder 1978). The noritoid bodies that host the disseminated copper sulfides exhibit a strong association with steep structures and megabreccias that transect the generally rather flat-lying structure of the various gneissic and granitic lithounits. Both the steep structures and the associated mafic units exhibit a strong east-west linear orientation.

Of the approximately 700 noritoid bodies that have been found scattered through the O'Kiep copper district, only about 27 contain economic copper concentrations (Stumpfl et al. 1976). The latter consist of three petrographic types, hypersthenite, hyperstene diorite, and mica diorite, and the copper sulfides they contain are mainly chalcopyrite and bornite. A deep-seated magmatic origin for these mafic bodies is indicated by their composition and setting, but rubidium-strontium isotope studies indicate high initial strontium ratios (0.719, Stumpfl et al. 1976), and an age of metamorphism of close to 1.2 Ga.

Within the last decade over 150 million tons of copper ore (1.04% Cu) have been discovered in a similar lithologic and high-grade metamorphic setting at Caraiba, State of Bahia, Brazil (Townend et al. 1980). The norites and hypersthenites that contain the copper sulfides (mainly chalcopyrite and bornite) are steeply dipping and are interlayered with a series of gneisses,

migmatites, and charnockites of probable early Proterozoic age. Some copper also occurs in calc-silicate rocks that contain significant amounts of anhydrite (Leake et al. 1979). The original depositional setting of these rocks is unclear, but the combination of copper-rich mafic rocks and lithologies suggestive of evaporites (see Leake et al. 1979) is certainly compatible with a rift environment.

Chapter 8 Metal Deposits Related to Advanced Stages of Rifting

8.1 General Observations

The variability in styles of rifting makes generalization of the more advanced stages of rifting a hazardous exercise. Nevertheless, broad patterns can be recognized. If the rifting is destined to result in creation of a new ocean basin, it will at a certain point produce a narrow seaway similar to that of the present Red Sea (Martinez and Cochran 1988). Other rifts that fail may only do so after they have evolved from an early stage of subaerial and very shallow-marine deposition to deep, starved basin-type environments. Still others may receive sufficient supplies of sediment to build up great thicknesses of sedimentary rocks ($>$ 10 km) without acquiring deep-marine environments.

Pretorius (1981a) has argued that many Proterozoic basins resulted from half-graben development, and he demonstrated that such basins tend to have a sedimentary fill that is symmetrical about a pivotal, fine clastic and chemical facies developed roughly at the midpoint of the total succession (Fig. 7.18A). Although such basins cannot perhaps be considered rifts sensu stricto, they do represent a manifestation of extensional tectonics in continental environments.

Another variable in terms of continental rifting and basin development is that of time, and many of these features appear to have existed as, at least intermittent, repositories for sediment accumulation for hundreds of millions of years. The most logical explanation for such gradual, long-lived subsidence is gradual cooling and contraction of the asthenospheric wedge, postulated by many to be the initial cause of rifting or extension (e.g., Sleep and Snell 1976).

In metallogenic terms, advanced rifting environments are of extreme importance, for they generate some of the world's most important base metal orebodies. Thus, clastic-hosted massive sulfide deposits provide 31% of the world's zinc production and 25% of the world's lead production (Tikkanen 1986). More importantly, these ore types account for 54% of the world's zinc reserves and 61% of the lead reserves. In addition, the sedimentary basins that develop in advanced rifting environments probably contribute critical fluid and metal components for the generation of many carbonate-hosted ores (see next chapter).

8.2 Metalliferous Deposits of the Red Sea

The discovery of hot brine pools in the median valley of the Red Sea in the mid-1960's generated considerable interest (Degens and Ross 1969), especially when it was shown that sulfide-rich muds of considerable economic potential existed below one of these pools (Hackett and Bischoff 1973). Thirteen occurrences are known of either brine pools and/or metalliferous sediments, scattered along the northern and central segments of the Red Sea (Fig. 8.1). All are located along the axis of spreading where the median valley is best

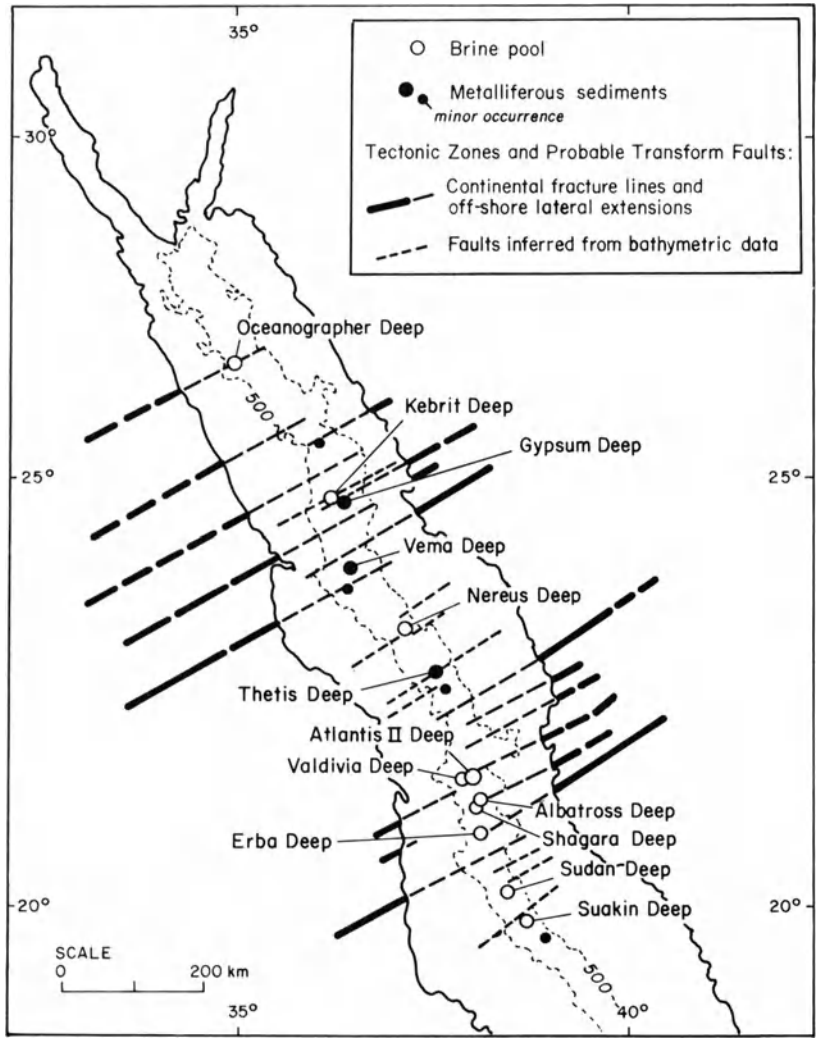

Fig. 8.1. Location of brine pools, metalliferous sediments, and probable transform faults and related structures in central and northern Red Sea (After Bignell 1975)

developed, and Bignell (1975) has pointed out that most of these occurrences are located where faults, inferred either from bathymetric data or from continuation of continental fracture lines, cross the median valley.

Studies of the history of the Red Sea (Girdler 1969; Martinez and Cochran 1988) have shown that the main Red Sea graben formed in earliest Miocene time and that a sequence of clastics and evaporites were deposited within it. Opening of the Red Sea to its present width has been a somewhat episodic process, but indications are that spreading has been occurring at about 1 cm/yr over the last 3 Ma (Vine 1966). Furthermore, the Red Sea appears to provide an excellent example of an asymmetric rift developed by low-angle detachment (Voggenreitter et al. 1988). Micropaleontologic analysis of cores taken from the Red Sea (Berggren 1969) suggest that increased salinity episodes occurred several times during the last 85 000 years, and these episodes probably correlate with times when connection with the Indian Ocean was restricted.

Although a number of occurrences of hot brines are known in the Red Sea axial trough, it should be emphasized that they exhibit considerable variation in terms of chemistry and brine temperature, and their associated metalliferous sediments vary in mineralogy and sulfide and metal contents. Of those known, only the metalliferous sediments of the Atlantis II deep are of possible economic interest (Shanks 1983).

8.2.1 Metalliferous Deposits of the Atlantis II Deep

Core sampling of the sediments below the Atlantis II hot brine pool, which lie at a depth of close 2000 m, has demonstrated that metalliferous sediments averaging 20 m in thickness occur over an area of approximately 50 km^2 (Hackett and Bischoff 1973; Shanks 1983). The sulfide-rich layers are a meter to several meters thick, but form beds several kilometers long, and are estimated to contain 100 to 200 million tons of material grading 3.5% zinc, 0.8% copper, and significant silver values, on a dry, salt-free basis. The overlying brines have a salinity of 256 g/kg, and exhibit maximum temperatures of about 60°C. It is believed that subsurface brine temperatures are $>$ 200°C (Shanks and Bischoff 1977).

The metalliferous sediments within the Atlantis II Deep form a relatively thin veneer above the basaltic basement (Fig. 8.2), and these sediments consist of fine-grained, thin-bedded oxides, silicates, sulfides, sulfates, and carbonates, although two main sulfidic layers contain the bulk of the zinc and copper. The oxidized units contain geothite, Fe-montmorillonite, manganese oxides, and carbonate. Radiocarbon dating reported by Shanks and Bischoff (1980) indicates that the oldest sediments in the Deep were deposited about 28 000 years ago. In addition, a much slower sedimentation rate is indicated for the basal detrital-oxide-pyrite zone than for the overlying sulfidic, oxide, and silicate zones (Fig. 8.3).

Isotope and chemical studies of the hot brines (Craig 1969; Shanks and Bischoff 1977, 1980; Pottorf and Barnes 1983; Zierenberg and Shanks, 1988)

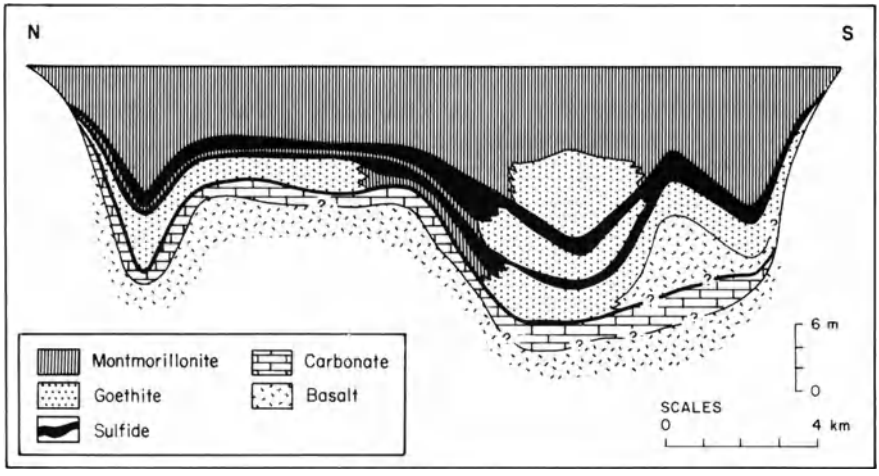

Fig. 8.2. Generalized cross-section of the geothermal deposits in the Atlantis II Deep, Red Sea. Note strong vertical exaggeration (After Hackett and Bischoff 1973)

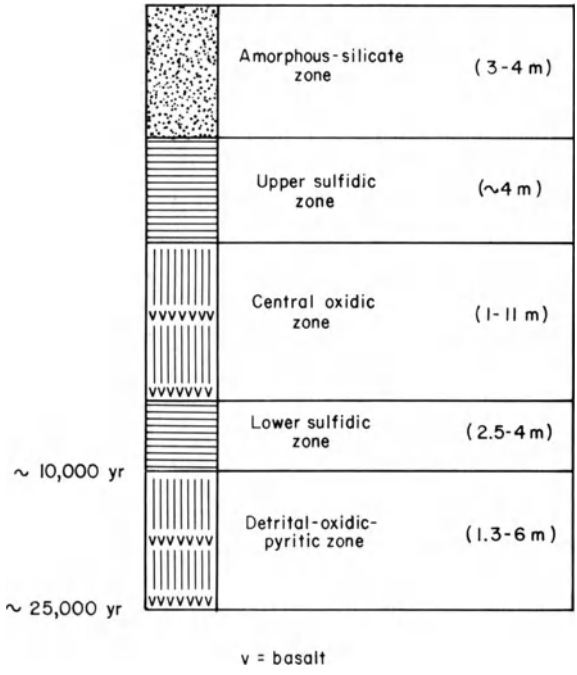

Fig. 8.3. Simplified lithostratigraphic sequence of Atlantis II Deep metalliferous sediments (After Backer and Richter 1973)

suggest that the metals and sulfide in the brines were transported by seawater that achieved enhanced salinity from circulation through Miocene evaporites. The heat to drive such convective circulation was probably derived from hot basaltic rocks in the slowly spreading axial zone, and such rocks are also a logical source for the base metals now concentrated in the sulfidic layers of the Atlantis II Deep sediments. The absence of significant amounts of zinc and copper in the sediments below other brine pools is probably due to the fact that circulating brines in those systems did not reach sufficiently high temperatures to effectively leach copper and zinc from the basaltic "basement". Some flux of juvenile material into these sites is, however, indicated by the very high He^3/He^4 ratios in the brine pools (Lupton et al. 1977). Studies of lead isotopes in the brine pool materials (Dupré et al. 1988) indicate that the lead present came from Miocene evaporites and not from underlying basalts.

8.2.2 Discussion

The slow spreading rate of the Red Sea and the presence of extensive evaporite beds in the sedimentary sections on both sides of the axial rift create a geologic setting that is not directly comparable to that of true oceanic spreading systems. Also, the lack of clear analogs of the Atlantis II Deep deposits in the geologic record in puzzling, despite the suggestion of Shanks (1977) that Besshi-type deposits may be representative of this type of mineralization. In this respect, it is instructive to consider the geologic future of these Red Sea deposits: whether the Red Sea continues to spread or not, the deposits lie approximately 250 km from a passive continental margin and would thus eventually be buried under a thick wedge of miogeoclinal sediments. It follows that their eventual reappearance at or near the surface would require a collision event at that continental margin. By that stage inevitably they would have suffered a certain degree of tectonism and metamorphism and their original setting would be obscure (Sawkins 1982a).

8.3 Sediment-Hosted Massive Sulfide Deposits

A number of world-class base metal deposits (Table 8.1) can be related, in terms of their lithologic settings, to the more advanced stages of continental rifting. Sawkins (1976c) suggested the name Sullivan-type deposits for this group of sediment-hosted massive sulfide ores, but in view of the variability exhibited by the different deposits that fall into this category, the more general term "sediment-hosted massive sulfide deposits" is preferable and has recently achieved wide usage (Large 1980; Sangster 1983). The deposits are massive to semimassive, conformable sulfide ores that occur most typically within marine shales or siltstones or their metamorphic equivalents. Volcanic materials are either minor or absent in the immediate host rocks, but carbonates and cherts are present in some cases.

Table 8.1. Sediment-hosted Pb-Zn massive sulfide deposits

Deposit or district	Age	Metal Composition[a]	Tonnage (10^6)	Host rocks	Reference
Lik, NW Alaska	Miss.	Zn,Pb	25+	Carb. shale, short	Forrest and Sawkins (1983)
Red Dog	Miss.	Zn,Pb	85+	Carb. shale	D.M. Moore et al. (1986)
Rammelsburg, Germany	Devonian	Zn,Pb,Cu	22	Carb. slates	Hannak (1981)
Meggen, Germany	Devonian	Zn,Pb	50	Carb. slates	Krebs (1981)
Macmillan Pass	Devonian	Zn,Pb	20	Carb., siliceous shale	Carne and Cathro (1982)
Gataga	Devonian	Zn,Pb	30	Siliceous pyrite shale	MacIntyre (1982)
Howards Pass	Silurian	Zn,Pb	?	Carb. sandstone, chert	Carne and Cathro (1982)
Anvil	Cambrian	Zn,Pb	140	Graphitic phyllite	Carne and Cathro (1982)
Sillivan, B.C.	Prot. (1.4)	Zn,Pb	155	Argillite	Ethier et al. (1976)
Mt. Isa, Aust. (Zn,Pb)	Prot. (1.65)	Zn,Pb	88.6	Carb. shale, dolomite	Mathias and Clark (1975)
Hilton, Aust.	Proterozoic	Zn,Pb	35.6	Carb. shale	Mathias et al. (1973)
Lady Loretta, Aust.	Proterozoic	Zn,Pb	8.6	Carb. shale	Loudon et al. (1975)
McArthur River, Aust.	Prot. (1.65)	Zn,Pb	190	Dolomite, shale	R.N. Walker et al. (1977)
Metamorphosed Equivalents					
Broken Hill, NSW	Prot. (1.7–2.0)	Pb,Zn	180	Felsic gneiss	Johnson and Klingner (1975)
Gamsberg, S. Africa	Prot.	Zn,Pb	93	Meta-pelites	Rozendaal (1980)
Big Syn, S. Africa	Prot.	Zn,Pb	101[b]		
Black Mountain, S. Africa	Prot.	Cu,Pb	82[b]	Mica schist	Ryan et al. (1982)
Broken Hill, S. Africa	Prot.	Pb,Zn	85[b]	Iron formation	

[a] Metals listed in order of decreasing abundance. Most deposits contain significant silver values.
[b] Grades in these deposits are low compared with the others listed.

8.3.1 Settings of Sediment-Hosted Massive Sulfide Deposits

The deposits tend to occur in settings characterized by thick to very thick sequences (5–15 km) of continentally derived clastics that are considered indicative of either intracontinental rifts or passive continental margins (e.g., Hoy 1982a). In both instances, there are linear zones of long-lived subsidence in which contemporaneous extensional faulting can be expected (Fig. 8.4).

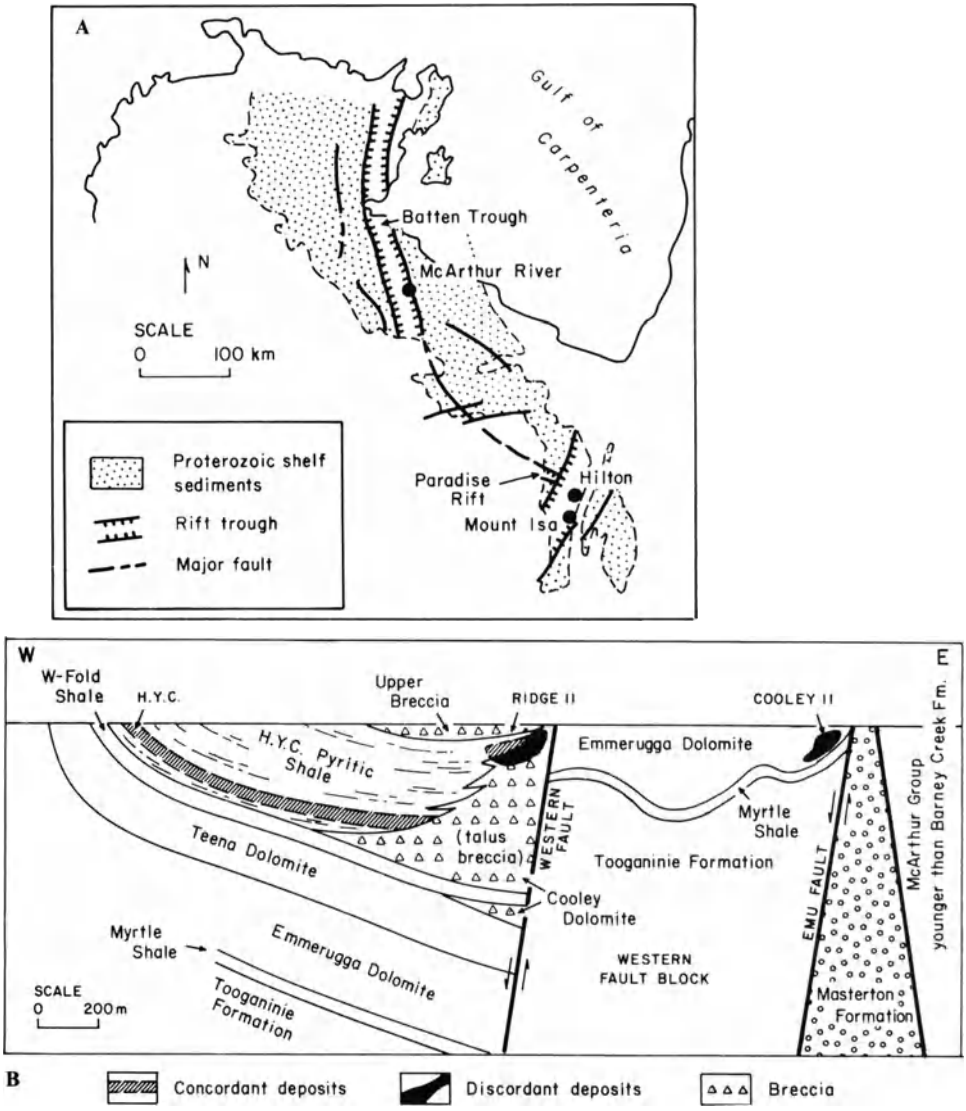

Fig. 8.4A. Map showing locations of Batten Trough, Paradise Rift, and the related sediment-hosted massive sulfide deposits of Mt. Isa and McArthur River (After Dunnet 1976). **B** Cross-section of the *H.Y.C.* and related carbonate replacement deposits associated with the Batten Trough, McArthur River (N. Williams 1978)

Large (1980, 1983) has suggested that the major first-order basins in which sediment-hosted massive sulfide deposits are generated form as either fault-controlled embayments in continental margins, or as intracratonic rift basins. The sedimentary facies manifest within such basins can be quite variable and include black shales, siltstones, carbonates, and turbidites (see Table 8.1). Within such first-order basins, second- and third-order basins tend to develop as a result of contemporaneous vertical tectonics during the period of first-order basin development. Proximity to the bounding structures of these first-, second-, and third-order basins is reflected by facies and thickness variations in the sediments and local intraformational breccias.

Although later deformation has generally rendered precise location of basin-controlling faults and hinge zones difficult, in most cases the massive sulfide deposits can be inferred to lie close to such structures (see Large 1980, pp.94–95; Krebs and Gwosdz 1985). The absence of deformation in the terrane that hosts the HYC deposit at McArthur River, Australia, makes this relationship particularly clear (Fig. 8.4B). It seems very probable that the basin-bounding structures were active at the times of mineralization, and thus may have exerted an important control on the plumbing systems utilized by the ore-generating fluids. Sibson et al. (1975) have suggested that seismic pumping, related to contemporaneous fault movements, is an important mechanism for promoting large-scale movement of hydrothermal fluids in such environments, and Sawkins (1984) noted that the stacked lens aspect of many major sediment-hosted lead-zinc deposits presumably reflects the episodic nature of earthquake-related basin-dewatering events (Fig. 8.5).

The relationship of major sediment-hosted deposits to rift environments is particularly apparent in the cases of Mt. Isa, Hilton and McArthur River deposits in Australia, and Dunnet (1976) has pointed out the position of the ore deposits in relation to major Proterozoic rift structures (Fig. 8.4). The Devonian, Atasu-type sediment-hosted massive sulfide deposits of central Kazakhstan (Shcherba et al. 1981) occur within dark shales, containing chert and carbonate units, deposited in troughs related to extensional tectonics. Stratiform lead-zinc ores of similar age also occur in China (Degi 1988).

The evidence for a rifting environment for Rammelsberg and Meggen, and other Paleozoic massive sulfide deposits in Europe, has been discussed by Sawkins and Burke (1980). More recently, Krebs (1981), Krebs and Gwosdz (1985), and Thein (1985) have suggested an environment of extensional block faulting during the formation of the Meggen ores (Fig. 8.6), and Hannak (1981) has emphasized the position of the Rammelsberg ore lenses on the hinge zone between the Goslar Trough and the Westharz Rise (Fig. 8.7). It is also noteworthy that both Rammelsberg and Meggen lie close to the hinge zone between the external shelf of the Old Red Continent to the northwest and a mid-Devonian trough to the south (Fig. 8.8). A rift setting for these deposits has been supported by detailed petrochemical studies of Hercynian basalts (Floyd 1982), but recent thinking on the paleoenvironment has focused on a complex backarc situation (Leeder 1987).

The question of water depth during formation of sediment-hosted massive sulfide deposits is largely unanswered and controversial. The presence of

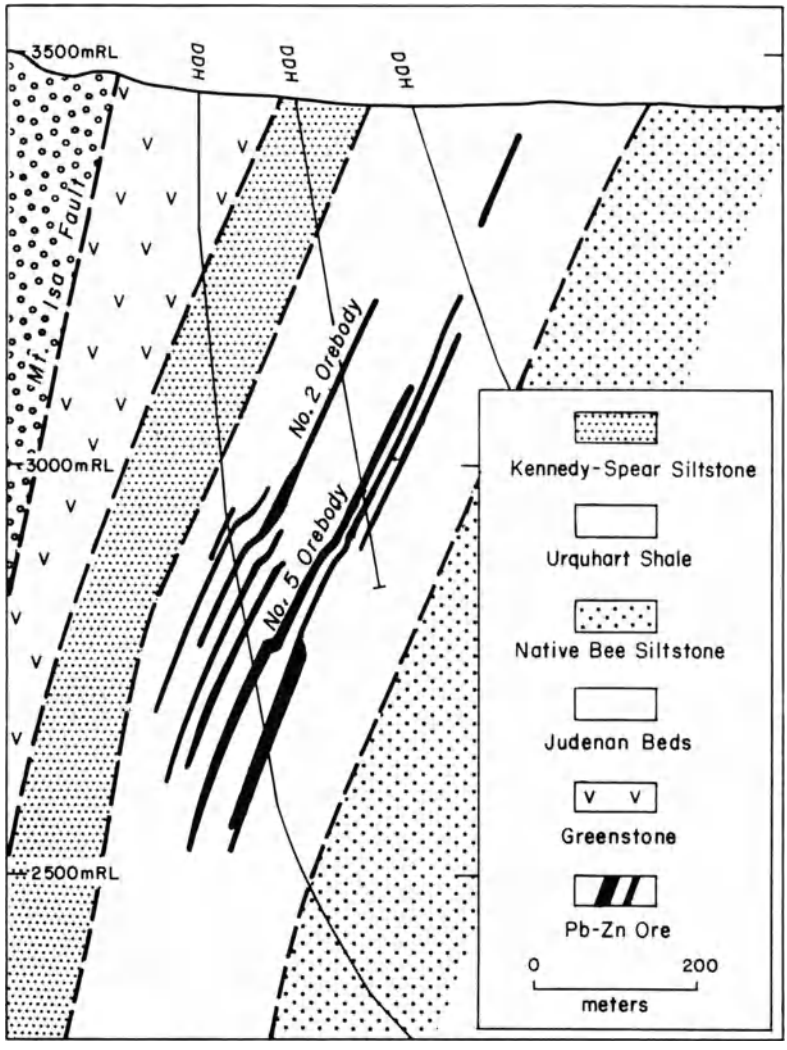

Fig. 8.5. Cross-section of the Hilton sediment-hosted, lead-zinc deposit near Mt. Isa, Queensland, to illustrate the stacked lens nature of many such deposits (After Sawkins 1984)

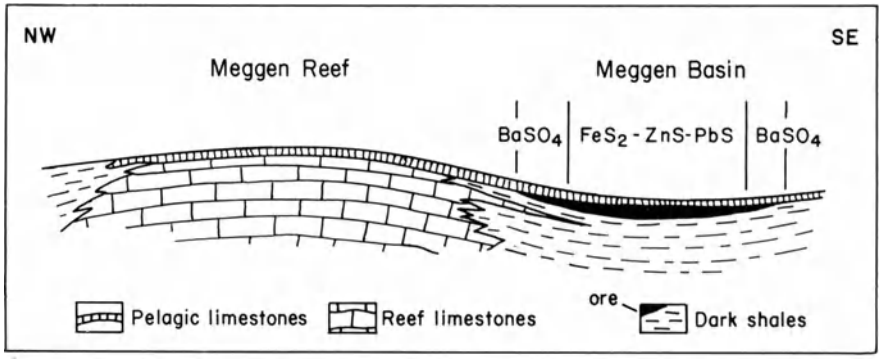

Fig. 8.6. Pre-orogenic position of the Meggen Basin and the Meggen Reef (After Krebs 1981)

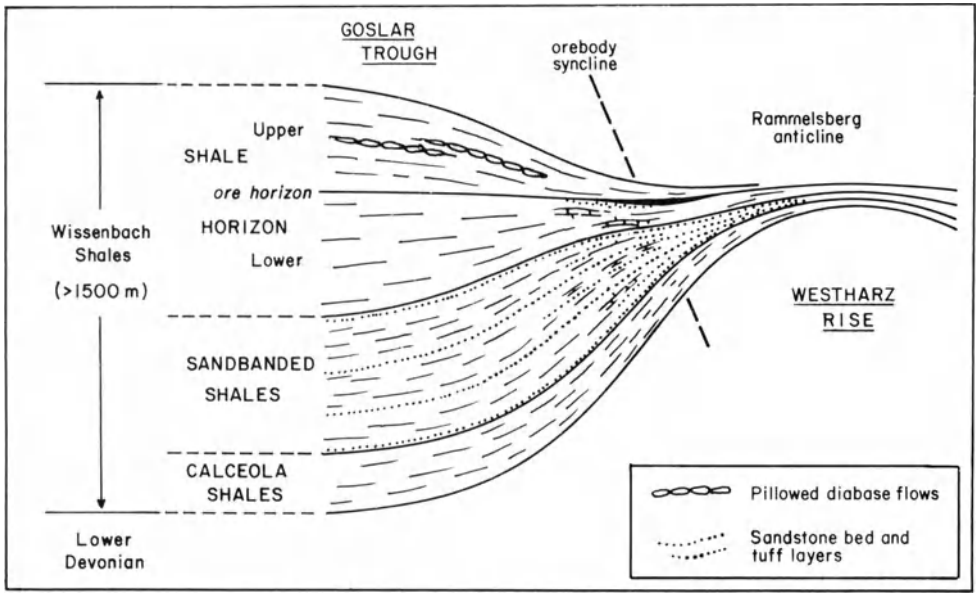

Fig. 8.7. Reconstruction of the structural and stratigraphic relationships pertaining to the Rammelsberg orebody, Harz Mountains, West Germany (After Hannak 1981)

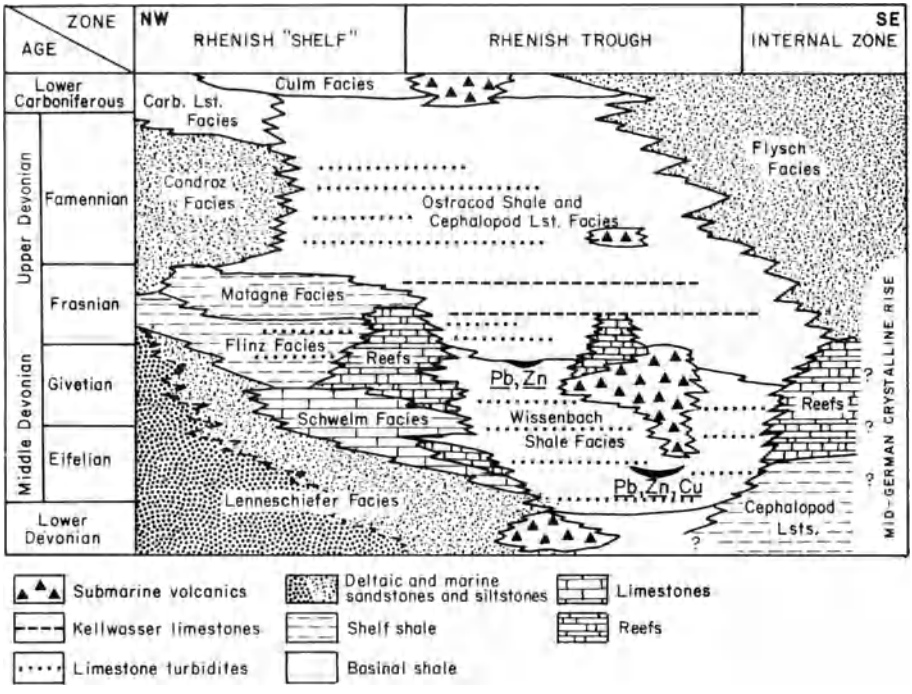

Fig. 8.8. Highly schematic section through the Devonian of the Rhenish Schiefergebirge showing facies relationships, and position of submarine volcanics and massive sulfide ores (After Krebs 1981)

stromatolitic dolomites in the host Barney Creek Formation at McArthur River suggests relatively shallow-water environments (Muir 1983), as does the evidence for evaporites in the Mt. Isa sequence (Neudert and Russell 1981). In all other examples of this type of deposit, no valid indicators of water depth are known, although Finlow-Bates and Large (1978) have pointed out that water depths must have been approximately 400 m or more to prevent boiling of the ore fluids and precipitation of metals prior to exhalation. The delicate banding present in some sediment-hosted massive sulfide ores certainly indicates the tranquil bottom conditions associated with deeper marine environments.

Despite their development in sedimentary sequences lacking significant volumes of volcanic material, it is demonstrable in many cases that some contemporaneous igneous activity was occurring in the general region during the formation of these ores. For example, felsic tuffite horizons have been recognized at Mt. Isa, McArthur River, Rammelsberg and Meggen (Large 1980) and, at Sullivan, intrusion of the Moyie Sills overlaps the time of ore formation (Ethier et al. 1976). No evidence for contemporaneous volcanism has yet been found in connection with the sediment-hosted massive sulfide deposits in the Selwyn Basin, but the sediments that host the Tom deposit are underlain by several mafic volcanic units (Dawson 1977). Overall, it seems clear that high geothermal gradients characterized the ore-forming environments.

8.3.2 Mineralization

Most sediment-hosted massive sulfide deposits consist of multiple stacked lenses of pyritic galena-sphalerite ore (see Fig. 8.5). The majority contain economically important amounts of silver, but virtually without exception they contain little or no copper or gold. The important copper orebodies of the Mt. Isa mine in Queensland are now viewed as the result of later, syntectonic hydrothermal activity (see Chap. 9). The lateral extent of mineralization is considerable in the larger deposits and ore zones can extend for several kilometers. At Mt. Isa and McArthur River, conformable mineralization occurs over a considerable vertical interval, 650 and 130 m, respectively. In such cases, shale beds are interlayered with massive or semimassive sulfides and, inasmuch as the shales at least must have accumulated relatively slowly, time periods over which intermittent mineralization occurred presumably totaled millions of years. This time span is in strong contrast to many volcanic-hosted massive sulfide deposits where indications are that mineralization occurred relatively rapidly. The iron and lead-zinc sulfides in sediment-hosted ores are typically fine-grained unless recrystallized as a result of metamorphism. Deformation, both syndepositional and postlithification, has in some deposits (e.g., Sullivan and Mt. Isa) produced spectacular fold and flowage structures in thinly banded massive sulfide ore (McClay 1982).

Certain sediment-hosted massive sulfide deposits have significant amounts of barite associated with them, and this is especially true of Paleozoic examples such as Meggen, Rammelsberg, Tom, and Red Dog. However, the

three very large Proterozoic deposits of sediment-hosted type, Sullivan, Mt. Isa, and McArthur River, lack barite. Chert horizons are also present in a number of these massive sulfide deposits and are particularly prominent in association with the ores in northwestern Alaska (Red Dog, Su-Lik), the Tom deposit, and at Lady Loretta and McArthur River in Australia. Oxygen isotope and crystallite size studies of the cherts in the Red Dog and Lik areas of northwestern Alaska (Harrover et al. 1982) have demonstrated that cherts near mineralization exhibit lower $\delta^{18}O$ values and larger crystallite size than cherts distal to mineralization.

Sediment-hosted massive sulfide deposits tend to exhibit zonation of metals in either lateral or vertical directions or both, and at Rammelsberg, for example, a well-defined vertical zonation from Cu → Zn → Pb → Ba has been demonstrated (Hannak 1981). At Sullivan, Mt. Isa, and McArthur River, a lateral zonation with increasing Zn/Pb ratios toward the margins of orebodies is manifest (see Large 1980, Table 9).

Some authors (e.g., Plimer 1978) have referred to sediment-hosted massive sulfide deposits as being of distal type, apparently in terms of their distance from volcanic or igneous centers. This usage is confusing; the terms "proximal" and "distal" should be used with reference to distances from exhalative centers, for in many instances it can be demonstrated that sediment-hosted massive sulfide deposits lie directly above the sites at which the hydrothermal fluids vented. This is certainly true for Sullivan (see Sect. 8.3.3). Furthermore, the siliceous kneist ores at Rammelsberg (Hannak 1981), the footwall alteration zones at Meggen (Krebs 1981) and Tom (Carne 1979), and the sphalerite veins at Red Dog (D.M. Moore et al. 1986) all suggest the presence of subjacent feeder zones. In all cases, breccia textures are associated with these zones.

8.3.3 The Sullivan Massive Sulfide Deposit, British Columbia

This important sediment-hosted metal deposit has been the subject of a number of recent studies (Ethier et al. 1976; F.A. Campbell et al. 1978, 1980), and excellent summaries of its geologic setting and features can be found in Hoy (1982a) and J.M. Hamilton et al. (1982, 1983). The Sullivan mine is located in the Purcell Mountains of southeastern British Columbia and its ores, together with several much smaller conformable massive sulfide deposits, occur within graywackes and argillites of the Lower Aldridge Formation. This unit occurs near the base of the exposed portion of the Purcell Supergroup, a very thick sequence of marine, predominantly clastic rocks that represents the equivalent of the Belt Supergroup in Montana and Idaho (Harrison 1972). Kanasewich (1968) has noted that the Sullivan deposit occurs close to the northern boundary of an east-west-trending, buried Precambrian rift structure that can be postulated on the basis of geophysical data.

Volcanic rocks in the Purcell Supergroup are restricted to the Purcell Lavas that occur at least 5000 m higher in the stratigraphic succession. The

Lower Aldridge, however, is copiously intruded by thick sills of basaltic composition (Edmunds 1973). In places these intrusions account for over half the measured section, and they appear to be concentrated in the general area of the Sullivan deposit. The age of emplacement of these Moyie Sills overlaps that of the emplacement of the Sullivan ores (~ 1.4 Ga, see Ethier et al. 1976, Fig. 3).

The orebody (Fig. 8.9), which contains a massive pyrrhotite lens up to 50 m thick in its western portion, consists mainly of massive to poorly banded lead-zinc ore, and is underlain by tourmalinized footwall conglomerate and breccia. At its eastern extremity, pyrrhotite is absent, and the ores consist of well-banded lead, zinc, and iron sulfides, in part interlayered with argillites. The tourmalinization and brecciation that are concentrated under the west end of the Sullivan deposit appear to extend at least 450 m below the sulfide ore lens (Jardine 1966). There is some tin mineralization in this area, and in places the massive exhalative ores also contain small amounts of tin. The footwall conglomerates (see Fig. 8.9), which are thought to have resulted from penecontemporaneous faulting and resultant slumping, attain a thickness of 60 m locally, and appear to have filled a newly created seafloor depression. A zone of intense albitization in the hanging wall, above the western

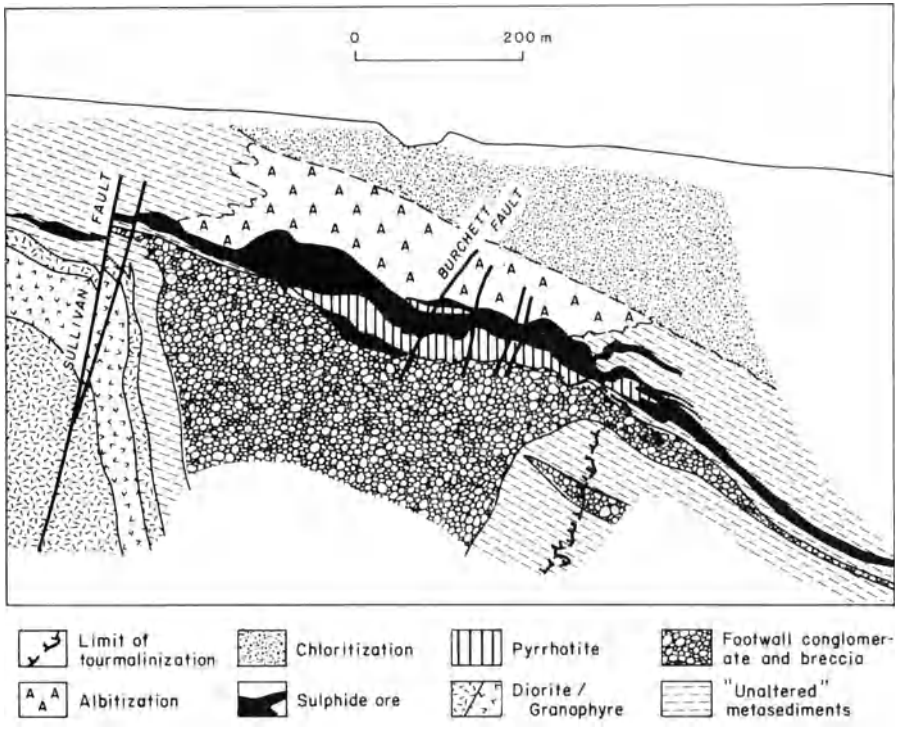

Fig. 8.9. Cross-section of the Sullivan lead-zinc orebody at Kimberley, British Columbia (Hoy 1982b)

portion of the ore lens, which caused many to view the deposit as epigenetic, is now thought to have been related to the emplacement of the postore Sullivan sill (Ethier et al. 1976).

Sulfur isotope studies of the Sullivan ores (F.A. Campbell et al. 1978, 1980) indicate a range in $\delta^{34}S$ of the sulfides from −10.4 to +4.7. These values exhibit variations both laterally and vertically through the ore lens, and are interpreted by the workers involved to indicate both higher temperatures during deposition of the iron sulfide-rich areas in the western portion of the orebody, and an increase in oxygenation of the ambient marine waters toward the final stages of sulfide deposition. They also conclude that the metals were transported by a dense sulfide-deficient brine at temperatures estimated at 150–200°C. The requisite H_2S for sulfide deposition is thought to have been produced under euxinic conditions in a local seafloor depression. It is noteworthy that a thin carbonaceous unit characterized by banded pyrrhotite occurs throughout the Purcell-Belt basin at the same stratigraphic level as the orebody (Huebschman 1973). This indication of widespread stagnant conditions suggests that the Lower Aldridge Formation accumulated in a basin related to rifting rather than along a continental slope, facing a large ocean.

Oxygen isotope studies of the Sullivan deposit (Nesbitt et al. 1984) indicate that little interaction occurred between the ore fluids and the surrounding sedimentary units. A synthesis of geologic, isotopic, and geochemical arguments suggests an early migration of low ($< 100°C$) temperature, boron-rich fluids that produced the tourmalinization at Sullivan and elsewhere in the Aldridge basin. Later fluids were hotter ($\sim 150°C$) and caused the deposition of the lead-zinc sulfides. The final hydrothermal event was the alteration of all units, including the hanging-wall sedimentary units, to produce the albite-rich alteration facies.

8.3.4 The Red Dog Zinc-Lead-Silver Deposit, Western Brooks Range, Alaska

One of the most significant discoveries of sediment-hosted massive sulfide ore in recent years is that of the Red Dog deposit in extreme northwestern Alaska (Fig. 8.10). Drilling has indicated Red Dog reserves to be 77 million tons of 17% Zn, 5% Pb, and 82 g/ton Ag (D.M. Moore et al. 1986). Furthermore, just 20 km to the west-northwest of Red Dog lies the Su-Lik deposit, which contains at least 50 million tons of zinc-lead-silver ore of somewhat lower grade (Forrest and Sawkins 1987). A number of other occurrences of sediment-hosted massive sulfide are known in the Mississippian-Pennsylvanian black shales of this area, which promises to become a major lead-zinc-producing district once the requisite infrastructure to permit mining and shipping of concentrate has been developed.

Structural studies in the De Long Mountains (Mayfield et al. 1983) have shown the presence of eight stacked and folded thrust sheets, six of which contain Devonian through Cretaceous sedimentary rocks and two of which contain Jurassic or older mafic and ultramafic igneous rocks. The host rocks of

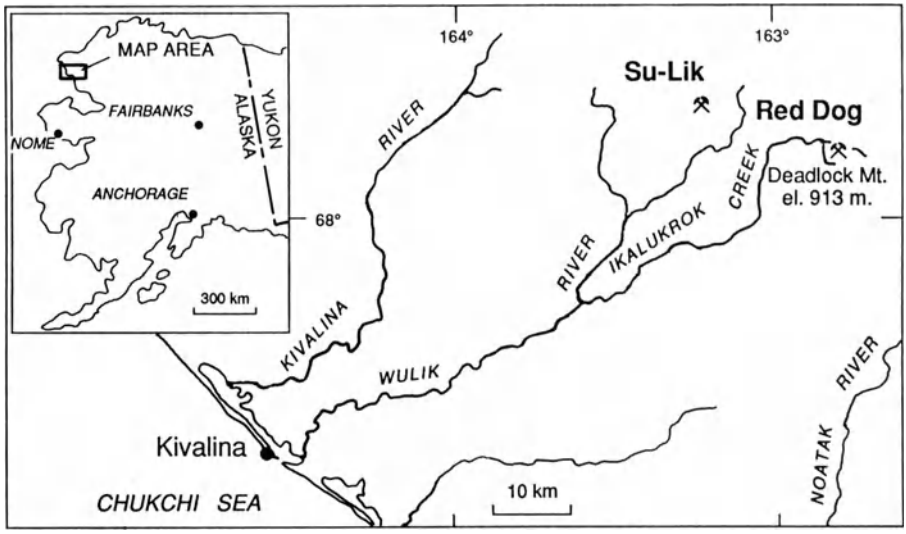

Fig. 8.10. Map showing the location of the important Red Dog and Su-Lik lead-zinc deposits in northwestern Alaska (After D.M. Moore et al. 1986)

the Red Dog deposit consist of a starved basin section of black shales, cherts, and lesser limestones, with the entire period of early Mississippian to early Cretaceous represented by a mere 400 m of continuous section (Fig. 8.11). This section overlies a much more robust fluvial-deltaic complex of Devonian age (Noatak Sandstone) and, based on observations elsewhere in the Brooks Range, a thick sequence of Paleozoic shales (Hunt Fork Shale; Mayfield et al. 1983).

The Red Dog deposit is contained in the upper portion of the Kuna Formation (Ikalukrok Unit, see Fig. 8.11), and consists of a stratabound accumulation of sulfides, siliceous material, and barite. The sulfides exhibit banding only locally, and predominant textures in the sulfides are massive or fragmental. The siliceous material occurs within and peripheral to the main sulfide concentration, and the barite is concentrated toward the top and periphery of the sulfide mass. Sphalerite, pyrite, marcasite, and galena, in that order of abundance, are the major sulfide phases. Boulangerite occurs in galena, and trace amounts of chalcopyrite and pyrrhotite occur within sphalerite. The fine-grained nature of the sulfides is ubiquitous except where coarse-grained, crustiform sphalerite feeder veins occur in the lower part of the system.

The structural complexity of the Red Dog deposit, with its stacked thrust slices is essentially similar to that of the structure of the De Long Mountains in general. However, restoration of the mineralized slices to their original positions indicates that the deposit contained a lead-zinc-rich central core surrounded by a halo with higher iron sulfide content.

Sulfur isotope data for sulfides and sulfates from the Red Dog deposit (Lange et al. 1980) indicate unusually light values for sulfide sulfur (−16.6 to

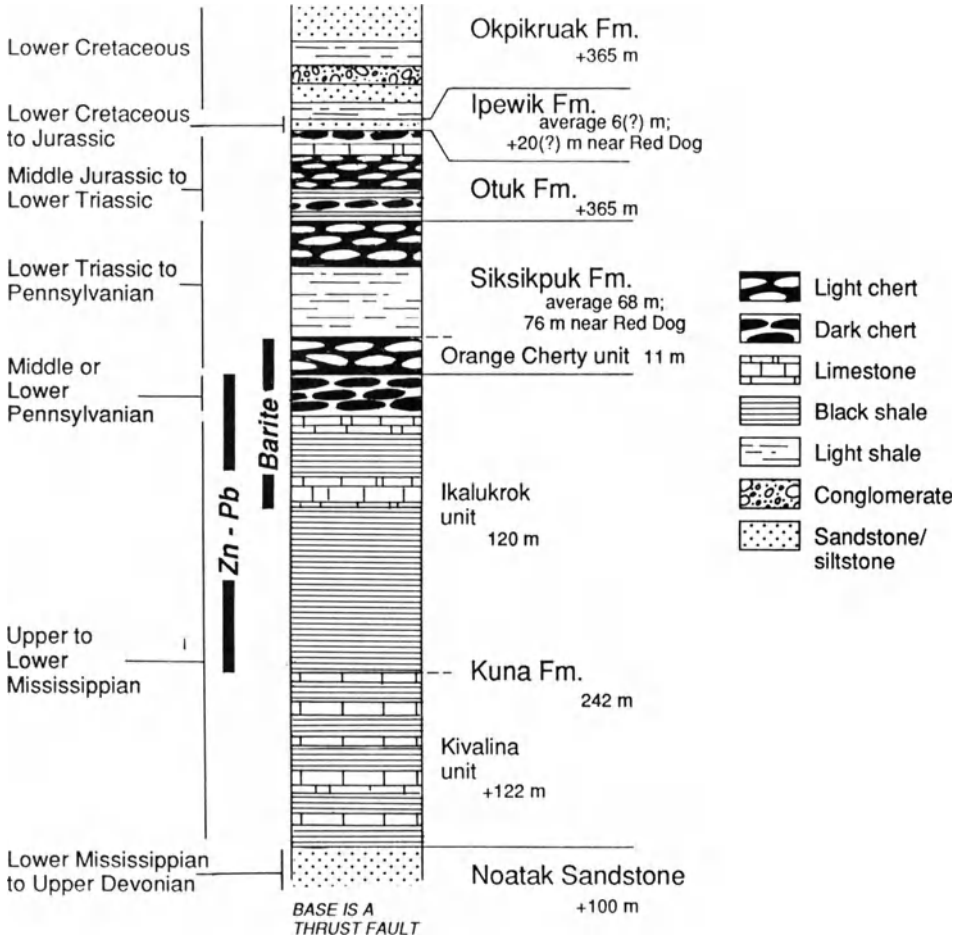

Fig. 8.11. Generalized stratigraphic column for the mineralized lithologic sequence in the DeLong Mountains, northwestern Alaska (After D.M. Moore et al. 1986)

+3.6%), which are in contrast to those reported by Forrest (1983) for sulfide from the nearby Su-Lik deposit and from analyses of basin-wide sulfides. These results suggest that the Red Dog deposit formed on the partially oxygenated flank of a Mississippian rift basin, whereas the Su-Lik deposit, with its greater development of finely laminated sulfide textures, formed within the deeper, anoxic parts of the basin (Fig. 8.12).

One particularly interesting feature of the Red Dog deposit reported by D.M. Moore et al. (1986) is the presence of a well-developed vent biota, particularly in the siliceous units, which exhibit similarities to the alvinillid worms observed around modern seafloor hydrothermal vents. This, and the overall stratiform aspect of the deposit, indicate an essentially syngenetic origin for the mineralization, but it is clear from the massive texture of much

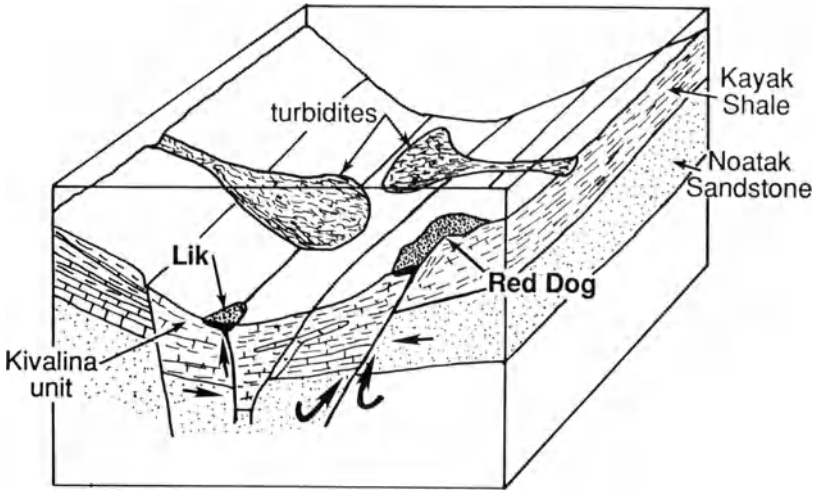

Fig. 8.12. Conceptual model illustrating the relative positions of the Red Dog and Lik deposits within a late-Paleozoic rift basin (After D.M. Moore et al. 1986)

of the deposit that a considerable amount of replacement of either sedimentary or exhalative material must have occurred prior to the cessation of metallization.

In genetic terms, this important deposit seems to fit admirably into the basin-dewatering model. D.M. Moore et al. (1986) note that disseminated pyrite, lesser galena, and rare sphalerite are widespread in the Noatak Sandstone underlying the mineralized black shales. This unit would have served as an aquifer to transmit basinal fluids from underlying shale packages (Hunt Fork Shale) that are widespread in northern Alaska. The trigger mechanism for initiation of dewatering events in this area is still not clear, but could have involved igneous events or, more likely perhaps, tectonic events involving continental margin accretion (see next chapter).

8.3.5 Discussion and Suggestions for Exploration

The considerable size of many sediment-hosted massive sulfide deposits and their relative rarity suggests that a rather special combination of circumstances is required for their generation. Although the precise origins of the metals and ore fluids involved in their genesis remain obscure, the size and protracted mineralization intervals indicated for these deposits are such that metal-rich formation waters represent the only logical candidate for the fluids involved in ore generation (Badham 1981; Large 1983; Lydon 1983, 1986). In addition, it seems clear that efficient plumbing systems and heat sources must have been available for long periods of time during their formation. The logical explanation for these parameters are the normal faulting and emplacement of

mafic magmas at deeper levels that characterize active rifting environments. With regard to the latter, not only are the rocks of the Lower Aldridge Formation copiously intruded by sills in the Sullivan area, but at Mt. Isa the sedimentary units below the sulfide ores contain numerous north-south-trending basaltic dikes.

Carbonaceous units containing syngenetic iron sulfides mark stratigraphic levels at which sediment-hosted massive sulfide deposits tend to occur in many basins related to the advanced stages of rifting. In the case of the Selwyn Basin, Goodfellow and Jonasson (1984) have demonstrated from analyses of sulfur isotopes in barites and sedimentary pyrites that a series of basin-wide stagnation and ventilation events took place during Paleozoic sedimentation (Fig. 8.13). Furthermore, the timing of formation of stratiform lead-zinc ores correlates most closely with major stagnation events. Euxinic bottom conditions will certainly favor preservation of exhalative sulfide ores, but they may be a common result of the faulting that creates both subbasins within rift environments and critical plumbing for the ore fluids. Whether euxinic environments produced by stagnation events are mandatory in terms of the supply of reduced sulfur is not clear. It is clear, however, that the results of Goodfellow and Jonasson (1984) have important implications in terms of mineral exploration, whether anoxic events are important in terms of availability of reduced sulfur, or merely reflect episodes of active rifting and

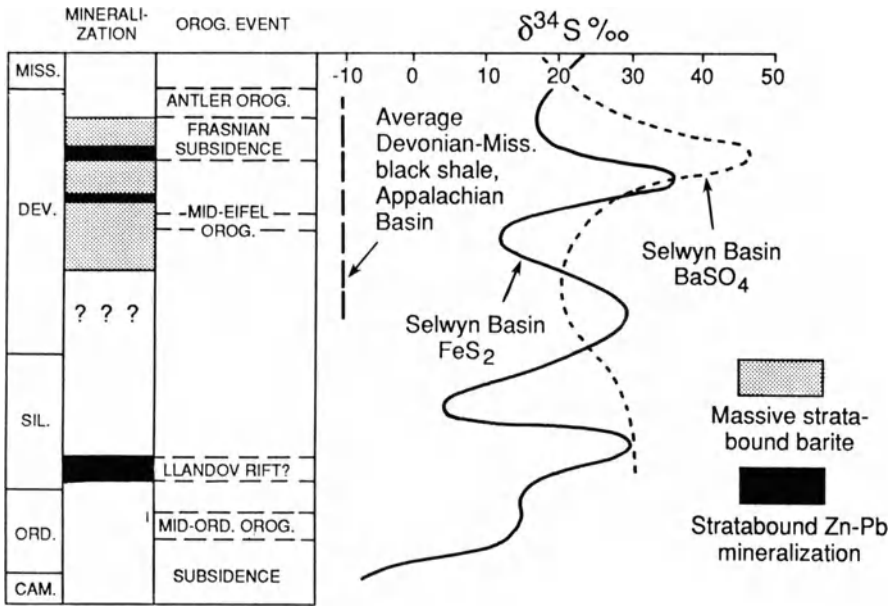

Fig. 8.13. Relationship of $\delta^{34}S$ values in disseminated pyrite and barite compared to stratigraphic position in the units of the Selwyn Basin northwestern Canada. Note that both major periods of massive sulfide mineralization are marked by strongly positive $\delta^{34}S$ values in rock pyrite (After Goodfellow and Jonasson 1984)

consequent deepening of rift basins. Episodic tectonic activity is also reflected by the intraformational conglomerates associated with many sediment-hosted massive sulfide deposits of this type.

Despite increased understanding of the environments and genetic systems that give rise to sediment-hosted massive sulfide deposits, most of the more recent discoveries of these deposits, such as those in northwestern North America, have resulted from the utilization of applied geochemistry, followed by application of exploration geophysics and drilling.

8.4 Massive Sulfide Deposits in High-Grade Metamorphic Terranes

8.4.1 General Comments

A significant proportion of the world's reserves of zinc and lead occur in stratiform massive sulfide bodies hosted by amphibolite- and granulite-grade metamorphic rocks. For a long time these ores were poorly understood in genetic terms, but with advances in our understanding of the setting in which sediment-hosted stratiform lead-zinc ores form, it is now clear that the majority of these deposits in high-grade terranes are merely their metamorphosed equivalents. This is of significance to the exploration geologist for it opens up major tracts of high-grade metamorphic terrane that were considered formerly to be barren of sulfide mineralization (Sawkins 1986b). Major examples include the huge lead-zinc sulfide lodes of Broken Hill, New South Wales (Johnson and Klingner 1975), and large tonnages of massive sulfide ore in the Proterozoic Namaqua Metamorphic Complex in South Africa (Tankard et al. 1982). The conformable ores in high-grade metamorphic rocks along the Singhbum Shear Zone in India (Banerji 1981) are presumably also of this type.

8.4.2 The Lead-Zinc Orebodies of Broken Hill, New South Wales

The orebodies at Broken Hill originally contained 180 million tons of ore grading 0.2% Cu, 11.3% Pb, 9.8% Zn, and 175 g/ton Ag (Gustafson and Williams 1981), and represent the greatest economic concentration of these metals known. The metamorphic rocks that host the lead-zinc-silver orebodies consist of a series of felsic gneisses containing lesser amounts of amphibolite and local iron formation. Detailed investigations of the structural complexities in the area (Laing et al. 1978; Marjoribanks et al. 1980) led to recognition of three major episodes of deformation, the earliest of which produced regional-scale, isoclinal, recumbent folds and a high-grade metamorphic axial-planar fabric. As a result of this folding, large domains of overturned stratigraphy were produced. Subsequent deformations produced mainly upright fold sets at various scales, and finally a series of retrograde schist zones were developed that divided the Broken Hill Block into a number of subblocks.

In recent years, considerable attention has been focused on the stratigraphy of the sequence of units (the Willyama Supergroup) exposed in the Broken Hill and adjacent Proterozoic structural blocks (Willis et al. 1983; Wright et al. 1987; Haydon and McConachy 1987). The Willyama Supergroup has been divided into eight suites totaling an estimated aggregate thickness of 5 to 6 km (Fig. 8.14). Some investigators of the sequence (e.g., Laing et al. 1984) have postulated a major felsic volcanic component to the original rocks, especially at the level of the lead-zinc lodes, but more recent work (Wright et al. 1987; Haydon and McConachy 1987) indicates that the succession is made up almost entirely of shales, siltstones, and sandstones, with the exception of some basaltic sills (now amphibolites) in the lower groups. The critical evidence cited for this conclusion involves both zircon morphologies, and major-element analysis of several 1000 whole-rock samples.

The six ore lenses at Broken Hill are stacked approximately one above another, and form a mineralized zone 7.3 km long, 850 m wide, and 250 m thick

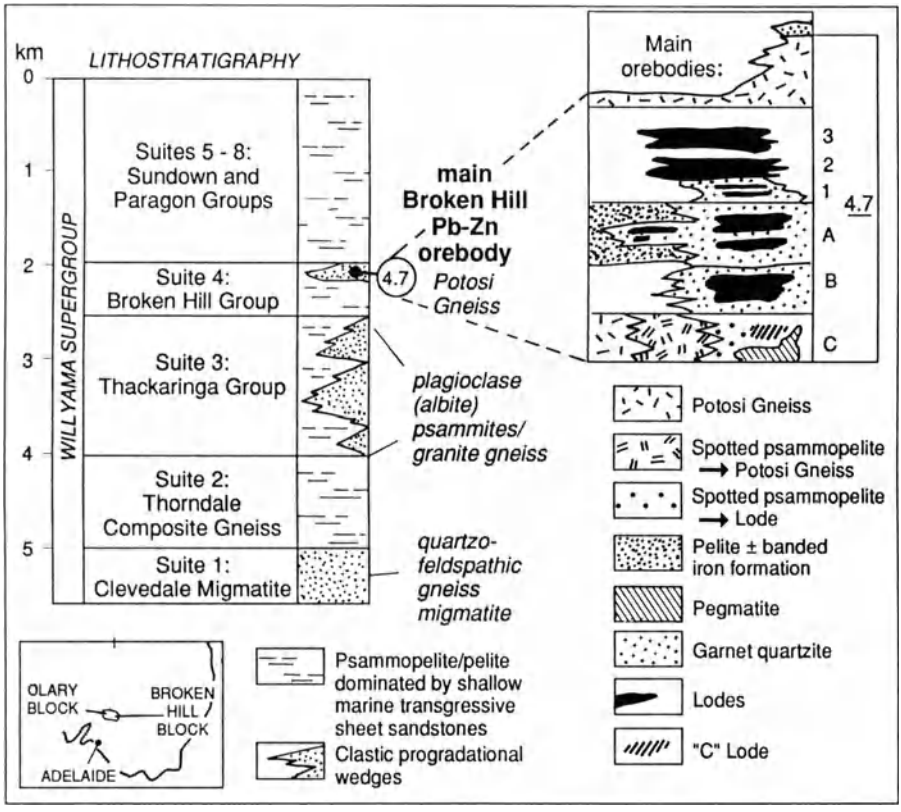

Fig. 8.14. Lithostratigraphy of the Willyama Supergroup, and details of the uppermost parts of Suite 4, the Broken Hill Group that hosts the Broken Hill Pb-Zn orebodies (After Wright et al. 1987). Note that a clastic sedimentary protolith is presumed, a position not shared by all Broken Hill geologists

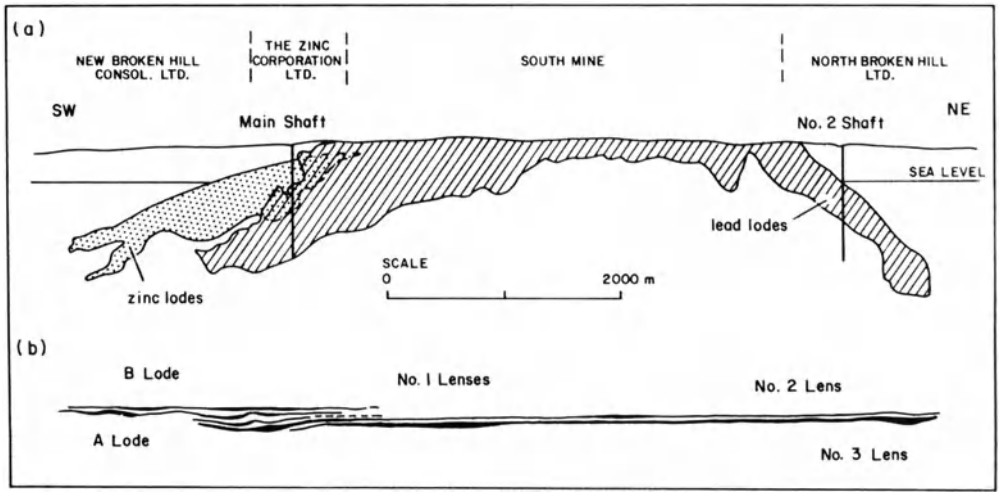

Fig. 8.15. Longitudinal projection of the Broken Hill ore deposit (**a**) and longitudinal projection through unfolded orebodies (**b**) (After Johnson and Klingner 1975)

(Fig. 8.15). Intensive exploration in the Broken Hill and surrounding Blocks has failed to uncover any ore of significance outside of this richly mineralized zone. The immediate host rocks to the lode horizon consist of coarse blue-quartz granite, garnet quartzite, sillimanite gneiss, concordant pegmatite, and garnet sandstone. The load horizon occurs at the top of suite 4 (see Fig. 8.14) and is associated with "Potosi"-type gneiss and local iron formation. The remaining, lower sequences of suite 4 consist of interbedded pelitic and psammitic metasediments and amphibolite layers.

The gangue mineralogy and typical mining grades of the six ore lenses are summarized in Table 8.2. Ore mineralogy is relatively simple, with galena and iron-rich (~ 10 wt% Fe) sphalerite dominating. Silver occurs in galena, tetrahedrite, dyscrasite, and as the native metal, and pyrrhotite and chalcopyrite are minor constituents. Minor copper, gold, antimony, and cadmium are also recovered from the ores. Uranium-lead and lead-lead isotope studies (Gulson 1984) have established an age of 1663 Ma for granulite metamorphism at Broken Hill, and suggest either a second metamorphic event at 1595 Ma, or an extended (~60–70 Ma) period at high temperatures for the rocks and ores prior to cooling. This latter scenario would provide an explanation for the extremely coarse textures that characterize the Broken Hill ores.

Genetic theories regarding this giant Proterozoic metal deposit have run the gamut from hydrothermal replacement to volcanic exhalation, but it is now recognized that metal-bearing basinal brines were generated within the lower units of the Willyama Supergroup at about the time the sand and shale precursors of the Broken Hill Group were accumulating. These brines migrated upward across the stratigraphic sequence along rift faults, and either exhaled into seafloor depressions or, as suggested recently by Wright et al.

Table 8.2. Mineralogy and grades of the six orebodies that constitute the Broken Hill massive sulfide deposit

Orebody	Gangue mineralogy	Typical mining grade %Pb	g/t Ag	%Zn	%Cu
Zinc lodes					
"C" Lode	Quartz, garnet, biotite, gahnite Manganoanhedenbergite, clinozoisite, actinolite, tremolite	3	25	7	0.17
"B" Lode	Quartz, feldspar, garnet, apatite, gahnite damourite, rhodonite, calcite manganoanhedenbergite	5	30	17	0.20
"A" Lode	Rhodonite, manganoanhedenbergite, quartz, garnet, calcite, cummingtonite	4	30	10	0.12
Lead lodes					
No. 1 Lenses	Quartz, calcite, wollanstonite, bustamite	8	50	20	0.09
No. 2 Lens	Calcite, rhodonite, bustamite, manganoanhedenbergite, knebelite, roepperite, quartz, garnet, fluorite, apatite, jacobsite	14	100	11	0.14
No. 3 Lens – S.W.	Quartz, fluorite, rhodonite, garnet	11	180	13	0.14

After Operations Handbook (1983) Australian Mining and Smelting Ltd.

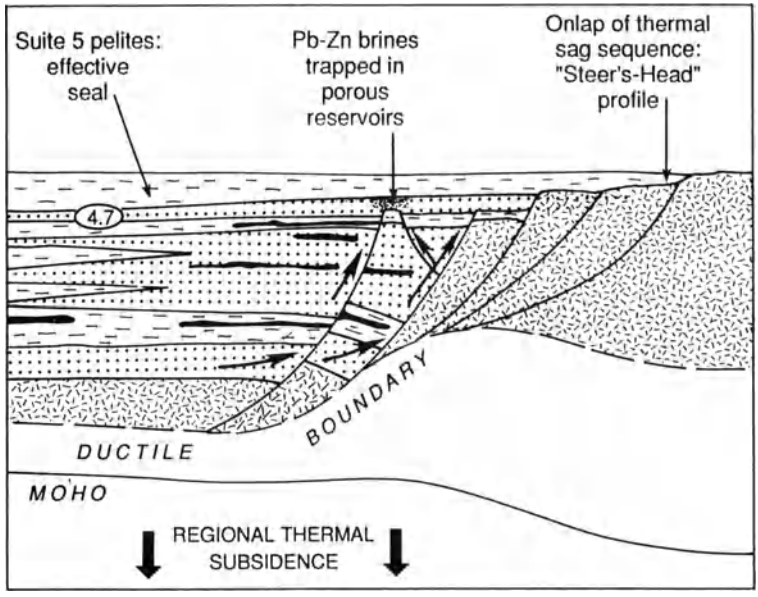

Fig. 8.16. The genetic concept of Wright et al. (1987) for the formation of the Broken Hill orebodies. Whether the orebodies formed within porous sandbodies, as they suggest, or were truly exhalative is secondary to the central concept of metal transport by basinal brines

(1987), mineralized porous sandstone bodies beneath the seawater interface (Fig. 8.16). These authors see a number of critical factors converging to allow the formation of this huge metal concentration. These factors include the timing of brine generation, the availability of both across-basin aquifers and cross-strata basin-margin fault pathways, the presence of highly porous reservoir sands adjacent to growth faults, and some chemical trap (? subinterface reducing conditions) to induce deposition of sulfides.

8.4.3 Additional Examples of Massive Sulfide Deposits in High-Grade Terranes

Almost 300 million tons of massive sulfide ore have been discovered in recent years in the Namaqualand Metamorphic Complex, South Africa. Previously, the only significant sulfide ores known from this terrane were the disseminated copper ores present in noritoid lenses in the O'Kiep district at the western extremity of this high-grade metamorphic belt (Fig. 8.17). At the eastern end of the belt is the Copperton deposit containing 47 million tons of ore grading 1.7% Cu and 3.8% Zn, with only minor lead (Wagener 1980). Lead isotope systematics indicate an age of 1.35 Ga for this deposit (Koeppel 1980), which occurs in a quartz-rich horizon that is probably metachert. Carbonates and calc-silicates are also closely associated with the sulfides, as are mica-rich

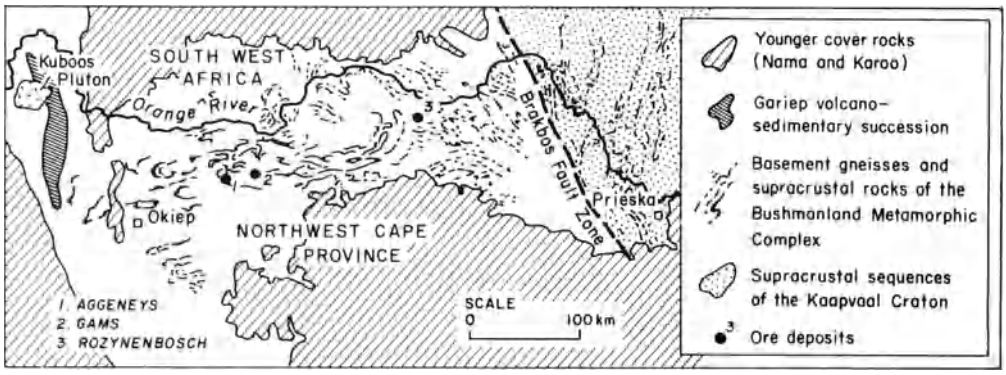

Fig. 8.17. Generalized map of Namaqualand and Bushmanland metamorphic complexes showing localities of major massive sulfide deposits and the O'Kiep copper district (After Anhauesser and Button 1974)

zones. Although Middleton (1976) concluded on textural evidence that the surrounding rocks were largely metavolcanics, Wagener (1980) and Wagener and Van Schalkwyk (1986) demonstrate that the lithosetting prior to metamorphism was more likely one of fine-grained clastic and chemical sedimentary rocks. At Aggeneys, farther west, 200 million tons of massive Cu-Pb-Zn-Ag sulfide ore, present as three orebodies, have been discovered. Unfortunately, further details on this important district have yet to be published.

The Gamsberg deposit (see Fig. 8.18) contains 143 millions tons of zinc ore grading 7.41% zinc and 0.55% lead (Rozendaal 1980; Rozendaal and Stumpfl 1984). Here, as elsewhere in the Namaqualand terrane, the host rocks and ores have been subjected to polyphase deformation and medium- to high-grade metamorphism. The sulfides are associated with the Gams Iron Formation, which exhibits lateral oxide through carbonate to sulfide transitions. In addition, graphite, manganese carbonates, and barite are present in the ore, which occurs as a steeply dipping lens (Fig. 8.18) within an overturned syncline. Rozendaal (1980) interprets the various felsic gneisses in the footwall as originally having been an upward-fining sequence of arkose, quartzite, and shale deposited in a restricted basin without significant volcanic components. These units were succeeded by chemical sediments that mark the time of ore deposition (Moore 1980). If this reconstruction is correct, then the environment was not atypical of those in which less-metamorphosed sediment-hosted massive sulfide deposits formed.

An additional important example of stratiform sediment-hosted, lead-zinc ore in high-grade metamorphic rocks is the Balmat-Edwards deposit in northwestern New York State (deLorraine and Dill 1982). The zinc-rich ores occurred as stacked lenses in a sequence of strongly deformed dolomitic and layered silicate-rich marbles that also host lenses of anhydrite. This sequence of metamorphic rocks forms part of the mid-Proterozoic Grenville Series, a

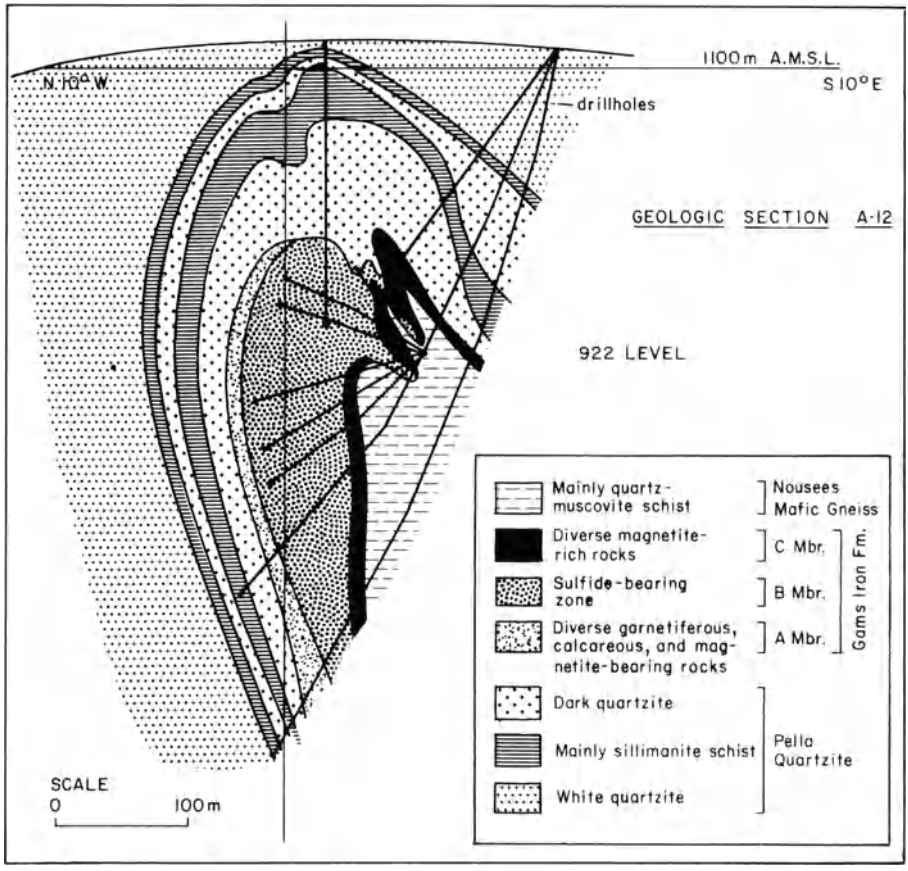

Fig. 8.18. Cross-section of the Gamsberg orebody, northern Cape, South Africa. Note association of sulfide zone with iron formation and calcareous metasediments (After Rozendaal 1980)

sequence of 5 to 6 km of marbles and paragneisses with minor amphibolites and quartzite. On the basis of isotope studies, Whelan et al. (1984) concluded that the anhydrite lenses were of evaporite origin and that the sequence of units in which they occur was deposited in a rift basin.

The orebodies at Balmat-Edwards are massive, tabular to podiform, and in most places conform to the metastratigraphy. Individual ore lenses range from 5 to 15 m in thickness, 15 to 240 m in strike length, and can extend for hundreds of meters down-plunge. Pyrite, sphalerite, and galena are the principal sulfide minerals, and only very minor amounts of chalcopyrite and pyrrhotite have also been identified. Gangue in the ore is composed of admixed rock fragments, massive quartz, calcite, and local barite, and textural relationships between ore and gangue are typical of those recognized to be the result of metamorphism (Vokes 1969; Stanton 1972).

The isotope studies of Whelan et al. (1984) have demonstrated that the $\delta^{34}S$ values of sphalerites from the orebodies all lie very close to +15‰, whereas the $\delta^{34}S$ values of anhydrites vary from +8 to +30‰, although values for anhydrite associated with sulfides are restricted to a 25.6 to 27.0‰ range. Whelan et al. (1984) interpret their data to indicate that the ore fluids were evolved basinal brines similar to Mississippi Valley-type ore fluids. These fluids must have been generated in episodic fashion to account for the sporadic ore horizons over 600 m of carbonate stratigraphy.

8.5 Rift-Related Mississippi Valley-Type Deposits

As noted in the next section, most major Mississippi Valley-type (MVT) ore districts can be viewed best in terms of tectonic settings linked to collisional events, and a full treatment of their main characteristics will be given there. However, certain examples appear to have formed in advanced rift settings without any relationship to collisional orogeny. Furthermore, MVT mineralization is now being discovered along passive continental margins, and these are best treated as former environments of advanced rifting type.

8.5.1 Mississippi Valley-Type Deposits in Advanced Rifting Environments

Clear examples of MVT deposits that formed in rift settings (Fig. 8.19) are provided by the minor lead deposits in Miocene sedimentary rocks along the Red Sea coast of Egypt (Dadet et al. 1970; El Aref 1984), and the more

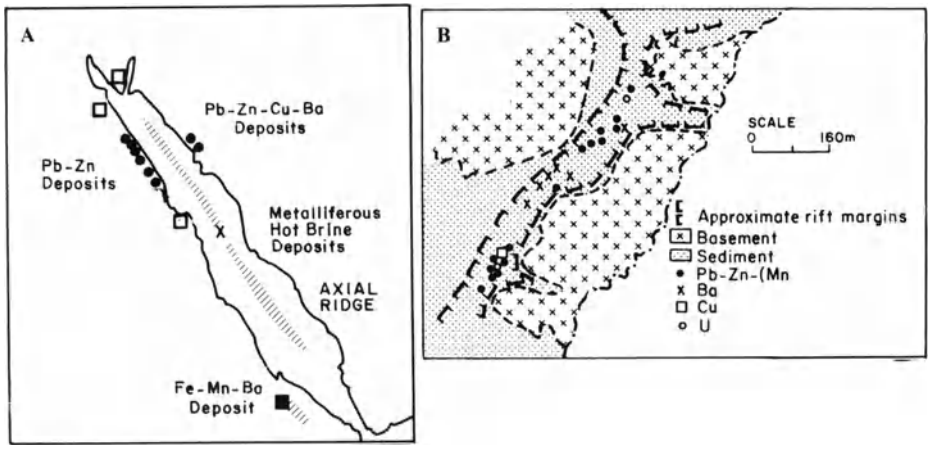

Fig. 8.19. Distribution of Mississippi Valley-type and manganese deposits adjacent to the Red Sea and within the Benue Trough rift systems. These are perhaps the best examples of a relationship between rifting and generation of Mississippi Valley-type deposits (After Olade 1980)

substantial lead-zinc deposits along the axis of the Benue Trough, Nigeria (Farrington 1952; Grant 1971; Akande et al. 1988). Recent studies of these latter deposits in Nigeria (Akande et al. 1988) have shown them to be of typical Mississippi Valley type. The lead-zinc-fluorite-bearing veins are hosted by Lower Cretaceous carbonate units that overlie several 1000 m of feldspathic sandstones and sandy clays.

MVT lead-zinc mineralization in advanced rifting environments is mainly in the form of veins, but some stratiform bodies and porosity infillings are known. Mineralogy of the deposits is simple, with galena and sphalerite accompanied by lesser tetrahedrite and rare native silver. Marcasite and chalcopyrite occur in minor amounts, and the gangue minerals are quartz and fluorite. Fluid inclusion studies (Olade and Morton 1985; Akande et al. 1988) confirm the presence of typical MVT fluids with temperatures in the 100–150°C range and salinities that average 20 wt% alkali chlorides. Eutectic temperatures observed during freezing studies indicate a high $CaCl_2$ content for the brines. These deposits provide a good example of mineralization by fluids derived by dewatering of a relatively thick succession of clastic sediments deposited in a rift. Cretaceous magmatism (Umeji and Caen-Vachette 1983) may have been a causative factor for dewatering events.

The series of lead-zinc deposits hosted by mid-Triassic carbonate units in the eastern Alps (Maucher and Schneider 1967) have come to be known as Alpine-type deposits, and essentially similar deposits also occur in the Atlas Mountains in northern Africa. These deposits appear to be of fairly typical Mississippi Valley-type affiliation, but their tectonic setting can be related to widespread rifting events in the area.

From early Triassic times until the early Cretaceous the Mediterranean area was characterized by a series of continental rifting events, followed by oceanic rifting (D'Argenio and Alvarez 1980), and although the precise ages of Alpine-type lead-zinc mineralization are not known, the deposits must have formed during this time interval. Furthermore, they typically occur in reef or back-reef facies carbonate units that developed on highstanding crustal blocks adjacent to deep shale basins (Fig. 8.20), and it appears probable that fluids migrating upward from these basins to the adjacent reefs formed the deposits. While more remains to be learned about these deposits, they do appear to represent a good example of carbonate-hosted MVT deposits generated in an environment characterized by rifting.

8.5.2 Mississippi Valley-Type Mineralization at Passive Continental Margins

A surprising variant of MVT mineralization involving the emplacement of lead-zinc sulfides in the cap rocks of salt domes has come to light recently (Rouvier et al. 1985; Kyle and Price 1986). Such base metal sulfide occurrences have been reported from Southern Europe, North Africa, and in the cap rocks of 16 salt domes along the Gulf Coast of the southern United States, and in the

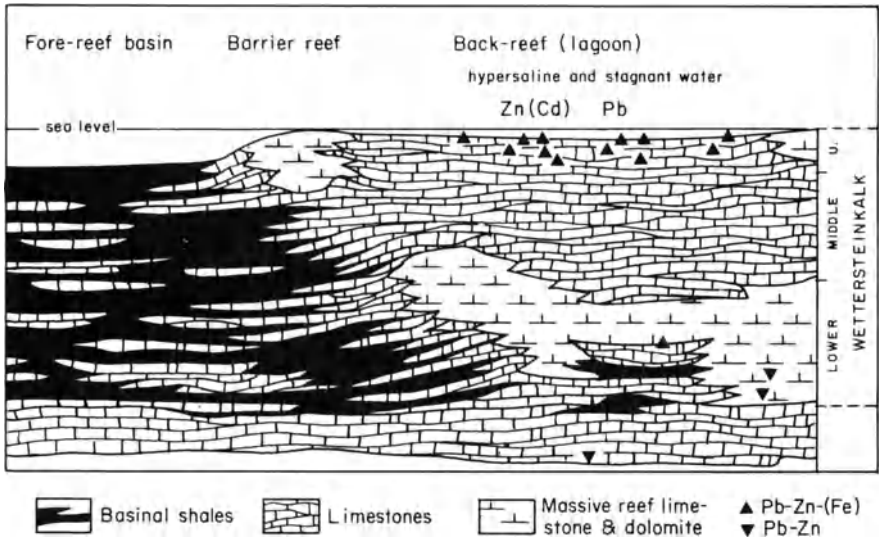

Fig. 8.20. Generalized cross-section illustrating geologic setting of many of the Alpine lead-zinc deposits (Simplified from Maucher and Schneider 1967)

case of the Hockley Dome in south-central Texas (Fig. 8.21) a multimillion ton Zn-Pb-Ag resource has been identified (Kyle and Price 1986). Saline formation waters enriched in lead and zinc have long been known to occur in Gulf Coast sedimentary units (Carpenter et al. 1974) and, as noted earlier, such waters are now widely accepted as the ore fluids responsible for both stratiform sediment-hosted lead-zinc deposits and Mississippi Valley-type deposits.

Along the Gulf Coast and offshore, literally hundreds of salt diapirs have intruded upward through Cretaceous and younger rocks from the thick Middle Jurassic Louann Salt. Many of these structures form foci for oil and gas accumulations, but in addition a number of the shallow domes with well-developed cap rocks are mined for sulfur. The presence of base metal sulfides in some of these attracted little attention until Price et al. (1983) and Kyle and Price (1986) reported their findings. The geologic relationships at the Hockley Dome (Fig. 8.21) indicate that deposition of lead and zinc sulfides can take place in a ring around the anhydrite portion of the cap rock and along fracture-controlled pathways within the anhydrite. Some replacement of carbonate rocks in the upper portions of the cap rock system also takes place, and barite is preferentially concentrated at this higher level.

The significance of salt dome-related Pb-Zn-Ag mineralization at this point in time is the confirmation of the mineralizing potential of certain oil field brines and related formation waters. It would appear that such fluids can develop within any thick accumulation of detrital sedimentary rocks that includes rift-related evaporite sequences (see Burke 1975).

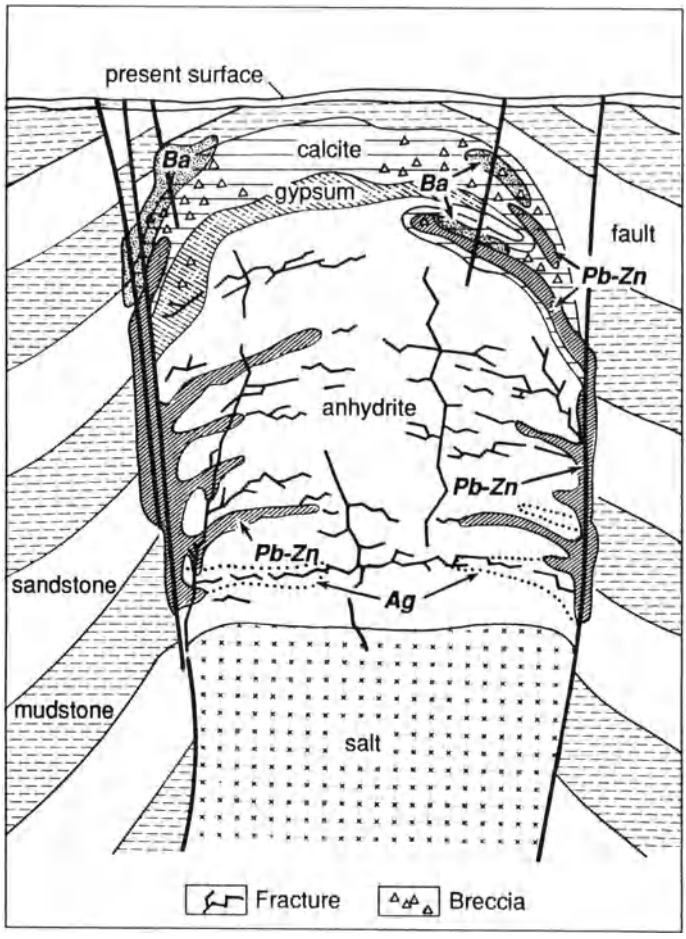

Fig. 8.21. Diagrammatic cross-section of a mineralized salt dome, based on the Hockley Dome, Texas (After Kyle and Price 1986)

8.6 Additional Facets of Rift-Related Metallogeny

In places where continental rifting leads to successful ocean-opening events, the newly created spreading-ridge system gradually retreats from the adjacent young continental margins. Over time periods of about 50 million years, these young continental margins tend to subside gradually and be covered by transgressive, shallow-marine sedimentary sequences (Sleep and Snell 1976). In addition, old flaws inherited from the time of continental fragmentation, especially along the continuation of transform faults in the new ocean, tend to be loci of earthquake activity and alkalic magmatism (Sykes 1978). Many of the kimberlites of Africa, Brazil, and Australia exhibit a relationship to such transverse structures (Mitchell and Garson 1981).

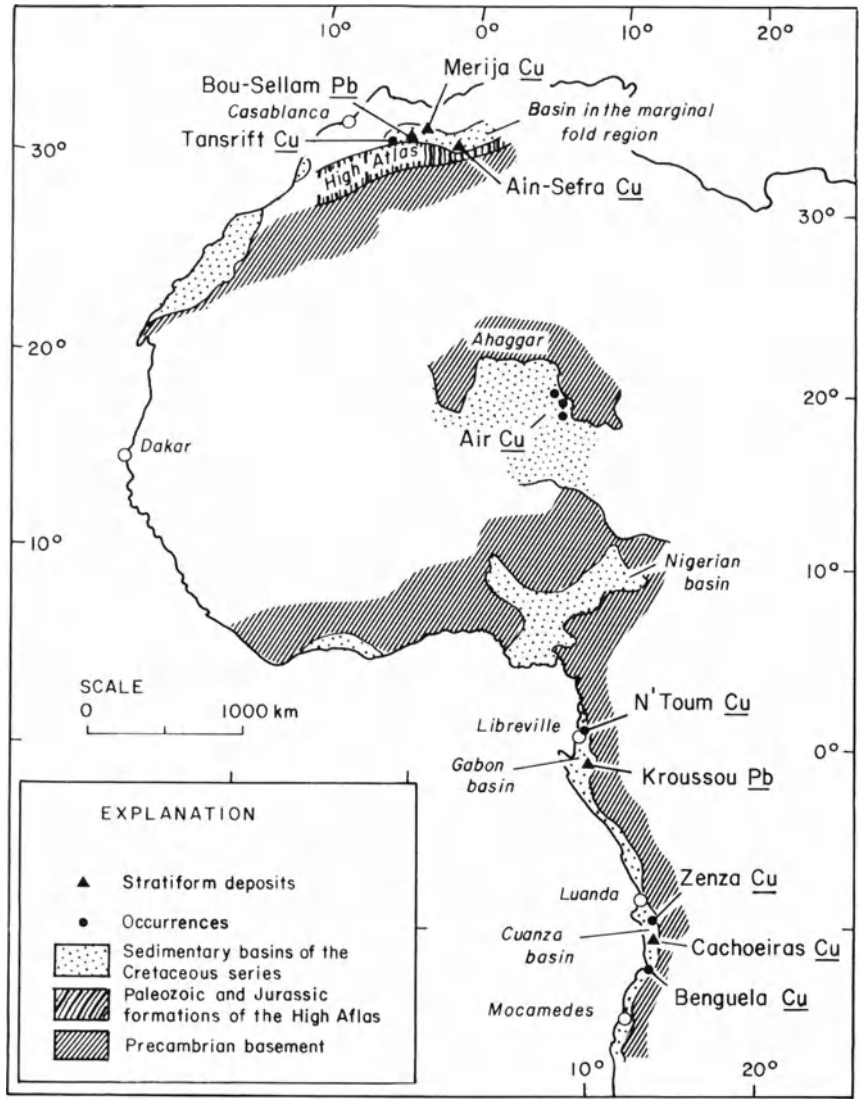

Fig. 8.22. Locations of the principal occurrences of stratiform copper and lead mineralization associated with the Lower Cretaceous unconformity in western Africa (After Caia 1976)

A number of small stratiform copper and lead deposits occur along the western edge of Africa (Fig. 8.22). These deposits occur mainly in Lower Cretaceous sandstones that discordantly overlie older rocks (Caia 1976; Van Eden 1978). The paleogeographic setting of the clastics is interpreted as deltaic and lagoonal, and clearly relates to a marine transgression over the subsiding continental edge some tens of millions of years after continental breakup. Whether the mineralization is truly syngenetic or was introduced into the

sediments along the unconformity is not clear, but in many respects the copper deposits exhibit similarities to the stratiform copper deposits discussed in the previous chapter, and may be variant of them (Bjorlykke and Sangster 1981). Similarly, the lead and zinc deposits exhibit a relationship to either limestones or the presence of a calcareous cement in the sandstones, and may thus be a variant of Mississippi Valley-type deposits.

Some of the major high-grade manganese deposits of the world occur in sedimentary rocks above a basal unconformity (Cannon and Force 1983; Force and Cannon 1988). The Oligocene Nikopol and Chiatura deposits north of the Black Sea, USSR (Varentsov 1964) (Fig. 8.23) and the Cretaceous Groote Eylandt deposits in northern Australia (McIntosh et al. 1975; Fig. 8.24) are important examples. Analysis of the environments in which the host rocks

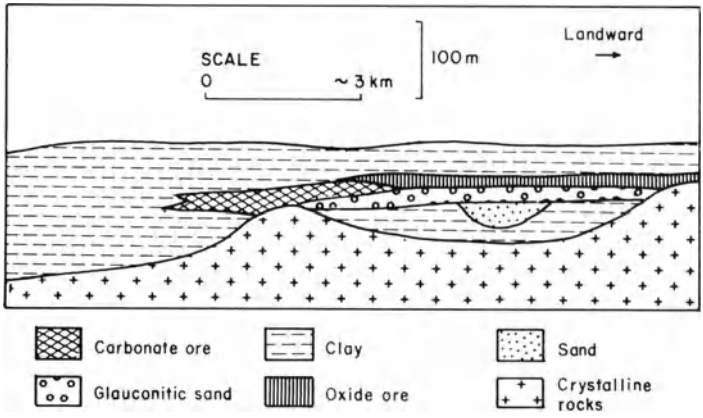

Fig. 8.23. Generalized cross-section of the Nikopol manganese district, Black Sea region, USSR (After Cannon and Force 1983)

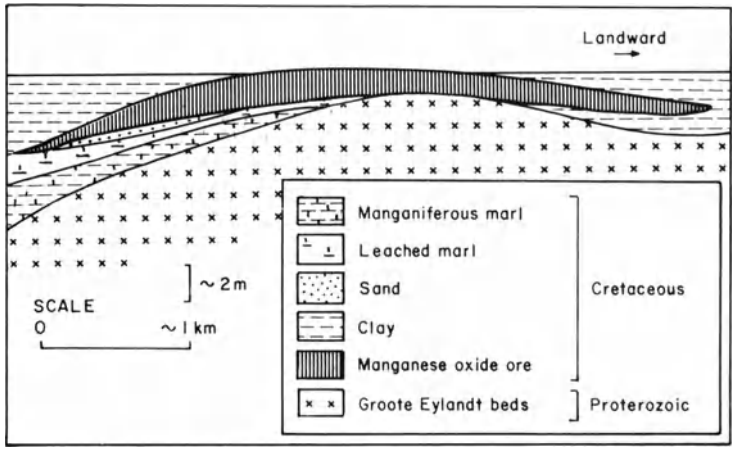

Fig. 8.24. Generalized cross-section of the Groote Eylandt manganese deposit, Gulf of Carpentaria, Australia (After Cannon and Force 1983)

of these deposits formed indicates littoral and shallow-marine conditions along irregular coastlines during marine transgressions. Such conditions may also apply to some of the carbonate-hosted manganese deposits of Morocco (Varentsov 1964) and eastern Mexico, and an unequivocal rift setting with similar lithologic characteristics is manifest for the manganese ores of the Boleo district, Baja California, Mexico (I.F. Wilson 1955).

It is now generally accepted that many of the well-documented marine transgressive episodes of later Phanerozoic time relate to displacement of seawater by increased activity at spreading ridge systems (Valentine and Moores 1972; Turcotte and Burke 1978). Furthermore, these transgressive episodes have been correlated with anaerobic events in world oceans, conditions that are recognized as an important factor in the creation of organic-rich source rocks for petroleum. The chemistry of manganese is such that its solubility relative to iron increases substantially under low Eh conditions (Fig. 8.25), and Cannon and Force (1983) and Force and Cannon (1988) suggest a correlation between the presence of such conditions in the world oceans and periods of major manganese ore accumulation. Whether the manganese was derived originally from hydrothermal activity at not-too-distant spreading ridge systems or from continental hinterlands, or both, is not clear at present. What does emerge, however, is a relationship, albeit indirect, between plate tectonics, in the form of increased spreading ridge activity, and conditions conducive to the formation of an important class of manganese deposit.

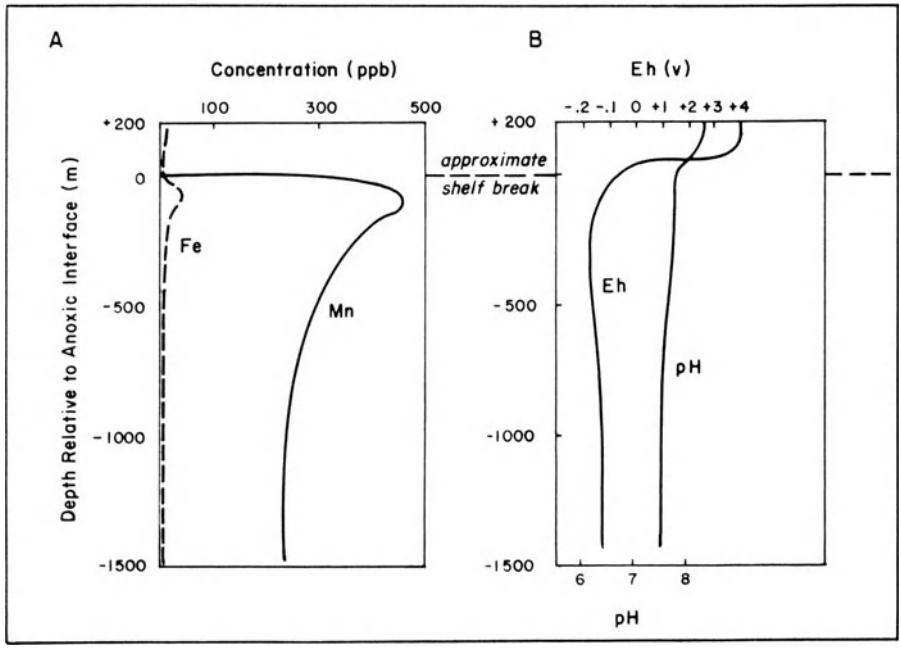

Fig. 8.25. Concentration-depth and Eh/pH-depth plots for the Black Sea showing a sharp increase in manganese solubility of anoxic interface (After Cannon and Force 1983)

8.6.1 Major Occurrences of Banded Iron Formation in Relation to Rifting Events

It was accepted formerly that the great period of early Proterozoic development of banded iron formations was concentrated rather sharply at or close to 2.0 Ga ago. Recently, Gole and Klein (1981) have demonstated that a continuum of deposition of banded iron formations existed from early Archean time until approximately 1.8 Ga ago, and that the major early Proterozoic development of banded iron formations should not be viewed as a more or less synchronous event. Despite this caveat, it is still probably correct to attribute the widespread early Proterozoic iron formations to the presence of increasing levels of oxygen in shallow-marine environments. As detailed by Holland (1973), this factor of increasing oxygen availability caused the ferrous iron budget of the world's oceans to be essentially used up by about 1.8 Ga ago. It has also been suggested that local evaporation may have aided this process of iron deposition (Trendall 1973; Button 1976).

Condie (1982) has attempted to classify early and middle Proterozoic supracrustal successions into three basic lithologic assemblages: (I) a quartzite-carbonate-shale, (II) bimodal volcanics-quartzite-arkose, and (III) continuous volcanics-graywacke. Group I assemblages, which include the Krivoy Rog Supergroup, USSR, the Transvaal Supergroup, South Africa, the Animikie Group, USA and Canada, and the Minas Series, Brazil, all of which contain important iron formations, are considered to represent paleocontinental shelf environments. However, why these particular successions, all of which have aggregate thicknesses of 6 km or more, should have developed important iron formations and other basins of broadly similar age and lithology did not, is unclear. An important factor may have been ocean circulation patterns at the time and their control of the sites of upwelling of deep ocean water. This would be essentially analogous to the controls of marine phosphorite deposition during Phanerozoic time (Cook and McElhinny 1979).

A relationship to plate tectonics in the above examples of iron formation may only be an indirect one, involving the control of continental geography, but it can be argued that the iron formations of the Hammersley Range, Australia, the Labrador Trough, and the Marquette Range, Michigan, are more directly related to continental rifting environments. The Hammersley Range contains the most extensive known accumulation of sedimentary iron deposits (Trendall and Blockley 1970; Trendall 1973), and the Mt. Bruce Supergroup, within which the Hammersley Group occupies a medial position, is about 10 km thick, and contains both basaltic and rhyolitic volcanics. In addition to this evidence for a rift environment, Horwitz and Smith (1976) have noted that the Supergroup coincides with a marked gravity high. They interpret this, together with similarities between the neighboring Yilgarn and Pilbara Archean terranes, as indicative of an early Proterozoic separation event that created the basin in which the Mt. Bruce Supergroup accumulated.

The initial accumulation of volcanics, sediments, and iron formations in the Labrador Trough also appears to have taken place in a rift environment (Dimroth 1981; Franklin and Thorpe 1982), and Larue and Sloss (1980) have deduced that rifting accompanied deposition of the Marquette Supergroup, which contains the Menominee and Baraga Group iron formations. A number of late Proterozoic iron formations also occur within well-defined rift environments (Young 1976). These include iron formations in the Rapitan Group, northwestern Canada, and iron formations in the upper part of the Adelaidian succession in South Australia. The clearest example of iron ore accumulation in a rift setting, however, is provided by the Devonian Lahn-Dill deposits in West Germany (Quade 1976) that are associated with bimodal basalt-rhyolite volcanics (Lehmann 1972; Sawkins and Burke 1980).

8.6.2 Sediment-Hosted Copper-Zinc Deposits

A few sediment-hosted, copper-zinc deposits are known and appear to represent a distinct subgroup of stratiform deposits related to the advanced stages of rifting. The most important example is the Ducktown district, Tennessee (Magee 1968; LeHuray 1984; Fig. 8.26), where nine highly folded orebodies comprise a total reserve in excess of 180 million tons of material grading about 2% Cu + Zn, with only trace amounts of lead. The deposits, which are dominated by pyrrhotite, occur in a thick sequence of metagraywacke, metasiltstone, and quartzite of the Ocoee Supergroup (Rast and Kohles 1986). This very thick clastic sequence contains local amphibolites, in particular in the vicinity of the orebodies, and has been interpreted as having accumulated in an intracratonic rift during incipient development of the Iapetus ocean (Rankin 1975; Sawkins 1976b; Gair and Slack 1980; Feiss and Hauck 1980).

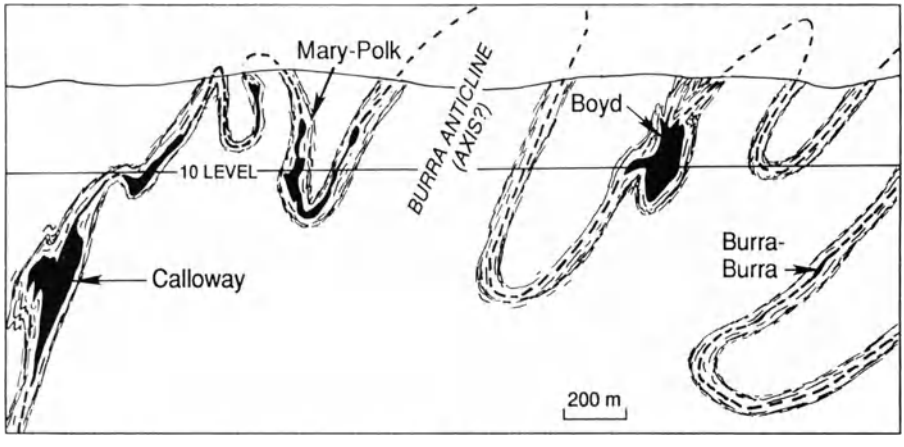

Fig. 8.26. Cross-section of the orebearing horizon at Ducktown, Tennessee (After Magee 1968)

Additional stratiform Cu-Zn deposits that occur in essentially similar lithotectonic settings are the Ore Knob and Gossan Lead in North Carolina and Virginia, respectively (Gair and Slack 1984 and references therein), the Elizabeth mine in Vermont (Annis et al. 1983), the Otjihase and related deposits along the Matchless Amphibolite Belt in Namibia (Goldberg 1976; Klemd et al. 1987), and the mid-Proterozoic Prieska zinc-copper deposit in northwestern Cape Province, South Africa (Wagener and Van Schalkwyk 1986).

Lead and sulfur isotope studies of the Ducktown deposits (LeHuray 1984) indicate that much of the sulfur was of seawater origin and much of the lead of crustal origin. However, the data also indicate an additional deep-seated source for some of the sulfur that could relate to mafic magmatism within the postulated rift basin.

These examples of copper-zinc deposits appear to have fundamental similarities to the Besshi deposits in Japan (Fig. 8.27) and can be grouped together as Besshi-type deposits (Scott 1983, 1985; Fox 1984).

8.6.3 Stratiform Tungsten Deposits

Stratiform concentrations of scheelite have been reported from many metamorphic terranes, including the Spanish Hercynian (Arribas-Rosado 1986), the Namaqua Mobile Belt (Tankard et al. 1982), the Malene supracrustals in West Greenland (Appel 1985, 1986), and from exhalite horizons in the Broken Hill Block, New South Wales (Plimer 1987). Major producers from stratiform tungsten ores are the Felbertal deposit in Austria (Holl 1977) and numerous deposits in northeastern Brazil (Reid 1983).

Plimer (1987) has noted that most stratiform scheelite concentrations exhibit a relationship to tourmalinites, and that such scheelite occurrences are found most typically in calc-silicate rocks deposited originally as impure carbonates in rift settings. Such calc-silicate units, although enriched in tungsten, do not achieve economic levels of tungsten mineralization unless fluid focusing and further concentration has occurred during deformation events. This two-stage aspect of the genesis of these deposits is supported by the extensive nature of stratiform tungsten enrichments in certain calc-silicate rocks, and by the obvious structural control of many specific scheelite orebodies within these metasedimentary horizons.

Concepts involving the movement of tungsten in hotspring environments are strongly supported by the association of tourmalinites with many stratiform scheelite occurrences (Appel 1986; Arribas-Rosado 1986; Plimer 1987), and the development of major concentrations of tungsten in the late Quaternary evaporites of Searles Lake, California (G.T. Smith 1979). Recognition of the fundamental stratiform aspect of many tungsten concentrations is of considerable import in terms of planning exploration strategies for this metal, especially within paleorift environments.

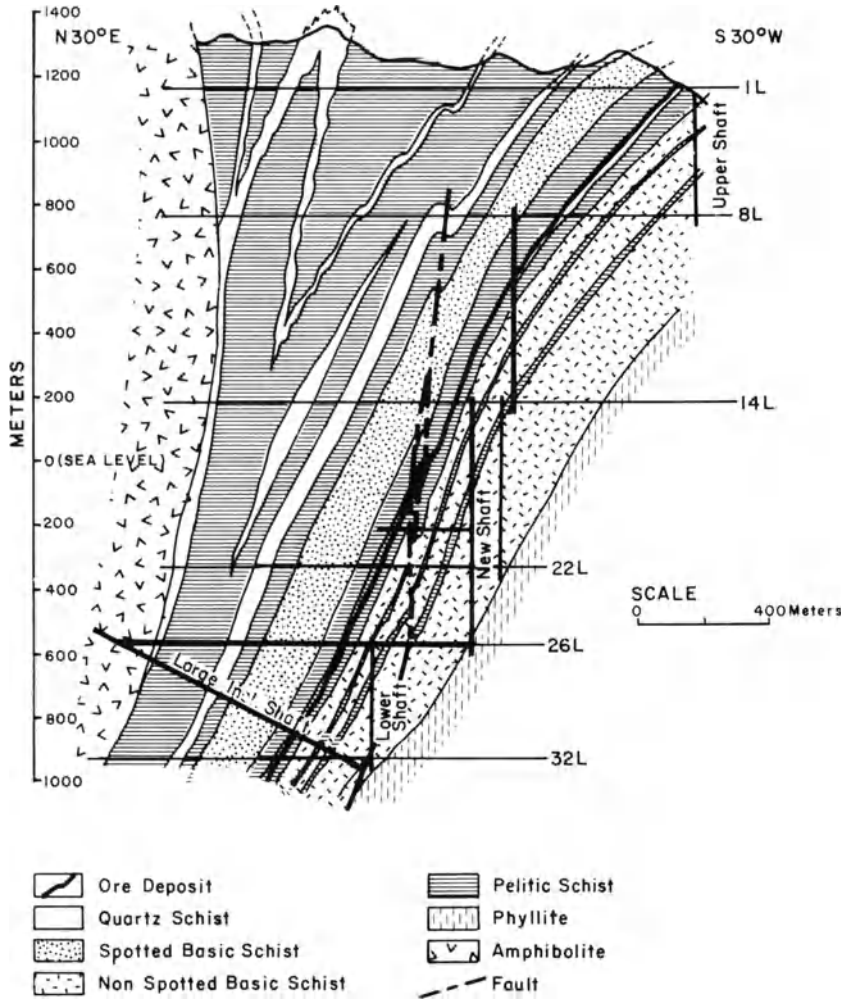

Fig. 8.27. Cross-section of the Besshi massive sulfide deposit, Japan. Note extreme elongation of the sulfide zone (After Franklin et al. 1981)

8.7 Metallogenesis and Rifting – Some Final Thoughts

The interrelationship between sedimentation in rift basins and the generation of specific types of metal deposits, especially those of lead and zinc, has come into increasingly clearer focus within the last decade. Many lines of evidence, geologic, hydrologic, and geochemical, appear to converge to reinforce the concept that basinal brines have the ability, under favorable conditions, to

develop into ore fluids. Given the impetus to migrate, suitable aquifers within which to migrate, and favorable conditions to precipitate their metallic constituents, such fluids can give rise to a significant array of sediment-hosted ore deposits, including some to be discussed in the following chapter.

A valid question remains as to why rift-related sequences seem to generate ore fluids and metal deposits so much more readily than other sedimentary sequences. The answer to this question presumably relates to several features of rift environments: the initial rapid sedimentation of clastics, the accumulation of thick clastic sequences, the tendency for evaporites to form at some stage of basin development, the high heat flow regimes of many rift basins, the active extensional faulting during basin filling, and the development of anoxic episodes in many advanced rifts. These factors all contribute in different ways to the development of metalliferous brines, their movement, and the eventual formation of sulfide deposits. The final mechanism of ore formation (exhalative, "inhalative," replacement of carbonates) and form of orebodies is in one sense secondary to these fundamental principles of ore fluid generation and migration.

In this and the previous chapter a distinction has been made between the copper-rich metallogeny associated with the earlier stages of continental rifting, and the lead-zinc-rich metallogeny of the more advanced stages of rifting. It is of interest nonetheless to note that few specific rift systems contain major examples of both copper and lead-zinc deposits. In the geologic record copper-dominated, rift-related metallogenesis occurred approximately 2 Ga ago and again between 1.2 and 0.9 Ga (see Sawkins 1976b), whereas Pb-Zn rift-related metallogenesis occurred primarily 1.8–1.4 Ga ago, especially in the southern continents (see Sawkins 1989).

The fundamental control on these two distinctive types of rift-related metallogeny are here considered to be the tectonomagmatic events that precede ore generation. The major copper-dominated metallogenesis associated with late Proterozoic rifting is clearly related to the extensive basaltic magmatism that accompanied those rifting events (see Sawkins 1976a).

The mid-Proterozoic magmatic events that preceded major lead-zinc metallogenesis in North America, southern Africa, and Australia were dominated by potassium-rich felsic volcanism (see Wyborn 1988; Sawkins 1989). In this latter case, the magmatism appears to have been generated by large-scale crustal underplating events that in turn produced major volumes of felsic magma by crustal melting processes. This scenario has been particularly well documented in Australia where very widespread felsic magmatism occurred between 1880 and 1840 Ma (Wyborn 1988). It is of no small consequence that the world's largest lead deposit formed in rift-related sediments that started to accumulate shortly thereafter (Stevens et al. 1988), and that major lead concentrations also occur in mid-Proterozoic sedimentary sequences at Mt. Isa and McArthur River. Much the same scenario can be used to explain the major concentrations of lead at Sullivan, British Columbia in North America, and those at Aggenys, Northern Cape in South Africa (see Sawkins 1989).

The fundamental control of continental rift metallogeny therefore appears to rest with the nature of crust-mantle interaction during attempted breakup events. In some instances basaltic melts from the mantle break through the crust to spawn major basaltic magmatic episodes and eventual copper-dominated metallogenetic events. In other instances the mantle-derived basalts collect at the base of the crust and induce large-scale crustal melting that in turn can generate important Pb-Zn metallogenesis. In both instances secondary processes involving basinal brine migration are required to generate the actual sediment-hosted metal deposits.

Unlike young Cordilleran terranes, most paleorift sequences now lie within continental interiors or are even covered by a veneer of younger rocks. As a result, exposures tend to be limited or nonexistent. Furthermore, many such sequences have borne the full brunt of later orogenesis. Meaningful exploration of such terranes will require the integration of surface, subsurface, and geophysical data, and enlightened programs of basin analysis, not unlike those practised by the petroleum industry, will be increasingly needed.

Chapter 9 Metal Deposits in Relation to Collision Events

9.1 Introduction

Although the Alpine-Himalayan belt provides a clear example of the consequences of Cenozoic collision tectonics, and the Caledonide-Appalachian belt an example of Paleozoic collision tectonics, the interpretation of the tectonic history of many Paleozoic and older orogenic belts is fraught with uncertainty. Wilson Cycle concepts provide a cogent explanation for the history of Iapetus, but there are many orogenic belts where the bulk of the evidence seems to militate against the former operation of a full Wilson Cycle. The problem is exacerbated by the fact that the large majority of orogenic belts provide reasonably clear evidence of an initial extensional phase followed eventually by a compressional phase, although the two events may be separated by large time intervals. It is also now recognized that many orogenic events are caused by accretional collisions that may involve just a fragment of continental-type crust or a relatively young arc system (Hoffmann 1988).

The formation and eventual subduction of an oceanic tract much wider than the present Red Sea can be expected to leave telltale evidence of its prior existence in the form of obducted ophiolites, provided erosion levels are not too deep. More significantly, irrespective of erosion levels, some evidence for the former presence of a calc-alkaline volcanoplutonic arc should be manifest along one side of the collision orogen. In some orogenic belts, such as the Damarides, much of this evidence is lacking, and paleomagnetic studies (McWilliams and Kroner 1981) provide no support for significant separation at any stage of the flanking, older cratonic blocks.

For reasons of exposure, access, and mineral potential the Damara Province has been the subject of considerable study (see Tankard et al. 1982 and references therein), and represents a key area in terms of understanding certain Proterozoic and perhaps Paleozoic orogenic belts that do not appear to fit a simple Wilson Cycle model. Tankard et al. (1982) provide and excellent summary of the sedimentation and tectonics of the Damara Province and the Gariep Province to the south, and also review the various models proposed for it.

The Damara Province represents a three-armed asymmetric orogenic system in which lithologic and structural continuity is observable between each arm (Fig. 9.1). Two of these arms parallel the Atlantic coast and may represent original depositional basins whose western flanks are now represented in part by lithosequences in the Ribera Province of Brazil (Porada

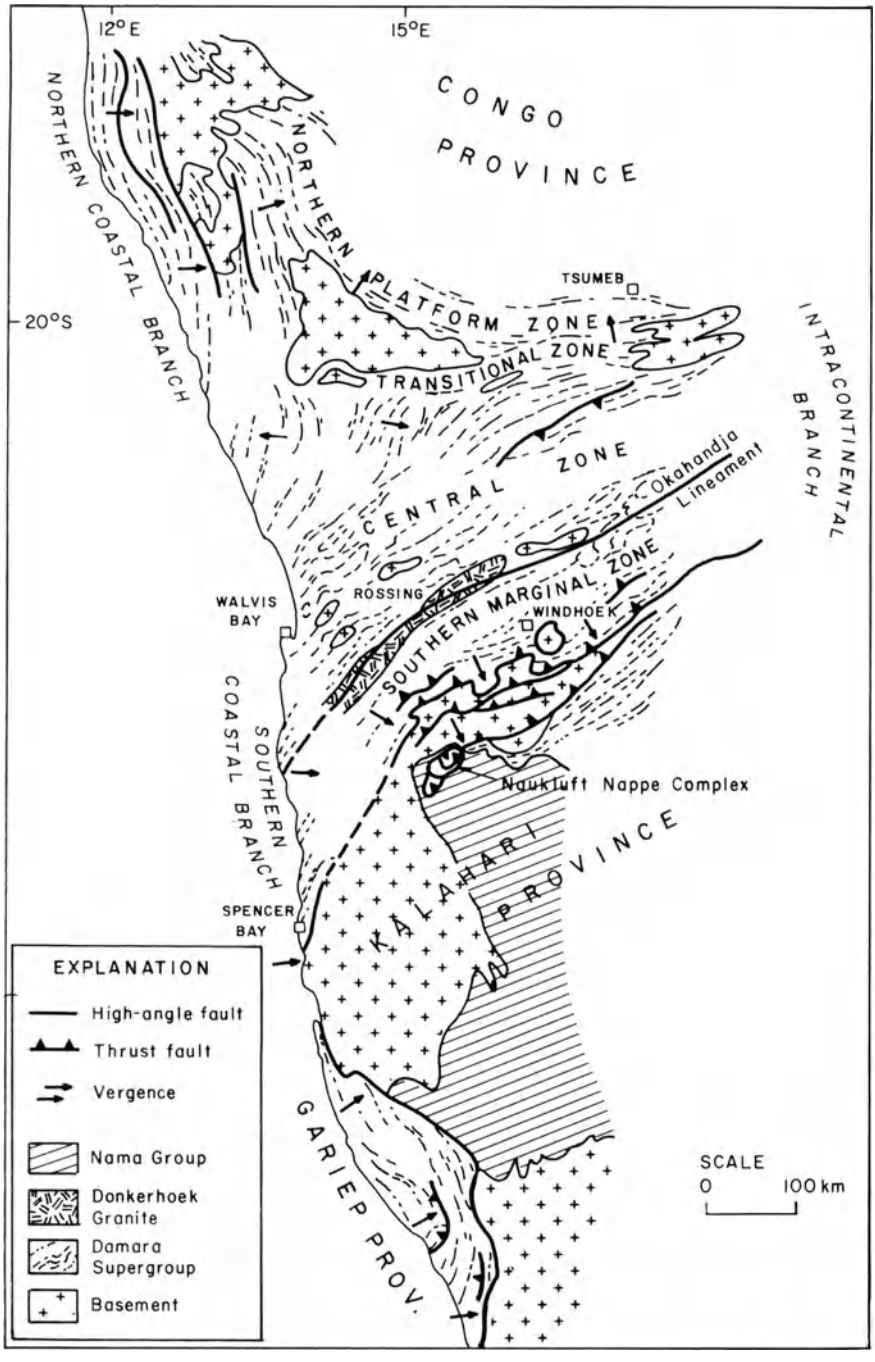

Fig. 9.1. Map of the Damara Province showing major tectonic elements (After Tankard et al. 1982)

1979). The three-armed nature of this orogenic system is highly suggestive of the hotspot-associated rift geometries documented by Burke and Dewey (1973). In fact, initial sedimentation of the Damara Supergroup, represented by arkosic arenites (Nosib Group) appears to have been on continental crust, and commenced about 1000 Ma ago. Locally, rhyolites were erupted and at one locality a considerable thickness of volcanic rocks of alkali-basaltic composition (Naauwpoort Formation, see Fig. 9.2) developed. Not only is this sequence of sediments and volcanics typical of the early stages of continental rifting, but stratiform copper deposits were formed at the interface between continental red beds and marine sediments (Martin 1978; see Chap. 7). By about 730 Ma ago a much broader trough developed and sedimentation across the entire width of the Damara Province commenced (see Fig. 9.2). Subsidence was more concentrated in a northern graben and in the south, where a very thick flysch sequence accumulated (~ 10 km). On the northern platform a substantial thickness of stromatolitic dolomitic limestones (Otavi Group) was deposited. Copper-zinc massive sulfide ores are associated with a brief, but extensive, pulse of basaltic volcanism (Matchless Amphibolite Belt) within the southern flysch belt, whereas Mississippi Valley-type lead-zinc mineralization is hosted by the carbonate rocks in the north. Uplift in the northwestern Kaoko zone of the province caused molasse sedimentation (Mulden Group) on the northern platform, and by this stage (650 Ma) major tectonism of the province was initiated. Syntectonic granites intruded from 650 to 540 Ma and metamorphism was at or close to its peak of intensity at about 530 Ma.

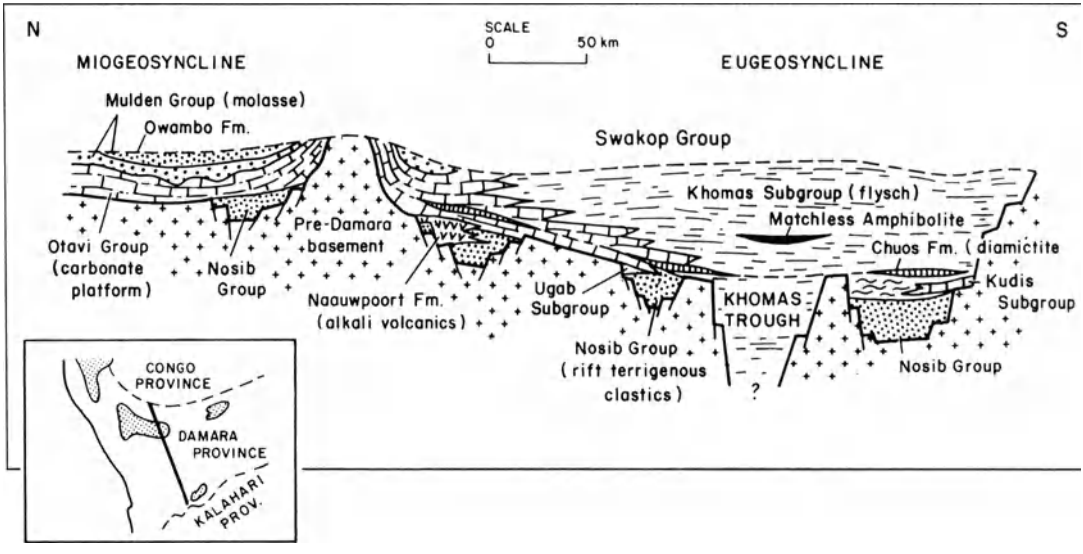

Fig. 9.2. North-south cross-section of the Damara Province showing control of stratigraphic elements by extensional (rift) faulting (After Tankard et al. 1982)

Final gravity emplacement of the high-level Naukluft Nappe Complex onto the Nama Foreland (see Fig. 9.1) occurred in response to posttectonic isostatic uplift of the orogen at about 490 Ma. Farther north in the Central Zone, posttectonic emplacement of high level, S-type granites continued until 460 Ma. The Rossing uraniferous alaskites were formed 460 Ma ago, and by this time sufficient uplift and cooling had occurred such that no further significant disruption of Sr-Rb isotope systems is evident.

Approximately 50 Ma later nappe tectonics were taking place in the Southern Marginal Zone and Nama Foreland, while farther north the Okahandja lineament became active and there was additional emplacement of granites. This was followed (~510–480 Ma ago) by the rise of mantled gneiss domes and emplacement of late granitoids. The Rossing uraniferous alaskites were formed 460 Ma ago, and by 400 Ma ago sufficient uplift and cooling had occurred such that no further disruption of the Sr-Rb isotope systems is evident.

Overall, the geology of the Damara Province has many of the features associated with Wilson Cycle collisional orogens – early rifting, development of basalts with MORB-like chemistry (Matchless Amphibolite Belt), major asymmetric thrusting, and basement reactivation – but lacks clear evidence of ocean opening and closing events. Despite this, Kasch (1979) and Barnes and Sawyer (1980) have suggested a continental collision model for it, in which they envisage northward subduction leading progressively from an Andean phase to a Zagros phase, followed by a Himalayan phase, and finally an Alpine phase of tectonism and magmatism. The two most telling arguments against this model come from the most recent, precision paleomagnetic data (McWilliams and Kroner 1981), and the relative paucity of intermediate, low initial Sr ratio granitoid bodies that would be products of the subduction process. In fact, the plutonic granitoid suite is clearly Hercynotype (Pitcher 1979) and dominated by granites (senso stricto).

Martin and Porada (1978) and Porada (1979) have championed a strictly ensialic model for the Damara Province, while acknowledging that the northern and southern coastal arms of the Province, with their strong eastward vergence of structures and a paired high P/low P metamorphic belt in the north, probably resulted from a true Wilson Cycle collision event that closed a proto-South Atlantic Ocean. Evidence for an initial divergence includes early bimodal igneous activity along both the northern (e.g., Chela Group, Angola; Kroner and Correia 1980) and southern (e.g., Stinkfonkein Formation; Tankard et al. 1982) arms of the system.

Porada (1979) notes that similar tectonic activity (graben formation) occurred within the Ribeira Province of Brazil, which was probably contiguous to the Damara Province approximately 1 billion years ago. The model suggested by Martin and Porada (1978) for the ensialic Damara Province arm involves foundering of a dense eclogitic upper mantle to provide the compressional forces for orogenic shortening and thrust tectonics during the metamorphic culmination.

The concepts favored by Kroner (1980) to explain Pan-African tectonic belts in general, and the Damara Province in particular, represent an extension of those of Martin and Porada (Fig. 9.3). Kroner envisages prolonged early rifting culminating in crustal thinning and extrusion of primitive tholeiitic basalts into basins (e.g., Matchless Amphibolite Belt). Subsequently, delamination and sinking of the dense subcrustal lithosphere occurs and the

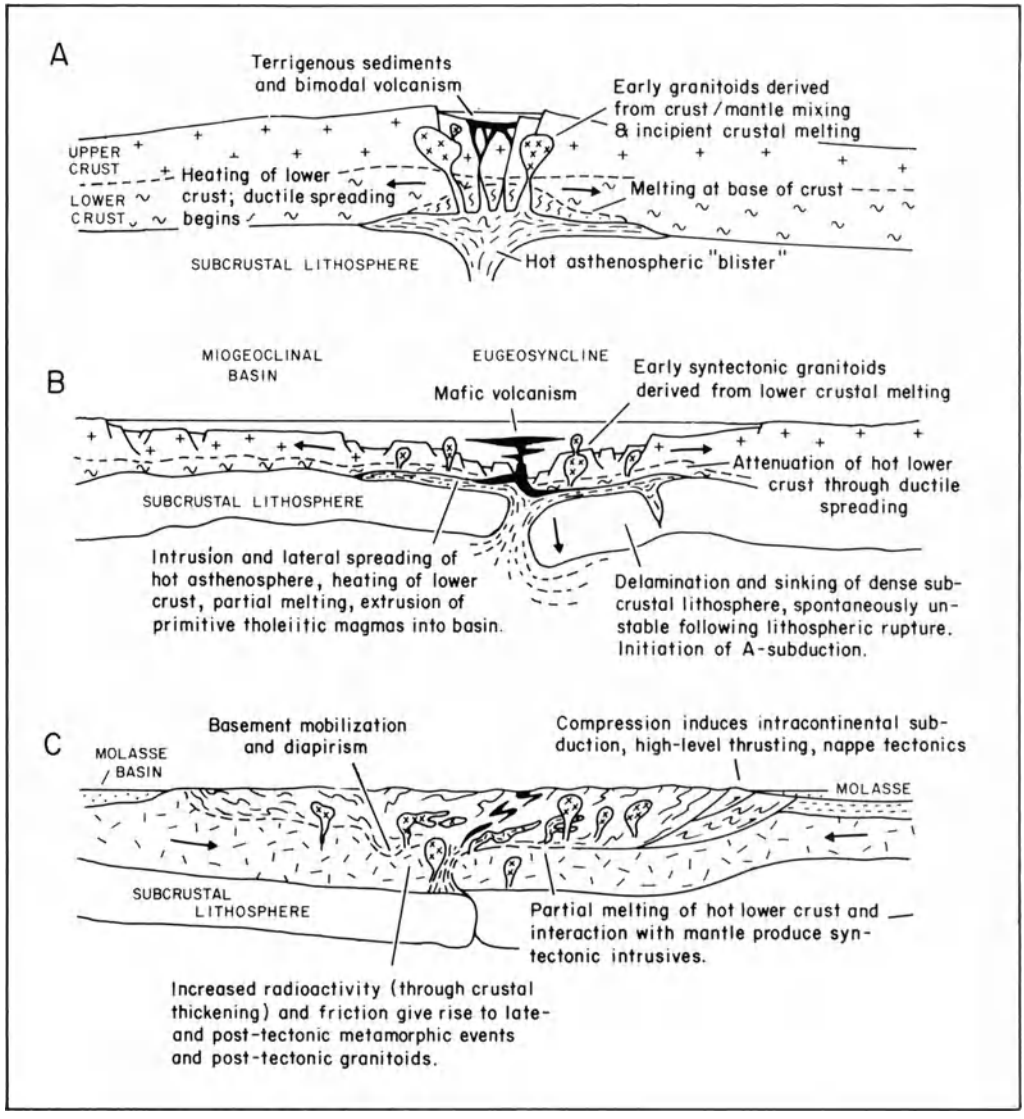

Fig. 9.3. Simplified schematic sections to show inferred evolution of Proterozoic ensialic mobile belts, as suggested by the geology of the Damara Province. Note initial phase of extension, followed by a compressional (collision) phase (After Tankard et al. 1982)

onset of compression leads to flat "subduction" of continental crust along the zone of delamination. The thickened crust thus produced leads eventually to uplift and exposure of the deep portions of the orogen where considerable metamorphism and S-type magmatism have occurred.

These models of ensialic orogeny certainly explain the geologic relationships and paleomagnetic data, but the source of the compressive forces involved remains obscure. It is, however, this very compression that generates the similarities of these belts to collision orogens of Wilson Cycle type. Perhaps the softening of these zones due to attenuation and strong heating makes them susceptible to forces transmitted across plates from their far edges. Whatever the ultimate causes, it appears that both Wilson Cycle and ensialic orogens merit designation as collisional tectonic belts and I plan to consider both as such.

This rather extended discussion of the Damaride Province is considered warranted because resolution of the broad dichotomy between concepts of Wilson Cycle orogeny and those of ensialic orogeny, and the fundamental differences and similarities between the two, is central to a fuller understanding of ancient orogenic belts. A key issue here is that initial rifting stages and final collisional stages appear to be common to both, and this has significant implications in terms of the metal deposits we can expect to find in such belts.

The metal deposits in collisional orogenic belts can be divided into two types: those formed prior to the main pulse of tectonism, and those generated as a result of the tectonic and associated metamorphic activity. We have dealt with the former, mainly in the two previous chapters, but it is worth reemphasizing that the tectonic events associated with collision are important from a metallogenic perspective in terms of dewatering of rift and foreland sedimentary basins, of aiding the alteration and leaching of certain packages of metal-rich volcanic rocks, and in terms of exhuming rifting-related deposits formerly deeply buried along passive continental margins or within deep rift troughs. This explains why sediment-hosted massive sulfide deposits younger than mid-Paleozoic are unknown, although possible contemporary examples of such ore deposits are represented by the Red Sea sulfide muds and sulfide mounds in the Guaymas Basin. In addition, the tendency of collision orogens produced by closure of an oceanic tract to contain a spectrum of juxtaposed ore deposit types, formed initially in a variety of tectonic settings has been well documented by Sillitoe (1978) in Pakistan.

9.2 Ophiolite-Hosted Metal Deposits

True Wilson Cycle collisions, and arc-arc or arc-continent collisions tend to result in the obduction of ophiolite complexes and thus are critical to the preservation of slices of oceanic crust and mantle. However, because strong uplift and subsequent deep erosion are typically attendant on collision events,

these ophiolite complexes tend to have a limited preservation potential. Thus, the Cenozoic Alpine-collision belt has numerous ophiolite complexes scattered along its length, and contains many of the most significant examples of ophiolite-hosted metal deposits (see Chap. 5). Paleozoic age collision belts of Wilson Cycle-type such as the Urals and Caledonide/Appalachian orogeny also contain a number of mineralized ophiolite complexes, but relative to the Alpine-Himalayan belt, they are less numerous. Proterozoic ophiolite complexes are rare, probably because the level of erosion in Proterozoic orogens tends to be deep, and any such complexes they may have harbored have been largely lost to the forces of erosion. Despite this, more and more examples of Precambrian ophiolites are being recognized (see Introduction and Chap. 5).

9.3 Mississippi Valley-Type Deposits in Relation to Collisional Orogeny

9.3.1 General Considerations

Mississippi Valley-type (MVT) deposits represent one of the subgroups of a broad class of carbonate-hosted, lead-zinc deposits. Other members of the class include the so-called Alpine-type and Irish-type deposits. These geographically oriented names are unfortunate and tend to confuse rather than elucidate fundamental types of metal deposits. However, the designation of epigenetic lead-zinc deposits emplaced in the carbonate rock sequences of continental interiors as MVT deposits has become so entrenched in the literature (see Kisvarsanyi et al. 1983) that it will be used here.

Despite considerable research attention for many decades, it is only recently that adequate genetic and tectonic models for MVT deposits have surfaced, and the details of these will no doubt be contested well into the future. In particular, the geographic position of most MVT districts well within stable continental interiors seemed to negate any connection of these examples with plate tectonic mechanisms. It is now becoming apparent that collision events

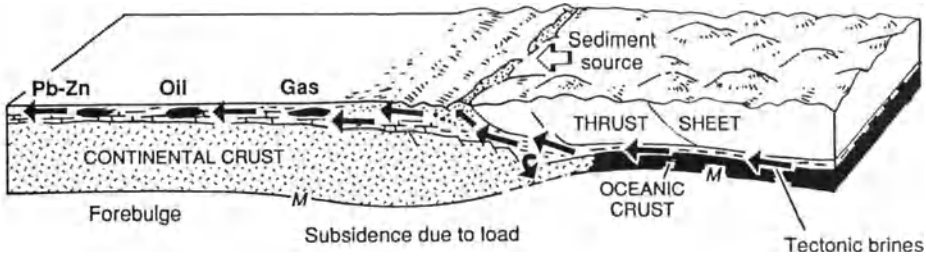

Fig. 9.4. The postulated relationship between the thrusting generated by continental collision and the migration of tectonic brines into continental interiors. Continental crust is ~ 35 km thick and horizontal dimension of diagram is ~ 500 km (After Oliver 1986)

at continental margins play an important role in terms of driving sedimentary brines out of either earlier rift or foreland basins, and that such tectonically driven brines can migrate hundreds of kilometers through cover rocks into continental interiors (Fig. 9.4; Oliver 1986; Duane and deWit 1988). The extent to which this tectonic explusion model can be applied to MVT deposits worldwide is as yet unclear, but it certainly fits the observational data for a number of major MVT districts, and is applicable to a number of other types of lead-zinc deposits (see following sections). Furthermore, an explanation is provided for the problem of timing of mineralization events versus original accumulation of host sedimentary sequences (Sangster 1986).

9.3.2 Occurrence and Distribution of MVT Deposits

MVT districts are typically of considerable areal extent but are present only over a relatively limited stratigraphic interval. Lead-zinc deposits of this type are, not surprisingly, widely distributed within the stable central region of the United States (Fig. 9.5), but important examples (Guild 1974) are also known in Arctic Canada (Kerr 1977), northwest Canada (Kyle 1981), northern England (Sawkins 1966), Poland (Sass-Gustkiewicz et al. 1982; Wodzicki 1987), and in the USSR (Smirnov 1977). In addition, important carbonate-hosted zinc deposits occur in the southern Appalachians (Kyle 1976; Hoagland 1976) outside of the Mississippi Valley proper. A variant of Mississippi Valley-type deposits are sandstone-hosted lead deposits (Bjorlykke and Sangster 1981), but these will be discussed briefly in a later section. The US deposits occur within essentially undeformed cover rocks ranging in age from

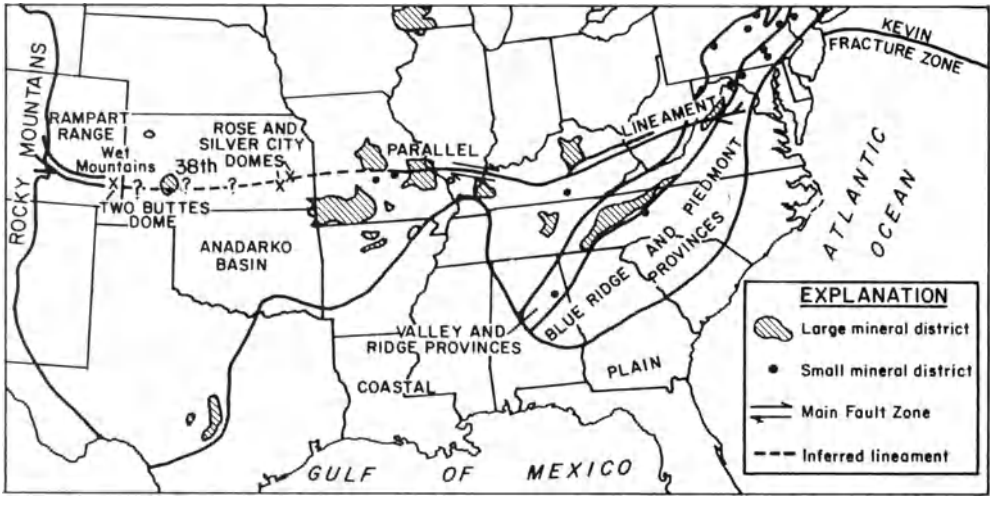

Fig. 9.5. Location of the 38th Parallel Lineament illustrating its spatial relationship to a number of major Mississippi Valley ore districts (After Heyl 1972)

Cambrian to Carboniferous and are unequivocally epigenetic in origin. Despite their broad similarity in lithologic setting, low temperature of formation (Roedder 1976), and basic lead-zinc composition, Mississippi Valley-type deposits display considerable variability. For example, zinc-lead ratios in some ore districts are > 10 and in others < 1, some deposits contain important amounts of copper, and the association of the lead and zinc sulfides with barite and/or fluorite is pronounced in some instances and essentially nonexistent in others. Despite these perturbations, and wide variations in the morphology of individual orebodies (Fig. 9.6), Mississippi Valley-type deposits do form a distinctive ore type linked by a common genetic thread.

Although much remains to be learned about the precise details of their genesis (Ohle 1980; Lydon 1986), several important points can be extracted from the available data base on Mississippi Valley-type deposits. For example, they tend to form on the flanks of or above basement highs, and from fluid inclusion studies it is clear that saline connate waters expelled from adjacent basins form a major component of the ore-forming fluids. In addition, the deposits in many districts occur in carbonate rocks adjacent to either sandstone beds, paleokarst features, or faults; all capable of acting as aquifers for large-scale fluid movement.

As detailed in the preceding chapter, a clear time-space relationship to rifting can be indicated for the lead-zinc deposits in Cretaceous sediments of the Benue Trough, and for the minor deposits of lead and zinc in Miocene sediment along the Red Sea (see Fig. 8.19). Such cannot be claimed for the deposits within the Mississippi Valley area proper, although some of these lie along the 38th parallel lineament (Heyl 1972) (see Fig. 9.5), a zone characterized by repeated fault activity and minor alkalic magmatism. Similarly,

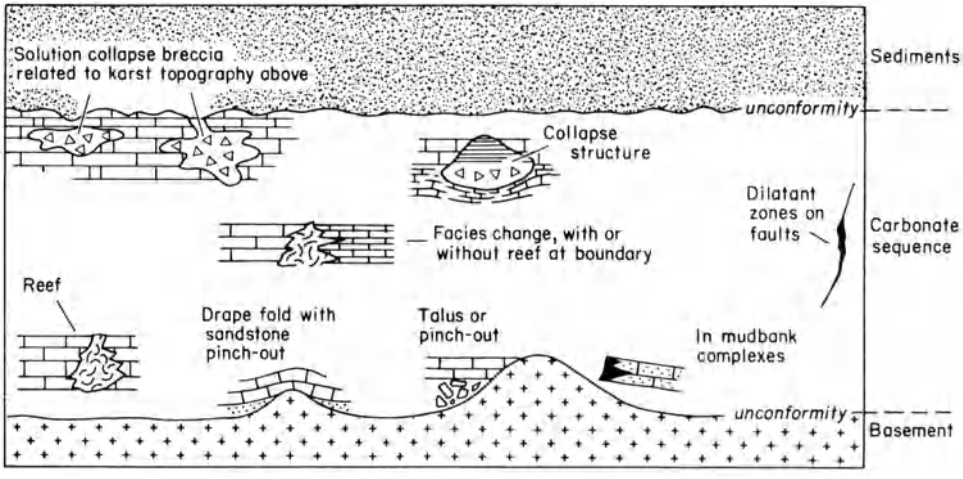

Fig. 9.6. The various types of geologic situations in which carbonate-hosted, lead-zinc deposits of Mississippi Valley type can occur (After Callahan 1967)

the Mississippi Valley-type deposits of the Pennines in England (Dunham 1948; Sawkins 1966) apparently developed during latest Carboniferous time (Moorbath 1962), when mafic and alkali magmatism was prevalent in the Midland Valley of Scotland just to the north (Francis 1968). Despite these examples, in broad terms it is safe to say that no significant spatial or temporal relationship between MVT deposits and magmatism is apparent.

9.3.3 MVT Deposits of the Viburnum Trend, Southwest Missouri

In economic terms the most important Mississippi Valley ore district is that of the Viburnum Trend, southwest Missouri (see Vineyard 1977, Econ. Geol., vol. 72, no. 3). Here, over 100 million tons of lead-zinc ore have been discovered, mainly within the last three decades, and the Viburnum Trend is currently the world's most productive lead district (Vineyard 1977). In 1974, the district accounted for 85% of US, and 15% of world lead production. The district consists of a virtually continuous, narrow, north-south-trending belt of mineralization west of the St. Francois Mountains, a Precambrian basement high (Fig. 9.7).

The ores are distinctly lead rich and lead/zinc ratios vary from about 3 to > 10, and locally, they contain significant amounts of copper and minor nickel and cobalt-bearing sulfides. The ore trend occurs within the Cambrian Bonneterre Formation, a complex unit consisting mainly of calcareous micrites and calcarenites. Algal reef facies are present in the Bonneterre Formation along parts of the Viburnum Trend and are locally important as an ore-bearing lithology. Below the Bonneterre Formation is the Lamotte Sandstone, lying unconformably on the Precambrian volcanic and crystalline rocks (Fig. 9.8). This unit is a typical transgressive basal sand of irregular thickness, consisting primarily of fine- to medium-grained rounded quartz particles (Thacker and Anderson 1977).

The Buick ore zone (Rodgers and Davies 1977) runs for over 8 km along the north-central portion of the Viburnum Trend, and is demarcated to the north and south by property lines rather than grade considerations. The sulfide ores occur largely in solution-collapse breccias within dolomitized calcarenites of the upper Bonneterre Formation, which, in the mine area, overlies algal stromatolite reef facies of the lower Bonneterre.

The main orebodies within the Buick Mine consist of narrow, continuous zones of sulfide mineralization developed in breccia bodies that are sinuous and locally branch or rejoin along the trend (Fig. 9.9). These collapse breccias are thought to have developed along lithologies representative of paleointratidal, drainage channels, and they attain dimensions of almost 100 m in width and 25 m in thickness (Rodgers and Davies 1977). A typical section across the mineralization trend in the Buick Mine indicates three breccia ore zones, each with distinctive metal content and zoning characterizations (Fig. 9.10). In detail, paragenetic relationships are complex and include evidence of periodic sulfide leaching.

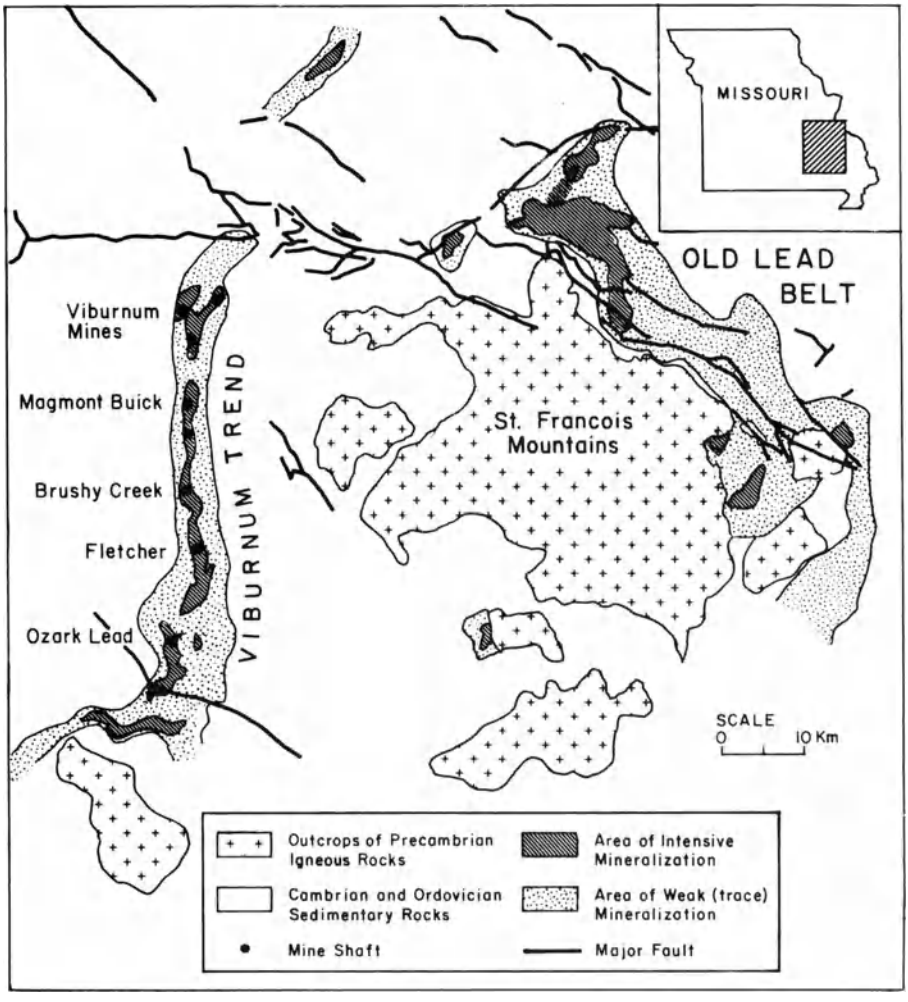

Fig. 9.7. Generalized map of southeast Missouri showing location of major Mississippi Valley ore districts surrounding the St. Francois Mountains basement high. The entire Viburnum Trend, which currently accounts for major lead, zinc, and lesser copper production, lies entirely in the subsurface (After Kisvarsanyi 1977)

Fluid inclusion data on sphalerites from Viburnum Trend ores (Roedder 1977) indicate the ore fluids were very saline brines at temperatures mainly in the range 94–120°C, and as such, they appear to be typical Mississippi Valley-type ore fluids. Sverjensky (1981) carried out detailed studies on the Buick ores, including sulfur and lead isotope work, and found that $\delta^{34}S$ values for sulfides exhibit a range of values from 21.3 to 0.9‰ and exhibit covariance with lead isotope data. These results led Sverjensky to conclude that both the sulfur and lead were transported by the same ore fluids, and that much of the sulfur was of evaporitic (sulfate) origin. Deloule et al. (1986) have investigated

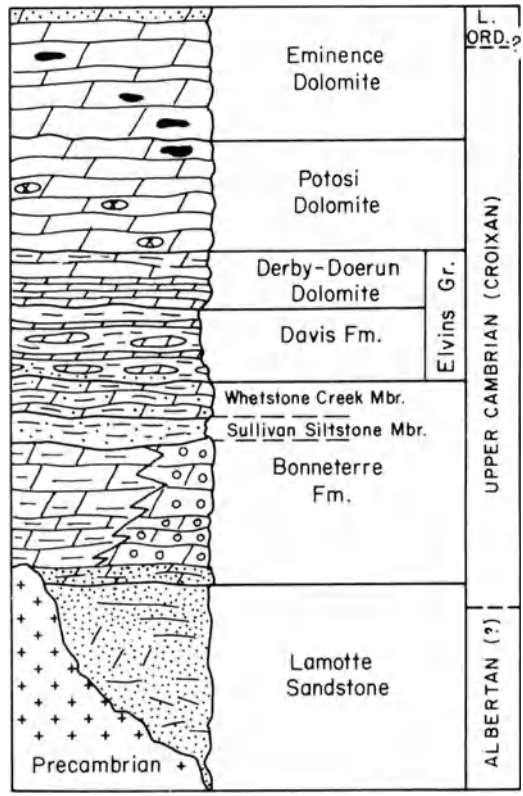

Fig. 9.8. Composite stratigraphic column of Upper Cambrian sedimentary rocks in southeastern Missouri. The Virburnum Trend ores occur within the Bonneterre Formation (After Thacker and Anderson 1977)

the microstratigraphy of galena crystals from the Picher mine, Tristate district, Oklahoma, and from the Buick mine. Frequent changes of lead and sulfur isotope compositions were observed on the microscale, indicating frequent changes in the precise sources of lead and sulfur. These were presumed to be different units within the sedimentary package that generated the ore fluids.

9.3.4 Discussion and Considerations for Exploration

As studies of fluid inclusions in samples from MVT deposits became more widespread (see Roedder 1984), it became increasingly apparent that these fluids exhibited marked similarities to oilfield brines. This concept is reinforced by reports of lead- and zinc-rich formation waters at Cheleken, USSR (Lebedev 1972), in central Mississippi (Carpenter et al. 1974), and in Alberta, Canada (Billings et al. 1969). However, the acceptance of brines of sedimentary origin as the ore fluids involved in MVT genesis (Hanor 1979;

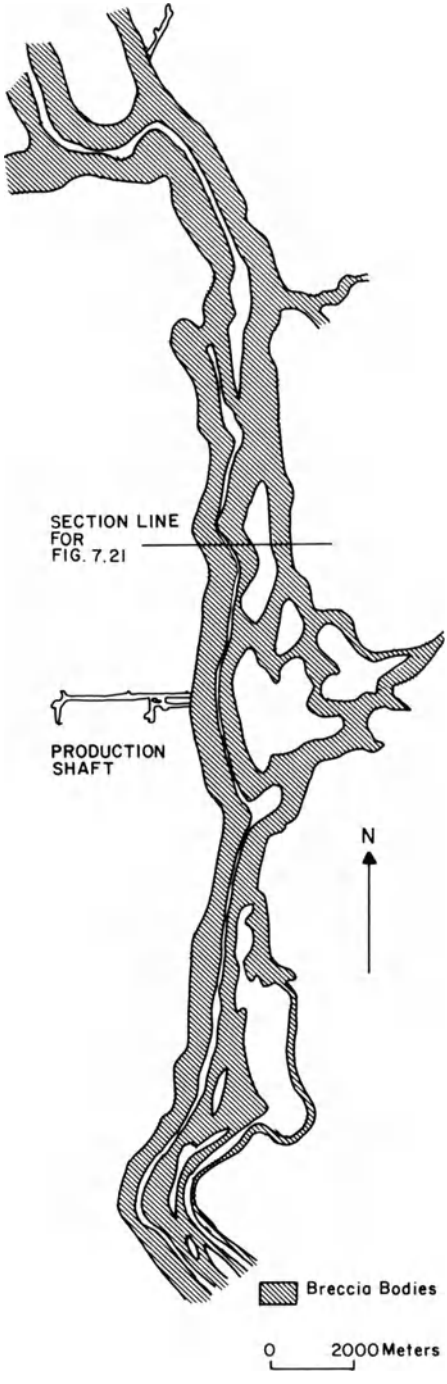

Fig. 9.9. Plan of major mineral zones showing their relation to the breccia bodies, Buick Mine, Viburnum Trend (After Rogers and Davis 1977)

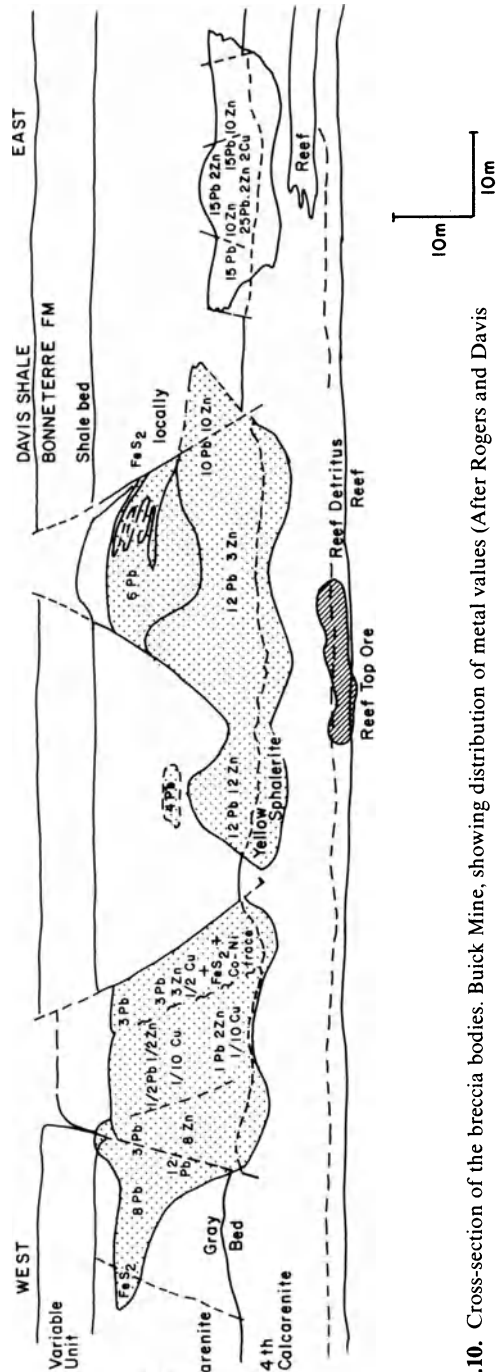

Fig. 9.10. Cross-section of the breccia bodies. Buick Mine, showing distribution of metal values (After Rogers and Davis 1977)

Sverjensky 1981, 1984) still left unresolved problems related to the timing and position of MVT districts. Some specific mechanism to initiate basin dewatering was required, especially after the thermal analyses of Cathles and Smith (1983) demonstrated the need for episodic, rapid, dewatering events.

As noted in an earlier section, the concept of fluid migration enforced by collisional events (Oliver 1986; Duane and deWit 1988) provides an attractive solution to these problems (see Fig. 9.4). It may not be a unique one, however, for although some kind of tectonic disturbance is undoubtedly required to promote rapid dewatering events these could be related to extensional faulting or due to gravity-driven flow caused by uplift of one margin of a basin. This latter scenario has been suggested by Garven (1985) for the Pine Point MVT deposits, and by Bethke (1985, 1986) for the Upper Mississippi Valley deposits. In both of these studies the hydrologic analyses were based on computer modeling.

The recognition that collision events may play an important role in the generation of MVT deposits and other types of Pb-Zn deposits (see following sections) is concept of particular value to the exploration geologist, which will be increasingly utilized in the future. Virtually all the significant discoveries of MVT deposits in the last three decades have been of orebodies that are completely blind in terms of surface exposure. Continental interiors are areas of both low physical and structural relief, and thus outcrops are limited and major portions of the cover-rock section hidden. The recognition of potential aquifers for MVT fluids (basal sands, paleokarst horizons), the location of basement highs, and limestone-dolostone interfaces within units, all provide aids to target development. However, the recognition of major paths and vectors of collision-induced fluid flow may prove invaluable in future basin analysis and subsurface exploration.

9.4 The Lead-Zinc Deposits of Ireland

9.4.1 Occurrence and General Considerations

Within just a few decades Ireland has emerged from near dormancy in mining terms to become a major producers of lead, zinc, and silver. The carbonate-hosted Zn-Pb deposits that have been discovered in central Ireland during this period (Fig. 9.11) represent a cohesive and yet varied group of orebodies that have received excellent documentation and attracted considerable research attention (see Andrew et al. 1986). Of the ~ 130 million tons of carbonate-hosted lead-zinc ore that has been discovered in Ireland in recent decades, most occur in the form of sediment-hosted massive sulfide deposits (Hitzman and Large 1986), and the lion's share of those is represented by the world-class ($>$ 70 million tons) Navan deposit. A relatively small amount occurs in clearly epigenetic MVT deposits.

Essentially all of the lead-zinc mineralization and the units that host it are of early Carboniferous age (Fig. 9.12), and can be divided into a group of

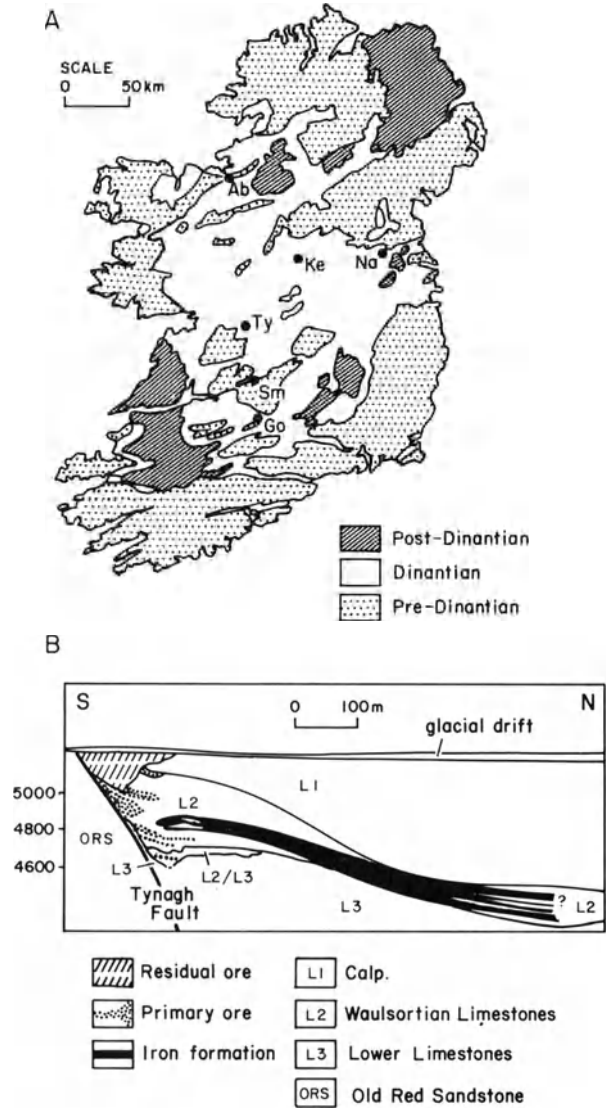

Fig. 9.11A. Map showing principal base metal deposits of Ireland. *Ty* Tynagh; *Ab* Abbeytown; *Go* Gotdrum; *Ke* Keel; *Na* Navan; *Ke* Keel (After Boast et al. 1981). **B** Geologic cross-section of the Tynagh deposit (After Boast et al. 1981)

deposits associated with the Walsortian mudbank micrite facies, and those deposits of the Navan group (Hitzman and Large 1986). Further evidence for the age of mineralization has come from U-Pb dating of uraninite (from the Gortdrum Cu deposit, Duane et al. 1986). The whole question of tectonic activity during the time of metallogenesis is pivotal to a full understanding of the central Ireland Pb-Zn province, but unfortunately some of the details are

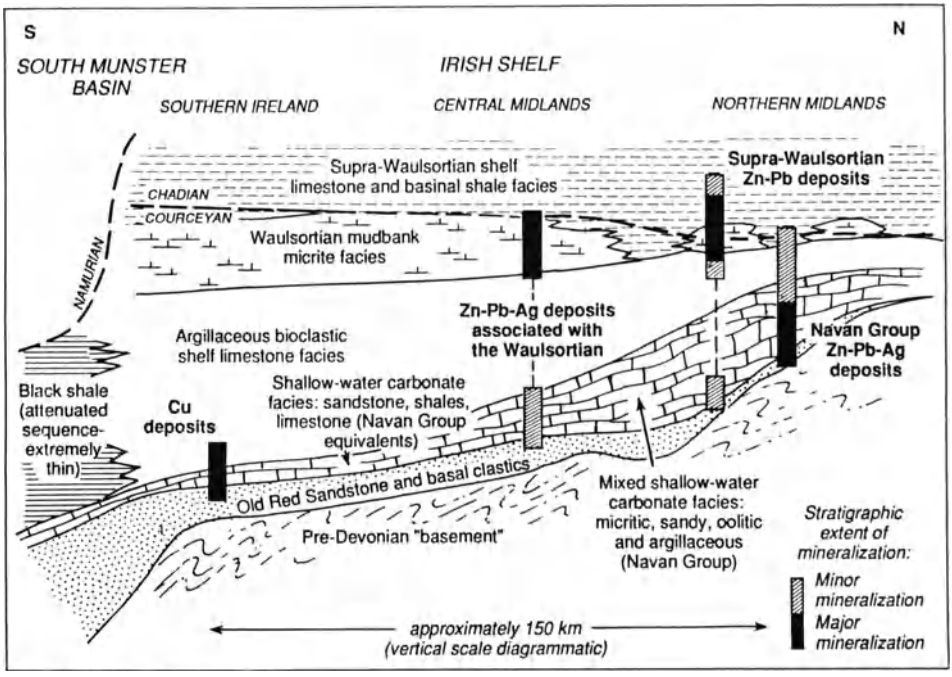

Fig. 9.12. Generalized north-south stratigraphic section across southern and central Ireland. Note position of South Munster Basin and the presence of basal clastics above the pre-Devonian basement. These provide both a source of basinal fluids and a potential conduit for them to reach the stratigraphic pinch-downs in the north (After Hitzman and Large 1986)

contentious. What is clear is that a period of subsidence and extensional faulting occurred in central Ireland during late Devonian and earliest Carboniferous time (Boyce et al. 1983; Philcox 1984; Andrew 1986a; Phillips and Sevastopulo 1986; Russell 1986). In addition, thicknesses of clastic rocks of up to 6 km developed in basins to the south (Munster Basin, South Munster Basin) and southeast (Shannon-Dingle Basin).

The salient features of the Irish base metal province are its relatively limited areal extent, the restriction of timing of mineralization to 350 ± 20 Ma, range of mineralization styles from syngenetic through diagenetic to epigenetic, lack of any obvious association with magmatism, and position of major deposits at the edge of subbasins (B. Williams and Brown 1986). In addition, fluid inclusion studies (Samson and Russell 1987) indicate saline ore fluids (10–25 equiv. wt% NaCl) with temperatures in the 100–200°C range, while isotope studies (Caulfield et al. 1986; LeHuray et al. 1987) indicate derivation of sulfur from both local and deep-seated sources, and lead from underlying Caledonide sources or from first-cycle sediments derived from such sources. Another noteworthy aspect of early Carboniferous metallogenesis in Ireland is a zoning of metals with copper and silver prominent in the south and zinc prominent in the north (see Fig. 9.11). This suggests, when

taken together with a narrow time window within which mineralization occurred, that the deposits are all the result of a series of tectonically-driven hydrothermal events.

9.4.2 Geology of the Navan Zn-Pb Deposit, County Meath, Ireland

The Navan orebodies, which contain at least 70 million tons of ore grading 10.1% Zn and 2.6% Pb, were discovered in 1970 and are expected to produce 2.3 million tons of ore annually. The stratigraphic sequence within which the ores occur, the Navan Group, consists of a relatively thin interval of clastic units overlying a major unconformity, which is in turn overlain by a series of shallow-water carbonate units (Fig. 9.13). It is the lower part of this carbonate sequence, the Pale Beds, that hosts the Navan ores (Andrew and Ashton 1985; Ashton et al. 1986). In regional terms the basal clastics thicken to the southwest and are overlain by a northerly-younging carbonate sediment package. It is an upward-fining clastic sequence that becomes increasingly carbonate-rich and passes into pale, oncolitic micrites. The uppermost part of the Navan Group consists of fine-grained bioclastic, muddy limestones and siltstones. Overlying groups are Walsortian mudbank Reef limestones and additional pale, shelf calcarenites and darker basinal limestones and shales (see Fig. 9.12). A major

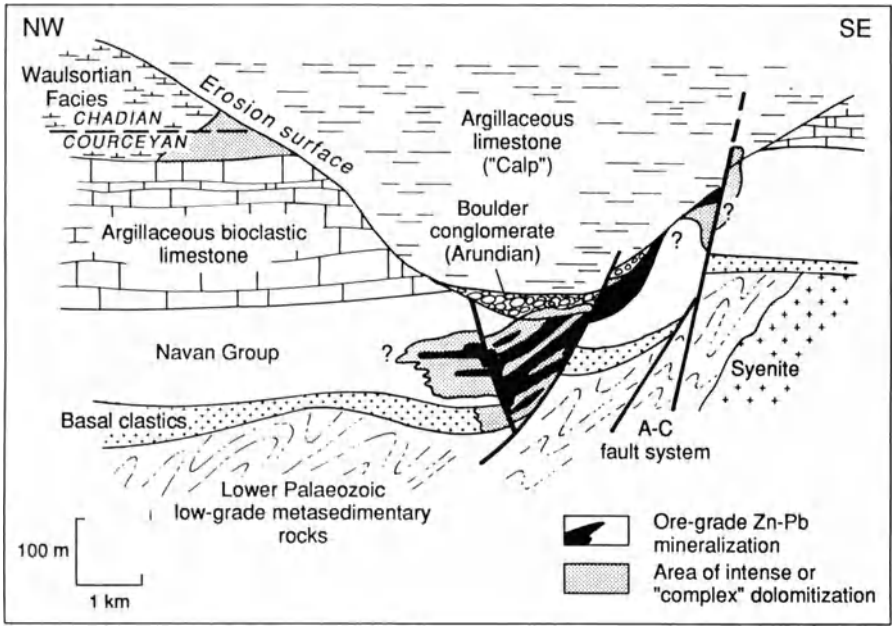

Fig. 9.13. Highly schematic regional cross-section through the Navan area. Note the presence of basal clastics and position of ore adjacent to faults just above these clasts (After Hitzman and Large 1986)

erosion event removed the entire lower Carboniferous sequence locally, and this surface is overlain by a variable thickness (0–45 m) of debris-flow material known as the Boulder Conglomerate.

The Navan ores exhibit a primary structural control in the form of ENE- to NE-trending mineralized fractures. Development of these fractures was followed by a series of ENE-trending normal and transcurrent faults that clearly developed subsequent to mineralization. These faults, which developed largely prior to the Boulder Conglomerate, divide the Navan ores into three structural zones (Fig. 9.13).

More than 95% of the ore at Navan is developed within a series of five stacked stratiform lenses in the lowermost 130 m of the Pale Beds. The ores are characterized by simple mineralogy and consist of low-iron sphalerite and galena, accompanied by variable amounts of marcasite and lesser pyrite. The sphalerite is typically very fine-grained, whereas the closely associated galena is coarser-grained. Trace amounts of sulfosalts, mainly semseyite and bournonite have been observed, in addition to freibergite and pyrargyrite, the two principal silver-bearing minerals.

The ore textures at Navan are complex in detail, but can be broadly divided into bedding-parallel styles and crosscutting styles. The former in their simplest form consist of layers of well-laminated, fine-grained, pale sphalerite interlayered with smaller quantities of coarser galena. These layers display evidence of strong disruption in many cases and bedding contortions and pull-apart structures indicate deformation of synsedimentary layers and perhaps selective replacement of unlithified chemical sediments. Other bedding-parallel features are dilational veins, some of which contain stalactitic sulfide growths. These indicate the former presence of hydraulically dilated cavities and provide evidence for fluid overpressures. Crosscutting mineralization occurs in discrete veins and breccia zones developed along NE and ENE directions. The larger of the vein structures display banded sulfides with a central zone of coarser galena, and in many instances the crosscutting mineralization appears to represent feeder zones to overlying stratiform sulfides. It is noteworthy that rare sulfide-filled veinlets and fractures are found in the clastic section below the limestones.

Metal distribution patterns at Navan emphasize the wide distribution of Lens 5 mineralization and the relatively restricted nature of mineralization in the overlying lenses. Changes in these patterns are most pronounced in a vertical sense and embody decreases in the Pb and Ag content of the ore lenses upwards and increases in their iron content. Overall, there is an indication that crosscutting mineralization was important in terms of upgrading the metal contents of earlier stratiform ores.

Fluid inclusion and isotope data for the Navan ores are only fragmentary at this time, but the numbers available are similar to those pertaining to other Irish carbonate-hosted Zn-Pb deposits. No consensus regarding the genesis of the Navan deposit has been reached, but it seems more fruitful to discuss the genesis of the Lower Carboniferous base metal event in Ireland in its entirety, as will be attempted in the next section.

9.4.3 A Model for Zn-Pb Metallogenesis in Central Ireland

The plethora of models that have been advanced to account for the genesis of the base metal deposits of central Ireland (see Andrew et al. 1986 and references therein) fall into two basic groups; those that favor some variant of basin dewatering (Lydon 1986), and those that appeal to concepts of fracture-controlled convective leaching of the pre-Carboniferous basement (Russell 1978, 1986). As noted in previous sections, basin dewatering has gained wide acceptance as a mechanism for production of the ore fluids responsible for the formation of both stratiform Zn-Pb massive sulfide and MVT deposits. Given the geologic, geochemical, and isotope data available from the Irish deposits, and their essential similarity to those pertaining to sediment-hosted Pb-Zn massive sulfide and MVT deposits elsewhere, it is appropriate to examine the basin-dewatering model for early Carboniferous metallogenesis in Ireland. In addition, Lydon (1986) presents an array of cogent arguments that cast serious doubt upon the viability of convective leaching models.

Factors that favor the basin-dewatering model are the presence of basins with significant thicknesses of clastic sediments to the south and southwest of the central Irish orefield, the narrow time window within which major ore deposition occurred, the presence of potential aquifer formations just above the major unconformity (see Fig. 9.12), the suggestion of progressive temperature and redox-dependent changes in metal ratios from south to north (Cu→ Pb→ Zn), and the presence of major mineralization (Navan group of deposits) close to a stratigraphic pinch-out (see Fig. 9.12).

To this list can be added the evidence for hydraulic overpressures at Navan (Ashton et al. 1986) and fault activity contemporaneous to mineralization in many of the deposits. One aspect that has received little attention is the fundamental cause of late Devonian-early Carboniferous rifting and basin development in Ireland (C. Brown and Williams 1985), although Mitchell (1985) has suggested that both it and the Irish mineralization are related to an arc-continent collision. This interesting postulate has been strengthened by refinements in our understanding of the relationship of rifting to collision events (Burke and Sengor 1986), and the results of both geophysical (Day 1986) and age-dating studies in southwest England and its adjacent continental margin. The former indicate the presence of major Hercynian thrust structures extending from the Lizard west-south-west to due south of Ireland, and the latter date the Lizard Thrust at 370 Ma. It is inconceivable that Ireland, just 200 km to the north, was in some way insulated from these major tectonic events. They provide, if nothing else, a mechanism for brine expulsion from the relatively deep South Munster Basin at precisely the right time and in the manner suggested by Oliver (1986) and Duane and deWit (1988).

It seems likely that the initial brines were somewhat oxidizing because of their Old Red Sandstone provenance and were responsible for the Cu-Ag deposits in the south (Sverjensky 1988). Further migration of these brines up onto the central Irish platform through less oxidized aquifers would result in

acquisition of lead and in particular zinc. Major deposits resulted at sites where these metalliferous brines escaped upward to the seafloor along faults (e.g., Silvermines; Andrew 1986b) or where they were trapped in stratigraphic pinchouts and utilized fracture systems to produce a combination of syngenetic, syndiagenetic, and epigenetic ore (e.g., Navan; Ashton et al. 1986).

This model for central Ireland metallogenesis differs from other basin dewatering models (Lydon 1986; B. Williams and Brown 1986) mainly in terms of the emphasis on lateral migration of basinal fluids just above the major unconformity separating subsurface Caledonide terranes from the overlying late Devonian-early Carboniferous cover rocks. Some may argue that the maximum temperatures of ore deposition (~200° C) are too high, and thus rule out fluid migrations of the order of 200 km. This objection may be questioned in view of the considerable thickness of cover rocks overlying the postulated basal aquifer (up to 1.7 km, Philcox 1984), and the evidence for Courceyan volcanism within the South Munster Basin (Phillips and Sevastopulo 1986). Furthermore, if the SW-NE-trending block-trough model of C. Brown and Williams (1985) is a valid interpretation of their geophysical data, then some potent linear zones for fluid flow would have been created by the presence of coarse clastics deposited adjacent to fault scarps.

LeHuray et al. (1987) have chosen to interpret their lead isotope data, which reflect the nature of the Caledonide and pre-Caledonide basement, as evidence for leaching of the basement terranes by the ore fluids. However, it should be noted that lead isotope data cannot be used to discriminate between basement rocks and first-cycle sedimentary units derived directly from them as lead sources for ore deposition.

The foregoing model for metallogenesis of the central Irish orefield will undoubtedly be subject to change with the acquisition of new data, but it provides a scenario that is consistent with the empirical data at scales ranging from broad tectonic settings to ore textures to isotopes.

9.5 Sandstone-Hosted Lead Deposits in Relation to Collisional Orogeny

9.5.1 General Aspects

As noted by Bjorlykke and Sangster (1981), deposits of galena in the form of disseminations in basal quartzitic sandstones represent a distinct and locally important ore type. The most important and best-studied examples occur in shallow marine sandstones in the eastern and southeastern margins of the Caledonides where they border on the Baltic Shield (Fig. 9.14). Additional examples are known in Carboniferous sandstones in Nova Scotia, eastern Canada, and possibly in quartzites and conglomerates of the Wollaston Group in northern Saskatchewan, Canada (see Bjorlykke and Sangster 1981). However, the lead deposits that are hosted by Triassic sandstones in West Germany, France, and Morocco (Samama 1976), and the lead and copper

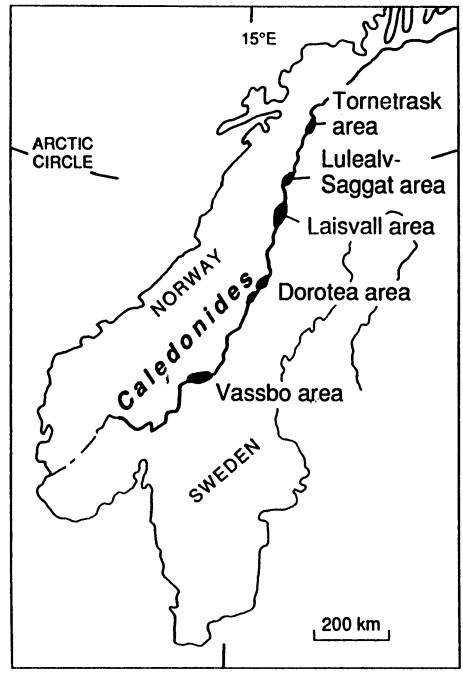

Fig. 9.14. Map illustrating the position of Pb-Zn deposits of Laisvall type at the forward edge of the Caledonide thrust belt (After Rickard et al. 1979)

deposits in Cretaceous sandstones in North and West Africa (see Fig. 8.22) are more appropriately viewed as related to continental rifting environments.

The presence of scattered occurrences of disseminated lead mineralization in sandstones for a distance of almost 2000 km along the Caledonide front in Sweden and Norway suggest the operation of a mineralizing system of dimensions similar to the Caledonide orogen itself. These ores, and those of the Yava deposit in Nova Scotia, can be viewed simply as low-grade, but commonly extensive, sandstone-hosted variants of collision-related MVT deposits. This scenario is further strengthened by the available fluid inclusion data which indicate ore deposition from saline brines at temperatures in the 120–180°C range (Lindblom 1986). The fact that these deposits are notably lead-rich in comparison to most MVT deposits could reflect the sandstone aquifers through which the basinal brines were impelled (see Lydon 1983).

9.5.2 The Pb-Zn Ores of the Laisvall Deposit, Sweden

The Laisvall deposit represents 80 million tons of ore grading 3.5% Pb and 0.44% Zn emplaced in Eocambrian sandstones that lie a short distance (30–60 m) above a major unconformity (Rickard et al. 1979). The sandstones and the Proterozoic granitic basement they overlie are autochtonous, but have been overridden by Caledonide thrust sheets (Fig. 9.15). Textural studies of the ores indicate that they were already in place at the time of deformation (Rickard et

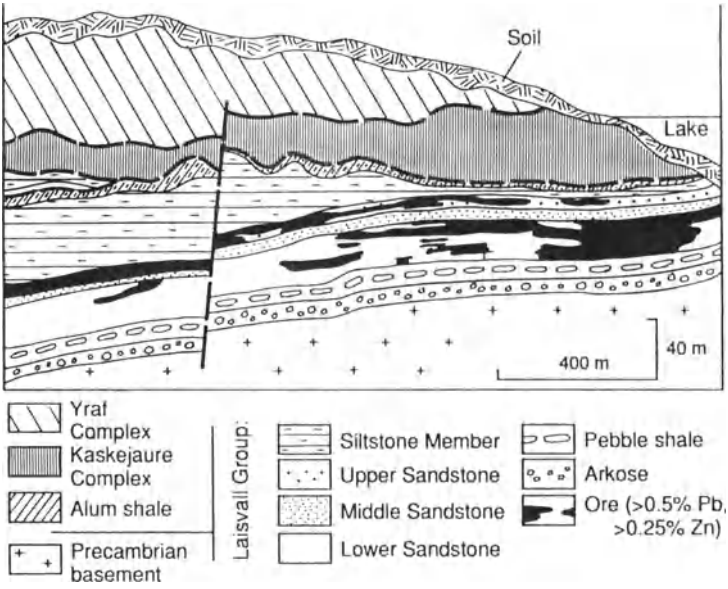

Fig. 9.15. Schematic section through the mine area at Laisvall, Sweden (After Rickard et al. 1979)

al. 1979). The host sandstones were deposited on a peneplained Precambrian surface that formed the stable eastern margin of the Iapetus Ocean. In a reconstruction of the paleogeography of the immediate Laisvall area, Rickard et al. (1979) note that the Lower and Middle Sandstones were deposited between basement hills, whereas the Upper Sandstone is continuous over the entire area. Orebodies occur as thin but extensive elongate sheets in the Lower and Upper Sandstones and exhibit distinctly different areal geometries in each.

The galena, sphalerite, quartz, barite, calcite, and fluorite that represent the phases introduced by mineralization, primarily occupy the pore spaces within the sandstone but small amounts of ore also occur in joints and tension cracks. Orebody contacts are in some instances very abrupt but are mostly the result of a gradual decrease in galena content of the sandstone host. Pb/Zn ratios are much higher (19) in the Lower Sandstone than those in the Upper Sandstone, where Pb/Zn ratios are lower and variable.

In his fluid inclusion study of the Laisvall ores, Lindblom (1986) was able to demonstrate that the sequence of deposition of minerals was calcite-barite-fluorite-sphalerite-galena, that this succession was repeated several times, and that sulfide deposition was accompanied by calcite dissolution. Ore deposition occurred within the temperature range 120–180°C and involved fluids of 24 equiv. wt% NaCl that are thought to have mixed with cool, local groundwater. On balance, this deposit and the Vassbo (5 million tons 5.5% Pb) and Guttusjo (2.5 million tons 3.5% Pb) deposits in the Vassbo district (Christofferson et al. 1979; see Fig. 9.14) clearly have close similarities and a common genetic heritage with MVT deposits.

9.6 Tin-Tungsten Deposits Associated with Collisional Granites

9.6.1 General Aspects

One of the hallmarks of collisional orogenic belts, both those of Wilson Cycle-type and intracratonic-type, is the generation of considerable volumes of anatectic (S-type) granites. These intrusions are in many instances two-mica granites and, as opposed to the I-type granitic intrusions of arc systems, tend to exhibit diffuse contact zones characterized by migmatites. Granites of this type are particularly prevalent along the Hercynian belt of western Europe (Fig. 9.16). Pitcher (1979) characterizes such granitic complexes as Hercynotype as opposed to those of Andinotype, which are subduction related (Fig. 9.17). He further points out that relative amounts of gabbro-diorite/tonalite-granodiorite/granite are quite distinctive for each type. In Hercynotype settings the relative proportions of these rock types are judged to be 2:18:80, whereas in Andinotype settings the ratios are closer to 15:50:35. Interestingly, the controversy that raged in petrologic circles several decades ago (Read 1957) regarding the origin and emplacement of granite was largely between those workers whose field experience was limited to Hercynotype granites, and those whose experience was limited to Andinotype granitic rocks.

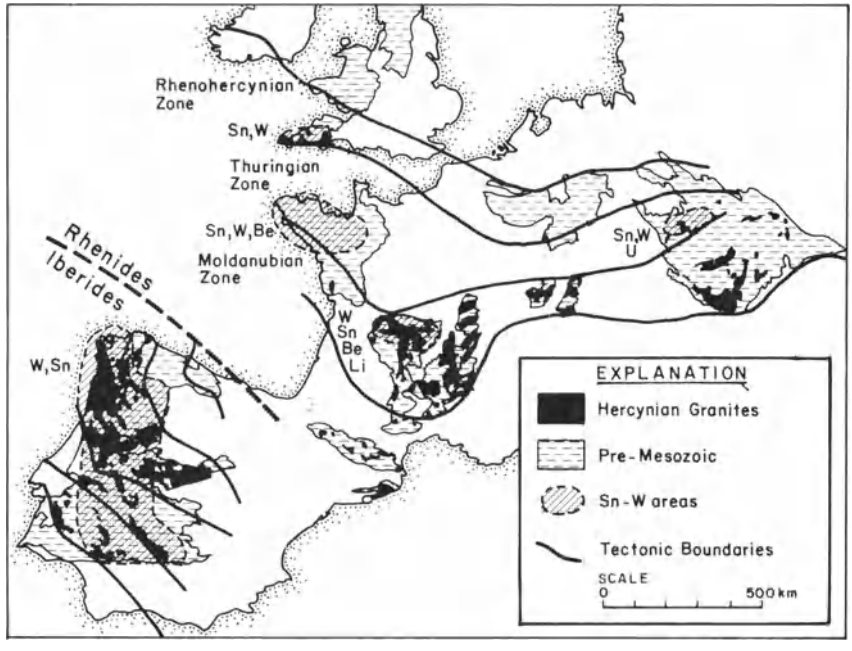

Fig. 9.16. Map of pre-Mesozoic and Hercynian granitoids in western and central Europe beyond the Alpine orogen. Granitoids shown in *black* (After Stemprok 1980)

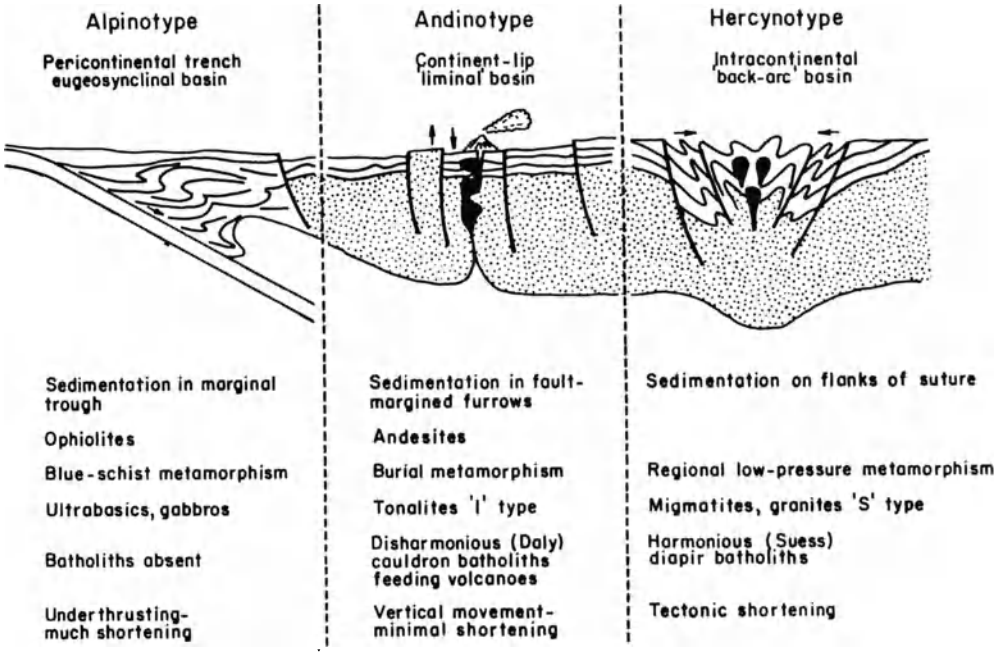

Fig. 9.17. Pitcher's conceptual depiction of the tectonic settings in which Andinotype and Hercynotype granitic intrusives are generated (After Pitcher 1979)

Important tin and tungsten deposits are associated with Hercynian granites in southwest England (Dines 1956), the Erzegebirge-Krusne Hory area, Germany and Czechoslovakia (Tischendorf et al. 1978), and the western Iberian Peninsula (Cotelo Neiva 1972), and lesser deposits are associated with Hercynian granites in Brittany and the Massif Central in France (Stemprok 1981; see Fig. 9.16). Numerous attempts have been made to interpret the Hercynides in terms of a collisional event preceded by closing of the Rheic Ocean (e.g., Dewey and Burke 1973; Mitchell 1974; Bromley 1976). However, the lack of a well-defined Andinotype arc on either flank of the Hercynian belt, and the evidence of a rifting event only about 70 million years prior to collision (Sawkins and Burke 1980) support the concept that the Hercynian belt is more appropriately viewed as a predominantly ensialic-type collision belt, of the type detailed in the opening section of this chapter. Transcurrent faulting may also have been important in the evolution of this belt (Badham 1982), as noted in the preceding chapter. If the Lizard Complex is in fact a true ophiolite, however, (Kirby 1979), then some oceanic crust must have been generated during the antecedent rifting events. S-type granites of Hercynian age (Middle Devonian to Carboniferous) that have tin-tungsten-molybdenum greisen and skarn deposits associated with them are also known in Nova Scotia and New Brunswick (Ruitenberg and Fyffe 1982). The best-known deposit in this area is that at Mt. Pleasant (Petruk 1973), a subvolcanic porphyry deposit containing 9 million tons of close to 0.4% WO_3 and 0.2% MoS_2, and considerable

potential for additional ore. Sillitoe (pers. comm.) suggests, however, that the intrusive which spanned this deposit is related to a major post-collisional transform.

The Central Tin Belt in Southeast Asia (Mitchell 1977) is a less controversial example of a collisional orogen, and contains major tin deposits associated with S-type granites. As depicted in Fig. 9.18, it is flanked to the west by the younger backarc magmatic tin belt (see Chap. 3), and to the east by a precollision magmatic arc of Permo-Triassic age (Mitchell and Garson 1981). This eastern belt is puzzling, however, because lead and strontium data indicate that the tin granites of Indonesia, which lie within this belt, are of crustal origin (M.T. Jones et al. 1977). Nevertheless, it also contains a porphyry copper deposit at Loci in Thailand, a typical product of subduction-related magmatism (Hutchinson and Taylor 1978) that appears to belong to an arc system sandwiched between the Central and Eastern Tin Belts (Sillitoe, pers. comm.).

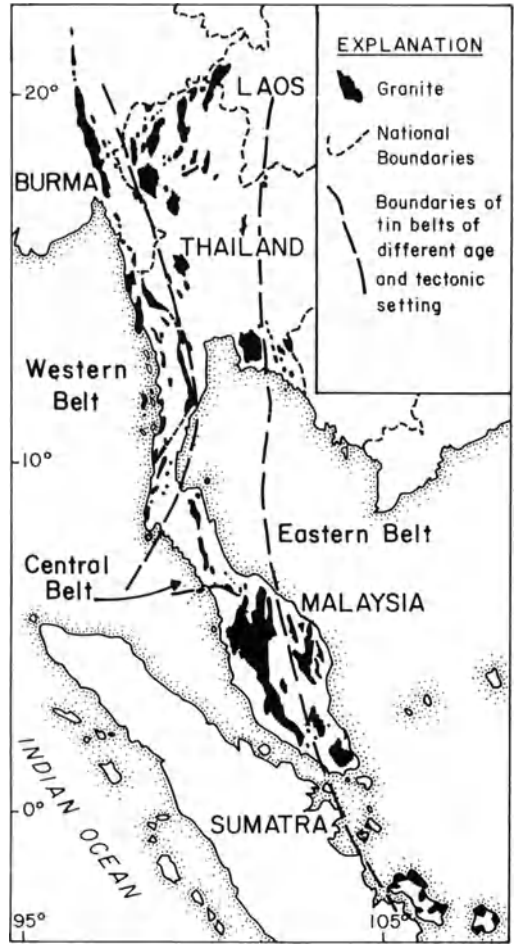

Fig. 9.18. Map of granitoid bodies associated with the tin belts of Southeast Asia (After Beckinsale et al. 1979)

The Central Tin Belt accounts for about half the tin production of the Western world, although most of this comes from placer deposits (Mitchell and Garson 1981). The tin-bearing granites are primarily peraluminous two-mica granites and adamellites of late Triassic age, and exhibit high initial $^{87}Sr/^{86}Sr$ ratios (Beckinsale et al. 1979). They are thus of characteristic S-type.

9.6.2 Mineralization

The tin and tungsten mineralization of the Hercynian belt is closely associated with the younger group of granitic intrusions (260–300 Ma), which are predominantly alumina-rich alaskites and lithium albite granites. The most important deposits are closely associated in space with intrusive contacts and occur as stockworks, vein complexes, or single veins characterized by greisen-type alteration and the presence of tourmaline (Stemprok 1981). Where limestones occur adjacent to igneous contacts, skarn-type deposits are formed locally. Vein deposits only loosely related to igneous contacts exhibit a control by regional structural directions and fissure systems. These veins are less important economically, but tend to be more extensive vertically.

Vein fillings consist predominantly of quartz with lesser amounts of micas, topaz, tourmaline, K-feldspar, fluorite, and siderite. The metallic minerals are cassiterite and wolframite, accompanied by variable amounts of the sulfides arsenopyrite, pyrite, pyrrhotite, sphalerite, galena, chalcopyrite, bismuthinite, and stannite. The sulfosalt association that characterizes the backarc tin deposits of Boliva is essentially absent in Hercynian tin deposits (Stemprok 1981). However, zoning, a feature of most arc-related hydrothermal deposits, is also developed in these collision-related ores, and is manifest as a change from tin-dominated veins in the central portions of districts to base metal sulfide-dominated veins on their peripheries. Such zoning is particularly well developed around the tin centers in Devon and Cornwall (Fig. 9.19). In greisen and skarn deposits the tunsten-bearing mineral is typically scheelite rather than wolframite.

9.6.3 The Panasqueira Tin-Tungsten Deposits, Northern Portugal

The Panasqueira district is of interest on two counts: it is the largest producer of tungsten in western Europe, and is almost certainly the most thoroughly studied collision-related hydrothermal deposit in the world. The ores in the Panasqueira district average 0.3% W, and in 1978 mine production represented 1450 tons of tungsten concentrate (75% WO_3), 62 tons of cassiterite concentrate (75% SnO_2), and 1101 tons of chalcopyrite concentrate (22% Cu). The geology, mineralogy, and fluid inclusions of the deposit have been extensively studied by Kelly over a period of several years (Kelly and Rye 1979), and the following descriptions and data are taken from that work.

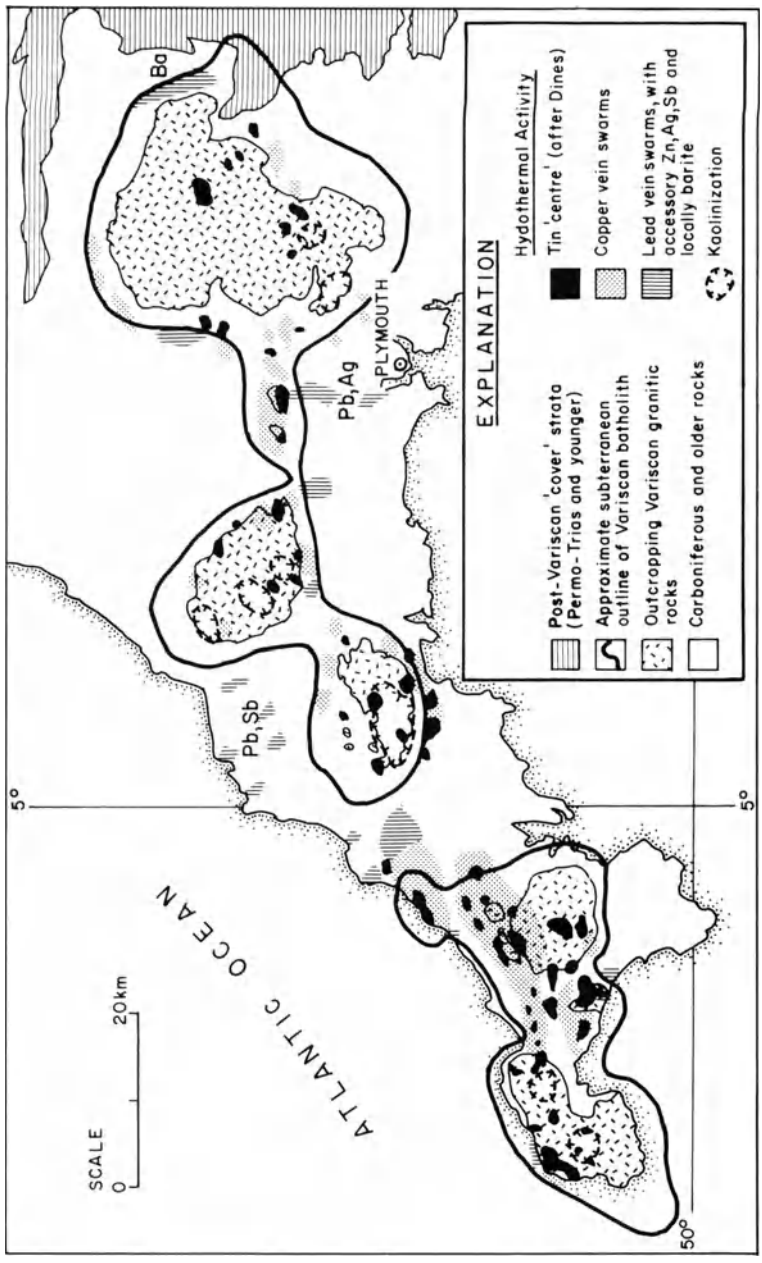

Fig. 9.19. Map of the mineralized centers of southwest England showing broad zonal relationships of tin, copper, and lead mineralization. Note clear indication of a spatial association of mineralization with the roof zones of the Variscan (Hercynian) granites (After Moore 1982)

The Panasqueira veins overlie a hidden cupola of strongly altered and greisenized two-mica granite. The granite was intruded about 290 Ma ago into a sequence of dark schists which exhibit a rather broad aureole of contact metamorphism (mainly spotting), indicative of a more extensive intrusion at depth. The area is also intruded by postgranite dolerite and aplite dikes.

The Panasqueira vein system is unusual in that the veins occupy horizontal dilation structures thought to have formed by the reduction of overburden pressure. The mineralization consequently is restricted to a narrow vertical interval (100–300 m) in the schists above the cupola, but is laterally extensive (Fig. 9.20). Kelly and Rye (1979) note that the veins, which formed by open-space filling, are clearly later than emplacement of the Panasqueira Granite, which they view as a structural conduit for ore fluids of deeper provenance.

Four stages of mineralization have been identified (Fig. 9.21), each of which appears to be contemporaneous throughout most of the vein system. The silica cap immediately above the apex of the granite cupola is thought to have been formed by early precipitation of quartz in a void created by slight withdrawal of magma, and is weakly mineralized. The vein apatites are fluorapatite, and all the white micas are fluormuscovites of rather uniform composition.

Fluid inclusion studies indicate that the ore solutions were sodium chloride brines (5–10 wt%) that ranged in temperature from 230° to 360°C during mineralization stages I, II, and III (see Fig. 9.21). During the final stage

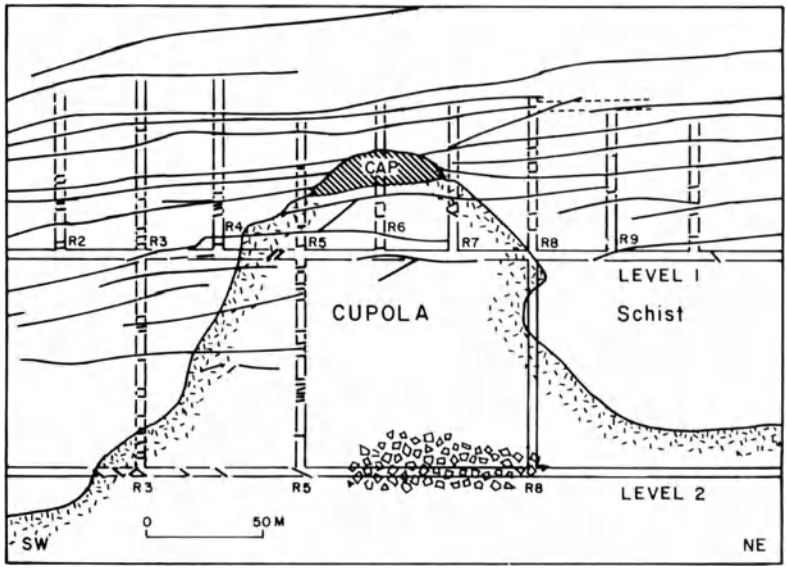

Fig. 9.20. Cross-section of the Panasqueira cupola showing flat vein structures and silica cap (After Kelly and Rye 1979)

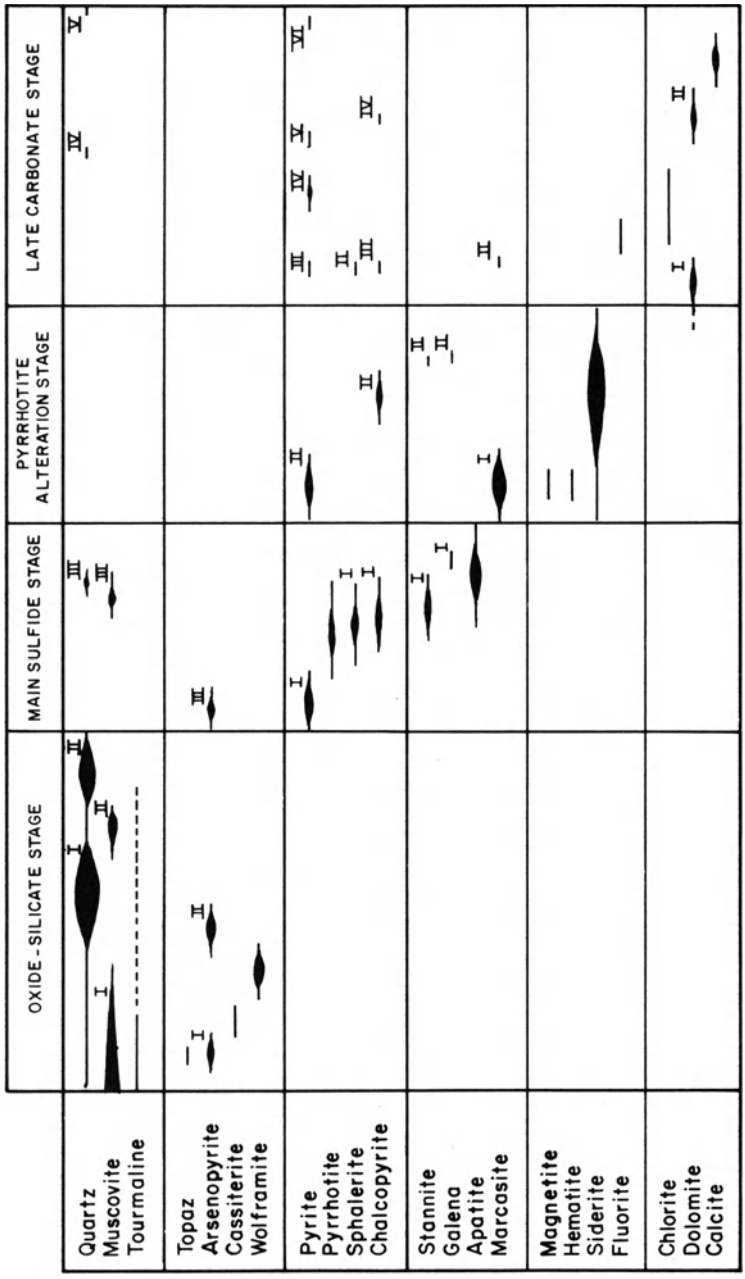

Fig. 9.21. General paragenesis of the tin-tungsten veins of the Panasqueira deposit. *Roman numerals* identify multiple generations of a given mineral (After Kelly and Rye 1979)

of vein deposition the temperatures dropped to below 120°C and the salinity of the fluids was less than 5 wt%. The carbon dioxide contents of the ore solutions declined with time, but were as high as 9 mol% during formation of the silica cap, although through most of the mineralization CO_2 contents were less than 2 mol%. Calculations based on the fluid inclusion data indicate that fluid pressure must have attained 1000 bar at times, and depth estimates for the vein system during mineralization provide a range of 600–1300 m below the water table.

$\delta^{18}O_{H_2O}$ data from the deposit indicate a high degree of ore fluid exchange with the schist country rocks and/or the underlying granite, and Kelly and Rye (1979) conclude the earlier stage fluids could have been either magmatic in origin or highly exchanged meteoric water. Based on their $\delta^{18}O_{H_2O}$ values, the late-stage fluids appear to have contained a dominant meteoric component. The available δD data are puzzling in that they indicate two isotopically distinct waters during stage I mineralization, one with values in the range -41 to -63‰ δD_{H_2O}, another with values in the range -67 to -124‰. $\delta^{34}S$ data derived from sulfide minerals indicate a narrow range of 0.1 to -0.9‰, and are interpreted to indicate H_2S-dominated solutions and sulfur of possible magmatic provenance. $\delta^{13}C$ values of carbonates in the veins imply a graphitic or organic carbon component for the carbon contained in the hydrothermal solutions. Overall, the stable isotope data appear to indicate a strong country rock signature in the mineralizing fluids, but inasmuch as the underlying granite is of S-type (i.e., formed by anatexis of crustal materials) a magamatic origin of the ealier stage ore fluids and the metals seems probable.

The Hercynian tin-tungsten veins are cut by steep, later faults that contain weak base metal mineralization of uncertain age and provenance, but in general the ores have not suffered tectonic or significant thermal disturbance since their formation. In view of the indicated shallow depth at which they formed, it is somewhat surprising that they have not been eroded away, but it can be surmised that they were protected by postore cover rocks that have since been removed.

9.6.4 Discussion and Suggestions for Exploration

The tin and tungsten deposits associated with S-type granitoid intrusives in collision belts resemble the magmatic hydrothermal vein-type deposits associated with I-type granitoid intrusives in subduction-related terranes in many respects (e.g., morphology and zoning). This is not surprising for both are almost certainly formed in large measure by hydrothermal fluids emanating from shallow-seated magmatic systems. The main difference between the two groups lies in the predominance of tin and tungsten in the former, and base and precious metals in the latter. As noted earlier, where tin and tungsten metallization does occur in arc systems, the deposits tend to be confined to the innermost zones of continental margin arcs where the intrusives manifest a distinct S-type character.

The tin-tungsten deposits in question exhibit a close spatial association with the roof zones of collision-related granites, especially those that are emplaced during the late stages of orogenesis. Granitic bodies of this class, which exhibit high degrees of differentiation and some postmagmatic alteration, are obvious, broad exploration targets. Also, because of the zoning characteristics of such systems, diffuse base metal vein mineralization in collision orogens deserves attention, for it may represent the distal manifestation of subsurface tin-tungsten mineralization. Unfortunately, neither geochemical nor geophysical techniques have much utility in such situations, although Yeates et al. (1982) have reported encouraging results from the application of gamma-ray spectrometry to prospecting for tin and tungsten granites in the Lachlan Fold Belt. Apparently in this area mineralized granites contain on average significantly higher U (5 ppm) than nonmineralized granites. Also, careful gravity surveys could help to locate shallow, subsurface granitic intrusives, and their uppermost portions could be subsequently tested by diamond drilling. Attention should also be focused on broad areas of greisenization, in the event that they host low-grade tin-tungsten ores amenable to bulk mining techniques. The East Kempville deposit in southwest Nova Scotia is an example of this, and contains 38 million tons of 0.2% Sn in a greisen zone developed along the contact of a monzogranite of late Devonian age (J.M.G. Richardson et al. 1982).

9.7 Uranium Deposits Associated with Collisional Granites

The S-type granites that are generated in collision orogens are also in some instances associated with uranium deposits. The major examples of such uranium mineralization occur in the Massif Central of France (Cuney 1978), the Bohemian Massif in Czechoslovakia (Ruzicka 1971; Fig. 9.22) and at Rossing in Namibia (Berning et al. 1976). Although the hydrothermal uranium deposits of the Hercynian terranes of Europe exhibit a strong spatial association with granites, their age of formation is in some instances distinctly younger than the granitic masses exposed at the surface (Leroy 1978). As with the Hercynian tin-tungsten deposits, mineralization ages tend to be in the 280–295 Ma range, coincidental with the very last phase of Hercynian magmatism.

Uranium deposits in collision settings are predominantly of vein type, but in some cases also occur in breccia zones. In the Margnac-Fanay district of the Central Massif, the vein deposits occur within an area of older two-mica granite (Saint Sylvestre granite) that is laced with faults, microgranite dikes, lamprophyre dikes, and mineralized veins (Fig. 9.23; Leroy 1978). Here, and also in the Boise Noirs-Limouzat vein system (Cuney 1978), detailed studies indicate multistage mineralization of the vein structures with quartz, pitchblende, sulfides, hematite, and carbonates arrayed in complex paragenetic sequences. In the case of the Bohemian Massif ores, uranium mineralization tends to represent a distinct stage that postdates an earlier

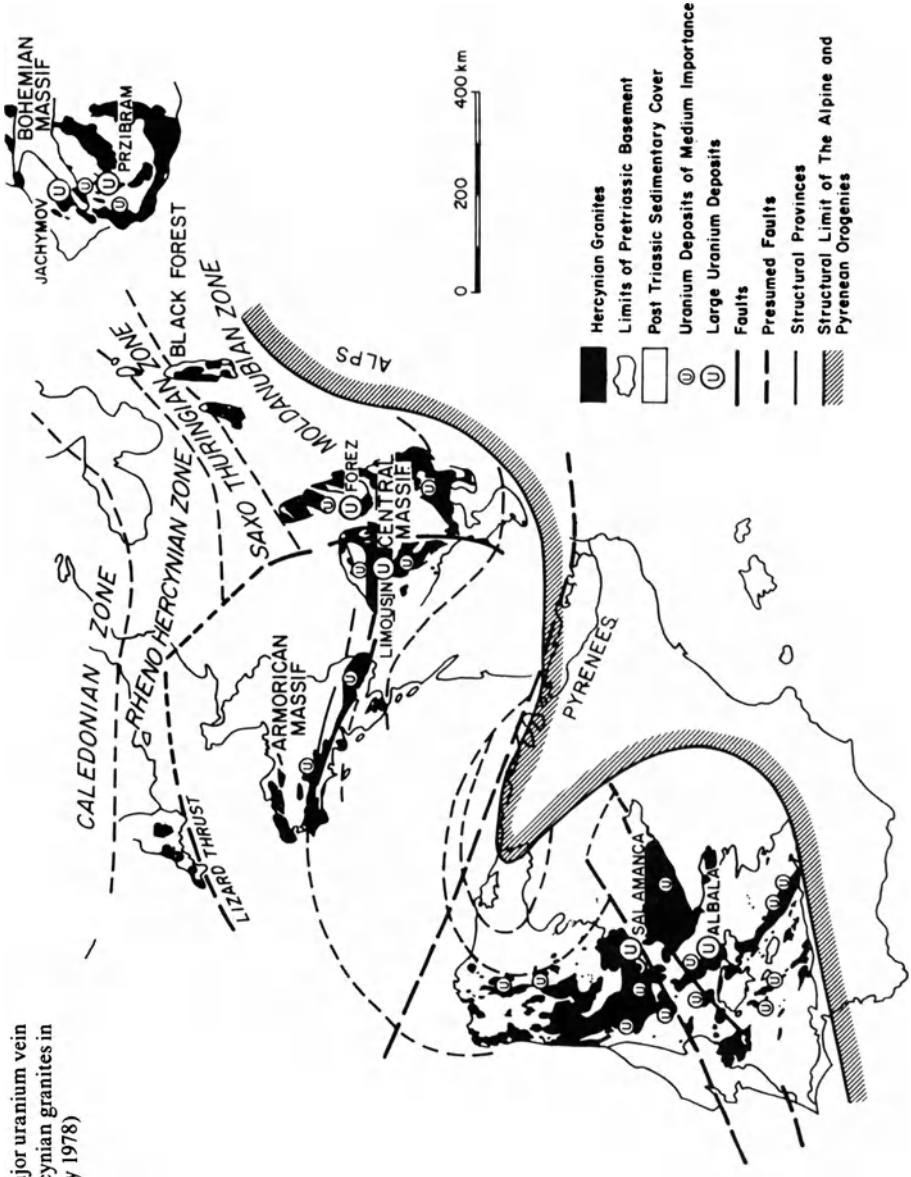

Fig. 9.22. Location of the major uranium vein deposits associated with Hercynian granites in western Europe (After Cuney 1978)

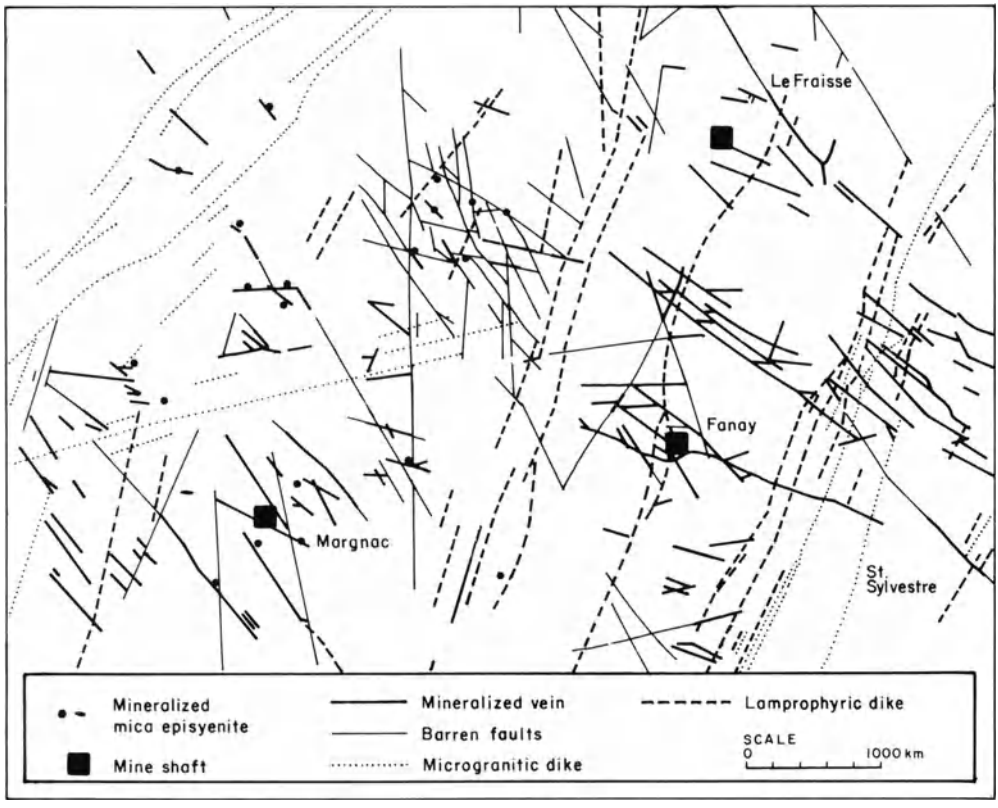

Fig. 9.23. Distribution of veins, faults, and dikes in the Margnac and Fanay uranium districts, developed within the Bois Noirs granite, central France (After Leroy 1978)

quartz-carbonate-sulfide stage of mineralization (Ruzicka 1971). Here, too, detailed paragenetic relationships are complex, and short uranium ore shoots occur within larger vein systems.

Fluid inclusion studies on the French deposits cited above provide data that seem to mirror the paragenetic complexity of the veins. Ore fluid temperatures varied from over 300° to less than 100° C, and variations also occur in salt and CO_2 contents of the fluids. The genetic model that has evolved from these studies suggests a mixing of meteoric water with deep-seated (magmatic) CO_2, and the leaching and concentration of uranium from the host granites. However, the manifestations of late Hercynian magmatism in these areas (mainly microgranite and lamprophyre dikes) conceivably provided a proportion of the aqueous fluids and metals involved in mineralization, in addition to the CO_2 and heat.

9.7.1 The Rossing Uranium Deposit, Namibia

Although grade and tonnage figures for the Rossing orebody are not known to the author, this deposit is generally conceded to be the largest uranium producer in the free world. It lies in the central, high-grade metamorphic zone of the Damaride orogenic belt, where granitized sedimentary rocks, and possibly volcanics, of the Etusis and Khan Formations, and remobilized early Precambrian basement (Abbabis Formation) have been intruded by anatectic granites. The Abbabis Formation includes a variety of gneisses, phyllites, marbles, and biotite schist, and is exposed in the cores of anticlines and domal structures (D.A.M. Smith 1965; Fig. 9.24). The overlying rocks of the Damara Supergroup consist of clastic and calcareous sediments now metamorphosed to gneisses, schists, and marbles, and all strongly deformed.

The uranium mineralization occurs within a migmatite zone characterized by largely concordant relationships between uraniferous pegmatitic granites and the gneisses, schists, and marbles of the Khan and Rossing Formations (Fig. 9.25). The granitic rocks that contain the uranium mineralization are termed alaskites by mine geologists, and they display a spectrum of textures ranging from aplitic to granitic and pegmatitic. The alaskite intrusions vary from thin conformable dikes, typically in closely spaced arrays, to more robust intrusions of discordant character. Relationships of the alaskite with country rocks, detailed by Berning et al. (1976) and Berning (1986), lead these authors to deduce a passive, metasomatic emplacement of the alaskite. However, contact metamorphic effects between alaskite and adjacent country rock are clearly evident, and the local presence of a melt phase cannot be totally discounted.

Most of the alaskite in the area is unmineralized or only weakly mineralized. Economic grade uranium mineralization is concentrated where the alaskite was emplaced in a garnet gneiss/amphibole unit (northern ore zone) or into the amphibole-biotite schist/lower marble/lower cordierite gneiss sequence of the central ore zone. The controls of ore localization in this manner are not understood. Uraninite is the main primary ore mineral, and is confined to alaskite as very small grains (several microns to 0.3 mm), occurring either occluded within quartz, feldspar, and biotite, or within cracks or interstitially to these minerals. It also exhibits a preferential association with biotite and zircon. Associated with the uraninite are much lesser amounts of betafite, whereas fluorite, sulfides (pyrite, chalcopyrite, bornite, molybdenite, and arsenopyrite), and oxides (magnetite, hematite, and ilmenite) occur somewhat sporadically in the ore. Secondary uranium minerals, mainly beta-uranophane, represent 40% of the uranium present in the orebody (Berning et al. 1976).

A precise genetic model for the Rossing deposit is not at hand, but clearly the formation of the alaskite must have involved a concentration of uranium, probably abetted by enhanced uranium levels in the basement rocks, where the alaskite or the metasomatizing fluids that produced it were generated.

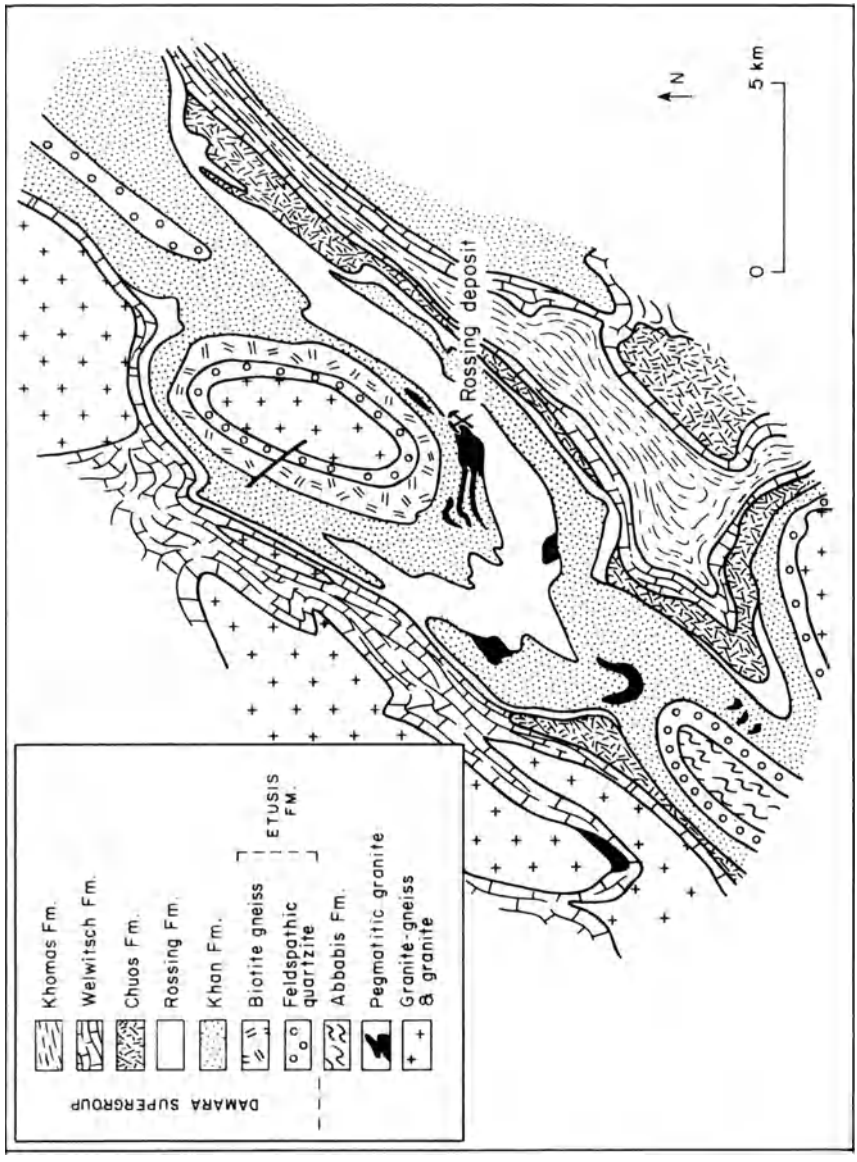

Fig. 9.24. Map of the Rossing uranium district, Damara Province, Namibia (After D.A.M. Smith 1965)

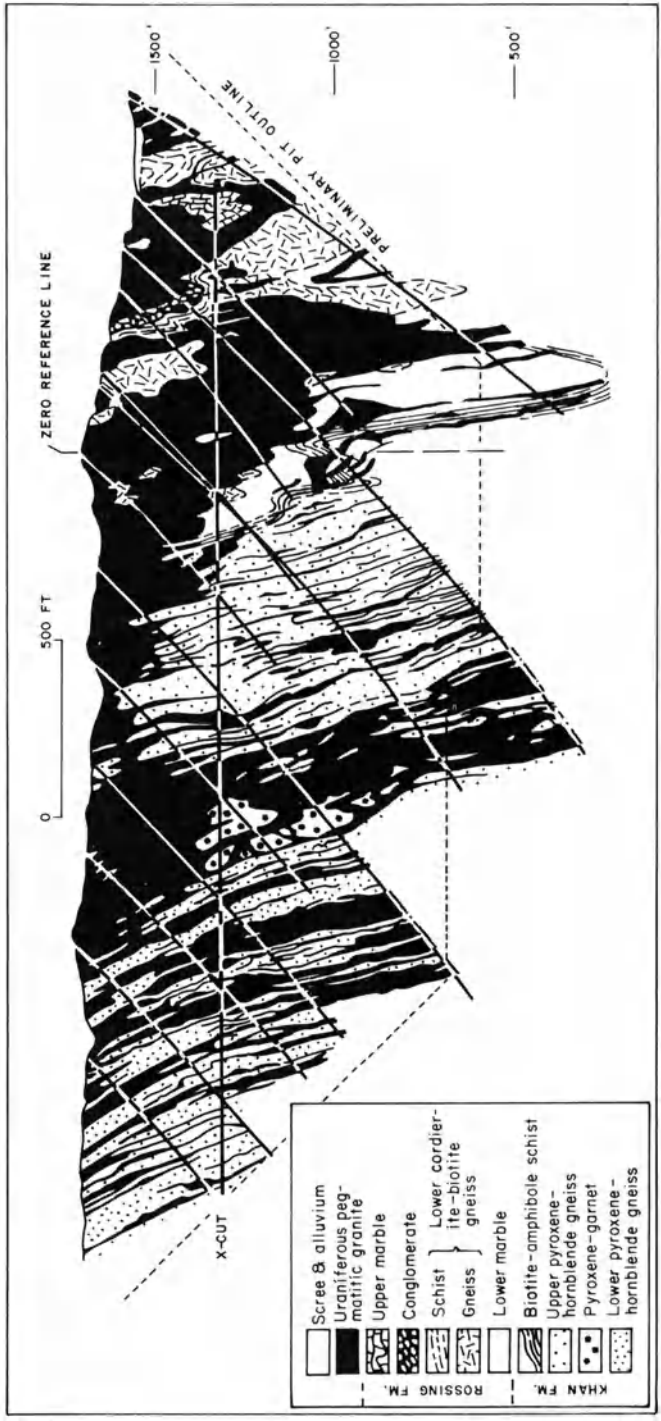

Fig. 9.25. Cross-section of the Rossing uranium deposit (After Berning et al. 1976)

9.7.2 Discussion and Suggestions for Exploration

The fact the collision-related S-type granites generate uranium deposits in some areas, tin-tungsten deposits in others, and neither in still others, presumably reflects the geochemical characteristics of the protolith from which they themselves originated, and their subsequent crystallization history. It follows that uranium deposits of this general type are best sought within terranes of demonstrably enhanced uranium content.

Clearly, deposits of Rossing-type that contain large tonnages of bulk-minable uranium ore are attractive exploration targets, but their recognition in nonarid climatic environments would be extremely difficult. Not only are the uranium minerals very fine-grained, but in areas of higher rainfall they would be leached downward from the surface. Notwithstanding these difficulties, the fact that a number of smaller deposits comparable to Rossing have been found in the core zone of the Damaride belt (Mouillac et al. 1986) would indicate that deposits of this type are not uncommon, and that examples will be found in other collisional orogens.

9.8 Additional Examples of Collision-Related Ore-Generating Systems

The nature of continental collision events (Dewey 1977) is such that a considerable array of geologic environments can be generated. Thus, in addition to the deformation and metamorphism that occur in the core of the collision belt, sedimentation will occur in collision-related basins. These include remanent basins, foreland and hinterland basins, and intermountane troughs. Apart from small sandstone-type uranium, vanadium, or copper deposits which tend to form in sequences of subaerial clastics, such as those in the Siwaliks of the Sulaiman Range of Pakistan (Moghal 1974), major metal deposits are not apparently generated in such environments. Furthermore, such sedimentary sequences are largely restricted to young collision belts (Mitchell and Garson 1981) and, unlike the precollision rift sequences, tend to be missing from older collision-related terranes where erosion has cut deeper.

Collision events involving the accretion of oceanic arcs or microcontinents to continental margins are now recognized as the fundamental mechanism by which continents are assembled (see Hoffman 1988). It is now appreciated, for example, that a significant fraction of the North American Cordillera from southern Mexico to Alaska is composed of discrete terranes accreted to the continental edge by plate tectonic rafting (Coney 1981). Interpretation of the accretion history of these terranes is obscured by later transform faulting, but Coney estimates that the North American continent has grown by as much as 30% through accretionary additions since the mid-Jurassic. The probability of a significant number of suspect (allochthonous) terranes in the Appalachian orogen has also been proposed (H. Williams and Hatcher 1982). The metallogenic implications of such events are not fully understood, but it is patently

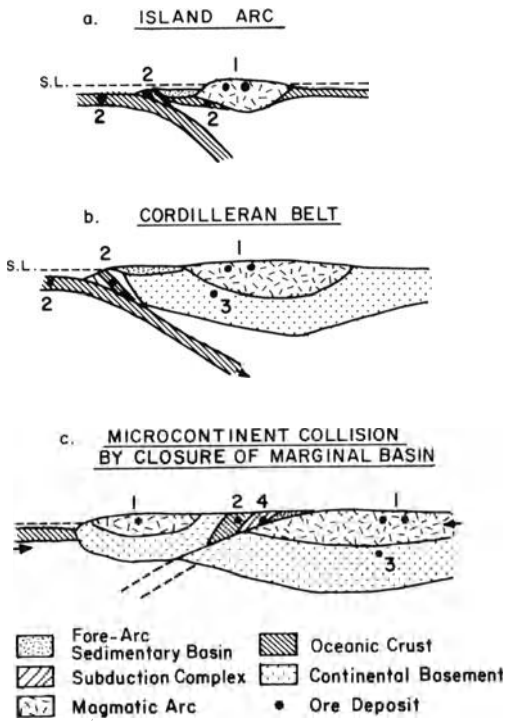

Fig. 9.26. Schematic metallogenic consequences of superposition of: **a** principal-arc deposits (*1*) on ophiolitic deposits (*2*), and **b** pre-arc, rift-related deposits (*3*); **c** juxtaposition of: **a** and **b** principal-arc deposits with accreted ophiolitic deposits in subduction complex (*2*), and with obducted ophiolitic deposits during collision, and of two belts of principal-arc deposits during collision; and generation of metamorphic-hydrothermal deposits (*4*) as a consequence of collision (After Sillitoe 1981a)

obvious that coherent metallogenic relationships cannot be expected to extend beyond the margins of a single terrane unless they were developed after accretion, and the search for broad metallogenic patterns in such areas would be futile in many cases. From the exploration viewpoint each separate terrane must obviously be considered on its own merits (Fig. 9.26).

9.8.1 The Copper Ores of the Kennecott Mine, Alaska

The now mined-out Kennecott deposits of Alaska represent an important example of world-class orebodies in an accreted terrane. D.L. Jones et al. (1977) define a Wrangellia terrane, named after the Wrangell Mountains in Alaska, that occurs in a number of discreet areas from Alaska to Oregon (Fig. 9.27). Each of these areas contains a distinctive sequence of middle to upper Triassic rocks consisting predominantly of thick tholeiitic flows and pillow lavas, overlain by platform carbonates. Paleomagnetic data from the Alaska

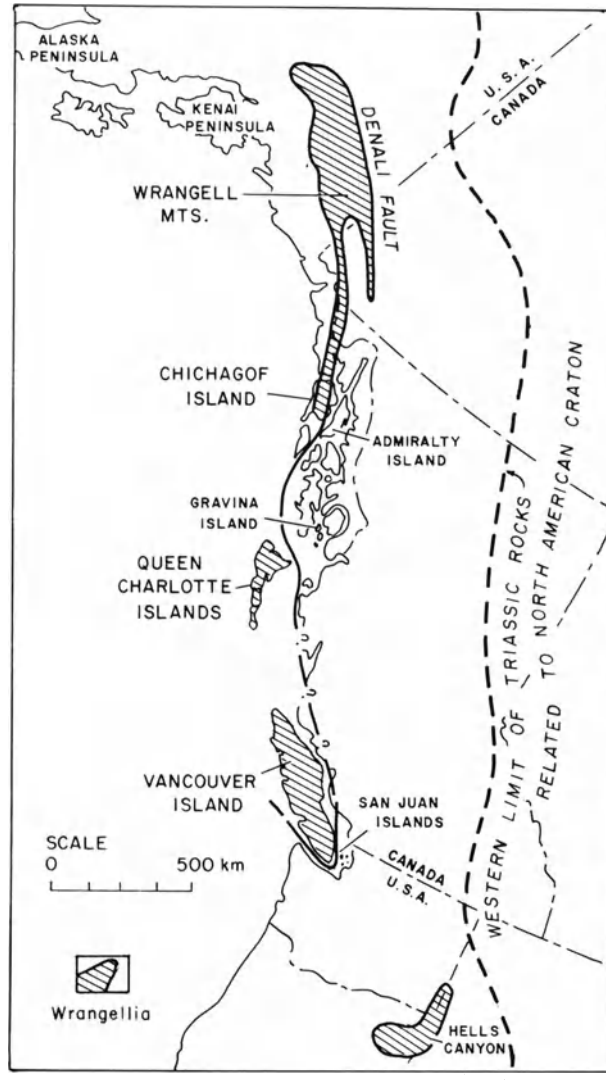

Fig. 9.27. Map showing distribution of terranes of Triassic age that are considered to represent fragments of Wrangellia (After D.L. Jones et al. 1977)

segment volcanics (Hillhouse 1977) indicate that this terrane has been translated at least 3000 km northward and rotated about 90°. The Wrangellia terranes thus appear to represent an enormous, presumably rift-related, outpouring of continental basalts, which was disrupted and translated northward between late Triassic and early Cretaceous time.

The Nikolai Greenstones of the Alaska Wrangellia fragment have an intrinsic copper content of 155 ppm (MacKevett et al. 1980), a value indicative of rift-related basalts (Sawkins 1976b). The rich Kennecott ores occur either in

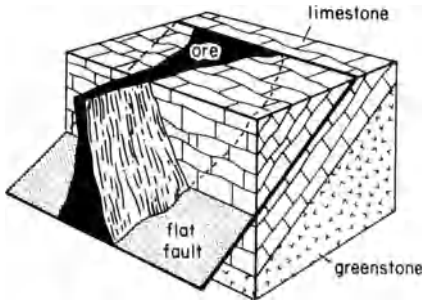

Fig. 9.28. Typical occurrence of replacement ores of the Kennecott Mine, Alaska. Note position of ores just above copper-rich Nikolai greenstones and their structural control (After Bateman and McLaughlin 1920)

the Middle to Upper Nikolai Greenstone or, more typically, in the immediately overlying Upper Triassic Chitistone Limestone. In terms of their mineralogy these deposits are completely dominated by Cu and Cu-Fe sulfides, but the deposits in the dolomitized limestones contain only the copper sulfides digenite, chalcocite, djurleite, and covellite (Sood et al. 1986). These latter deposits are localized along a fault-truncated limb of a syncline as massive wedges of chalcocite and lesser copper oxides (Fig. 9.28), which probably reflect the filling of voids and caverns produced during an earlier karstification event (MacKevett et al. 1980).

Silberman et al. (1981) present stable isotope data for the Nikolai Greenstones near the Kennecott deposits that indicate a metamorphic-segregation origin for vein-flow, top-copper mineralization within these volcanics. They also report potassium-argon results indicative of a thermal-metamorphic episode at approximately 112 Ma. This date agrees with the timing of accretion deduced from structural and stratigraphic evidence. The mineralization within the volcanics and the Chitistone Limestone can thus be viewed as the direct result of hydrothermal processes set in motion by collision-induced, low-grade metamorphism of a sequence of copper-rich basalts. If this scenario is correct, then these unique Kennecott ores represent an important example of collision-related metallogeny.

9.8.2 The Copper Orebodies of the Mt. Isa Mine, Queensland, Australia

The copper orebodies at Mount Isa represent a worldwide deposit in their own right (190 million tons ~ 2% Cu). However, their occurrence within brecciated silica-dolomite rock and consistent spatial separation from the shale-hosted stratiform Zn-Pb ores (Fig. 9.29) were always problematic (Mathias and Clark 1975). In recent years a major reinterpretation of the timing and genesis of these copper orebodies has occurred (Gulson et al. 1983; Perkins 1984; Swager 1985; Bell et al. 1988), and much evidence has been accumulated in support of a syndeformational hydrothermal model for copper mineralization.

The copper ore and its envelopes of silica dolomite protrude upward from the faulted contact of the Urquhart Shale and the greenstones of the Has-

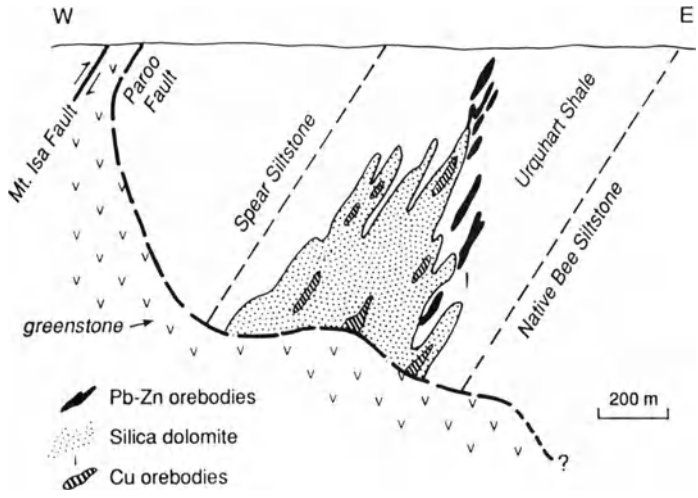

Fig. 9.29. Generalized cross-section of the Mt. Isa deposit, Queensland, illustrating the relationship of the copper orebodies and their silica dolomite envelope to underlying mafic volcanics with which they are in fault contact (After Mathias and Clark 1975)

lingden Group (see Fig. 9.29). This fault is considered to be the overturned portion of a lateral D-thrust ramp within the mine area (Bell et al. 1988). These authors consider that this and other structural complications, in part engendered by geometry and in part by competency factors, allowed a large imbalance in fluid pressure to develop across the faulted greenschist-shale contact during D-tectonism and low-grade metamorphism. This in turn caused explosive fracturing and ingress of copper-bearing fluids. Analysis of the greenstones near the fault and at increasing distances from it (I.H. Wilson et al. 1984) demonstrate a remarkable decrease in the Cu contents of the copper-rich basalts (from 150 ppm down to 10 ppm) as the fault is approached.

In genetic terms, the situation bears strong similarities to that at Kennecott in Alaska. Furthermore, the complex history of deformation evident in the Mount Isa terrane is almost certainly the result of some mid-Proterozoic collision event or events.

9.8.3 Lode Gold Deposits in Relation to Collision Events

We have dealt with the localization of certain Archean and possibly some younger mesothermal gold deposits in an earlier chapter, but it bears repeating that many of the major "breaks" in Superior Province of Canada and the Yilgarn Province of Western Australia, together with younger gold-bearing structures such as the Mother Lode in California, resulted in the first instance from collision events.

9.9 Metallogenesis and Collision Events – Some Final Thoughts

The spectrum of deposits that has been related to collision events in this chapter is considerably broader than that envisioned just a few years ago (Sawkins 1984). However, in that same interval of time the importance of collision events to understanding the manner in which continents are assembled has been more fully appreciated (see Hoffman 1988). With this has come the realization that a wide spectrum of geologic processes, including some involving major movements of fluids (Oliver 1986; Fyfe 1986) must result from collisional orogeny.

Given the multiplicity of collision events that are now recognized and their obvious frequency in the geologic record, it is important to realize that all of the pre-Mesozoic deposit types discussed in previous chapters, especially those formed in relation to rifting events, will probably have been involved in some way in collision events.

One cannot help but wonder what metal deposits will be found when the extensive collisional terranes present on all the continents are subjected to careful scrutiny by exploration geologists. As the need to carry out subsurface exploration becomes more acute, the utilization of concepts involving plate tectonic environments and plate interactions should prove to be increasingly fruitful.

Chapter 10 Metal Deposits and Plate Tectonics – An Attempt at Perspective

Two decades have now passed since an integrated model of plate tectonics (Le Pichon 1968) changed forever the way in which earth scientists view the planet earth. In the interim period plate tectonic theory has grown considerably more complex in its details, but has not lost the elegant simplicity of its original tenets. In terms of providing a framework within which metal deposits can be classified, I would offer the foregoing chapters as manifest testimony to its utility. The concept of plate tectonics as a basic control for metallogenesis has had some detractors (Sangster 1979), but now that Archean and Proterozoic terranes are being increasingly interpreted in terms of accreted arc systems and collision events (e.g. Hoffman 1988) the utility of plate tectonic theory for understanding the space-time distribution of most metal sulfide deposits has, I believe, been validated.

10.1 Lineaments and Metal Deposits

A number of authors have maintained that lineaments, representing fundamental flaws in the continental crust, are major factors in the control of metallogenesis (e.g., Favorskaya 1977; Noble 1980; Kutina 1980; O'Driscoll 1986). The availability of high quality earth imagery has also provided an impetus to the recognition and interpretation of continental lineaments (e.g., Norman 1980). Although many of these efforts do not stand up well to scrutiny (see Gilluly 1976), the whole question of the possible significance of deep crustal flaws to certain groups of metal deposits cannot be summarily dismissed.

Sykes (1978, 1980) has demonstrated that the reactivation of zones of weakness in continental crust can be related to the development of transform faults in nascent ocean basins, and that these zones tend to control sites of intracontinental alkaline magmatism in west Africa and elsewhere (see also Marsh 1973; Culver and Williams 1979). Such structures do not appear to be overly important in terms of metallogenesis, although associated kimberlites may be diamond-bearing, and carbonatites may have potential for niobium or fluorite deposits (Mitchell and Garson 1981, p. 311). Also, Heyl (1972) has documented the structures, alkaline rocks, and Mississippi Valley-type deposits that lie along the 38th parallel lineament (see Fig. 9.5). Whether certain Mississippi Valley deposits that lie close to this structure are genetically

related to it is somewhat contentious, but it is noteworthy that major amounts of fluorite are present in some of the deposits that lie along this structure, and fluorine enrichment is characteristic of many alkaline rocks.

The Colorado Lineament represents a major crustal flow of considerable antiquity (Warner 1978), and it is clear that it exerted a control on the magmatism that is associated with the ores of the Colorado Mineral Belt (see Fig. 3.4). Furthermore, the Walker Lane is a lineament that in some manner controlled the sites of major Miocene precious metal deposits in the western Great Basin (see Fig. 4.4). Hoy (1982b) noted that all significant stratabound lead-zinc deposits in southeastern British Columbia, regardless of age and host-rock type, seem to be regionally controlled by a northeast-trending tectonic zone. Thus, middle Precambrian sediment-hosted massive sulfide deposits (e.g., Sullivan), late Proterozoic mineralization in marbles and calc-silicate rocks of the Shuswap Metamorphic Complex, and deposits in carbonate rocks of the Kootenay Arc (Lower Cambrian) in the Salmo and Duncan areas all fall within this zone. Hoy suggests that the zone is underlain by northeast-trending basement fractures that were the loci for recurrent faulting that controlled the discharge of metal-bearing fluids.

O'Driscoll (1981, 1986) has been a leading advocate of the utility of lineament studies in attempting to understand the spatial distribution of major metal deposits. His application of lineament analysis to the Australian continent is certainly of interest, especially as it applies to Archean and Proterozoic terranes, but the credibility of his approach decreases sharply when he attempts to apply it on a more global scale.

The Russian ore deposits literature is replete with references to the importance of deep crustal flaws as important controls of metallogeny (e.g., Smirnov 1977), but in most cases these concepts result from an unwillingness of Soviet geologists (at least until recently) to accept plate tectonic interpretations of many geologic features. Much the same applies to the concepts of metallogeny in relation to geosynclinal theory (Bilibin 1968; Smirnov 1977) that prevail(ed) in that country. Kerrich (1986) discusses various aspects of fluid transport in lineaments but includes a somewhat disparate array of structures in his treatment. For example, he ranges from major transcurrent shear zones in the Abitibi Belt, to boundary thrusts in the Grenville, to the crustal detachment faults of the southwest USA.

It is reasonable to postulate that certain long-lived flaws in the continental lithosphere have repeatedly controlled geologic processes such as rise of magma and fluid flow across the brittle-ductile transition. Furthermore, metallogenesis may be related locally to such processes, but lineaments simply do not provide adequate models for understanding the space-time distribution of metal deposits. Conversely, models based on plate tectonic theory permit the division of most metal deposits into subtypes that are distinctive in tectonic, lithologic, and genetic terms.

10.2 Transform Faults and Metal Deposits

Not only are transform faults a major type of plate boundary, but as demonstrated by Woodcock (1986), most (59%) plate boundaries have a relative velocity that is markedly oblique ($> 22°C$). Plate interactions thus spawn a considerable array of strike-slip faults as well as true transform faults. True transform faults appear to have limited importance in metallogenesis because, except where "leaky", they have no magmatism associated with them.

Thus, major structures such as the Sagainy-Namyin Fault, Burma (Curray et al. 1980), and the Central Range Fault, Taiwan (Biq 1971) have no known mineralization directly associated with them. However, Sillitoe (1978) has noted a possible genetic relationship between the Cenozoic Chaman transform fault in Pakistan and stibnite vein deposits, and compared this setting with that of late Cenozoic mercury deposits in the Coast Ranges of California. Albers (1981), however, suggests a relationship of these mercury deposits to the Coast Range Thrust, a subduction-related feature.

The intersections of a spreading axis and transform faults also appear to be important in terms of localizing the metalliferous brine pools in the Red Sea (see Fig. 8.1). There is reason to suppose that similar situations accompanied the development of nascent ocean basins at other times in the geologic past, even though the lack of documented examples is puzzling (Shanks 1977).

10.2.1 The McLaughlin Gold Deposit, Northern California

The McLaughlin hot-spring gold deposit in the California Coast Ranges north of San Francisco, contains 20 million tons grading 4.6 g/ton Au (Lehrman 1988). This well-preserved, gold-bearing, hot-spring system is less than 2.2 Ma old and is hosted by a major thrust fault that has been subject to reactivation by the San Andreas right-lateral, strike-slip system.

The late Cenozoic geologic history of this area is dominated by transform faulting and volcanism. The Clear Lake volcanics (Hearn et al. 1982) represent the northernmost and youngest (0.01 to 2.1 Ma) group of a series of late Cenozoic igneous, extrusive rocks that are strung out along the central Coast Ranges of California. All of these volcanics exhibit a spatial association with the San Andreas transform and associated faults to the east, and a general northward younging (23.5 to 0.01 Ma) of volcanism is apparent (see Fig. 4.11; see Hearn et al. 1982 and references therein). Although these volcanics range in composition from basalt to rhyolite and are essentially of calc-alkaline type, they exhibit complex strontium isotope variations suggestive of multiple magma sources in the upper mantle and lower crust (Futa et al. 1982).

The northward migration of volcanism referred to above has led to the suggestion of a hotspot control of igneous activity (Hearn et al. 1982), but Isherwood (1982) sees the main control of magmatism as the downward settling of a subducted slab after its detachment from the Farallon Plate by the San Andreas transform (see Fig. 4.12). Geophysical studies (Isherwood 1982)

indicate that magma bodies are still present under the Clear Lake volcanic field and heat from these is responsible for the Geysers system, a major geothermal energy resource. Whatever the ultimate triggering mechanism for the magmatism, its association with transform faulting is clear, as is the relation of the mercury and gold deposits to this magmatism. The gold mineralization at McLaughlin is of typical hotspring type, consisting of a vent complex made up of chalcedonic sinter and hydrothermal explosion breccias overlying a silica-flooded cap cut and underlain by a stockwork of chalcedonic veins. The deposit extends 1.5 km, attains a width of 200 m, and extends down to depths of about 250 m. The gold is present as submicroscopic particles of native Au disseminated through the pervasive silicification and veining. Silver, present in sulfosalts, averages about three to four times gold content, and forms part of the geochemical signature which includes Sb, Hg, As, Tl, Ba, and W.

The Mesquite gold deposit in southeasternmost California (Willis 1988) contains 41 million tons of ore grading 1.74 g/ton. The gold occurs in epithermal breccias, veins, and fractures cutting Jurassic orthogneiss and Mesozoic pegmatites. Structural relationships suggest that the mineralized ground developed in a dilatant jog between two en echelon segments of a larger strike-slip fault (Willis et al. 1987). The gold deposit at Mesquite thus could relate to mid-Tertiary development of the Cenozoic strike-slip fault systems in this part of California.

10.2.2 The Salton Sea Geothermal System, Imperial Valley, California

The Salton Sea geothermal area sits astride short spreading segments that connect offset strands of the San Andreas transform system in southern California (see Fig. 5.7). A good deal of research effort has been focused on this geothermal system because of its energy potential and because of the metalliferous nature of the saline brines it contains (McKibben and Elders 1985; McKibben et al. 1988 and references therein). The actual mineralization in the deltaic sediments that underlie the area involves only weak development of stratiform iron and base metal sulfides at shallow levels under diagenetic conditions, and formation of sulfide-bearing veinlets at depths greater than 700 m under hydrous metamorphic conditions.

The hypersaline fluids present in the reservoir have temperatures as high as 365 °C, and both fluid inclusion studies, and actual monitoring of boreholes (McKibben et al. 1988), indicate that fluid mixing mechanisms are important to the development of the vein mineralization. The Salton Sea hydrothermal system provides a natural laboratory in which to study water-rock interactions, but the jury is still out regarding the significance of this system to actual ore deposits. Given the metal content of the Salton Sea brines and the development of the system in a pull-apart basin, the closest ore deposit analogs one can envisage for this system are the Cu-Zn massive sulfide ores (Ducktown, Tennessee) discussed in Chapter 8.

10.3 Plate Tectonics and Metal Deposits of Surficial Origin

Metal deposits in which the prime cause of metal concentration is due to surficial (weathering) processes are obviously dependent primarily on climatic factors for their origin, but plate tectonics can play a critical role in the emplacement or elevation of the protolith of certain deposits. Laterite-type nickel deposits provide a case in point, for all are formed in areas where tropical weathering processes act on the mantle portions of ophiolite complexes (Coleman 1977; Golightly 1981). Major examples include the laterite nickel deposits in New Caledonia, Cuba, the Dominican Republic, Columbia, Indonesia, and the Philippines (Boldt 1967).

In deposits of this type the ultramafic protolith typically contains about 0.2% nickel but weathering results in the development of a mantle of low-grade lateritic nickel ore that in many instances is separated from unweathered peridotite by a zone of garnierite-bearing, semidecomposed rock containing up to 3% Ni (Fig. 10.1). Clearly the initial crucial step in the history of the formation of these deposits is the emplacement of ophiolite complexes resulting from plate interactions.

Henley and Adams (1979) have noted that the formation of giant gold placer deposits around the Pacific basin can be related to erosion and sequential hydraulic concentration, and pointed out that the tectonic uplifts that initiated the erosion can be related to Mesozoic and Tertiary plate motions. These include changes in spreading rate (Pitman and Hayes 1973) that influence global sea levels, and thus impact on the sequential erosion-deposition stages that are important to the evolution of giant placer deposits. Thus, here again we are confronted with the far-reaching effects of plate tectonics on ore formation.

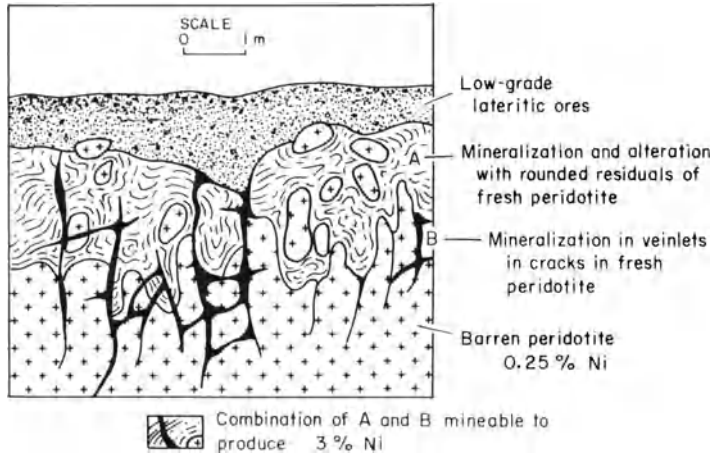

Fig. 10.1. Schematic section of laterite-type nickel deposits such as those developed in New Caledonia and other tropical areas where ophiolites are exposed (After Boldt 1967)

10.4 An Enigmatic Class of Uranium Deposits

Within the last two decades a major new type of uranium deposit, the so-called unconformity type, has come to be recognized, and additional discoveries of such deposits have had a major impact on the uranium resources of the Western World. The known deposits of this type occur almost exclusively in two terranes of Proterozoic age, the Pine Creek Geosyncline in northernmost Australia and the Athabasca Basin in west-central Canada. Although there are perhaps some fundamental, but hitherto unrecognized, differences between the uranium deposits in each of these areas, the two districts exhibit similarities in geologic setting and age, host-rock alteration, mineralogy, geochemistry, and spatial association with graphitic or carbonaceous rocks (Hoeve et al. 1980; Needham et al. 1980).

In both areas metamorphosed lower Proterozoic sedimentary sequences overlie Archean rocks, and are themselves unconformably overlain by essentially undeformed middle Proterozoic sandstone-dominated sequences. In both areas tholeiitic mafic magmatism is broadly synchronous with the major period of uranium emplacement, and background uranium levels are high in the metamorphosed units below the unconformity. Within the Athabasca Basin (Fig. 10.2) the deposits occur both within carbon-rich metamorphics just below the unconformity and within the lowermost units of the overlying Athabasca Formation (Fig. 10.3), especially where east-northeast trending faults are present. The deposits thus exhibit a very strong relationship (control?) with respect to the unconformity. In the Pine Creek Geosyncline (Fig. 10.4) the deposits occur within carbonaceous metapelites (Cahill Fm) below the unconformity (Fig. 10.5; Hegge et al. 1980), and most Australian workers have tended to minimize the significance of the unconformity at the base of the mid-Proterozoic sandstones (Kombolgie Fm) as a factor in ore genesis.

Mineralogic and geochemical research on these unconformity-type uranium deposits has produced a considerable data base and certain constraints regarding genetic models (e.g., Ypma and Fuzikawa 1980), but little concensus regarding the source of the uranium. What does seem to be clear is that the fluids involved were of connate or meteoric rather than magmatic origin, that redox reactions were important in the transportation and eventual deposition of the uranium, and that chlorite was an important alteration product associated with ore deposition. Furthermore, paragenesis and element associations in these deposits are complex (Ferguson and Winer 1980; Hoeve et al. 1980).

Genetic models that have been put forward for these deposits run the gamut from leaching of uranium and associated elements from the rocks above the unconformity (Hoeve et al. 1980), to derivation of the uranium from the adjacent subunconformity metamorphics (Ferguson et al. 1980), to a deeper seated origin related to convective geothermal systems (Binns et al. 1980). Whatever the precise mechanisms collection, transport, and deposition of the uranium may be, however, it is noteworthy that both areas exhibit high

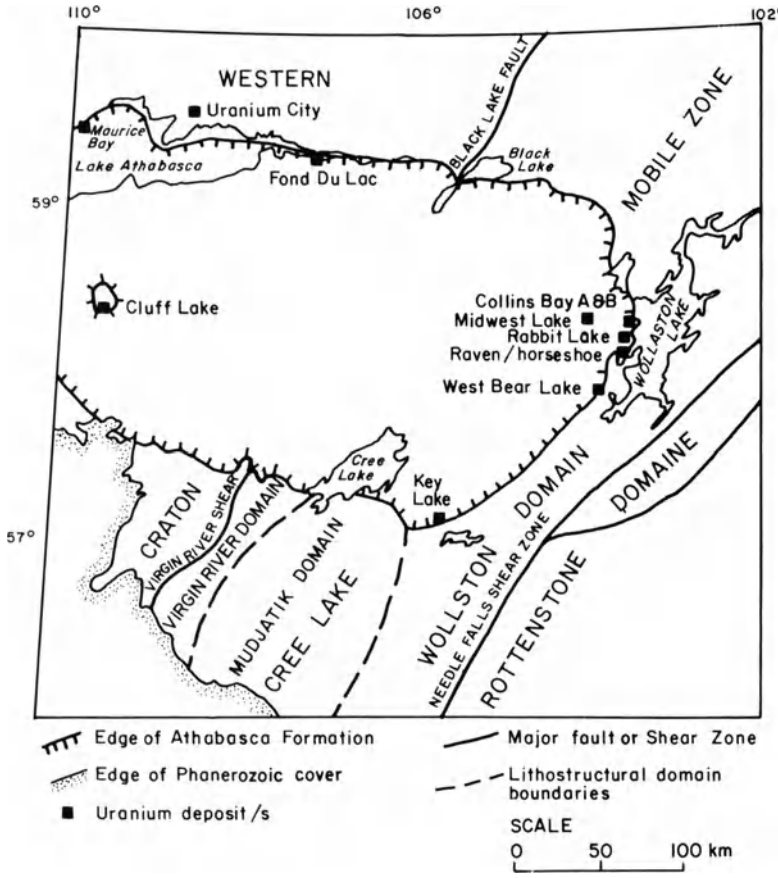

Fig. 10.2. Map showing the major unconformity-type uranium deposits of the Athabasca Basin, Canada (After Sibbald et al. 1977)

uranium background levels and that the deposits themselves represent only the final stage of uranium concentration.

Rossiter and Ferguson (1980) have attempted a geotectonic synthesis of the Proterozoic metal deposits of northern Australia, and, with respect to the Pine Creek Geosyncline and its uranium ores, suggest that during the Proterozoic rifting of the Pine Creek region away from a paleocontinental margin occurred, with resultant emplacement of uraniferous granitic rocks due to mantle plume activity. In support of their model they note that the petrochemistry of the Proterozoic mafic igneous rocks in the region is supportive of this rifting plus hotspot scenario.

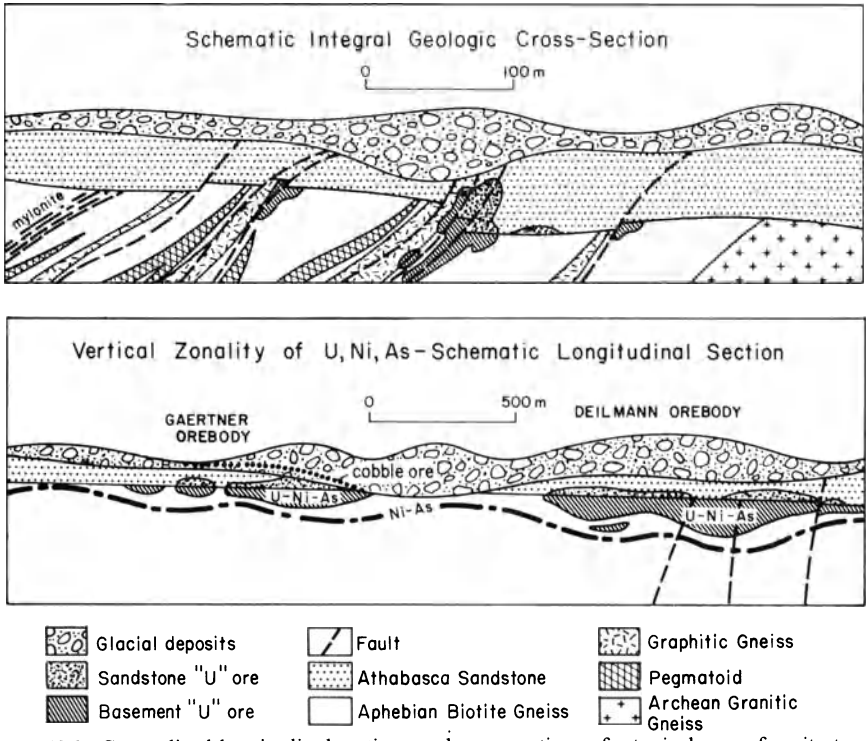

Fig. 10.3. Generalized longitudinal sections and cross-sections of a typical unconformity-type uranium deposit in the Athabasca Basin (After Kirchner et al. 1980)

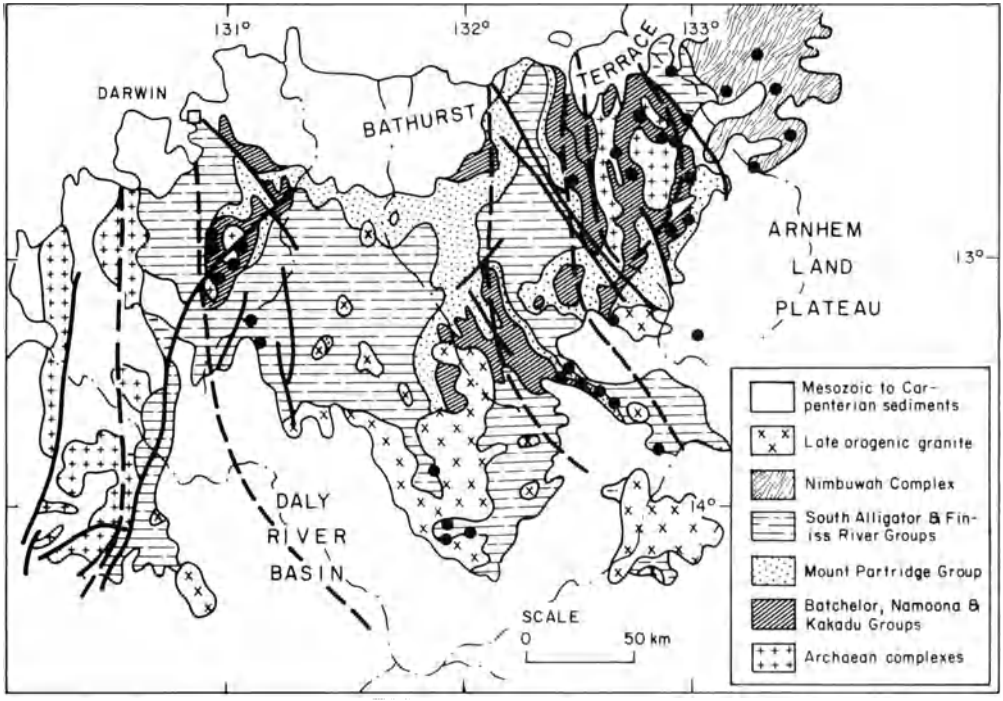

Fig. 10.4. Generalized geology and location of major uranium deposits (*solid circles*), Pine Creek Geosyncline, northern Australia (After Needham et al. 1980)

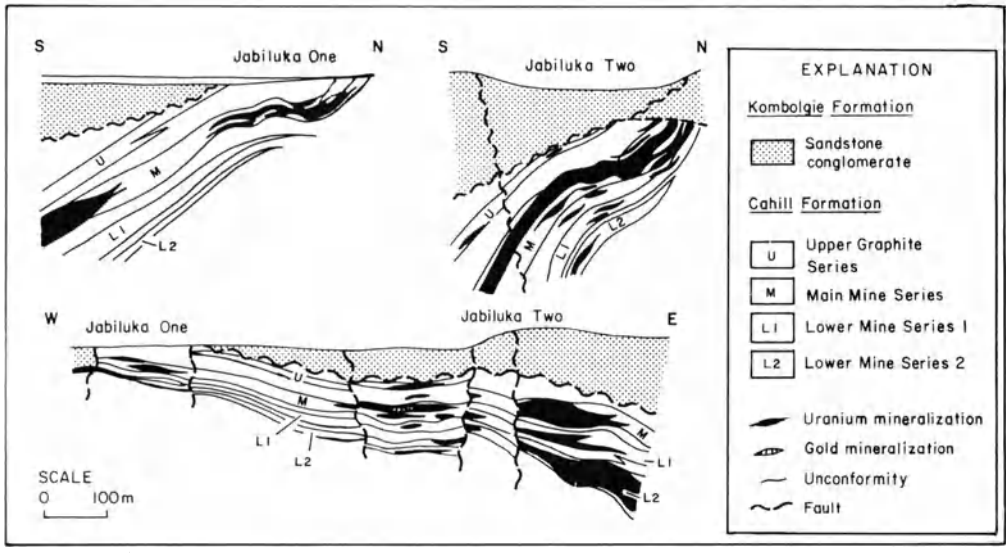

Fig. 10.5. Geologic sections of the Jabiluka One and Two, Pine Creek Geosyncline, northern Australia. Note that ores extend for a considerable distance below the Kombolgie unconformity (After Hegge et al. 1980)

10.5 Metal Deposits and Plate Tectonics: Geochemical Perspectives

In the preceding chapters two mechanisms have emerged as preeminent in terms of the genesis of nonferrous metal deposits; the crystallization of intermediate to felsic magmatic systems, and the dewatering of rifting-related sedimentary sequences. Although these two processes operate at virtually opposite ends of the upper crustal temperature spectrum, both are characterized by fluid chemistries in which alkali chlorides are the dominant species, and both are controlled by redox reactions.

The large bulk of the metal deposits related to magmas occur within subduction-related arc systems, and much of the chloride present in the eventual magmatic-hydrothermal ore fluids probably represents recycled seawater chloride. The characteristic high oxidation state of productive I-type magmatic systems may also relate to the involvement of oxidized materials in subduction zones.

In the case of ore fluids generated by the dewatering of rift sequences, the original source of chlorides is also seawater, and as noted by Sverjensky (1987) redox reactions related to the presence or absence of significant amounts of sulfate-rich evaporites will tend to dictate whether copper, on the one hand, or lead and zinc, on the other, will be the main metals transported by basin-dewatering events. These scenarios are admittedly simplistic, but they do explain why such as overwhelmingly large fraction of the planet's nonferrous metal resources come from two environments that are so dramatically distinctive in virtually all aspects of their tectonic and lithologic settings.

10.6 Metal Deposits and Plate Tectonics: Time-Space Perspectives

The relationships of metal deposits to various types of plate activity explored in the preceding chapters are impressive. In view of the thermal requirements of virtually all ore-generating systems, such a relationship is hardly surprising if one accepts that plate activity is primarily the result of the continuing requirement of the mantle to dissipate heat. The convective transfer of this heat to the surface and upper crust via magmatism or tectonic activity sets in motion a variety of potential ore-generating mechanisms, and it is thus predictable that most major metal concentrations will exhibit time-space relationships to active or nascent (e.g., continental rifting) plate boundaries.

Some workers (e.g., Pereira and Dixon 1963; Laznicka 1973) have attempted to demonstrate that the fundamental nature of ore genesis has changed with the passage of geologic time. Although I reject this concept in favor of a more uniformitarian approach to ore genesis, it is clear that certain types of metal deposits are unevenly distributed with respect to the geologic time scale (Meyer 1981), and such irregularities require explication. Many of these time patterns, such as the strong concentration of porphyry-type deposits to the latter third of the Phanerozoic, can logically be viewed as the result of erosion of the upper portions of arc systems. However, in explaining other age anomalies one has to take cognizance of both crustal and atmospheric evolution. Thus, metal deposits that tend to form in continental rifting environments are absent from Archean terranes, because stable continental blocks of any consequence had not developed until the time of the Archean-Proterozoic transition. The one exception to this is represented by southern Africa where essentially stable Proterozoic regimes appear to have been ushered in by 2.8 Ga ago (e.g., Witwatersrand Supergroup).

Another nonuniformitarian aspect of earth history is the evolutionary change of the earth's atmosphere (Schidlowski 1976 and references therein). These changes had important effects on those deposits whose formation was critically dependent on redox reactions in near-surface environments. Thus low partial pressures of oxygen were a factor in the detrital concentration of uraninite in paleoplacers, whereas more oxidized oceans and hence sulfate-bearing evaporites were almost certainly a factor in the formation of stratiform copper deposits, early Proterozoic banded iron formations, and unconformity-type uranium deposits. Also, sandstone-type uranium deposits related to concentrations of plant material in permeable sandstones could not form until the evolution of land plants in Devonian time. It is noteworthy that these are the deposit types that exhibit the strongest degree of time dependency.

Finally, as noted in Chapter 8, the paucity of sediment-hosted massive sulfide deposits in post-Paleozoic terranes is best explained by the deep burial of any such deposits within untectonized failed rifts or continental margins.

10.7 Metal Deposits and Plate Tectonics: Exploration Perspectives

There are two contrasting statements that can be made regarding the implications of plate tectonics to mineral exploration that are both inherently correct: (1) utilization of plate tectonics has never resulted in the discovery of a metal deposit, and (2) the use of plate tectonic principles has enormous significance to the exploration for metal deposits. The contradictory nature of these two statements is apparent rather than real. Metal deposits are found by the investigation of mineralized or altered outcrops, and more and more in recent years by the followup of geochemical and/or geophysical anomalies. The primary conceptual tool that is used in exploration planning is that of the lithologic association. For example, it has long been recognized that certain massive sulfide deposits are associated with felsic pyroclastics erupted in submarine environments, and that stratiform copper deposits are associated with clastic sedimentary rocks deposited in continental settings. Similarly, the association of porphyry copper and base metal skarn deposits with shallow-seated, felsic calc-alkaline stocks is well documented.

The main impact of plate tectonics on all this has been to broaden and deepen our understanding of the tectonic environments in which many of these lithologic associations develop (Dickinson 1980), and to provide insights into their relative spatial positions. Thus, once a particular tectonic setting, perhaps blurred by metamorphism and deformation, is recognized, the exploration geologist can have a much clearer idea of the various potential ore-generating environments that could have existed within that setting. Metallogenesis can now be understood within the fundamental context of continental evolution, and this in turn permits the conception of exploration programs aimed at specific types of deposits.

Not only are metal deposits becoming increasingly difficult to find, but rising exploration costs have far outstripped increases in the prices of most metals in the past two decades. This is particularly true with respect to deep exploration targets, and it is this third dimension (downwards) that will increasingly represent the frontier of future mineral exploration. As noted by Boldy (1981), the range of the diamond drill and the depth to which mining can be carried out (given economic viability) considerably exceeds the penetration range of relevant geophysical techniques.

The utilization of plate tectonic concepts in exploration is obviously no panacea, but does provide a meaningful framework within which the geologic and geochemical processes that lead to economic metal concentrations can be more fully understood. On a more specific level, plate tectonics have formed the backdrop to progress in our understanding of paleogeography, metallogenic zoning in arc systems, arc segmentation, intraplate magmatism, and the nature and products of rifting. All of this can be translated into the currency of fresh ideas by the imaginative mineral explorationist, much as has been done by those involved in the search of oil. Undoubtedly the future will see

refinements, and perhaps some significant corrections, in the theory of plate tectonics, but each step along the way will have implications in terms of mineral exploration strategy.

10.8 Afterword

The writing of a book such as this one is a humbling experience, for one is constantly confronted with the gaps that exist in one's knowledge, and the awesome amount of information, even outside the field of economic geology, that is pertinent to a full understanding of metallogenesis. Although some of my interpretations will probably not stand the test of time, I am convinced that the study of metallogenesis must be approached within the context of plate tectonic theory. This approach has given a tangible sense of excitement and enrichment to my efforts in this field, and if this book achieves the same for the bulk of those students, teachers, and explorationists who use it, it will have succeeded in its primary purpose.

References

Adamides NG (1980) The form and environment of formation of the Kalavasos ore deposits, Cyprus. In: Panayiotou A (ed) Ophiolites. Int Ophiolite Symp, Cyprus 1979, pp 117–178

Agar RA (1981) Copper mineralization and magmatic hydrothermal brines in the Rio Pisco section of the Peruvian Coastal Batholith. Econ Geol 76:677–693

Aguirre L, Charrier R, Davidson J, Mpodozis A, Rivano S, Thiele R, Tidy E, Vergara M, Vicente JC (1974) Andean magmatism: its paleogeographic and structural setting in the central part (30°–35° S) of the southern Andes. Pac Geol 8:1–35

Ahmad M, Solomon M, Walshe JL (1987) Mineralogic and geochemical studies of the Emperor gold telluride deposit, Fiji. Econ Geol 82:345–370

Ahmad Z, Bilgrami SA (1987) Chromite deposits and ophiolites of Pakistan. In: Stowe CW (ed) Evolution of the chromium ore fields. Van Nostrand Reinhold, New York, pp 238–264

Akande SO, Zentilli M (1984) Geologic, fluid inclusion and stable isotopic studies of the Gays River lead-zinc mineralization, Nova Scotia, Canada. Econ Geol 79:1187–1211

Akande SO, Horn EE, Reutel C (1988) Mineralogy, fluid inclusion and genesis of the Arufu and Akwana Pb-Zn-F mineralization, middle Benue Trough, Nigeria. J Afr Earth Sci 7:167–180

Alabaster T, Pearce JA (1985) The interrelationship between magmatic and ore-forming hydrothermal processes in the Oman ophiolite. Econ Geol 80:1–16

Alabaster T, Pearce JA, Mallick DIJ, Elboushi IM (1980) The volcanic stratigraphy and location of massive sulfide deposits in the Oman ophiolite. In: Panayiotou A (ed) Ophiolites. Int Ophiolite Symp, Cyprus 1979, pp 751–757

Alabaster T, Pearce JA, Malpas J (1982) The volcanic stratigraphy and petrogenesis of the Oman ophiolite complex. Contrib Mineral Petrol 81:168–183

Albers JP (1981) A lithologic-tectonic framework for the metallogenic provinces of California. Econ Geol 76:765–790

Albers JP, Robertson JF (1961) Geology and ore deposits of East Shasta copper-zinc district, Shasta County, California. US Geol Surv Prof Pap 338:1–107

Albinson TF (1988) Geologic reconstruction of paleosurfaces in the Sombrerete, Colorado and Fresnillo districts, Zacatecas State, Mexico. Econ Geol 83:1975–1984

Aldous RTH (1986) Copper-rich fluid inclusions in pyroxenes from the Guide copper mine, a satellite intrusion of the Palabora Igneous Complex, South Africa. Econ Geol 81:143–155

Allerton S, Vine FJ (1987) Spreading structure of the Troodos ophiolite, Cyprus: some paleomagnetic constraints. Geology 15:593–597

Allmendinger RW, Hauge TA, Hauser EC, Potter CJ, Klemperer SL, Nelson KD, Knuepfer P, Oliver J (1987) Overview of the COCORP 40° N transect, western United States. Geol Soc Am Bull 98:308–319

Alt JC, Honnorez J, Laverne C, Emmermann R (1986) Hydrothermal alteration of a 1 km section through the upper oceanic crust. Deep Sea Driling Project Hole 504 B: mineralogy, chemistry, and the evolution of seawater-basalt interactions. J Geophys Res 91:10309–10335

Anderson DL (1975) Chemical plumes in the mantle. Geol Soc Am Bull 86:1593–1600

Anderson JA (1982) Characteristics of leached capping and techniques of appraisal. In: Titley SR (ed) Advances in geology of the porphyry copper deposits, vol 12. Univ Arizona Press, Tuscon, pp 274–295

Anderson JL (1983) Proterozoic anorogenic granite plutonism of North America. Geol Soc Am Mem 161:133–154

Anderson P, Guilbert JM (1979) Precambrian massive sulfide deposits of Arizona – a distinct metallogenic epoch and province. Nev Bur Mines Geol Rep 33:39–48
Anderson RN, Delong SE, Schwarz WM (1978) Thermal model for subduction with dehydration in the downgoing slab. J Geol 86:731–739
Anderson WB, Muchito A, Davis B, Jones GFP, Setterfield TN, Tua P (1987) The Emperor epithermal gold deposit, Vatukoula, Fiji. Pacific Rim Congr 87:9–12
Andrew AJ (1986) Silver vein deposits: summary of recent research. Can J Earth Sci 23:1459–1462
Andrew AS, Baker EM (1987) The nature and origin of the ore-forming fluid in the Kidston gold deposit, North Queensland. Pac Rim Congr 87:13–16
Andrew CJ (1986a) A diagrammatic representation of the Courceyan stratigraphy of the Irish Midlands. In: Geology and genesis of mineral deposits of Ireland. Irish Assoc Econ Geol, Dublin, pp 239–242
Andrew CJ (1986b) The tectono-stratigraphic controls to mineralization in the Silvermines area, County Tipperary, Ireland. In: Geology and genesis of mineral deposits of Ireland. Irish Assoc Econ Geol, Dublin, pp 377–417
Andrew CJ, Ashton JH (1985) Regional setting, geology and metal distribution patterns of Navan orebody, Ireland. Inst Min Metall Trans 94:B66–B93
Andrew CJ, Crowe RWA, Finlay S, Pennell WM, Pyne JF (eds) (1986) Geology and genesis of mineral deposits of Ireland. Irish Assoc Econ Geol, Dublin, 711 pp
Anhaeusser CR (1976) The nature and distribution of Archean gold mineralization in southern Africa. Mineral Sci Eng 8:46–84
Anhaeusser CR (1986) Archean gold mineralization in the Barberton Mountain Land. In: Anhaeusser CR, Maske S (eds) Mineral deposits of southern Africa. Geol Soc S Afr 1:113–154
Anhaeusser CR, Button A (1974) A review of southern African stratiform ore deposits – their position in time and space. Econ Geol Res Unit Univ Witwatersrand Inf Circ 85:1–48
Annels AE (1974) Some aspects of the stratiform ore deposits of the Zambian copper belt and their genetic significance. In: Bartholome P (ed) Gisements stratiformes et provinces cuprifères. Soc Geol Belg, Leige, pp 235–254
Annels AE (1984) The geotectonic environment of the Zambian copper-cobalt mineralization. Geol Soc London J 141:279–289
Annels AE, Simmonds JR (1984) Cobalt in the Zambian copper belt. Precambrian Res 25:75–98
Annis MP, Slack JF, Rolph AL (1983) Stratabound massive sulphide deposits of the Elizabeth mine, Orange County, Vermont. Can Geol Surv Misc Rep 36:41–51
Appel PWU (1985) Stratabound tourmaline in the Archean Malene supracrustals, West Greenland. Can J Earth Sci 22:1485–1491
Appel PWU (1986) Stratabound scheelite in the Archean Malene supracrustal belt, West Greenland. Mineral Depostita 21:207–215
Appel PWU, Secher K (1984) On a gold mineralization in the Precambrian Tartoq Group, South West Greenland. J Geol Soc London 141:273–278
Archibald DA, Clark AH, Farrar E, Zaw UK (1978) Potassium-argon ages of intrusion and scheelite mineralization, Cantung, Tungsten, Northwest Territories. Can J Earth Sci 15:1205–1207
Arculus RJ, Powell R (1986) Source component mixing in the regions of arc magma generation. J Geophys Res 91:5913–5926
Argo-Rise Group (1988) Geological mapping of the East Pacific Rise axis (10° 19′–11° 53′ N) using the Argo and Angus imaging systems. Can Mineral 26:467–486
Armstrong FC (1974) Uranium resources of the future – 'porphyry' uranium deposits. In: IAEA (ed) Formation of uranium ore deposits. IAEA, Vienna, pp 625–634
Armstrong RL (1982) Metamorphic core complexes – from Arizona to southern Canada. Annu Rev Earth Planet Sci 10:129–154
Arribas-Rosado A (1986) The significance of tourmaline in stratabound tungsten deposits in Spain. Abstr Gisements Tungstene, Toulouse, p 33
Ashley RP (1982) Occurrence model for enargite-gold deposits. US Geol Surv Open File Rep 82–795
Ashton JH, Downing DT, Finlay S (1986) The geology of the Navan Zn-Pb orebody. In: Geology and genesis of mineral deposits of Ireland. Irish Assoc Econ Geol, Dublin, pp 243–280

Atkinson WW, Jr., Einaudi MT (1978) Skarn formation and mineralization in the contact aureole at Carr Fork, Bingham, Utah. Econ Geol 73:1326–1365
Bache JJ (1987) World gold deposits: a geological classification. Elsevier, Amsterdam New York, 178 pp
Backer H, Lange J (1987) Recent hydrothermal metal accumulation products and conditions of formation. In: Teleki PG, Dobson MP, Moore JR, von Stackelberg (eds) Marine minerals. Reidel, Dordrecht, pp 317–337
Backer H, Richter H (1973) Die rezente hydrothermal-sedimentäre Lagerstätte Atlantis-II-Tief im Roten Meer. Geol Rundsch 62:697–741
Badham JPN (1981) Shale-hosted Pb-Zn deposits: products of exhalation of formation waters? Trans Inst Mining Metall 90:B70–B76
Badham JPN (1982) Strike slip orogens – an explanation for the Hercynides. J Geol Soc 139:495–506
Bahnemann KP (1972) A review of the stratigraphy and the metamorphism of the basement rocks in the Messina district, Northern Transvaal. Thesis, Univ Pretoria
Bahnemann KP (1986) A review of the geology of the Messina copper deposits, Northern Transvaal. In: Anhaeusser CR, Maske S (eds) Mineral deposits of southern Africa. Geol Soc S Afr 2:1671–1688
Bailey DK (1980) Volatile flux, geotherms, and the generation of the kimberlite-carbonate-alkaline magma spectrum. Min Mag (Tokyo) 43:695–700
Bakken BM, Einaudi MT (1986) Spatial and temporal relations between wall rock alteration and gold mineralization, Main pit, Carlin gold mine, Nevada, U.S.A. In: Proc Gold '86 Symp, Toronto, pp 388–403
Balce GR, Crispin OA, Samaniego CM, Miranda CR (1981) Metallogenesis in the Philippines: explanatory text for the CGMW metallogenic map of the Philippines. In: Metallogeny of Asia. 1981 Geol Soc Jpn Rep 261:125–148
Baldock JW (1969) Geochemical dispersion of copper and other elements at the Bukusu carbonatite complex, Uganda. Trans Inst Min Metall 78:B12–B28
Baldwin JT, Swain HD, Clark GH (1978) Geology and grade distribution of the Panguna porphyry copper deposit, Bougainville, Papua New Guinea. Econ Geol 73:690–702
Ballard RD, Francheteau J (1982) The relationship between active sulfide deposits and the axial processes of the mid-ocean ridge. Mar Tech Soc J 16:8–22
Ballard RD, Francheteau J, Juteau T, Rangan C, Normark W (1981) East Pacific Rise at 21° N: the volcanic, tectonic and hydrothermal processes of the central axis. Earth Planet Sci Lett 55:1–10
Ballhaus CG, Stumpfl EF (1985) Occurrence and petrological significance of graphite in the upper critical zone, western Bushveld Complex, South Africa. Earth Planet Sci Lett 74:58–68
Ballhaus CG, Stumpfl EG (1986) Sulfide and platinum mineralization in the Merensky Reef: evidence from hydrous silicates and fluid inclusions. Contrib Mineral Petrol 94:193–204
Banerji AK (1981) Ore genesis and its relationship to volcanism, tectonism, granitic activity, and metasomatism along the Singhbum Shear Zone, eastern India. Econ Geol 76:905–912
Baragar WRA (1969) The geochemistry of Coppermine River basalts. Geol Surv Can Pap 69-44:1–43
Baragar WRA, Lambert MR, Baglow L, Gibson I (1988) Sheeted dykes of the Troodos ophiolite complex. In: Mafic dyke swarms. Geol Assoc Can Spec Pap 34:257–272
Barangazi M, Brown L (1986) Reflection seismology: the continental crust. Am Geophys Un Geodyn Ser 14:339 pp
Barker F, Millard HT, JR., Knight RJ (1979) Reconnaisance geochemistry of Devonian island-arc and intrusive rocks, West Shasta district, California. In: Barker F (ed) Trondhjemites, dacites, and related rocks. Elsevier, Amsterdam, pp 531–545
Barley ME (1982) Porphyry-style mineralization associated with early Archean calc-alkaline igneous activity, eastern Pilbara, western Australia. Econ Geol 77:1230–1235
Barnes HL (ed) (1979) Geochemistry of hydrothermal ore deposits, 2nd edn. John Wiley & Sons, New York, 798 pp
Barnes SJ, Sawyer EW (1980) An alternative model for the Damara Mobile Belt: ocean crust subduction and continental convergence. Precambrian Res 13:297–336

Barnes SJ, Coats CJA, Naldrett AJ (1982) Petrogenesis of a Proterozoic nickel-sulfide-komatiite association: the Katiniq Sill, Ungava, Quebec. Econ Geol 77:413–429

Barnett ES, Hutchinson RW, Adamcik A, Barnett R (1982) Geology of the Agnico-Eagle gold deposit, Quebec. Geol Assoc Can Spec Pap 25:403–426

Barr DA, Fox PE, Northcote KE, Preto VA (1976) The alkaline suite porphyry copper deposits – a summary. In: Sutherland Brown A (ed) Porphyry deposits of the Canadian Cordillera. Can Inst Min Metall Spec Vol 15:359–367

Barrero LD (1976) Mapa metalogenico de Colombia 1:5,000,000. Inst Nacl Invest Geol-Mineras, Bogata, Colombia

Barton BP, Jr., Bethke PM, Roedder E (1977) Environment of ore deposition in the Creede mining district, San Juan mountains, Colorado. Part III: Progress toward interpretation of the chemistry of the ore-forming fluid for the OH vein. Econ Geol 72:1–24

Barton JM, Cawthorn RG, White J (1986) The role of contamination in the evolution of the Platreef of the Bushveld Complex. Econ Geol 81:1096–1104

Bateman AM, McLaughlin DH (1920) Geology of the ore deposits of Kennecott, Alaska. Econ Geol 15:1–80

Baum W, Gobel VM (1980) Investigations on metallogeny, calc-alkaline magmatism, and related tectonism in a continental margin province, western Cordillera of Colombia. U.S.A. In: Proc 5th IAGOD Symp, Utah, pp 591–605

Baumer A, Fraser RB (1975) Panguna porphyry copper deposit, Bougainville. In: Knight CL (ed) Economic geology of Australia and Papua New Guinea. I Metals. Aust Inst Min Metall Mon 5:855–866

Beane RE, Titley SR (1981) Porphyry copper deposits. Econ Geol 75th Anniv Vol, pp 214–269

Bear LM (1963) The geology and mineral resources of the Akaki-Lythrodondha area. Cyprus Geol Surv Dep Mem 3:122 pp

Beaty DW, Taylor HP, Jr. (1982) Some petrologic and oxygen isotopic relationships in the Amulet Mine, Noranda, Quebec, and their bearing on the origin of Archean massive sulfide deposits. Econ Geol 77:95–108

Beaty DW, Taylor HP, Jr., Coad PR (1988a) An oxygen isotope study of the Kidd Creek, Ontario, volcanogenic massive sulfide deposit: evidence for a high ^{18}O ore fluid. Econ Geol 83:1–17

Beaty DW, Hahn GA, Threlkeld WE (1988b) Field, isotopic, and chemical studies of tourmaline-bearing rocks in the Belt-Purcell Supergroup: genetic constraints and exploration significance for Sullivan type ore deposits. Can J Earth Sci 25:392–402

Beckinsale RD, Suensilpong S, Nakapaduncrat S, Walsh JN (1979) Geochronology and geochemistry of granite magmatism in Thailand in relation to a plate tectonic model. J Geol Soc London 136:529–537

Behrendt JC, Green AG, Cannon WF, Hutchinson DR, Lee MW, Milkereit B, Agena WF, Spencer C (1988) Crustal structure of the Midcontinent rift system: results from GLIMPCE deep seismic reflection profiles. Geology 16:81–85

Bell K, Blenkinsop J (1981) A geochronological study of the Buchans area, Newfoundland. Geol Assoc Can Spec Pap 22:91–112

Bell TH, Perkins WG, Swager CP (1988) Structural controls on development and localization of syntectonic copper mineralization at Mount Isa, Queensland. Econ Geol 83:69–85

Bellido BE, de Montreuil DL (1972) Aspectos generales de la metalogenia – del Peru. Peru Serv Geol Min. Geol Econ 1:1–149

Belyayev KV, Uyad'yev LI (1978) Paleozoic dike complexes of the Kola peninsula and northern Karelia. Int Geol Rev 20:273–280

Benes K, Hanus V (1967) Structural control and history of origin of hydrothermal metallogeny in western Cuba. Mineral Deposita 2:318–338

Berggren WA (1969) Micropaleontologic investigations of Red Sea cores – summation and synthesis of results. In: Degens ET, Ross DA (eds) Hot brines and recent heavy metal deposits in the Red Sea. Springer, Berlin Heidelberg New York, pp 329–335

Bernasconi A (1981) The Marinkas Kwela alkali granite intrusive, a probable porphyry molybdenum system of Cambrian age, Namibia. Mineral Deposita 16:447–454

Bernier L, Pouliot G, Maclean WH (1987) Geology and metamorphism of the Montauban North gold zone: a metamorphosed polymetallic exhalative deposit, Grenville Province, Quebec. Econ Geol 82:2076–2091

Berning J (1986) The Rossing uranium deposit, South West Africa/Namibia. In: Anhaeusser CR, Maske S (eds) Mineral deposits of southern Africa. Geol Soc S Afr 11:1819–1832
Berning J, Cooke R, Hiemstra SA, Hoffman U (1976) The Rossing uranium deposit, South West Africa. Econ Geol 71:351–368
Bethke CM (1985) A numerical model of compaction-driven groundwater flow and heat transfer and its application to the paleohydrology of intracratonic sedimentary basins. J Geophys Res 90B:6817–6828
Bethke CM (1986) Hydrologic constraints on the genesis of the Upper Mississippi Valley mineral district from Illinois basin brines. Econ Geol 81:233–249
Bethke PM, Rye RO (1979) Environment of ore deposition in the Creede mining district, San Juan mountains, Colorado. Part IV: Source of fluids, from oxygen, hydrogen, and carbon isotope studies. Econ Geol 72:1832–1851
Bethke PM, Barton PB Jr, Lanphere MA, Steven TA (1976) Environment of ore deposition in the Creede mining district, San Juan mountains, Colorado. Part II: Age of mineralization. Econ Geol 71:1006–1011
Bichan R (1969) Chromite seams in the Hartley Complex of the Great Dyke of Rhodesia. In: Magmatic ore deposits. Econ Geol Monogr 4:95–113
Bickel MJ (1978) Heat loss from the earth: a constraint on Archean tectonics from the relation between geothermal gradients and the rate of plate production. Earth Planet Sci Lett 40:301–315
Biddle KT, Christie-Blick N (eds) (1985) Strike-slip deformation, basin formation, and sedimentation. Soc Econ Paleont Mineral Spec Publ 37:1–386
Bignell RD (1975) Timing, distribution and origin of submarine mineralization in the Red Sea. Inst Min Metall Trans 84: B1-B6
Bignell RD, Cronan DS, Tooms JS (1976) Red Sea metalliferous brine precipitates. Geol Assoc Can Spec Pap 14:147–179
Bilibin YA (1968) Metallogenic provinces and metallogenic epochs. Queens Coll Press, Flushing, New York, pp 1–35
Billings GK, Kesler SE, Jackson SA (1969) Relation of zinc-rich formation waters, northern Alberta, to the Pine Point ore deposit. Econ Geol 64:385–391
Binns RA, McAndrew J, Sun S-S (1980) Origin of uranium mineralization at Jabiluka. In: IAEA (ed) Uranium in the Pine Creek geosyncline. IAEA, Vienna, pp 543–562
Biq Chingchang (1971) Dual-trench structure in the Taiwan-Luzon region. Proc Geol Soc China 15:65–75
Bird JM, Dewey JF, Kidd WSF (1971) Proto-Atlantic Ocean crust and mantle: Appalachian/Caledonian ophiolites. Nature Phys Sci 231:28–31
Bischoff JL, Rosenbauer RJ, Aruscavage PJ, Baedeckerr PA, Crock JG (1983) Seafloor massive sulfide deposits from 20° N East Pacific Rise, Juan de Fuca Ridge, and Galapagos Rift: bulk chemical composition and economic implications. Econ Geol 78:1711–1720
Bjorlykke A, Sangster DF (1981) An overview of sandstone lead deposits and their relation to red-bed copper and carbonate-hosted lead-zinc deposits. Econ Geol 75th Anniv Vol, pp 179–213
Bjorlykke K (1978) The eastern marginal zone of the Caledonide orogen, Norway. Norges Geol Undersokelse 305:1–81
Black R, Lameyre J, Bonin B (1985) The structural setting of alkaline complexes. J Afr Earth Sci 3:5–16
Blake DW, Kretschmer EL, Theodore TG (1978) Geology and mineralization of the Copper Canyon deposits, Lander County, Nevada. Nev Bur Mines Geol Rep 32:45–48
Blecha M (1965) Geology of the Tribag Mine. Can Min Metall Bull 58:1077–1082
Boast MA, Coleman ML, Halls C (1981) Textural and stable isotopic evidence for the genesis of the Tynagh base metal deposit, Ireland. Econ Geol 76:27–55
Bogdanov YV (1986) Major types of copper-bearing zones in the Soviet Union. In: Friedrich GH, Genkin AD, Naldrett AJ, Ridge JD, Sillitoe RH, Voices FM (eds) Geology and metallogeny of copper deposits. Springer, Berlin Heidelberg New York Tokyo, pp 492–503
Bogodanov B, Dachev H, Vulchanov A (1974) Metallogeny of Bulgaria in the context of plate tectonics. In: Problems of ore deposition, vol. 2. In: 4th IAGOD Symp, Varna, Bulgaria, pp 435–443

Bohlke JK, Kistler RW (1986) Rb-Sr, K-Ar, and stable isotope evidence for the ages and sources of fluid components of gold-bearing quartz veins in the northern Sierra Nevada foothills metamorphic belt, California. Econ Geol 81:296–322

Boldt JR, Jr. (1967) The winning of nickel. Van Nostrand, Princeton, NJ, 487 pp

Boldy J (1981) Prospecting for volcanogenic ore. Can Inst Min Bull 74/834:55–65

Bollingberg H, Brooks CK, Noe-Nygaard A (1975) Trace element variations in Faeroes basalts and their possible relationships to oceanfloor spreading history. Bull Geol Soc Denm 24:55–60

Bonham HF, Jr. (1986) Models for volcanic-hosted epithermal precious metal deposits: a review. In: Hamilton NZ (ed) Proc Int Volcanism Congress, New Zealand Symp 5:13–17

Bonham HF, Jr. (1988) Models for volcanic-hosted epithermal precious metal deposits. In: Bulk mineable precious metal deposits of the western United States. Geol Soc Nev, Reno, pp 259–272

Bonham HF, Jr., Garside LJ (1979) Geology of the Tonapah, Lone Mountain, Klondike, and northern Mud Lake quadrangles, Nevada. Nev Bur Mines Geol Bull 82:1–142

Bonham HF, Papke KG (1969) Geology and mineral deposits of Washoe and Storey Counties, Nevada. Nev Bur Mines Geol Bull 70:1–140

Bonin B (1986) Ring complex granites and anorogenic magmatism. Elsevier, Amsterdam New York, 188 pp

Bonin B, Bowden P, Vialette Y (1979) Le comportement des éléments Rb et Sr au cours des phases de minéralisation, l'example de Ririwai (Liruei) Nigeria. C R Acad Sci Paris Ser D 289:707–710

Bookstrom AA (1977) The magnetite deposits of El Romeral, Chile. Econ Geol 72:1101–1130

Bookstrom AA (1981) Tectonic setting and generation of Rock Mountain porphyry molybdenum deposits. In: Dickinson WR, Payne WD (eds) Relations of tectonics to ore deposits in the southern Cordillera. AR Geol Soc Digest 14:215–226

Bor-Ming Jahn, Chen PY, Yen TP (1976) Rb-Sr ages of granitic rocks in south-eastern China and their tectonic significance. Bull Geol Soc Am 86:763–776

Borg G (1988) The Koras-Sinclair-Ghanzi rift in southern Africa. Volcanism, sedimentation, age relationships and geophysical signature of a late Proterozoic rift system. Precambrian Res 38:75–90

Bortolotti V, Lapierre H, Piccardo GB (1976) Tectonics of the Troodos Massif (Cyprus): preliminary results. Tectonophysics 35:T1–T6

Bosworth B (1987) Off-axis volcanism in the Gregory Rift, east Africa: implications for models of continental rifting. Geology 15:397–400

Boudreau AE (1988) Investigations of the Stillwater Complex. IV: The role of volatiles in the petrogenesis of the J-M Reef, Minneapolis Adit section. Can Mineral 26:193–208

Boulter CA, Fotios MG, Phillips GN (1987) The Golden Mile, Kalgoorlie: a giant gold deposit localized in ductile shear zones by structurally induced infiltration of an auriferous metamorphic fluid. Econ Geol 82:1661–1678

Bowden P (1982) Magmatic evolution and mineralization in the Nigerian Younger Granite Province. In: Evans AM (ed) Metallization associated with acid magmatism. John Wiley & Sons, New York, pp 51–62

Bowden P (1985) The geochemistry and mineralization of alkaline ring complexes in Africa (a review). J Afr Earth Sci 3:17–39

Bowden P, Kinnaird JA (1978) Younger granites of Nigeria – a zinc-rich tin province. Trans Inst Min Metall 87:B66–B69

Bowers TS, Taylor HP Jr (1985) An integrated chemical and stable isotope model of the origin of mid-ocean ridge hot spring systems. J Geophys Res 90:12583–12606

Bowman JR, Covert JJ, Clark AH, Mathieson GA (1985) The Can Tung E Zone scheelite skarn orebody, Tungsten, Northwest Territories: oxygen, hydrogen, and carbon isotope studies. Econ Geol 80:1872–1895

Boyce AJ, Anderton R, Russell MJ (1983) Rapid subsidence and early Carboniferous base-metal mineralization in Ireland. Inst Min Metall Trans 92:B55–B66

Boyle RW (1979) The geochemistry of gold and its deposits. Geol Surv Can Bull 280:584 pp

Breitkopf JH, Maiden KJ (1988) Tectonic setting of the Matchless Belt pyritic copper deposits, Namibia. Econ Geol 83:710–723

Bridgewater D, Windley BF (1973) Anorthosites, postorogenic granites, acid volcanic rocks, and crustal development in the North Atlantic Shield during the mid-Proterozoic. In: Lister LA (ed) Symp Granites, gneisses and related rocks. Geol Soc S Afr Spec Publ 3:307–318

Bridgewater D, Sutton J, Watterson J (1974) Crustal downfolding associated with igneous activity. Tectonophysics 21:57–77

Brimhall GH, Jr. (1979) Lithologic determination of mass transfer mechanisms of multiple-stage porphyry copper mineralization at Butte, Montana: vein formation by hypogene leaching and enrichment of potassium-silicate protore. Econ Geol 74:556–589

Brimhall GH (1980) Deep hypogene oxidation of porphyry copper potassium-silicate protore at Butte, Montana: a theoretical evaluation of the copper remobilization hypothesis. Econ Geol 75:384–409

Brimhall GH, Ghiorso MS (1983) Origin and ore-forming consequences of the advanced argillic alteration process in hypogene environments by magmatic gas contamination of meteoric fluids. Econ Geol 78:73–90

Brimhall GH, Alpers CN, Cunningham AB (1985) Analysis of supergene ore-forming processes and groundwater solute transport using mass balance principles. Econ Geol 80:1227–1256

Briske JA, Dingess PR, Smith F, Gilbert RC, Armstrong AK, Cole GP (1986) Localization and source of Mississippi Valley-type zinc deposits in Tennessee, USA, and comparisons with Lower Carboniferous rocks in Ireland. In: Geology and genesis of mineral deposits of Ireland. Irish Assoc Econ Geol, Dublin, pp 635–661

Brock BB, Pretorius DA (1964) Rand basin sedimentation and tectonics. In: Haughton SH (ed) The geology of some ore deposits in southern Africa. Geol Soc S Afr 1:549–599

Bromley AV (1976) Granites in mobile belts – the tectonic setting of the Cornubia batholith. J Camborne School Mines 76:40–47

Brooks C, Thayer P (1981) Rb/Sr geochronology in the Thompson belt, Manitoba: implications for Aphebian crustal development and metallogenesis. Can J Earth Sci 18:932–943

Brown AC (1971) Zoning in the White Pine copper deposit, Ontonagon County, Michigan. Econ Geol 66:543–573

Brown AC (1980) The diagenetic origin of stratiform copper deposits. In: Proc 5th IAGOD Symp, Utah, vol 1, pp 81–90

Brown AC (1984) Alternate sources of metals for stratiform copper deposits. Precambrian Res 25:61–74

Brown C, Williams B (1985) A gravity and magnetic interpretation of the Irish Midlands and its relation to ore genesis. J Geol Soc London 142:1059–1076

Brown GC (1980) Calc-alkaline magma genesis: the Pan-African contribution to crustal growth? In: Al-Shanti (ed) Evolution and mineralization of the Arabian-Nubian Shield, vol 3. Pergamon, Oxford, pp 19–30

Brown M (1980) Textural and geochemical evidence for the origin of chromite deposits in the Oman ophiolite. In: Panayiotou A (ed) Ophiolites. Proc Int Ophiolite Symp, Cyprus 1979, pp 714–721

Brown PE, Lamb WM (1986) Mixing of H_2O-CO_2 in fluid inclusions: geobarometry and Archean gold deposits. Geochim Cosmochim Acta 50:847–852

Brown PE, Bowman JR, Kelly WC (1985) Petrologic and stable isotope constraints on the source and evolution of skarn-forming fluids at Pine Creek, California. Econ Geol 80:72–95

Bryner L (1969) Ore deposits of the Philippines – an introduction to their geology. Econ Geol 64:644–666

Buchanan L (1981) Precious metal deposits associated with volcanic environments in the southwest. AR Geol Soc Digest 14:237–262

Bugge JAW (1978) Norway. In: Bowie SHU, Kualheim A, Haslam HW (eds) Mineral deposits of Europe, vol 1. Northwest Europe. Inst Min Metall, pp 199–249

Buisson G, Leblanc M (1986) Gold-bearing listwaenites (carbonatized ultramafic rocks) from ophiolite complexes. In: Gallagher MJ, Ixer RA, Neary CR, Prichard HM (eds) Metallogeny of basic and ultrabasic rocks. Inst Min Metall 121–132

Buisson G, Leblanc M (1987) Gold in mantle peridotites from Upper Proterozoic ophiolites in Arabia, Mali, and Morocco. Econ Geol 82:2091–2098

Buntin TJ, Grandstaff DE, Ulmer GC, Gold DP (1985) A pilot study of geochemical and redox relationships between potholes and adjacent normal Merensky Reef of the Bushveld Complex. Econ Geol 80:975–987

Burchfield BC (1979) Geologic history of the central western United States. Nev Bur Mines Geol Rep 33:1–12

Burgath K, Weiser TH (1980) Primary textures and genesis of Greek podiform chromite deposits. In: Panayiotou A (ed) Ophiolites. Proc Int Ophiolite Symp, Cyprus 1979, pp 675–690

Burk R, Hodgson CJ, Quartermain RA (1986) The geological setting of the Teck-Corona Au-Mo-Ba deposit, Hemlo, Ontario, Canada. In: Proc Gold '86 Symp, Toronto, pp 311–326

Burke K (1975) Atlantic evaporites formed by evaporation of water spilled from Pacific, Tethyan, and southern oceans. Geology 3:613–616

Burke K (1976) The Chad Basin: an active intra-continental basin. Tectonophysics 36:197–206

Burke K (1977) Aulocogens and continental breakup. Annu Rev Earth Planet Sci 5:371–396

Burke K, Dewey JF (1973) Plume-generated triple junctions: key indicators in applying plate tectonics to old rocks. J Geol 81:406–433

Burke K, Kidd WSF (1980) Volcanism on earth through time. In: Strangway DW (ed) The continental crust and its mineral deposits. Geol Assoc Can Spec Pap 20:503–522

Burke K, Sengor C (1986) Tectonic escape in the evolution of continental crust. In: Reflection seismology: the continental crust. Am Geophys Un Geodyn Ser 14:41–53

Burke K, Whiteman AJ (1973) Uplift, rifting and breakup of Africa. In: Tarling DH, Runcorn SK (eds) Implications of continental drift to the earth sciences, vol 2. Academic Press, New York London, pp 735–755

Burke K, Dewey JF, Kidd WSF (1976) Dominance of horizontal movements, arc and microcontinental collisions during the later permobile regime. In: Windley BF (ed) The early history of the earth. John Wiley & Sons, New York London, pp 133–129

Burke K, Dewey JF, Kidd WSF (1977) World distribution of sutures – the sites of former oceans. Tectonophysics 40:69–99

Burke K, Kidd WSF, Kusky TM (1986) Archean foreland basin tectonics in the Witwatersrand, South Africa. Tectonics 5:439–456

Burke KC, Kidd WSF, Turcotte DL, Dewey JF, Mouginis-Mark PJ, Parmentier EM, Sengor AM, Tapponier PE (1981) Tectonics of basaltic volcanism. In: Basaltic volcanism on the terrestrial planets. Basaltic Volcanism Study Project, Pergamon, New York, pp 803–898

Burnham CW (1981) Physicochemical constraints on porphyry mineralization. In: Dickinson WR, Payne WD (eds) Relations of tectonics to ore deposits in the southern Cordillera. AR Geol Soc Digest 14:71–77

Burnham CW (1985) Energy release in subvolcanic environments: implications for breccia formation. Econ Geol 80:1515–1522

Burrows DR, Spooner ETC (1986) The McIntyre Cu-Au deposit, Timmins, Ontario, Canada. In: Proc Gold '86 Symp, Toronto, pp 23–39

Burrows DR, Spooner ETC (1987) Generation of a magmatic H_2O-CO_2 fluid enriched in Mo, Au, and W within an Archean sodic granodiorite stock, Mink Lake, northwestern Ontario. Econ Geol 82:1931–1957

Burrows DR, Wood PC, Spooner ETC (1986) Carbon isotope evidence for a magmatic origin for Archean gold-quartz vein ore deposits. Nature (London) 321:851–854

Burt DM (1974) Metasomatic zoning in Ca-Fe-Si exoskarns. Carnegie Inst Washington 634:287–293

Burton B (1975) Paragenetic study of the San Martin mine, Durango, Mexico. MS Thesis, Univ Minn

Buseck PR (1966) Contact metasomatism and ore deposition. Concepcion del Oro, Mexico. Econ Geol 61:97–136

Button A (1976) Iron-formation as an end-member in carbonate sedimentary cycles in the Transvaal Supergroup, South Africa. Econ Geol 71:193–201

Byers AR, Kirkland SJT, Pearson WJ (1965) Geology and mineral deposits of the Flin Flon area, Saskatchewan. Sask Deposits Mineral Resourc Rep 62

Cahen L (1970) Igneous activity and mineralization episodes in the evolution of the Kibaride and Katangide orogenic belts of Central Africa. In: Clifford TN, Gass IG (eds) African magmatism and tectonics. Oliver & Boyd, Edinburgh, pp 97–118

Cahen L, Francois A, Ledent D (1971) Sur l'age des uraninites de Kambove ouest et de Kamato principal et revision des reconnaissances relatives aux minéralisations uranfières du Katanga et du Copperbelt de Zambia. Soc Geol Belg Ann 94:185–198

Cahen L, Snelling NJ, Delhal J, Vail JR (1984) The geochronology and evolution of Africa. Oxford Univ Press, 512 pp

Caia J (1976) Paleogeographical and sedimentological controls of copper, lead, and zinc mineralizations in the Lower Cretaceous sandstones of Africa. Econ Geol 71:409–422

Cailteux J (1986) Diagenetic sulphide mineralization within the stratiform copper-cobalt deposit of West Kambove (Shaba-Zaire). Sequence of mineralization in sediment-hosted copper deposits, Part 2. In: Friedrich GH, Genkin AD, Naldrett AJ, Ridge JD, Sillitoe RH, Vokes FM (eds) Geology and metallogeny of copper deposits. Springer, Berlin Heidelberg New York Tokyo, pp 398–411

Callahan WH (1967) Some spatial and temporal aspects on the localization of Mississippi Valley-Appalachian type ore deposits. Econ Geol Monogr 3:14–19

Callow KJ, Worley HW, Jr. (1965) The occurrence of telluride minerals at the Acupan gold mine, Mountain Province, Philippines. Econ Geol 60:251–268

Cameron EM, Hattori K (1987) Archean gold mineralization and oxidized hydrothermal fluids. Econ Geol 82:1177–1191

Cameron EN (1980) Evolution of the lower critical zone, eastern Bushveld Complex, and its chromite deposits. Econ Geol 75:845–871

Cameron EN, Desborough GA (1969) Occurrence and characteristics of chromite deposits – Eastern Bushveld Complex. Econ Geol Monogr 4:23–40

Campbell AR, Rye DM, Petersen U (1984) A hydrogen and oxygen isotope study of the San Cristobal mine, Peru: implications of the role of water to rock ratio for the genesis of wolframite deposits. Econ Geol 79:1818–1832

Campbell FA, Ethier VG, Krouse HR, Both RA (1978) Isotopic composition of sulfur in the Sullivan orebody, British Columbia. Econ Geol 73:246–268

Campbell FA, Ethier VG, Krouse HR (1980) The massive sulfide zone: Sullivan orebody. Econ Geol 75:916–926

Campbell IH (1986) A fluid dynamic model for the potholes of the Merensky Reef. Econ Geol 81:1118–1125

Campbell IH, Naldrett AJ, Barnes SJ (1983) A model for the origin of the platinum-rich sulfide horizons in the Bushveld and Stillwater Complexes. J Petrol 24:133–165

Candela PA, Holland HD (1986) A mass transfer model for copper and molybdenum in magmatic hydrothermal systems: origin of porphyry-type deposits. Econ Geol 81:1–19

Cann JR, Strens MR, Rice A (1985) A simple magma-driven thermal balance model for the formation of volcanogenic massive sulfides. Earth Planet Sci Lett 76:123–134

Cannon WF, Force ER (1983) Potential for high-grade shallow-marine manganese deposits in North America. In: Shanks WC (ed) Unconventional mineral deposits. AIME, New York, pp 175–190

Card KD, Gupta VK, McGrath PH, Grant FS (1984) The Sudbury Structure: its regional geological and geophysical setting. In: The geology and ore deposits of the Sudbury Structure. Ontario Geol Surv Spec Vol 1:25–43

Carlson SR, Sawkins FJ (1980) Mineralogic and fluid inclusion studies of the Turmalina Cu-Mo-bearing breccia pipe, Northern Peru. Econ Geol 75:1233–1238

Carne RC (1979) Geological setting and stratiform mineralization Tom Claims, Yukon Territory. Dep Indian N Aff EGS 1979-4:1–30

Carne RC, Cathro RJ (1982) Sedimentary exhalative (Sedex) zinc-lead-silver deposits, northern Canadian Cordillera. Can Inst Mining Bull 75/840:66–78

Carpenter AB, Trout ML, Pickett EE (1974) Preliminary report on the origin and chemical evolution of lead- and zinc-rich oilfield brines in central Mississippi. Econ Geol 69:1191–1206

Carpenter LG, Garrett DE (1959) Tungsten in Searles Lake. Min Eng 11: 301–303

Carten RB, Geraghty EP, Walker BM, Shannon JR (1988) Cyclic development of igneous features and their relationship to high-temperature hydrothermal features in the Henderson porphyry molybdenum deposit, Colorado. Econ Geol 83:266–296

Carvahlo D (1988) Case history of the Neves-Corvo massive sulfide deposit, Portugal. Geol Soc Am Abstr Prog Annu Meet, Denver, A32

Casadevall T, Ohmoto H (1977) Sunnyside Mine, Eureka mining district, San Juan County, Colorado: geochemistry of gold and base metal ore deposition in a volcanic environment. Econ Geol 72:1285–1320

Casey JF, Dewey JF (1984) Initiation of subduction zones along transform and accreting plate boundaries, triple junction evolution, and forearc spreading centers-implications for ophiolitic geology and obduction. In: Gass IG, Lippard SJ, Shelton AW (eds) Ophiolites and oceanic lithosphere. Geol Soc. Blackwell, Oxford, pp 269–290

Cessard D, Rabinovitch M, Nicolas A, Moutte J, Leblanc M, Prinzhofer A (1981) Structural classification of chromite pods in southern New Caledonia. Econ Geol 76:805–831

Cathles LM (1986) The geologic solubility of gold from 200–350°C, and its implications for gold-base metal ratios in vein and stratiform deposits. In: Clark LA (ed) Gold in the Western Shield. Can Inst Min Metall Spec Vol 38:187–211

Cathles LM, Smith AT (1983) Thermal constraints on the formation of Mississippi Valley-type lead-zinc deposits and their implications for episodic basin dewatering and deposit genesis. Econ Geol 78:983–1002

Cathles LM, Guber AL, Lenagh TC, Dundas FO (1983) Kuroko-type massive sulfide deposits of Japan: products of an aborted island-arc rift. Econ Geol Monogr 5:96–114

Caulfield JBD, LeHuray AP, Rye DM (1986) A review of lead and sulfur isotope investigations of Irish sediment-hosted base-metal deposits with new data from the Kell, Ballinalack, Moyvoughly and Tatestown deposits. In Andrew CJ, Crowe RWA, Finlay S, Pennell WM, Pyne JF (eds) The geology and genesis of mineral deposits in Ireland. Irish Assoc Econ Geol, Dublin, pp 591–615

Cawthorn RG, Molyneux TG (1986) Vanadiferous magnetite deposits of the Bushveld Complex. In: Anhaeusser CR, Maske S (eds) Mineral deposits of southern Africa. Geol Soc S Afr 2:1251–1266

Chafee MA (1982) Geochemical prospecting techniques for porphyry copper deposits. In: Titley SR (ed) Advances in the geology of the porphyry copper deposits, vol 13. Univ Arizona Press, Tucson, pp 297–307

Chapman HJ, Spooner ETC (1977) ^{87}Sr enrichment of ophiolitic sulfide deposits in Cyprus confirms ore formation by circulating seawater. Earth Planet Sci Lett 35:71–78

Chappell BW, White AJR (1974) Two contrasting granite types. Pac Geol 8:173–174

Charef A, Sheppard SMF (1988) The Malines Cambrian carbonate-shale-hosted Pb-Zn deposit, France: thermometric and isotopic (H, O) evidence for pulsating hydrothermal mineralization. Mineral Deposita 23:86–95

Chase CG, Gilmer TH (1973) Precambrian plate tectonics: the midcontinent gravity high. Earth Planet Sci Lett 21:70–78

Chavez WX, Jr. (1983) The geologic setting of disseminated copper sulfide mineralization of the Mantos Blancos copper-silver district, Antofagasta Province, Chile. SME-AIME Annu Meet, Atlanta, Georgia, Preprint 83–193:1–20

Chavez WX, Jr. (1984) Alteration mineralogy and chemistry of rhyolitic and andesitic volcanic rocks of the Mantos Blancos copper-silver district, Chile. SME-AIME Annu Meet, Los Angeles, Cal, Preprint 84–153:1–6

Cherry ME (1983) Association of gold and felsic intrusions-examples from the Abitibi belt. In: Colvine AC (ed) The geology of gold in Ontario. Ontario Geol Surv Misc Pap 110:48–55

Chivas AR, Wilkins RWT (1977) Fluid inclusion studies in relation to hydrothermal alteration and mineralization at the Koloula porphyry copper prospect, Guadacanal. Econ Geol 72:153–169

Chongke H, Zenggi X (1986) A general review of the tungsten deposits of China. In: Bues AA (ed) Int Geol Correl Prog Proj 26:157–165

Chown EH, Hicks J, Phillips GN, Townend R (1984) The disseminated Archaean Big Bell gold deposit, Murchison Province, western Australia: an example of pre-metamorphic hydrothermal alteration. In: Foster RP (ed) Gold '82: the geology, geochemistry and genesis and gold deposits. Balkema, Rotterdam, pp 305–324

Christiansen FG (1986) Structural classification of ophiolitic chromite deposits. In: Gallagher MJ, Ixer RA, Neary CR, Prichard HM (eds) Metallogeny of basic and ultrabasic rocks. Inst Min Metall, pp 279–290

Christofferson HC, Wallin B, Selkman S, Richard DT (1979) Mineralization controls in the sandstone lead-zinc deposits at Vassbo, Sweden. Econ Geol 74:1239–1249
Churchill RK (1980) Meteoric water leaching and ore genesis at the Tayoltita silver-gold mine, Durango, Mexico. Ph D Thesis, Univ Minn, 162 pp
Clauge DA, Straley PF (1977) Petrologic nature of the oceanic Moho. Geology 5:133–136
Clark KF, Foster CT, Damon PE (1982) Cenozoic mineral deposits and subduction related magmatic arcs in Mexico. Bull Geol Soc Am 93:533–544
Clark WB (1969) Gold districts of California. Cal Div Mines Geol Bull 193:1–186
Clarke AH, Caelles JC, Farrar E, Haynes SJ, Lortie RB, McBride SL, Quirt SG, Robertson RCR, Zentilli M (1976) Longitudinal variations in the metallogenic evolution of the Central Andes. Geol Soc Can Spec Pap 14:23–58
Clayton RH, Thorpe L (1982) Geology of the Nanisivik zinc-lead deposit. Geol Assoc Can Spec Pap 25:739–760
Clemmey H (1974) Sedimentary geology of a late Precambrian copper deposit at Kitwe, Zambia. In: Bartholome P (ed) Gisements stratiformes et provinces cypriferes. Soc Geol Belg Leige, pp 255–266
Clemmey H (1985) Sedimentary ore deposits. In: Brenchley PJ, Williams BPJ (eds) Sedimentology: recent developments and applied aspects. Geol Soc Spec Publ 18:229–248
Clendenin CW, Charlesworth EG, Maske S (1988) An early Proterozoic three-stage rift system, Kaapvaal Craton, South Africa. Tectonophysics 145:73–86
Clifford JA, Ryan P, Kucha H (1986) A review of the geological setting of the Tynagh orebody, Co. Galway. In: Geology and genesis of mineral deposits of Ireland. Irish Assoc Econ Geol, Dublin, pp 419–439
Coad PR (1985) Rhyolite geology at Kidd Creek: a progress report. Can Inst Metall Min Trans 78 874:70–83
Cole JW (1979) Structure, petrology and genesis of Cenozoic volcanism, Taupo Volcanic Zone, New Zealand – a review. N Z J Geol Geophys 22:631–657
Cole JW (1984) Taupo-Totorua depression – an ensialic marginal basin of North Island, New Zealand. In: Kokelaar BP, Howath MF (eds) Marginal basin geology. Geol Soc London Spec Publ 16:109–120
Coleman RG (1977) Ophiolites: ancient oceanic lithosphere. Springer, Berlin Heidelberg New York, 229 pp
Coleman RG (1981) Tectonic setting of ophiolite obduction in Oman. J Geophys Res 86:2497–2508
Colley H, Greenbaum D (1980) The mineral deposits and metallogenesis of the Fiji Platform. Econ Geol 75:807–829
Collins WJ, Beams SD, White AJR, Chappell BW (1982) Nature and origin of A-type granites with particular reference to southeastern Australia. Contrib Mineral Petrol 80:189–200
Colvine AC, Fyon JA, Heather KB, Marmont S, Smith PM, Troop DG (1988) Archean lode gold deposits in Ontario. Ontario Geol Surv Misc Pap 139:136 pp
Condie KC (1981) Archean greenstone belts. Elsevier, Amsterdam 434 pp
Condie KC (1982) Early and middle Proterozoic supracrustal successions and their tectonic settings. Am J Sci 282:341–357
Coney PJ (1972) Cordilleran tectonics and North American plate motion. Am J Sci 272:603–628
Coney PJ (1981) Accretionary tectonics in western North America. In: Dickinson WR, Payne WD (eds) Relations of tectonics to ore deposits in the southern Cordillera. AR Geol Soc Digest 14:23–38
Coney PJ, Reynolds SJ (1977) Cordilleran Benioff zones. Nature (London) 270:403–406
Conn HK (1979) The Johns-Manville platinum-palladium prospect, Stillwater Complex, Montana, U.S.A. Can Mineral 17:463–468
Constantinou G (1976) Genesis of the conglomerate structure, porosity and collomorphic textures of massive sulfide ores of Cypurs. Geol Assoc Can Spec Pap 14:187–210
Constantinou G (1980) Metallogenesis associated with the Troodos ophiolite. In: Panayioutou A (ed) Ophiolites. Int Ophiolite Symp, Cyprus 1979, pp 663–674
Constantinou G, Govett GJS (1972) Genesis of sulfide deposits, ochre and umber of Cyprus. Inst Mining Metall Trans 8:B36–B46

Converse DR, Holland HD, Edmond JM (1984) Flow rates in the axial hot springs of the East Pacific Rise (21°N): implications for the heat budget and the formation of massive sulfide deposits. Earth Planet Sci Lett 69:159–175

Cook PJ, McElhinny MW (1979) A re-evaluation of the spatial and temporal distribution of sedimentary phosphate deposits in the light of plate tectonics. Econ Geol 74:315–330

Corbett KD (1981) Stratigraphy and mineralization in the Mt. Read volcanics, western Tasmania. Econ Geol 76:209–230

Corliss JG, Dymond J, Gordon LI, Edmond JM, von Herzen RP, Ballard RD, Green K, Williams D, Bainbridge A, Crane K, van Andel TjH (1979) Submarine thermal springs on the Galapagos rift. Science 203:1073–1083

Cornwall HR, Rose HJ Jr (1957) Minor elements in Keweenawan lavas, Michigan. Geochim Cosmochim Acta 12:209–224

Cotelo Neiva JM (1972) Tin-tungsten deposits and granites from northern Portugal. 24th Int Geol Congr Sect 4:282–288

Cotterill P (1969) The chromite deposits of Selukwe, Rhodesia. Econ Geol Monogr 4:154–186

Cousins CA (1969) The Merensky Reef of the Bushveld Igneous Complex. Econ Geol Monogr 4:239–251

Coveney RM, Jr (1981) Gold quartz veins and auriferous granite at the Oriental Mine, Alleghany district, California. Econ Geol 76:2176–2199

Coward MP (1986) Heterogeneous stretching, simple shear and basin development. Earth Planet Sci Lett 80:325–336

Coward MP, Dewey JF, Hancock PL (eds) (1987) Continental extensional tectonics. Geol Soc London Spec Publ

Cox KG, Johnson RL, Monkman LJ, Stillman CJ, Vail JR, Wood DN (1965) The geology of the Nuanetsi Igneous Province. Proc Soc Philos Trans 257A:71–218

Craig H (1966) Isotopic composition and origin of the Red Sea and Salton Sea geothermal brines. Science 154:1544–1547

Craig H (1969) Geochemistry and origin of the Red Sea brines. In: Degens ET, Ross DA (eds) Hot brines and recent heavy metals in the Red Sea. Springer, Berlin Heidelberg New York, pp 208–242

Crane K, Aikman F III, Embley R, Hammond S, Malahoff A, Lupton J (1985) The distribution of geothermal fields on the Juan de Fuca Ridge. J Geophys Res 90:727–744

Crocker IT (1985) Volcanogenic fluorite-hematite deposits and associated pyroclastic rock suite at Vergenoeg, Bushveld Complex. Econ Geol 80:1181–1200

Crocker IT (1986) The Zaaiplaats tinfield, Pogietersrust district. In: Anhaeusser CR, Maske S (eds) Mineral deposits of southern Africa. Geol Soc S Afr 2:1287–1300

Cronan DS (1987) Controls on the nature and distribution of manganese nodules in the western equatorial Pacific. In: Teleki PG, Dobson MP, Moore JR, von Stackelberg U (eds) Marine minerals. Reidel, Dordrecht, pp 177–188

Cross TA, Pilger RH Jr (1978) Constraints on absolute plate motion and plate interaction inferred from Cenozoic igneous activity in the western United States. Am J Sci 278:865–902

Crough ST (1979) Hotspot epeirogeny. Tectonophysics 61:321–333

Crough ST (1983) Hotspot swells. Annu Rev Earth Planet Sci 11:165–193

Crowell JC (1979) The San Andreas fault system through time. J Geol Soc London 136:293–302

Culver SJ, Williams HR (1979) Late Precambrian and Phanerozoic geology of Sierra Leone. J Geol Soc London 136:604–618

Cuney M (1978) Geological environment, mineralogy, and fluid inclusions of the Bois Noirs-Limouzat uranium vein, Forez, France. Econ Geol 73:1567–1610

Curray JR, Emmel FJ, Moore DG (1980) Structure, tectonics and geological history of the northeastern Indian Ocean. In: Nairn AEM, Stehli FG (eds) The ocean basins and continental margins, vol 6. The Indian Ocean. Plenum, New York, pp 399–450

Dadet P, Marchesseau J, Millon R, Motti E (1970) Mineral occurrences related to stratigraphy and tectonics in Tertiary sediments near Umm Lajj, eastern Red Sea area, Saudi Arabia. Philos Trans R Soc London Ser A 267:99–106

Daly MC (1986) Crustal shear zones and thrust belts: their geometry and continuity in central Africa. Philos Trans R Soc London A 317:111–127

Dalziel IWD (1981) Back-arc extension in the southern Andes – a review and critical discussion. Philos Trans R Soc London Ser A 300:319–336
Damasco FV, de Guzman MT (1977) The GW gold orebodies in the Acupan mine of Benguet Corporation. In: 6th Symp Min Res Dev, Baguio City, Philippines 1977. Proc Sec 6 Pap, 76 pp
D'Argenio B, Alvarez W (1980) Stratigraphic evidence for crustal thickness changes on the southern Tethyan margin during the Alpine cycle. Geol Soc Am Bull 91:681–689
Darnley AG (1960) Petrology of some Rhodesian Copperbelt orebodies and associated rocks. Trans Inst Min Metall London 69:137–173; 371–398; 540–569
Date J, Tanimura S (1974) Dacite and rhyolite associated with the Kuroko mineralization. Mining Geol Spec Issue 6. Soc Mining Geol Jpn, pp 261–265
Date J, Wanatabe Y, Saeki Y (1983) Zonal alteration around the Fukazawa Kuroko deposit, Akita Prefecture, Northern Japan. Econ Geol Monogr 5:365–386
Davies JL, Fyffe LR, Irrinki RR (1973) The geology of the Miramachi zone (north) northeastern New Brunswick. Can Inst Mining Metall Annu Conf, Preprint, pp 1–26
Davies RM, Ballantyne GH (1987) Geology of the Ladolam gold deposit, Lihir Island, Papua New Guinea. Pac Rim Congr 87:943–949
Davis GA, Lister GS (1988) Detachment faulting in continental extension: perspectives from the southwestern U.S. Cordillera. Geol Soc Am Spec Pap 218:133–160
Davis GR (1969) Aspects of the metamorphosed sulfide ores at Kilembe, Uganda. Sedimentary ores. In: Proc 15th Inter-Univ Geol Congr Spec Publ 1: Univ Leicester, pp 273–296
Dawson KM (1977) Regional metallogeny of the northern Cordillera. Geol Surv Can Pap 77 1A:1–4
Day GA (1986) The Hercynian evolution of the southwest British continental margin. In: Reflection seismology; the continental crust. Am Geophys Un Geodyn Ser 14:233–242
de Cserna Z (1976) Geology of the Fresnillo area, Zacatecas, Mexico. Geol Soc Am Bull 87:1191–1199
Deen JA, Drexler JW, Rye RO, Munoz JL (1987) A magmatic fluid origin for the Julcani district, Peru: stable isotope evidence. Geol Soc Am Abstr with Prog, Annu Meet, Phoenix, p 638
Degens ET, Ross DA (eds) (1969) Hot brines and recent heavy metal deposits in the Red Sea: a geophysical and geochemical account. Springer, Berlin Heidelberg New York
Degi S (1988) Sedimentary facies, paleogeography, and the formation of mineral deposits in the Middle and Late Devonian, South China. Mineral Deposita 23:77–85
de Laeter JR, Martyn JE (1986) Age of molybdenum-copper mineralization at Coppin Gap, western Australia. Aust J Earth Sci 33:65–72
Delaney JR, Mogk DW, Mottle MJ (1988) Quartz-cemented breccias from the Mid-Atlantic Ridge: samples of a high salinity upflow zone. J Geophys Res 92:9175–9192
Delong SE, Schwarz WM (1979) Thermal effects of ridge subduction. Earth Planet Sci Lett 44:239–246
deLorraine W, Dill DB (1982) Structure, stratigraphic controls and genesis of the Balmat zinc deposits, northwest Adirondacks, New York. Geol Assoc Can Spec Pap 25:571–596
Deloule E, Allegre C, Doe B (1986) Lead and sulfur microstratigraphy in galena crystals from Mississippi Valley-type deposits. Econ Geol 81:1307–1321
Denisenko VK (1986) Tungsten-bearing provinces in the USSR. In: Bues AA (ed) Int Geol Correl Prog Proj 26:127–156
DePaolo DJ, Wasserberg GJ (1979) Sm-Nd age of the Stillwater Complex and the mantle evolution curve for neodymium. Geochim Cosmochim Acta 43:999–1008
Dewey JF (1977) Suture zone complexities: a review. Tectonophysics 40:53–68
Dewey JF (1980) Episodicity, sequence and style at convergent plate boundaries. In: Strangway DW (ed) The continental crust and its mineral deposits. Geol Assoc Can Spec Pap 20:553–573
Dewey JF, Burke KC (1973) Tibetan, Variscan and Precambrian basement reactivation: products of continental collision. J Geol 81:683–692
Dewey JF, Burke KC (1974) Hotspots and continental breakup: implications for continental orogeny. Geology 2:57–60
de Wit MJ, Ashwal LD (eds) (1986) Tectonic evolution of greenstone belts. LPI Tech Rep No 86-10 227 pp

de Wit MJ, Stern CR (1981) Variations in the degree of crustal extension during formation of a back arc basin. Tectonophysics 72:229–260
de Wit MJ, Hart R, Martin A, Abbott P (1982) Archean abiogenic and probable biogenic structures associated with mineralized hydrothermal vent systems and regional metasomatism, with implications for greenstone belt studies. Econ Geol 77:1783–1802
de Wit MJ, Hart RA, Hart RJ (1987) The Jamestown ophiolite complex, Barberton mountain belt: a section through 3.5 Ga oceanic crust. J Afr Earth Sci 6:681–730
Dick HLB (1982) The petrology of two back-arc basins of the northern Philippine Sea. Am J Sci 282:644–700
Dick LA (1976) Metamorphism and metasomatism at the MacMillan Pass tungsten deposit, Yukon and District of MacKenzie, Canada. MS Thesis, Queens Univ, Kingston, Ontario, 226 pp
Dick LA (1979) Tungsten and base metal skarns in the northern Cordillera. Geol Surv Can Pap 79-1A:259–266
Dick LA, Hodgson CJ (1982) The MacTung W-Cu(Zn) contact metasomatic and related deposits of the northeastern Canadian Cordillera. Econ Geol 77:845–867
Dickey JS (1975) A hypothesis of origin for podiform chromite deposits. Geochim Cosmochim Acta 39:1061–1074
Dickinson WR (1980) Plate tectonics and key petrologic associations. In: Strangway DW (ed) The continental crust and its mineral deposits. Geol Assoc Can Spec Pap 20:341–360
Dickinson WR, Seely DR (1979) Structure and stratigraphy of fore-arc regions. Am Assoc Petrol Geol Bull 63:2–31
Dickinson WR, Snyder WS (1979) Geometry of triple junctions related to San Andreas transform. J Geophys Res 84:604–628
Dietz RS (1964) Sudbury structure as an astrobleme. J Geol 72:412–434
Dimroth E (1981) Labrador Geosyncline: type example of early Proterozoic cratonic reactivation. In: Kroner A (ed) Precambrian plate tectonics. Elsevier, Amsterdam, pp 331–352
Dines HG (1956) The metalliferous mining region of southwest England. Mem Geol Surv UK, 2 vols, HMSO, London
Distler VV, Genkin AD, Dyuzhikov OA (1986) Sulfide petrology and genesis of copper-nickel ore deposits. In: Friedrich GH, Genkin AD, Naldrett AJ, Ridge JD, Sillitoe RH, Vokes FM (eds) Geology and metallogeny of copper deposits. Springer, Berlin Heidelberg New York Tokyo, pp 111–123
Djumhani (1981) Metallic mineral deposits of Indonesia: a metallogenic approach. Geol Surv Jpn Rep 261: (Metallog Asia) 107–124
Dodge FCW, Loyd RC (1984) Gold deposits of the western Sierra Nevada. Soc Econ Geol Field Trip Guide Annu Meet, Los Angeles 1984, 25 pp
Doe BR, Zartman RE (1979) Plumbotectonics, the Phanerozoic. In: Barnes HL (ed) Geochemistry of hydrothermal ore deposits. John Wiley & Sons, New York, pp 22–70
Doe BR, Steven TA, Delevaux MH, Stacey JS, Lipman PW, Fisher FS (1979) Genesis of ore deposits in the San Juan volcanic field, southwestern Colorado: lead isotope evidence. Econ Geol 74:1–26
Dokka RK (1986) Patterns and modes of early Miocene crustal extension, central Mojave Desert, California. Geol Soc Am Spec Pap 208:75–95
Donnelly ME, Hahn GA (1981) A review of the Precambrian massive sulfide deposits in central Arizona, and the relationship to their depositional environment. AR Geol Soc Digest 14:11–21
Dressler BO (1984) General geology of the Sudbury area. In: The geology and ore deposits of the sudbury structure. Ontario Geol Surv Spec Vol 1:57–82
Drexler JW, Munoz JL (1985) Highly oxidized, pyrrhotite-anhydrite-bearing silicic magmas from the Julcani Ag-Cu-Bi-Pb-Au-W district, Peru: physicochemical conditions of a productive magma. In: Taylor RP, Strong DF (eds) Granite-related mineral deposits. Can Inst Min, pp 87–100
Duane MJ (1988) Genesis, mineralogy and geochemistry of uranium in the Gortdrum stratiform copper deposit, Ireland. Mineral Deposita 23:50–57
Duane MJ, de Wit MJ (1988) Pb-Zn ore deposits of the northern Caledonides-products of continental-scale fluid mixing and tectonic expulsion during continental collision. Geology 16:999–1002

Duane MJ, Welke HJ, Allsop HL (1986) U-Pb age for some base-metal sulfide deposits in Ireland: genetic implications of Mississippi Valley-type mineralization. Geology 14:477–480
Dubois RL, Brummett RW (1968) Geology of the Eagle Mountain mine area. In: Ridge JD (ed) Ore deposits of the United States 1933–1967. New York Am Inst Mining Metall Petrol Eng (Graton-Sales vol): 1592–1606
Duke NA, Hodder RW (1987) Stratabound base metals and gold in iron-rich rocks of a late Proterozoic-early Paleozoic rift setting, central Appalachia, U.S.A. Trans Geol Soc S Afr 89:233–252
Duke NA, Hutchinson RW (1974) Geological relationships between massive sulfide bodies and ophiolitic volcanic rocks near York Harbour, Newfoundland. Can J Earth Sci 11:53–69
Duncan RA, Green DH (1980) Role of multistage melting in the formation of oceanic crust. Geology 8:22–26
Dunham KC (1948) Geology of the North Pennine orefield: V.1 Tyne to Stainmore. Mem Geol Surv UK, 357 pp
Dunnet D (1976) Some aspects of the Panantarctic cratonic margin in Australia. Philos Trans R Soc London Ser A 280:641–654
Dupuy C, Dostal J, Leblanc M (1981) Geochemistry of an ophiolite complex from New Caledonia. Contr Min Pet 76:71–83
East Pacific Rise Study Group (ed) (1981) Crustal processes of the mid-ocean ridge. Science 13:31–40
Eastoe CJ (1978) A fluid inclusion study of the Panguna porphyry copper deposit, Bougainville, Papua New Guinea. Econ Geol 73:721–742
Eastoe CJ (1982) Physics and chemistry of the hydrothermal system at the Panguna porphyry copper deposit, Bougainville, Papua New Guinea. Econ Geol 77:127–153
Eastoe CJ, Solomon M, Garcia Palomero F (1986) Sulphur isotope study of massive and stockwork pyrite deposits at Rio Tinto, Spain. Trans Inst Min Metall 95:B201–207
Easton RM (1986) Geochronology of the Grenville Province; Part I: Compilation of data. Part II: Synthesis and interpretation. Geol Assoc Can Spec Pap 31:127–174
Eaton GP (1979) A plate tectonic model for late Cenozoic crustal spreading in the western United States. In: Riecker RE (ed) Rio Grande Rift: tectonics and magmatism. Am Geophys Union, pp 7–32
Eaton GP (1982) The Basin and Range province: origin and tectonic significance. Annu Rev Earth Planet Sci 10:409–440
Edmond JR, Measures C, Mangum B, Grant B, Selater R, Collier R, Hudson A, Gordon LI, Corliss JB (1979) On the formation of metal-rich deposits at ridge crests. Earth Planet Sci Lett 46:19–30
Edmond JR, Von Damm KL, McDuff RE, Measures CI (1982) Chemistry of hot springs on the East Pacific Rise and their effluent dispersal. Naure (London) 297:187–191
Edmunds FR (1973) Stratigraphy and lithology of the Lower Belt Series in the southern Purcell Mountains, British Columbia. In: Belt Symp, Moscow 1973, vol 1. Idaho Bur Mines Geol, pp 230–234
Egin D, Hirst DM, Phillips R (1979) The petrology and geochemistry of volcanic rocks from the north Harsit River area, Pontid volcanic province, northeast Turkey. J Volcanic Geotherm Res 6:105–123
Einaudi MT (1977a) Petrogenesis of the copper-bearing skarn at the Mason Valley Mine, Yerington district, Nevada. Econ Geol 72:769–795
Einaudi MT (1977b) Environment of ore deposition at Cerro de Pasco, Peru. Econ Geol 72:893–924
Einaudi MT, Meinert LD, Newberry RJ (1981) Skarn deposits. Econ Geol 75th Anniv Vol, pp 317–391
Eisbacher GH (1977) Tectono-stratigraphic framework of the Redstone Copper Belt, District of Mackenzie. Geol Surv Can Pap 77-35:1–21
El Aref MM (1984) Strata-bound and stratiform iron sulfides, sulfur, and galena in the Miocene evaporites, Ranga, Red Sea, Egypt (with special emphasis on their diagenetic crystallization rhythmites). In: Wauschkuhn A, Kluth C, Zimmermann RA (eds) Syngenesis and epigenesis in the formation of mineral deposits. Springer, Berlin Heidelberg New York, pp 457–467

Eldridge CS, Barton PB Jr, Ohmoto H (1983) Mineral textures and their bearing on ore formation of the Kuroko orebodies. Econ Geol Monogr 5:241–281

Ellis AJ (1979) Explored geothermal systems. In: Barnes HL (ed) Geochemistry of hydrothermal ore deposits, 2nd edn. John Wiley & Sons, New York, pp 623–683

Ellis MW, MacGregor JA (1967) The Kalengwa copper deposit in northwestern Zambia. Econ Geol 62:781–797

Emslie RF (1978a) Elsonian magmatism in Labrador: age, characteristics and tectonic setting. Can J Earth Sci 15:438–453

Emslie RF (1978b) Anorthosite massifs, Rapakivi granites, and late Proterozoic rifting of North America. Precambrian Res 7:61–98

Engebretson DC, Cox A, Gordon RG (1985) Relative motions between oceanic and continental plates in the Pacific Basin. Geol Soc Am Spec Pap 206:1–59

Engin T, Ozkocak O, Artan U (1987) General geological setting and character of chromite deposits in Turkey. In: Stowe CW (ed) Evolution of the chromium ore fields. Van Nostrand Reinhold, New York, pp 194–219

Eriksson SC (1984) Age of carbonatite and phoscorite magmatism of the Phalaborwa Complex (South Africa). Isotope Geosci 2:291–299

Ernst WG (ed) (1981) The geotectonic development of California (Rubey vol). Prentice-Hall, Englewood Cliffs, NJ, 706 pp

Ernst WG (1988) Metamorphic terranes, isotopic provinces, and implications for continental growth of the western United States. J Geophys Res 93:7634–7642

Etheridge MA (1986) On the reactivation of extensional fault systems. Phil Trans R Soc Lond A317:179–194

Etheridge MA, Rutland RWR, Wyborn LAI (1987) Orogenesis and tectonic process in the Early to Middle Proterozoic of northern Australia. Am Geophys Un Geodyn Ser 17:131–148

Ethier VG, Campbell FA, Both RA, Krouse HR (1976) Geological setting of the Sullivan orebody and estimates of temperature and pressure of metamorphism. Econ Geol 71:1570–1588

Evernden JF, Kriz SJ, Chervoni C (1977) Potassium-argon ages of some Bolivian rocks. Econ Geol 72:1042–1061

Fahley MP (1981) Fluid inclusion study of the Tonapah district, Nevada. MS Thesis, Colorado School of Mines

Fahrig WF (1987) The tectonic settings of continental mafic dyke swarms: failed arm and early passive margin. Geol Assoc Can Spec Pap 34:331–348

Fahrig WF, Wanless RK (1963) Age and significance of diabase dyke-swarms of the Canadian shield. Nature (London) 200:934–937

Fahrig WF, Christie KW, Chown EH. James D, Machado N (1986) The tectonic significance of some basic dyke swarms in the Canadian Superior Province with special reference to the geochemistry and paleomagnetism of the Mistassini swarm, Quebec, Canada. Can J Earth Sci 23:238–253

Farmer GL, DePaolo DJ (1983) Origin of Mesozoic and Tertiary granite in the western United States and implications for pre-Mesozoic crustal structure 1. Nd and Sr isotopic studies in the geocline of the northern Great Basin. J Geophys Res 8:3379–3401

Farmer GL, DePaolo DJ (1987) A Nd and Sr isotopic study of hydrothermally altered granite at San Manuel, Arizona: implications for element migration paths during the formation of porphyry-copper ore deposits. Econ Geol 82:1142–1151

Farr JE, Scott SD (1981) Geochemistry of the Uwamuki #2 stockwork, Hokuroku district, Japan (Abstr.). Geol Soc Am Abstr with Prog 13:449

Farrar E, Clark AH, Haynes SJ, Quirt GS, Conn H, Zentilli M (1970) K-Ar evidence for the post = Paleozoic migration of granitic intrusion foci in the Andes of northern Chile. Earth Planet Sci Lett 9:17–28

Farrington JL (1952) A preliminary description of the Nigerian lead-zinc field. Econ Geol 47:583–608

Favorskaya MA (1977) Metallogeny of deep lineaments and new global tectonics. Mineral Deposita 12:163–169

Fehlberg B, Giles CW (1984) Archeaen volcanic exhalative gold mineralization at Spargoville, Western Australia. In: Foster RP (ed) Gold '82: the geology, geochemistry and genesis of gold deposits. Balkema, Rotterdam, pp 285–304

Fehn U (1986) The evolution of low-temperature convection cells near spreading centers: a mechanism for the formation of the Galapagos mounds and similar manganese deposits. Econ Geol 81:1396–1407

Fehn U, Cathles LM (1986) The influence of plate movement on the evolution of hydrothermal convection cells in the oceanic crust. Tectonophysics 125:289–312

Feiss PG, Hauck SA (1980) Tectonic setting of massive-sulfide deposits in the southern Appalachians, USA. In: Proc 5th IAGOD Symp, Utah, pp 567–580

Feraud G, Giannerini G, Campredon R (1987) Dyke swarms as paleostress indicators in areas adjacent to continental collision zones: examples from the European and northwestern Arabian Plates. Geol Assoc Can Spec Pap 34:273–278

Ferencic A (1971) Metallogenic provinces and epochs in southern Central America. Mineral Deposita 6:77–88

Ferguson J, Winer P (1980) Pine Creek geosyncline: statistical treatment of whole rock chemical data. In: IAEA (ed) Uranium in the Pine Creek geosyncline. IAEA, Vienna, pp 191–208

Ferguson J, Ewers GR, Donnelly TH (1980) Model for the development of economic uranium mineralization in the Alligator Rivers uranium field. In: IAEA (ed) Uranium in the Pine Creek geosyncline. IAEA, Vienna, pp 563–574

Fernandez HE, Damasco FV (1979) Gold deposition in the Baguio gold district and its relationship to regional geology. Econ Geol 74:1852–1868

Ferrario A, Garuti G (1980) Copper deposits in the basal breccias and volcano-sedimentary sequences of the eastern Ligurian Ophiolites (Italy). Mineral Deposita 15:291–303

Field CW, Fifarek RH (1985) Light stable-isotope systematics in the epithermal environment. Rev Econ Geol 2:99–128

Field CW, Gustafson LB (1976) Sulfur isotopes in the porphyry copper deposit at El Salvador, Chile. Econ Geol 71:1533–1548

Finlow-Bates T, Large DE (1978) Water depth as a major control on the formation of submarine exhalative ore deposits. Geol Jahrb D30:27–39

Finucane KJ (1965) Geology of the Sons of Gwalia gold mine. In: McAndrew J (ed) Geology of Australian ore deposits. 8th Commun Min Metall Congr, Melbourne, pp 95–97

Fleischer VD, Garlick WG, Haldane R (1976) Geology of the Zambian Copper Belt. In: Handbook of stratabound and stratiform ore deposits, vol 6. Elsevier, Amsterdam New York, pp 223–352

Fleming AW, Handley GA, Williams KL, Hills AL, Corbett GJ (1986) The Porgera gold deposit, Papua New Guinea. Econ Geol 81:660–680

Fletcher CJN (1977) The geology, mineralization and alteration of Ilkwang mine, Republic of Korea: a Cu-W-bearing tourmaline breccia pipe. Econ Geol 72:753–768

Floyd PA (1982) Chemical variation in Hercynian basalts relative to plate tectonics. J Geol Soc 139:507–522

Floyd PA, Winchester JA (1975) Magma type and tectonic setting discrimination using immobile elements. Earth Planet Sci Lett 27:211–218

Foose M, Weiblen P (1986) The physical and petrologic setting and textural and compositional characteristics of sulfides from the South Kawishiwi intrusion, Duluth Complex, Minnesota, U.S.A. In:Friedrich GH, Genkin AD, Naldrett AJ, Ridge JD, Sillitoe RH, Vokes FM (eds) Geology and metallogeny of copper deposits. Springer, Berlin Heidelberg New York Tokyo, pp 8–24

Force ER, Cannon WF (1988) Depositional model for shallow marine manganese deposits around black shale basins. Econ Geol 83:93–117

Ford AB (1975) Stratigraphy and whole-rock chemical variation in the stratiform Dufek intrusion, Pensacola Mountains, Antarctica (Abstr). Geol Soc Am Annu Meet, Salt Lake City, pp 1077–1078

Ford JH (1978) A chemical study of alteration at the Panguna porphyry copper deposit, Bougainville, Papua New Guinea. Econ Geol 73:703–720

Forrest K (1983) Geologic and isotopic studies of the Lik deposit and the surrounding mineral district, De Long Mountains, western Brooks Range, Alaska. PhD Thesis, Univ Minn, 161 pp

Forrest K, Sawkins FJ (1987) Geologic setting and mineralization of the Lik deposit: implications for the tectonic history of the western Brooks Range. In:Thailleur I, Weimer P (eds) Alaskan north shore geology. Pac Sec SEPM, Cal 1:295–306

Foster RP, Furber FMW, Gilligan JM, Green D (1986a) Shamva gold mine, Zimbabwe: a product of the calc-alkaline-linked exhalative, volcaniclastic, and epiclastic sedimentation in the late Archean. Geol Assoc Can Spec Pap 32:41–66

Foster RP, Mann AG, Stowe CW, Wilson JF (1986b) Archaean gold mineralization in Zimbabwe. In: Anhaeusser CR, Maske S (eds) Mineral deposits in southern Africa 1:43–112

Fourie PJ, de Jager DH (1986) Phosphate in the Phalaborwa Complex. In: Anhaeusser CR, Maske S (eds) Mineral deposits of southern Africa. Geol Soc S Afr 2:2239–2253

Fox JS (1979) Host rock geochemistry and massive volcanogenic sulfide ores. Can Inst Min Bull 72:127–134

Fox JS (1984) Besshi-type volcanogenic sulphide deposits – a review. Can Inst Min Metall Bull 77:57–68

Fox PJ, Detrick RS, Purdy GM (1980) Evidence for crustal thinning near fracture zones: implications for ophiolites. In: Panayiotou A (ed) Proc Int Ophiolite Symp, Cyprus 1979, pp 161–168

Francis EH (1968) Review of Carboniferious-Permian volcanicity in Scotland. Geol Rundsch 57:219–246

Francois A (1974) Stratigraphie, tectonique et minéralisations dans l'arc cuprifère du Shaba (Republique du Zaire). In: Bartholome P (ed) Gisments stratiformes et provinces cuprifères. Geol Soc Belg, Leige, pp 79–101

Franklin JM, Thorpe RI (1982) Comparative metallogeny of the Superior, Slave and Churchill Provinces. Geol Assoc Can Spec Pap 25:3–90

Franklin JM, Lydon JW, Sangster DF (1981) Volcanic-associated massive sulfide deposits. Econ Geol 75th Anniv Vol, pp 485–627

Franklin JM, Kissin SA, Smyk MC, Scott SD (1986) Silver deposits associated with the Proterozoic rocks of the Thunder Bay district, Ontario. Can J Earth Sci 23:1576–1591

Frarey MJ, Roscoe SM (1970) The Huronian Supergroup north of Lake Huron. Geol Surv Can Pap 70-40:143–158

Freiberg DA (1983) Geologic setting and origin of the Lucifer manganese deposit, Baja California Sur, Mexico. Econ Geol 78:931-943

French BM (1970) Possible relationship between meteorite impact and igneous petrogenesis as indicated by the Sudbury structure, Ontario, Canada. Bull Volcanol 34:466–517

Freund R, Garfunkel Z (eds) (1981) The Dead Sea Rift. Int Symp Rift Zones Earth. Tectonophys (Spec Issue) 80:1–30

Frietsch R, Papunen H, Vokes FM (1979) The ore deposits in Finland, Norway and Sweden – a review. Econ Geol 74:975–1001

Fripp REP (1976) Stratabound gold deposits in Archean banded iron formation, Rhodesia. Econ Geol 71:58–75

Frost JE (1965) Controls of ore deposition for the Larap mineral deposits, Camarines Norte, Philippines. PhD Diss, Stanford Univ, 173 pp

Fujii K (1974) Tectonics of the Green Tuff region, northern Honshu, Japan. Min Geol Spec Issue 6, Soc Min Geol Jpn, pp 251–260

Fulp MS, Renshaw JL (1985) Volcanogenic-exhalative tungsten mineralization of Proterozoic age near Santa Fe, New Mexico, and implications for exploration. Geology 13:66–69

Furnes H, Roberts D, Sturt BA, Thon A, Gale GH (1980) Ophiolite fragments in the Scandinavian Caledonides. In: Panayiotou A (ed) Proc Int Ophiolite Symp, Cyprus 1979, pp 582–600

Futa K, Hedge CE, Hearn BC, Donnelly-Nodan JM (1982) Strontium isotopes in the Clear Lake Volcanics. US Geol Surv Prof Pap 1141:61–66

Fyfe WS (1980) Crust formation and destruction. In: Strangway DW (ed) The continental crust and its mineral deposits. Geol Assoc Can Spec Pap 20:77–88

Fyfe WS (1986) Fluids in deep continental crust. In: Reflection seismology: the continental crust. Am Geophys Un Geodyn Ser 14:33–40

Gablina IF (1986) Genetic types of copper mineralization in the Igarka area, west of the Siberian Platform. In: Friedrich GH, Genkin AD, Naldrett AJ, Ridge JD, Sillitoe RH, Vokes FM (eds) The geology and metallogeny of copper deposits. Springer, Berlin Heidelberg New York Tokyo, pp 524–539

Gabrielse H (1985) Major dextral transcurrent displacements along the northern Rocky Mountain trench and related lineaments in north-central British Columbia. Geol Soc Am Bull 96:1–14
Gabrielse H, Reesor JE (1974) The nature and setting of granitic plutons in the central and eastern parts of the Canadian Cordillera. Pac Geol 8:109–138
Gair JE (1962) Geology and mineral deposits of the Nova Lima and Rio Acima quadrangles, Minas Gerais, Brazil. US Geol Surv Prof Pap 341-A:1–67
Gair JE, Slack JF (1980) Stratabound massive sulfide deposits of the U.S. Appalachians. Geol Surv Irel Spec Pap 5:67–81
Gair JE, Slack JF (1984) Deformation, geochemistry, and origin of the massive sulfide deposits, Gossan Lead district, Virginia. Econ Geol 79:1483–1520
Gale GH, Pearce JA (1982) Geochemical patterns in Norwegian greenstones. Can J Earth Sci 19:386–397
Gale GH, Roberts A (1974) Trace element geochemistry of Norwegian Lower Paleozoic basic volcanics and its tectonic implications. Earth Planet Sci Lett 22:380–390
Gallagher MJ (1984) Methods of exploration for strata-bound mineral deposits in the Appalachian-Caledonian orogen. Econ Geol 79:1749–1758
Gallon ML (1986) Structural re-interpretation of the Selebi-Phikwe nickel-copper sulphide deposits, eastern Botswana. In: Anhaeusser CR, Maske S (eds) Mineral deposits of southern Africa. Geol Soc S Afr 2:1663–1669
Gandhi SS, Brown AC (1975) Cupriferous shales of the Adeline Island Formation, Seal Lake Group, Labrador. Econ Geol 70:145–163
Garcia Palomero F (1980) Carateres geologicos y relaciones morfologicas y geneticas de los yaciminentos del "Anticlinal de Riotinto." Inst Estud Onubenes "Padre Marchena", Huelva, Spain, 262 pp
Garcia Palomero F (1983) Geologia de las mineralizaciones de Riotinto y su modelo genetico. In: Libro Homenaje a Carlos Felguroso, Madrid. Cia General de Sondeos, SA, pp 43–53
Gardiner PRR, MacCarthy IAJ (1981) The late Paleozoic evolution of southern Ireland in the context of tectonic basins and their transatlantic significance. In: Kerr JWM, Fergusson AJ (eds) Geology of the North Atlantic borderlands. Can Soc Petrol Geol Mem 7:683–726
Garlick WG (1981) Sabkhas, slumping and compaction at Mufulira, Zambia. Econ Geol 76:1817–1847
Garlick WG, Fleischer VD (1972) Sedimentary environment of Zambian copper deposition. Geol Mijnbouw 51:277–298
Garson MS, Krs M (1976) Geophysical and geological evidence of the relationship of Red Sea transverse tectonics to ancient fractures. Geol Soc Am Bull 87:169–181
Garven G (1985) The role of regional fluid flow in the genesis of the Pine Point deposit, western Canada sedimentary basin. Econ Geol 80:307–324
Garven G, Freeze RA (1984a) Theoretical analysis of the role of groundwater flow in the genesis of stratabound ore deposits. 1. Mathematical and numerical model. Am J Sci 284:1085–1124
Garven G, Freeze RA (1984b) Theoretical analysis of the role of groundwater flow in the genesis of stratabound ore deposits. 2. Quantitative results. Am J Sci 284:1125–1174
Gaskarth JW, Parslow GR (1987) Proterozoic volcanism in the Flin Flon greenstone belt, east-central Saskatchewan, Canada. In: Paraoh TC, Beckinsale RD, Rickard D (eds) Geochemistry and mineralization of Proterozoic volcanic suites. Geol Sci Spec Publ 33:183–200
Gass IG (1980) The Troodos massif: its role in the unravelling of the ophiolite problem and its significance in the understanding of constructive plate margin processes. In: Panayiotou A (ed) Ophiolites. Int Ophiolite Symp, Cyprus 1979, pp 23–35
Gaut A (1981) Field relations and the petrography of the biotite granites of the Oslo region. Norges Geol Under 367:39–64
Gealey WK (1980) Ophiolite obduction mechanism. In: Panayiotou A (ed) Ophiolites. Int Ophiolite Symp, Cyprus 1979, pp 228–243
Gemmell JB, Simmons SF, Zantop H (1988) The Santo Niño silver-lead-zinc vein, Fresnillo, Zacatecas, Mexico, Part I: structure, vein stratigraphy, and mineralogy. Econ Geol 83:1597–1618
Gervasio FS (1971) Ore deposits of the Philippines mobile belt. J Geol Soc Philipp 25:1–24

Geyti A, Schoenwandt HK (1979) Bordvika – a possible porphyry molybdenum occurrence within the Oslo Rift, Norway. Econ Geol 74:1211–1230

Geyti A, Thomassen B (1984) Molybdenum and precious metal mineralization at Flammefjeld, southeast Greenland. Econ Geol 79:1921–1929

Gibbs A (1976) Geology and genesis of the Baqf lead-zinc deposits, Iran. Inst Mining Metall Trans 85:B205–B220

Giggenbach WF (1981) Geothermal mineral equilibria. Geochim Cosmochim Acta 45:393–410

Giles DL (1982) Gold mineralization in the laccolithic complexes of central Montana. In: The genesis of Rocky Mountain ore deposits: changes with time and tectonics. Proc Denver Region Explor Geol Soc Symp, pp 157–162

Giles DL, Nelson CE (1983) Principal features of epithermal lode gold deposits of the circum-Pacific Rim. In: Circum-Pacific energy and minerals resource Conf Proc, Honolulu 1982

Gill JB (1981) Orogenic andesites and plate tectonics. Minerals and rocks, vol 16. Springer, Berlin Heidelberg New York, 390 pp

Gilligan LB (1978) Mineral deposits in the New South Wales part of the Lachlan fold belt. A review. Geol Surv NSW Rep GS 1978/320:1–7

Gilligan LB, Felton EA, Olgers F (1979) The regional setting of the Woodlawn deposit. Geol Soc Aust J 26:135–140

Gilluly J (1976) Lineaments – ineffective guides to ore deposits. Econ Geol 71:1507–1514

Girdler RW (1969) The Red Sea – a geophysical background. In Degens ET, Ross DA (eds) Hot brines and recent heavy metal deposits in the Red Sea. Springer, Berlin Heidelberg New York, pp 38–58

Girdler RW (1983) Processes of planetary rifting as seen in the rifting and breakup of Africa. Tectonophys 95:241–252

Glaskovsky AA, Gorbunov GI, Sysoev FA (1977) Deposits of nickel. In: Smirnov VI (ed) Ore deposits of the USSR, vol 2. Pitman, London, pp 3–79

Godlevskii MN, Grinenko LN (1963) Some data on the isotopic composition of sulfur in sulfides of the Noril'sk deposit. Geochemistry 1:35–41

Godwin CI, Sinclair AS, Ryan BD (1982) Lead isotope models for the genesis of carbonate-hosted Zn-Pb, shale-hosted Ba-Zn-Pb, and silver-rich deposits in the northern Canadian Cordillera. Econ Geol 77:82–94

Goldberg I (1976) A preliminary account of the Otjihase copper deposit, South West Africa. Econ Geol 71:384–390

Goldfarb RJ, Leach DL, Miller ML, Pickthorn WJ (1986) Geology, metamorphic setting, and genetic constraints of epigenetic lode-gold mineralization within the Cretaceous Valdez Group, south-central Alaska. Geol Assoc Can Spec Pap 32:87–105

Goldfarb RJ, Leach DL, Pickthorn WJ, Paterson CJ (1988) Origin of lode gold deposits of the Juneau gold belt, southeastern Alaska. Geology 16:440–443

Goldie RJ (1979) Metamorphism of the Flavrian and Powell plutons, Noranda area, Quebec. J Petrol 20:227–238

Goldie RJ, Kotila B, Seward D (1979) The Don Rouyn mine; an Archean porphyry copper deposit near Noranda, Quebec. Econ Geol 74:1680–1684

Golding SD, Wilson AF (1983) Geochemical and isotope studies of the No. 4 lode, Kalgoorlie, western Australia. Econ Geol 78:438–450

Gole MJ, Klein C (1981) Banded iron-formations through much of Precambrian time. J Geol 89:169–184

Golightly JP (1981) Nickeliferous laterite deposits. Econ Geol 75th Anniv Vol, pp 710–734

Goodell PC, Petersen U (1974) Julcani mining district, Peru: a study of metal ratios. Econ Geol 69:347–361

Goodfellow WD, Jonasson IR (1984) Ocean stagnation and ventilation defined by $\delta^{34}S$ secular trends in pyrite and barite, Selwyn Basin, Yukon. Geology 12:583–586

Goodwin AM, Riddler RH (1970) The Abitibi orogenic belt. Geol Surv Can Pap 70-40:1–28

Goossens PJ (1972) Metallogeny in Ecuadorian Andes. Econ Geol 67:458–468

Goossens PJ (1976) Lithologic, geochemical, and metallogenic belts in the northern Andes, and their structural relationships. Soc Min Eng AIME Trans 260:60–67

Gordon MB, Hempton MR (1986) Collision induced rifting: the Grenville orogeny and Keweenawan Rift of North America. Tectonophysics 127:1–25
Gordon PSL (1973) The Selebi-Kitwe nickel-copper deposits, Botswana. Geol Soc S Afr Spec Publ 3:167–187
Graham SA, Dickinson WR, Ingersoll RV (1975) Himalayan-Bengal model for flysch dispersal in the Appalachian-Ouchita System. Geol Soc Am Bull 86:273–286
Grainger DJ, Grainger RL (1974) Explanatory notes on the 1:2,500,000 mineral deposits map of Papua New Guinea. Bur Min Geol Geophys Bull 148:1–171
Grammelvedt G (1979) The geology of the Lokken-Holdal area IGCP Project 60. Caledonian-Appalachian stratabound sulfides. Trondheim Norges Geol Unders Presymp Excurs Guideb, pp 106–120
Grant JN, Halls C, Avila W, Avila G (1977) Igneous geology and the evolution of hydrothermal systems in some sub-volcanic tin deposits of Bolivia. Geol Soc London Spec Publ 7:117–126
Grant JN, Halls C, Avila Salinas W, Snelling NJ (1979) K-Ar ages of igneous rocks and mineralization in part of the Bolivian tin belt. Econ Geol 74: 838–851
Grant JN, Halls C, Sheppard SMF, Avila W (1980) Evolution of the porphyry tin deposits of Bolivia. In: Granitic magmatism and related mineralization. Min Geol Spec Issue 8:151–174
Grant NK (1971) South Atlantic, Benue Trough, and the Gulf of Guinea Cretaceous triple junction. Bull Geol Soc Am 82:2295–2298
Gray RF, Hoffmann VJ, Bagan RJ, McKinley HL (1968) Bishop tungsten district, California. In: Ridge JD (ed) Ore deposits of the United States, 1933–1967 New York Am Inst Min Metall Petrol Eng (Graton-Sales vol):1531–1554
Graybeal FT, Smith DM Jr (1988) Regional distribution of silver deposits on the Pacific Rim. Pacific Rim Congr 87. Gold Coast, Aust pp 404–411
Green AH, Naldrett AJ (1981) The Langmuir volcanic peridotite-associated nickel deposits: Canadian equivalents of the western Australian occurrences. Econ Geol 76:1503–1523
Green JC (1983) Geologic and geochemical evidence for the nature and development of the Precambrian Midcontinent Rift of North America. Tectonophysics 94:413–437
Grenne T, Grammeltvedt G, Vokes FM (1980) Cyprus-type sulfide deposits in the western Trondheim district, central Norwegian Caledonides. In: Panayiotou A (ed) Ophiolites. In: Int Ophiolite Symp, Cyprus 1979, pp 727–743
Gresens RL, Nisbet PC, Cool CA (1982) Alkali enrichment haloes and nickel depletion haloes around gold-bearing silica-carbonate veins in serpentinite, Washington State. In: Precious metals in the northern Cordillera. Assoc Explor Geochem Can 107–119
Griffin TJ (1983) Granitoids of the Tertiary continent-island arc collision zone, Papua New Guinea. Geol Soc Am Mem 159:61–76
Gross GA (1967) Geology of the iron deposits of Canada, vol 2. Geol Surv Can Econ Geol Rep 22:1–11
Groves DI, Barrett FM, McQueen KG (1979) The relative roles of magmatic segregation, volcanic exhalation and regional metamorphism in the generation of volcanic-associated nickel ores of western Australia. Can Mineral 17:319–336
Guber AL, Merrill S (1983) Paleobathymetric significance of the foraminifera from the Hokuroku district. Econ Geol Monogr 5:55–70
Guilbert JM (1981) A plate tectonic-lithotectonic classification of ore deposits. In: Dickinson WR, Payne WD (eds) Relations of tectonics to ore deposits in the southern Cordillera. AR Geol Soc Digest 14:1–10
Guilbert JM, Lowell JD (1974) Variations in zoning pattern in porphyry copper deposits. Can Inst Min Metall Bull 67(Feb):99–109
Guild PW (1974) Distribution of metallogenic provinces in relation to major earth structures. In: Petrascheck WE (ed) Metallogenetische und geochemische Provinzen. Springer, Berlin Wien, pp 10–24
Guild PW (1978) Metallogenesis in the western United States. J Geol Soc London 135:355–376
Gulson BL (1984) Uranium-lead and lead-lead investigations of minerals from the Broken Hill lodes and mine sequence rocks. Econ Geol 79:476–490
Gulson BL, Perkins WG, Mizon KJ (1983) Lead isotope studies bearing on the genesis of copper orebodies at Mount Isa, Queensland. Econ Geol 78:1466–1504

Gupta HK (1987) Deep seated processes in collision zones. Tecton Spec Issue 134:1–175
Gustafson LB, Hunt JP (1975) The porphyry copper deposit at El Salvador, Chile. Econ Geol 70:857–912
Gustafson LB, Williams N (1981) Sediment-hosted stratiform deposits of copper, lead and zinc. Econ Geol 75th Anniv Vol, pp 139–178
Guthrie JO, Cockle AR, Branham AD (1987) Geology of the American Girl – Padre y Madre gold deposits, Imperial County, California. Annu Meet, Denver, Feb 1987. Soc Min Eng Preprint
Haapala I (1977) The controls of tin and related mineralization in the rapakivi granite areas of south-eastern Fennoscandia. Geol Foren Stock Forh 99:130–142
Haapala I (1985) Metallogeny of the Proterozoic rapakivi granites of Finland. In: Taylor RP, Strong DF (eds) Granite-related mineral deposits. Can Inst Min Geol Div, pp 123–131
Hackett JP, Bischoff JL (1973) New data on the stratigraphy, extent and geologic history of the Red Sea geothermal deposits. Econ Geol 68:533–564
Hall WE, Mackevett EM, Jr. (1962) Geology and ore deposits of the Darwin quadrangle, Inyo County, California. US Geol Surv Prof Pap 368:1–87
Hallager WS (1984) Geology of gold-bearing metasediments near Jardine, Montana. In: Foster RP (ed) Gold '82: the geology, geochemistry and genesis of gold deposits. Balkema, Rotterdam, pp 191–218
Halls HC (1986) Paleomagnetism, structure and longitudinal correlation of Middle Precambrian dykes from northwestern Ontario and Minnesota. Can J Earth Sci 23:142–157
Halsall C, Sawkins FJ (1989) Magmatic-hydrothermal origin for fluids involved in generation of massive sulfide deposits at Rio Tinto, Spain. Ext Abst, Sixth Int Conf Water-Rock Interaction. Bath, England
Hamilton J (1977) Sr isotope and trace element studies of the Great Dyke and Bushveld mafic phase and their relation to early Proterozoic magma genesis in southern Africa. J Petrol 18:24–52
Hamilton JM, Bishop DT, Morris HC, Owens OE (1982) Geology of the Sullivan orebody, Kimberley, BC, Canada. Geol Assoc Can Spec Pap 25:597–665
Hamilton JM, Delaney GD, Hauser RL, Ransom PW (1983) Geology of the Sullivan deposit, Kimberley, BC, Canada. In: Sangster DF (ed) Sediment-hosted stratiform lead-zinc deposits. Min Assoc Can Short Course Handb 8:31–84
Hamilton JV, Hodgson CJ (1986) Mineralization and structure of the Kolar Gold Field, India. In: Macdonald AJ (ed) Proc Gold '86 Symp, Toronto, pp 270–283
Hamilton W (1970) The Uralides and the motion of the Russian and Siberian platforms. Bull Geol Soc Am 81:2553–2576
Hammond P (1952) Allard Lake ilmenite deposits. Econ Geol 47:634–649
Hannak WW (1981) Genesis of the Rammelsberg ore deposit near Goslar/Upper Harz, Federal Republic of Germany. Handbook of Strata-bound and stratiform ore deposits, vol 9. Elsevier, Amsterdam, pp 551–642
Hannington MD, Scott SD (1988) Mineralogy and geochemistry of a hydrothermal silica-sulfide-sulfate spire in the caldera of Axial Seamount, Juan de Fuca Ridge. Can Min 26:603–626
Hannington MD, Peter JM, Scott SD (1986) Gold in polymetallic seafloor sulfide deposits. Econ Geol 81:1867–1883
Hanor JS (1979) The sedimentary genesis of hydrothermal fluids. In: Barnes HL (ed) Geochemistry of hydrothermal ore deposits, 2nd edn. John Wiley & Sons, New York, pp 137–172
Hargraves RB (1962) Petrology of the Allard Lake anorthosite suite. Petrologic studies. Geol Soc Am (Buddington Vol) 163–190
Hargraves RB (1978) Punctuated evolution of tectonic style. Nature (London) 276:459–461
Harley DN (1979) A mineralized Ordovician resurgent caldera complex in the Bathurst-Newcastle mining district, New Brunswick, Canada. Econ Geol 74:786–796
Harmer RE, Sharpe MR (1985) Field relations and strontium isotope systematics of the marginal rocks of the eastern Bushveld Complex. Econ Geol 80:813–837
Harper GD (1980) The Josephine Ophiolite – remains of a late Jurassic marginal basin in northwestern California. Geology 8:333–337

Harper GD (1984) The Josephine ophiolite, northwestern California. Geol Soc Am Bull 95:1009–1026
Harper GD (1986) Dismembered Archean ophiolite in the southeastern Wind River mountains, Wyoming: remains of Archean oceanic crust. Lunar Planet Inst Tech Rep 86–10:108–115
Harris DC (1986) Mineralogy and geochemistry of the main Hemlo gold deposit, Hemlo, Ontario, Canada. In: Proc Gold 86 Symp, Toronto, pp 297–310
Harris JF (1961) Summary of the geology of Tanganyika, Part IV: economic geology. Geol Surv Tanganyika Mem 1:1–143
Harris LB (1987) A tectonic framework for the Western Australian Shield and its significance to gold mineralization: a personal view. Univ W Aust Publ 11:1–27
Harrison JE (1972) Precambrian Belt basin of northwestern United States. Geol Soc Am Bull 83:1215–1240
Harrison JE (1974) Copper mineralization in miogeosynclinal clastics of the Belt Supergroup, northwestern United States. In: Bartholome P (ed) Gisements stratiformes et provinces cuprifères. Soc Geol Belg, Leige, pp 353–366
Harrover RD, Norman DI, Savin SM, Sawkins FJ (1982) Stable oxygen isotope and crystallite size analysis of the De Long Mountain, Alaska cherts: an exploration tool for submarine exhalative deposits. Econ Geol 77:1761–1766
Hassan MA, Al-Sulaimi JS (1979) Copper mineralization in the northern part of Oman Mountains near Al Furaijah, United Arab Emirates. Econ Geol 74:919–924
Hastings JS (1987) Ore deposits of the Little Rocky Mountains, Montana. AIME 115th Annu Meet 1987, Denver, Preprint 87–22
Hatton CJ, Von Gruenewaldt G (1987) The geological setting and petrogenesis of the Bushveld chromitite layers. In: Stowe CW (ed) Evolution of the chromium ore fields. Van Nostrand Reinhold, New York, pp 109–143
Hattori K, Muehlenbachs K (1980) Marine hydrothermal alteration at a Kuroko ore deposit, Kosaka, Japan. Contrib Mineral Petrol 74:285–292
Hattori K, Sakai H (1979) D/H ratios, origins, and evolution of the ore-forming fluids for the Neogene veins and Kuroko deposits of Japan. Econ Geol 74:535–555
Haug JL (1976) Geology of the Merry Widow and Kingfisher contact metasomatic skarn-magnetite deposits, northern Vancouver Island, British Columbia. Ms Thesis, Univ Calgary, 174 pp
Hawkins JW (1980) Petrology of back-arc basins and island arcs: their possible role in the origin of ophiolites. In: Panayiotou A (ed) Ophiolites. Int Ophiolite Symp, Cyprus 1979, pp 224–254
Hayba DO (1987) Fluid-inclusion evidence for hydrologic and hydrothermal processes in the Creede mineralizing system, Colorado. Geol Soc Am Abstr with Prog 19:282
Hayba DO, Bethke PM, Heald P, Foley NK (1985) Geologic, mineralogic, and geochemical characteristics of volcanic-hosted epithermal precious-metal deposits. Rev Econ Geol 2:129–167
Haydon RC, McConachy GW (1987) The stratigraphic setting of Pb-Zn-Ag mineralization at Broken Hill. Econ Geol 82:826–856
Heald P, Foley NK, Hayba DO (1987) Comparative anatomy of volcanic-hosted epithermal deposits: acid-sulfate and adularia-sericite types. Econ Geol 82:1–27
Hearn BC, Donnelly-Nolan JM, Goff FE (1982) The Clear Lake volcanics: tectonic setting and magma sources. US Geol Surv Prof Pap 1141:25–46
Hearn PP, Jr, Sutter JF, Belkin HE (1987) Evidence for late Paleozoic brine migration in Cambrian carbonate rocks of the central and southern Appalachians: implication for Mississippi Valley-type sulfide mineralization. Geochim Cosmochim Acta 51:1323–1334
Heaton THE, Sheppard SMF (1977) Hydrogen and oxygen isotope evidence for seawater-hydrothermal alteration and ore deposits, Troodos complex, Cyprus. In: Volcanic processes in ore genesis. Geol Soc London Spec Publ 7:42–57
Hegge MR, Mosher DV, Eupene GS, Anthony PJ (1980) Geologic setting of the East Alligator uranium deposits and prospects. In: IAEA (ed) Uranium in the Pine Creek geosyncline. IAEA, Vienna, pp 259–272
Hekinian R, Fouquet Y (1985) Volcanism and metallogenesis of axial and off-axis structures on the East Pacific Rise near 13° N. Econ Geol 80:221–249

Hekinian R, Renard V, Cheminee JL (1983) Hydrothermal deposits on the East Pacific Rise near 13° N: geological setting and distribution of active sulfide chimneys. In: Rona PA, Bostrom K, Laubier L, Smith KL Jr (eds) Hydrothermal processes at seafloor spreading centers. Plenum, New York, pp 571–594

Helmstaedt H (1973) Structural geology of the Bathurst-New castle district. In: Rast N (ed) Field guide to excursions. N Engl Intercoll Geol Conf 1973, pp 34–43

Helmstaedt H, Padgham WA (1986) Stratigraphic and structural setting of gold-bearing shear zones in the Yellowknife greenstone belt. In: Clark LA (ed) Gold in the Western Shield. Can Inst Min Metall Spec Vol 38:322–346

Helmstaedt H, Padgham WA, Brophy JA (1986) Multiple dikes in the Lower Cam Group, Yellowknife greenstone belt: evidence for Archean seafloor spreading? Geology 14:562–566

Hemley JJ, Cygan GL, D' Angelo WM (1986) Effect of pressure on ore mineral solubilities under hydrothermal conditions. Geology 14: 377–379

Hendry DAF, Chivas AR, Long JVP, Reed SJB (1985) Chemical differences between minerals from mineralizing and barren intrusions from some North American porphyry copper deposits. Contrib Mineral Petrol 89:317–329

Henley RW (1985) The geothermal framework for epithermal systems. In: Geology and geochemistry of epithermal systems. Rev Econ Geol 2:1–24

Henley RW, Adams J (1979) On the evolution of giant gold placers. Inst Min Metall Trans 88:B41–B50

Henley RW, Ellis AJ (1983) Geothermal systems, ancient and modern. Earth Sci Rev 19:1–50

Henley RW, Hoffman CF (1987) Gold: sources to resources. Pac Rim Congr 87:159–168

Henley RW, McNabb A (1978) Magmatic vapor plumes and groundwater interaction in porphyry copper emplacement. Econ Geol 73:1–20

Henley RW, Thornley P (1981) Low grade metamorphism and the geothermal environment of massive sulfide ore formation, Buchans, Newfoundland. Geol Assoc Can Spec Pap 22:205–228

Henley RW, Norris RJ, Paterson CJ (1976) Multistage ore genesis in the New Zealand geosyncline; a history of post-metamorphic lode emplacement. Mineral Deposita 11:180–196

Hernon RM, Jones WR (1968) Ore deposits of the Central Mining district, New Mexico. In: Ridge JD (ed) New York Am Inst Min Metall Petrol Eng (Graton-Sales Vol):1211–1238

Hervig R, Dunbar NW, Westrich H, Kyle P (1986) Direct determination of initial H_2 and F contents of rhyolitic magmas by ion microprobe. Geol Soc Am Abstr with Prog, p 17

Herz N (1969) Anorthosite belts, continental drift, and the anorthosite event. Science 164:944–947

Herz N (1977) Timing of spreading in the South Atlantic: information from Brazilian alkalic rocks. Bull Geol Soc Am 88:101–112

Hess HH (1960) Stillwater igneous complex – a quantitative mineralogical study, Montana. Geol Soc Am Mem 80:1–230

Hewton RS (1982) Gayna River: a Proterozoic Mississippi Valley-type zinc-lead deposit. Geol Assoc Can Spec Pep 25:667–700

Heyl AV (1972) The 38th parallel lineament and its relationship to ore deposits. Econ Geol 67:879–894

Hiemstra SA (1985) The distribution of some platinum-group elements in the UG-2 chromitite layer of the Bushveld Complex. Econ Geol 80:944–957

Hilde TWC (1983) Sediment subduction versus accretion around the Pacific. Tectonophysics 99:381–397

Hillhouse JW (1977) Paleomagnetism of the Triassic Nikolai Greenstone, McCarthy Quadrangle, Alaska. Can J Earth Sci 14:2578–2592

Hitzman MW, Large D (1986) A review and classification of the Irish carbonate-hosted base metal deposits. In: Geology and genesis of mineral deposits in Ireland. Irish Assoc Econ Geol, Dublin, pp 217–238

Hitzman MW, Proffett JM, Jr., Schmidt JM, Smith TE (1986) Geology and mineralization of the Ambler district, northwestern Alaska. Econ Geol 81:1592–1618

Ho SE, Groves DI, Phillips GN (1985) Fluid inclusions as indicators of the nature and source of ore fluids and ore depositional conditions for Archean gold deposits of the Yilgarn block, western Australia. Geol Soc S Afr Trans 88:149–158

Hoagland AD (1976) Appalachian zinc-lead deposits. In: Wolf KH (ed) Handbook of stratabound and stratiform ore deposits, vol 6. Elsevier, New York, pp 495–534
Hochstein MP (1976) Estimation of geothermal resources, Taupo Volcanic Zone. In: 25th Int Geol Congr, Sydney, Excursion Guide 55A and 56C, pp 44–48
Hodgson CJ (1986) Place of gold ore formation in the geological development of Abitibi greenstone belt, Ontario, Canada. Inst Min Metall Trans 95:B185–B194
Hodgson CJ, Lydon JW (1977) Geological setting of volcanogenic massive sulfide deposits and active hydrothermal systems: some implications for exploration. Can Min Metall Bull 70:360–366
Hoeve J, Sibbald TII, Ramaekers P, Lewry JF (1980) Athabasca Basin unconformity-type uranium deposits: a special class of sandstone-type deposits. In: IAEA (ed) Uranium in the Pine Creek geosyncline. IAEA, Vienna, pp 575–594
Hoffman PE (1980) Wopmay Orogen: a Wilson cycle of early Proterozoic age in the northwest of the Canadian Shield. Geol Assoc Can Spec Pap 20:523–552
Hoffman PE (1988) United plates of America, the birth of a craton: early Proterozoic assembly and growth of Laurentia. Annu Rev Earth Planet Sci 16:543–603
Hohmann GW, Ward SH (1981) Electrical methods in mining geophysics. Econ Geol 75th Anniv Vol pp 806–828
Holl R (1977) Early Paleozoic ore deposits of the Sb-W-Hg formation in the eastern Alps and their genetic interpretation. In: Klemm DD, Schneider HJ (eds) Time- and strata-bound ore deposits. Springer, Berlin Heidelberg New York, pp 169–198
Holl R, Ivanova G, Grinenko V (1987) Sulfur isotope studies of the Felbertal scheelite deposit, eastern Alps. Mineral Deposita 22:301–308
Holland HD (1973) The oceans: a possible source of iron in iron-formations. Econ Geol 68:1169–1172
Hollister LS, Crawford ML (1986) Melt enhanced deformation: a major tectonic process. Geology 14:558–561
Hollister VF (1978) Geology of the porphyry copper deposits of the western hemisphere. AIME, New York, 219 pp
Hollister VF, Potter RR, Barker AL (1974) Porphyry-type deposits of the Appalachian orogen. Econ Geol 69:618–630
Horn DR, Horn BM, Delach MN (1973) Ocean manganese nodules, metal values and mining sites. Nat Sci Found, Washington, Tech Rep 4 Gx 33616, pp 1–57
Horton DJ (1978) Porphyry-type copper-molybdenum mineralization belts in eastern Queensland, Australia. Econ Geol 73:904–921
Horwitz RC, Smith RE (1976) Bridging the Yilgarn and Pilbara Blocks, western Australia Shield (Abstr). In: Int Geol Congr Abstr Vol, Sydney, p 12
Howard PF (1959) Structure and wallrock alteration at the Elizabeth Mine, Vermont. Econ Geol 54:1214–1249; and 1414–1443
Hoy T (1982a) The Purcell Supergroup in southeastern British Columia: sedimentation, tectonics and stratiform lead-zinc deposits. Geol Assoc Can Spec Pap 25:127–147
Hoy T (1982b) Stratigraphic and structural setting of stratabound lead-zinc deposits in southeastern B.C. Can Inst Min Bull 75/840:114–134
Hsü KJ, Shu S, Jiliang L, Haihong C, Haipo P, Sengor AMC (1988) Mesozoic ovethrust tectonics in South China. Geology 16:418–421
Hudson T (1983) Calc-alkaline plutonism along the Pacific rim of southern Alaska. In: Circum-pacific plutonic terranes. Geol Soc Am Mem 159:159–169
Hudson T, Plafker G, Peterman ZE (1979) Paleogene anatexis is along the Gulf of Alaska margin. Geology 7:573–577
Huebschman RP (1973) Correlation of fine carbonaceous bands across a Precambrian stagnant basin. J Sediment Petrol 43:688–699
Hughes MJ, Welke HJ, Allsopp HL (1984) Lead isotopic studies of some late Proterozoic stratabound ores of central Africa. Precambrian Res 25:137–139
Hugon H (1986) The Hemlo gold deposit, Ontario, Canada: a central portion of a large scale, wide zone of heterogeneous ductile shear. In: Macdonald AJ (ed) Proc Gold'86 Symp, Toronto pp 379–387

Huhtala T (1979) The geology and zinc-copper deposits of the Pyhasalmi-Pielavesi district, Finland. Econ Geol 74:1069–1083

Hulston J, Lupton JE, Rosenberg N (1986) Variations of $^{3}He/^{4}He$ isotope ratios within the Broadlands geothermal field, New Zealand. In: Proc 8th Geotherm Worksh, Univ Auckland Geotherm Inst, pp 13–16

Humphris SE, Thompson G (1978) Hydrothermal alteration of oceanic basalts by seawater. Geochim Cosmochim Acta 42:107–125

Hunter DR (1973) Localization of tin mineralization with reference to southern Africa. Minerals Sci Eng 5:53–77

Hunter DR (1976) Some enigmas of the Bushveld Complex. Econ Geol 71:229–248

Huot D, Sattran V, Zida P (1987) Gold in Birrimian greenstone belts of Burkina Faso, West Africa. Econ Geol 82:2033–2044

Huspeni JR, Kesler SE, Ruiz J, Tuta Z, Sutter JF, Jones LM (1984) Petrology and geochemistry of rhyolites associated with tin mineralization in northern Mexico. Econ Geol 79:87–105

Hutchinson CS (1983) Multiple Mesozoic Sn-W-Sb granitoids of southeast Asia. In: Circum-pacific plutonic terranes. Geol Soc Am Mem 159:35–60

Hutchinson CS, Taylor D (1978) Metallogenesis in South East Asia. J Geol Soc London 135:407–428

Hutchinson RW (1980) Massive base metal sulfide deposits as guides to tectonic evolution. Geol Assoc Can Spec Pap 20:659–684

Hutchinson RW (1987) Metallogeny of Precambrian gold deposits: space and time relationships. Econ Geol 82:1993–2007

Hutchinson RW, Burlington JL (1984) Some broad characteristics of greenstone belt gold lodes. In: Foster RP (ed) Gold '82: the geology, geochemistry and genesis of gold deposits. Balkema, Rotterdam, pp 339–372

Hynes A, Francis DM (1982) A transect of the early Proterozoic Cape Smith foldbelt, New Quebec. Tectonophysics 88:23–60

Ihlen PM, Vokes FM (1977) Metallogeny associated with the Oslo rifting: the Oslo Paleorift. Part 2: Guide to excursions NATO Adv Study Inst, Oslo, pp 147–174

Iijima A (1974) Clay and zeoloitic alteration zones surrounding Kuroko deposits in the Hokuroku District, northern Akita, as submarine hydrothermal-diagenetic alteration products. Min Geol Spec Issue 6:267–289

Imeokparia EG (1985) Mesozoic granite magmatism and tin mineralization in Nigeria. In: Taylor RP, Strong DF (eds) Granite-related mineral deposits. Can Inst Min Geol Div Halifax, Canada, pp 137–140

Ingersoll RV (1982) Triple-junction instability as cause for late Cenozoic extension and fragmentation of the western United States. Geology 10:621–624

Instituto Geologico y Minero de España (ed) (1982) Sintesis geologica de la Faja Piritica del SO de España. Mem Inst Geol Min Esp 98:1–106

Isherwood WF (1982) Geophysical overview of the Geysers. US Geol Surv Prof Pap 1141:83–95

Ishihara S (1977) The magnetite-series and ilmenite-series granitic rocks. Min Geol (Tokyo) 27:293–305

Ishihara S (1978) Metallogenesis in the Japanese island-arc system. J Geol Soc 135:389–406

Ishihara S (1981) The granitoid series and mineralization. Econ Geol 75th Anniv Vol, pp 458–484

Ishihara S, Sasaki A (1978) Sulfur in Kuroko deposits – a deep seated origin? Min Geol 28:361–367

Ishihara S, Sawata H, Shibata K, Terashima S, Arrykul S, Sato K (1980) Granites and Sn-W deposits of Peninsular Thailand. In: Granitic magmatism and related mineralization. Min Geol Spec Issue 8:223–241

Ito E, Harris DM, Anderson AT Jr (1983) Alteration of oceanic crust and geologic recycling of chlorine and water. Geochim Cosmochim Acta 47:1613–1624

Ixer RA, Alabaster T, Pearce JA (1984) Ore petrography and geochemistry of massive sulfide deposits within the Semail ophiolite, Oman. Inst Min Metall Trans 93:B107–125

Jackson ED (1969) Chemical variation in coexisting chromite and olivine in chromitite zones of the Stillwater Complex. Econ Geol Monogr 4:41–71

Jackson ED, Silver EA, Dalrymple GB (1972) Hawaiian-Emperor chain and its relation to Cenozoic circum-Pacific tectonics. Geol Soc Am Bull 38:601–618
Jackson GD, Ianelli TR (1981) Rift-related cyclic sedimentation in the Neohelikian Borden Basin, northern Baffin Island. In: Proterozoic basins of Canada. Geol Surv Can Pap 81–10:269–302
Jacobsen JBE, McCarthy TS (1976) An unusual hydrothermal copper deposit of Messina, South Africa. Econ Geol 71:117–130
Jacobsen JBE, McCarthy TS, Laing CJ (1976) The copper-bearing breccia pipes of the Messina district, South Africa. Mineral Deposita 11:33–45
Jacobson RRE, MacLeon WN, Black R (1958) Ring complexes in the younger Granite Province of northern Nigeria. Mem Geol Soc London 1:1–72
Janecky DR, Seyfried WE Jr (1984) Formation of massive sulfide deposits on oceanic ridge crest: incremental reaction models for mixing between hydrothermal solutions and seawater. Geochim Cosmochim Acta 48:2723–2738
Jankovic S (1980) Porphyry-copper and massive-sulfide ore deposits in the northeastern Mediterannean. In: Ridge JD (ed) Proc 5th IAGOD Symp Snowbird, Utah, pp 431–444
Jankovic S, Putnik S (1980) Copper deposits in southeastern Europe connected with the ophiolite complexes. In: Jankovic S, Sillitoe RH (eds) European copper deposits. Spec Publ SGA 1:117–123
Jardine DE (1966) An investigation of brecciation associated with the Sullivan mine orebody of Kimberley, BC. M Sc Thesis, Univ Manitoba, 121 pp
Jarrard RD (1986) Relations among subduction parameters. Rev Geophys 24:217–284
Jensen A (1982) The distribution of Cu across three basaltic lava flows from the Faeroe Islands. Bull Geol Soc Denm 31:1–10
John TU (1963) Geology and mineral deposits of east-central Balabac Island, Palawan Province, Philippines. Econ Geol 58:107–130
John YW (1978) Sangdong mine, Korea. In: Imai H (ed) Geological studies of the mineral deposits of Japan and East Asia. Univ Press, Tokyo, pp 196–200
Johnson IR, Klingner GD (1975) Broken Hill ore deposit and its environment. In: Knight CL (ed) Economic geology of Australia and Papua New Guinea I. Metals. Australas Inst Min Metall Monogr 5:476–491
Johnson WP, Lowell JD (1961) Geology and origin of mineralized breccia pipes in Copper Basin, Arizona. Econ Geol 56:916–940
Johnston WD, Jr. (1940) The gold-quartz veins of Grass Valley, California. US Geol Surv Prof Pap 194:101 pp
Jones DL, Silbering NJ, Hillhouse JW (1977) Wrangellia – a displaced terrane in northwestern North America. Can J Earth Sci 14:2565–2577
Jones JP, Yamada EH, Marques CGM, Yokoi OY, Yamamoto MF (1986) Some aspects of the geology of the newly discovered tin deposits of Brazil. Mining Latin America/Mineria Latinoamerica. Inst Min Metall, London, pp 165–182
Jones MT, Reed BL, Doe BR, Lanphere MA (1977) Age of tin mineralization and plumbotectonics, Belitung, Indonesia. Econ Geol 72:745–752
Jones WR, Peoples JW, Howland AL (1960) Igneous and tectonic structures of the Stillwater Complex, Montana. US Geol Surv Bull 1071-H:281–340
Jowett EC (1986) Genesis of Kupferschiefer Cu-Ag deposits by convective flow of Rotliegende brines during Triassic rifting. Econ Geol 81:1823–1837
Jowett EC (1987) Formation of sulfide-calcite veinlets in the Kupferschiefer Cu-Ag deposits in Poland by natural hydrofracturing during basin subsidence. J Geol 95:513–526
Jowett EC, Jarvis GT (1984) Formation of foreland rifts. Sediment Geol 40:51–72
Jowett EC, Rydzewski A, Jowett RJ (1987a) The Kupferschiefer Cu-Ag ore deposits in Poland: a re-appraisal of the evidence of their origin and presentation of a new genetic model. Can J Earth Sci 24:2016–2037
Jowett EC, Pearce GW, Rydzewski A (1987b) A mid-Triassic paleomagnetic age of the Kupferschiefer mineralization in Poland, based on a revised apparent polar wander path for Europe and Russia. J Geophys Res 92:581–598
Kamilli RJ (1978) The genesis of stockwork molybdenite deposits: implications from studies at the Henderson Mine (Abstr). Geol Soc Am Abstr with Prog 10:431

Kamilli RJ, Ohmoto H (1977) Paragenesis, zoning, fluid inclusion, and isotopic studies of the Finlandia Vein, Colqui District, Central Peru. Econ Geol 71:950–982
Kanasewich ER (1968) Precambrian rift: genesis of stratabound ore deposits. Science 161:1002–1005
Kanehira K, Tatsumi T (1970) Bedded cupriferous deposits in Japan, a review. In: Tatsumi T (ed) Volcanism and ore genesis. Univ Press, Tokyo, pp 51–76
Karig DE (1971) Origin and development of marginal basins in the western Pacific. J Geophys Res 76:2542–2561
Karig DE (1983) Accreted terranes in the northern part of the Philippine archipelago. Tectonics 2:211–236
Karson J, Dewey JF (1978) Coastal Complex, western Newfoundland: an early Ordovician oceanic fracture zone. Geol Soc Am Bull 89:1037–1049
Karson JA (1984) Variations in structure and petrology in the Coastal Complex, Newfoundland: anatomy of an oceanic fracture zone. In: Gass IG, Lippard SJ, Shelton AW (eds) Ophiolites and oceanic lithosphere. Geol Soc, Blackwell, Oxford, pp 131–146
Karson JA, Elthon D (1987) Evidence for variations in magma production along oceanic spreading centers: a critical appraisal. Geology 15:127–131
Karvinen WO (1981) Geology and evolution of gold deposits, Timmins area, Ontario. In: Pye EG, Roberts RG (eds) Genesis of Archean, volcanic hosted gold deposits. Ontario Geol Surv Misc Pap 97:29–46
Kasch KW (1979) A continental collision model for the tectonothermal evolution of the (southern) Damara belt. Precambrian Res Unit Univ Cape Town Annu Rep 16:101–107
Keen CE, Stock GS, Welsink H, Quinlan G, Mudford B (1987) Deep crustal structure and evolution of the rifted margin northeast of Newfoundland: results from LITHOPROBE East. Can J Earth Sci 24:1537–1549
Keith SB (1978) Paleosubduction geometries inferred from Cretaceous and Tertiary magmatic patterns in southwestern North America. Geology 6:516–521
Keith SB, Swan MM (1987) Oxidation state of magma series in the southwestern US: implications for geographic distribution of base, precious, and lithophile metal metallogeny (Abstr). Geol Soc Am Annu Meet Prog, Phoenix, AR, pp 723–724
Kelley DS, Delaney JR (1987) Two-phase separation and fracturing in mid-ocean ridge gabbros at temperatures greater than 700°C. Earth Planet Sci Lett 83:53–66
Kelly WC, Goddard EN (1969) Telluride ores of Boulder County, Colorado. Geol Soc Am Mem 109:1–237
Kelly WC, Rye RO (1979) Geologic, fluid inclusion and stable isotope studies of the tin-tungsten deposits of Panasquiera, Portugal. Econ Ecol 74:1721–1822
Kelly WC, Turneaure FS (1970) Mineralogy, paragenesis and geothermometry of the tin and tungsten deposits of the eastern Andes, Bolivia. Econ Geol 65:609–680
Kelsey GL, Glavinovich PS, Sheridan MF (1980) High-potassium metarhyolites associated with volcanogenic sulfides, Ambler district, northwest Alaska. Geol Soc Am Abstr with Prog 12:114
Kerr JW (1977) Cornwallis lead-zinc district, Mississippi Valley-type deposits controlled by stratigraphy and tectonics. Can J Earth Sci 14:1402–1426
Kerrich R (1983) Geochemistry of gold deposits in the Abitibi greenstone belt. Can Inst Min Metall Spec Vol 27:1–75
Kerrich R (1986) Fluid transport in lineaments. Philos Trans R Soc London Ser A 317:219–252
Kerrick DM (1970) Contact metamorphism in some areas of the Sierra Nevada. Geol Soc Am Bull 81:2913–2938
Kesler SE (1973) Copper, molybdenum and gold abundances in porphyry-copper deposits. Econ Geol 68:106–113
Kesler SE (1977) Geochemistry of manto fluorite deposits, northern Coahuila, Mexico. Econ Geol 72:204–218
Kesler SE (1978) Metallogenesis of the Caribbean region. J Geol Soc London 135:429–441
Kesler SE, Jones LM, Ruiz J (1988) Strontium isotopic geochemistry of Mississippi Valley-type deposits, east Tennessee: implications for age and source of mineralizing brines. Geol Soc Am Bull 100:1300–1307

Kiltin DA, Pavlova TG (1974) Ophiolite complex of the Baikal fold zone. Dokl Akad Nauk SSR 215:413–416 (p 33–36 in translation)
Kimbach FW, Cruson MG, Brooks RA (1981) Geology of stockwork gold deposits as exemplified by the Cinola deposit. Col Min Assoc 1981 Mining Yearb, pp 122–129
Kindle ED (1972) Classification and description of copper deposits, Coppermine River area, District of Mackenzie. Geol Surv Can Bull 214:1–109
Kinkel AR, Jr., Hall WE, Albers JP (1956) Geology and base-metal deposits of west Shasta copper-zinc district, Shasta County, California. US Geol Surv Prof Pap 285:1–156
Kinneard JA (1985) Hydrothermal alteration and mineralization of the alkaline anorogenic ring complexes of Nigeria. J Afr Earth Sci 3:229–251
Kirby GA (1979) The Lizard Complex as an ophiolite. Nature (London) 282:58–61
Kirchner G, Lehnert-Thiel K, Rich J, Strand JG (1980) The Key Lake U-Ni deposit: a model for lower Proterozoic uranium deposition. In: IAEA (ed) Proc Int Uranium Symp Pine Creek geosyncline. IAEA, Vienna, pp 617–629
Kirkham RV (1972) Geology of copper and molybdenum deposits. Can Geol Surv Pap 72-1A:82–87
Kirkham RV (1987) Tectonic setting of the Buchans Group. In: Kirkham RV (ed) Buchans geology, Newfoundland. Geol Surv Can Pap 86-24:23–34
Kirkham RV, Thurlow JG (1987) Evaluation of a resurgent caldera and aspects of ore deposition and deformation at Buchans. In: Kirkham RV (ed) Buchans geology, Newfoundland. Geol Surv Can Pap 86-24:177–196
Kissin SA (1988) Nickel-cobalt-native silver (five element) veins: a rift-related ore type. In: Kisvarsanyi G, Grant SK (eds) North American conference on tectonic control of ore deposits. Proc Vol Univ Missouri Rolla, Missouri, pp 268–279
Kisvarsanyi EB (1980) Granitic ring complexes and Precambrian hot-spot activity in the St. Francois terrane, midcontinent region, United States. Geology 8:43–47
Kisvarsanyi G (1977) The role of Precambrian igneous basement in the formation of the stratabound lead-zinc-copper deposits in southeast Missouri. Econ Geol 72:435–442
Kisvarsanyi G, Grant SK, Pratt WP, Koenig JW (eds) (1983) Proc Int Conf Mississippi Valley-type lead-zinc deposits, Univ Missouri, Rolla, 603 pp
Klemd R, Maiden KJ, Okrusch M (1987) The Matchless copper deposit, South West Africa/Namibia; a deformed and metamorphosed massive sulfide deposit. Econ Geol 82:587–599
Kloosterman JB (1969) A two-fold analogy between the Nigerian and Amazonian tin provinces. In: Fox W (ed) 2nd Conf Tin, vol 2, Bangkok, Intnl Tin Council London, pp 197–222
Knopf A (1929) The Mother Lode system of California. US Geol Surv Prof Pap 157:103 pp
Knutson J, Ferguson J, Roberts WMB, Donnelly HT, Lambert IB (1979) Petrogenesis of the copper bearing breccia pipes Redbank, Northern Territory, Australia. Econ Geol 74:814–826
Koeppel V (1980) Lead isotope studies of stratiform ore deposits of the Namaqualand, NW Cape Province, South Africa, and their implications on the age of the Bushmanland sequence. In: 5th IAGOD Symp, Utah, pp 195–208
Konstantynowicz E (1973) Genesis of Permian copper deposits in Poland. Int Geol Rev 15:1054–1066
Kooiman GJA, McLeod MJ, Sinclair WD (1986) Porphyry tungsten-molybdenum orebodies, polymetallic veins and replacement bodies, and tin-bearing greisen zones in the Fire Tower Zone, Mount Pleasant, New Brunswick. Econ Geol 81:1356–1373
Korneliussen A, Robins B (1985) Titaniferous magnetite, ilmenite and rutile deposits in Norway. Norges Geol Unders Bull 402 98 pp
Koski RA (1987) Sulfide deposits on the sea floor: geological models and resource perspectives based on studies in ophiolite sequences. In: Teleki PG, Dobson MP, Moore JR, von Stackelberg U (eds) Marine minerals. Reidel, Dordrecht, pp 301–316
Kovalenko VA, Glaskyshev GD, Nosik LP (1975) Isotopic composition of sulfide sulfur from deposits of Talnakh ore node in relation to their selenium content. Int Geol Rev 17:725–736
Kovalev AA, Karyakin YuV (1980) Volcanism, subvolcanic processes and ore deposits of the Caucasian collision orogen. In: 5th IAGOD Symp, Utah, pp 313–324

Kowalik J, Rye RO, Sawkins FJ (1981) Stable isotope study of the Buchans polymetallic sulphide deposits. Geol Assoc Can Spec Pap 22:229–254

Kratz K, Mitrofanov F (1980) Main type reference sequences of the early Precambrian in the USSR. Earth Sci Rev 16:295–301

Kravchenco GG (1986) Factors that affect the distribution of chromite deposits in folded belts. In: Gallagher MJ, Ixer RA, Neary CR, Prichard HM (eds) Metallogeny of basic and ultrabasic rocks. Inst Min Metall London, pp 355–360

Krebs W (1981) The geology of the Meggen ore deposit. Handbook of strata-bound and stratiform ore deposits, vol 9. Elsevier, Amsterdam, pp 509–550

Krebs W, Gwosdz W (1985) Ore-controlling parameters of Devonian stratiform lead-zinc-barite ore in central Europe. Geol Jahrb D70:9–36

Kreczmer MJ (1977) The geology and geochemistry of the Fortuna mineralization, Fresnillo, Zacatecas, Mexico. MSc Thesis, Univ Toronto 115 pp

Krogh TE, Davis GL (1971) Zircon U-Pb ages of Archean metavolcanics rocks in the Canadian Shield. Carnegie Inst Washington Yearb 70:241–242

Krogh TE, Davis DW, Corfu F (1984) Precise U-Pb zircon and baddeleyite ages for the Sudbury area. In: The geology and ore deposits of the Sudbury Structure. Ontario Geol Surv Spec Vol 1:431–447

Kroner A (1977a) Precambrian mobile belts of southern and eastern Africa – ancient sutures or sites of ensialic mobility? A case for crustal evolution towards plate tectonics. Tectonophysics 40:101–135

Kroner A (1977b) The Precambrian geotectonic evolution of Africa: plate accretion versus plate destruction. Precambrian Res 4:163–213

Kroner A (1980) Pan African crustal evolution. Episodes. Int Un Geol Sci 2:3–8

Kroner A (ed) (1987) Proterozoic lithospheric evolution. Geodyn Ser 17:273 pp

Kroner A, Correia H (1980) Continuation of the Pan African Damara belt into Angola: a proposed correlation of the Chela Group in southern Angola with the Nosib Group in northern Namibia/S.W.A. Geol Soc S Afr Trans 83:5–16

Krupp RE, Seward TM (1987) The Rotokawa geothermal system, New Zealand: an active epithermal gold-depositing environment. Econ Geol 82:1109–1129

Kuehn CA, Rose AW (1986) Temporal framework for the evolution of fluids at the Carlin gold mine, Eureka County, Nevada. Geol Soc Am Abstr with Prog 18:663

Kuhn TH (1941) Pipe deposits of the Copper Creek area, Arizona. Econ Geol 36:512–538

Kuhns RJ (1986) Alteration styles and trace element dispersion associated with the Golden Giant deposit, Hemlo, Ontario, Canada. In: Proc Gold '86 Symp, Toronto, pp 340–354

Kuhns RJ (1988) The Golden Giant deposit, Hemlo, Ontario: geologic, and geochemical relationships between mineralization, alteration, metamorphism, magmatism and tectonism. PhD Thesis, Univ Minnesota 381 pp

Kuhns RJ, Baitis HW (1987) Preliminary study of the Turner Albright Zn-Cu-Ag-Au-Co massive silfide deposit, Josephine county, Oregon. Econ Geol 82:1362–1376

Kuhns RJ, Kennedy P, Cooper P, Brown P, Mackie B, Kusins R, Friessen R (1986) Geology and mineralization associated with the Golden Giant deposit, Hemlo, Ontario, Canada. In: Proc Gold '86 Symp, Toronto, pp 327–339

Kuran VM, Godwin CI, Armstrong RL (1982) Geology and geochemistry of the Scheelite Dome tungsten-bearing skarn property, Yukon Territory. Can Inst Min Bull 75:137–142

Kuroda Y, Suzuoki T, Matsuo S (1983) Hydrogen isotope study of Japanese granitic rocks. In: Circum-Pacific plutonic terranes. Geol Soc Am Mem 159:123–128

Kurtz RD, DeLaurier JM, Gupta JC (1986) A magnetotelluric sounding across Vancouver Island detects the subducting Juan de Fuca plate. Nature 321:596–599

Kutina J (1980) Regularities in the distribution of ore deposits along the Mendocino Latitude, western United States. Global Tecton Metall 1:134–193

Kwak TAP (1978) The conditions of formation of the King Island scheelite contact skarn, King Island, Tasmania, Australia. Am J Sci 278:969–999

Kwak TAP (1987) W-Sn skarn deposits. Developments in economic geology, vol 24. Elsevier, Amsterdam, 451 pp

Kwak TAP, Tan TH (1981) The geochemistry of zoning of skarn minerals at the King Island (Dolphin) mine. Econ Geol 76:468–497
Kyle RJ (1976) Brecciation, alteration, and mineralization in the central Tennessee zinc district. Econ Geol 71:892–903
Kyle RJ (1981) Geology of the Pine Point lead-zinc district. In: Wolfe KH (ed) Handbook of stratabound and stratiform ore deposits, vol 9. Elsevier, Amsterdam, pp 643–741
Kyle RJ, Price PE (1986) Metallic sulfide mineralization in salt-dome cap rocks, Gulf Coast, U.S.A. Trans Inst Min Metall 95:B6–B16
Lago BL, Robinowicz M, Nicolas A (1982) Podiform chromite orebodies: a genetic model. J Petrol 23:103–125
Laing WP, Marjoribanks RW, Rutland RWR (1978) Structure of the Broken Hill mine area and its significance for the genesis of the orebodies. Econ Geol 73:1112–1136
Laing WP, Sun SS, Nesbitt RW (1984) Acid volcanic precursor to Potosi gneiss at Broken Hill and its implication for ore genesis. In: Geol Soc Aust, 7th Aust Geol Congr Abstr, pp 318–321
Lambe RN, Rowe RG (1987) Volcanic history, mineralization, and alteration of the Crandon massive sulfide deposit, Wisconsin. Econ Geol 82:1192–1203
Lambert IB, Sato T (1974) The Kuruko and associated ore deposits of Japan: a review of their features and metallogenesis. Econ Geol 69:1215–1236
Lambert IB, Knutson J, Donnelly TH, Etminan H (1986) The diverse styles of sediment-hosted copper deposits in Australia. In: Friedrich GH, Genkin AD, Naldrett AJ, Ridge JD, Sillitoe RH, Vokes FM (eds) The geology and metallogeny of copper deposits. Springer, Berlin Heidelberg New York Tokyo, pp 540–558
Lambert IB, Knutson J, Donnelly TH, Etminan H (1987) Stuart shelf-Adelaide geosyncline copper province, South Australia. Econ Geol 82:108–123
Landis GP, Rye RO (1974) Geologic, fluid inclusion and stable isotope studies of the Pasto Bueno tungsten-base metal ore deposit, northern Peru. Econ Geol 69:1025–1037
Lang B (1979) The base metals-gold hydrothermal ore deposits of Baia Mare, Romania. Econ Geol 74:1336–1351
Lang B, Steinitz G, Sawkins FJ, Simmons SF (1988) K-Ar dating studies in the Fresnillo silver district. Econ Geol 83:1642–46
Lange IM, Nokleberg WJ, Plahuta JT, Krouse HR, Doe BR, Jansons U (1980) Isotopic geochemistry of stratiform zinc-lead-barium deposits, Red Dog Creek and Drenchwater Creek areas, northwestern Brooks Range, Alaska. US Geol Surv Open File Rep 81–355:1–16
Large DE (1980) Geological parameters associated with sediment-hosted, submarine exhalative Pb-Zn deposits: an empirical model for mineral exploration. Geol Jahrb 40:59–129
Large DE (1983) Sediment-hosted massive sulfide lead-zinc deposits: an empirical model. In: Sangster DF (ed) Sediment-hosted stratiform lead-zinc deposit. Mineral Assoc Can Short Course Handb, pp 1–29
Large RR (1977) Chemical evolution and zonation of massive sulfide deposit in volcanic terrains. Econ Geol 72:549–572
Large RR, Huston D, McGoldrick P (1987a) Gold concentration in eastern Australian volcanic-hosted massive sulfide ores (Abstr). Geol Soc Am Annu Meet, Phoenix, AR, Abstr with Prog:740
Large RR, Herrmann W Corbett KD (1987b) Base metal exploration of the Mount Read Volcanics, western Tasmania, Part I: Geology and exploration, Ellitt Bay. Econ Geol 82:267–290
Larue DK, Sloss LL (1980) Early Proterozoic sedimentary basins of the Lake Superior region: summary. Geol Soc Am Bull 91:450–452
Latvalahti U (1979) Cu-Zn-Pb ores in the Aijala-Orijarvi area, southwest Finland. Econ Geol 74:1035–1059
Laurent A (1980) Environment of formation, evolution and emplacement of the Appalachian ophiolites of Quebec. In: Panayiotou A (ed) Ophiolites. Int Ophiolite Symp Proc, Cyprus 1979, pp 628–636
Laznicka P (1973) Development of nonferrous metal deposits in geological time. Can J Earth Sci 10:18–25

Laznicka P (1976) Porphyry copper and molybdenum deposits of the U.S.S.R. and their plate tectonic settings. Trans Inst Min Metall 85:B14–32
Lea ER, Dill DB (1968) Zinc deposits of the Balmat-Edwards district. AIME, New York, Graton-Sales Vol (1):20–48
Leach DL, Rowan EL (1986) Genetic link between Ouachita foldbelt tectonism and Mississippi Valley-type lead-zinc deposits of the Ozarks. Geology 14:931–935
Leake BE, Farrow CM, Townend RA (1979) A pre-2000 m yr old granulite facies metamorphosed evaporite from Caraiba, Brazil? Nature (London) 277:49–50
LeBas MJ (1977) Carbonatite-nephelinite volcanism. John Wiley & Sons, New York London, pp 1–347
Lebedev LM (1972) Minerals of contemporary hydrotherms of Cheleken. Geochem Int 9:485–504
Leblanc M (1976) Oceanic crust at Bou Azzer. Nature (London) 261:34–35
Leblanc M (1981) The late Proterozoic ophiolites of Bou Azzer (Morocco): evidence for Pan-African plate tectonics. In: Kroner A (ed) Precambrian plate tectonics. Elsevier, Amsterdam, pp 435–451
Leblanc M (1987) Chromite in oceanic arc environments: New Caledonia. In: Stowe CW (ed) Evolution of the chromium ore fields. Van Nostrand Reinhold, New York, pp 265–296
Leblanc M, Billaud P (1982) Cobalt arsenide orebodies related to an Upper Proterozoic ophiolite: Bou Azzer (Morocco). Econ Geol 77:162–175
Lee MS (1986) Tungsten deposits of the Korean Peninsula. In: Bues AA (ed) Int Geol Correl Prog Proj 26:167–186
Lee WHK (1967) Thermal history of the earth. PhD Thesis, Univ Cal, Los Angeles
Leeder MR (1987) Tectonic and paleogeographic models for Lower Carboniferous Europe. In: Miller J, Adams AR, Wright VP (eds) European Dinantian environments. John Wiley & Sons, New York, pp 1–20
Leeman WP (1983) Tectonic and magmatic significance of strontium isotopic variations in Cenozoic volcanic rocks from the western United States. Geol Soc Am Bull 93:487–503
Leeman WP, Hawkesworth CJ (1986) Open magma systems: trace element and isotopic constraints. J Geophy's Res 91:5901–5912
Lee-Moreno JL (1980) The metallogenic tin province of Mexico. In: Metallogensis in Latin America. Prog with Abstr, Mexico City Int Symp, p 8
Lehmann E (1972) On the source of the iron in the Lahn ore deposits. Mineral Deposita 7:247–270
Lehrman NJ (1988) Geology and geochemistry of the McLaughlin hot-spring precious metal deposit, California coast ranges (Abstr). In: Schafer RW, Cooper JJ, Vikre PG (eds) Bulk mineable precious metal deposits of the western United States. Geol Soc Nev, Reno, p 732
LeHuray AP (1984) Lead and sulfur isotopes and a model for the origin of the Ducktown deposit, Tennessee. Econ Geol 79:1561–1573
LeHuray AP, Caulfield JBD, Rye DM, Dixon PR (1987) Basement controls on sediment-hosted lead-zinc deposits; a Pb isotope study of Carboniferous mineralization in central Ireland. Econ Geol 82:1695–1709
Leitch CHB (1981) Mineralogy and textures of the Lahanos and Kizilkaya massive sulfide deposits, northeastern Turkey, and their similarity to Kuroko ores. Mineral Deposita 16:241–257
Lenthall DH (1974) Tin production from the Bushveld Complex. Inf Circ 93 Econ Geol Res Unit, Univ Witwatersrand, pp 1–15
Le Pichon X (1968) Seafloor spreading and continental drift. J Geophys Res 73:3661–3697
Leroy J (1978) The Margnac and Fanay uranium deposits of the La Crouzille District (Western Massif Central, France): geologic and fluid inclusion studies. Econ Geol 73:1611–1634
Lesher CM, Goodwin AM, Campbell IH, Gorton MP (1986) Trace element of ore-associated and barren, felsic metavolcanic rocks in the Superior Province, Canada. Can J Earth Sci 23:222–241
Lewis BR (1965) Gold deposit of Hill 50 mine. In: McAndrew J (ed) Geology of Australian ore deposits. 8th Commonwealth Min Metall Congr Melbourne, pp 98–100
Licence PS, Terrill JE, Fergusson LJ (1987) Epithermal gold mineralization, Ambitle Island, Papua New Guinea. Pac Rim Congr 87:273–278

Lindblom S (1986) Textural and fluid inclusion evidence for ore deposition in the Pb-Zn deposit at Laisvall, Sweden. Econ Geol 81:46–64
Lindgren W (1933) Mineral deposits. McGraw-Hill, New York
Lindgren W, Ross CP (1916) The iron deposits of Daiquiri, Cuba. Am Inst Min Eng Trans 53:40–66
Lindsey DA (1977) Epithermal beryllium deposits in water-laid tuff, western Utah. Econ Geol 72:219–232
Lipman PW (1980) Cenozoic volcanism in the western United States: implication for continental tectonics. In: Geophysics: continental tectonics. Natl Acad Sci, Washington, pp 161–174
Lipman PW, Steven TA, Mehnert HH (1970) Volcanic history of the San Juan Mountains, Colorado, as indicated by potassium-argon dating. Geol Soc Am Bull 81:2329–2352
Lipman PW, Fisher FS, Mehnert HH, Naeser CW, Luedke RG, Steven TA (1976) Multiple ages of mid-Tertiary mineralization and alteration in the western San Juan Mountains, Colorado. Econ Geol 71:571–588
Lipman PW, Doe BR, Hedge CE, Steven TA (1978) Petrologic evolution of the San Juan volcanic field, southwestern Colorado: lead and strontium evidence. Geol Soc Am Bull 89:59–82
Lippard SJ, Shelton AW, Gass IG (1986) The ophiolite of northern Oman. Geol Soc Mem 11. Blackwell, Oxford, 178 pp
Lister CRB (1972) On the thermal balance of an oceanic ridge. Geophys J R Astron Soc 26:515–535
Lister CRB (1980) Heat flow and hydrothermal circulation. Annu Rev Earth Planet Sci 8:95–117
Lister CRB (1983) The basic physics of water penetration into hot rock. In: Rona PA, Bostrom K, Laubier L, Smith KL Jr (eds) Hydrothermal processes at seafloor spreading centers. Plenum, New York, pp 141–168
Lister GS, Etheridge MA, Symonds PA (1986) Detachment faulting and the evolution of passive continental margins. Geology 14:246–250
Livaccari RF (1979) Reply on Late Cenozoic tectonic evolution of western United States. Geology 7:371–373
Ljundgren P, Meyer HC (1964) The copper mineralization in the Corocoro Basin, Bolivia. Econ Geol 59:110–125
Locke A (1926) The formation of certain orebodies by mineralization stoping. Econ Geol 21:431–453
Lombaard AF, Schreuder FJG (1978) Distribution pattern and general geological features of steep structures, megabreccias and basic rocks in the Okiep copper district. In: Verwoerd WJ (ed) Mineralization in metamorphic terrains. Geol Soc S Afr Spec Publ 4:269–296
Lombaard AF, Gunzel A, Innes J, Kruger TL (1986) The Tsumeb lead-copper-zinc-silver deposit, South West Africa/Namibia. In: Anhaeusser CR, Maske S (eds) Mineral deposits in southern Africa. Geol Soc S Afr 11:1761–1787
Lonsdale PF, Bischoff JL, Burns VM, Kastner M, Sweeney RE (1980) A high-temperature hydrothermal deposit on the seabed at a Gulf of California spreading center. Earth Planet Sci Lett 49:8–20
Lonsdale PF, Batiza R, Simkin T (1982) Metallogensis at seamounts on the East Pacific Rise. Mar Technol Soc J 16:54–61
Lorenz V, Nicholls IA (1976) The Permocarboniferous Basin and Range Province of Europe. An application of plate tectonics. In: Falke H (ed) The continental Permian in central, west, and south Europe. Reidel, Dordrecht, pp 313–342
Lorinczi GI, Miranda JC (1978) Geology of the massive sulfide deposits of Campo Morado, Guerrero, Mexico, Econ Geol 73:180–191
Lortie RB, Clark AH (1987) Strata-bound cupriferous sulfide mineralization associated with continental rhyolitic volcanic rocks, northern Chile, I: the Jardin copper-silver deposit. Econ Geol 82:546–570
Loudon AG, Lee MK, Dowling JF, Bourn R (1975) Lady Loretta silver-lead-zinc deposit. In: Economic geology of Australia and Papua New Guinea. Australas Min Metal Monogr 5:377–382
Lovering TS, Tweto O, Lovering TG (1978) Ore deposits of the Gilman district, Eagle County, Colorado. US Geol Surv Prof Pap 1017:1–90

Lowell GR (1976) Tin mineralization and mantle hotspot activity in southeastern Missouri. Nature (London) 261:482–483

Lowell JD, Guilbert JM (1970) Lateral and vertical alteration-mineralization zoning in porphyry ore deposits. Econ Geol 65:373–408

Lowell RP, Rona PA (1985) Hydrothermal models for the generation of massive sulfide ore deposits. J Geophys Res 90:8769–8783

Luff WM (1977) Geology of Brunswick 12: mine. Can Inst Min Bull 70–782:109–119

Luhr JF, Carmichael ISE, Varekamp JC (1984) The 1982 eruptions of El Chicon volcano, Chiapas, Mexico: mineralogy and petrology of the anhydrite-bearing pumices. J Volcan Geotherm Res 23:69–108

Lupton JE, Weiss RF, Craig HC (1977) Mantle helium in the Red Sea brines. Nature (London) 266:244–246

Lusk J (1972) Examination of volcanic-exhalative and biogenic origins of sulfur in the stratiform massive sulfide deposits in New Brunswick. Econ Geol 67:169–183

Lusk J, Crocket JH (1969) Sulfur isotope fractionation in coexisting sulfides from the Heath Steele B-1 orebody, New Brunswick, Canada. Econ Geol 64:147–155

Lydon JW (1983) Chemical parameters controlling the origin and deposition of sediment-hosted stratiform lead-zinc deposits. In: Sangster DF (ed) Sediment-hosted stratiform lead-zinc deposits. Min Assoc Can Short Course Handb 8:175–250

Lydon JW (1986) Models for the generation of metalliferous hydrothermal systems within sedimentary rocks, and their applicability to the Irish Carboniferous Zn-Pb deposits. In: Andrew CJ, Crowe RWA, Finlay S, Pennell WM, Pyne JF (eds) Geology and genesis of mineral deposits in Ireland. Irish Assoc Econom Geol, pp 555–578

Lydon JW (1988) Ore deposit models # 14. Volcanogenic massive sulfide deposits, Part 2: genetic models. Geosci Can 15:43–65

Lydon JW, Galley A (1986) Chemical and mineralogical zonation of the Mathiati alteration pipe, Cyprus, and its genetic significance. In: Gallagher, Ixer RH, Neary CR, Prichard HM (eds) Metallogeny of basic and ultrabasic rocks. Inst Min Metall, pp 49–86

Lydon JW, Goodfellow WD, Jonasson IR (1985) A general genetic model for stratiform baritic deposits of the Selwyn Basin, Yukon Territory and District of Mackenzie. Geol Soc Can Pap 85–1A:651–660

Maas R, McCulloch MT, Campbell IH, Coad PR (1986) Sm-Nd and Rb-Sr dating of a Archean massive sulfide deposit: Kidd Creek, Ontario. Geology 14:585–588

Macdonald AJ (1987) Ore deposit models # 12. The platinum group element deposits: classification and genesis. Geosci Can 14:155–166

Macdonald AJ, Krezmer MJ, Kesler SE (1986) Vein, manto, and chimney mineralization at the Fresnillo silver-lead-zinc mine, Mexico. Can J Earth Sci 23:1603–1614

Macdonald KC, Becker K, Spiess FN, Ballard RD (1980) Hydrothermal heat flux of the "black smoker" vents on the East Pacific Rise. Earth Planet Sci Lett 48:1–7

MacGeehan PJ, Hodgson CJ (1982) Environments of gold deposition in the Campbell Red Lake and Dickenson mines, Red Lake district, Ontario. In: Hodder RW, Petruk W (eds) Geology of Canadian gold deposits. Can Inst Min Metall Spec Vol 24:184–210

MacGeehan PJ, Maclean WH (1980) Tholeiitic basalt-rhyolite magmatism and massive sulfide deposits at Matagami, Quebec. Nature (London) 283:153–157

MacGeehan PJ, Maclean WH, Bonenfaut AJ (1981) Exploration significance of the emplacement and genesis of massive sulfides in the Main Zone at the Norita Mine, Matagami, Quebec. Can Inst Min Metall Bull 74/828:59–75

MacIntyre DG (1982) Geologic setting of recently discovered stratiform barite-sulfide deposits in northeast British Columbia. Can Inst Min Bull 75/840:99–113

MacKenzie WB (1970) Hydrothermal alteration associated with the Urad and Henderson molybdenite deposits, Clear Creek County, Colorado. PhD Thesis, Univ Mich, 208 pp

MacKevett EM, Jr., Armstrong AK, Potter RW, Silberman ML (1980) Kennecott-type copper deposits, Wrangell Mountains, Alaska – an update and summary (Abstr). Mineral deposits of the Pacific Northwest. Symp Proc US Geol Surv Open File Rep 81–355:50–51

Magee M (1968) Geology and ore deposits of the Ducktown district, Tennessee. Ore deposits of the United States, 1933–1967. AIME Graton-Sales Vol 1:207–241

Maiden KJ (1984) Metamorphic features of stratiform gold ores in the Barberton greenstone belt, eastern Transvaal. In: Foster RP (ed) Gold '82: the geology, geochemistry and genesis of gold deposits. Balkema, Rotterdam, pp 325–338

Maiden KJ, Innes AH, King MJ, Mater S, Pettitt I (1984) Regional controls on the localization of stratabound copper deposits: Proterozoic examples from southern Africa and south Australia. Precambrian Res 25:99–118

Mainwaring PR, Naldrett AJ (1977) Country-rock assimilation and the genesis of Cu-Ni sulfides in the Waterhen intrusion, Duluth Complex, Minnesota. Econ Geol 72:1269–1284

Maliotis G, Khan MA (1980) The applicability of the induced polarization method of geophysical exploration in the search for sulfide mineralization within the Troodos ophiolite complex of Cyprus. In: Panayiotou A (ed) Ophiolites. Proc Int Ophiolite Symp, Cyprus 1979, pp 129–138

Mangan M, Craig JR, Rimstidt JD (1984) Submarine exhalative gold mineralization at the London-Virginia mine, Buckingham County, Virginia. Mineral Deposita 19:227–236

Mangini A, Halbach P, Puteanus D, Segl M (1987) Chemistry and growth history of central Pacific Mn-crusts and their economic importance. In: Teleki PG (eds) Marine minerals. Reidel, Dordrecht, pp 9–19

Manske SL, Mallack WF, Springett NW, Strakele AE, Watowich SN, Yeomans B, Yeomans E (1987) Geology of the Mesquite deposit, Imperial County, California. Soc Min Eng Annu Meet, Denver, Feb 1987, Preprint:87–107

Manton WI (1968) The origin of associated basic and acid rocks in the Lebombo-Nuanetsi igneous province, southern Africa, as implied by strontium isotopes. J Petrol 9:23–39

Marcotte D, David M (1981) Target definition of Kuroko-type deposits in Abitibi by discriminant analysis of geochemical data. Canadian Inst Min Metall Bull 74/828:102–108

Marjoribanks RW, Rutland RWR, Glen RA, Laing WP (1980) The structure and tectonic evolution of the Broken Hill region, Australia. Precambrian Res 13:209–240

Marsh JS (1973) Relationship between transform directions and alkaline igneous rock lineaments in Africa and South America. Earth Planet Sci Lett 18:317–323

Marshak RS, Karig DE (1977) Triple junctions as a cause for anomously near-trench igneous activity between the trench and volcanic arc. Geology 5:233–236

Marston RJ, Groves DL, Hudson DR, Ross JR (1981) Nickel sulfide deposits in western Australia: a review. Econ Geol 76:1330–1363

Martin H (1978) The mineralization of the ensialic Damara orogenic belt. Geol Soc S Afr Spec Publ 4:405–415

Martin H, Porada H (1978) The intracratonic branch of the Damara Orogen in southwest Africa. I Discussion of geodynamic models. Precambrian Res 5:311–338

Martin RF, Piwinskii AJ (1972) Magmatism and tectonic setting. J Geophys Res 77:4966–4975

Martinez F, Cochran JR (1988) Structure and tectonics of the northern Red Sea: catching a continental margin between rifting and drifting. Tectonophysics 150:1–32

Mason R, Melnik N (1986) The anatomy of an Archean gold system – the McIntyre-Hollinger Complex at Timmins, Ontario, Canada. In: Proc Gold '86 Symp, Toronto, pp 40–55

Materikov MP (1977) Deposits of tin. In: Smirnov VI (ed) Ore deposits of the USSR, vol 3. Pitman, London, pp 229–294

Mathews D, Smith C (eds) (1987) Deep seismic reflection profiling of the continental lithosphere. R Astron Soc Geophys J 89:497 pp

Mathias BV, Clark GJ (1975) Mount Isa copper and silver-lead-zinc orebodies – Isa and Hilton Mines. In: Knight CL (ed) Economic geology of Australia and Papua New Guinea. Australas Inst Min Metall Monogr 5:351–371

Mathias BV, Clark GJ, Morris D, Russell RE (1973) The Hilton deposit – stratiform silver-lead-zinc mineralization of the Mt. Isa type. In: Metallogenic provinces and mineral deposits in the southwest Pacific. Bur Mineral Res Australas Bull 141:33–58

Mathieson GA, Clark AH (1984) The Cantung E Zone scheelite skarn orebody, Tungsten Northwest Territories: a revised genetic model. Econ Geol 79:883–901

Matoba V (1983) A discussion on the estimation of the sea depth in the Hokuroku district during the time of the Kuroko deposition. Mining Geol Spec Issue 11:251–262 (in Japanese with English Abstr)

Matty DJ, Lipman PW, Stormer JC, Jr. (1987) Common-Pb isotopic characteristics of Central San Juan ash flow tuffs. Geol Soc Am Abstr with Prog 19:319–320
Maucher A, Schneider HJ (1967) The Alpine lead-zinc ores. Econ Geol Monogr 3:71–89
May ER, Schmidt PG (1982) The discovery, geology and mineralogy of the Crandon Precambrian massive sulfide deposit, Wisconsin. Geol Assoc Can Spec Pap 25:447–480
Mayfield CF, Tailleur IL, Ellersieck I (1983) Stratigraphy, structure and palinspastic analysis of the western Brooks Range, northwestern Alaska. US Geol Surv Open File Rep 83–779:58 pp
McBirney AR (1987) Constitutional zone refining of layered intrusions. In: Parsons I (ed) Origins of igneous layering. Reidel, Dordrecht, pp 437–452
McCallum IS, Raedeke LD, Mathez EA (1980) Investigations of the Stillwater Complex, Part I: stratigraphy and structure of the banded zone. Am J Sci 280A:59–87
McCallum ME (1985) Experimental evidence for fluidization processes in breccia pipe formation. Econ Geol 80:1523–1543
McClay KR (1982) Tectonic and sedimentary deformation in the sulphide orebodies of Mount Isa (Australia) and Sullivan (Canada). Inst Min Metall Trans 91:B146–B151
McConnell RB (1974) Evolution of taphrogenic lineaments in continental platforms. Geol Rundsch 63:389–430
McDougall I (1976) Geochemistry and origin of basalt of the Columbia River Group, Oregon and Washington. Geol Soc Am Bull 87:777–792
McDougall I, Lovering JF (1963) Fractionation of chronium, nickel, cobalt, and copper in a differential dolerite-granophyre sequence at Red Hill, Tasmania. J Geol Soc Aust 10:325–338
McGetchin TR, Burke KC, Thompson GA, Young RA (1980) Mode and mechanism of plateau uplifts. Dynamics of plate interiors. Am Geophys Un Geodyn Ser 1:99–110
McIlveen GR (1974) The Eden-Comerong-Yalwal rift zone and the contained gold mineralization. Rec Geol Surv NSW 16:245–277
McIntosh JL, Farag JS, Slee KJ (1975) Groote Eylandt manganese deposits. In: Knight CL (ed) Economic geology of Australia and Papua New Guinea. Metals. Australasian Inst Min Metall Victoria, Austr, pp 815–821
McKay MJ, Hazeldene RK (1987) Woodlawn Zn-Pb-Cu sulfide deposit, New South Wales, Australia: an interpretation of ore formation from field observations and metal zoning. Econ Geol 82:141–164
McKee EH (1979) Ash-flow sheets and calderas: their genetic relationship to ore deposits in Nevada. Geol Soc Am Spec Pap 180:205–211
McKelvey VE (1986) Subsea mineral resources. US Geol Surv Bull 1689:106
McKenzie DP (1967) Some remarks on heat flow and gravity anomalies. J Geophys Res 72:6261–6273
McKenzie D (1978) Some remarks on the development of sedimentary basins. Earth Planet Sci Lett 40:25–32
McKibben MA, Elders WA (1985) Fe-Zn-Cu-Pb mineralization in the Salton Sea geothermal system, Imperial Valley, California. Econ Geol 80:539–559
McKibben MA, Andes JP, Williams AE (1988) Active ore formation at a brine interface in metamorphosed deltaic lacustrine sediments: the Salton Sea geothermal system, California. Econ Geol 83:511–523
McLaughlin RJ (1981) Tectonic setting of pre-Tertiary rocks and its relation to geothermal resources in the geysers – Clear Lake area. US Geol Surv Prof Pap 1141:3–24
McLelland JM (1986) Pre-Grenvillian history of the Adirondacks as an anorogenic, bimodal caldera complex of mid-Proterozoic age. Geology 14:229–233
McLelland JM, Isachsen YW (1986) Synthesis of the geology of the Adirondack Mountains, New York, and their tectonic setting within the southwestern Grenville Province. Geol Assoc Can Spec Pap 31:75–94
McLeod WN, Turner DC, Wright EP (1971) The geology of the Jos Plateau. Geol Surv Nigeria Bull 32 2:1–168
McNaughton K, Smith TE (1986) A fluid inclusion study of sphalerite and dolomite from the Nanisivik lead-zinc deposit, Baffin Island, Northwest Territories, Canada. Econ Geol 81:713–720

McNeil AM, Kerrich R (1986) Archean lamprophyre dykes and gold mineralization, Matheson, Ontario: the conjuction of LILE-enriched mafic magmas, deep crustal structures, and Au concentration. Can J Earth Sci 23:324–342
McWilliams MO, Kroner A (1981) Paleomagnetism and tectonic evolution of the Pan-African Damara Belt, southern Africa. J Geophys Res 86:5147–5162
Meinert LD (1984) Mineralogy and petrology of iron skarns in western British Columbia, Canada. Econ Geol 79:869–882
Meinert LD, Newberry R, Einaudi MT (1980) An overview of tungsten, copper and zinc-bearing skarns in western North America. In: Silberman ML, Field CW, Berry AL (eds) Symp Mineral deposits of the Pacific Northwest. USGS Open File Rep 81-355:303–327
Melson WG, Vallier TL, Wright TL, Byerly G, Nelson J (1976) Chemical diversity of abyssal volcanic glass erupted along Pacific, Atlantic, and Indian Ocean sea-floor spreading centers. Am Geophys Un Monogr 19:351–368
Menard HW (1967) Sea-floor spreading, topography and the second layer. Science 157:923–924
Menard HW, Atwater T (1969) Origin of fracture zone topography. Nature (London) 222:1037–1040
Mendelsohn F (1961) The geology of the northern Rhodesian Copper Belt. MacDonald, London, 523 pp
Metz PA, Freeman CJ, Calvin JS (1987) Bulk mineable vein type and disseminated gold mineralization of the Fairbanks mining districts, Alaska. Pac Rim Congr 87:333–342
Meyer C (1981) Ore-forming processes in geologic history. Econ Geol 75th Anniv Vol, pp 6–41
Meyer C (1988) Ore deposits as guides to the geologic history of the earth. Annu Rev Earth Planet Sci 16:147–172
Middleton RC (1976) The geology of Prieska Copper Mines Limited. Econ Geol 71:328–350
Milanovsky EE (1981) Aulacogens of ancient platforms: problems of their origin and tectonic development. Tectonophysics 73:213–248
Miller CF, Bradfish LJ (1980) An inner Cordilleran belt of muscovite-bearing plutons. Geology 8:412–416
Miller RMcG (ed) (1983a) Evolution of the Damara Orogen, South West Africa/Namibia. Spec Publ Geol Soc South Africa, Johannesberg, South Africa, 293 pp
Miller RMcG (1983b) A possible model for the Damara Orogen in the light of recent data. In: Profiles of orogenic belts. Am Geophys Un Geodyna Ser 10:31–34
Minniti M, Bonavia FF (1984) Copper-ore grade hydrothermal mineralization discovered in a seamount in the Tyrrhenian Sea (Mediterranean): is the mineralization related to porphyry-coppers or to base metal lodes? Mar Geol 59:271–282
Minnitt RCA (1986) Porphyry copper-molybdenum mineralization at Haib River, South West Africa/Namibia. In: Anhaeusser CR, Maske S (eds) Mineral deposits of southern Africa. Geol Soc S Afr 2:1567–1586
Mitchell AHG (1974) Southwest England granites: magmatism and tin mineralization in a post-collision tectonic setting. Trans Inst Min Metall 83:B95–97
Mitchell AHG (1977) Tectonic settings for emplacement of Southeast Asian tin granites. Bull Geol Soc Malaysia 9:123–140
Mitchell AHG (1985) Mineral deposits related to tectonic events accompanying arc-continent collision. Inst Min Metall Trans 94:B115–B125
Mitchell AHG, Garson MS (1981) Mineral deposits and global tectonic settings. Academic Press, New York London, 405 pp
Moghal MY (1974) Uranium in Siwalik sandstones, Sulaiman Range, Pakistan. In: IAEA (ed) Formation of uranium ore deposits. IAEA, Vienna, pp 383–403
Mohr P (1982) Musings on continental rifts. In: Palmason G (ed) Continental and oceanic rifts. Am Geophys Un Geodyn Ser 8:293–309
Montoya JW, Hemley JJ (1975) Activity relations and stabilities in alkali feldspar and mica alteration reactions. Econ Geol 70:577–594
Moorbath S (1962) Lead isotope abundance studies on mineral occurrences in the British Isles and their geological significance. Philos Trans R Soc London, Series A, 254:295–360

Moorbath S (1980) Aspects of the chronology of ancient rocks related to continental evolution. In: Strangway DW (ed) The continental crust and its mineral deposits. Geol Assoc Can Spec Pap 20:89–115

Moore DM, Young LE, Modene JS, Plahuta JT (1986) Geologic setting and genesis of the Red Dog zinc-lead-silver deposit, western Brooks Range, Alaska. Econ Geol 81:1696–1727

Moore JM, Davidson A, Baer AJ (eds) (1986) The Grenville Province. Geol Assoc Can Spec Pap 31:358 pp

Moore JM (1980) A study of certain paragneiss associations and their metallogenic characteristics in Namaqualand and Bushmanland. Univ Cape Town Precambrian Res Unit Annu Rep 1979:65–73

Moore JM (1982) Mineral zonation near the granitic batholiths of south-west and northern England and some geothermal analogues. In: Evans AM (ed) Metallization associated with acid magmatism. John Wiley & Sons, New York, pp 229–241

Moores E (1969) Petrology and structure of the Vourinos ophiolite complex, northern Greece. Geol Soc Am Spec Pap 118:1–74

Morgan BA (1975) Mineralogy and origin of skarns in the Mount Morrison roof pendant, Sierra Nevada, California. Am J Sci 275:119–142

Morgan WJ (1972) Plate motions and deep mantle convection. Geol Soc Am Mem 132:7–22

Mortimer GE, Cooper JA, Paterson HL, Cross K, Hudson GRT, Uppill RK (1988) Zircon U-Pb dating in the vicinity of the Olympic Dam Cu-U-Au deposit, Roxby Downs, South Australia. Econ Geol 83:694–709

Morton JL, Sleep NH (1985) A mid-ocean ridge thermal model: constraints on the volume of axial hydrothermal heat flux. J Geophys Res 90:11345–11353

Mottl MJ (1983) Metabasalts, axial hot springs, and the structure of hydrothermal systems at mid-ocean ridges. Geol Soc Am Bull 94:161–180

Mouillac JL, Valois J-P, Walgenwitz F (1986) The Goanikontes uranium occurrence in South West Africa/Namibia. In: Anhaeusser CR, Maske S (eds) Mineral deposits of southern Africa. Geol Soc S Afr 11:1833–1843

Mueller AG, Harris LB (1987) An application of wrench tectonic models to mineralized structures in the Golden Mile district, Kalgoorlie, western Australia. Univ W Aust Publ 11:97–107

Muff R (1978) The Antimony deposits in the Murchison Range of the northeastern Transvaal, Republic of South Africa. Monograph Series on Mineral deposits, vol 16. Borntraeger, Berlin, pp 1–90

Muir MD (1983) Depositional environments of host rocks to northern Australian lead-zinc deposits, with special reference to McArthur River. In: Sangster DF (ed) Sediment-hosted stratiform lead-zinc deposits. Mineral Assoc Can Short Course Handb, pp 141–174

Muir TL (1984) The Sudbury structure: considerations and models for an endogenetic origin. In: The geology and ore deposits of the Sudbury structure. Ontario Geol Surv Spec Vol 1:449–489

Muir TL (1985) Geology of the Hemlo-Heron Bay area. In: McMillan RH, Robinson DJ (eds) Gold and copper-zinc metallogeny, Hemlo-Manitouwadge-Winston Lake, Ontario, Canada. Joint Publ Geol Assoc Can, Can Inst Min Metall, pp 30–38

Mukasa SB, Ludden JN (1987) Uranium-lead isotopic ages of plagiogranites from the Troodos ophiolite, Opyrus, and their tectonic significance. Geology 15:825–828

Mulligan R (1971) Lithophile metals and the Cordilleran tin belt. Can Min Metall Bull 64:714, 68–71

Mumpton FA, Thompson CS (1975) Mineralogy and origin of the Coalinga asbestos deposit. Clays Clay Mineral 23:131–143

Munha J (1979) Blue amphiboles, metamorphic regime and plate tectonic modelling in the Iberian pyrite belt. Contrib Mineral Petrol 69:279–289

Munha J (1983) Hercynian magmatism in the Iberian Pyrite Belt. Serv Geol Portugal Mem 29:39–81

Munha J, Barriga FJAS, Kerrich R (1986) High ^{18}O ore-forming fluids in volcanic-hosted base metal massive sulfide deposits: geologic $^{18}O/^{16}O$, and D/H evidence from the Iberian Pyrite Belt: Crandon, Wisconsin and Blue Hill, Maine. Econ Geol 81:530–552

Mutschler FE, Griffen ME, Stevens SD, Shannon SS, Jr. (1985) Precious metal deposits related to alkaline rocks in the North American Cordillera – an interpretative review. Trans Geol Soc S Afr 88:355–377

Naganna C (1987) Gold mineralization in the Hutti mining are, Karnataka, India. Econ Geol 82:2008–2016

Naldrett AJ (1981a) Platinum-group element deposits. In: Cabri LJ (ed) Platinum-group elements: mineralogy, geology, recovery. CIM Spec Vol 23:197–231

Naldrett AJ (1981b) Nickel sulfide deposits: classification, composition, and genesis. Econ Geol 75th Anniv Vol, pp 628–685

Naldrett AJ (1984) Mineralogy and composition of the Sudbury ores. In: The geology and ore deposits of the Sudbury Structure. Ontario Geol Surv Spec Vol 1:309–326

Naldrett AJ, Hewins RH (1984) The main mass of the Sudbury Igneous Complex. In: The geology and ore deposits of the Sudbury Structure. Ontario Geol Surv Spec Vol 1:235–251

Naldrett AJ, Kullerud G (1967) A study of the Strathcona mine and its bearing on the origin of the nickel-copper ores of the Sudbury district, Ontario. J Petrol 8:453–531

Naldrett AJ, MacDonald AJ (1980) Tectonic settings of some Ni-Cu sulfide ores: their importance in genesis and exploration. Geol Assoc Can Spec Pap 20:633–657

Naldrett AJ, Hewins RH, Breenman L (1972) The main irruptive and the sublayer at Sudbury. Int Geol Congr 24th Montreal Proc Sect 4:206–214

Naldrett AJ, Hewins RH, Dressler BO, Rao BV (1984) The contact sublayer of the Sudbury Igneous Complex. In: The geology and ore deposits of the Sudbury Structure. Ontario Geol Surv Spec Vol 1:253–274

Naldrett AJ, Gasparrini EC, Barnes SJ, von Gruenewaldt G, Sharpe MR (1986a) The Upper Critical Zone of the Bushveld Complex and the origin of Merensky-type ores. Econ Geol 81:1105–1117

Naldrett AJ, Rao BV, Evensen NM (1986b) Contamination at Sudbury and its role in ore formation. In: Gallagher MJ, Ixer RA, Neary CR, Prichard HM (eds) Metallogeny of basic and ultrabasic rocks. Inst Min Metall, pp 75–92

Naldrett AJ, Cameron G, von Gruenewaldt G, Sharpe MR (1987) The formation of stratiform PGE deposits in layered intrusions. In: Parsons I (ed) Origins of igneous layering. Reidel, Dordrecht Amsterdam, pp 313–397

Narayanaswami S, Zinuddin M, Ramachandra AV (1960) Structural control and localization of gold-bearing lodes, Kolar Gold Field, India. Econ Geol 55:1429–1459

Nash JT (1976) Fluid inclusion petrology-data from porphyry copper deposits and applications to exploration. US Geol Surv Prof Pap 907-D: 1–16

Nash JT, Cunningham CG, Jr. (1973) Fluid inclusion studies of the fluorspar and gold deposits, Jamestown district, Colorado. Econ Geol 68:1247–1262

Nasseef AO, Bakor AR, Hashad AH (1980) Petrography of possible ophiolite rocks along the Qift-Quseir road, Eastern Desert, Egypt. In: Al-Shanti AMS (ed) Evolution and mineralization of the Arabian-Nubian Shield, vol 4. Pergamon, New York Oxford, pp 157–168

Needham RS, Crick IH, Stuart-Smith PG (1980) Regional geology of the Pine Creek geosyncline. In: IAEA (ed) Uranium in the Pine Creek geosyncline. IAEA, Vienna, pp 1–22

Nelson CE, Giles DL (1985) Hydrothermal eruption mechanims and hot spring gold deposits. Econ Geol 80:1633–1639

Nelson G (1986) Gold mineralization at the Homestake gold mine, Lead, South Dakota. In: Clark LA (ed) Gold in Western Shield. Can Inst Min Metall Spec Vol 38:347–358

Nesbitt BE, Longstaffe FJ, Shaw DR, Muehlenbachs K (1984) Oxygen isotope geochemistry of the Sullivan massive sulfide deposit, Kimberley, British Columbia. Econ Geol 79:933–946

Nesbitt BE, Murowchick JB, Muehlenbachs K (1986) Dual origins of lode gold deposits in the Canadian Cordillera. Geology 14:506–509

Neudert MK, Russell RE (1981) Shallow water and hypersaline festures from the Middle Proterozoic Mt. Isa sequence. Nature (London) 293:284–286

Neugebauer HJ (1987) Models of lithospheric thinning. Annu Rev Earth Planet Sci 15:421–444

Newberry RJ, Einaudi MT (1981) Tectonic and geochemical setting of tungsten skarn mineralization in the Cordillera. In: Dickinson WR, Payne WD (eds) Relations of tectonics to ore deposits in the southern Cordillera. AR Geol Soc Digest 14:19–111

Newham WDN (1986) The Lomagundi and Sabi metallogenic provinces of Zimbabwe. In: Anhaeusser CR, Maske S (eds) Mineral deposits of southern Africa. Geol Soc S Afr 2:1351–1393

Ney CS, Hollister VF (1976) Geologic setting of porphyry deposits of the Canadian Cordillera. In: Sutherland Brown A (ed) Porphyry deposits of the Canadian Cordillera. Can Inst Min Metall Spec Vol 15:21–29

Nicolas A, Violette JF (1982) Mantle flow at oceanic spreading centers: models derived from ophiolites. Tectonophysics 81:319–339

Nielsen BL (1976) Geology of Greenland:economic minerals. Gron Geol Unders Denm, pp 461–486

Nilsen O (1978) Caledonian massive sulfide deposits and minor iron-formations from the southern Trondheim region, Norway. Norges Geol Unders 340:35–85

Noble DC, Silberman ML (1984) Evolucion volcanica e hidrothermal y cronologica de K-Ar del distrito minero de Julcani, Peru. Soc Geol Peru Vol Jubilar LX Anniv, pp 1–35

Noble DC, McCormack JK, McKee EH, Silberman ML, Wallace AB (1988) Timing of mineralization of the McDemitt caldera complex, Nevada–Oregon, and the relation of the middle Miocene mineralization in the northern Great Basin to coeval regional basaltic magmatic activity. Econ Geol 83:859–863

Noble JA (1980) Two metallogenic maps for North America. Geol Rundsch 69:594–609

Noble SR, Spooner ET, Harris FR (1984) The Logtung large tonnage, low-grade W (scheelite)-Mo porphyry deposit, south central Yukon Territory. Econ Geol 79:848–868

Noe-Nygaard A, Pedersen AK (1974) Progressive chemical variation in a tholeiitic lava sequence at Kap Stosch, northern East Greenland. Bull Geol Soc Denm 23:175–190

Nokleberg WJ (1981) Geologic setting, petrology, and geochemistry of zoned tungsten-bearing skarns at the Strawberry Mine, central Sierra Nevada, California. Econ Geol 76:111–133

Nokleberg WJ, Winkler GR (1982) Stratiform zinc-lead deposits in the Drenchwater Creek area, Howard Pass quadrangle, northwestern Brooks Range, Alaska. US Geol Surv Prof Pap 1209:22 pp

Nolan TB (1933) Epithermal precious metal deposits. In: Ore deposits of the western States (Lindgren Volume). Am Inst Mining Metall Eng, New York, pp 623–640

Norman DI (1977) Geology and geochemistry of Tribag Mine, Batchawana Bay, Ontario. PhD Thesis, Univ Minn, 257 pp

Norman DI (1978) Ore deposits related to the Keweenawan Rift. In: Neumann ER, Ramberg IB (eds) Petrology and geochemistry of continental rifts. Reidel, Dordrecht, pp 245–254

Norman DI, Landis GP (1983) Source of mineralizing components in hydrothermal ore fluids as evidenced by $^{87}Sr/^{86}Sr$ and stable isotope data from the Pasto Bueno deposit, Peru. Econ Geol 78:451–465

Norman DI, Sawkins FJ (1985) The Tribag breccia pipes: Precambrian Cu-Mo deposits, Batchawana Bay, Ontario. Econ Geol 79:1493–1621

Norman DI, Wupoa T, Putnam BR, Smith RW (1985) Mineralization of the Hansonburg Mississippi Valley-type deposit, New Mexico: insight from composition of gases in fluid inclusions. Can Mineral 23:353–368

Norman JW (1980) Causes of some old crustal failure zones interpreted from Landstat images and their significance in regional exploration. Trans Inst Min Metall 89:B63–B72

Normark WR, Morton JL, Koski RA, Clague DA, Delaney JR (1983) Active hydrothermal vents and sulfide deposits on the southern Juan de Fuca Ridge. Geology 11:158–163

Northern Miner (ed) (1982) Major zinc-lead Alaska deposit now under study by Cominco. N Miner 67/49: Al,A6

Northolt AJG (1979) The economic geology and development of igneous phosphate deposits in Europe and the USSR. Econ Geol 74:339–350

Norton D (1978) Source-lines, source-regions, and pathlines for fluids in hydrothermal systems related to cooling plutons. Econ Geol 73:21–28

Norton D (1979) Transport phenomena in hydrothermal systems – the redistribution of chemical components around cooling magmas. Bull Mineral 102:471–486

Norton DL, Cathles LM (1973) Breccia pipes – products of exsolved vapor from magmas. Econ Geol 68:540–546

Nozawa T (1983) Felsic plutonism in Japan. In: Circum-pacific plutonic terranes. Geol Soc Am Mem 159:105–122
Nunes PD, Pyke DR (1980) Geochronology of the Abitibi metavolcanic belt, Timmins-Matachewan area – progress report. Ontario Geol Surv Misc Pap 92:34–39
Nutt THC (1984) Archean gold mineralization in the Nando and Pinkun mines, Kadoma district, Zimbabwe. In: Foster RP (ed) Gold '82: the geology, geochemistry and genesis of gold deposits. Balkema, Rotterdam, 261–284
Oba N, Miyahisa M (1977) Relations between chemical composition of granitic rocks and metallization in the Outer Zone of southwest Japan. Bull Geol Soc Malaysia 9:67–74
O'Driscoll EST (1981) A broad-scale structural characteristic of major nickel sulfide deposits of western Australia. Econ Geol 76:1364–1372
O'Driscoll EST (1986) Observations on the lineament-ore relation. Philos Trans R Soc London Ser A 317:179–194
Ohle EL (1980) Some considerations in determining the origin of ore deposits of the Mississippi Valley type, Part II. Econ Geol 75:161–172
Ohmoto H (1978) Submarine calderas: a key to the formation of volcanogenic massive sulfide deposits. Min Geol 28:219–231
Ohmoto H (1986) Stable isotope geochemistry of ore deposits. Rev Mineral 16:491–570
Ohmoto H, Rye RO (1974) Hydrogen and oxygen isotopic compositions of fluid inclusions in the Kuroko deposits, Japan. Econ Geol 69:947–953
Ohmoto H, Hart SR, Holland HD (1966) Studies of the Providencia area, Mexico, II, K-Ar and Rb-Sr ages of intrusive rocks and hydrothermal minerals. Econ Geol 61:1205–1213
Ohmoto H, Mizukami M, Drummond SE, Eldridge CS, Pisutha-Arnond V, Lenagh TC (1983) Chemical processes of Kuroko formation. Econ Geol Monogr 5:570–604
Ojeda JM (1986) Escondida porphyry copper deposit, II Region, Chile: exploration drilling and current geological interpretation. Mining Latin America/Mineria Latinoamerica. Inst Min Metall, London, pp 299–318
O'Keeffe WG (1986) Age and postulated source rocks for mineralization in central Ireland, as indicated by lead isotopes. In: Geology and genesis of mineral deposits of Ireland. Irish Assoc Econ Geol, Dublin, pp 617–624
Olade MA (1980) Plate tectonics and metallogeny of intracontinental rifts and aulocogens, with special reference to Africa. In: Proc 5th IAGOD Symp, Utah, pp 91–112
Olade MA (1985) Aspects of primary tin-niobium mineralization in Nigeria's Younger Granite Province. In: Taylor RP, Strong DF (eds) Granite-related mineral deposits. Can Inst Min Geol Div, pp 200–202
Olade MA, Morton RD (1985) Origin of lead-zinc mineralization in the southern Benue Trough, Nigeria – fluid inclusion and trace element studies. Mineral Deposita 20:76–80
Oliver J (1986) Fluids expelled tectonically from orogenic belts: their role in hydrocarbon migration and other geologic phenomena. Geology 14:99–102
O'Neil JR, Silberman ML (1974) Stable isotope relations in epithermal Au-Ag deposits. Econ Geol 69:902–909
Padgham WA, Brophy JA (1986) Gold deposits of the Northwest Territories. In: Clark LA (ed) Gold in the Western Shield. Can Inst Min Metall Spec Vol 38:2–25
Page RW, McDougall I (1972) Geochronology of the Panguna porphyry copper deposit, Bougainville Island, New Guinea. Econ Geol 67:1065–1074
Palabora Mining Company Ltd Mine geological and mineralogical staff (1976) The geology and economic deposit of copper, iron, and vermiculite in the Palabora Igneous Complex: a brief review. Econ Geol 71:177–192
Pallister JS (1984) Parent magmas of the Semail ophiolite. In: Gass IG, Lippard SJ, Shelton AW (eds) Ophiolites and oceanic lithosphere. Geol Soc. Blackwell, Oxford, pp 63–70
Pallister JS, Stacey JS, Fischer LB, Premo WR (1987) Arabian Shield ophiolites and Late Proterozoic microplate accretion. Geology 15:320–323
Panayiotou A (ed) (1980) Cu-Ni-Co-Fe sulfide mineralization, Limassol Forest, Cyprus. In: Ophiolites. Proc Int Ophiolite Symp, Cyprus 1979, pp 102–116
Pansze AJ (1975) Geology and ore deposits of the Silver City-Delamar-Flint region, Omyhee County, Idaho. Idaho Bur Mines Geol Pamphlet 161

Panteleyev A (1986) Ore deposits # 10. A Canadian Cordilleran model for epithermal gold-silver deposits. Geosci Can 13:101–112
Paraoh TC, Beckinsale RD, Rickard D (eds) (1987) Geochemistry and mineralization of Proterozoic suites. Geol Soc Spec Publ 33:575 pp
Park AF (1988) Nature of the early Proterozoic Outokumpu assemblage, eastern Finland. Precambrian Res 38:131–146
Park CF, Jr. (1961) A magnetite 'flow' in northern Chile. Econ Geol 56:431–436
Park CF, Jr. (1972) The iron deposits of the Pacific basin. Econ Geol 67:339–349
Paterson R (1976) Ardlethan tin mine. In: Ore deposits of the Lachlan fold belt, New South Wales. 25th Int Geol Congr Excursion Guide 15C: 36–43
Pattison EF (1979) The Sudbury sublayer. Can Mineral 17:257–274
Pearce JA (1980) Geochemical evidence for the genesis and eruptive setting of lavas from Tethyan ophiolites. In: Panayiotou A (ed) Ophiolites. Proc Int Ophiolite Symp, Cyprus 1979, pp 261–272
Pearce JA, Cann JR (1973) Tectonic setting of basic volcanic rocks determined using trace element analyses. Earth Planet Sci Lett 19:290–300
Pearce JA, Lippard SJ, Roberts S (1984) Characteristics and tectonic significance of supra-subduction zone ophiolites. In: Kokelaar BP, Howells MF (eds) Marginal basin geology. Geol Soc London Spec Publ 16:77–96
Pearson WN (1979) Copper metallogeny, North Shore region of Lake Huron, Ontario. Geol Surv Can Pap 79-1A: 289–303
Pearton TN (1982) Gold and antimony mineralization in altered komatiites of the Murchison greenstone belt, South Africa. In: Arndt TN, Nisbet EG (eds) Komatiites. Allen & Unwin, London, pp 459–475
Pearton TN, Viljoen MJ (1986) Antimony mineralization in the Murchison greenstone belt – an overview. In: Anhaeusser CR, Maske S (eds) Mineral deposits of southern Africa. Geol Soc S Afr 1:293–320
Pedersen FD (1980) Remobilization of the massive sulfide ore of the Black Angel Mine, central west Greenland. Econ Geol 75:1022–1041
Percival TJ, Bagby WC, Radtke AS (1988) Physical and chemical features of precious metal deposits hosted by sedimentary rocks in the western United States. In: Bulk mineable precious metal deposits of the western United States. Geol Soc Nev, Reno, pp 11–34
Peredery WV (1982) Geology and nickel sulfide deposits of the Thompson Belt, Manitoba. Geol Assoc Can Spec Pap 25:165–209
Peredery WV, Morrison GG (1984) Discussion of the origin of the Sudbury Structure. In: The geology and ore deposits of the Sudbury Structure. Ontario Geol Surv Spec Vol 1:491–511
Pereira J, Dixon CJ (1963) Evolutionary trends in ore deposition. Inst Min Metall Trans 74:505–527
Perkins WG (1984) Mount Isa silica dolomite and copper orebodies: the result of a syntectonic hydrothermal alteration system. Econ Geol 79:601–637
Perry VD (1961) The significance of mineralized breccia pipes. Min Eng 13:367–376
Petersen U (1965) Regional geology and major ore deposits of central Peru. Econ Geol 60:407–476
Petersen U (1970) Metallogenic provinces of South America. Geol Rundsch 59:834–897
Petersen U, Noble DC, Arenas MJ, Goodell PC (1977) Geology of the Julcani district, Peru. Econ Geol 72:931–949
Petruk W (1973) The tungsten-bismuth-molybdenum deposit of Brunswick Tin Mines Ltd, its mode of occurrence, mineralogy, and amenability to mineral beneficiation. Can Inst Min Bull 66:113–130
Philcox ME (1984) Lower Carboniferous lithostratigraphy of the Irish Midlands. Irish Assoc Econ Geol Spec Publ, Dublin, 89 pp
Phillips GN (1986) Geology and alteration of the Golden Mile, Kalgoorlie. Econ Geol 81:779–808
Phillips GN, Groves DI, Martyn JE (1984) An epigenetic origin for Archean banded iron-formation-hosted gold deposits. Econ Geol 79:162–171
Phillips GN, Groves DI, Brown IJ (1987) Source requirements for the Golden Mile, Kalgoorlie: significance to the metamorphic replacement model for Archean gold deposits. Can J Earth Sci 24:1643–1651

Phillips WEA, Sevastopulo GD (1986) The stratigraphic and structural setting of Irish mineral deposits. In: Geology and genesis of mineral deposits in Ireland. Irish Assoc Econ Geol, Dublin, pp 1–30

Pienaar PJ (1961) Mineralization in the Basement Complex. In: Mendelsohn F (ed) The geology of the northern Rhodesian Copperbelt. MacDonald, London, pp 30–41

Pilcher SH, McDougall JJ (1976) Characteristics of some Canadian porphyry prospects. Can Inst Min Metall Spec Vol 15:79–82

Piper JDA (1982) The Precambrian paleomagnetic record. The case for the Proterozoic supercontinent. Earth Planet Sci Lett 59:61–89

Pipino G (1980) Gold in Liqurian ophiolites (Italy). In: Panayiotou A (ed) Ophiolites. Intl Ophiolite Symp, Cyprus 1979, pp 765–774

Pirie J (1982) Regional geological setting of gold deposits, Eastern Red Lake area, northwestern Ontario. In: Hodder RW, Petruk W (eds) Geology of Canadian gold deposits. Can Inst Min Metall Spec Vol 24:171–183

Pisutha-Arnond V, Ohmoto H (1983) Thermal history, and chemical and isotopic compositions of the ore-forming fluids responsible for the Kuroko massive sulfide deposits in the Hokuroku district of Japan. Econ Geol Monogr 5:523–558

Pitcher WS (1979) The nature, ascent and emplacement of granitic magmas. J Geol Soc London 136:627–662

Pitman WC III, Hayes JD (1973) Upper Cretaceous spreading rates and the great transgression. Abstr Progr Geol Soc Am 5:768

Platt JW (1977) Volcanogenic mineralization at Avoca, Co. Wicklow, Ireland, and its regional implications. In: Volcanic processes in ore genesis. Geol Soc London; and Inst Mining Metall, pp 163–170

Plimer IR (1978) Proximal and distal stratabound ore deposits. Mineral Deposita 13:345–353

Plimer IR (1987) The association of tourmalinite with stratiform scheelite deposits. Mineral Deposita 22:282–291

Ploshko VV (1963) Lizwaenitization and carbonation at terminal stages of Urushten Igneous Complex, North Caucasus. Int Geol Rev 7:446–463

Porada H (1979) The Damara-Ribeira orogen of the Pan-African Brasiliano cycle in Namibia (Southwest Africa) and Brazil as interpreted in terms of continental collision. Tectonophysics 57:237–265

Porter EW, Ripley E (1985) Petrologic and stable isotope study of the gold-bearing breccia pipe at the Golden Sunlight deposit, Montana. Econ Geol 80:1689–1706

Potgieter GA, de Villiers JPR (1986) Controls of mineralization at the Fumani gold deposit, Sutherland greenstone belt. In: Anhaeusser CR, Maske S (eds) Mineral deposits of southern Africa. Geol Soc S Afr 1:197–203

Pottorf RJ, Barnes HL (1983) Mineralogy, geochemistry, and ore genesis of hydrothermal sediments from the Atlantis II Deep, Red Sea. Econ Geol Monogr 5:198–223

Pouba Z (1971) Relations between iron and copper-lead-zinc mineralizations in submarine volcanic ore deposits in the Jeseniky Mts. Czechoslovakia. IAGOD, Soc Mining Geol Jpn Spec Issue 3:186–192

Poulsen KH (1986) Auriferous shear zones with examples from the Western Shield. In: Clark LA (ed) Gold in the Western Shield. Can Inst Min Metall Spec Vol 38:86–103

Poulsen KH, Franklin JM (1981) Copper and gold mineralization in an Archean trondhjemitic intrusion, Sturgeon Lake, Ontario. Geol Surv Can Pap 81-1A:9–14

Powar KB, Patwarchan AM (1984) Tectonic evolution and base-metal mineralization in the Arvalli-Delhi belt, India. Precambrian Res 25:309–323

Pretorius DA (1975) The depositional environment of the Witwatersrand goldfields: a chronological review of speculations and observations. Minerals Sci Eng 7:18–47

Pretorius DA (1981a) Gold and uranium in quartz-pebble conglomerates. Econ Geol 75th Anniv Vol, pp 117–138

Pretorius DA (1981b) Gold, geld, gilt: future supply and demand. Econ Geol Res Unit Univ Witwatersrand Inf Circ 152:1–15

Pretorius DA (1986) The goldfields of the Witwatersrand Basin. In: Anhaeusser CR, Maske S (eds) Mineral deposits of southern Africa. Geol Soc S Afr 1:489–495

Price PE, Kyle JR, Wessel GR (1983) Salt dome-related zinc-lead deposits. In: Kisvarsanyi G, Grant SK, Pratt WP, Koenig JW (eds) Proc Int Conf Mississippi Valley type lead-zinc deposits, Univ Missouri, Rolla, pp 558–571

Priem HNA, Boelrijk NA, Hebeda EH, Verdurmen EA, Verschure RH, Bon EH (1971) Granitic complexes and associated tin mineralizations of 'Grenville' age in Rondonia, western Brazil. Geol Soc Am Bull 82:1095–1102

Prinz M (1967) Geochemistry of basaltic rocks: trace elements. Basalts, the Poldervaart treatise on rocks of basaltic composition I. Wiley Interscience, New York, pp 271–323

Proffett JM, Jr. (1979) Ore deposits of the western United States – a summary. Nev Bur Mines Geol Rep 33:13–32

Pye EG, Naldrett AJ, Giblin PE (eds) (1984) The geology and ore deposits of the Sudbury Structure. Ontario Geol Surv Spec Vol 1:1–603

Quade H (1976) Genetic problems and environmental features of volcano-sedimentary iron-ore deposits of the Lahn-Dill type. In: Wolfe KH (ed) Handbook of strata-bound and stratiform ore deposits. Elsevier, Amsterdam, pp 255–294

Radtke AS (1985) Geology of the Carlin deposit. US Geol Surv Prof Pap 1267:124 pp

Radtke AS, Rye RO, Dickson FW (1980) Geology and stable isotope studies of the Carlin gold deposit. Econ Geol 75:641–672

Raedeke LD, Vian RW (1986) A three-dimensional view of mineralization in the Stillwater J-M Reef. Econ Geol 81:1187–1195

Rambau Perez F (1969) El sinclinal carbonifero de Riotinto y sus mineralizaciones assiadas. Mem Inst Geol Min Esp 71:1–229

Rankin DW (1975) The continental margin of North America in the southern Appalachians: the opening and closing of the proto-Atlantic. Am J Sci 275-A:298–336

Ransom PW (1977) Geology of the Sullivan orebody. Geol Assoc Canada Ann Mtg Vancouver B.C. Field Trip Guidebook 1:7–21

Rast N, Kohles KM (1986) The origin of the Ocoee Supergroup. Am J Sci 286:593–617

Ravenhurst CE, Reynolds PH, Zentilli M, Akande S (1987) Isotopic constraints on the genesis of Zn-Pb mineralization at Gays River, Novia Scotia, Canada. Econ Geol 83:1294–1308

Raybould JG (1978) Tectonic controls on Proterozoic stratiform mineralization. Trans Inst Min metall 87:B79–B86

Read HH (1957) The granite controversy. Murby, London, pp 1–430

Reid DL (1977) Geochemistry of Precambrian igneous rocks in the lower Orange River region. Precambrian Res Unit, Univ Cape Town Bull 22:1–397

Reid DL, Welke HJ, Erlank AJ, Moyes A (1987) The Orange River Group: a major Proterozoic calcalkaline volcanic belt in the western Namaqua Province, southern Africa. In: Paraoh TC, Beckinsale RD, Rickard D (eds) Geochemistry and mineralization of proterozoic volcanic suites. Geol Soc Spec Publ 33:327–346

Reid J (1983) Stratabound tungsten deposits in metamorphic terranes: stratabound scheelite deposits of northeast Brazil. Soc Min Eng AIME, Atlanta, Georgia Preprint 83–128: 1–43

Reinsbakken A (1980) Geology of the Skorovass mine: a volcanogenic massive sulfide deposit in the central Norwegian Caledonides. Norges Geol Unders Bull 57:123–154

Renfro AR (1974) Genesis of evaporite-associated stratiform metalliferous deposits – a Sabkha process. Econ Geol 69:33–45

Rentzsch J (1974) The Kupferschiefer in comparison with the deposits of the Zambian copperbelt. In: Bartholome P (ed) Gisments stratiformes et provinces cuprifères. Soc Geol Belg, Leige, pp 395–418

Reynolds IM (1985) The nature and origin of titaniferous magnetite-rich layers in the Upper Zone of the Bushveld Complex: a review and synthesis. Econ Geol 80:1089–1108

Rhodes RC (1975) New evidence for the impact origin of the Bushveld Igneous Complex. Geology 3:549–554

Richards DNG (1980) Paleozoic granitoids of northeastern Australia. In: Henderson RA, Stephenson PJ (eds) The geology and geophysics of northeastern Australia. Brisbane Geol Soc Aust, Queensland Div, pp 229–246

Richards JP, Krogh TE, Spooner ETC (1988) Fluid inclusion characteristics and U-Pb rutile age of late hydrothermal alteration and veining at the Musoshi stratiform copper deposit, central African Copper Belt, Zaire. Econ Geol 83:118–139

Richardson CJ, Cann JR, Richards HG, Cowan JG (1987) Metal-depleted root zones of the Troodos ore-forming hydrothermal systems, Cyprus. Earth Planet Sci Lett 84:243–253

Richardson JMG, Spooner ETC, McAuslan DA (1982) The East Kemptville tin deposit, Nova Scotia: an example of a large tonnage, low grade, greisen-hosted deposit in the endocontact zone of a granite batholith. Curr Res Part B, Geol Surv Can Pap 82-1B:27–32

Richardson SV, Kesler SE, Essene EJ, Jones LM (1986) Origin and geochemistry of the Chapada Cu-Au deposit, Goias, Brazil: a metamorphosed wall-rock porphyry copper deposit. Econ Geol 81:1884–1898

Rickard DT, Zweifel H (1975) Genesis of Precambrian sulfide ores, Skellefte district, Sweden. Econ Geol 70:255–274

Rickard DT, Willden MY, Marinder NE, Donnell TH (1979) Studies of the genesis of the Laisvall Sandstone lead-zinc deposit, Sweden. Econ Geol 74:1255–1285

Ridler RH (1970) Relationship of mineralization to volcanic stratigraphy in the Kirkland-Larder Lakes area, Ontario. Geol Assoc Can 21:33–42

Ripley EM (1986) Application of stable isotopic studies to problems of magmatic sulfide ore genesis with special reference to the Duluth Complex, Minnesota. In: Friedrich GH, Genkin AD, Naldrett AJ, Ridge JD, Sillitoe RH, Vokes FM (eds) Geology and metallogeny of copper deposits. Springer, Berlin Heidelberg New York Tokyo, pp 25–42

Ripley EM, Lambert MW, Berendsen P (1980) Mineralogy and paragenesis of red-bed copper mineralization in the Lower Permian of south central Kansas. Econ Geol 75:722–729

Riverin G, Hodgson CJ (1980) Wall-rock alteration at the Millenbach Cu-Zn mine, Noranda, Quebec. Econ Geol 75:424–444

Robbins EI (1983) Accumulation of fossil fuels and minerals in active and ancient rifts. Tectonophysics 94:633–658

Robert F, Brown AC (1986a) Archean gold-bearing quartz veins at the Sigma mine, Abitibi greenstone belt, Quebec: Part 1. Geologic relations and formation of the vein system. Econ Geol 81:578–592

Robert F, Brown AC (1986b) Archean gold-bearing quartz veins at the Sigma mine, Abitibi greenstone belt, Quebec, Part II: vein paragenesis and hydrothermal alteration. Econ Geol 81:593–616

Robert F, Kelly WC (1987) Ore-forming fluids in Archean gold-bearing quartz veins at the Sigma mine, Abitibi greenstone belt, Quebec, Canada. Econ Geol 82:1464–1482

Roberts DE, Hudson GRT (1983) The Olympic Dam copper-uranium-gold deposit, Roxby Downs, South Australia. Econ Geol 78:799–822

Roberts RG (1987) Ore deposit models #11 – Archean lode gold deposits. Geosci Can 14:37–52

Robertson AHF (1977) Tertiary uplift history of the Troodos Massif, Cyprus. Geol Soc Am Bull 88:1763–1772

Robertson JM (1975) Geology and mineralogy of some copper sulfide deposits near Mount Bohemia, Keweenawan County, Michigan. Econ Geol 70:1202–1224

Robinson RW, Norman DI (1984) Mineralogy and fluid inclusion study of the southern Amethyst vein system, Creede mining district, Colorado. Econ Geol 79:439–447

Rock NMS, Groves DI (1988) Do lamprophyres carry gold as well as diamonds? Nature (London) 332:253–255

Rock NMS, Duller P, Haszeldine RS, Groves DI (1987) Lamprophyres as potential gold exploration targets: some preliminary observations and speculations. Publ 11 Geol Dep; and Univ Exten, Univ West Aust, pp 271–286

Roddick JA (1983) Circum-Pacific plutonic terranes: an overview. Mem Geol Soc Am 159:1–4

Roedder E (1971) Fluid inclusion studies on the porphyry-type ore deposits at Bingham, Utah; Butte, Montana; and Climax, Colorado. Econ Geol 66:98–120

Roedder E (1976) Fluid inclusion evidence in the genesis of ores in sedimentary and volcanic rocks. In: Wolf KH (ed) Handbook of stratabound and stratiform ore deposits, vol 4. Elsevier, Amsterdam, pp 67–110

Roedder E (1977) Fluid inclusion studies of ore deposits in the Viburnum Trend, southeast Missouri. Econ Geol 72:474–479
Roedder E (1984) Fluid inclusions. Rev Mineral 12:10–644
Rogers RK, Davis JM (1977) Geology of the Buick Mine, Viburnum Trend, southeast Missouri. Econ Geol 72:372–380
Rona PA (1978) Criteria for recognition of hydrothermal mineral deposits in oceanic crust. Econ Geol 73:135–160
Rona PA (1984) Hydrothermal mineralization at seafloor spreading centers. Earth Sci Rev 20:1–104
Roobol MJ, Hackett D (1987) Paleovolcanic facies and exhalite geochemistry: guides for selecting exploration areas in volcano-sedimentary complexes. Econ Geol 82:691–705
Roobol MJ, Ramsay CR, Jackson NJ, Darbyshire DPF (1983) Late Proterozoic lavas of the central Arabian Shield: evolution of an ancient volcanic arc system. J Geol Soc London 140:185–202
Rose AW, Burt DM (1979) Hydrothermal alteration. In: Barnes LH (ed) Geochemistry of hydrothermal ore deposits. John Wiley & Sons, New York, pp 173–235
Rosendahl BR (1987) Architecture of continental rifts with special reference to East Africa. Annu Rev Earth Planet Sci 15:445–504
Ross JR, Travis GA (1981) The nickel sulfide deposits of western Australia in global perspective. Econ Geol 76:1291–1329
Rossiter AG, Ferguson J (1980) A Proterozoic tectonic model for northern Australia and its economic implications. In: IAEA (ed) Uranium in the Pine Creek geosyncline. IAEA, Vienna, pp 209–232
Routhier P, Aye F, Boyer C, Lecolle M, Moliere P, Picot P, Roger G (1979) La ceinture sud-ibérique à amas sulfures dans sa partie espagnole médiane. Tableau géologique et metallogénique. Synthèse sur le type amas sulfures volcano-sédimentaires. Mem Bur Rech Geol Min 94:1–266
Rouvier H, Perthuisot V, Mansouri A (1985) Pb-Zn deposits and salt-bearing diapirs in southern Europe and North Africa. Econ Geol 80:666–687
Rowlands NJ (1974) The gitology of some Adelaidean stratiform copper occurrences. In: Batholome P (ed) Gisements stratiformes et provinces cuprifères. Soc Geol Belg, Leige, pp 419–427
Rowlands NJ (1980) Discussions and contributions: tectonic controls on Proterozoic stratiform mineralization. Trans Inst Min Metall 89:B167–B168
Rowlands NJ, Blight PG, Jarvius DM, von der Borch CC (1980) Sabkha and playa environments in late Proterozoic grabens, Willouran Ranges, South Australia. J Geol Soc Aust 27:55–68
Roy DW, Woussen G, Dimroth E, Chown EH (1986) The central Grenville Province: a zone of protracted overlap between crustal and mantle processes. Geol Assoc Can Spec Pap 31:51–60
Royden L, Sclater JG (1981) The Neogene intra-Carpathian basins. Philos Trans R Soc London Ser A 300:373–381
Rozendaal A (1980) The Gamsberg zinc deposit, South Africa: a banded stratiform base-metal sulfide deposit. In: Proc 5th IAGOD Symp, Utah, pp 619–633
Rozendaal A, Stumpfl EF (1984) Mineral chemistry and genesis of Gamsberg zinc deposit, South Africa. Trans Inst Min Metall 93:B161–B175
Rozendaal A, Toros MS, Anderson JR (1986) The Rooiberg tin deposits, west-central Transvaal. In: Anhaeusser CR, Maske S (eds) Mineral deposits of southern Africa. Geol Soc S Afr 2:1307–1328
Rubright RD, Hart OJ (1968) Non-porphyry ores of the Bingham district, Utah. In: Ridge JD (ed) Ore deposits of the United States 1933–1967, vol 1. AIME, New York, pp 886–908
Ruegg NR (1976) Characteristicas de distribuicao e teor de elementos tracos dosados em rochas basalticas de bacia do Parana. Naturalia 2:23–45
Ruelle JC (1982) Depositional environments and genesis of stratiform copper deposits of the Redstone Copper Belt, Mackenzie Mountains, NWT. Geol Assoc Can Spec Pap 25:701–737
Ruitenberg AA, Fyffe LR (1982) Mineral deposits associated with granitoid intrusions and related subvolcanic stocks in New Brunswick and their relationship to Appalachian tectonic evolution. Can Inst Min Bull 75/842:83–97

Ruiz C, Aguilar A, Egert E, Espinoza W, Peebles F, Quezada R, Serrano M (1971) Strata-bound copper deposits of Chile. In: 3rd IAGOD Symp Kyoto, Japan, pp 252–260
Ruiz F (1965) Geologia y yacimientos metaliferos de Chile. Santiago Inst Invest Geol 305 pp
Russell MJ (1968) Structural controls of base metals mineralization. In: Ireland in relation to continental drift. Trans Inst Min Metall 77:B117–B128
Russell MJ (1975) Lithogeochemical environment of the Tynagh base-metal deposit, Ireland, and its bearing on ore deposition. Trans Inst Min Metal 84:B128–B133
Russell MJ (1978) Downward-excavating hydrothermal cells and Irish-type ore deposits: importance of an underlying thick Caledonian prism. Trans Inst Min Metal 87:B168–B171
Russell MJ (1986) Extension and convection: a genetic model for the Irish Carboniferous base metal and barite deposits. In: Geology and genesis of mineral deposits of Ireland. Irish Assoc Econ Geol, Dublin, 545–553
Russell N, Seaward M, Rivera J, McCurdy J, Kesler SE, Cloke PL (1981) Geology and geochemistry of the Pueblo Viejo gold-silver oxide ore deposit, Dominican Republic. Trans Inst Min Metall 90:B178–B201
Rutland RWR (1971) Andean orogeny and ocean floor spreading. Nature 233:252–255
Ruvalcaba-Ruiz D, Thompson TB (1988) Ore deposits at the Fresnillo Mine, Zacatecas, Mexico. Econ Geol 83:1583–1596
Ruxton PA, Clemmey H (1986) Late Proterozoic stratabound red bed-copper deposits of the Witvlei area, South West Africa/Namibia. In: Anhaeusser CR, Maske S (eds) Mineral deposits of southern Africa. Geol Soc S Afr 2:1739–1754
Ruzicka V (1971) Geological comparisons between East European and Canadian uranium deposits. Geol Surv Can Pap 70–48:1–196
Ryan PJ, Lawrence AL, Lipson RD, Moore JM, Paterson A, Stedman DP, Van Zyl D (1982) The Aggenys base metal sulfide deposits, Namaqualand, South Anrica. Econ Geol Res Unit, Univ Witwatersrand Inf Circ 160:1–33
Rye DM, Rye RO (1974) Homestake gold mine, South Dakota, I: stable isotope studies. Econ Geol 69:293–317
Rye RO (1966) The carbon, hydrogen, and oxygen isotopic composition of the hydrothermal fluids responsible for the lead-zinc deposits at Providencia, Zacatecas, Mexico. Econ Geol 61:1399–1427
Rye RO (1974) A comparison of sphalerite-galena sulfur isotope temperatures with filling temperatures of fluid inclusions. Econ Geol 69:26–32
Rye RO (1985) A model for the formation of carbonate-hosted disseminated gold deposits based on geologic, fluid inclusion and stable-isotope studies of the Carlin and Cortez deposits, Nevada. US Geol Surv Bull 1646:35–42
Rye RO, Haffty J (1969) Chemical composition of the hydrothermal fluids responsible for the lead-zinc deposits at Providencia, Zacatecas, Mexico. Econ Geol 64:629–643
Rye RO, O'Neil JR (1968) The O^{18} content of water in primary fluid inclusions from Providencia, north-central Mexico. Econ Geol 63:232–238
Rye RO, Sawkins FJ (1974) Fluid inclusion and stable isotope studies on the Casapalca Ag-Pb-Zn-Cu deposit, central Andes, Peru. Econ Geol 69:181–205
Rye RO, Hall WE, Ohmoto H (1974) Carbon, hydrogen and sulfur isotope study of the Darwin lead-silver-zinc deposit, southern California. Econ Geol 69:468–481
Rytuba JJ (1981) Relation of calderas to ore deposits in the western United States. AR Geol Soc Digest 14:227–236
Saager R, Meyer M, Muff R (1982) Gold distribution in supracrustal rocks from Archean greenstone belts of southern Africa and from Paleozoic ultramafic complexes of the European Alps: metallogenic and geochemical implications. Econ Geol 77:1–24
Saager R, Oberthur T, Tomschi H-P (1987) Geochemistry and mineralogy of banded iron-formation-hosted gold mineralization in the Gwanda greenstone belt, Zimbabwe. Econ Geol 82:2017–2032
Sabir H (1979) Precambrian polymetallic sulfide deposits in Saudi Arabia and their metallogenic significance. In: Al-Shanti (ed) Evolution and mineralization of the Arabian-Nubian Shield, vol 2. Pergamon, Oxford, pp 83–92
Saito M, Sato E (1978) On the recent exploration at the Iwato gold mine. Min Geol 28:191–202

Salas GP (1975) Carta y provincias metalogeneticas de la Republica Mexicana. Mex Cons Recurs Minerales Publ 21E, 242 pp
Saleeby JB, Harper GD, Snoke AW, Sharp WD (1982) Time relations and structural-stratigraphic patterns in ophiolite accretion, west central Klamath Mountains, California. J Geophys Res 87:3831–3848
Samama JC (1976) Comparative review of the genesis of the copper-lead sandstone-type deposits. In: Wolf KH (ed) Handbook of strata-bound and stratiform ore deposits, vol 6. Elsevier, Amsterdam, pp 1–20
Samanov IZ, Pozharisky IF (1977) Deposits of copper. In: Smirnov VI (ed) Ore deposits of the USSR, vol 2. Pitman, London, pp 106–181
Samson IM, Russell MJ (1987) Genesis of the Silvermines zinc-lead-barite deposit, Ireland: fluid inclusion and stable isotope evidence. Econ Geol 82:371–394
Sangster DF (1969) The contact metasomatic magnetite deposits of southwestern British Columbia. Geol Surv Can Bull 172:1–85
Sangster DF (1976) Carbonate-hosted lead-zinc deposits. In: Wolf KH (ed) Handbook of strata-bound and stratiform deposits, vol 6, Elsevier, Amsterdam, pp 447–456
Sangster DF (1979) Plate tectonics and mineral deposits: a view from two perspectives. Geosci Can 6:185–188
Sangster DF (1980) Quantitative characteristics of volcanogenic massive sulfide deposits. Can Inst Min Bull 73:74–81
Sangster DF (1981) Three potential sites for the occurrence of stratiform, shale-hosted lead-zinc deposits in the Canadian Arctic. Geol Surv Can Pap 81-A:1–8
Sangster DF (ed) (1983) Sediment-hosted stratiform lead-zinc deposits. Min Assoc Can Short Course Handb 8:309
Sangster DF (1984) Grade-tonnage summaries of massive sulfide deposits relative to paleotectonic settings in the Appalachian-Caledonian orogen. Econ Geol 79:1479–1482
Sangster DF (1986) Age of mineralization in Mississippi Valley-type (MVT) deposits: a critical requirement for genetic modelling. In: Geology and genesis of mineral deposits of Ireland. Irish Assoc Econ Geol, Dublin, pp 625–634
Sangster DF, Brook WA (1977) Primitive lead in an Australian Zn-Pb-Ba deposit. Nature (London) 270:423
Sano Y, Wakita H, Giggenbach W (1987) Island arc tectonics of New Zealand manifested in helium isotope ratios. Geochim Cosmochim Acta 51:1855–1860
Sass-Gustkiewicz M, Dzulynski S, Ridge JD (1982) The emplacement of zinc-lead sulfide ores in the Upper Silesian District – a contribution to the understanding of Mississippi Valley-type deposits. Econ Geol 77:392–412
Sassos MP (1986) Echo Bay's Lupin Mine. Eng Min Jour Dec 1986:24–28
Sato K, Sasaki A (1973) Lead isotopes of the Black Ores ("Kuroko") deposits of Japan. Econ Geol 68:547–552
Sato T (1974) Distribution and geological setting of the Kuroko deposits. In: Soc Min Geol Jpn (ed) Min Geol Spec Issue 6:1–9
Sato T (1975) Unilateral isotope variation of Miocene ore leads from Japan. Econ Geol 70:800–805
Sato T, Tanimura S, Ohtagaki T (1974) Geology and ore deposits of the Hokuroku District, Akita Prefecture. In: Ishihara S (ed) Geology of Kuroko deposits. Min Geol Spec Issue 6:11–18
Saunders JA, May ER (1986) Bessie G: a high-grade epithermal gold telluride deposit, La Plata county, Colorado, U.S.A. In: Macdonald AJ (ed) Proc Symp Gold '86, Toronto 1986, pp 445–456
Sawkins FJ (1964) Lead-zinc ore deposition in the light of fluid inclusion studies. Providencia Mine, Zacatecas, Mexico. Econ Geol 59:883–919
Sawkins FJ (1966) Ore genesis in the north Pennine orefield, in the light of fluid inclusion studies. Econ Geol 61:385–401
Sawkins FJ (1976a) Widespread continental rifting: some considerations of timing and mechanism. Geology 4:427–430
Sawkins FJ (1976b) Metal deposits related to intracontinental hotspot and rifting environments. J Geol 80:1028–1041

Sawkins FJ (1976c) Massive sulfide deposits in relation to geotectonics. Geol Assoc Can Spec Publ 14:221–240
Sawkins FJ (1977) Fluid inclusion studies of the Messina copper deposits, Transvaal, South Africa. Econ Geol 72:619–631
Sawkins FJ (1979) Fluid inclusion studies of copper-bearing breccia pipes, Inguaran Mine, Michoacan, Mexico. Econ Geol 74:924–928
Sawkins FJ (1980) Single-stage versus two-stage ore deposition in subduction-related volcano-plutonic arc. In: Proc 5th Quadrennial IAGOD Symp. Schweizerbarth, Stuttgart, pp 143–154
Sawkins FJ (1982a) Metallogenesis in relation to rifting. In: Palmason G (ed) Continental and oceanic rifts. Geodyn Ser 8:259–270
Sawkins FJ (1982b) The formation of Kuroko-type deposits viewed within the broader context of ore genesis theory. Min Geol 32:25–33
Sawkins FJ (1983) Tectonic controls of the time-space distribution of Proterozoic metal deposits. Geol Soc Am Mem 161:179–189
Sawkins FJ (1984) Ore genesis by episodic dewatering of sedimentary basins: application to giant Proterozoic lead-zinc deposits. Geology 12:451–454
Sawkins FJ (1986a) Some thoughts on the genesis of Kuroko-type deposits. In: Geology in the real world – the Kingsley Dunham volume. Inst Min Metall, London, pp 387–394
Sawkins FJ (1986b) The recognition of paleorifting in mid- to late-Proterozoic terranes.: implications for the exploration geologist. Trans Geol Soc S Afr 89:223–232
Sawkins FJ (1988) Anatomy of a world-class silver system, and implications for exploration: Fresnillo district, Zacatecas, Mexico. In: Silver – exploration, mining, treatment. Inst Min Metall London, pp 33–40
Sawkins FJ (1989) Anorogenic felsic magmatism, rift sedimentation, and giant Proterozoic Pb-Zn deposits. Geology 17:657–660
Sawkins FJ, Burke K (1980) Extensional tectonics and mid-Paleozoic massive sulfide occurrences in Europe. Geol Rundsch 69:349–360
Sawkins FJ, Kowalik J (1981) The source of ore metals at Buchans: magmatic versus leaching models. Geol Assoc Can Spec Pap 22:255–268
Sawkins FJ, Rye DM (1974) Relationship of Homestake-type gold deposits to iron-rich Precambrian sedimentary rocks. Trans Inst Min Metall 83: B56-B60
Sawkins FJ, Rye RO (1976) Fluid inclusion and stable isotope studies of the Caudalosa Ag deposit: evidence for the mixing of magmatic and meteoric fluids. Proc 4th IAGOD Symp, Varna, Bulg, pp 110–116
Sawkins FJ, Rye RO (1979) Additional geochemical data on the Messina copper deposits, Transvaal, South Africa. Econ Geol 74:684–689
Sawkins FJ, Scherkenbach D (1981) High copper contents of fluid inclusions in quartz from northern Sonora: implications for ore genesis theory. Geology 9:37–40
Sawkins FJ, O'Neil JR, Thompson JM (1979) Fluid inclusion and geochemical studies of gold vein deposits, Baguio District, Philippines. Econ Geol 74:1420–1434
Scherkenbach DA, Sawkins FJ, Seyfried WE, Jr. (1985) Geologic, fluid inclusion, and geochemical studies of the mineralized breccia at Cumobabi, Sonora, Mexico. Econ Geol 80:1566–1592
Schermer ER, Howell DG, Jones DL (1984) The origin of allochtonous terranes: perspectives on the growth and shaping of continents. Ann Rev Earth Planet Sci 12:107–131
Schermerhorn LJG (1975) Spilites, regional metamorphism and subduction in the Iberian Pyrite Belt: some comments. Geol Mijnbouw 54:23–25
Schidlowski M (1976) Archaean atmosphere and evolution of the terrestrial oxygen budget. In: Windley BF (ed) The early history of the earth. John Wiley & Sons, New York London, pp 525–535
Schiffries CM (1982) The petrogenesis of a platiniferous dunite pipe in the Bushveld Complex: infiltration metasomatism by a chloride solution. Econ Geol 77:1439–1453
Schmidt JM (1986) Stratigraphic setting and mineralogy of the Arctic volcanogenic massive sulfide prospect, Ambler district, Alaska. Econ Geol 81:1619–1643
Schmidt JM (1988) Mineral and whole-rock compositions of seawater-dominated hydrothermal alteration at the Arctic volcanogenic massive sulfide prospect, Alaska. Econ Geol 82:822–842

Scholl DW, Vallier TL, Stevenson AJ (1986) Terrane accretion, production, and continental growth: a perspective based on the origin and tectonic fate of the Aleutian-Bering Sea region. Geology 14:43–47

Schulz KL, Laberge GL (1986) The Wisconsin magmatic terrane: An early Proterozoic greenstone-granite terrane formed by plate tectonic processes. LPI Tech Rep 86-10:182–184

Schütz W, Ebneth J, Meyer K-D (1987) Trondjemites, tonalites, and diorites in the south Portugese zone and their relations to the vulcanites and mineral deposits of the Iberian Pyrite Belt. Geol Rundsch 76:201–212

Sclater JG, Von Herzen RP, Williams DL, Anderson RN, Klitgord K (1974) The Galapagos spreading center: heat flow on the north flank. R Astron Soc Geophys J 38:609–626

Sclater JG, Jaupart C, Galson D (1980) The heat flow through oceanic and continental crust and the heat loss of the earth. Rev Geophys Space Phys 18:269–311

Scott SD (1980) Geology and structural control of Kuroko-type massive sulphide deposits. Geol Assoc Can Spec Pap 20:705–722

Scott SD (1983) Basalt and sedimentary hosted seafloor polymetallic sulfide deposits and their ancient analogues. Proc Oceans '83/2:813–824

Scott SD (1985) Seafloor polymetallic sulfide deposits: modern and ancient. Mar Min 5:191–212

Scott SD (1987) Seafloor polymetallic sulfides: scientific curiosities or mines of the future. In: Teleki PG, Dobson MP, Moore JR, von Stackelberg U (eds) Marine minerals. NATO ASI Ser C 194:277–300

Scott SD, Edmond J, Lonsdale P (1983) Modern analogue of a Besshi-type massive sulfide deposit on the sea floor, Guaymas Basin, Gulf of California (Abstr). Am Inst Min Eng Annu Meet, Atlanta, Abstr with Prog: 84

Searle DL, Panayiotou A (1980) Structural implications in the evolution of the Troodos massif, Cyprus. In: Panayiotou A (ed) Ophiolites. Int Ophiolite Symp, Cyprus 1979, pp 50–60

Semenov EI (1974) Economic mineralogy of alkaline rocks. In: Sorenson H (ed) The alkaline rocks. John Wiley & Sons, New York London, pp 543–554

Sengor AMC, Burke K, Dewey JF (1978) Rifts at high angles to orogenic belts: tests for their origin and the upper Rhine graben as an example. Am J Sci 278:24–40

Seyfried WE, Jr. (1987) Experimental and theoretical constraints on hydrothermal alteration processes at mid-ocean ridges. Annu Rev Earth Planet Sci 15:317–335

Seyfried WE, Jr., Bischoff JL (1979) Low temperature basalt alteration by seawater: an experimental study at 70°C and 150°C. Geochim Cosmochim Acta 43:1937–1947

Seyfried WE, Jr., Janecky DR (1985) Heavy metal and reduced sulfur transport during subcritical and supercritical hydrothermal alteration of basalt: influence of fluid pressure and basalt composition and crystallinity. Geochim Cosmochim Acta 49:2545–2560

Seyfried WE, Jr., Mottl MJ (1982) Hydrothermal alteration of basalt by seawater under seawater-dominated conditions. Geochim Cosmochim Acta 45:985–1002

Shanks WC (1977) Massive sulfide deposits at divergent plate boundaries: origin and subsequent emplacement (Abstr). Geol Soc Am, Abstr with Prog 9:1170

Shanks WC, Bischoff JL (1977) Ore transport and deposition in the Red Sea geothermal system: a geochemical model. Geochim Cosmochim Acta 41:1507–1519

Shanks WC, Bischoff JL (1980) Geochemistry, sulfur isotope composition, and accumulation rate of Red Sea geothermal deposits. Econ Geol 75:445–459

Shanks WC, Seyfried WE, Jr. (1987) Stable isotope studies of vent fluids and chimney minerals, southern Juan de Fuca Ridge: sodium metasomatism and seawater sulfate reduction. J Geophys Res 92:11387–11399

Shanks WC III, Woodruff LG, Jilson GA, Jennings DS, Modene JS, Ryan BD (1987) Sulfur and lead isotope studies of stratiform Zn-Pb-Ag deposits, Anvil Range, Yukon; basinal brine exhalation and anoxic bottom-water mixing. Econ Geol 82:600–634

Sharp JE (1979) Cave Peak, a molybdenum-mineralized breccia pipe complex in Culberson County, Texas. Econ Geol 74:517–534

Shatski NS (1947) Structural correlations of platforms and geosynclinal folded regions. SSR Akad Nauk Izv Geol Ser 5:37–56

Shcherba GN, Mukanov KM, Mitryayeva NM (1980) Ore-formation in Atasu-type deposits. In: Proc 5th IAGOD Symp, Utah 1978, pp 337–345

Shelnutt JP, Noble DC (1985) Premineralization radial dikes of tourmalinized fluidization breccia, Julcani district, Peru. Econ Geol 80:1622–1632
Sheppard SMF, Gustafson LB (1976) Oxygen and hydrogen isotopes in the porphyry copper deposit at El Salvador, Chile. Econ Geol 71:1549–1559
Sheppard SMF, Taylor HP, Jr. (1974) Hydrogen and oxygen evidence for the origin of water in the Boulder Batholith and the Butte ore deposit, Montana. Econ Geol 69:926–946
Sheppard SMF, Nielsen RL, Taylor HP (1971) Hydrogen and oxygen isotope ratios in minerals from porphyry copper deposits. Econ Geol 66:515–542
Sheppard WA (1980) The ores and host rock geology of the Avoca mines, Co Wicklow, Ireland. Norges Geol Unders Bull 57:269–283
Sheridan MF (1979) Emplacement of pyroclastic flows: a review. In: Ash flow tuffs. Geol Soc Am Spec Pap 180:125–136
Shikazono N, Tsunakawa H (1982) K-Ar ages of Hosokura Pb-Zn and Sado Au-Ag vein-type deposits, northeastern part of Japan. Min Geol 32:479–482 (in Japanese with English Abstr)
Shimazaki H (1980) Characteristics of skarn deposits and related acid magmatism in Japan. Econ Geol 75:173–183
Shimazaki Y (1974) Ore minerals of the Kuroko-type deposits. In: Soc Min Geol Jpn (ed) Min Geol Spec Issue 6:311–322
Shreve RL, Cloos M (1986) Dynamics of sediment subduction, melange formation, and prism accretion. J Geophys Res 91:10229–10245
Siapno WP (1987) Nodule exploration: accomplishments, needs and problems. In: Teleki PG, Dobson MP, Moore JR, von Stackelberg U (eds) Marine minerals. Reidel, Dordrecht, pp 247–248
Sibbald TII, Munday RJC, Lewry JF (1977) Setting of uranium mineralization in northern Saskatchewan. Spec Publ Geol Soc Sask 3:51–98
Sibson RH (1987) Earthquake rupturing as a hydrothermal mineralizing agent. Geology 15:701–704
Sibson RH, Moore JM, Rankin AH (1975) Seismic pumping – a hydrothermal fluid transport mechanism. J Geol Soc London 131:653–659
Sibson RH, Robert F, Poulsen KH (1988) High angle reverse faults, fluid pressure cycling, and mesothermal gold-quartz deposits. Geology 16:551–555
Siddeley G, Araneda R (1986) The El Indio-Tambo gold deposits, Chile. In: Macdonald AJ (ed) Proc Symp Gold '86, Toronto 1986, pp 445–456
Silberman ML (1982) Hot-spring type, large tonnage, low-grade gold deposits. US Geol Surv Open File Rep 82–795
Silberman ML, McKee EH (1974) Ages of Tertiary volcanic rocks and hydrothermal precious-metal deposits in central and western Nevada. Nev Bur Mines Geol Rep 19:67–72
Silberman ML, Stewart JH, McKee EH (1976) Igneous activity, tectonics, and hydrothermal precious-metal mineralization in the Great Basin during Cenozoic time. Soc Min Eng AIME Trans 260:253–263
Silberman ML, MacKevett EM, Jr., Connor CL, Mathews A (1981) Metallogenic and tectonic significance of whole-rock potassium-argon ages of the Nikolai Greenstone, McCarthy Quadrangle, Alaska. In: Silberman ML, Field CW, Berry AL (eds) Proc Symp Mineral deposits of the Pacific Northwest. USGS Open File Rep 81-355:53–73
Sillitoe RH (1972a) A plate tectonic model for the origin of porphyry copper deposits. Econ Geol 67:184–197
Sillitoe RH (1972b) Formation of certain massive sulfide deposits at sites of seafloor spreading. Inst Min Metall Trans 81:B141–B148
Sillitoe RH (1973) The tops and bottoms of porphyry copper deposits. Econ Geol 68:799–815
Sillitoe RH (1974a) Tectonic segmentation of the Andes: implications for magmatism and metallogeny. Nature (London) 250:542–545
Sillitoe RH (1974b) Tin mineralization above mantle hotspots. Nature (London) 248:497–499
Sillitoe RH (1976a) A reconnaissance of the Mexican porphyry copper belt. Trans Inst Min Metall 85:B170–B189
Sillitoe RH (1976b) Andean mineralization: a model for the metallogeny of convergent plate margins. Geol Assoc Can Spec Pap 14:59–100

Sillitoe RH (1977) Metallic mineralization affiliated to subaerial volcanism: a review. Geol Soc London Spec Publ 7:99–116
Sillitoe RH (1978) Metallogenic evolution of a collisional mountain belt in Pakistan: a preliminary analysis. J Geol Soc London 135:377–387
Sillitoe RH (1979) Some thoughts on gold-rich porphyry copper deposits. Mineral Deposita 14:161–174
Sillitoe RH (1980a) Types of porphyry molybdenum deposits. Min Mag (Tokyo) 142:550–553
Sillitoe RH (1980b) Are porphyry copper and Kuroko-type massive sulfide deposits incompatible? Geology 8:11–14
Sillitoe RH (1980c) Cauldron subsidence as a possible inhibitor of porphyry copper formation. In: Granitic magmatism and related mineralization. Mining Geol Spec Issue 8:85–93
Sillitoe RH (1980d) Strata-bound ore deposits related to infra-Cambrian rifting along northern Gondwanaland. In: Proc 5th IAGOD Symp, Utah, pp 163–172
Sillitoe RH (1981a) Ore deposits in Cordilleran and island-arc settings. AR Geol Soc Digest 14:49–70
Sillitoe RH (1981b) Regional aspects of the Andean porphyry copper belt in Chile and Argentina. Trans Inst Min Metall 90:B15–B36
Sillitoe RH (1982) Extensional habits of rhyolite-hosted massive sulfide deposits. Geology 10:403–407
Sillitoe RH (1983a) Enargite-bearing massive sulfide deposits high in porphyry copper systems. Econ Geol 78:348–352
Sillitoe RH (1983b) Unconventional metals in porphyry deposits. In: Shanks WC (ed) Cameron volume on unconventional mineral deposits. AIME, New York, pp 207–221
Sillitoe RH (1985) Ore-related breccias in volcanoplutonic arcs. Econ Geol 80:1467–1514
Sillitoe RH (1987) Copper, gold and subduction: a trans-Pacific perspective. Pac Rim Congr 87. Gold Coast Aust, pp 399–403
Sillitoe RH (1988a) Epochs of intrusion related copper mineralization in the Andes. In: Magmatic evolution of the Andes. J S Am Earth Sci 1:89–108
Sillitoe RH (1988b) Gold and silver deposits in porphyry systems. In: Bulk-mineable precious metal deposits of the western United States. Geol Soc Nev Symp, Reno, pp 233–258
Sillitoe RH, Bonham HF, Jr. (1984) Volcanic landforms and ore deposits. Econ Geol 79:1286–1298
Sillitoe RH, Gappe IM, Jr. (1984) Philippine porphyry copper deposits: geologic setting and characteristics. Commun Coordination Joint Prosp Resourc (CCOP) Tech Publ 14:1–89
Sillitoe RH, Sawkins FJ (1971) Geologic, mineralogic, and fluid inclusion studies relating to the origin of copper-bearing tourmaline breccia pipes, Chile. Econ Geol 66:1028–1041
Sillitoe RH, Halls C, Grant NJ (1975) Porphyry tin deposits in Bolivia. Econ Geol 70:913–927
Sillitoe RH, Baker EM, Brook WA (1984) Gold deposits and hydrothermal eruption breccias associated with a maar volcano at Wau, Papua New Guinea. Econ Geol 79:638–655
Simmons SF, Sawkins FJ (1983) Mineralogic and fluid inclusion studies of the Washington Cu-Mo-W breccia pipe, Sonora, Mexico. Econ Geol 78:521–526
Simmons SF, Gemmell JB, Sawkins FJ (1988) The Santo Nino silver-lead-zinc vein Fresnillo district, Zacatecas, Part II: physical and chemical nature of ore forming solutions. Econ Geol 83:1619–1641
Simpson ESW (1970) The anorthosite of southern Angola: a review of present data. In: Clifford J, Gass I (eds) African magmatism and tectonics. Oliver & Boyd, Edinburgh, pp 89–96
Simpson PR, Gang Y, Gao B (1987) Metallogeny, magmatism and structure in Jiangxi Province, China: a new interpretation. Inst Min Metall Trans 96:B77–B83
Sims PK, Card KD, Lumbers SB (1981) Evolution of early Proterozoic basins of the Great Lakes region. In: Proterozoic basins of Canada. Geol Surv Can Pap 81–10:379–397
Sinclair AJ, Drummond AD, Carter NC, Dawson KM (1982) A preliminary analysis of gold and silver grades of porphyry-type deposits in western Canada. In: Levison AA (ed) Precious metals in the northern Cordillera. Assoc Explor Geochem 157–172
Skinner BF, White DE, Rose HJ, Mays RE (1967) Sulfides associated with the Salton Sea geothermal brine. Econ Geol 62:316–330

Slack JF (1980) Multistage vein ores of the Lake City district, western San Juan Mountains, Colorado. Econ Geol 75:963–991
Slaughter AL (1968) The Homestake mine. In: Ridge JD (ed) Ore deposits of the United States 1933–1967 (Graton-Sales Vol). New York Am Inst Min Metall Petrol Eng, pp 1436–1459
Sleep NH, Snell NS (1976) Thermal contraction and flexure of mid-continent and Atlantic marginal basins. Geophys J R Astron Soc 45:125–154
Sleep NH, Windley BF (1982) Archean plate tectonics: constraints and inferences. J Geol 40:363–380
Sleep NH, Morton JL, Burns LE, Wolery TJ (1983) Geophysical constraints on the volume of hydrothermal flow at ridge crests. In: Rona PA, Bostrom K, Laubier L, Smith KL, Jr. (eds) Hydrothermal processes at seafloor spreading centers. Plenum, New York, pp 53–70
Smirnov VI (1970) Pyritic deposits, Parts 1 and 2. Int Geol Rev 12:881–908; and 1039–1058
Smirnov VI (ed) (1977) Ore deposits of the USSR. Pitman, London
Smith DAM (1965) The geology of the area around the Khan and Swakop Rivers in South West Africa. S Afr Geol Surv Dep Mines Johannesburg, pp 1–113
Smith DM, Jr., Albinson T, Sawkins FJ (1982) Geologic and fluid inclusion studies of the Tayoltita silver-gold vein deposits, Durango, Mexico. Econ Geol 77:1120–1145
Smith GI (1979) Subsurface stratigraphy and geochemistry of Late Quaternary evaporites, Searles Lake, California. US Geol Surv Prof Pap 1043:1–130
Smith RB, Christiansen RL (1980) Yellowstone Park as a window on the earth's interior. Sci Am 242:84–95
Smith TJ, Cloke PL, Kesler SE (1984) Geochemistry of fluid inclusions from the McIntyre-Hollinger gold deposit, Timmins, Ontario. Econ Geol 79:1265–1285
Smith TK, Loyd RC, Schull HW (1987) Precious metal deposits of the central California coast ranges and Sierra Nevada foothills region. In: Johnson JL (ed) Guidebook for field trips, bulk-mineable precious metal deposits of the western United States. Geol Soc Nev Symp, Reno 1987, pp 179–222
Snyder WS, Dickinson WR, Silberman MC (1976) Tectonic implications of space-time patterns of Cenozoic magmatism in the western United States. Earth Planet Sci Lett 32:91–106
So C-S, Shelton KL, Rye DM (1983) Geologic, sulfur isotopic, and fluid inclusion study of the Sang Jeon tungsten mine, Republic of Korea. Econ Geol 78:1057–1063
Sohnge PG (1946) The geology of the Messina copper mines and surrounding country. S Afr Geol Surv Mem 40:1–280
Sokolov GA, Grigorev VM (1977) Deposits of iron. In: Smirnov VI (ed) Ore deposits of the USSR, vol 1. Pittman, London, pp 7–113
Soler E (1973) L'association spilites-quartz keratophyres du sud-oest de la Peninsule Iberique. Geol Mijnbouw 52:277–288
Soler E (1980) Spilites et métallogénie: la province pyritocuprifère de Huelva (SW Espagne). Mem Sci Terre 39:1–461
Solomon M (1976) "Volcanic" massive-sulfide deposits and their host rocks – a review and an explanation. In: Wolf KH (ed) Handbook of stratabound and stratiform ore deposits, vol 6. Elsevier, Amsterdam, pp 21–54
Solomon M (1981) An introduction to the geology and metallic ore deposits of Tasmania. Econ Geol 76:194–208
Sood MK, Wagner RJ, Markazi HD (1986) Stratabound copper deposits in east south-central Alaska. In: Friedrich GE, Genkin AD, Naldrett AJ, Ridge JD, Sillitoe RH, Vokes FM (eds) Geology and metallogeny of copper deposits. Springer, Berlin Heidelberg New York Tokyo, pp 422–442
Souch BE (1969) The sulfide ores of Sudbury: their particular relationship to a distinctive inclusion-bearing facies of the Nickel Irruptive. Econ Geol Monogr 4:252–261
Southwick DL, Halls HC (1987) Compositional characteristics of the Kenoran-Kabetogama dyke swarm (Early Proterozoic), Minnesota and Ontario. Can J Earth Sci 24:2197–2205
Southwick DL, Sims PK (1979) The Vermilion granitic complex – a new name for old rocks in northern Minnesota. U.S. Geol Surv Shorter Contrib Mineral Petrol A1–A11
Sparks RSJ, Wright JV (1979) Welded air fall tuffs. In: Ash fall tuffs. Geol Soc Am Spec Pap 180:155–166

Spence CD, de Rozen-Spence AF (1975) The place of sulfide mineralization in the volcanic sequence at Noranda, Quebec. Econ Geol 70:90–101
Spooner ETC, Bray CJ (1977) Hydrothermal fluids of seawater salinity in ophiolitic sulfide ore deposits in Cyprus. Nature (London) 266:808–812
Stagman JG (1978) An outline of the geology of Rhodesia. Geol Surv Rhod Bull 80:1–126
Stakes D, Vanko DA (1986) Multistage hydrothermal alteration of gabbroic rocks from the failed Mathematician Ridge. Earth Planet Sci Lett 79:75–92
Stakes DS (1989) The mineralogy, structure and oxygen isotopic characteristics of marginal basin-island-arc crust: the diachronous hydrothermal system of the northern Semail Ophiolite (in prep)
Stanton RL (1972) Ore petrology. McGraw Hill, New York, 713 pp
Stein HJ, Hannah JL (1985) Movement and origin of ore fluids in Climax-type systems. Geology 13:469–474
Stein HJ, Kish SA (1985) The timing of ore formation in southeast Missouri: Rb-Sr glauconite dating at the Magmont mine, Viburnum Trend. Econ Geol 80:739–753
Stemprok M (1980) Tin and tungsten deposits of the west central European Variscides. In: Proc 5th IAGOD Symp, Utah, pp 495–512
Stephens MB, Swinden HS, Slack JF (1984) Correlation of massive sulfide deposits in the Appalachian-Caledonian orogen on the basis of paleotectonic setting. Econ Geol 79:1442–1487
Stern TA (1987) Asymmetric back-arc spreading, heat flux and structure associated with the central volcanic region of New Zealand. Earth Planet Sci Lett 85:265–276
Sterne EJ, Zantop H, Reynolds RC (1984) Clay mineralogy and carbon-nitrogen geochemistry of the Lik and Competition Creek zinc-lead-silver prospects, De Long Mountains, Alaska. Econ Geol 79:1406–1411
Steven TA, Eaton GP (1975) Environments of ore deposition in the Creede mining district, San Juan Mountains, Colorado: 1. Geologic, hydrologic and geophysical setting. Econ Geol 70:1023–1037
Steven TA, Lipman PW (1976) Calderas of the San Juan volcanic field, southwestern Colorado. US Geol Surv Prof Pap 958:35 pp
Steven TA, Ratte JC (1960) Geology and ore deposits of the Summitville district, San Juan Mountains, Colorado. US Geol Surv Prof Pap 343:1–70
Steven TA, Laedke RG, Lipman PW (1974) Relation of mineralization to calderas in the San Juan volcanic field, southwestern Colorado. J Res US Geol Surv 2:405–409
Stevens BJP, Barnes RG, Brown RE, Stroud WJ, Willis IL (1988) The Willyama Supergroup in the Broken Hill and Eurowie Blocks, New South Wales. Precambrian Res 40/41:298–328
Stewart PW (1987) Geology and genesis of granitoid clasts in the MacLean Extension transported orebody. In: Kirkham RV (ed) Buchans geology, Newfoundland. Geol Surv Can Pap 86-24:149–176
Stillman CJ, Williams CT (1978) Geochemistry and tectonic setting of some Upper Ordovician volcanic rocks in east and southeast Ireland. Earth Planet Sci Lett 41:288–310
Stoffregen R (1987) Genesis of acid-sulfate alteration and Au-Cu-Ag mineralization at Summitville, Colorado. Econ Geol 82:1575–1591
Stone JB, McCarthy JC (1948) Mineral and metal variations in the veins of Fresnillo, Zacatecas, Mexico. AIME Trans 148:91–106
Stone JG (1959) Ore genesis in the Naica district, Chihuahua, Mexico. Econ Geol 54:1002–1034
St-Onge MR, Lucas SB, Scott DJ, Begin NJ (1988) Thin-skinned imbrication and subsequent thick-skinned folding of rift-fill, transitional-crust, and ophiolite suites in the 1.9 Ga Cape Smith belt, northern Quebec. In: Current research, Part A. Geol Surv Can Pap 88-1A: pp 1–18
Stowe CW (1974) Alpine-type structures in the Rhodesian basement complex at Selukwe. J Geol Soc London 130:411–426
Stowe CW (1984) The early Archaean Selukwe nappe, Zimbabwe. In: Precambrian Tectonics Illustrated. Kroner A and Greiling R (eds) Scheizerbartsche Verlagsbuchhandlung, Stuttgart, pp 41–56
Stowe CW (ed) (1987a) Evolution of chromium ore fields. Van Nostrand Reinhold, New York, 340 pp

Stowe CW (ed) (1987b) Chromite host rocks and their tectonic environments. In: Evolution of chromium ore fields. Van Nostrand Reinhold, New York, pp 23–48
Stowe CW (ed) (1987c) Chromite deposits of the Shurugwi greenstone belt. In: Evolution of the chromium ore fields. Van Nostrand Reinhold, New York, pp 71–88
Strachan DM, Moffett R (1985) Geology of the Lupin gold deposit, N.W.T. Preprint 11 NW Min Assoc 91st Annu Conv, Spokane
Strong DF, Saunders CM (1988) Ophiolitic sulfide mineralization at Tilt Cove, Newfoundland: controls by upper mantle and crustal processes. Econ Geol 83:239–255
Stuckless JS, Troeng B (1984) Uranium mineralization in response to regional metamorphism at Lilljuthatten, Sweden. Econ Geol 79:509–528
Stumpfl EG, Rucklidge JC (1982) The platiniferous dunite pipes of the eastern Bushveld. Econ Geol 77:1419–1431
Stumpfl EE, Clifford TN, Burger AJ, van Zyl D (1976) The copper deposits of the O'okiep District, South Africa. Mineral Deposita 11:46–70
Sturt BA, Roberts D, Furnes HA (1984) A conspectus of Scandinavian Caledonian ophiolites. In: Gass IG, Lippard SJ, Shelton AW (eds) Ophiolites and oceanic lithosphere. Geol Soc. Blackwell, Oxford, pp 381–392
Styles MT, Rundle CC (1984) The Rb-Sr isochron age of the Kennack Gneiss and its bearing on the age of the Lizard Complex, Cornwall. J Geol Soc London 141:15–19
Sutherland Brown A (ed) (1976) Porphyry deposits of the Canadian Cordillera. Can Inst Min Metall Spec Vol 15
Sutherland Brown A, Cathro RJ, Panteleyev A, Ney CS (1971) Metallogeny of the Canadian Cordillera. Can Inst Min Metall Trans 74:121–145
Sverjensky DA (1981) The origin of a Mississippi Valley-type deposit in the Viburnum Trend, southeast Missouri. Econ Geol 76:1848–1872
Sverjensky DA (1984) Oil field brines as ore-forming solutions. Econ Geol 79:23–37
Sverjensky DA (1986) Genesis of Mississippi Valley-type lead-zinc deposits. Annu Rev Earth Planet Sci 14:177–199
Sverjensky DA (1987) The role of migrating oil field brines in the formation of sediment-hosted Cu-rich deposits. Econ Geol 81:1130–1141
Swager CP (1985) Syndeformational carbonate-replacement model for the copper mineralization at Mount Isa, northwest Queensland: a microstructural study. Econ Geol 80:107–125
Swanson CO (1925) The genesis of the Texada Island magnetite deposits. Geol Surv Can Summary, Rep 1924 A:106–144
Swinden HS, Strong DF (1976) A comparison of plate tectonic models of metallogenesis in the Appalachians, the North America Cordillera, and the east Australian Paleozoic. Geol Assoc Can Spec Pap 14:443–471
Swinden HS, Thorpe RI (1984) Variations in style of volcanism and massive sulfide deposition in early and middle Ordovician island-arc sequences of the Newfoundland Central Mobile Belt. Econ Geol 79:1596–1619
Sykes LR (1978) Intraplate seismicity, reactivation of existing zones of weakness, alkaline magmatism, and other tectonism postdating continental fragmentation. Rev Geophys Space Phys 16:621–688
Sykes LR (1980) Earthquakes and other processes within lithospheric plates and the reactivation of pre-existing zones of weakness. Geol Assoc Can Spec Pap 20:215–238
Takahashi M, Aramaki S, Ishihara S (1980) Magnetite-series/ilmenite series vs. I-type/S-type granitoids. In: Granitic magmatism and related mineralization. Min Geol Spec Issue 8:13–28
Tamrazyn GP (1971) Siberian continental drift. Tectonophysics 11:433–460
Tankard AJ, Jackson MPA, Eriksson KA, Hobday DK, Hunter DR, Minter WEL (1982) Crustal evolution of Southern Africa. Springer, Berlin Heidelberg New York, 523 pp
Tankut A (1980) The Orhaneli massif, Turkey. In: Panayiotou A (ed) Ophiolites. Proc Int Ophiolite Symp, Cyprus 1979, pp 702–713
Tapponnier P, Peltzer G, LeDain AY, Armijo R (1982) Propagating extrusion tectonics in Asia: new insights from simple experiments with plasticine. Geology 10:611–617
Tarney J, Windley BF (1978) Chemistry, thermal gradients and evolution of the lower continental crust. J Geol Soc London 134:153–172

Tarney J, Windley BF (1981) Marginal basins throughout geologic time. Philos Trans R Soc London Ser A 301:217–231

Tarney J, Dalziel I, DeWit M (1976) Marginal basin 'Rocas Verdes' complex from S. Chile: a model for Archean greenstone belt formation. In: Windley BF (ed) The early history of the earth. John Wiley & Sons, New York London, pp 131–146

Taube A (1986) The Mount Morgan gold-copper mine and environment: a volcanogenic massive sulfide deposit with penecontemporaneous faulting. Econ Geol 81:1322–1340

Taylor BE (1986) Magmatic volatiles: isotopic variations of C, H, and S. Rev Mineral Stable Isotopes High Temp Geol Processes 16:185–226

Taylor BE, O'Neil JR (1977) Stable isotope studies of metasomatic Ca-Fe-Al-Si skarns and associated metamorphic and igneous rocks, Osgood Mountains, Nevada. Contrib Mineral Petrol 63:1–50

Taylor GR (1976) Styles of mineralization in the Solomon Islands – a review. In: Glasby GP, Katz HR (eds) Marine geophysical investigations in the southwest Pacific and adjacent areas. ESCAP COOP/SOPAC Tech Bull 2:83–91

Taylor HP, Jr. (1973) O^{18}/O^{16} evidence for meteoric-hydrothermal alteration and ore deposition in the Tonapah, Comstock Lode, and Goldfield mining districts, Nevada. Econ Geol 68:747–764

Taylor HP, Jr. (1979) Oxygen and hydrogen isotope relationships in hydrothermal ore deposits. In: Barnes HL (ed) Geochemistry of hydrothermal ore deposits, 2nd edn. John Wiley & Sons, New York, pp 236–277

Taylor RG (1979) Geology of tin deposits. Elsevier, Amsterdam, 543 pp

Templeman-Kluit D (1981) Geology and mineral deposits of the southern Yukon. In: Yukon geology and exploration 1979–80. Dep Indian Aff Can, Whitehorse, pp 7–31

Thacker JL, Anderson KH (1977) The geologic setting of the southeast Missouri lead district – regional geologic history, structure and stratigraphy. Econ Geol 72:339–348

Thayer TP (1942) Chromite resources of Cuba. US Geol Surv Bull 935-A:1–74

Thayer TP (1964) Principal features and origin of chromite deposits and some observations of the Guleman-Soridag district, Turkey. Econ Geol 59:1479–1524

Thayer TP (1969) Gravity differentiation and magmatic re-emplacement of podiform chromite deposits. In: Wilson HDB (ed) Magmatic ore deposits. Econ Geol Monogr 4:132–146

Thein J (1985) Geochemistry and origin of the stratiform sulfide ore deposit of Meggen (Middle Devonian, Rheinisches Schiefergebirge). Geol Jahrb D70:37–51

Theodore TG, Howe SS, Blake DW, Wotruba PR (1986) Geochemical and fluid zoning in the skarn environment at the Tomboy-Minnie gold deposits, Lander County, Nevada. J Geochem Explor 25:99–128

Thiessen R, Burke K, Kidd WSF (1979) African hotspots and their relation to the underlying mantle. Geology 7:263–266

Thomas JA, Galey JT, Jr. (1982) Exploration and geology of the Mt. Emmons molybdenite deposits, Gunnison County, Colorado. Econ Geol 77:1085–1104

Thomas MD, Gibb RA (1985) Proterozoic plate subduction and collision: processes for reactivation of Archean crust in the Churchill Province. Geol Assoc Canada Spec Pap 28:263–280

Thompson TB, Arehardt GB, Johansing RJ, Osborne LW, Jr, Landis GP (1983) Geology and geochemistry of the Leadville district, Colorado. In: Proc Denver Region Explor Geol Soc Symp. The genesis of Rocky Mountain ore deposits: changes with time and tectonics, pp 101–115

Thompson TB, Arehart GB Origin of ore deposits in the Leadville district, Colorado. Part 1. Geologic studies of orebodies and wallrocks. In: Carbonate-hosted sulfide deposits of the Central Colorado Mineral Belt. Econ Geol Monogr (in press)

Thompson TB, Beaty DW Origin of the ore deposits in the Leadville district, Colorado. Part II. Oxygen, hydrogen, carbon, sulfur and lead isotope data and development of a genetic model. In: Carbonate-hosted sulfide deposits of the Central Colorado Mineral Belt. Econ Geol Monogr (in press)

Thompson TB, Trippel AD, Dwelley PC (1985) Mineralized veins and breccias of the Cripple Creek district, Colorado. Econ Geol 80:1669–1689

Thurlow JG, Swanson EA (1981) Geology and ore deposits of the Buchans area, central Newfoundland. Geol Assoc Can Spec Pap 22:113–142
Thurlow JG, Swanson EA (1987) Stratigraphy and structure of the Buchans Group. In: Kirkham RV (ed) Buchans geology, Newfoundland. Geol Surv Can Pap 86-24:35–46
Thurlow JG, Swanson EA, Strong DF (1975) Geology and lithogeochemistry of the Buchans polymetallic sulfide deposits, Newfoundland. Econ Geol 70:130–144
Thy P (1977) Petrogenetic implications of mineral crystallization trends of Troodos cumulates, Cyprus. Geol Mag 124:1–11
Thy P, Brooks CK, Walsh JN (1985) Tectonic and petrogenetic implications of major and rare earth element chemistry of Troodos glasses, Cyprus. Lithos 18:165–178
Tikkanen GD (1986) World resources of and supply of lead and zinc. In: Bush WR (ed) Economics of internationally traded minerals. Soc Min Eng Inc, Littleton, Col, pp 242–250
Tilton GR, Hopson CA, Wright JG (1981) Uranium-lead isotopic ages of the Semail ophiolite with applications to Tethyan ocean ridge tectonics. J Geophys Res 86:2763–2775
Tingley JV, Berger BR (1985) Lode gold deposits of Round Mountain, Nevada. Nev Bur Mines Geol Bull 100:62 pp
Tischendorf G, Schust F, Lange H (1978) Relation between granites and tin deposits in the Erzegebirge, GDR. Metallization associated with acid magmatism. IGCP 3:123–138
Titley SR, Beane RE (1981) Porphyry copper deposits, Part 1: geologic settings, petrology, and tectogenesis. Econ Geol 75th Anniv Vol, pp 214–234
Toens PD (1975) The geology of part of the southern foreland of the Damara Orogenic Belt in S.W.A. and Botswana. Geol Rundsch 64:175–192
Tokunaga M, Honma H (1974) Fluid inclusions in the minerals from some Kuroko deposits. In: Soc Min Geol Jpn (ed) Min Geol Spe Issue 6:385–388
Townend R, Ferreira PM, Franke ND (1980) Caraiba, new copper deposit in Brazil. Trans Inst Min Metall 89: B159–164
Tremblay LP (1976) Geology of northern Contwoyto Lake area, District of MacKenzie. Geol Surv Can Mem 381
Trendall AF (1973) Iron-formations of the Hamersley Group in western Australia: type examples of varved Precambrian evaporites. In: Genesis of Precambrian iron and manganese deposits. Proc Kiev Symp 1970 UNESCO, Paris, pp 257–268
Trendall AF, Blockley JG (1970) The iron formations of the Precambrian Hamersley Group, western Australia. W Aust Geol Surv Bull 119:366 pp
Trettin HP (1979) Middle Ordovician to Lower Devonian deep-water succession at southeastern margin of Hazen Trough, Canon Fiord, Ellsemere Island. Geol Surv Can Bull 272:1–84
Tu KC, Wang ZG, Yu XY (1980) Genesis of granitic rocks in South China and related mineralization. In: Granitic magmatism and related mineralization. Min Geol Spec Issue 8:189–196
Tuach J, Kennedy MJ (1978) The geologic setting of the Ming and other sulfide deposits, Consolidated Rambler Mines, northeast Newfoundland. Econ Geol 73:192–206
Tupper WM (1969) The geology of the Orvan Brook sulfide deposits, Restigouche County, New Brunswick. Geol Surv Can Pap 66-59:1–11
Turcotte DL, Burke KCA (1978) Global sea-level changes and the thermal structure of the earth. Earth Planet Sci Lett 41:341–346
Turneaure FS (1935) The tin deposits of Llallagua, Bolivia. Econ Geol 30:14–60; and 170–190
Turneaure FS (1971) The Bolivian tin-silver province. Econ Geol 66:215–225
Turneaure FS, Welker KK (1974) The ore deposits of the eastern Andes of Bolivia. The Cordillera Real. Econ Geol 42:595–625
Turner DC, Webb PK (1974) The Daura igneous complex, N. Nigeria: a link between the Younger Granite district of Nigeria and S. Niger. J Geol Soc London 130:71–77
Turner RJW, Einaudi MT (eds) (1986) The genesis of stratiform sediment-hosted lead and zinc deposits: conference proceedings. Stanford Univ Publ Geol Sci 20:227 pp
Tweto O, Sims PK (1963) Precambrian ancestry of the Colorado mineral belt. Geol Soc Am Bull 74:991–1014
Ueda A, Sakai H (1984) Sulfur isotope study of Quaternary volcanic rocks from the Japanese Islands arc. Geochim Cosmochim Acta 48:1837–1848

Umeji AC, Caen-Vachette (1983) Rb-Sr isochron from Gboko and Ikuyen rhyolites and its implications for the age and evolution of the Benue Trough, Nigeria. Geol Mag 120:529–533
Upadhyay HD, Strong DF (1973) Geological setting of the Betts Cove copper deposits, Newfoundland: an example of ophiolite sulfide mineralization. Econ Geol 68:161–167
Urabe T (1985) Aluminous granite as a source magma of hydrothermal ore deposits: an experimental study. Econ Geol 80:148–157
Urabe T (1987) Kuroko deposit modeling based on magmatic hydrothermal theory. Min Geol 37:159–176
Urabe T, Sato T (1978) Kuroko deposits of the Kosaka Mine, northeast Honshu, Japan – products of submarine hotsprings on Miocene sea floor. Econ Geol 73:161–179
Urabe T, Scott SD, Hattori K (1983) A comparison of footwall-rock alteration and geothermal systems beneath some Japanese and Canadian volcanogenic massive sulfide deposits. Econ Geol Monogr 5:345–364
Urashima Y, Saita M, Sato E (1981) The Iwato gold ore deposits, Kagoshima Prefecture, Japan. Min Geol Spec Issue 10
US Geological Survey Juan de Fuca Study Group (ed) (1986) Submarine fissure eruptions and hydrothermal vents on the southern Juan de Fuca Ridge: preliminary observations from the submarine ALVIN. Geology 14:823–827
Uyeda S, Nishiwaki C (1980) Stress field, metallogenesis and mode of subduction. In: Strangway DW (ed) The continental crust and its mineral deposits. Geol Assoc Can Spec Pap 20:323–339
Vail JR (1977) Further data on the alignment of basic igneous intrusive complexes in southern and eastern Africa. Trans Geol Soc S Afr 80:87–92
Vail JR (1985) Pan-African (late Precambrian) tectonic terranes in the reconstruction of the Arabian-Nubian Shield. Geology 13:839–842
Valentine JW, Moores EM (1972) Global tectonics and the fossil-record. J Geol 80:167–184
Valliant RI, Bradbrook CJ (1986) Relationship between stratigraphy, faults and gold deposits, Page-Williams mine, Hemlo, Ontario, Canada. In: Proc Gold '86 Symp, Toronto, pp 355–361
Van Alstine RE (1976) Continental rifts and lineaments associated with major fluorspar districts. Econ Geol 71:977–987
Van Biljon WJ (1980) Plate-tectonics and the origin of the Witwatersrand basin. In: Proc 5th IAGOD Symp, Utah 1979, pp 217–226
Vance RK, Condie KC (1987) Geochemistry of footwall alteration associated with the early Proterozoic United Verde massive sulfide deposit, Arizona. Econ Geol 82:571–586
Van Eden JG (1978) Stratiform copper and zinc mineralization in the Cretaceous of Angola. Econ Geol 73:1154–1160
Vanko DA (1986) High-chlorine amphiboles from oceanic rocks: product of highly saline hydrothermal fluids? Am Mineral 71:51–59
Van Schmus WR, Hinze WJ (1985) The Midcontinent Rift system. Annu Rev Earth Planet Sci 13:345–383
Van Staal CR (1987) Tectonic setting of the Tetagouche Group in northern New Brunswick: implications for plate tectonic models of the northern Appalachians. Can J Earth Sci 24:1329–1351
Van Staal CR, Williams PF (1984) Structure, origin, and concentration of the Brunswick 12 and 6 orebodies. Econ Geol 79:1669–1693
Van Straaten HP (1984) Gold mineralization in Tanzania – a review. In: Foster RP (ed) Gold '82: the geology, geochemistry and genesis of gold deposits. Balkema, Rotterdam, pp 673–685
van Vuuren CJJ (1986) Regional setting and structure of the Rosh Pinah zinc-lead deposit, South West Africa/Namibia. In: Anhaeusser CR, Maske S (eds) Mineral deposits in southern Africa. Geol Soc S Afr 2:1593–1607
Varekamp JC, Luhr JF, Prestegaard KL (1984) The 1982 eruptions of El Chichon volcano (Chiapas, Mexico): character of the eruptions, ash-fall deposits, and gas phase. J Volcan Geothem Res 23:39–68
Varentsov IM (1964) Sedimentary manganese ores. Elsevier, Amsterdam, 119 pp
Varga RJ, Moores EM (1985) Spreading structure of the Troodos ophiolite, Cyprus. Geology 13:846–850

Vermaak CF (1976) The Merensky Reef – thoughts on its environment and genesis. Econ Geol 71:1270–1298
Vermaak CF (1981) Kunene Anorthosite complex. In: Hunter DR (ed) Precambrian of the southern hemisphere, Elsevier, Amsterdam, pp 578–598
Vermaak CF, Von Gruenewaldt G (1986) Introduction to the Bushveld Complex. In: Anhaeusser CR, Maske S (eds) Mineral deposits of southern Africa. Geol Soc S Afr 2:1021–1029
Verwoerd WJ (1986) Mineral deposits associated with carbonatites and alkaline rocks. In: Anhaeusser CR, Maske S (eds) Mineral deposits of southern Africa. Geol Soc S Afr 2:2173–2191
Vetter SK, Stakes DS (1988) The northern Semail plutonic suite: field and trace element evidence for repeated magma injection in the construction of back-arc crust. Troodos 87 Ophiolites and ocean crust special vol (in press)
Vikre PG (1987) Fluid-mineral relationships in the Comstock Lode, Storey, Washoe, and Lyon Counties, Nevada, U.S.A. Pac Rim Congr 87:603–606
Vikre PG, McKee EH, Silberman ML (1988) Chronology of Miocene hydrothermal and igneous events in the western Virginia Range, Washoe, Storey, and Lyon Counties, Nevada. Econ Geol 83:864–874
Viljoen MJ, Scoon RN (1985) The distribution and main geologic features of discordant bodies of iron-rich ultramafic pegmatite in the Bushveld Complex. Econ Geol 80:1109–1128
Viljoen RP, Saager R, Viljoen MJ (1969) Metallogenesis and ore control in the Steynsdorp goldfield, Barberton Mountain Land, South Africa. Econ Geol 64:778–797
Vine FJ (1966) Spreading of the ocean floor: new evidence. Science 154:1405–1410
Vine FJ, Smith AG (1981) Extensional tectonics associated with convergent plate boundaries. Philos Trans R Soc London on Ser A 300:217–442
Vineyard JD (1977) Preface to Viburnum Trend issue. Econ Geol 72:337–338
Voggenreitter W, Hotzl H, Mechie J (1988) Low-angle detachment origin for the Red Sea Rift System? Tectonophys 150:51–75
Vokes FM (1968) A review of the metamorphism of sulphide ore deposits. Earth Sci Rev 5:99–143
Vokes FM (1969) Regional metamorphism of the Paleozoic geosynclinal sulfide ore deposits of Norway. Trans Inst Min Metall 77:B53–B59
Vokes FM (1973) Metallogeny possibly related to continental breakup in southwest Scandinavia. In: Tarling DH, Runcorn SK (eds) Implications of continental drift to the earth sciences, vol 1. Academic Press, New York London, pp 573–579
Vokes FM (1976) Caledonian massive sulfide deposits in Scandinavia: a comparative review. In: Wolf KH (ed) Handbook of strata-bound and stratiform ore deposits, vol 6. Elsevier, Amsterdam, pp 79–127
Vokes FM (1980) Some aspects of research into the Caledonian stratabound sulphide deposits of Scandinavia. Norges Geol Unders Bull 57:77–93
Vokes FM, Gale GH (1976) Metallogeny relatable to global tectonics in southern Scandinavia. Geol Assoc Can Spec Pap 14:413–441
Von der Borch CC (1980) Evolution of late Proterozoic to early Paleozoic Adelaide Foldbelt, Australia: comparison with post-Permian rifts and passive margins. Tectonophysics 70:115–134
von Drach V, Marsh BD, Wasserberg GJ (1986) Nd and Sr isotopes in the Aleutians: multicomponent parenthood of island-arc magmas. Contr Min Pet 92:13–34
Von Gruenewaldt G (1977) The mineral resources of the Bushveld Complex. Mineral Sci Eng 9:83–95
Von Gruenewaldt G (1979) A review of some recent concepts of the Bushveld Complex with particular reference to sulfide mineralization. Can Mineral 17:233–256
Von Gruenewaldt G, Sharpe MR, Hatton CJ (1985) The Bushveld Complex: introduction and review. Econ Geol 80:803–812
Von Gruenewaldt G, Hatton CJ, Merkle RKW, Gain SB (1986) Platinum-group element-chromitite associations in the Bushveld Complex. Econ Geol 81:1067–1079
von Stackelberg U (1987) Growth history and variability of manganese nodules of the equatorial North Pacific. In: Teleki PG, Dobson MP, Moore JR, von Stackelberg U (eds) Marine Minerals. Reidel, Dordrecht, pp 189–204

Wagener J (1980) The Prieska zinc-copper deposit, Cape Province, South Africa. In: Proc 5th IAGOD Symp, Utah 1979, pp 635–651

Wagener JHF, Van Schalkwyk L (1986) The Prieska zinc-copper deposit, northwestern Cape Province. In: Anhaeusser CR, Maske S (eds) Mineral deposits of southern Africa. Geol Soc S Afr 2:1503–1527

Wakefield J (1978) Samba: a deformed porphyry-type copper deposit in the basement of the Zambian copperbelt. Trans Inst Min Metall 87:B43–B52

Walford P, Stephens J, Strecky G, Barnett R (1986) The geology of the 'A' Zone, Page-Williams mine, Hemlo, Ontario, Canada. In: Proc Gold '86 Symp, Toronto, pp 362–378

Walker PN, Barbour DM (1981) Geology of the Buchans ore horizon breccias. Geol Assoc Can Spec Pap 22:161–186

Walker RG (1970) Review of the geometry and facies organization of turbidites and turbidite-bearing basins. In: Lajoie J (ed) Flysch sedimentology in North America. Geol Assoc Can Spec Pap 7:219-252

Walker RN, Logan RG, Binnekamp JG (1977) Recent geological advances concerning the H.Y.C. and associated deposits, McArthur River, N.T. Geol Soc Aust J 24:365–380

Walker RR, Matulich A, Amos AC, Watkins JJ, Mannard GW (1975) The geology of the Kidd Creek Mine. Econ 70:80–89

Wallace SR, Muncaster NK, Johnson DC, Mackenzie WB, Bookstrom AA, Surface VE (1968) Multiple intrusion and mineralization at Climax, Colorado. In: Ridge JD (ed) Ore deposits of the United States, 1933–1967. AIME, New York, pp 606–640

Wallace SR, Mackenzie WB, Blair RG, Muncaster NK (1978) Geology of the Urad and Henderson molybdenite deposits, Clear Creek County, Colorado, with a section on a comparison of these deposits with those at Climax, Colorado. Econ Geol 73:325–368

Walthier TN, Sirvas E, Araneda R (1985) The El Indio gold, silver, copper deposit. Eng Min J 186 (10):38–42

Wang K (1984) Geochemical characteristics of sedimentation and metamorphism of the Dongchuan copper deposit, Yunnan Province, China. Precambrian Res 25:135–136

Warnaars FW, Holmgren D, Barassi S (1985) Porphyry copper and tourmaline breccias at Los Bronces-Rio Blanco, Chile. Econ Geol 80:1544–1565

Warner LA (1978) The Colorado Lineament: a middle Precambrian wrench fault system. Geol Soc Am Bull 89:161–171

Weiblen PW, Morey GB (1980) A summary of the stratigraphy, petrology, and structure of the Duluth Complex. Am J Sci 280-A:88–133

Weir RH, Jr., Kerrick DM (1987) Mineralogic, fluid inclusion, and stable isotope studies of several gold mines in the Mother Lode, Tuolumne, and Mariposa counties, California. Econ Geol 82:328–344

Weissberg BG (1969) Gold-silver ore-grade precipitates from New Zealand thermal waters. Econ Geol 64:95–108

Wellman P, McDougall I (1974) Cenozoic igneous activity in eastern Australia. Tectonophysics 23:301–335

Wells PRA (1979) Chemical and thermal evolution of Archean sialic crust, southern West Greenland. J Petrol 20:187–226

Wells RE, Heller PL (1988) The relative contribution of accretion, shear, and extension to Cenozoic tectonic rotation in the Pacific northwest. Geol Soc Am Bull 100:325–338

Werle JL, Ikramuddin M, Mutscher FE (1984) Allard stock, La Plata Moutains, Colorado – an alkaline rock-hosted porphyry copper-precious metal deposit. Can J Earth Sci 21:630–641

Wernicke B, Burchfiel BC (1982) Modes of extensional tectonics. J Struct Geol 4:105–115

Westra G, Keith SB (1981) Classification and genesis of stockwork molybdenum deposits. Econ Geol 76:844–873

Whalen JB, Currie KL, Chappell BW (1987) A-type granites: geochemical characteristics, discrimination and petrogenesis. Contrib Mineral Petrol 95:407–419

Wheatley CJV, Whitfield GG, Kenny KJ, Birch A (1986) The Pering carbonate-hosted lead-zinc deposit, Griqualand West. In: Anhaeusser CR, Maske S (eds) Mineral deposits of southern Africa. Geol Soc S Afr 1:867–874

Whelan JF, Rye RO, deLorraine W (1984) The Balmat-Edwards zinc-lead deposits – syn-sedimentary ore from Mississippi Valley-type fluids. Econ Geol 79:239–265
White AJR (1979) Sources of granite magmas. Geol Soc Am Abstr with Prog 11:539
White ARJ, Clemenn JD, Holloway JR, Silver LT, Chappell BW, Wall VJ (1986) S-type granites and their probable absence in southwestern North America. Geology 14:115–118
White DE (1968) Environments of generation of some base-metal ore deposits. Econ Geol 63:301–335
White DE (1974) Diverse origins of hydrothermal fluids. Econ Geol 69:954–973
White WM, Dupre B (1986) Sediment subduction and magma genesis in the Lesser Antilles: isotopic and trace element constraints. J Geophys Res 91:5927–5941
White DE, Anderson ET, Grubbs DK (1963) Geothermal brine well: mile-deep drill hole may tap ore-forming magmatic water, rocks undergoing metamorphism. Science 139:919–922
White WH, Bookstrom AA, Kamilli RJ, Ganster MW, Smith RP, Ranta DE, Steininger RC (1981) Character and origin of Climax-type molybdenum deposits. Econ Geol 75th Anniv Vol, pp 270–316
Whitehead RES, Goodfellow WD (1978) Geochemistry of volcanic rocks from the Tetagouche Group, Bathurst, New Brunswick, Canada. Can J Earth Sci 15:207–219
Wiebe RA (1980) Anorthositic magmas and the origin of Proterozoic anorthosite massifs. Nature (London) 286:564–567
Willemse J (1964) A brief outline of the Bushveld igneous complex. In: Some ore deposits of southern Africa, vol 2. Geol Soc S Afr Publ, Johannesberg, South Africa, pp 19–128
Willemse J (1969) The geology of the Bushveld Igneous Complex, the largest repository of magmatic ore deposits in the world. Econ Geol Monogr 4:1–22
Williams B, Brown C (1986) A model for the genesis of Zn-Pb deposits in Ireland. In: Geology and genesis of mineral deposits of Ireland. Irish Assoc Econ Geol, Dublin, pp 579–589
Williams D, Stanton RL, Rambaud F (1975) The Planes-San Antonion pyritic deposit of Rio Tinto, Spain: its nature, environment and genesis. Inst Min Metall Trans 84:B73–84
Williams H, Hatcher RD, Jr. (1982) Suspect terranes and accretionary history of the Appalachian orogen. Geology 10:530–536
Williams N (1978) Studies of the base metal sulfide deposits at McArthur River, Northern Territory, Australia I: the Cooley and Ridge deposits. Econ Geol 73:1005–1035
Williamson HC, Barr DJ (1965) Gold mineralization in the Yilgarn Goldfield. In: McAndrew J (ed) Geology of Australian ore deposits. 8th Commun Min Metall Congr, Melbourne, pp 87–94
Willis GF (1988) Geology and mineralization of the Mesquite open pit gold mine. In: Schafer RW, Cooper JJ, Vikre PG (eds) Bulk mineable precious metal deposits of the western United States. Geol Soc Nev, Reno, pp 473–486
Willis GF, Holm VT (1987) Geology and mineralization of the Mesquite open pit gold mine. In: Johnson JL (ed) Guidebook for field trips, bulk-mineable precious metal deposits of the western United States. In: Geol Soc Nev Symp, Reno 1987, pp 52–56
Willis GF, Tosdal RM, Manske SL (1987) The Mesquite Mine, southeastern California: epithermal gold mineralization in a strike-slip fault system (Abstr). Geol Soc Am Annu Meet, Phoenix, AR, p 892
Willis IL, Brown RE, Stroud WJ, Stevens BPJ (1983) The early Proterozoic Willyama Supergroup: stratigraphic subdivision and interpretation of high- to low-grade metamorphic rocks in the Broken Hill Block, New South Wales. Geol Soc Aust J 30:195–224
Wilse MA, McGlasson JA (1973) Prince William Sound, a volcanogenic massive sulfide province (Abstr). Geol Soc Am Annu Meet, Dallas 1973, p 865
Wilson CJN, Rojan AM, Smith IEM, Northey DJ, Nairn IA, Houghton BF (1984) Caldera volcanoes of the Taupo Volcanic Zone, New Zealand. J Geophys Res 89:8463–8484
Wilson IF (1955) Geology and mineral deposits of the Boleo copper district Baja California, Mexico. US Geol Surv Prof Pap 273:1–133
Wilson IH, Derrick GM, Perkin DJ (1984) Eastern Creek Volcanics: their geochemistry and possible role in copper mineralization at Mount Isa, Queensland. BMR J Aust Geol Geophys 9:317–328

Wilson JT (1963) Evidence from islands on the spreading of ocean floors. Nature (London) 197:536–538
Wilson JT (1965) A new class of faults and their bearing on continental drift. Nature (London) 207:343–347
Windley BF (1978) The evolving continents. John Wiley & Sons, New York, 385 pp
Windley BF (1983) Metamorphism and tectonics of the Himalaya. Geol Soc London J 140:849–865
Windley BF (1984) The evolving continents. 2nd edn, John Wiley & Sons, New York 399 pp
Wisser E (1966) The epithermal precious-metal province of northwest Mexico. Nev Bur Mines Geol Rep 13:63–92
Wodzicki A (1987) Origin of the Cracovian-Silesian Zn-Pb deposits. Ann Soc Geol Pol 57:3–36
Wold RJ, Hinze WJ (eds) (1982) The geology and tectonics of the Lake Superior Basin – a review. Geol Soc Am Mem 156:278 pp
Wolery TJ, Sleep NH (1976) Hydrothermal circulation and geochemical flux at mid-ocean ridges. J Geol 84:249–275
Wolfhard MR, Ney CS (1976) Metallogeny and plate tectonics in the Canadian Cordillera. Geol Assoc Can Spec Pap 14:361–392
Wood PC, Burrows DR, Thomas AV, Spooner ETC (1986) The Hollinger-McIntyre Au-quartz vein system, Timmins, Ontario, Canada: geologic characteristics, fluid properties and light stable isotope geochemistry. In: Proc Gold '86 Symp, Toronto, pp 56–80
Woodall R (1965) Structure of the Kalgoorlie goldfield. In: Commonw Min Metall Congr 8th, vol 1, Melbourne, pp 71–79
Woodall R (1975) Gold in the Precambrian Shield of western Australia. In: Knight CL (ed) Economic geology of Australia and Papua New Guinea. Aust Inst Min Metall Monogr 5:175–184
Woodcock NH (1986) The role of strike-slip fault systems at plate boundaries. Philos Trans R Soc London Ser A 317:13–29
Woodhead JD (1987) A geochemical study of island arc volcanism. In: Proc Pac Rim Congr Aust Inst Min Metall, pp 932–936
Woodhead JD, Fraser DG (1985) Pb, Sr and ^{10}Be isotopic studies of volcanic rocks from the northern Mariana Islands. Implications for magma genesis and crustal cycling in the western Pacific. Geochim Cosmochim Acta 49:1925–1930
Woodhead JD, Harmon RS, Fraser DG (1987) O, S, Sr and Pb isotope variations in volcanic rocks from the northern Mariana Islands: implications for crustal recycling in intra-oceanic arcs. Earth Planet Sci Lett 83:39–57
Worthington JE, Kiff IT (1970) A suggested volcanogenic origin for certain gold deposits in the slate belt of the North Carolina piedmont. Econ Geol 65:529–537
Wotruba PR, Benson RG, Schmidt KW (1988) Geology of the Fortitude gold-silver skarn deposit, Copper Canyon, Lander County, Nevada. In: Bulk mineable precious metal deposits of the western United States. Geol Soc Nev, Reno, pp 159–172
Wright A (1983) The Ortiz gold deposit (Cunningham Hill) – geology and exploration. Nev Bur Min Geol Rep 36:42–51
Wright JV, Haydon RC, McConachy GW (1987) Sedimentary model for the giant Broken Hill Pb-Zn deposit, Australia. Geology 15:598–602
Wu I, Petersen U (1977) Geochemistry of tetrahedrite and mineral zoning at Casapalca, Peru. Econ Geol 72:993–1016
Wyborn LAI, Page RW, Parker AJ (1987) The petrology and geochemistry of alteration assemblages in the Eastern Creek Volcanics, as a guide to copper and uranium mobility associated with regional metamorphism and deformation, Mount Isa, Queensland. In: Paraoh TC, Beckinsale RD, Rickard D (eds) Geochemistry and mineralization of Proterozoic volcanic suites. Geol Soc Spec Publ 33:425–434
Wyborn LAI (1988) Petrology, geochemistry and origin of a major Australian 1880–1840 Ma felsic volcano-plutonic suite: a model for intracontinental felsic magma generation. Precambrian Res 40/41:37–60
Wyllie PJ (1981) Magma sources in Cordilleran settings. In: Dickinson WK, Payne WD (eds) Relations of tectonics to ore deposits in the southern Cordillera. AR Geol Soc Digest 14:39–48

Wyman D, Kerrich R (1988) Alkaline magmatism, major structures and gold deposits: implications for greenstone belt metallogeny. Econ Geol 83:454–461

Wynne-Edwards HR (1976) Proterozoic ensialic orogenesis: the millipede model of ductile plate tectonics. Am J Sci 276:927–953

Yeates AN, Wyatt BW, Tucker DH (1982) Application of gamma-ray spectrometry to prospecting for tin and tungsten granites, particularly within the Lachan fold belt, New South Wales. Econ Geol 77:1725–1738

Young GM (ed) (1973) Huronian stratigraphy and sedimentation. Geol Assoc Can Spec Pap 12

Young GM (1976) Iron-formation and glaciogenic rocks of the Raptian Group, Northwest Territories, Canada. Precambrian Res 3:137–158

Young GM (1984) Proterozoic plate tectonics in Canada with emphasis on evidence for a late Proterozoic rifting event. Precambrian Res 25:233–256

Ypma PJM, Fuzikawa K (1980) Fluid inclusion and oxygen isotope studies of the Nabarlek and Jabiluka deposits, Northern Territory, Australia. In: IAEA (ed) Uranium in the Pine Creek geosyncline. IAEA, Vienna, pp 375–396

Ypma PJM, Simons JH (1970) Genetical aspects of the tin mineralization in Durango, Mexico. In: Fox W (ed) 2nd Tech Conf Tin, Bangkok 1969; Int Tin Council, London, pp 179–191

Yui S, Ishitoya K (1983) Some textures of the Ezuri Kuroko deposits, Akita Prefecture, Japan. Econ Geol Monogr 5:224–230

Zachos K (1969) The chromite mineralization of the Vourinos ophiolite complex, northern Greece. In: Wilson HDB (ed) Magmatic ore deposits. Econ Geol Monogr 4:147–153

Zachrisson E (1982) Spilitization, mineralization and vertical zonation at the Stekenjokk strata-bound sulfide deposit, central Scandinavian Caledonides. Trans Inst Min Metall 91:B192–B199

Zaw UK (1976) The Cantung E-zone ore body, Tungsten, Northwest Territories - a major scheelite skarn deposit. Thesis, Queens Univ, Kingston, Ontario, 327 pp

Ziegler PA (1978) North-western Europe: tectonics and basin development. Geol Mijnbouw 57:589–626

Zierenberg RA, Shanks WC (1988) Isotopic studies of epigenetic features in metalliferous sediment, Atlantis 11 deep, Red Sea. Can Mineral 26:737–753

Zierenberg RA, Shanks WC III, Seyfried WE, Jr., Koski RA, Strickler MD (1988) Mineralization, alteration, and hydrothermal metamorphism of the ophiolite-hosted Turner-Albright sulfide deposit, southwestern Oregon. J Geophys Res 93:4657–4674

Zoback ML, Thompson GA (1978) Basin and range rifting in northern Nevada: clues from a mid-Miocene rift and its subsequent offsets. Geology 6:111–116

Zuffardi P (1977) Ore/mineral deposits related to the Mesozoic ophiolites in Italy. In: Klemm DD, Schneider HJ (eds) Time- and strata-bound ore deposits. Springer, Berlin Heidelberg New York, pp 314–323

Subject Index

Page numbers in *italics* refer to citations in tables or figures.